

**Outcrop and forward modelling analysis of ice-house
cyclicality and reservoir lithologies**

David A. Pollitt

2008

UMI Number: U585144

All rights reserved

INFORMATION TO ALL USERS

The quality of this reproduction is dependent upon the quality of the copy submitted.

In the unlikely event that the author did not send a complete manuscript and there are missing pages, these will be noted. Also, if material had to be removed, a note will indicate the deletion.



UMI U585144

Published by ProQuest LLC 2013. Copyright in the Dissertation held by the Author.
Microform Edition © ProQuest LLC.

All rights reserved. This work is protected against
unauthorized copying under Title 17, United States Code.



ProQuest LLC
789 East Eisenhower Parkway
P.O. Box 1346
Ann Arbor, MI 48106-1346

DECLARATION

This work has not previously been accepted in substance for any degree and is not concurrently submitted in candidature for any degree.

Signed *David Platt* (candidate)
Date *20/06/08*

STATEMENT 1

This thesis is being submitted in partial fulfilment of the requirements for the degree of PhD.

Signed *David Platt* (candidate)
Date *20/06/08*

STATEMENT 2

This thesis is the result of my own independent work/investigation, except where otherwise stated.

Other sources are acknowledged by explicit references.

Signed *David Platt* (candidate)
Date *20/06/08*

STATEMENT 3

I hereby give consent for my thesis, if accepted, to be available for photocopying and for inter-library loan, and for the title and summary to be made available to outside organisations.

Signed *David Platt* (candidate)
Date *20/06/08*

STATEMENT 4: PREVIOUSLY APPROVED BAR ON ACCESS

I hereby give consent for my thesis, if accepted, to be available for photocopying and for inter-library loans **after expiry of a bar on access previously approved by the Graduate Development Committee.**

Signed *David Platt* (candidate)
Date *20/06/08*

SUMMARY

Combined outcrop and forward modelling studies were employed to improve upon conceptual sequence stratigraphic models of carbonate platform facies architecture during ice-house climate periods. The studied outcrops were chosen to reflect carbonate deposition in a range of sedimentary basin types of similar age (Moscovian); the Paradox Basin (Utah, USA), the Orogrande Basin (New Mexico, USA) and the Moscow-Mezen Basin (Arkhangel'sk Oblast, Russia). Results of outcrop studies were compared and contrasted with results of a one-dimensional stratigraphic forward model, designed to incorporate and test likely controls on carbonate icehouse systems.

Outcrop studies and microfacies interpretation of the Honaker Trail Section (Paradox Basin) reveals no evidence of a sedimentary hierarchy, despite previous interpretation. Existing qualitative conceptual models of a sedimentary hierarchy are found to be flawed and an improved quantitative definition of a sedimentary hierarchy is presented. Results of numerical forward modelling suggest that the existence of a rigorously identifiable sedimentary hierarchy in the stratigraphic record is highly improbable.

Comparison of sedimentary stacking patterns between the Orogrande Basin, the Moscow-Mezen Basin and numerical simulations suggest that although sedimentary cyclicity is highly likely to be forced by glacio-eustatic sea-level oscillations, the stacking patterns and intra-cycle facies distributions are controlled primarily by subsidence regime of the basin. Generally, it can be said that the best reservoir facies (net-to-gross thickness of grainstone) development will occur in moderately to rapidly subsiding extensional basins and moderately subsiding foreland basins.

The absence of peritidal facies within ice-house carbonate successions is a sedimentological distinction between ice-house and green-house periods. Numerical forward modelling reveals that peritidal facies are developed during ice-house periods but because of their position within accommodation cycles tend to have low preservation potential.

ACKNOWLEDGEMENTS

My sincere thanks go to those people who have provided invaluable assistance during fieldwork: Jerry Davies for giving up his free-time and providing valuable instruction in exposure surface identification, Peter and Dana Scholle for very helpful advice and logistical support in New Mexico. I'm also grateful to my fellow Cardiff post-graduate student Huw Williams for assisting me with the Honaker Trail section.

Thanks also to Pavel Kabanov and Anna Strezh, who facilitated access to some little known sections in the Russian north and continue to provide stimulating discussion about this and more.

Thanks too to those who provided excellent advice and discussion: Tom Algeo for advice concerning the Fresnal Canyon section, Gene Stevenson for providing invaluable information and fruitful discussion on the Honaker Trail section and Dan Lehrmann for insightful guidance whenever we've met.

David Emery deserves a special mention and my utmost thanks for developing the Fourier series function for asymmetric sinusoidal oscillations.

I am deeply indebted to my supervisors, Paul Wright, Peter Burgess and Giovanna Della Porta for their guidance – thank you.

Finally, I'd like to thank my family for their loving support over the duration of my studies.

Chapter 1:	Introduction	1
1.1	Rationale	1
1.2	Aims	2
1.3	Structure	3
1.4	Terminology	4
1.4.1	Cycles	4
1.4.2	Sea-level oscillations	4
1.4.3	High-frequency sequence definition	5
1.4.4	List of acronyms	7
<hr/>		
Chapter 2:	A review of Carboniferous sedimentary cyclicity and factors controlling cyclic sedimentation	9
2.1	Sedimentary cyclicity in Carboniferous carbonates	9
2.1.1	Orbital parameters and their effect on climate	14
2.1.2	Uncertainty in the interpretation of sedimentary cyclicity	20
2.2	Models for cyclic sedimentation	30
2.2.1	Autocyclicity	30
2.2.2	Tectonism	32
2.2.3	Allocyclicity	34
2.3	Interpretation of sedimentary cyclicity	35
2.4	Models of eustatic sea-level behaviour	39
2.4.1	An observation-based model	39
2.4.2	An insolation-based model	43
2.4.3	Forward modelling of eustatic sea-level	47
2.5	Evidence of chaotic behaviour of orbital parameters	55
2.6	Summary	61

Chapter 3:	Description of the numerical forward model “TED”	63
3.1	One-dimensional forward modelling	63
3.1.1	Precedents for one-dimensional forward modelling	63
3.1.2	Benefits of one-dimensional forward modelling	64
3.1.3	Limitations of one-dimensional forward modelling	65
3.2	Formulation of TED	67
3.2.1	Explanation of model	67
3.3	TED Parameter definition	71
3.3.1	Time-step Analysis	71
3.3.2	Runs	75
3.3.3	Accumulation	79
3.3.3.1	<i>Sub-tidal production regime</i>	84
3.3.3.2	<i>Peritidal production regime</i>	85
3.3.3.3	<i>Euphotic calcium carbonate production</i>	86
3.3.3.4	<i>Oligophotic calcium carbonate production</i>	87
3.3.3.5	<i>Aphotic calcium carbonate production</i>	88
3.3.3.6	<i>Marine Erosion</i>	88
3.3.3.7	<i>Lag-depth</i>	89
3.3.3.8	<i>Compaction</i>	90
3.3.4	Sub-aerial exposure	91
3.3.4.1	<i>Sub-aerial platform denudation</i>	94
3.3.4.2	<i>Sub-aerial pedogenesis</i>	95
3.3.4.3	<i>Sub-aerial diagenesis</i>	95
3.3.5	Accommodation	96
3.3.5.1	<i>Subsidence</i>	96

3.3.5.2	<i>Symmetric sea-level oscillations</i>	97
3.3.5.3	<i>Asymmetric sea-level oscillations</i>	97
3.4	Output from TED	99
3.4.1	Visualisation	99
3.4.2	Missed-beats	104
3.4.3	Facies taphonomy	107
3.4.4	Statistics	107
3.4.4.1	<i>Embedded Markov chain analysis</i>	108
3.4.4.2	<i>Facies & system entropy analysis</i>	118
3.4.4.3	<i>Runs tests</i>	120
3.4.4.4	<i>Durbin-Watson test</i>	124
<hr/>		
Chapter 4:	Disassembling hierarchies of stratigraphic cyclicity	127
4.1	A sedimentary hierarchy in carbonate successions	127
4.1.1	Lack of a formal definition of a hierarchy	127
4.1.2	Comparison of a new qualitative definition with that of Goldhammer <i>et al.</i> (1991)	129
4.1.3	A quantitative definition of a sedimentary hierarchy	133
4.2	One-dimensional forward modelling of sedimentary hierarchies	135
4.2.1	The objective basis of TED	135
4.2.2	Methodology	136
4.3	Results of modelling studies	141
4.3.1	Runs investigating eustatic amplitude	141
4.3.1.1	<i>A hierarchy of sedimentary thickness</i>	141
4.3.1.2	<i>A hierarchy of hiatal duration</i>	153
4.3.2	Runs investigating subsidence	160
4.3.3	Runs investigating carbonate accumulation	167

4.3.4	Runs investigating sub-aerial platform denudation	172
4.4	Interpretation	179
4.4.1	Examination of hierarchical groupings resulting from a quantitative definition	179
4.4.2	Scenarios where a hierarchy may exist	183
4.4.3	The likelihood of the existence of a hierarchy in the sedimentary record	185
4.5	Conclusions	190
<hr/>		
Chapter 5:	Subsidence-modulated glacio-eustasy: an example from Middle Pennsylvanian shelf carbonates of the Paradox Basin, USA	193
5.1	Introduction	193
5.2	Geological setting	197
5.2.1	Tectonic setting	197
5.2.2	The Middle Pennsylvanian carbonate succession	199
5.3	Facies analysis	202
5.3.1	Aims	202
5.3.2	Method	202
5.3.3	Black laminated mudstone	205
5.3.3.1	<i>Interpretation</i>	205
5.3.4	Sponge facies	208
5.3.4.1	<i>Interpretation</i>	210
5.3.5	Algal facies	213
5.3.5.1	<i>Interpretation</i>	213
5.3.6	Skeletal-silt facies	213
5.3.6.1	<i>Interpretation</i>	216
5.3.7	Skeletal facies	216
5.3.7.1	<i>Interpretation</i>	221

5.3.8	Non-skeletal facies	221
5.3.8.1	<i>Interpretation</i>	226
5.3.9	Quartz-sandstone facies	226
5.3.9.1	<i>Interpretation</i>	229
5.3.10	Discontinuity and sub-aerial exposure surfaces	233
5.3.11	Cycle boundaries	238
5.3.12	Statistical analysis of vertical facies transitions	238
5.4	Stratigraphic simulations	242
5.4.1	Aims	242
5.4.2	Method	242
5.4.3	Lithofacies-matching of the Honaker Trail sedimentary section	245
5.4.3.1	<i>Simulations investigating amplitude of eustatic oscillation</i>	245
5.4.3.2	<i>Simulations investigating rate of platform denudation</i>	248
5.4.3.3	<i>Simulations investigating rate of subsidence</i>	250
5.4.3.4	<i>Reasons for deviation between the HTS and simulated lithofacies</i>	250
5.4.3.5	<i>Summary</i>	253
5.4.4	High-frequency sequence matching	255
5.4.4.1	<i>Simulations investigating amplitude of eustatic oscillation</i>	255
5.4.4.2	<i>Evaluation of stacking patterns</i>	260
5.4.4.3	<i>Simulations investigating rate of subsidence</i>	261
5.4.4.4	<i>Simulations investigating production rate and platform denudation rate</i>	267
5.5	Interpretation	272
5.5.1	Evaluation of an ordered forcing-mechanism	272
5.5.2	Controlling parameters on sedimentation and stacking	275
5.5.3	Hierarchical stacking-patterns	279

5.5.4	Revised genetic stratigraphy	285
5.6	Conclusions	293
Chapter 6:	Tectonically-modulated glacio-eustatic forcing of carbonate successions: examples from the Pennsylvanian of New Mexico (USA) and Arkhangel'sk Oblast (Russia)	297
6.1	Introduction	297
6.2	Method	299
6.2.1	Facies analysis	299
6.2.2	Stratigraphic simulations	305
6.3	The Atokan/Derryan-Desmoinesian (Moscovian) Gobbler Formation, New Mexico, USA	307
6.3.1	Geological setting	307
6.3.1.1	<i>Tectonic setting</i>	307
6.3.1.2	<i>The carbonate succession of the Gobbler Formation</i>	310
6.3.2	Depositional facies	313
6.3.2.1	<i>Lithofacies</i>	313
6.3.2.2	<i>Cycle boundaries</i>	315
6.3.3	Stratigraphic simulation of high-frequency sequences	317
6.4	The Moscovian succession of Arkhangel'sk Oblast, Russia	332
6.4.1	Geological setting	332
6.4.1.1	<i>Tectonic setting</i>	332
6.4.1.2	<i>The carbonate succession of the Moscovian Moscow-Mezen Basin</i>	335
6.4.2	Depositional facies	336
6.4.2.1	<i>Lithofacies</i>	336
6.4.2.2	<i>Cycle boundaries</i>	340
6.4.3	Stratigraphic simulation of high-frequency sequences	342

6.5	Interpretation	352
6.5.1	Evaluation of controlling parameters on stacking patterns	352
6.5.2	Assessment of the presence of a sedimentary hierarchy	354
6.5.3	Reservoir Implications	356
6.6	Conclusions	360
<hr/>		
Chapter 7:	Peritidal facies in ice-house successions: rarity resulting from limited preservation potential	363
7.1	Introduction	363
7.1.1	Peritidal versus sub-tidal cyclicity	364
7.2	Method	367
7.3	Numerical modelling of peritidal carbonate accumulations	370
7.4	Interpretation	380
7.4.1	Accumulation of peritidal facies	380
7.4.2	Taphonomy of peritidal facies	381
7.5	Conclusions	386
<hr/>		
Chapter 8:	Conclusions	387
8.1	Major results	387
8.1.1	The improbability of a sedimentary hierarchy	387
8.1.2	Identification of possible parameter values for ancient successions	389
8.1.3	Subsidence as the primary control on ice-house stacking patterns	390
8.1.4	Poor preservation potential of peritidal facies	391
8.2	Wider implications of results	392
8.3	Future work	393
<hr/>		
References		395
<hr/>		
Appendices		419

Chapter 1: INTRODUCTION

1.1 RATIONALE

The rationale of this study was to use numerical forward modelling and outcrop studies to provide a generic model for understanding the controlling parameters on inner-platform, cyclic ice-house successions.

There are several fundamental problems regarding the study of these types of platform successions. Not least among these is the fact that despite significant study of outcrop and subsurface examples, the controlling parameters on their development are poorly constrained. There are limits to the knowledge that stratigraphy and the study of sedimentary successions can provide regarding depositional conditions in the interiors of ancient carbonate platforms. Similarly, studies of modern analogues are informative; yet modern systems are not perfect at providing insights into ancient successions for a number of reasons. Numerical forward modelling provides a tool with which the controlling parameters of carbonate deposition in ancient environments can be evaluated in terms of their potential to produce recognisably equivalent sections to modern outcrop and subsurface examples.

A further problem may be considered to be the behaviour of sea-level during ice-house periods. There exists a consensus that sea-level oscillations resulted in the deposition of ostensibly cyclic strata, a finding largely supported by sedimentary evidence. Secondary to this is the assumption by a number of authors that cyclic strata, by virtue of hierarchical sea-level oscillations themselves are arranged hierarchically. However, the degree to which stacking patterns are affected by these oscillations, and the conditions which may lead to the occurrence of a sedimentary hierarchy in ice-house sections, have rarely been quantitatively studied.

The relevance of these academic issues should not be under-estimated. Important inner-platform reservoirs exist globally, and there has been much emphasis recently on super-giant hydrocarbon accumulations within inner-platform strata of the Pricaspian Basin (e.g. Kenter *et al.*, 2006). Inner-platform strata are continually cited as being the overriding control on the vertical distribution of reservoir properties within such fields. Despite or perhaps because of this, there are a very limited number of studies investigating the controlling parameters on the distribution of reservoir properties in ice-house successions. This study attempts to redress this deficit in knowledge, with a particular emphasis on one-dimensional modelling of positionally-contemporaneous outcrop analogues for the Pricaspian Basin.

1.2 AIMS

In addition to the individual objectives listed in each chapter of this study; this research has two broad aims addressing the nature of inner-platform ice-house carbonate successions:

1. To quantify the controlling parameters on ice-house inner-platform carbonate successions.
2. To objectively assess the existence of a hierarchy in sedimentary successions.
3. To evaluate the disparity between abundant peritidal facies accumulation in greenhouse successions and the paucity of peritidal facies in ice-house successions.

1.3 STRUCTURE

The body of this thesis is structured thematically into a six chapters which contribute to the aims of the overall thesis. This chapter serves as an introduction. Chapter 2 addresses what is currently known about sea-level behaviour during ancient ice-house worlds which is regarded as the dominant control on sedimentary cyclicity in carbonate successions, and investigates other possible controls of cyclicity.

Chapter 3 is an explanation of the numerical forward model used to conduct simulations, and is described here for the first time. Chapter 4 uses the forward model to conduct a quantitative examination of the existence of a sedimentary hierarchy in ice-house platform strata. Chapters 5 and 6 apply the numerical forward model to try and replicate observed lithofacies and sequence thicknesses in different outcrop examples. As a result of the economic importance of Pricaspian ice-house hydrocarbon reservoirs, outcrops were found which were contemporaneous in their development with the subsurface reservoirs. These studied successions are from basins with different tectonic settings, and were chosen in order to better distinguish the effect of glacio-eustasy on sea-level (as opposed to tectonism). The sections chosen are the Honaker Trail in the southwestern Utah (presented in Chapter 4), the Gobbler Formation in New Mexico and sections in Arkhangel'sk Oblast of northern Russia (all broadly Moscovian in age; refer to individual chapters for precise ages). In addition the outcrops were selected for predominantly excellent exposure of inner-shelf successions, especially in the US sections.

Chapter 7 is a modelling-based study of conditions which lead to the accumulation and preservation of peritidal facies in the stratigraphic record, with an aim to improving our understanding of why these facies are a rarity among ice-house strata. Following this, Chapter 8 concludes by addressing what this study has contributed in terms of the original aims of the study.

This thesis also comprises three appendices. Appendix 1 is a pilot study of lateral variability in a Dinantian (Mississippian) ice-house carbonate platform from Anglesey. It is included here because importantly the Late Carboniferous ice-house period is represented in the UK at Anglesey by a carbonate platform (the morphology of the platform is poorly constrained) with ice-house cyclicity. However, the quality of the outcrop is not adequate for a detailed study quantifying this cyclicity. The sections in Anglesey do represent an opportunity, however, to study lateral variability in an inner-platform succession. This is particularly important given the use of a one-dimensional forward model in this thesis. Appendix 2 and 3 are detailed logs of the Honaker Trail section and Fresnal canyon section, respectively.

1.4 TERMINOLOGY

1.4.1 Cycles

For clarity, it is worthy of note at this point that the terms “rhythmic” and “cyclic” are not synonymous, and the term “cyclic sedimentation” is used here in its popular sense. That is to say: “A style of sedimentation where the sequence of sedimentary facies develops in a regular or repeated manner. The cycle of sediments may consist of two or more facies, and the cycles may be symmetrical or asymmetrical” (Allaby & Allaby, 1999; p142). It would be more accurate when describing ice-house cyclothem, to label them as “rhythmic”, as they represent a repetition of units (i.e. 12341234) rather than a symmetric succession (i.e. 1234321), which would be correctly termed “cyclic”. However, as the convention in contemporary literature is to use the term “cycle”, this will be maintained here to avoid confusion.

1.4.2 Sea-level oscillations

Contemporary studies of carbonate cyclicity make use of an ordinal system to classify both sea-level change and sedimentary cyclicity. This commonly takes the form of division into third-, fourth- and fifth-order (e.g. de Boer & Smith, 1994), although sixth-order has also been cited (Lerat *et al.*, 2000). First- and second-order cycles are variously ascribed to long-term (My-scale) climate change and global tectonic events (refer to de Boer & Smith, 1994). Higher-order divisions are based upon observations of quasi-periodic variation in climate (and therefore continental ice volume and subsequently base level) as a result of changes in the Earth’s orbit (Berger, 1978). This has become known as “Milankovitch theory”.

It is common for different studies to adopt different wavelengths. One of the most prominent examples of this is the difference of opinion over the wavelength of the eccentricity component, with some workers advocating a “long-term” component (c. 400ky; e.g. Heckel, 1986) and others a “short-term” component (c. 100ky; e.g. Goldammer *et al.*, 1991). Both the lack of consensus of the fundamental wavelength of the oscillations (not limited to those of “4th-order”) and the fact that different groups ascribe similar wavelength groups to different categories is confusing.

This problem is compounded by the fact that authors confer the same categorisation scheme to both sedimentary cycles and the sea-level fluctuations which they are deemed to be forced by. Furthermore, some workers apply the highest orders of cyclicity to cycles formed by autocyclic elements which have no corresponding sea-level

fluctuation (e.g. Lerat *et al.*, 2000). This is not constructive for objective analysis of the controls on sedimentary cyclicity.

The final and perhaps most damaging aspect, in terms of our understanding of the behaviour of the link between sea-level oscillation and sedimentary cyclicity, is that this classification scheme is fundamentally hierarchical. This stems from Milankovitch theory which dictates that the quasi-periodic secular variations in the orbit of the Earth are of different duration depending on their type. This topic is discussed further in Chapter 2. The usage of this scheme, even in sections which are not hierarchical implies that they are by virtue of their forcing, and as such may not be appropriate for all sedimentary successions.

Instead of this scheme, a new method of classifying periodic oscillations in eustatic sea-level is presented here (Table 1.1). Where appropriate, this scheme is also applied to cycles observed in sedimentary sections. The division is still made on the basis of wavelength of eustatic oscillations, and as such can be compared to the previous classification scheme. Importantly, however, it should not automatically invoke a hierarchy solely by its use.

1.4.3 High-frequency sequence definition

It is important to differentiate at this stage between parasequences and high-frequency sequences, and explain how this definition is applied within the forward model. A carbonate parasequence is defined by Lehrmann & Goldhammer (1999), after Van Wagoner *et al.* (1988) as “a relatively conformable succession of genetically related beds or bedsets bounded by marine flooding surfaces”. Lehrmann & Goldhammer (1999) go on to state that parasequences “may be subtidal, peritidal, symmetric or asymmetric” and show a “shallowing-upward progression from deeper-marine facies, above the flooding surface, to shallowing-subtidal to peritidal facies”. The boundaries of parasequences are defined where they are “capped by subaerial exposure surfaces, developed on peritidal facies, marine hardgrounds, or shallow-to-deeper-subtidal facies shifts”. This is a fundamentally qualitative sub-division of carbonate strata, and is founded on the tenuous basis of reliably inferring depositional water depth (Rankey, 2004) and in terms of ordered vertical facies transitions (e.g. Wilkinson *et al.*, 2003). Although it has been applied successfully in previous 1D models (e.g. Burgess, 2006), it is not a term used in the forward model presented here because of the subjectivity of its definition.

Consequently the cycles generated by the numerical model presented here, as well as those interpreted in sedimentary sections studied here, are better termed high-frequency sequences (HfSs).

Classification	Duration (My)	Contemporary equivalent (<i>sensu</i> Goldhammer <i>et al.</i> , 1991)
Low-order	>1	3 ^d -order
Intermediate-order	$1 > x > 0.1$	4 th -order
High-order	<0.1	5 th -order

Table 1.1: Classification scheme used for sea-level oscillations.

These, as defined by Lehrmann & Goldhammer (1999), are “a relatively conformable succession of genetically related strata bounded by unconformities or their correlative conformities”. The boundaries of HfSs are identified by “surfaces or facies shifts demonstrating relative fall in sea-level, such as (1) surface of abnormal subaerial exposure, (2) surface or deep subaerial erosional truncation, or (3) abrupt basinward facies offset”. The third criterion is not applied here since it requires two-dimensional control, and the identification of HfSs is therefore applied in its most rigorous, objective sense. This allows a quantitative examination of the occurrence of HfSs in both modelled and sedimentary sections.

1.4.4 List of acronyms

BSLM: Bug Scuffle Limestone Member

FC: Fresno Canyon

HfS: High-frequency Sequence

HTS: Honaker Trail Section

SDP: Severnaya Dvina – Pinega

Chapter 2: A REVIEW OF CARBONIFEROUS SEDIMENTARY CYCLICITY AND FACTORS CONTROLLING CYCLIC SEDIMENTATION

2.1 SEDIMENTARY CYCLICITY IN CARBONIFEROUS CARBONATES

Cyclic styles of sedimentation are characteristic of late Palaeozoic shallow-marine carbonate platform sequences, globally (Veevers & Powell, 1987; Walkden, 1987; Lehrmann & Goldhammer, 1999). This rhythmic sedimentation produces cyclothem which are typically three to 30 metres in thickness, composed principally of sub-tidal sediments and capped with a sub-aerial exposure surface (Walkden, 1987; Figure 2.1). The driving mechanism for this cyclic sedimentation has been extensively studied (refer to de Boer & Smith, 1994) with the current consensus highlighting 'Milankovitch' orbital forcing, and particularly the eccentricity component of this forcing (Horbury, 1989; Barnett, 2002).

Prior to the late Viséan (Asbian), there is no evidence for large-amplitude high-frequency glacio-eustatic sea-level oscillations in the Carboniferous (Wright, 1992). Prior to the Asbian, Carboniferous eustatic sea-level had been dictated according to low-order sea-level changes (Ross & Ross, 1987). These low-order oscillations (i.e. on the order of 1-2My) continued to occur throughout the Carboniferous, but after the Asbian are overprinted by apparent glacio-eustatic intermediate-order (i.e. 100-1000ky) oscillations. Elrick (1991) interpreted cyclic sedimentation in the Courceyan-Chadian of Wyoming and Montana to be linked with high-frequency moderate-amplitude glacio-eustatic oscillations. These cyclothem were not, however, seen in contemporaneous sequences in the British Isles (Wright, 1996). The fact that this cyclicality cannot be correlated with similar platform sequences at geographically distant locations is critical in disproving (or conversely, with correlative cyclothem; proving) a glacio-eustatic causal mechanism.

Smith & Read (2000) timed the onset of glacio-eustasy with relative precision, placing it 1.6My before the end of the Viséan, by counting the number of cyclothem in a given stratigraphic unit and deriving cyclothem duration from the assumed total depositional time. Their paper makes it clear, however, that they failed to take into account 'missed beats', therefore introducing an unknown degree of error into their calculations. The concept of 'missed beats' and their impact on the work of Smith & Read is discussed later.

Wright & Vanstone (2001) present the most reliable estimate for the onset of glacio-eustasy from simple sedimentological evidence. Wright & Vanstone noted that evidence of cyclicality was absent from the Holkerian of Southwest Britain, while the overlying Asbian and Brigantian is distinctly cyclic (Walkden, 1987; Horbury, 1989). This

would be unremarkable if the Holkerian comprised deep-water deposits, however it is primarily composed of very shallow-water limestones (Wright & Vanstone, 2001). Any absence of cyclicity, therefore, is an indictment of glacio-eustasy operating as a major forcing-factor of sedimentation at this time. In addition to this, the Holkerian is devoid of the sub-aerial exposure surfaces that are intrinsically associated with ice-house cyclothem (Wright & Vanstone, 2001; Figure 2.1). The obvious implication here is that glacio-eustasy began in the Asbian.

When glacio-eustasy (apparently) became the dominant forcing mechanism, distinct cyclothem were produced, involving the appearance of similar facies patterns in geographically well-separated areas. Cyclothem characteristically display a shoaling-upwards sequence which is ultimately terminated by lengthy phases of sub-aerial emergence during which the platforms experienced extensive meteoric diagenesis (Figure 2.2). Although the exact composition of facies in a cyclothem varies according to geographical locality, as well as with time through the Carboniferous, cyclothem generally conform to this shoaling-upwards formula.

An example of the changing nature of cyclicity, while still conforming to the shoaling-upwards regime, is apparent in the Asbian-Brigantian of the British Isles. Late Asbian cyclothem are dominated by massive-bedded, often bioturbated light-coloured crinoid-peloid packstones and grainstones (Walkden, 1987). The base of the cyclothem, may, however, comprise darker, more thinly-bedded packstones and wackestones, representing deeper-water sub-wave-base conditions (Walkden, 1987; Davies, 1991). These sediments contain a diverse array of shallow, open-platform flora and fauna. The tops of cyclothem are invariably capped by emergent surfaces, the characteristics of which have been well documented (Davies, 1991; Vanstone, 1996), and with morphologies ranging from gently undulating to heavily-pitted with depressions of half a metre or more (Davies, 1991). Walkden (1987) notes that exposure surface morphology alone is an insufficient diagnostic criterion for the identification of sub-aerial exposure of a platform, "particularly in wavy-bedded mudstones". Examples of this are in the Lower Brigantian of Anglesey, North Wales, where nodular bedding renders exposure surfaces particularly indistinct (Davies, 1991). Similarly, nodular bedding in sections of the Gobbler Formation in the Sacramento Mountains, New Mexico, disguises exposure surfaces as bedding planes (Algeo *et al.*, 1992). Other characteristic features (yet not always present) includes rhizoliths and palaeosols with calcretes, and where present, can be interpreted as being diagnostic of an exposure surface.



Figure 2.1: Photographs showing sedimentary sequences interpreted to be cyclic. This also illustrates the remarkable similarities of Upper Carboniferous cyclic successions, worldwide. A) 4-20m thick Viséan sub-tidal cycles from Derbyshire, UK. B) 3-15m thick Viséan sub-tidal cycles from Anglesey, UK. C) 5-20m thick Desmoinesian sub-tidal cycles from the Sacramento Mts., New Mexico, USA.

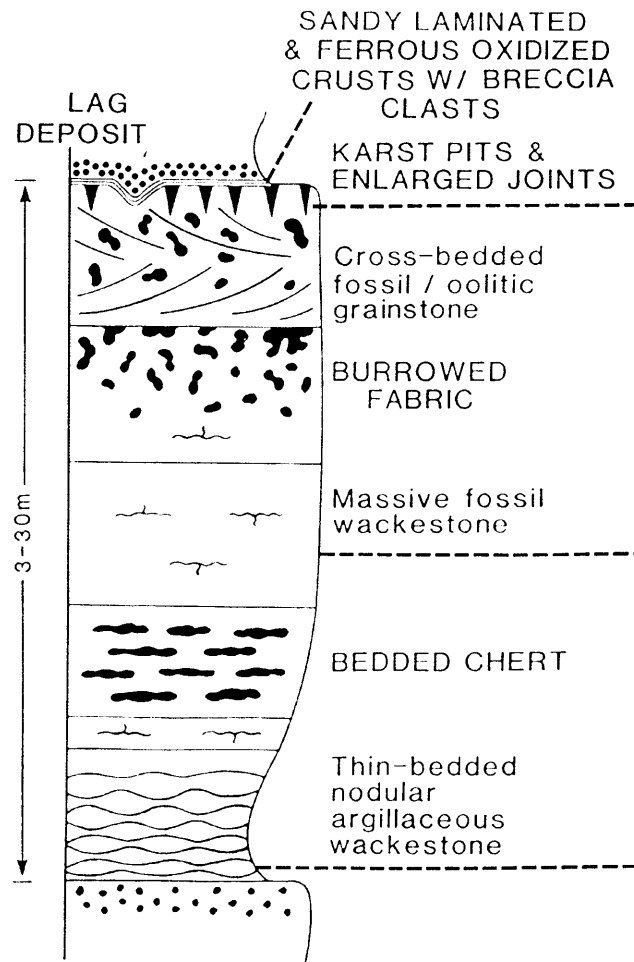


Figure 2.2: Cyclothem interpreted as shoaling-upwards from a facies thought to resemble deeper-sedimentation; primarily because of increased micrite content and relatively deep water biota, which shoals to sub-aerial exposure of sub-tidal shallow-water facies. From the Gobbler Fm., Desmoinesian, Sacramento Mountains, New Mexico (modified from Algeo *et al.*, 1992).

Cyclicality changes noticeably in the Brigantian with the darker wackestones and packstones comprising a significantly greater proportion of a cyclothem than in the Asbian, at the expense of cyclothem-top packstones and grainstones (Walkden, 1987). Shale interlayers are more common in lower sections of cyclothem, and give the appearance of nodular (or wavy) bedding at outcrop (Davies, 1991). Palaeokarstic surfaces and their associated features are still common, occurring on sub-tidal facies. The change in cyclothem characteristics between the Asbian and Brigantian has been interpreted to be the result of variations in the periodicity of orbital forcing components (Walkden, 1987; Wright, 1996).

Although the cyclic sequences in the British Isles are only representative of sections paleogeographically close to one another, similar ice-house cyclothem sequences have been described from locations and timeframes that are distinct from those in Britain. One such example comes from the Gobbler Formation of the Sacramento Mountains, New Mexico. Algeo *et al.* (1992) described strikingly similar cyclothem sequences in the Middle Pennsylvanian (Desmoinesian) New Mexico to those described by Walkden (1987) and others in the British Asbian-Brigantian. The Gobbler Formation is largely comprised of bioclastic wackestones and packstones, containing abundant and diverse open-marine flora and fauna (similar to that described in the British Asbian and Brigantian; Horbury & Adams, 1996). Basal sections of cyclothem sequences are dominated by mudstones and wackestones, representing deeper-water conditions, and containing significant proportions of sponges and brachiopods, and large amounts of nodular chert. These muddier facies grade up into clean, locally grainy although usually of packstone facies-type, limestones, occasionally showing cross bedding. Between these two end-members, algal-plate wackestones and packstones represent biohermal mounds within slope sequences (Algeo *et al.*, 1992; Figure 2.2). These cyclothem sequences are therefore seen to be genetically similar to those of the British Asbian-Brigantian, despite a relatively large difference both in terms of time and geographical separation. This is not restricted to sections from New Mexico, there has also been significant, well-documented studies of similar cyclicality, both in terms of sedimentary style and temporally, from the mid-continent of the United States (e.g. Heckel, 1986; Klein, 1994; Barrick & Heckel, 2000).

The global similarity of ice-house cyclothem sequences has led workers (e.g. Heckel, 1986; Walkden & Walkden, 1990; Wright & Vanstone, 2001) to conclude that orbital forcing was responsible for influencing climate, forcing fluctuations in the volume of water stored as ice at the poles, and ultimately, dictating eustatic sea level.

2.1.1 Orbital parameters and their effect on climate

The widely accepted view (cf. de Boer & Smith, 1994) is that the globally-similar sedimentary cyclothem characteristic of the Lower Carboniferous are the result of glacio-eustatic sea-level oscillations that developed as the Earth moved into an ice-house phase in the Early Carboniferous (Figure 2.3). This cyclicity is considered the result of secular variations in the orientation and position of the Earth (affecting the amount of solar energy received) during its orbit around the Sun (de Boer & Smith, 1994); a theory first proposed by Adhémar (1842), subsequently modified and expanded by Croll (1875) and Milankovitch (1941).

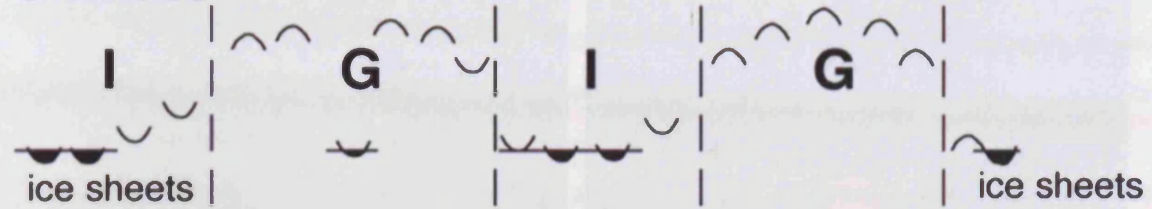
Using three major components; eccentricity, precession and obliquity, Milankovitch calculated the solar insolation of the Earth over the past 650ky. These orbital variations do not radically change the solar constant (the amount of solar energy received by a given area at the top of the stratosphere; which currently increases by 6.4% from aphelion to perihelion, (Berger, 1978b; 1978a); rather they significantly alter the latitudinal and seasonal distribution of solar radiation received by the Earth (Davis & Herzfeld, 1993). Each of the three components has a specific period and an extent to which it affects the amount of light the Earth receives, and hence, its insolation (Figure 2.4).

Eccentricity is the degree to which the Earth's orbit around the Sun deviates from circular (Figure 2.4). The eccentricity periodically ranges from relatively elliptical (0.0607 – where a value of 0 is perfectly circular) to nearly circular (0.0005; Berger, 1978b; 1978a). Eccentricity is primarily affected by the interactions of gravity on the Earth, Sun and Moon, but is also perturbed by interactions with other planets. Periodicities for the eccentricity motion have been dated at 413ky, 123ky, 100ky and 95ky, with secondary peaks thought to be eccentricity-related at 50ky and 53ky (Berger, 1978b; 1978a). The commonly used secular variation for the eccentricity period is 98ky, although some workers favour a 400ky period as well (e.g. Melnyk & Smith, 1989).

Precession can be considered as the deviation of the Earth's polar axis away from the plane of the elliptic due to the combined effects of solar and lunar attraction on the Earth's equatorial bulge; commonly referred to as a 'spinning top' effect (Figure 2.4). The secular period of this component is considered to be 23ky at the present day (Berger, 1978b; 1978a). The Sun's gravity impairs the Earth's ability to spin uniformly about its axis, causing the greatest increase on insolation at perihelion.

The obliquity of the Earth's axis varies from 21° to 24° (Berger, 1978b; 1978a), and the change of aspect causes the differences between the seasons to be more pronounced or dampened. The secular periodicity of the change in obliquity is judged to

Climate



PC	C	O	S	D	C	P	Tr	J	K	T
----	---	---	---	---	---	---	----	---	---	---

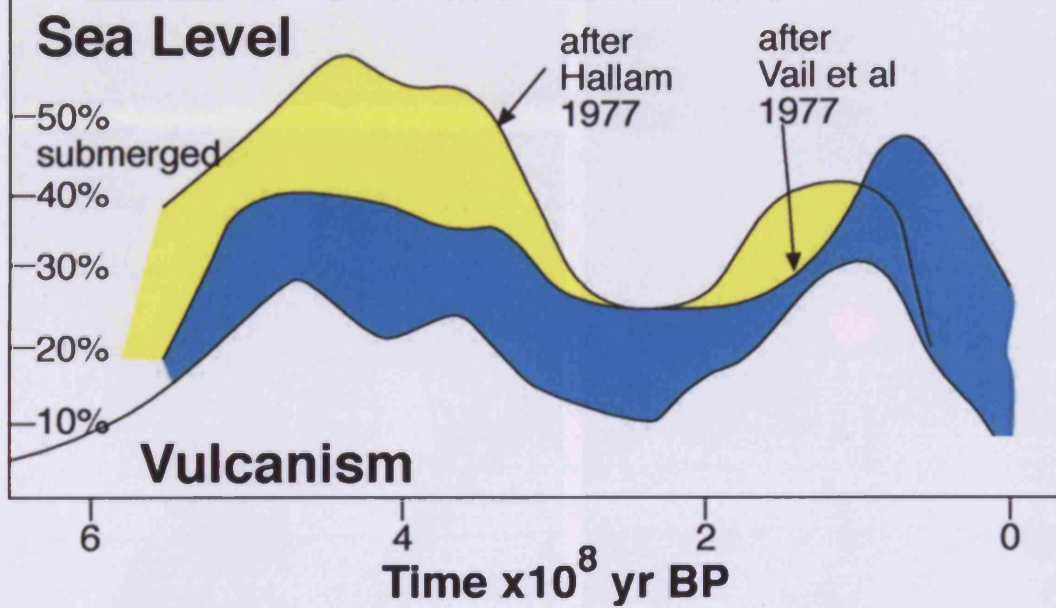


Figure 2.3: Diagram depicting changing levels of vulcanism and sea-level through time. Also represented are greenhouse and ice-house periods (legends G and I respectively). (From Wright, 2005).

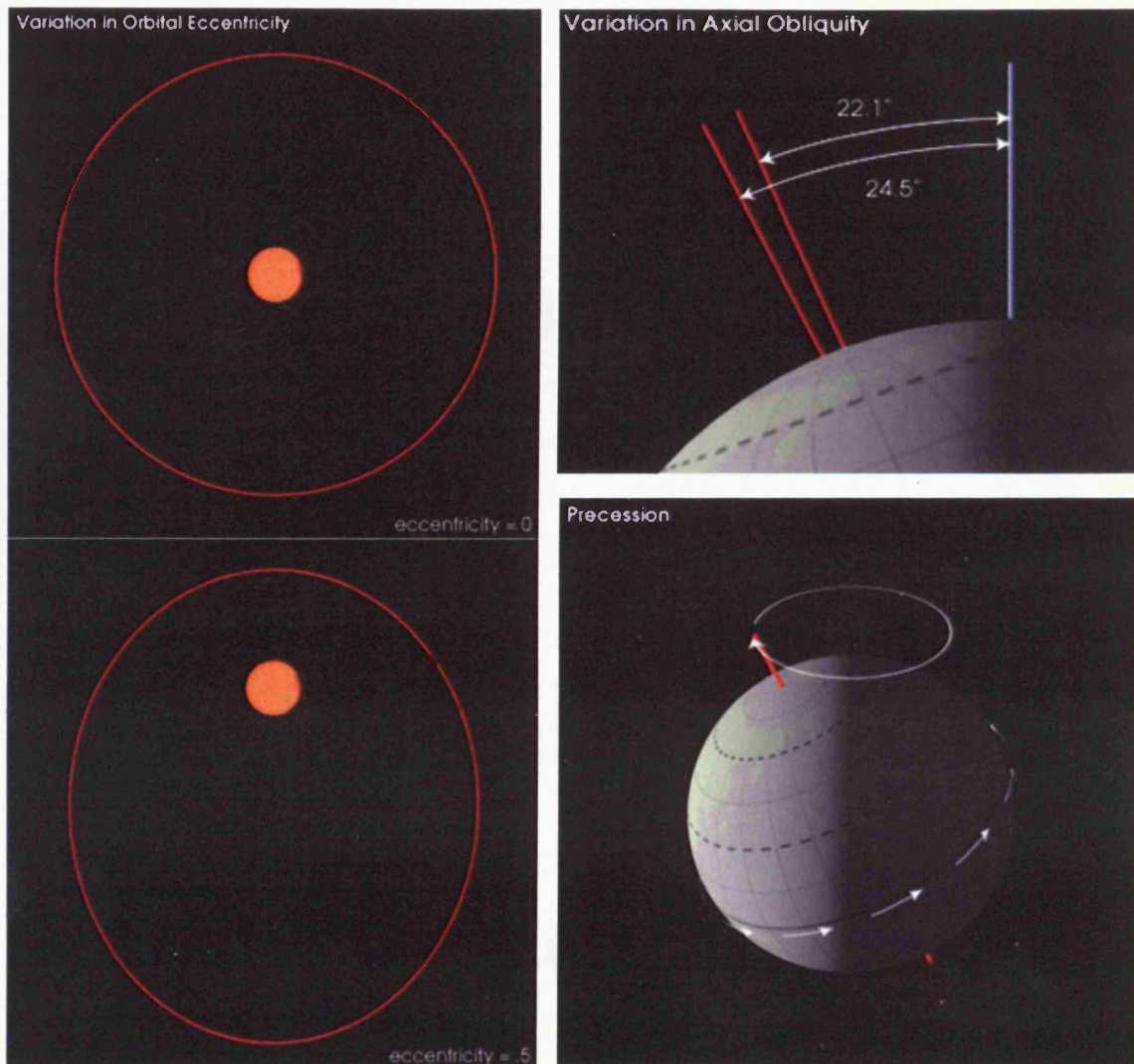


Figure 2.4: Schematic representation of the astronomical variables influencing the climate of the Earth. N.B. not to scale. (Riebeek, 2006).

occur on a 41ky basis (Berger, 1978b; 1978a). Laskar *et al.* (2004) computed the secular oscillations of obliquity over a 250Ma period (Figure 2.5).

Insolation at a given point on Earth depends on the position of the Earth in space, and on the orientation of the point relative to the sun and therefore on eccentricity, precession and obliquity. These factors cause variations in the solar constant and determine the amount of solar energy reaching the surface of the Earth at a given latitude. In turn this affects the location of the caloric equator (Figure 2.6), position of climatic belts and global atmospheric patterns, such as monsoons.

While insolation is likely to have a large effect in determining the climate of the Earth, on the basis that the Earth is not a closed system, and requires energy from the sun, it is difficult to quantify the extent of the effect. Imbrie & Imbrie (1980) attempted to do this for the Pleistocene. However, the degree to which insolation is crucial in determining the global climate of the Earth is unknown. Berger speculates that longer term variations in orbital cyclicity may lead to small variations of climate which can have a disproportionate effect at certain latitudes (Berger, 1978b; 1978a). Between the tropics, it is eccentricity, over-ridden by precession, which has the greatest effect: altering the latitude at which the caloric equator lies, and with it the latitude of climatic zones (de Boer & Smith, 1994). At mid-latitudes (20-40°) orbital variations have their greatest effect on the intensity of the monsoon (Kutzback & Otto-Bliesner, 1982), demonstrating that the energy received by the Earth from the Sun, can have a direct, and seasonal impact on climate. At the highest latitudes (greater than 40°), obliquity has a greater importance acting as a modulator for seasonality (Berger, 1978a; de Boer & Smith, 1994).

As de Boer & Smith (1994) note, most examples of sedimentary cyclicity are concentrated at palaeolatitudes of 20-40°. While this is likely to have a greater relationship with the temperature within these latitudinal bands, the effect of the orbital components is difficult to quantify. What seems apparent from current evidence is that the climatic implications of apparent orbital forcing are manifested most dramatically in the waxing and waning of polar glaciation (Smith & Read, 2000). Any glaciation on a global scale will cause eustatic sea-levels to rise and fall, and so ultimately dictates the accommodation space available to a carbonate factory (Goldhammer *et al.*, 1994).

In terms of accommodation for potential cyclothem development, rhythms operating at different frequencies and amplitudes (which equates to the height and duration of a sea-level rise-fall cycle) are recognised to have varying degrees of importance by differing authors (e.g. Collier *et al.*, 1990; Goldhammer *et al.*, 1991; Barnett *et al.*, 2002). Plotting methods, such as "Fischer" plots (cf. Boss & Rasmussen, 1995), are often interpreted to show a dominant eccentricity rhythm overprinted by a cycle of

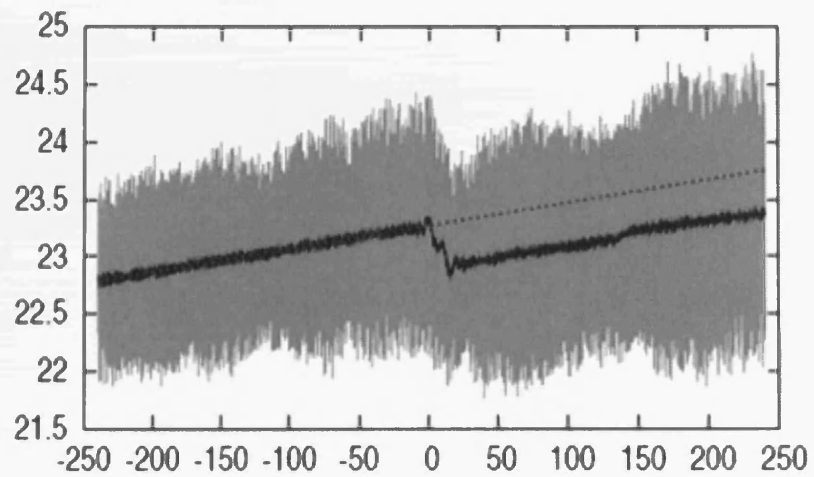


Figure 2.5: Evolution of the obliquity of the Earth in degrees from -250My to +250My. The grey zone is the actual obliquity, while the black curve is the averaged value of the obliquity over 0.5My time intervals. The dotted line is a straight line fitted to the average obliquity in the past. (From Laskar *et al.*, 2004).

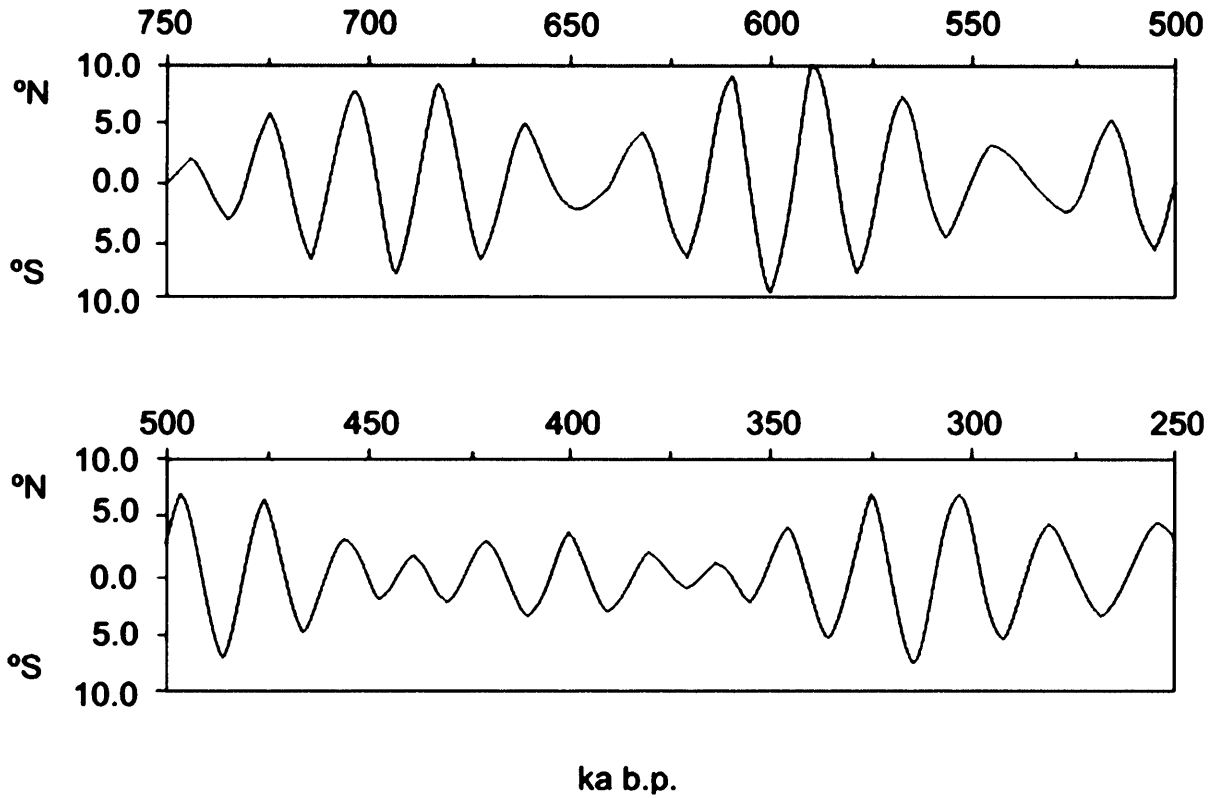


Figure 2.6: Changing position of the caloric equator between 750ka and 250ka. Note the varying frequency. Periods between extreme (north or south) latitudinal positions of the caloric equator vary between 14ky and 28ky. Redrawn from Berger (1978a).

precession (e.g. Osleger & Read, 1991). Subsequently the eccentricity rhythm is incorrectly perceived as imposing a greater effect on atmosphere and climate than that of precession. The true cause is that eccentricity has a much more regular cyclic period than that of the precession cycle, whose frequency varies by a factor of two (14-28ky; de Boer & Smith, 1994); diffusing, to an extent, its true effect (de Boer & Smith, 1994).

2.1.2 Uncertainty in the interpretation of sedimentary cyclicity

There are, however, fundamental problems when translating Milankovitch's work (1941) on the Pleistocene further back into geological time. Firstly, although the solar constant for a given point of the Earth's atmosphere is known, what is unclear is how, and how quickly, the ocean-atmosphere system responds to changes of the solar constant. As sedimentation does not depend on insolation alone, it is likely that a multitude of other factors are incorporated into the system before sediment is lithified (de Boer & Smith, 1994). In Pliocene sediment for instance, Hilgen (1991) showed evidence for a lag of approximately 5ky to precession and eccentricity rhythms, and suggested that a monsoonal climate may take this long to be affected. A further example of this lag effect was highlighted by Adams *et al.*, (1992). These workers showed that methane produced by peat during its formation may not reach a maximum until thousands of years after the corresponding insolation peak; implying that sedimentary systems take significant periods to respond to orbital change. A resolution of sedimentary cyclothem at this level on a thousand-year time-scale, in such a complex system, is very difficult to attain.

A much more complex problem exists, however, in calculating the periodicities of the three orbital parameters back to the Carboniferous. While these variables can be calculated accurately for the present day, there is no guarantee that they have remained static throughout geological time. Berger & Loutre (1994; see also Berger *et al.*, 1989) demonstrated that while tidal friction is gradually slowing the rate of rotation of the Earth, and therefore altering both the periodicities of obliquity and precession; eccentricity is not affected by tidal friction. Therefore the ratios between obliquity and eccentricity, and precession and eccentricity will have changed over time, essentially meaning that the number of higher-frequency rhythms per longer eccentricity cycle will increase further back into geological time. Berger & Loutre calculated that during the Early Palaeozoic secular values for precession were 16ky and 18.5ky, compared to the present day values of 19ky and 23ky. During the Early Carboniferous it is therefore likely that six precession rhythms could overprint one eccentricity rhythm, compared to five in the present day.

Berger's (1978a, 1978b) theory has a flaw, however. The values for the orbital parameters calculated in that work, while accounting for the fact that precession and obliquity are likely to change over time due to tidal friction, rely on the fact that

eccentricity has remained constant. If eccentricity were to change over time also, then the values for obliquity and precession are likely to be affected much more dramatically. Berger (1978b), however, assumed that the motion of the solar system was constant, and the solution could be obtained as quasi-periodic series, using perturbation theory.

Laskar (1989) demonstrated that the motion of bodies in the solar system did not remain constant over large periods of time (Figure 2.7). The motion of the planets could not, therefore, be calculated by perturbative series. Furthermore, Laskar (1989) showed strong evidence of divergence in the system of inner planets, demonstrating that initially close orbits diverge with a Lyapunov time (essentially the time for chaos to become apparent in an orbit; regular orbits have an infinite Lyapunov time; Figure 2.8) of 5Ma.

Laskar's (1989) findings are conveniently ignored in some geological literature. Perhaps this reflects the results that Laskar obtained, which means that if the variation of the Earth's orbit is chaotic, then there can be little confidence in the periodicities of orbital parameters beyond the Oligocene, which workers use to define from stacking pattern analysis. Laskar's work and its applications to sedimentary modelling are assessed in detail in section 2.5.

Critical to the understanding of high-frequency, high-amplitude glacio-eustasy is the question of whether the stratigraphic succession of sedimentary cyclothems was the result of rhythmic or arrhythmic processes. A distinction between the two is critical as rhythmic processes implies an ordered forcing mechanism, such as astronomically-forced sea-level oscillations, whereas arrhythmic process suggest an unordered controlling mechanism – such as non-uniform subsidence. This relationship was explicitly defined by Sander (1951, p. 16).

Sander deduced from a study of the Dachstein Limestone in the Northern Calcareous Alps, that it cannot be concluded “from sequences that are non-rhythmic in space that the control has been non-rhythmic in time but we must conclude from sequences that are rhythmic in space that there has been a time-rhythmic control (law of the rhythmic record)”. Schwarzacher (1975, p. 288) confirmed this statement through the use of statistical arguments, and defined the concept as Sander's Rule: “cyclicity in space (which means stratigraphical [*sic*] thickness) indicates cyclicity in time but the absence of cyclicity in the stratigraphical record does not indicate the absence of time cyclicity”.

This statement is fundamental to understanding the controls on stratigraphic cyclicity, and also highlights a further problem of the study of rhythmic sedimentation.

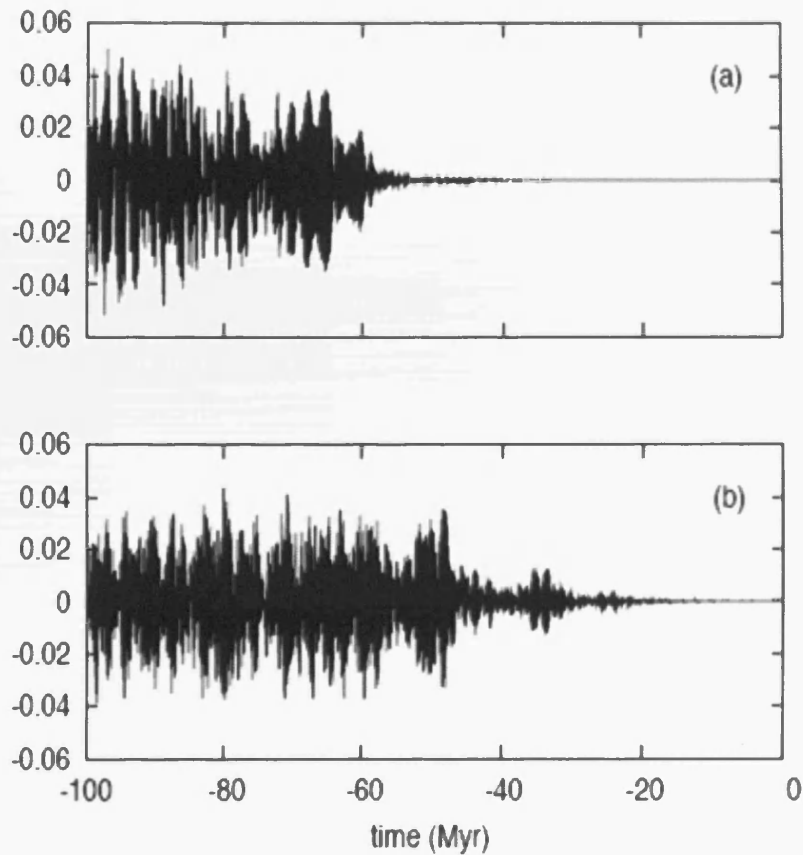


Figure 2.7: Stability of the solution for eccentricity of the Earth as computed by two numerical models: La2004 and La2004*. (a) Difference of the nominal solution La2004 (from Laskar, 2004) with stepsize $r = 5. \times 10^{-3}$ years, and La2004*, obtained with $r^* = 4.8828125 \times 10^{-3}$ years. (b) Difference of the nominal solution with the solution obtained while setting $J_2^S = 0$ for the Sun (instead of 2×10^{-7} in the nominal solution). The key point to take from this diagram is that up to 60Ma a solution can be generated with good stability – suggesting that the eccentricity component of the Earth’s orbit can be modelled up to this point. Beyond 60Ma the stability of the simulation decreases dramatically, indicating that beyond this point the veracity of numerical simulations in predicting the eccentricity component of the Earth’s orbit should be considered tenuous. (From Laskar *et al.*, 2004).

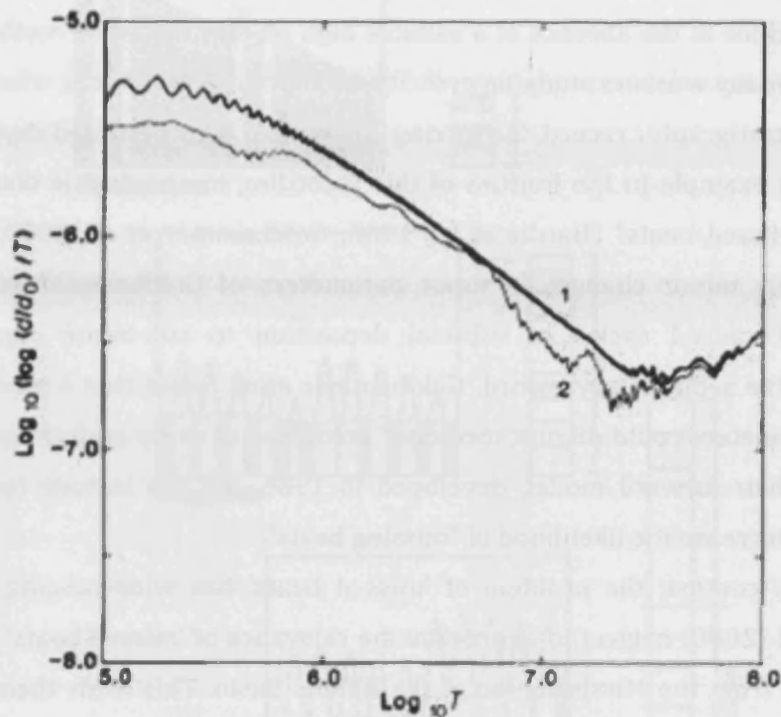


Figure 2.8: Computation of the maximum Lyapunov exponent. This plot shows $\log_{10}(\log(d/d_0)/T)$ versus $\log_{10}T$ (where T is time in years) over 100My with renormalisation every 40My (curve 1) or with renormalisation every 1My (curve 2). In the two cases, the same results are obtained for large values of T , which give a maximum Lyapunov exponent of about $10^{-6.7} \text{ y}^{-1}$ ($1/5\text{My}^{-1}$) for the secular system in eccentricity. This suggests that a critical divergence in terms of stability occurs after 5Ma, at which point the motion of the planets becomes unpredictable, and orbital parameters (eccentricity, obliquity and precession) may change from periodicities observed in the Pleistocene. (From Laskar, 1989).

Schwarzacher (1975) highlights the fact that a time-cyclic control is likely to have been more regular than its record in the stratigraphy, which because of the number of factors and variables involved, is at best a “faulty recording mechanism”. Sander’s Rule does not imply that the Milankovitch cyclicity hypothesis is, at present, untestable as time cyclicity cannot be tested for in the absence of a suitable high resolution dating method. Rather, it reaffirms what many workers studying cyclicity take for granted: that is, where cyclicity is present in the stratigraphic record, the forcing factor must have operated rhythmically.

A prime example in the frailties of this recording mechanism is displayed in the evidence for “missed beats” (Hardie *et al.*, 1986; Goldhammer *et al.*, 1990; Balog *et al.*, 1997). Relatively minor changes in input parameters of Goldhammer *et al.*’s (1990) forward model caused cycles of subtidal deposition to sub-aerial exposure to go unrecorded in the sedimentary record. Goldhammer *et al.* found that a modification of a number of parameters could disrupt the ‘ideal’ recording of every cyclothem (Figure 2.9). Furthermore, their forward model, developed in 1986, did not include factors such as erosion, which increase the likelihood of “missing beats”.

Put into context, the problem of ‘missed beats’ has wide-ranging implications. Smith and Read (2000) neglect to appreciate the relevance of ‘missed beats’ in calculating cycle durations from the Mississippian of the Illinois Basin. This leads them to deduce a period for intermediate-order cycles by simply dividing the total period of their study interval by the number of cycles; resulting in an average duration of 333ky. Regardless of the fact that there is a discrepancy of seventy thousand years between this figure and that of a 400ky eccentricity cycle (the period employed by Smith and Read (2000)), ‘missed beats’ could alter this conclusion dramatically. For instance, the 3My spanning the study period could feasibly accommodate one low-order cycle, which, in light of Goldhammer *et al.* (1990; 1991) could have as many as three ‘missed beats’ on each rising limb and falling limb. This would mean that instead of 9 sequences, there could be 15, giving a cycle duration of 200ky, which if a 70ky leeway is applied, as Smith and Read did in the opposite direction, could put the cycle period at around 130ky – reminiscent of the secular 112ky eccentricity period.

The method used by Smith & Read (2000) to calculate the average cycle period is also called into question by the work of Algeo & Wilkinson (1988). They are able to demonstrate that of more than 200 “meso-scale” (1m to 20m) sedimentary cyclothem, 98% can be shown to have a ‘mean’ accumulation rate; meaning that sedimentary cyclothem with thicknesses between 1m and 20m will generally produce values in the Milankovitch frequency range (21ky to 413ky). As cyclothem of similar thicknesses may be produced by mechanisms independent of orbitally-modulated climatic change (e.g. autocyclicity; Burgess, 2001), average periodicity in the Milankovitch range is not

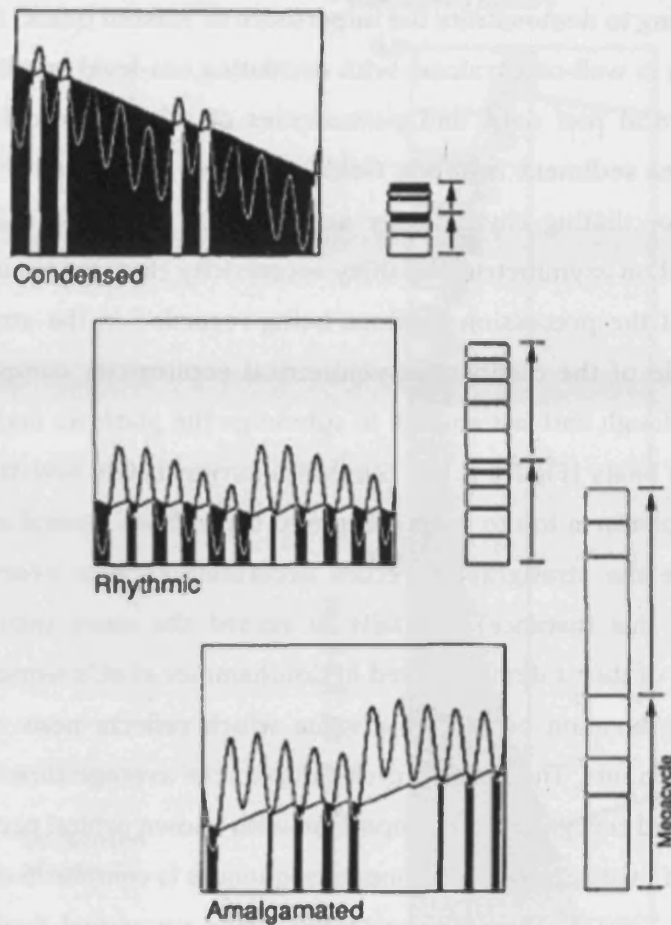


Figure 2.9: Graphical representation of high-frequency, composite sea-level oscillations (superimposed 100ky asymmetric fourth-order and 20ky sinusoidal fifth-order [sic]) and platform aggradation (panels on left) resulting in 'megacycle' (high-frequency sequence) packaging (columns on right). High-frequency composite eustasy combined with long term ("third-order") trends yields three classes of 'megacycles': 1) condensed 'megacycles' are produced when one or more 20ky oscillations are missed below the platform top. 2) Rhythmic 'megacycles' are produced when each successive 20ky oscillation is registered. 3) Amalgamated 'megacycles' are produced when 20ky oscillations are missed above the platform. (From Goldhammer *et al.*, 1990).

sufficient to prove Milankovitch-type forcing as a causal factor.

Goldhammer *et al.* (1990) used an example from the Pleistocene of South Florida, for forward modelling to demonstrate the importance of 'missed beats'. Pleistocene glacio-eustasy in this area is well-constrained; with oscillating sea-level amplitudes determined from Pleistocene coral reef data, and periodicities of sea-level oscillations derived by proxy from deep-sea sediment isotopes. Goldhammer *et al.* showed that a model which invoked sea-level oscillating rhythmically according to sinusoidal *c.*20ky precessional beats superimposed on asymmetrical *c.*100ky eccentricity rhythms, would result in only a small proportion of the precession rhythms being recorded in the stratigraphic record. The large amplitude of the distinctly asymmetrical eccentricity component forced sea-level to rise high enough and fast enough to submerge the platform and fail to record any of the precessional beats (Figure 2.10). Similarly, during 100ky low-stands sea-level fell quickly below the platform top to keep it exposed throughout several of the precessional rhythms. Therefore the stratigraphic record accurately reflects overriding Pleistocene orbital forcing (in this instance) but fails to record the more intricate higher-order cyclicity. The effect of this is demonstrated in Goldhammer *et al.*'s work, which records an average cyclothem duration of *c.*67ky; a value which reflects none of the Pleistocene Milankovitch components. The missing cycles distort the average time taken to deposit a parasequence beyond recognition in comparison with known orbital periodicities.

The issue of missing time in carbonate sequences is complicated by the findings of Burgess & Wright (2003). They demonstrated, using numerical forward models, that hiatuses could occur throughout a parasequence, not at the base and top alone (Figure 2.11). These hiatuses represent non-deposition due to the production of carbonate in a mosaic pattern (as their model was programmed to produce) as well as erosional scour. Burgess & Wright linked the triggers for these hiatuses to water depth and fetch, which in their 2D model displayed a complex relationship due to the formation of islands in the mosaic. Preserved strata represent between 15% and 60% of the time taken to deposit an individual parasequence; representing relatively small depositional periods. Burgess & Wright stated that: 'stratigraphic completeness therefore depends on subsidence rate and sediment transport rate, so that completeness generally increases with increasing subsidence rate and decreasing transport rate, but shows a non-linear relationship with subsidence rate.' The salient point is that the carbonate depositional systems of the past and their subsequent output of preserved strata may rely upon more than simply a constant subsidence rate and sea-level. This is likely to comprise a myriad of factors which interact with a considerable degree of complexity.

Stratigraphic column

Sea-level – sedimentation – subsidence history

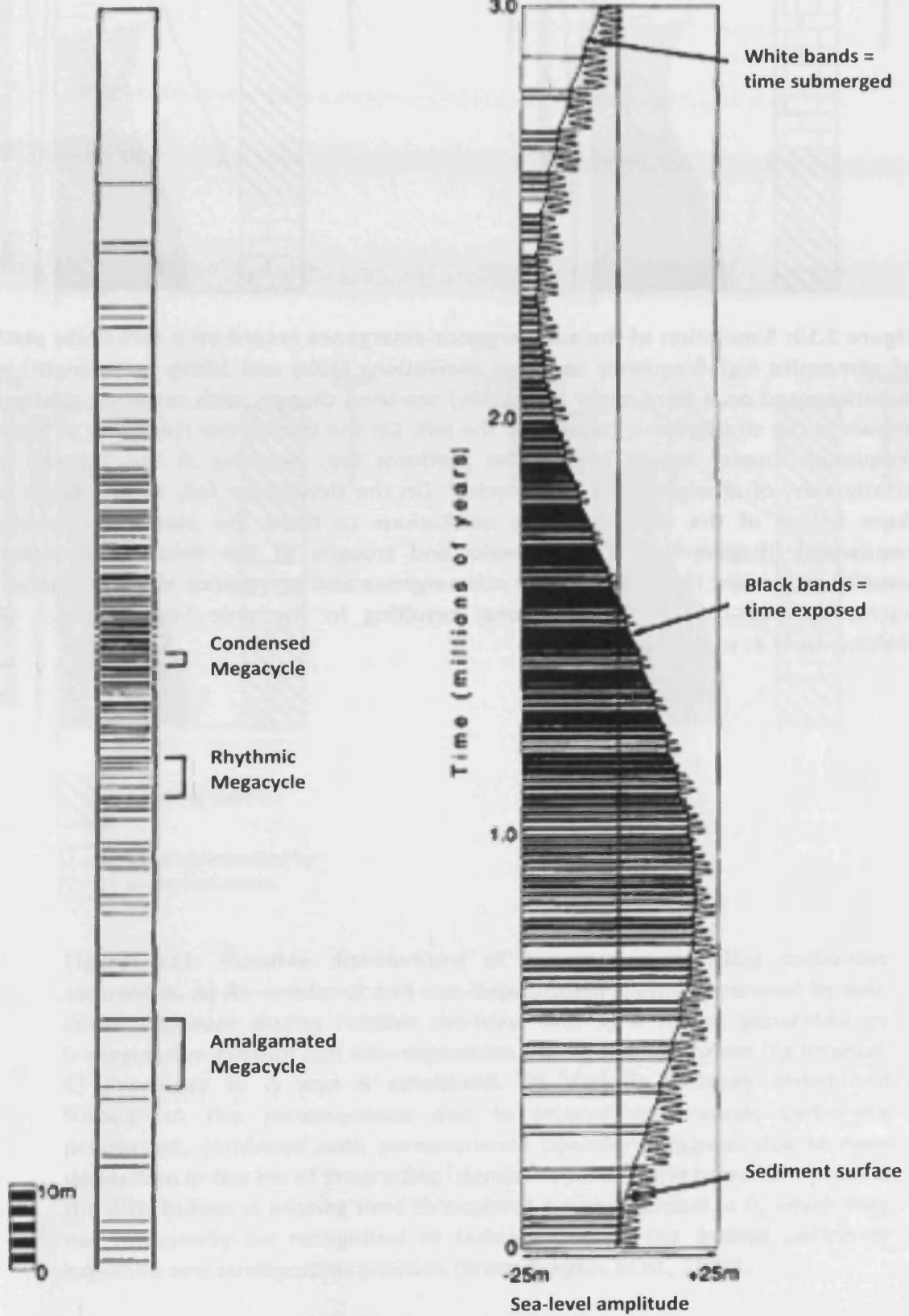


Figure 2.10: Caption overleaf.

Figure 2.10: Simulation of the submergence-emergence record on a carbonate platform of composite high-frequency sea-level oscillations (20ky and 100ky wavelength) when superimposed on a third-order [sic] (3My) sea-level change, with resulting stratigraphy shown in the stratigraphic column on the left. On the third-order rise some of the high-frequency “beats” fail to expose the platform top, resulting in the “missed beat” stratigraphy of amalgamated ‘megacycles’. On the third-order fall, missed beats result from failure of the high-frequency oscillations to flood the platform, resulting in condensed ‘megacycles’. At the peaks and troughs of the third-order oscillation, conditions are just right to allow for submergence and emergence of the platform with successive high-frequency oscillations, resulting in rhythmic ‘megacycles’. (From Goldhammer *et al.*, 1990).

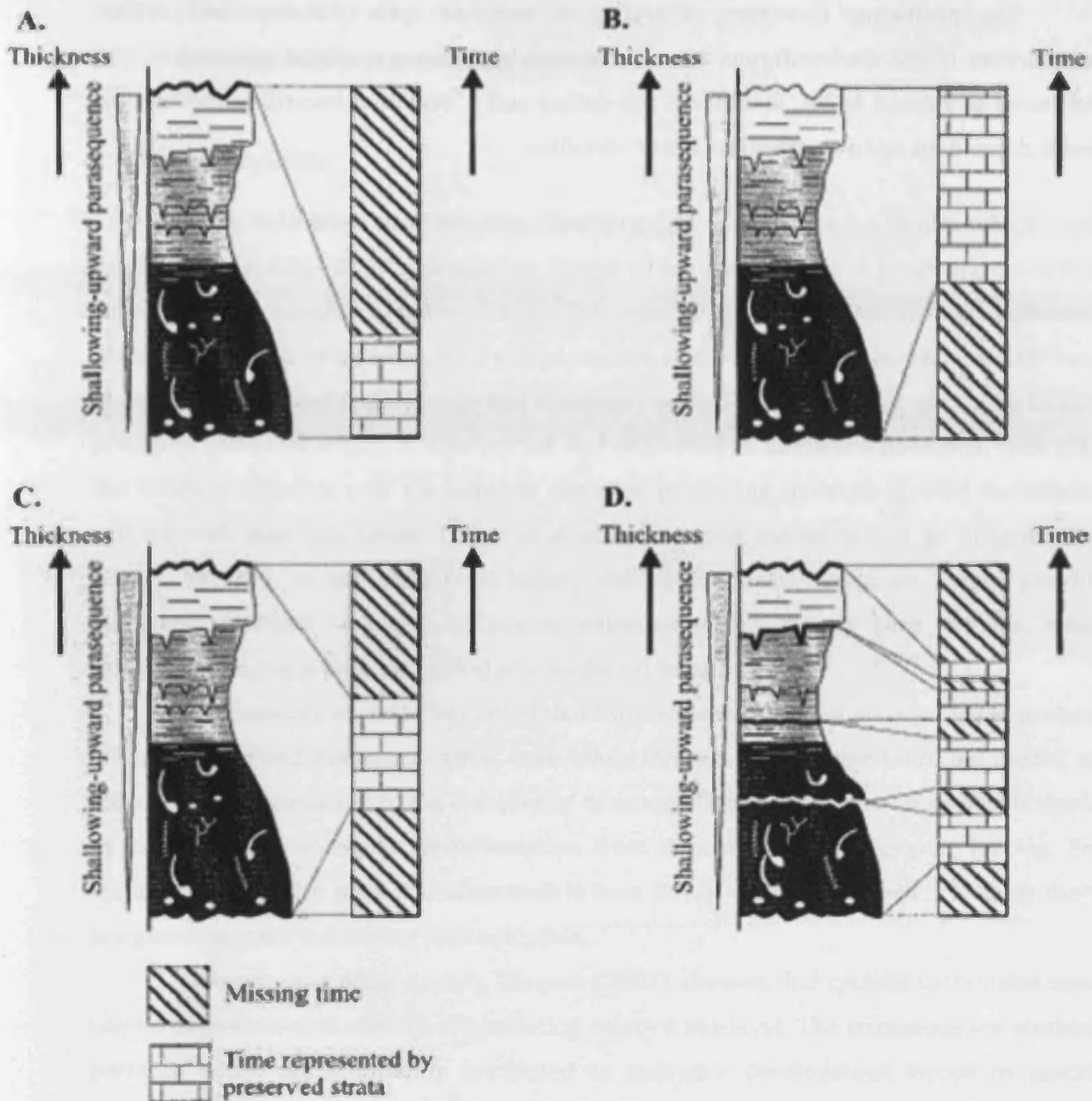


Figure 2.11: Possible distributions of hiatuses in peritidal carbonate sequences. A) An erosional and non-depositional hiatus generated by sub-aerial exposure during relative sea-level fall. B) A hiatus generated by transgressive erosion and non-deposition during the carbonate lag interval. C) Processes in A and B combined. D) Various hiatuses distributed throughout the parasequence due to intermittent mosaic carbonate production, combined with parasequence boundary hiatuses due to non-deposition in the lee of prograding islands. A particularly important point is the distribution of missing time throughout a parasequence in D, which may not necessarily be recognised at outcrop due to the limited period of exposure and stratigraphic position (From Burgess *et al.*, 2001).

The problems, therefore, of trying to estimate cycle duration and orbital periodicities in the Carboniferous are exacerbated by unknown orbital parameters, the likelihood of missed beats, inaccurate age-dating and a sensitive recording mechanism that is dependent upon an extensive list of variables.

2.2 MODELS FOR CYCLIC SEDIMENTATION

2.2.1 Autocyclicity

Using data from the Holocene, Ginsburg (1971) developed a model which could produce a stacking pattern simulating fourth order cyclicity via a progradation-driven autocyclic mechanism (Figure 2.12). This model envisages continuous carbonate accumulation and prograding tidal complexes on shallowly-dipping carbonate platforms, in conditions of steady subsidence and stationary eustatic sea-level. The carbonate factory produces sediment which is transported and deposited in landward positions, with tidal flat facies prograding over the subtidal deposits, producing shoaling-upward cyclothems capped with tidal flat facies. The critical concept of the model is that as progradation occurs, the size of the carbonate factory diminishes, until it can no longer provide sufficient sediment to match or exceed subsidence. The factory then drowns, while production begins after a lag period at a landward location.

Goldhammer *et al.* (1994) noted that time-series analysis of autocycles fail to show Milankovitch-band frequency ratios, even when they are programmed into the model; an effect which is attributed to the complexity of autocyclic progradation. This effect is useful in distinguishing autocyclic sedimentation from deposition with allocyclic forcing. For instance, if extensive meteoric diagenesis is seen to cap cyclothems, then it is likely there is a glacio-eustatic control on sedimentation.

Through modelling studies, Burgess (2001) showed that cyclical carbonates need not be deposited with the aid of oscillating relative sea-level. The parasequence stacking patterns which are commonly attributed to sequence development forced by glacio-eustasy may also occur in conditions of static sea-level but oscillating production and sediment-transport rates. The caveat to this is that where sub-aerial exposure of sub-tidal facies is evident, glacio-eustasy or tectonism must be given credit as the cause of such cyclicity. This does not rule out, however, the importance of autocyclic mechanisms as a contributory component in glacio-eustatic cycles (Barnett *et al.*, 2002).

Barnett *et al.* (2002) used the model of Burgess (2001) to generate autocycles in an ice-house environment. It is interesting to note that Barnett *et al.* found that autocycle development to be far less prolific in terms of cyclothem-generation, in an ice-house environment than in the greenhouse environment (i.e. periods of relatively static low-amplitude low-frequency sea-level) modelled by Burgess (2001). As Burgess (2001) concludes, many carbonate systems may represent a combination of both glacio-eustatic

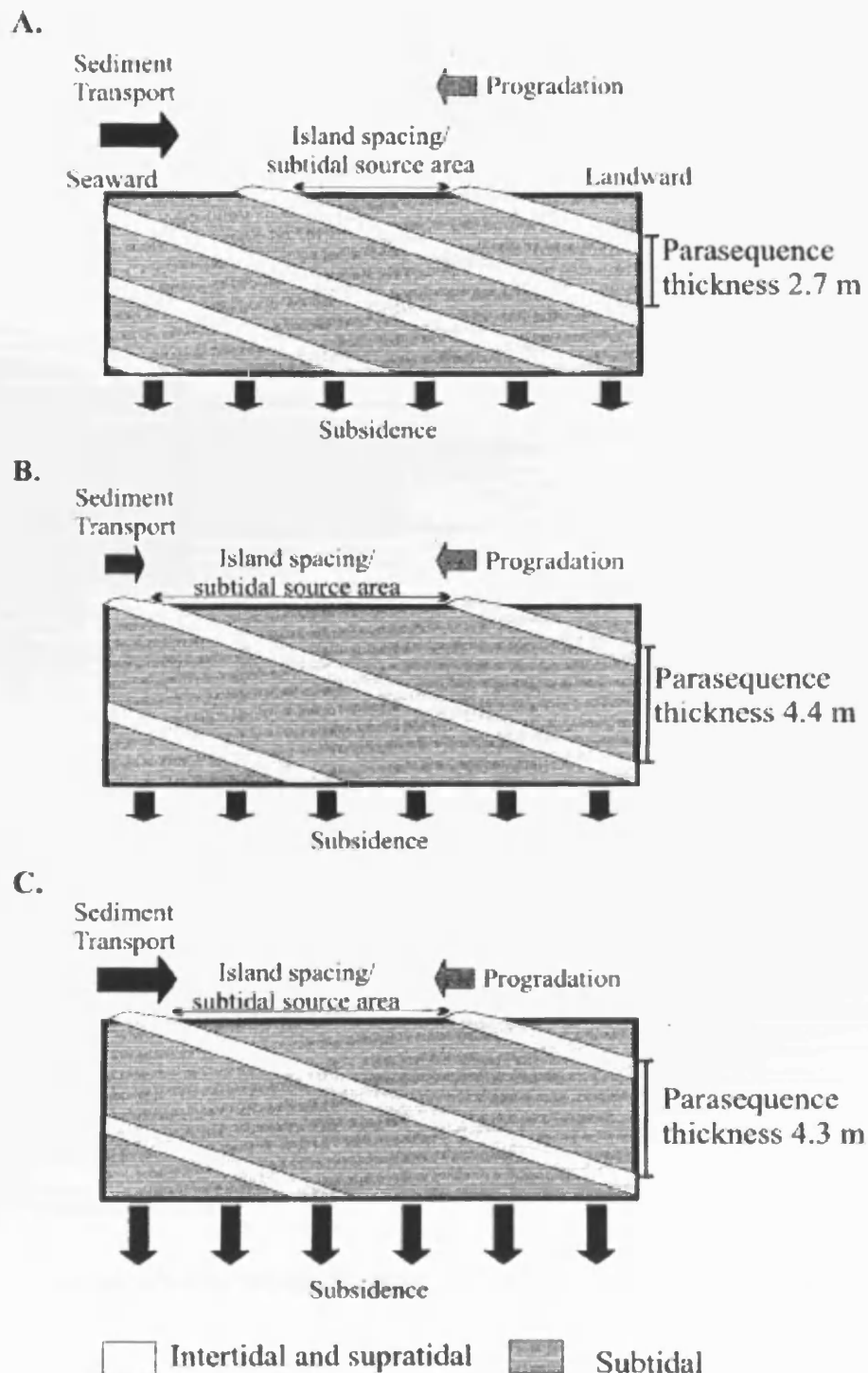


Figure 2.12: In the model of Burgess & Wright (2003) parasequence thickness varies with both the rate of relative sea-level rise and rate of sediment transport. Increasing subsidence rate, or decreasing sediment transport rate, decreases the rate of island progradation, allowing more accommodation to be created during progradation, and therefore generating a thicker parasequence. A) Sediment transport rate 1000m My^{-1} and subsidence rate 20m My^{-1} creates parasequences 2.7m thick. B) Sediment transport rate 500m My^{-1} and subsidence rate 20m My^{-1} creates parasequences 4.4m thick. C) Sediment transport rate 1000m My^{-1} and subsidence rate 40m My^{-1} creates parasequences 4.3m thick. (From Burgess & Wright, 2003).

and autocyclic forcing. Therefore as a component of glacio-eustatic cycles, autocyclic influence should not be discredited.

2.2.2 Tectonism

Despite the recent popularity of the theory that sedimentary cyclicity seen at outcrop is due to some form of rhythmic orbital forcing alternative mechanisms have been suggested (e.g. Ramsay, 1989). The importance of tectonics in cyclic sedimentation has also been noted by several workers (e.g. Gawthorpe, 1986; Horbury, 1989; Adams *et al.*, 1990). These authors suggested alternate periods of tectonic quiescence and activity during which the active faulting (equivalent to 3rd order eustatic variations) allowed accommodation to be created. It was only during the periods of relatively uniform subsidence that glacio-eustasy was envisaged to be able to produce shoaling-upward cyclothem in the newly-created accommodation. A fundamental problem with this theory is the requirement that accommodation must be reduced at the correct time-frequency in order to produce the strata seen in the rock record. One way workers have tried to account for this is by invoking 'yo-yo' tectonics as the forcing mechanism.

Intervals of repeated tectonic pulses of relatively rapid subsidence followed by uplift (reversal or 'yo-yo' tectonics) could induce cyclicity by alternately submerging and then sub-aerially exposing the carbonate platform (Goldhammer *et al.*, 1994). While this causal mechanism is possible, it is difficult to visualise as there are no modern analogues world-wide. An added problem is present in the fact that to create these sedimentary cyclothem, this mechanism has to be both pulsed, and operate on a global scale at the correct frequency; a set of criteria that no known tectonic mechanism can meet.

A key difference between the two types of tectonic model is the style of sedimentation that will be produced (Goldhammer *et al.*, 1994). Reversal tectonics will create cyclothem superficially similar to those apparently forced by orbital components, composed of shoaling-upwards cyclothem with a sub-aerial diagenetic cap. Comparatively, cyclothem controlled by episodic subsidence may shallow-upwards but would not show significant evidence of sub-aerial exposure.

Cisne (1986) proposed a model that accommodates reversal tectonism, but only in platforms that are fault-bounded. Modern examples of tectonic pulsing are confined to tectonically active settings; poor analogues for ancient mature passive margins (Osleger & Read, 1991). Indeed, Osleger & Read note that the applicability of such a model would be restricted to a local scale, not able to produce cyclicity or a regional, or global, scale. Notably however, throw and recurrence frequency cannot be estimated. Goldhammer (1994) notes that while a differential subsidence origin for sedimentary cyclicity is feasible, time-scale estimates are hard to constrain.

The importance of tectonism as a controlling factor in any sedimentary regime is beyond doubt; however, its relevance as a controlling mechanism for low-order sedimentary cyclicity was highlighted by Barnett *et al.* (2002). Titus & Riley (1997) correlated a major mid-Asbian transgression between two basins of differing tectonic regimes; the Antler Foreland Basin, Utah and the Craven Basin, Cumbria using ammonoid biostratigraphy. Using this method, a relatively high time-resolution was achieved (of less than 1My error), although this is still outside of the ideal 500ky resolution for the identification of low-order sequences, as recommended by Miall (1997). Nevertheless Titus & Riley correlated a major flooding event between two basins of different tectonic styles that were over 5000 kilometres apart during the Carboniferous. This suggests that the cause of sedimentation was eustatic, and while this does not preclude a tectonic cause, sea-level rise as a function of long-wavelength tectonic processes (at the correct frequency) is hard to envisage.

Furthermore, when considering tectonism as a forcing-mechanism for sedimentary cyclicity, it is useful to remember Sander's Rule (Schwarzacher, 1975). If a sedimentary succession displays ordered cyclicity, then the process dictating it must be ordered as well. In the case of tectonism, therefore, this would require a very strict threshold-stress which must be achieved in order to induce crustal movement. As fault-related tectonics has an under-riding principle of threshold-stress, its applicability as a forcing mechanism should not be precluded. This stress, however, would also have to remain relatively constant over a considerable duration to produce the style of cyclicity seen in the sedimentary record. Cloetingh (1986) cites intra-plate stress as a potential forcing mechanism for sea-level change, however this is too slow (0.01-0.1m/ky) and does not contain an inherent threshold stress needed for the production of rhythmic cyclothem.

More recently, De Benedictis *et al.* (2007) showed that Quaternary extensional faults with instantaneous and relatively small throw (0.4m to 4m) also had average slip rates of 0.05 to 2.8 m kyr⁻¹) and frequency of recurrence of less than 40ky. This places the frequency of these fault movements well within the range normally reserved for high-frequency Milankovitch cyclicity. Furthermore, De Benedictis *et al.* (2007) demonstrated using numerical modelling that simulated cyclothem were comparable to observed sedimentary peritidal cyclothem. These numerical simulations demonstrate that peritidal high-frequency cyclothem (if not ice-house) can potentially be generated by tectonic processes without oscillations of eustatic sea-level.

2.2.3 Allocyclicity

There is notable division between workers concerning the duration of orbital components, and therefore glacio-eustatic sea-level changes during the Carboniferous. Primarily, the distinction is between two camps; one which advocates a long-term (c. 400ky) eccentricity cycle (e.g. Heckel, 1986) and one which favours short-term (c. 100ky) eccentricity to be the dominant forcing mechanism (e.g. Barnett *et al.*, 2002). This issue is of critical importance not only in terms of understanding the presence of apparently ordered cyclothem in carbonate strata, but also in understanding the architecture of Lower Carboniferous reservoirs. Stacking patterns are defined by the allocyclic controls placed upon them, and therefore, so too is cyclothem-boundary related sub-aerial diagenesis, making this knowledge critical for the development of accurate models of ice-house reservoirs. Most recently, Barnett *et al.* (2002) critically compared the two conflicting theories through the development of an observation-based model based on the studies of Saller and co-workers (Saller *et al.*, 1994; Saller *et al.*, 1999a; Saller *et al.*, 1999b), and an alternative theoretical model based on the work of Collier *et al.* (1990) and Maynard & Leeder (1992). These two models are compared in section 2.4.

2.3 INTERPRETATION OF SEDIMENTARY CYCLICITY

The early work of Goldhammer *et al.* (1987; 1990) proposed that periods of sub-tidal carbonate deposition alternating with hiatuses would give rise to cyclic sedimentation (Figure 2.13). In this model, outputs such as cyclothem thickness and the duration of sub-aerial exposure are derived from long-term variations in the availability of accommodation space. Long periods of deposition are recorded when accommodation rates are high and recorded sub-aerial exposure is short. In contrast during times when rates of long-term accommodation are low, periods of sedimentation are short and sub-aerial exposure extended.

In a series of seminal studies, Goldhammer *et al.* (1987; 1990; 1991) described and demonstrated through computer modelling the concept of composite eustasy. This concept is commonly used in most modern computer models attempting to simulate high-frequency high-amplitude glacio-eustasy (Maynard & Leeder, 1992; Saller *et al.*, 1999a). Goldhammer *et al.* (1990) used a study of Middle Triassic platform carbonates in the Alps to demonstrate that composite eustasy provided the major control on the Middle Triassic cyclic stratigraphy of the Alps. This was attributed to intermediate-order eustasy as a function of Milankovitch variations. Goldhammer credits Milankovitch frequencies as the forcing mechanism because of the 5:1 (precession:eccentricity) stacking pattern observed in the Alpine Triassic. However, this assumption is dangerous: Laskar (1999) has shown that it is difficult to extrapolate these ratios so far back in time. While projecting orbital variations back up to 100 million years is possible, the further back in time; the greater the potential for error and likelihood that any ratios become highly distorted due to the relatively small time-frames (~20ky to ~100ky) involved. The problem of extracting the true Milankovitch ratios present in the Palaeozoic (if any) is further compounded by imprecise dating methods. To determine any precession:eccentricity stacking, relative dating resolution would need to be on the thousand-year scale.

Goldhammer *et al.* (1990) also highlighted important principles regarding systematic variations in the vertical stacking patterns in cyclic platform carbonates, which was later built upon by Saller *et al.* (1994) and which has implications for hydrocarbon reservoirs. As previously mentioned, Goldhammer *et al.* have shown that it was the lowest order that dictated the overall trend in sea-level and therefore the stacking patterns of higher-order eustatic oscillations (assuming, of course, that lower orders have higher amplitudes). Specifically it was interpreted that (independent of an allocyclic or autocyclic forcing mechanism) increase in accommodation potential on a low-order rising limb

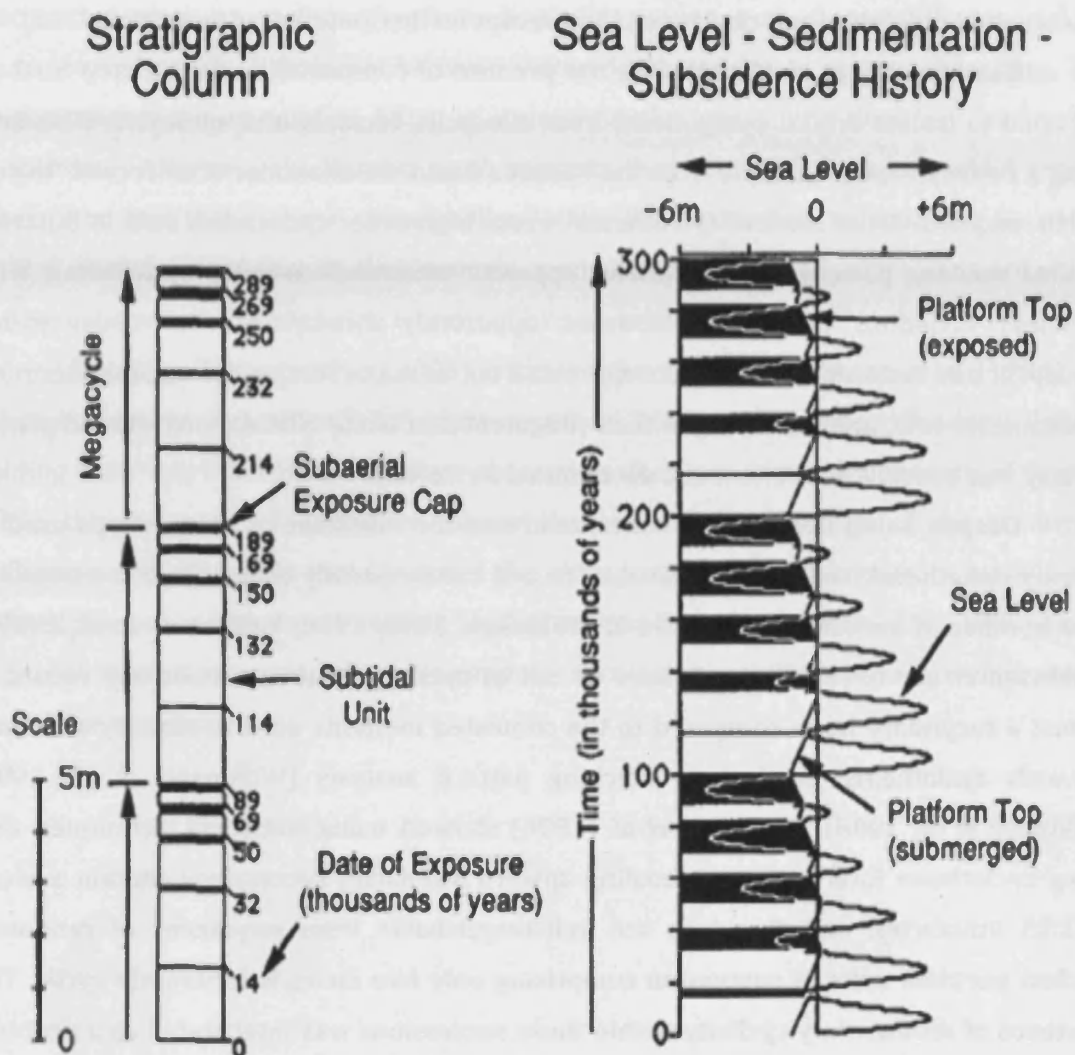


Figure 2.13: Simulated stratigraphic columns and sea-level curves using a superimposed oscillation periodicity ratio equal to 5:1. Dated black bars represent sub-aerial exposure, and white sections represent sub-tidal portions of a cycle. Sea-level fluctuations are plotted against time (x1000y). A positive (toward the right) trend of the platform surface indicates sediment accumulation. A negative trend represents shallow submergence (depth < lag depth) and no sediment accumulation. The black regions to the left of the dotted line represent exposure of the sediment column and formation of a diagenetic exposure cap. (From Goldhammer *et al.*, 1990).

resulted in thick cyclothems with extensive sub-marine diagenesis, along with exposure-related 'missed beats'. Conversely a low-order eustatic sea-level fall produces thin cyclothems, sub-aerial diagenesis and 'missed beats' due to rapid submergence of the platform. Saller *et al.* (1994) recognised the potential of this differential diagenesis for hydrocarbon reservoirs and developed the concept further (addressed in section 2.4.1).

Goldhammer *et al.* (1994) took the premise of composite eustasy a step further, and tried to isolate orbital components from allocyclic, tectonic and autocyclic elements. Using a Pennsylvanian example from the Paradox Basin, Goldhammer *et al.* record "third-, fourth- and fifth-order stacked cyclothems". From high-order cyclothems seen at outcrop, vertical stacking pattern analysis shows apparent intermediate-order cyclothems, with thickness variations of these cyclothems apparently displaying a low-order trend. Autocyclic and tectonic controls were also ruled out as major forcing factors. Furthermore Goldhammer *et al.* are discerning in their judgment that while Milankovitch-forced glacio-eustasy was possible it, could not be determined for certain.

Despite being in relatively widespread use, the relevance of the methods used to identify cyclothems from the sedimentary record has frequently been called into question by a number of authors (Drummond & Wilkinson, 1993; 1996; Wilkinson *et al.*, 1997a; Wilkinson *et al.*, 1998). The existence or not of cyclicity in the sedimentary record is almost a secondary issue compared to the contested methods used to identify shoaling-upwards cyclothems, particularly stacking pattern analysis (Wilkinson *et al.*, 1996; Wilkinson *et al.*, 1998). Wilkinson *et al.* (1996) showed, using statistical techniques, that many cyclothems interpreted as shoaling-upward lithofacies successions contain a mean of 2.25 lithofacies, and therefore are indistinguishable from sequences of randomly stacked peritidal units. A succession comprising only two facies is inherently cyclic. The existence of sedimentary cyclicity within these successions was interpreted as a problem of perception rather than a demonstrable reality in the stratigraphic record, with a majority of sedimentary successions showing no evidence for cyclicity.

Comparative studies of ice-house and green-house periods by Lehrmann & Goldhammer (1999) showed that the occurrence of demonstrable cyclicity in platform carbonate strata is strongly dependent on the position within the stratigraphic record. This work is interesting in that it supports that of Wilkinson *et al.* (1996; 1997b) in some respects, while contradicting it in others. For instance, both studies (Wilkinson *et al.*, 1996; Lehrmann & Goldhammer, 1999) concur that in ice-house periods, approximately 50% of their studied successions show non-random lithofacies successions. Lehrmann & Goldhammer also show that some of their greenhouse successions show high levels of randomness as a result of autocyclic processes.

Furthermore, Wilkinson *et al.* (1997b) show that in many ice-house successions, instances of sub-aerial exposure frequently occur on subtidal deposits. Similarly, Horbury (1989) noted sub-aerial exposure surfaces capping sub-tidal strata in the Asbian of Britain. Barnett *et al.* (2002) supported this finding through numerical forward modelling, stating that exposure surfaces (surfaces displaying evidence of sub-aerial diagenesis) can be generated on any lithologies between water depths of 0m to greater than 20m. This may represent the incomplete filling of accommodation space, and therefore 'incomplete cyclothems'. Alternatively, Barnett *et al.* suggests that with very high sub-aerial erosion rates (30m Myr⁻¹) the upper, more shallow-water lithofacies may be stripped. Barnett *et al.* also demonstrated that, in their models, many externally forced cyclothems are shown to deepen-upwards before being truncated by sub-aerial exposure.

Recently, Schwarzacher (2005) criticised the work of Wilkinson *et al.* (1996) and other authors as 'wasted efforts' (Schwarzacher, 2005; p104), citing Sander's Rule as voiding their work because a random succession does not prove the absence of forcing. While this is true, Schwarzacher misses the broader implications of the studies of Wilkinson and others. As already noted the issue in question is whether cyclicity can be defined from the sedimentary record. Studies such as that of Wilkinson *et al.* (1996) aim to illustrate that often random, or near-random, successions are interpreted over-zealously as cyclical successions.

2.4 MODELS OF EUSTATIC SEA-LEVEL BEHAVIOUR

2.4.1 An observation-based model

As a by-product of work examining effects of sub-aerial diagenesis on carbonate cyclothems, Saller *et al.* (1999b) examined the veracity of the sedimentation model employed by Goldhammer *et al.* (Goldhammer *et al.*, 1987; 1990). They studied how long-term changes in accommodation alter the deposition, diagenesis and porosity of carbonate strata. Using Fischer plots, changes in lithofacies, degree of sub-aerial exposure and carbon/oxygen isotope analyses stacking patterns and hierarchical architecture were defined in late Pennsylvanian and Permian strata. Saller *et al.* (1999b) proposed that cyclothem stacking patterns were controlled by low-order cyclicity with an overriding intermediate-order cycle, both of which operated as apparently uniform, sinusoidal curves. Sinusoidal curves are unlikely to be realistic, but are used in models such as that of Saller *et al.*, as they are more simplistic to model, and don't need to be based on a dataset, merely information regarding the frequency and amplitude of the sinusoids.

The use of lithofacies proportions in this study was crucial to determine the position of the strata within a low-order cycle, and this was found to be critical in determining where reservoir-grade porosity is likely to occur (Figure 2.14). Saller *et al.* (1999b) noted a change in parasequence character through a sequence. In the Pennsylvanian, from the base to the top of a sequence, they noted a shallowing of depositional facies (more grainstones), as well as a decrease in average thickness and increase in the amount of shale. Most notably they recorded decreases in bulk sediment ^{13}C and ^{18}O values, which suggests sub-aerial leaching, and an increase in pedogenic features. The overall trend through a sequence of these four factors drew Saller *et al.* to conclude that accommodation was decreasing 'upwards'. Furthermore, after a platform drowning episode, cyclothems in the Wolfcampian thicken through a sequence, contain more deep water facies and increase in ^{13}C and ^{18}O values, all caused by an increase in accommodation.

Saller *et al.* (1999b) highlighted the fact that the time represented by each cyclothem includes both the time when the sediment surface was below sea-level and accumulating sediment, and the time when it was exposed and subjected to meteoric diagenesis. The meteoric diagenesis is evident both in the lighter carbon and oxygen isotope compositions, and in the prominent soil textures displayed. Additionally, the disparity between the isotopic compositions of the Pennsylvanian and Wolfcampian (Lower Permian) intervals showed that the degree of sub-aerial exposure

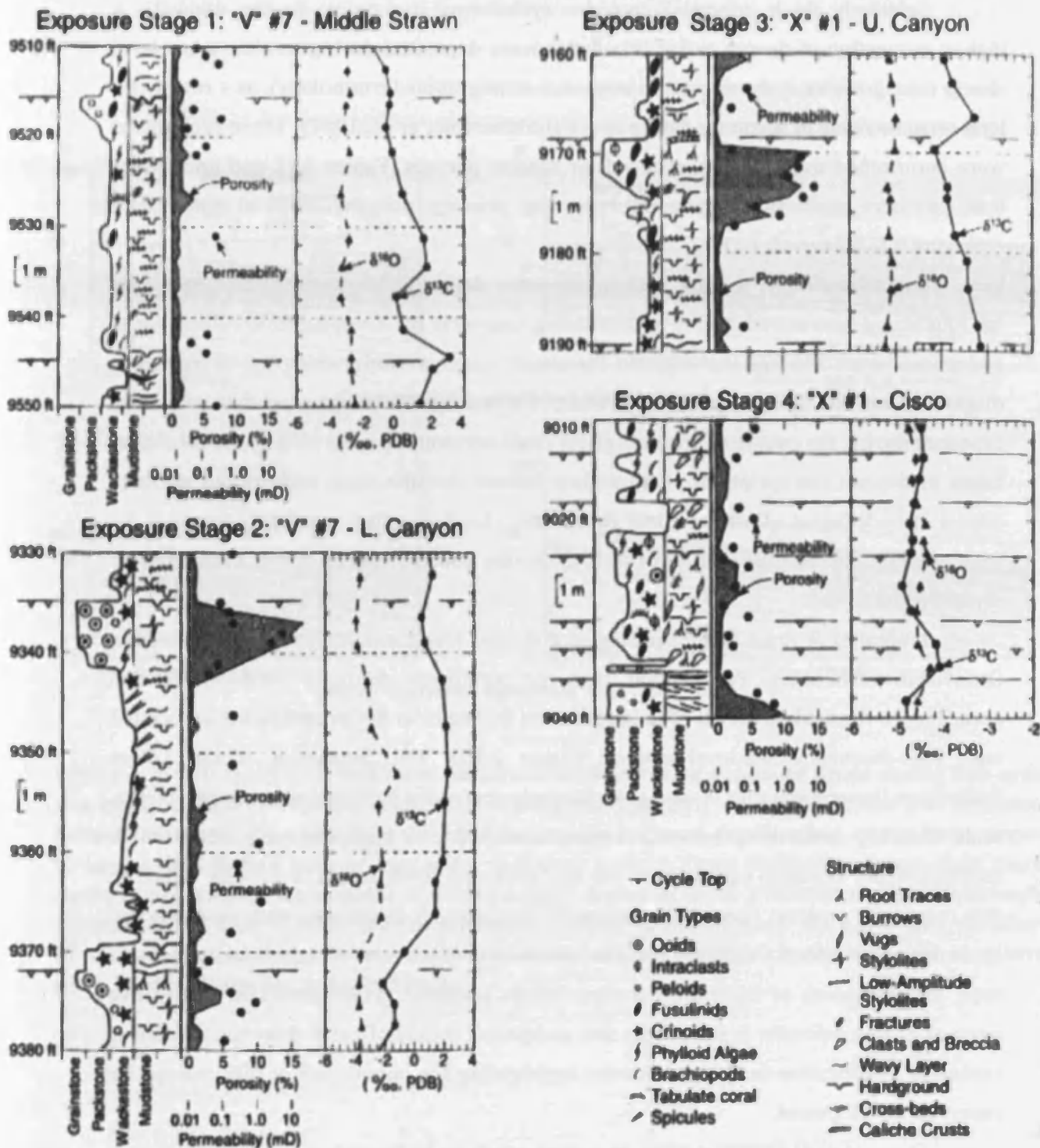


Figure 2.14: Depositional textures, grain types, sedimentary structures, porosity, permeability, and stable isotope compositions for cycles typical of different sub-aerial exposure stages. Note the distribution of porosity and permeability in relation to exposure surfaces (depicted symbolically on the depth scale). (From Saller *et al.*, 1999a).

(and therefore the duration between flooding events) varies between the two stages (assuming that diagenesis occurs at a constant rate).

Relatively thick intermediate-order cyclothem containing, in the majority, a higher proportion of deeper-water lithofacies were deposited during a relative sea-level rise (a transgressive systems-tract in sequence stratigraphic terminology), as a result of a long-term increase in accommodation space (Goldhammer *et al.*, 1987). These cyclothem were determined to have been exposed for shorter periods (Figure 2.9), and underwent less extensive meteoric diagenesis preserving primary porosity, and in some cases enlarging it (Saller *et al.*, 1994).

Correspondingly, thinner cyclothem were deposited during a relative sea-level fall (highstand systems-tract) due to decreasing long-term accommodation creation. These cyclothem were sub-aerially exposed for much longer periods which led to extensive diagenesis and the filling of primary porosity. Vanstone (1996) suggested that sub-aerial exposure during the course of one cyclothem could account for up to 80% of the total time taken to deposit the cyclothem. It therefore follows that the most widespread porosity occurs in cyclothem of intermediate (or greater) thickness that were only exposed for brief periods (those that had less opportunity for substantial sub-aerial diagenesis to cement pore-space).

Montañez & Read (1992) identified a similar trend in dolomitisation patterns in Ordovician carbonates. They found that the stratiform dolomite probably formed according to the sabkha model of dolomitisation during tidal-flat progradation associated with high-frequency sea-level events (Figure 2.15). The deposition of the Lower Ordovician Upper Knox unit is seen to be strongly controlled by composite eustasy. Metre-scale, shoaling-upwards cyclothem formed in response to high-frequency third, fourth and high-order sea-level oscillations. The evidence of dolomitisation is strongly linked to this composite eustasy. Specifically, dolomite is commonly associated with mud-cracked laminites and silicified evaporate nodules, dolomitic clasts occur in lags above cyclothem-tops, and instances of dolomite decrease below laminate cyclothem caps. Eighty five percent of this dolomite is stratiform and composed mainly of early dolomite exhibiting extensive modification to burial dolomite; highlighting the importance of this concept for reservoir development.

Bosence *et al.* (2000) outline, in a similar fashion to Montañez & Read (1992) how an understanding of the causes of sedimentary cyclicity can lead to a better understanding of effects apparent in the sedimentary record. Within the Lower Jurassic Gibraltar Limestone, Bosence *et al.* identify high-frequency cyclothem apparently conforming to a speculated third order oscillation. They credit this underlying fluctuation as the control of

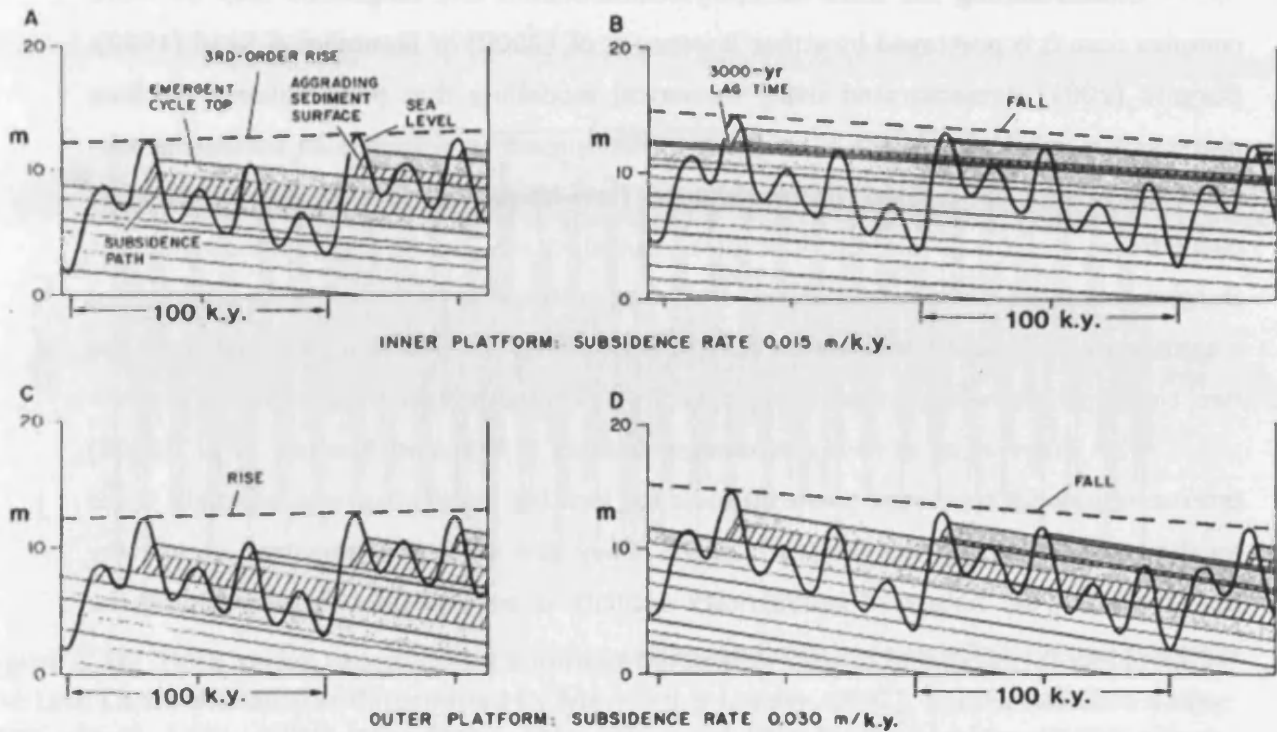


Figure 2.15: 1D models of sediment accumulation illustrating exposure times during low-order sea-level rise and fall for the Knox Gp. Cross-hatched pattern = sub-tidal facies (i.e. deposited below 2m depth), fine stipple = tidal flat facies (depositional depth < 2m). Steep lines sloping to upper-right define path of aggrading sediment surface. Lines inclined to lower-right marks paths of subsidence boundaries and cycles caps. A and B: inner platform models (0.015m/ky subsidence). C and D: outer platform models (0.03m/ky subsidence). Note the long durations of exposure associated with long-term falls versus shorter durations associated with long-term rises. (From Montañez & Read, 1992).

facies, biota, cyclothem-type and dolomitisation. They demonstrate that lowstands, typified by reduced accommodation space, comprise restricted inner-platform facies which underwent early reflux dolomitisation. Transgressive and highstand phases are associated with more accommodation space, and therefore have a more diverse, open-marine facies-assemblage and lack evidence of dolomitisation.

Understanding the links affecting sedimentation and diagenesis may be more complex than it is portrayed by either Bosence *et al.* (2000) or Montañez & Read (1992). Burgess (2001) demonstrated using numerical modelling that parasequence stacking patterns typically interpreted as sequence development in response to oscillating sea-level, may also be created in greenhouse (low-frequency, low-amplitude sea-level oscillations) systems as a result of oscillating productivity and sediment-transport rates. Burgess concludes that greenhouse and ice-house systems may represent end-members of a continuum, and carbonate systems may display a response that is a combination of the two, complicating the sequence-stratigraphic interpretations of such sequences.

The Saller *et al.* (1999b), Montañez & Read (1992) and Bosence *et al.* (2000) interpretations all represent powerful tools for locating reservoir-prone intervals, if the location within a systems-tract is known. They are also a demonstration of why understanding the nature of sedimentary cyclicity is so important for developing the reservoir potential of major hydrocarbon assets.

2.4.2 An insolation-based model

In contrast to the work of Saller *et al.* (1999b), Collier *et al.* (1990) (and subsequently; Maynard & Leeder, 1992) used data based on Imbrie & Imbrie's (1980) Pleistocene climate model which associates orbital forcing with climate changes at mid-latitudes (Figure 2.16). This data was modified and used to construct a sea-level curve applied to a simplified basin model, assuming a direct link between climate and ice volume. Maynard & Leeder (1992) assumed that the orbital parameters affecting insolation could be resolved easily mathematically, and the effects on climate drawn from Berger's (1978b) findings.

Maynard & Leeder (1992) used five secular orbital forcing periodicities as defined by $\delta^{18}\text{O}$ data (Imbrie & Imbrie, 1980). The obliquity and precession values were adjusted from Recent data, incorporating the shorter Earth-Moon distance in the Carboniferous (although Maynard & Leeder's values were still higher than those calculated by Berger & Loutre, 1994: values of 21ky and 17ky compared to 18.5ky and 16ky, respectively). However, the eccentricity models did not take into account tidal friction, later highlighted by Berger & Loutre, instead suggesting that eccentricity values were constant at 413ky

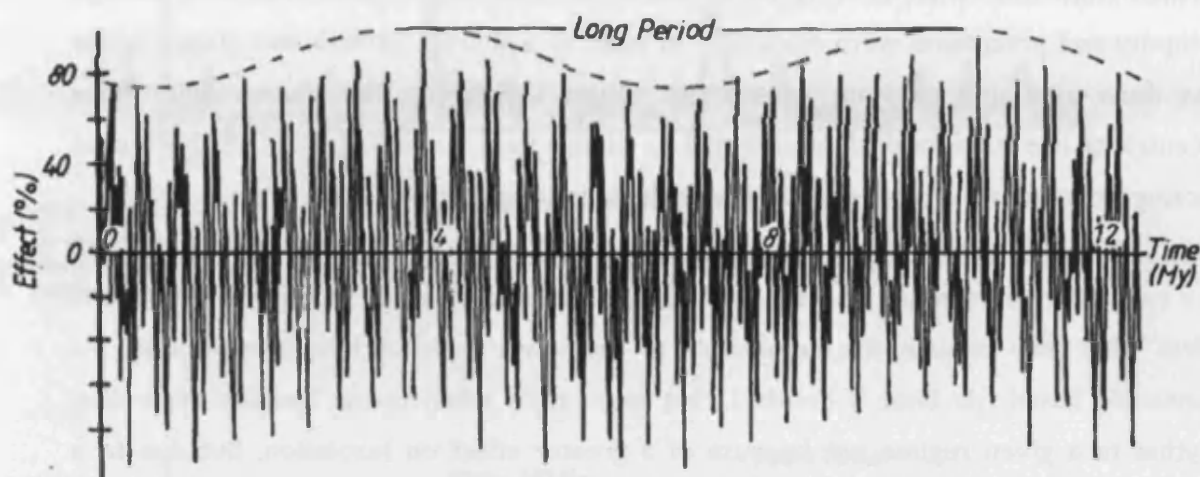


Figure 2.16: Time series representing summed parameters thought to control sea-level in the Late Carboniferous (as determined by Maynard & Leeder, 1992). Values used are 413ky (30% effect), 112ky (20%), 34ky (11%), 21ky (23%) and 17ky (16%); combined 100% effect. The vertical axis shows the relative effect, or amplitude, of the summed periodicities as derived from power spectra from Imbrie and Imbrie (1980). (From Maynard & Leeder, 1992).

and 112ky throughout the Phanerozoic. The corresponding amplitude for each of these cyclothem was derived from Walsh power spectral analysis (Figure 2.17), and combined to give a percentage of maximum reinforcement of all periodicities.

Maynard & Leeder (1992) note that from their own results the 112ky rhythm seems to have the dominant effect on their time series. However as the 413ky periodicity (as defined by Maynard & Leeder,) is based on values from the Pleistocene which have been shown to be untraceable further back in time by Laskar, and the 112ky periodicity is derived from this; what is truly being modelled? The fact remains that even though obliquity and precession were calculated in mind of a shorter Earth-Moon distance, this was done assuming constant eccentricity values throughout the Phanerozoic. Since eccentricity has since been demonstrated to change over geological time, all the orbital parameters used in Maynard and Leeder's calculations are likely to be wrong.

In addition to this problem, the amplitudes of the five periodicities were calculated as a cumulative percentage of a total, so a maximum reinforcement would result in 100% effect. This may explain the dominance of the lower order orbital periodicities. As previously noted (de Boer & Smith, 1994) eccentricity often seems like the overriding rhythm in a given regime not because of a greater effect on insolation, but due to a relatively static periodicity. In Maynard & Leeder's case, it is entirely likely that eccentricity appears dominant as obliquity and precession have periodicities four times smaller (112ky compared to 34ky, 21ky and 17ky). In this instance it could be argued that the reason these orbital parameters appear insignificant is that in a very short time-frame there are three strong orbital parameters operating against each other in negative feedback, and it is only when they happen to operate in conjunction that they have an effect on the eccentricity curve. The use of insolation curves as indicators of eustatic sea-level change is also discussed by Barnett *et al.* (2002; refer to section 2.4.3).

From the synthetic sea-level curve produced by Collier *et al.* (1990), combining the five periodicities, they identified an apparent 2nd-3rd order curve with a frequency of 2-6My. They identified the two eccentricity parameters as the most likely cause of the oscillation, and put it forward to explain distributions of sea-level rises in the Late Carboniferous. They logically deduced that due to the presence of periodicities within Upper Carboniferous successions, the process governing the cyclicity was non-random. As orbitally-controlled glacio-eustasy is apparently the only periodic mechanism in operation, they deduced that this must be the primary cause of the transgressions.

Klein (1994) argued against the applicability of Milankovitch parameters to Carboniferous sediments, due to the large margin of error and small periods of the parameters. Klein advocated the possible role of active faulting in producing cyclicity as an

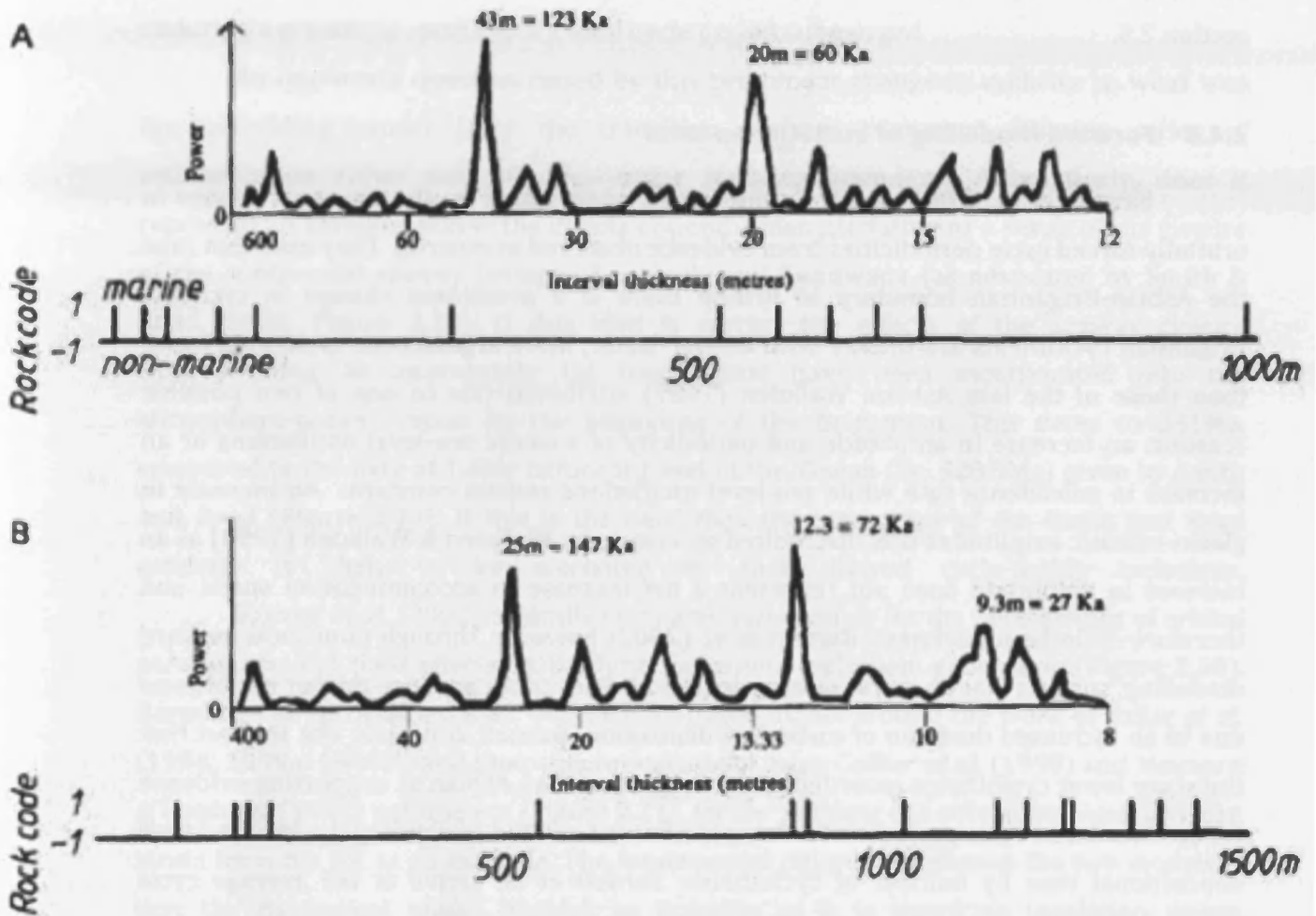


Figure 2.17: Smoothed Walsh power spectra and input time series. A) Data from a basin edge setting, Tynemouth, UK. B) Basin centre setting, Derbyshire, UK. Only major cycles are interpreted as 'recognised' in these power spectra. Cycle thicknesses are converted into time using mean decompacted deposition rates for the two areas of 0.17mm a^{-1} for Tynecastle and 0.35mm a^{-1} for Derbyshire. The decompacted rates are sources of significant error given uncertainty between sedimentation and accumulation (e.g. Pomar, 2001). (From Maynard & Leeder, 1992).

alternative mechanism to orbital forcing. Were this to be the case, Maynard and Leeder (1992) stated spectral analysis would show no clear peaks, in contrast with their findings. While this is true, since the peaks produced are simply the result of human-defined variables, based on Milankovitch parameters operating in conjunction, there is no guarantee that they represent the cause of cyclicity either, especially in light of the flaws intrinsic to the calculated values, highlighted by Laskar (1999), and outlined in detail in section 2.5.

2.4.3 Forward modelling of eustatic sea-level

Barnett *et al.* (2002) make an interesting observation on the apparent change in orbitally-forced cycle periodicities from evidence observed at outcrop. They note that in at the Asbian-Brigantian boundary in Britain there is a prominent change in cyclicity; Brigantian cyclothem are thicker with deeper-water, more argillaceous cyclothem bases than those of the late Asbian. Walkden (1987) attributed this to one of two possible reasons: an increase in amplitude and periodicity of eustatic sea-level oscillations or an increase in subsidence rate while sea-level oscillations remain constant. An increase in glacio-eustatic amplitudes was discredited as a cause by Walkden & Walkden (1990) as an increase in amplitude does not represent a net increase in accommodation space, and therefore cyclothem thickness. Barnett *et al.* (2002) however, through numerical forward modelling, suggest that an increase in cycle periodicities could produce thicker cyclothem due to an increased duration of carbonate deposition. Barnett *et al.* also cite the fact that there are fewer cyclothem recorded in the Brigantian than Asbian as supporting evidence for an increase in cycle periodicities. Using the flawed method of dividing the inferred total depositional time by number of cyclothem, Barnett *et al.* arrive at the average cycle duration of 225ky. Quite correctly, however, they state that this figure implies complete preservation, and the true period would lie closer to the 100ky cycle than the 400ky cycle suggested by Smith and Read (2000).

Sub-aerial exposure surface development corroborates Barnett *et al.*'s conclusion that cyclicity may have switched near the Asbian/Brigantian boundary. The degree of development exhibited by a palaeosol reflects the duration of sub-aerial exposure (Barnett *et al.*, 2002). Soils which develop as a consequence of a low-order regression show complex, polygenetic histories, due to the long exposure period, while those that developed at intermediate-order boundaries will show less development (Wright, 1996). Palaeosols, however, cannot be used to apply absolute temporal values to the duration of sub-aerial exposure, rather they can be used to distinguish between relatively more and less developed surfaces, and therefore between sequence boundaries.

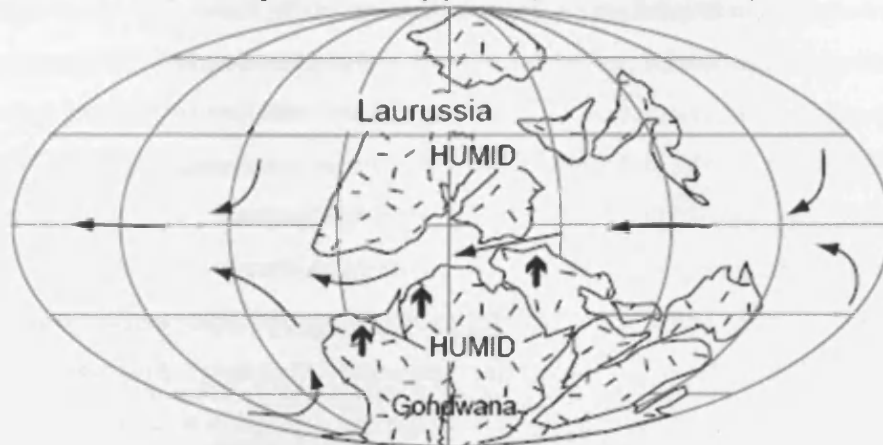
Using this principle Barnett *et al.* illustrated that 400ky cyclicity should be inherently associated with long periods (226-350ky) of sub-aerial exposure, evidence of which is not seen in the Brigantian of the UK. Consequently, Barnett *et al.* conclude that a significant transgression and deepening event at the Asbian-Brigantian boundary caused the change in cyclothem character. This conforms well with the less extensive exposure surface development in the Brigantian; interpreted as a consequence of the platform enduring a greater proportion of a total cycle period submerged.

An important question raised by this prominent change in cyclicity is: what was the overriding cause? Does the transition perhaps represent differing styles of sedimentation either side of a low-order sequence-boundary? Alternatively, does it represent an amplification of the effects of Gondwanan glaciation as a result of the closure of the continental seaway between Laurussia and Gondwana (as advocated by Smith & Read, 2000; Figure 2.18). If this idea is correct the effects of the seaway closure (incorporating an appropriate lag time) must have been incorporated into the atmosphere-ocean system by the beginning of the Brigantian. This dates to 331Ma, compared to the date of 1.6My before the end of the Viséan (i.e. 328.5Ma) given by Smith and Read (Figure 2.19). If this is the case, then the inaccuracy of the Smith and Read estimate is likely to be exacerbated by their flawed cycle-dating technique.

Barnett *et al.* (2002) critically compared two models for the periodicities of orbital parameters, and their effects on platform carbonate cyclothem generation (Figure 2.20). Barnett *et al.* constructed their observation-based model around the work of Saller *et al.* (1994; 1999a; 1999b), and their theoretical model using Collier *et al.* (1990) and Maynard & Leeder's (1992) parameters (Figure 2.21), for the purpose of a comparison using Viséan strata from the UK as an example. The fundamental difference between the two models is that the theoretical model 'should' be accurate as it is based on insolation values calculated from orbital parameters. The observation-based model is essentially built backwards from that of the theoretical model: the results of forcing are observed at outcrop and then orbital parameters are derived from it. This observational method results in a simpler sinusoidal curve than that of the highly 'specific' theoretical model (Figure 2.21).

Through computer modelling and sensitivity of these models to outcrop, Barnett *et al.* (2002) showed that there was little evidence to support the application of Collier *et al.*'s (1990) solar insolation curve to the Viséan, and in fact it is the more generic observational model that seemed to better fit the data (Figure 2.22). There are probably multiple

A) Early Mississippian (Greenhouse)



B) Early Pennsylvanian (Icehouse)

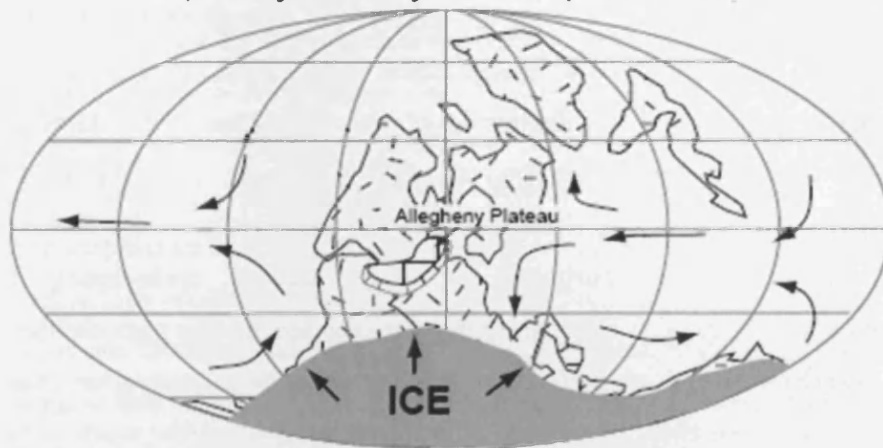


Figure 2.18: Palaeogeographic maps with schematic oceanic current trends (base map from McKerrow & Scotese, 1990). A: Ocean currents flowed freely through sub-equatorial seaway in Early Mississippian. B: Closure of seaway in Late Mississippian might have caused equatorial currents to be diverted south toward Gondwana and initiated onset of major southern hemisphere glaciation. (Modified from Smith & Read, 2000).

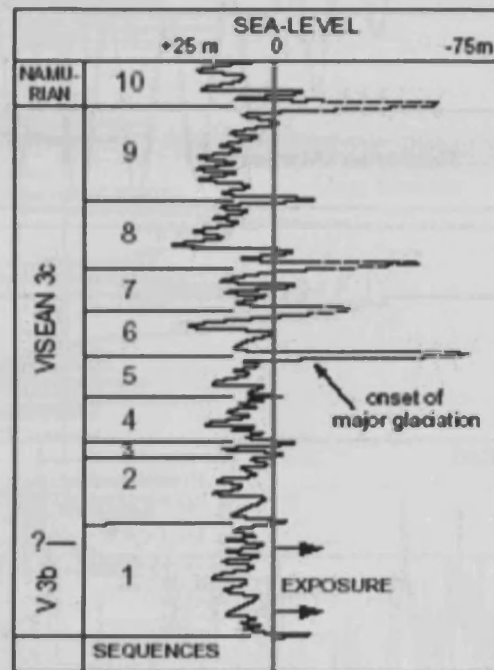


Figure 2.19: Sea Level curve based on interpreted water depths for different lithofacies types and depth of incision associated with each sequence boundary. Onset of major glaciation is inferred by abrupt increase from 20m to 30m sea-level changes of sequences 1-5 up to 95m for sequence 6. (From Smith & Read, 2000).

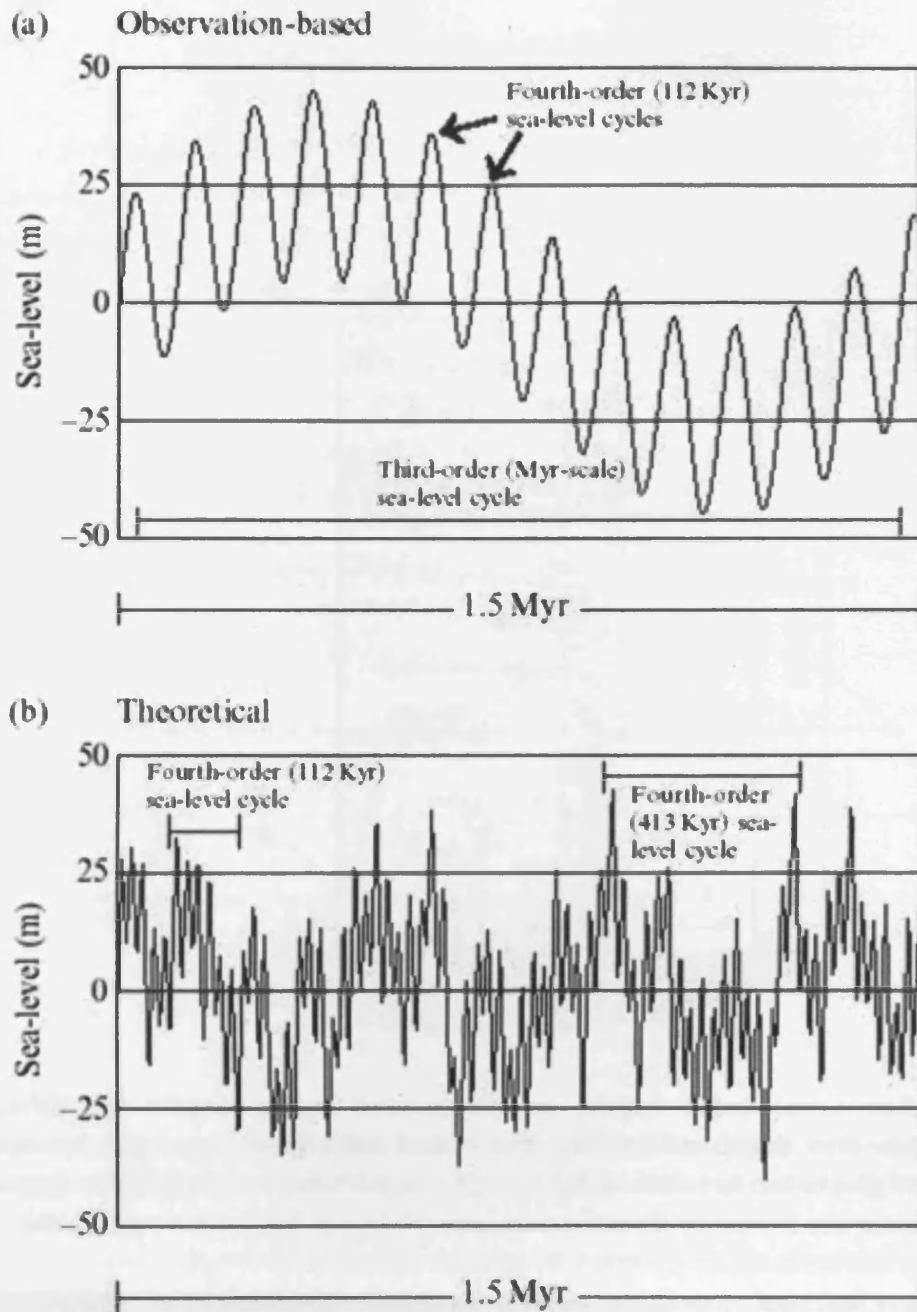


Figure 2.20: Models of cyclic sea-level change proposed for Carboniferous intermediate-order cycles. (a) Observation-based model from the work of Saller *et al.* (1994; 1999a; 1999b). Cycle stacking is controlled by the harmonics of low- and relatively uniform intermediate-order sea-level oscillations. (b) Theoretical model based on the synthetic solar insolation curve of Collier *et al.* (1990) and Maynard & Leeder (1992) (refer to Figure 2.16 and Figure 2.21 for an explanation). (From Barnett *et al.*, 2002).

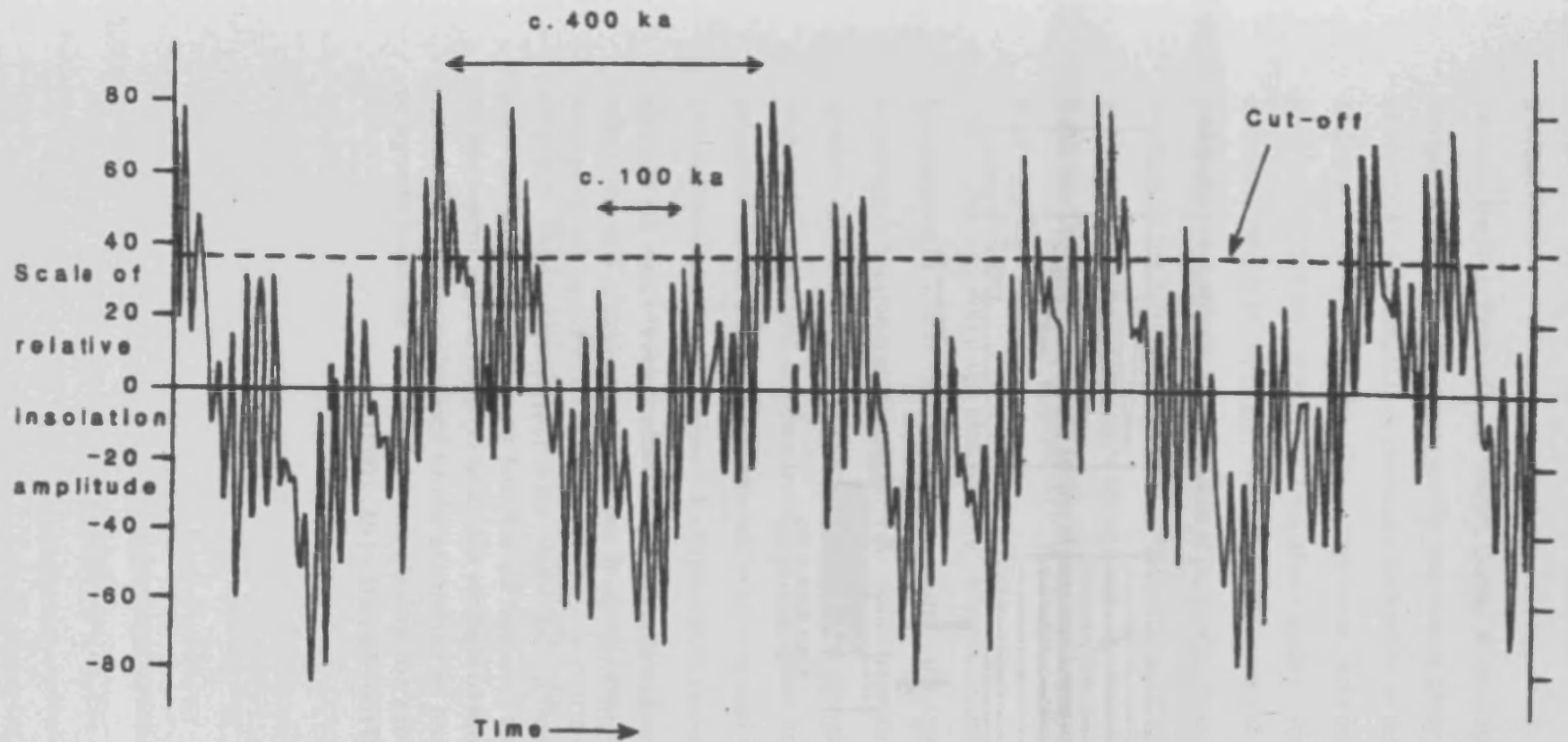


Figure 2.21: Synthetic curve of insolation, as calculated using Milankovitch parameters for the Carboniferous Period (based on spectral analysis of Quaternary data from Imbrie & Imbrie, 1980). Obliquity has been modified by a factor of 0.75. (From Collier *et al.*, 1990).

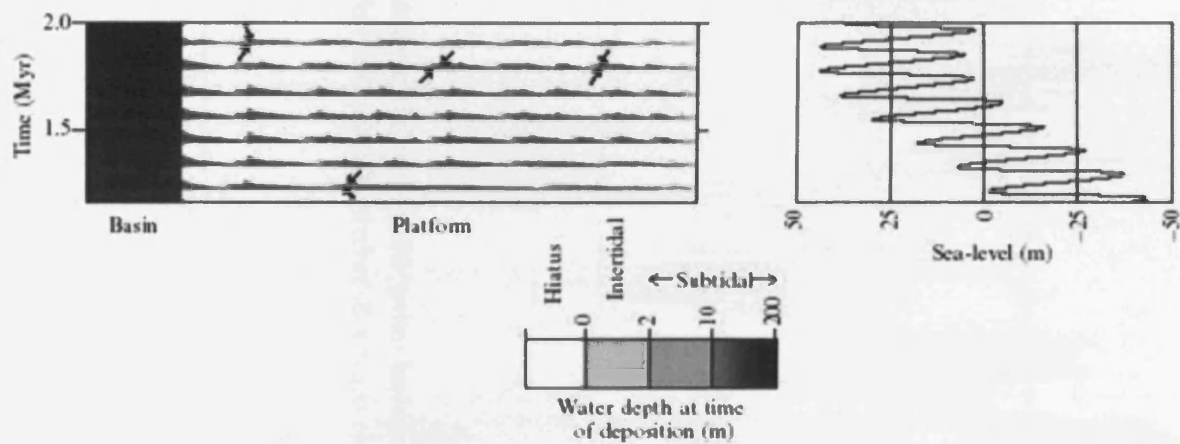


Figure 2.22: Enlarged section of a chronostratigraphic plot and sea-level curve for a model run simulating sedimentation under conditions of oscillating sea-level. The simulated stratigraphy comprises 7 “short-eccentricity-driven” (112ky) cycles dominantly composed of sub-tidal sediment (c.10-30m depth). Individual externally-forced cycles comprise numerous upward-shoaling autocycles (marked by arrows) characterised by an upward transition from relatively deep sub-tidal to shallow sub-tidal (2-10m) and/or inter-tidal (0-2m) sediment. Autocycles are produced by carbonate island formation and progradation. Note that the input sea-level curve does not include any higher-order sea-level change to produce this “hierarchy” of cyclicity. (From Barnett *et al.*, 2002).

reasons for this. Primarily, as stated, Collier *et al.* (1990) based their work on data from Berger (1978b), which, subsequently was shown likely to be flawed (Laskar, 1999; Laskar *et al.*, 2004). Any model they therefore derived from this data, particularly one as sensitive and specific as this theoretical insolation model, was destined to be inaccurate.

The detailed sensitivity of a given model may also be lost in translation to the sediment. Multiple workers note the sensitivity of cyclicity to original depositional conditions (e.g. Hilgen, 1991; Adams *et al.*, 1992; Klein, 1994), and the imperfect recording medium of the sedimentary record, which may give a result that bears little resemblance to the complicated forcing imposed upon it. To quote an obvious statement from Sander's Rule: the absence of cyclicity in the stratigraphic record does not indicate the absence of time cyclicity.

It may be that the observation-based model appears to fit the data better because the simple cumulative (and more importantly – fixed period) sinusoidal fluctuations act as a common denominator, whereas those of the theoretical model are lost as noise, because of more variable periods. In contrast, it could be that global climate shows such a complex response to changes in solar insolation that links between the causal factors and the response cannot be resolved. Alternatively, it is also possible that global climate in the Upper Palaeozoic may have been decoupled from changes in insolation, with climate being dictated by another mechanism. What is apparent, is that global climate in the Lower Carboniferous is not well understood at this time, but appears to not to bear an obvious relationship with interpreted palaeo-insolation rates.

2.5 EVIDENCE OF CHAOTIC BEHAVIOUR OF ORBITAL PARAMETERS

Laskar (1989) conducted a seminal numerical experiment on the chaotic behaviour of the Solar System which impacts any assumptions geologists make regarding Milankovitch-style cyclicity through geological time. Despite this, the work is under-referenced in the literature, perhaps reflecting the fact that it represents concepts contrary to the findings of most cyclostratigraphers.

Laskar demonstrated (through numerical modelling) that contrary to popular beliefs, the motion of the planets is not quasiperiodic but chaotic based on averaged differential equations for the secular evolution of the orbits of the eight main planets (i.e. excluding Pluto). Laskar found that a numerical integration of his system over 200My gave a chaotic solution, with a maximum Lyapunov exponent of $1/5\text{My}^{-1}$ (Figure 2.8). The Lyapunov exponent measures the exponential rate of divergence of two initially close orbits, meaning for quasiperiodic (i.e. the type of motion executed by a dynamical system containing two incommensurable frequencies) the value should be 0. Laskar therefore showed that it was possible to give a precise solution of the solar system over 10My but not over 100My. For instance, a perturbation as small as 10^{-10} of the initial conditions affecting an orbit, would lead to 100% discrepancy in the solution over 100My. The Lyapunov exponent of the outer planets is likely to be longer than that of the inner planets due to the regular behaviour of the solutions over 200My (Laskar, 1989). Therefore this chaotic behaviour comes mainly from the secular resonances among the inner planets (Figure 2.23).

Matthews *et al.* (1997) provide an extension to the work of Laskar (1989) by modifying the original computations to incorporate a greater degree of approximation. This involves the use of a trigonometric series expression for eccentricity to evaluate the effects that arise from artificially perturbing the orientation of planetary orbits (Figure 2.24). The benefit of this would be to sensitise, and in essence apply 'quality control' to a proposed eccentricity calculation. Whereas Berger and Loutre (1994) construct their representation of eccentricity through a trigonometric series of more than one thousand terms, Matthews *et al.*'s method uses a significantly simpler expression to calculate eccentricity. This allows for the prediction of more or less modulation of the effects of obliquity and precession. It therefore presents an opportunity to explore convergence of model results with observed stratigraphic data.

Laskar (1999) improved his solution and extended the possibility of obtaining an accurate solution for the orbital and precessional motion of the Earth over 35-50Ma. This

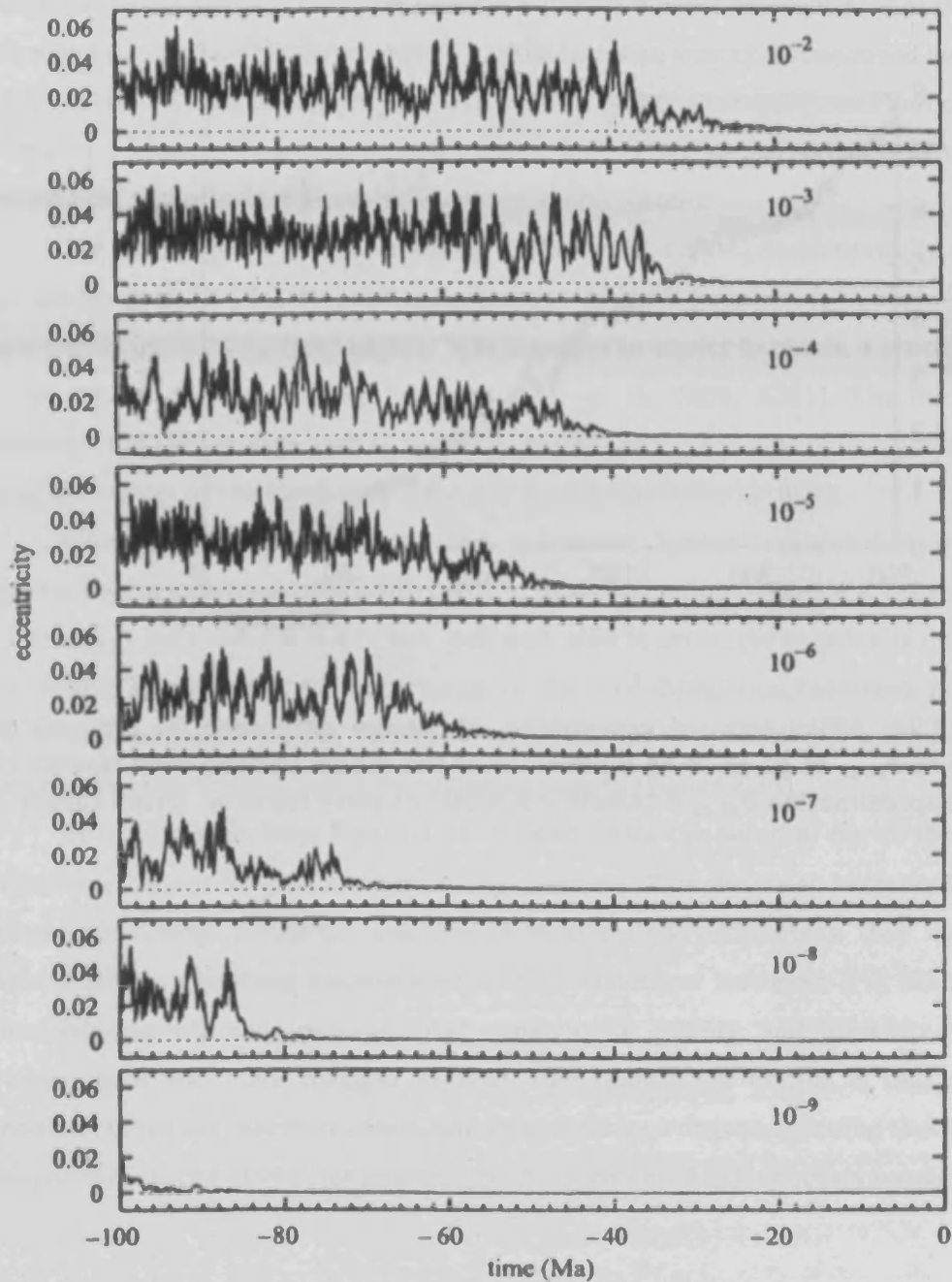


Figure 2.23: Error in the eccentricity of the Earth resulting from an initial change of 10^{-n} rad in the perihelion of the Earth at the origin. After approximately $n \times 20$ Ma, the exponential divergence of the orbits dominates, and the solutions are no-longer valid. Error in eccentricity is plotted versus time (Ma). (From Laskar, 1999).

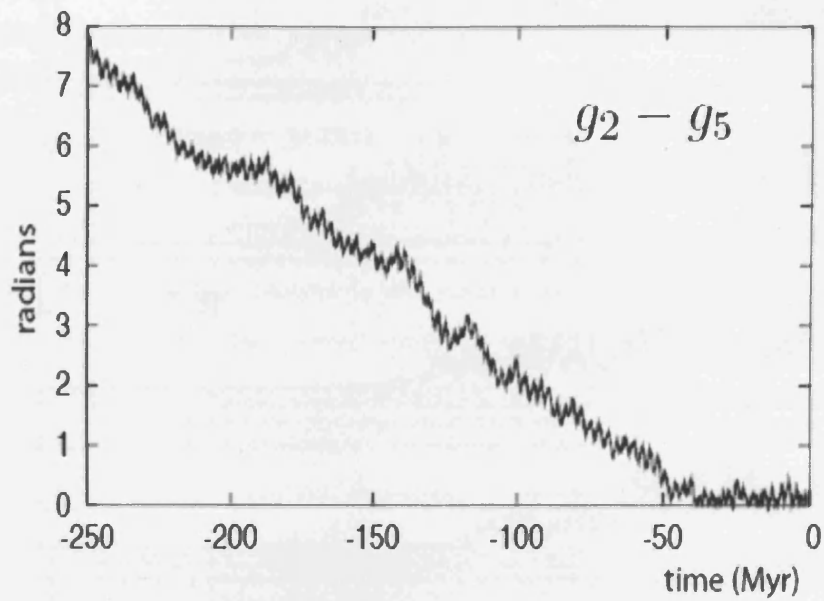


Figure 2.24: 405ky term of eccentricity. Maximum difference (in radians) of the argument $\vartheta_{g_2-g_5}$ of g_2-g_5 in all 6 solutions of the model La2004, with respect to the linear approximation $\vartheta_{g_2-g_5} = 243400 + 3.20000 t$ where t is in yr. (From Laskar *et al.*, 2004).

calculation is still limited by the sensitivity of the solution to initial conditions. Furthermore, Laskar states that the major source of error could come not from secular resonances in the orbits of the inner planets, but from the lack of knowledge of the value of precession due to the oblateness of the Sun. This solution was again improved by Laskar *et al.* (2004) by isolating and modelling independently the dissipative contributions. These dissipative components are parameters which may retard or perturb one of the orbital components, and principally involve the Earth-Moon system.

The orbital solution presented by Laskar *et al.* (2004) is successfully calibrated over the Neogene (0-23.03Ma) and is accurate to within 0.3 radians (or 20ky) up to 50Ma (Figure 2.7; Figure 2.25). Beyond this, "it is hopeless to expect to obtain a precise solution for the orbital elements of the Earth" (Laskar *et al.*, 2004; p281). The most regular components of the solution, that is, the outer planets, are resolvable over 250Ma, but have negligible impact on the insolation of the Earth or sedimentary cyclicity.

When considering obliquity and precession Laskar calculated two separate degrees of error resulting from a difference in tidal dissipation. With 5% error the solution of obliquity is valid over about 20Myr, but with a 10 % error, the solution is out of phase after 20Myr. Despite this, the uncertainty in the tidal dissipation manifests mostly as a small change of the precession frequency, which reveals in the obliquity solution as a time offset that does not change much the obliquity pattern (Figure 2.26).

As can be seen from Figure 2.26, beyond 50Ma the solution for all three orbital components cannot be calculated with any certainty. This does not necessarily imply a fundamental change in the periodicities of Milankovitch parameters; they may not be radically different to those encountered in the Pleistocene. However, it is likely that the orbital components have not remained constant for 300My, and therefore the ratios between them will have changed as well. One implication of this is that calculated insolation curves are therefore inaccurate to an unknown degree, meaning that the curves of Maynard & Leeder (1992) for example, have the potential to be entirely wrong.

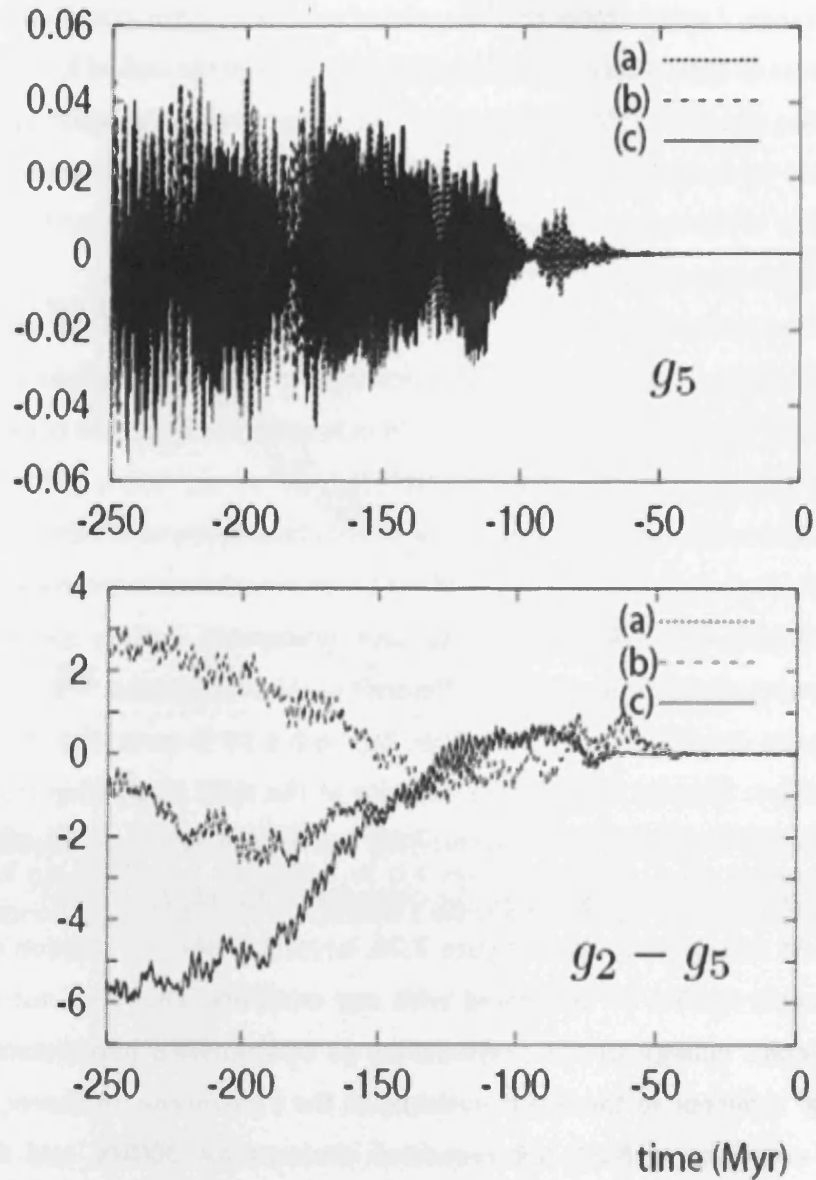


Figure 2.25: Stability of the g_5 (top) and $g_2 - g_5$ (bottom) arguments. The difference (in radians) of the angles related to g_5 and $g_2 - g_5$ from the nominal solution La2004 and an alternate solution for the models (a) La2004_{1.5}, (b) La2004₀ and (c) La2004*. Note the decrease in stability after 50Ma. (From Laskar *et al.*, 2004).

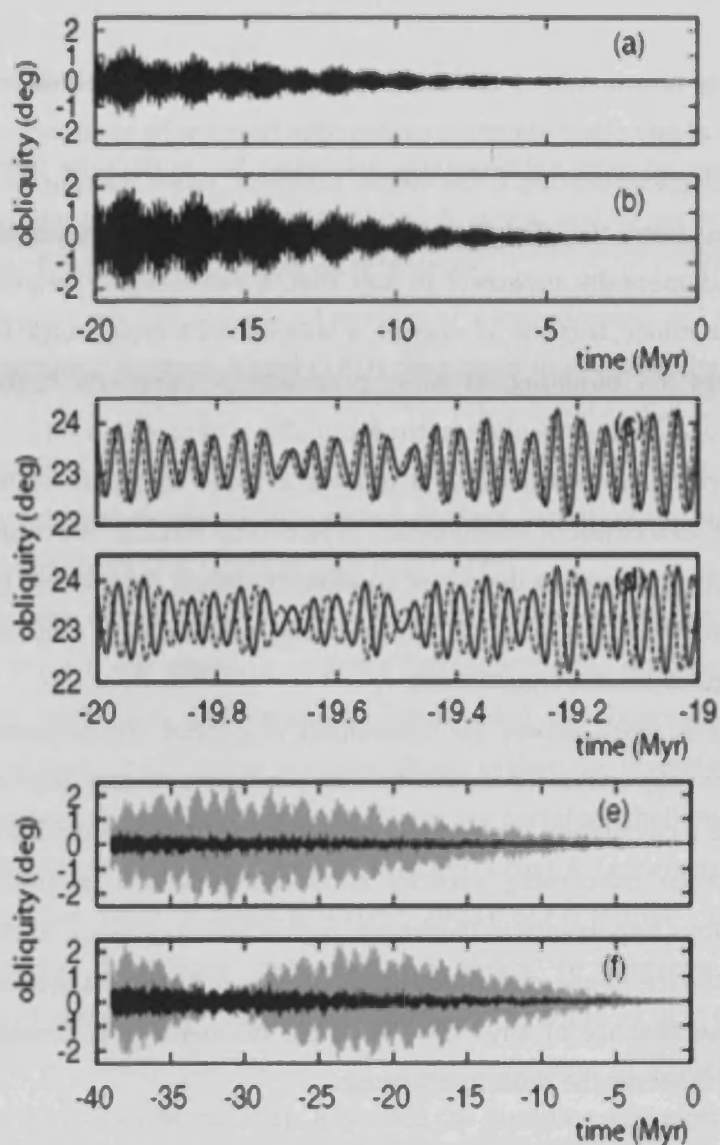


Figure 2.26: Difference in obliquity for different tidal dissipation factors: (a) $\text{La2004} - \text{La2004}^{(0.95)}$; (b) $\text{La2004} - \text{La2004}^{(0.90)}$. In (c) and (d), the nominal solution of the obliquity is plotted in full line, while $\text{La2004}^{(0.95)}$ (c) and $\text{La2004}^{(0.90)}$ (d) are in dotted line. After an adjustment of the time scale, the differences of the solutions are much smaller over 40 Myr : (e) $\text{La2004} - \text{La2004}^{(0.95)}$; (f) $\text{La2004} - \text{La2004}^{(0.90)}$. (From Laskar *et al*, 2004).

2.6 SUMMARY

It is perfectly reasonable to deduce from an ancient cyclic sedimentary sequence that, in the absence of any other plausible explanation (autocyclic sequences or tectonism) that orbitally-forced glacio-eustasy is the cause. However, when making this assumption, Milankovitch cycles from the Pleistocene must be treated as an imperfect modern analogue. It is fundamentally incorrect to say that a sedimentary sequence from the Carboniferous, for instance, is cyclic as a result of Milankovitch-type orbital forcing, simply because it evidences 5:1 bundling, as these precession/eccentricity ratios will almost certainly have changed through geological time. Equally, it cannot be said that a Palaeozoic sequence has an orbital-control because it follows a 40ky, 100ky or 400ky trend. This pattern may well be as a result of Milankovitch-type orbital forcing, but cannot be directly attributed to it with a reasonable degree of confidence unless the worker can isolate the effects of inaccurate dating, allocyclic and tectonic mechanisms, 'missed beats' and variable orbital amplitudes and frequencies.

While modern work allows for calculation of orbital components increasingly further back in time (e.g. Laskar *et al.*, 2004) with a relatively small degree of error, the further back in time a calculation is attempted; the greater the potential for error. The list of conflicting evidence concerning cyclicity is extensive, which is unfortunate when considering its obvious importance to Palaeozoic hydrocarbon systems. At the moment, all that can be said of the ice-house cyclothem in relation to orbital forcing and Milankovitch cycles, is that in the absence of any other plausible mechanism as a major controlling factor; orbital forcing seems the most likely cause.

Chapter 3: DESCRIPTION OF THE NUMERICAL FORWARD MODEL “TED”

3.1 ONE-DIMENSIONAL FORWARD MODELLING

Numerical simulations of carbonate accumulation may be used to develop and quantify conceptual models of carbonate platform strata, and to perform sensitivity tests that evaluate the fundamental controls on this strata.

This chapter describes the final version of a one-dimensional numerical process-response stratigraphic forward model (TED) developed to examine the origin of apparent cyclicity in ice-house carbonate platforms. To achieve this, the model assumes that controlling variables and parameters can be extracted from the geologic record. In a geological context, one-dimensional forward models are typically applied to examine vertical sections of strata (e.g. Goldhammer *et al.*, 1987).

The purpose of this modelling is to investigate the various mechanisms proposed for the origins of ice-house platform cyclicity. Representing the proposed mechanisms in a forward model, with rates and processes constrained by observation of modern and interpretation of ancient carbonate systems, allows systematic investigation to determine which products arise from what processes. There are certainly challenges involved in this process (Kendall & Lerche, 1988; Carey *et al.*, 1999; Cross & Lessenger, 1999; Perlmutter *et al.*, 1999; Steckler, 1999; Burgess & Wright, 2003), but if treated carefully this kind of modelling analysis does have demonstrated ability to improve our quantitative understanding of geological processes (Ginsburg, 1971; Dunn *et al.*, 1986; Watney *et al.*, 1991; Barnett *et al.*, 2002). One element of careful treatment of modelling study is a full appreciation of the model formulation, including the founding assumptions. Given this, the inputs and algorithms used in TED are examined here in detail.

3.1.1 Precedents for one-dimensional forward modelling

The desire to quantitatively explain sedimentary stacking patterns led workers from qualitative conceptual models to numerical forward models (Dunn *et al.*, 1986; Lerche *et al.*, 1987; Bice, 1988). These models used mathematical functions to describe the processes thought to be controlling factors on carbonate platform sediment accumulation. Bosence & Waltham (1990) provided a significant advance from these early models by further refining the controls on sedimentation and incorporating a greater number of variables into their model, including sub-aerial erosion, and vertical and lateral variability in production. These early examples of numerical forward models proved they could simulate strata relatively accurately by mimicking what were observed to be the controlling factors on carbonate platform sedimentations.

One-dimensional forward modelling has been applied to carbonate platform depositional systems previously, most notably the platforms of the Alpine Triassic (e.g. Goldhammer *et al.*, 1987; 1990) and the ice-house platforms of late-Mississippian and Pennsylvanian age globally (e.g. Walkden & Walkden, 1990; Watney *et al.*, 1991). Walkden & Walkden (1990) demonstrated that one-dimensional simulations could accurately reproduce lithologies from a range of mixed carbonate-siliciclastic systems. Building upon this, Goldhammer *et al.* (1991; 1994) showed the practical application of one-dimensional forward modelling; matching synthetic sections to lithological sections and subsequently deducing the controlling parameters for the succession.

The numerical forward model developed by Bosence & Waltham (1990) also represented a key development from models such as that of Walkden & Walkden (1990) by being two-dimensional. Two-dimensional models were a logical step in the quest to provide a quantitative and predictive tool to understand platform-basin patterns in carbonate systems. Later incarnations of 2D models have been successfully applied both as an interpretive tool (Aurell *et al.*, 1995; 1998) and to further conceptual models (Dunn *et al.*, 1991; Barnett, 2002; Barnett *et al.*, 2002).

Increases in technological capability coupled with the need for more complex models to explain issues arising from improved geological understanding have led to the abandonment of the development of stand-alone one-dimensional models. This stagnation has developed in the midst of increasing amounts of work with complex three-dimensional models and a discrete philosophy that a model is without value unless it can explain a sedimentary system as a whole. There are, however, some important benefits to one dimensional modelling that continue to make it a worthwhile technique to apply.

3.1.2 Benefits of one-dimensional forward modelling

The model presented here represents a significant advance over previous one-dimensional models, particularly in its ability to produce thousands of runs, diversity of input variables, intricacy of its algorithms and adaptability to different systems. The speed advantage of a one-dimensional model is conferred by saving the computational time required to calculate points in additional dimensions. This represents two orders of magnitude difference in the complexity of the calculation. Essentially, this is an expression of the scientific principle of *lex parsimoniae*; where a scenario does not necessitate a two- or three-dimensional control, a one-dimensional model is sufficient. This is the case for flat-topped carbonate platforms which display a dominantly aggradational architecture (e.g. Goldhammer *et al.*, 1990), and in these cases a one-dimensional model can be successfully applied.

One-dimensional modelling lends itself well to the evaluation of stacking-patterns in platform top carbonates. Aggradational stratal geometries are common throughout isolated platforms active during ice-house periods (e.g. Goldhammer *et al.*, 1991; Della Porta *et al.*, 2004). Under these conditions, inner-platform areas show little lateral facies variation (Stemmerik, 1996; Lehrmann & Goldhammer, 1999) despite complex variations in controlling factors (see Burgess & Wright, 2003). They can therefore be reliably modelled as one-dimensional stacks.

The relatively quick runtime of a simple model allows it to be used in ways that it is less convenient to use a more complex program, or in which a more complex program cannot be used. For example, TED, the model presented here, can complete 1000 simulations in 7 hours on an average personal computer. CARB3D+, a more complex three-dimensional forward model, takes 2000 hours to produce 100 simulations (processor capacity unknown; Paterson *et al.*, 2006). A very rapid run-time allows extremely long runs (tens of million years) to be conducted. It also allows for a large number of runs to be conducted to evaluate a criterion against a number of its parameters (a concept addressed in section 3.4.1).

Large numbers of runs provide a basis for quantitative statistical analysis of the model output. A quantitative method is essential for both assessing the influence of controlling factors on sedimentary stacking-patterns, and the intrinsic properties of the stacking-patterns themselves – particularly in terms of cyclicity. As demonstrated, this would be a cumbersome process in more complex models with a greater number of variables, which are not necessarily designed to quickly and efficiently output a large number of runs.

3.1.3 Limitations of one-dimensional forward modelling

The limitations, like the advantages, of a one-dimensional model stem from its simplicity. It fundamentally lacks some of the functionality of more advanced models programmed in two- or three-dimensions (compare with Burgess (2001) and Paterson *et al.* (2006)). However, this loss of functionality does not equate to a loss of usefulness (in a world comprising one-dimension any system will be simpler than the same system in a two- or three-dimensional world). This caveat remains true as long as the model in question is applied to a problem which does not need to be addressed in more than one dimension.

Any one-dimensional forward model is, by its nature, limited in its scope. In situations where facies exhibit significant lateral variability, use of a one-dimensional model would not be appropriate to evaluate stacking-patterns, as the sedimentary section at point *a* may differ significantly from point *b*, even if they are geographically close to

each other. The issue of apparently cyclic stacking-patterns in platform carbonate is an example of a problem that can be addressed by a 1D model. The high lateral continuity exhibited by beds from inner-platform successions (e.g. Goldhammer *et al.*, 1987; Goldhammer *et al.*, 1994; D'Argenio *et al.*, 1999; Della Porta *et al.*, 2002) allows cyclicity to be evaluated in the *z*-dimension, without addressing the horizontal *x*- and *y*-dimensions.

A criticism levelled at one-dimensional forward and conceptual models is their lack of two-dimensional control (Eberli, 2007, pers. comm. 24-04-2007). This criticism is valid, although it depends entirely upon the problem which the model is targeted and the context of the geological setting. The Paradox Formation in the Four Corners area of the U.S.A. is an example of a scenario to which a one-dimensional model can be usefully applied. The Paradox sequences and cycles are interpreted as largely aggradational in nature (Goldhammer *et al.*, 1994; Grammer *et al.*, 2000), lending themselves to being modelled as one-dimensional stacks. Lateral continuity of facies is demonstrable on a kilometre-scale in this section, and only varies where algal mounds create significant depositional topography (Grammer *et al.*, 2000; Lerat *et al.*, 2000). Where mounds are largely absent, such as at the land-proximal Honaker Trail section of the Paradox Formation, a one-dimensional forward model can be useful if it is capable of simulating the stacking-patterns of the geological record. In this type of scenario, as long as the scope of the problem does not extend beyond the 'layer-cake' platform top, two-dimensional control is not required.

The transport of carbonate sediment prior to lithification is a topic that has received significant study in recent years, and is increasingly seen to play an important role in the distribution of sediment on flat-topped carbonate platforms (Burgess & Wright, 2003; Quiquerez *et al.*, 2004). Studies employing forward models suggest there is a complex relationship between stratigraphic completeness, subsidence rate and sediment transport, and this relationship is likely to be considerably more complex in actuality than that predicted by numerical models (Burgess & Wright, 2003).

A one-dimensional model does not allow for complex transport functions to be included in accumulation algorithms as at any given iteration the conceptual world in model-space exists as only one point. In other words, sediment cannot be laterally transported in one-dimensional models as there is nowhere for it to go. This, however, does not constitute a critical problem for simple one-dimensional models as the loss or gain of sediment via lateral transport can be emulated in the sediment accumulation algorithm.

3.2 FORMULATION OF TED

The one-dimensional model described here was written in Microsoft Visual Basic for Applications 6.5, by the author, and is run from a Microsoft Excel host. TED distinguishes itself from previous one-dimensional forward models in a number of ways (refer to section 3.1.1). Fundamentally, it contains a significant degree of functionality previously unseen in one-dimensional models (Table 3.1). Typically, a numerical forward model increases in complexity through its development life-span as more complexity is added, usually in the form of additional dimensions and features. An increase in complexity, however, need not necessarily equate to an increase in dimensions. One dimensional models, as mentioned (section 3.1.2), have specific advantages when applied to certain problems which can be addressed without two- or three-dimensional control.

As TED represents a model with a significant number of interacting components, dependent upon user-defined controls, reflecting the state-of-the-art in one-dimensional lithological forward modelling, it is necessary to examine the algorithms and inputs of the model in detail.

3.2.1 Explanation of model

TED is a one-dimensional numerical process-response stratigraphic forward model of carbonate accumulation. Essentially, the model records the vertical movement (the z -dimension of a Cartesian coordinate system) of the top of a carbonate platform at a given geographic point. Processes affecting this movement can be thought of as one-dimensional vectors; they can either raise or lower the platform surface by a given magnitude. There are a number of processes which can cause the raising or lowering of the platform surface, the most important of which (based on previous modelling studies; e.g. Goldhammer *et al.*, 1990; Burgess, 2001; Barnett *et al.*, 2002; Burgess & Emery, 2004; Burgess, 2006) can be considered to be relative sea-level change, subsidence and carbonate sediment accumulation.

Carbonate accumulation is observed at each iteration of the model (referred to as a timestep) and changes through time during a model run according to the operation of several individually simple processes that can be summarised as the function

$$c_{(t)} = e_{(z)} + o_{(z)} + a_{(z)} + m_{(z)} \vee d_{(z)}$$

3.1

Capability	'Mr. Sediment' (Dunn <i>et al.</i> , 1986; Goldhammer <i>et al.</i> , 1987; Dunn, 1991)	'Milankovitch' (Walkden & Walkden, 1990)	'TED' (this volume)
Sinusoidal eustasy	Yes	Yes	Yes
Asymmetric sinusoids	Yes	Yes*	Yes
Variable eustatic amplitude	Yes	Yes	Yes
Linear subsidence	Yes	Yes	Yes
Pulsed subsidence	No	Yes	Yes
Random walks of eustasy	No	No	Yes
'Pomar' production style	No	No	Yes
'Bosscher & Schlager' Production Style	Yes	No	Yes
Variable production rates	Yes	Yes	Yes
Independently variable production curves	Yes	No	Yes
Sub-tidal production	Yes	Yes	Yes
Peritidal production	No	No	Yes
Wave-base	No	Yes	Yes
Marine erosion	No	Yes*	Yes
Variable marine erosion rate	No	Yes	Yes
Lag-depth	Yes	No	Yes
Sub-aerial platform denudation	No	No	Yes
Sub-aerial pedogenesis	No	No	Yes
Sub-aerial diagenesis	No	No	Yes
Missed-beat recognition	No	No	Yes
Facies taphonomy	No	No	Yes
Statistical package	Yes	No	Yes

Table 3.1: Comparison of TED with earlier one-dimensional models of carbonate accumulation and cyclicity. * denotes partial implementation.

where t is time, z is vertical movement of the platform surface, c is carbonate accumulation, e is euphotic production, o is oligophotic production, a is aphotic production, m is marine erosion and d is rate of surface lowering due to sub-aerial dissolution (platform denudation). All of the above components of the function, excluding time, are rates; and either raise or lower the platform surface over time according to the individual function determining that rate. These rates are usually expressed here in metres per million-years (m/My). Therefore, carbonate accumulation (or erosion) at a given time is dependent on a number of processes which may raise or lower the platform surface. These processes are explained further in section 0.

An important architectural consideration of the model is that it was constructed in a modular manner. Modularity is a concept that allows the program to run with non-essential processes disabled. Non-essential processes may be defined as those without which carbonate strata will still accumulate (sub-aerial erosion would fall into this category, but the carbonate production functions would not). If a process is not invoked by a particular model run, then that module is not loaded, saving memory and increasing performance. The modular programming of the model is described in Figure 3.1.

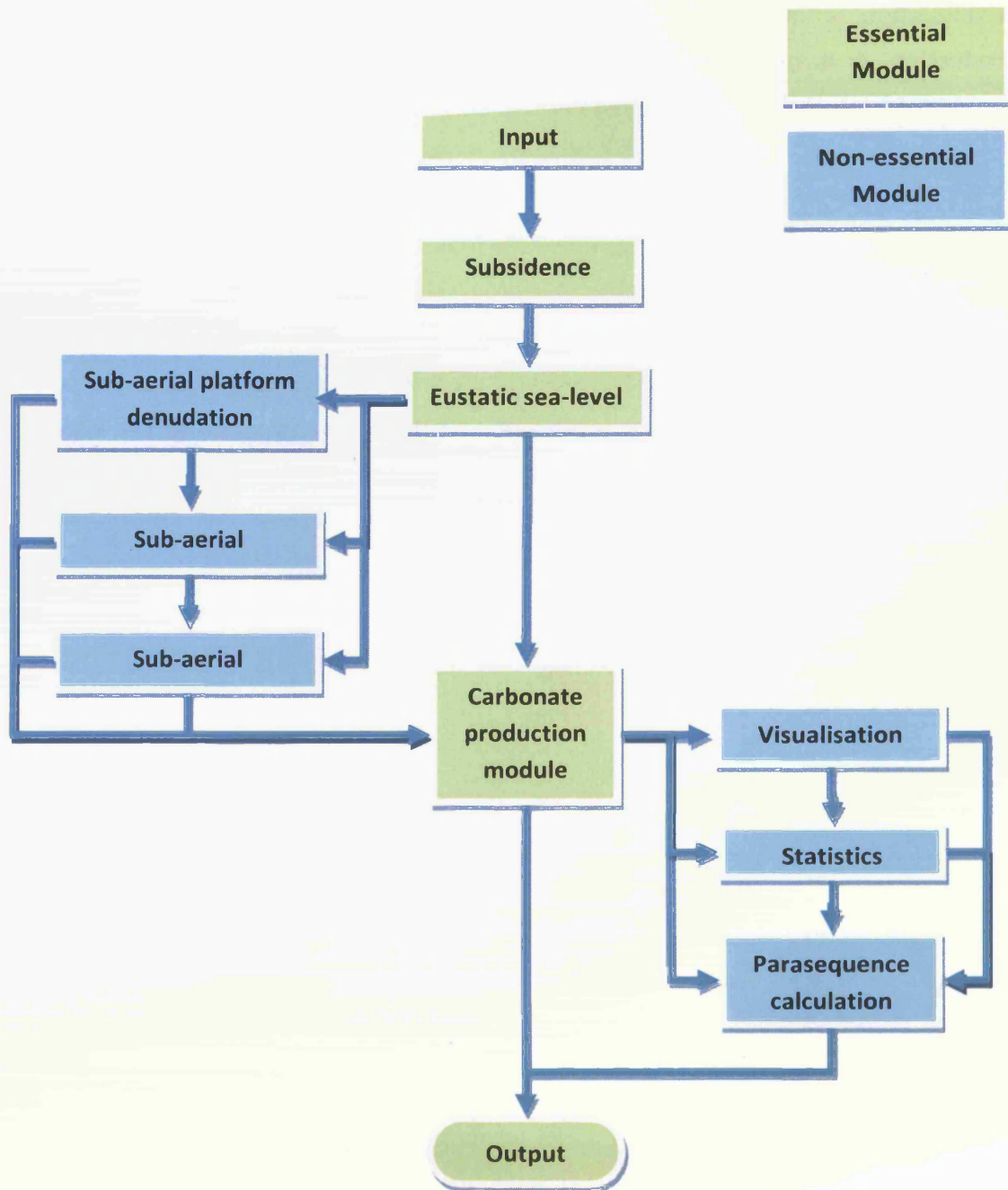


Figure 3.1: Conceptual flow-chart depicting modular elements of TED. Non-essential modules can be disabled according to the needs of individual simulations.

3.3 TED PARAMETER DEFINITION

There are demonstrable difficulties involved in extracting definitive values from the sedimentary record for parameters crucial to carbonate accumulation (Kendall & Lerche, 1988; Carey *et al.*, 1999; Cross & Lessenger, 1999; Perlmutter *et al.*, 1999; Steckler, 1999; Burgess & Wright, 2003). It is therefore crucial to examine the provenance of any values presented in a numerical forward model, and their reliability in representing discrete pre-, syn- and post-sedimentary processes. It is also necessary to consider how they are interpreted and represented in the numerical forward model as logical, deterministic procedures.

3.3.1 Time-step Analysis

Time-step analysis represents a critical formative iteration in the construction of any numerical model and dictates both the accuracy and performance of a model. A time-step in the context of computer modelling represents the period between model iterations. The compromise in selecting a time-step lies between the numerical accuracy and numerical stability of the simulation whilst also maximising the speed at which the simulation runs. A good time-step limits the approximation error within a model, and therefore the model can be said to have robust numerical stability (Figure 3.2).

This crucial stage receives scant mention in discussion of the parameters underpinning numerical forward models (e.g. Walkden & Walkden, 1990; Cross & Lessenger, 1999; Boylan *et al.*, 2002; Paterson *et al.*, 2006). Failure to recognise the importance of an appropriate time-step is likely to result in the use of a time-step which creates numerical artefacts (e.g. Figure 3.3) in the output of a model that are consequences of the timestep rather than accurate representations of the underlying formulations. A secondary benefit of time-step analysis is that it can identify errors in numerical algorithms that may not necessarily show up otherwise (Figure 3.3).

The process of time-step analysis (Figure 3.4) represents a search for numerical stability of a simulation's algorithms. If the time-step is too small then the data is accurately recorded but the simulation is needlessly slowed down by additional calculations. Conversely, if the time-step is too large, artefacts may result and the outcome may be unreliable. The most-desirable time-step exists at the upper-end of reasonable stability for a given confidence interval (Figure 3.2).

Time-step analysis for TED was conducted by running a single simulation multiple times with different time-steps until a measured criterion became stable (i.e. did not vary

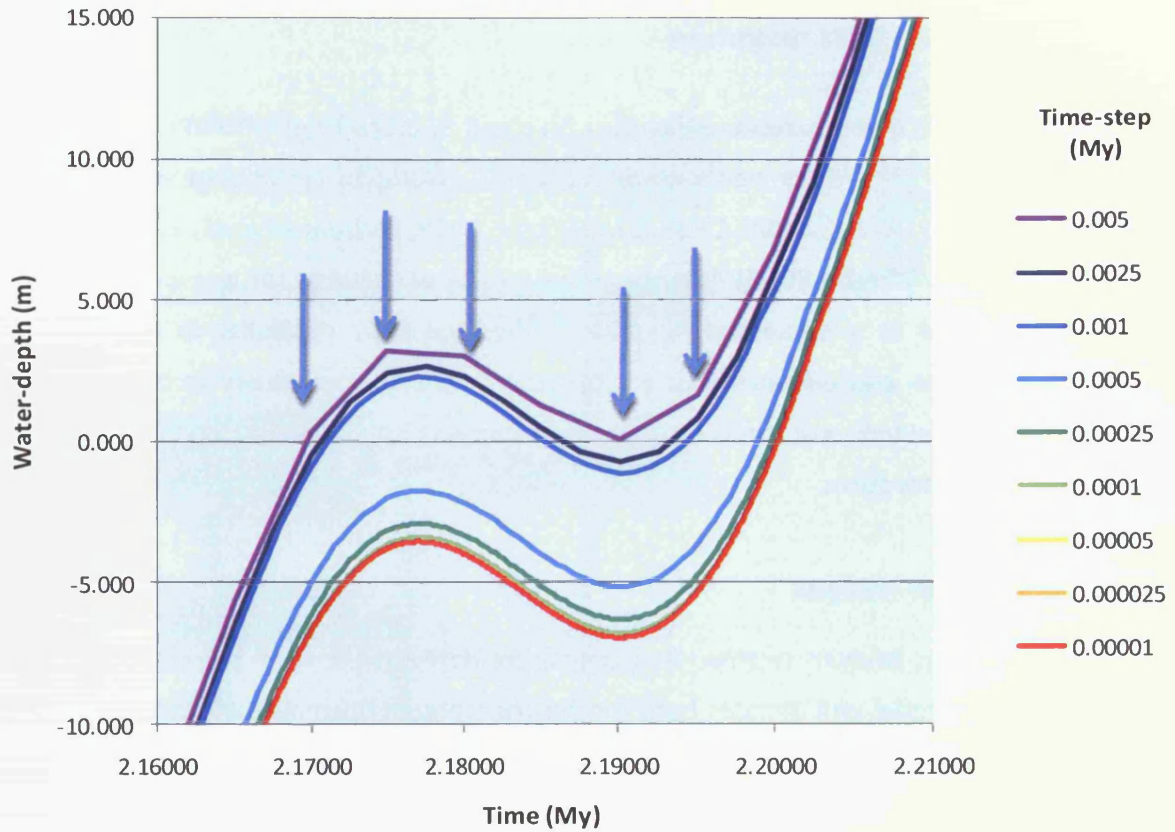


Figure 3.2: Diagram from a model run of TED showing the approximation error introduced through the utilisation of a time-step which is too large. Arrows identify points on the 0.005 time-step water-depth plot where visible approximation errors can be observed. Larger time-steps do a poorer job of defining the curve due to the fewer number of measured points. The shortest time-step (0.00005My) records the simulation with the highest fidelity. In this case shorter time-steps can be seen to incrementally reduce approximation error (timesteps 0.000025 and 0.00005 bear close resemblance to the 0.00001 curve, and as such, are depicted behind this curve).

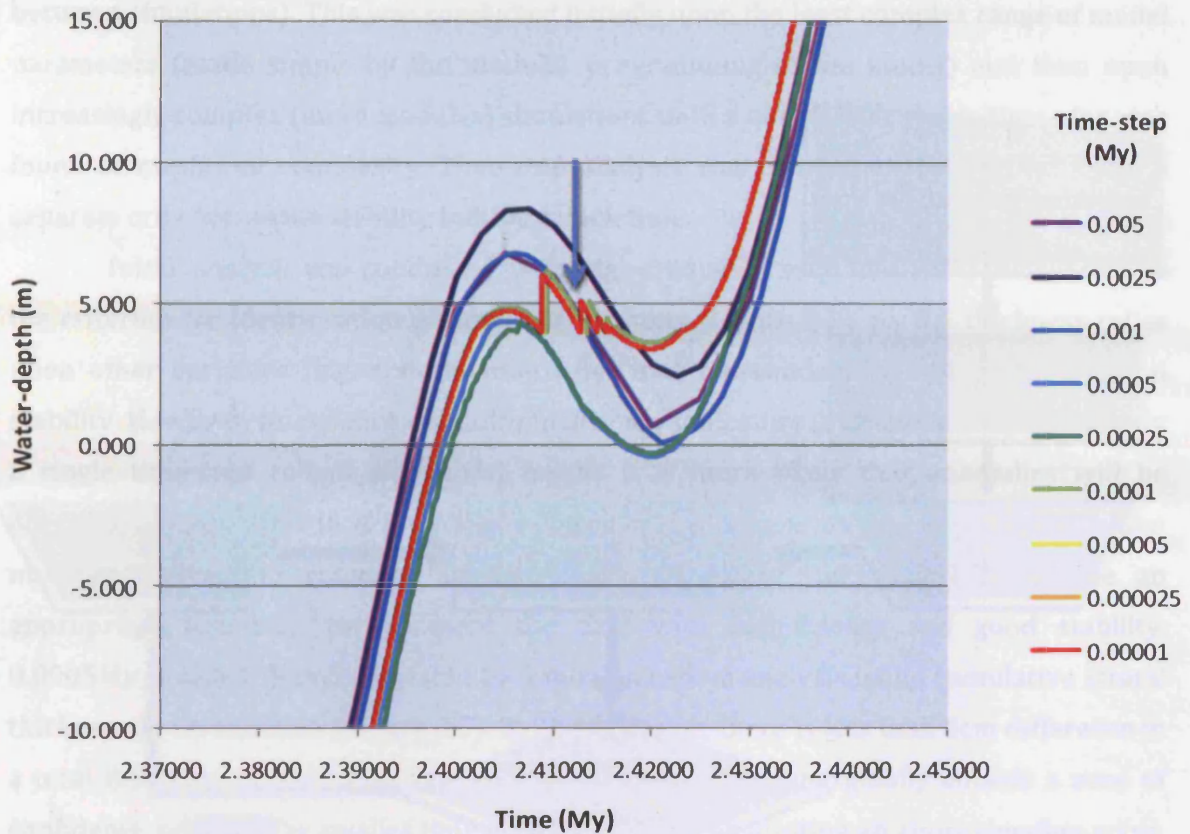


Figure 3.3: Diagram from a model run of TED showing an anomaly caused by erroneous program code (arrowed). This problem was caused by a section of code dedicated to sub-aerial denudation of the carbonate platform which, at very short time-steps, was continually implemented in a negative-feedback loop. This did not show up during the development phase as the time-step used was 0.00025My, which did not show the inherent instability in this piece of code. Time-step analysis allowed this problem to be identified and repaired.

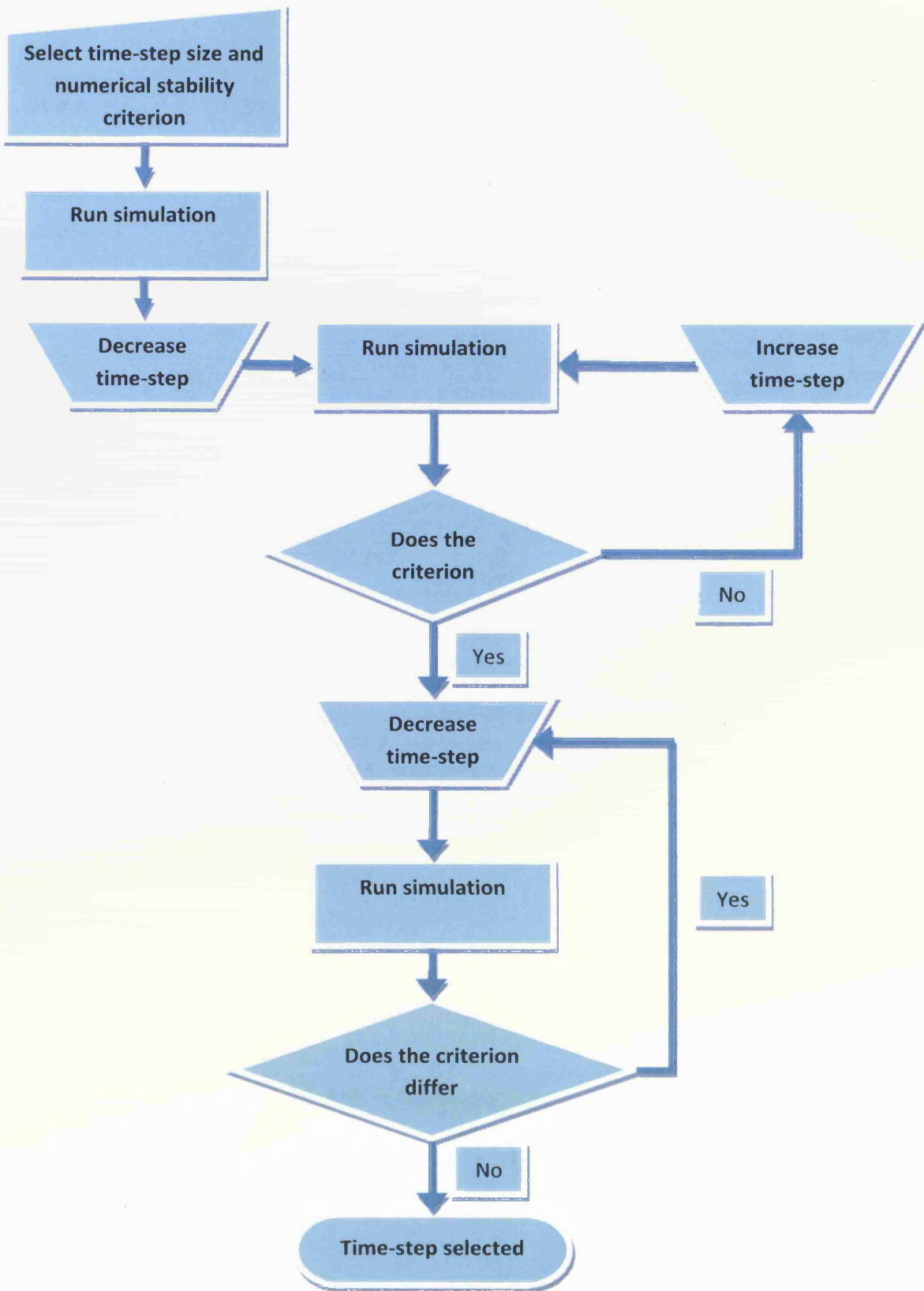


Figure 3.4: Workflow for time-step analysis.

between simulations). This was conducted initially upon the least complex range of model parameters (made simple by the modular programming of the model) and then upon increasingly complex (more modules) simulations until a numerically stable time-step was found at maximum complexity. Time-step analysis was conducted three times using a separate criterion as the stability indicator each time.

Initial analysis was conducted using high-frequency sequence (HfS) thicknesses as the criterion for identification of numerical stability (Figure 3.5). As HfS thickness relies upon other variables (e.g. accumulation rate) it is a secondary indicator of numerical stability. However, its reliance on multiple primary indicators (output values produced by a single time-step reliant algorithm) means it is more likely that anomalies will be manifest as disparities in HfS thickness. Analysis of a simple model scenario (minimum number of modules running) suggested that 0.0005My (500 years) would be an appropriate time-step to represent the data with high-fidelity and good stability. 0.0005My is also a figure suggested by a more sensitive analysis using cumulative stratal thickness as an indicator (Figure 3.5). By this criterion, there is less than 5cm difference in a total thickness of over 31m after 500ky. However, it lies marginally outside a zone of confidence provided by smaller time-steps, therefore constituting an approximation error. The distance from a grouping of smaller time-steps presents a warning that this time-step may still be unstable and further analysis is required to ensure a suitable time-step is adopted.

A time-step of 0.0005My therefore provides the basis for more sensitive analysis. Using water-depth increases the accuracy of the analysis as the water-depth output value is derived directly from a time-step dependent algorithm and does not involve other equations. It also allows the complexity to be increased up to a maximum, thereby testing all modules for approximation errors that may result from a poor choice of time-step. At maximum complexity, a time-step of 0.00025My constitutes less than a centimetre of error after 500ky (Figure 3.6). Confidence can be placed in the 0.00025My value as time-steps an order of magnitude smaller provide similar water-depth values, and it is this value which is used for all model runs.

3.3.2 Runs

The word 'run' refers to a single simulation as performed by the numerical forward model. It is synonymous with 'simulation' in this context and the two terms are used interchangeably here. The length of a run is a fundamental component of a simulation as it can profoundly affect results. For example, in Markov chain analysis (refer

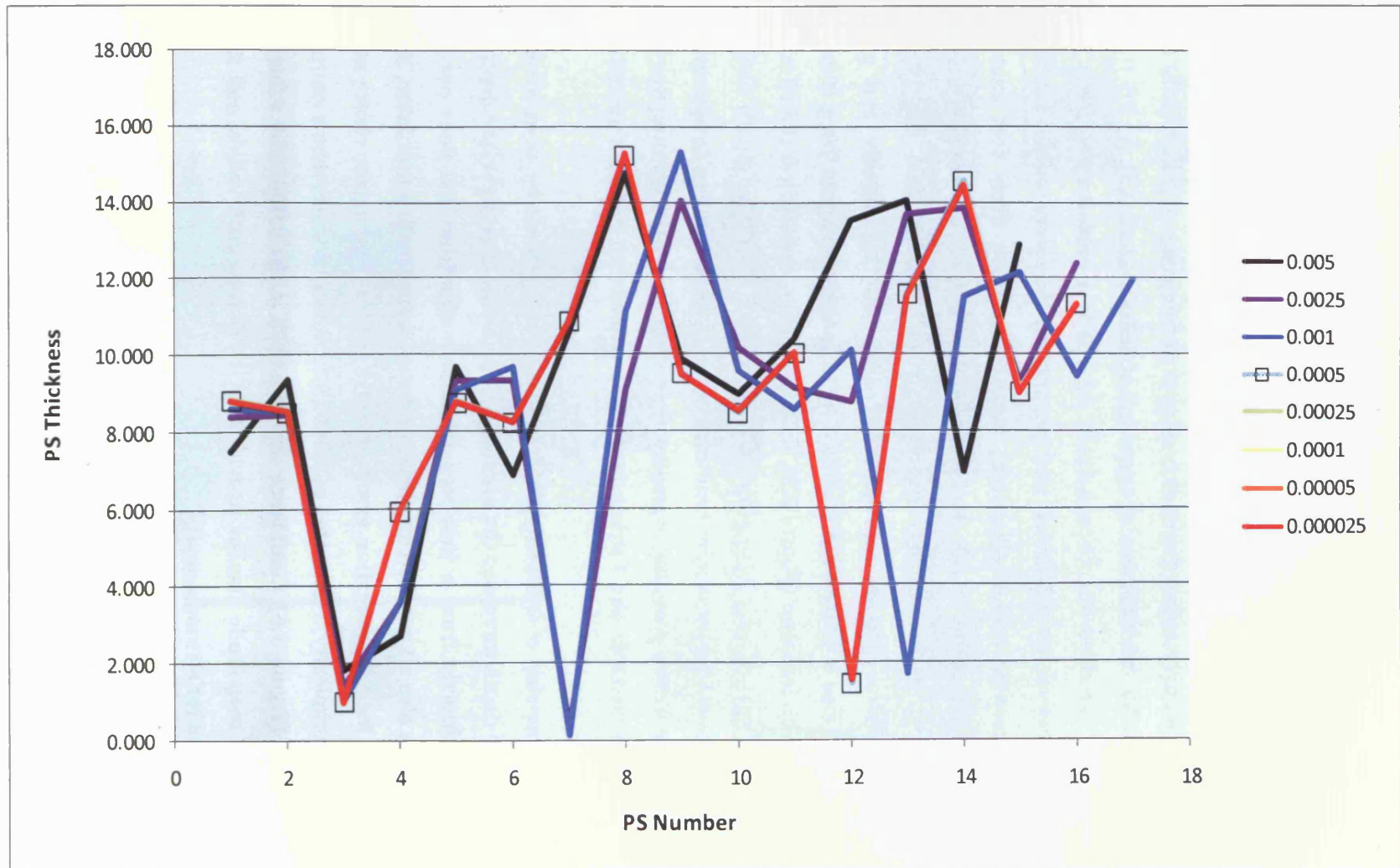


Figure 3.5: Graph showing variations in parasequence thickness over time as a result of approximation errors caused by inappropriate time-steps. Time-steps shorter than 0.0005My plot along the line with square markers due to their similarity, suggesting 0.0005 is at the upper limits of the confidence interval and is therefore an appropriate time-step.

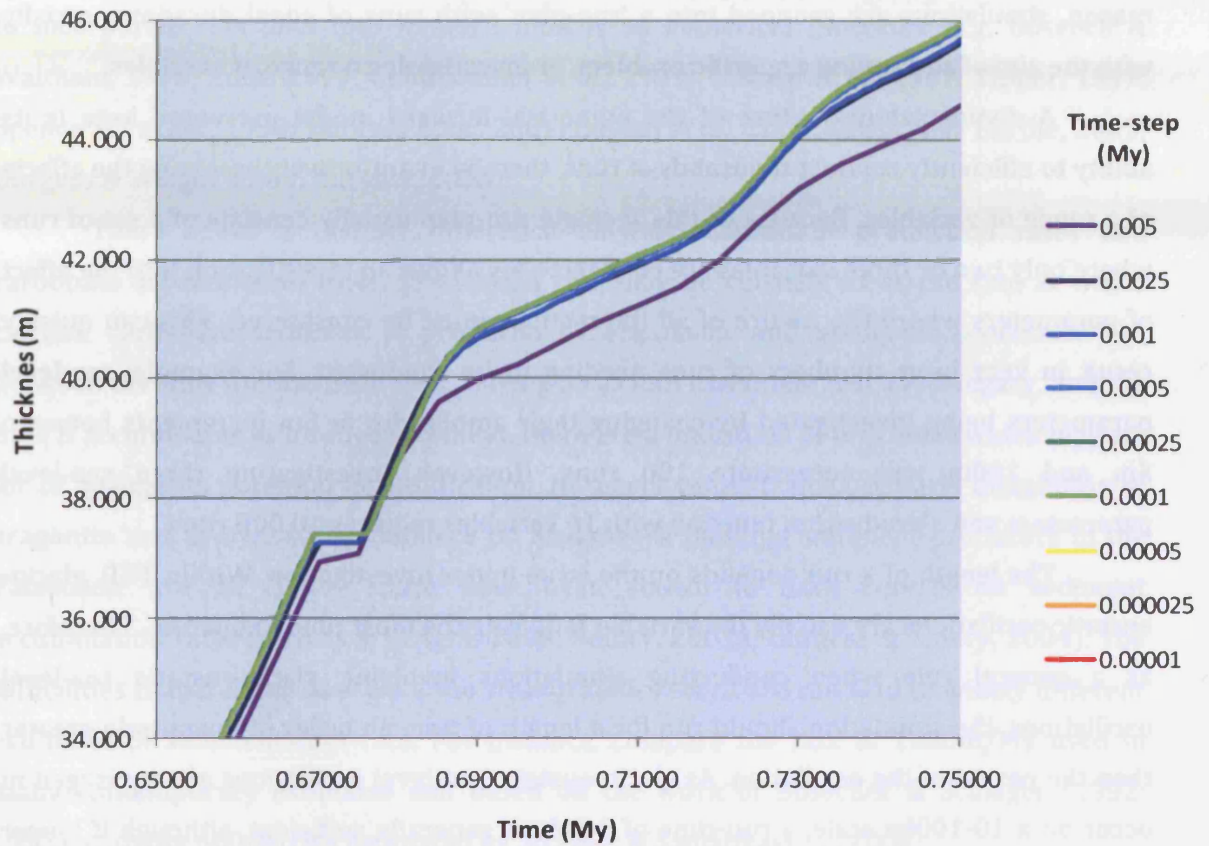


Figure 3.6: Graph plotting variations in thickness of carbonate accumulation over time. Time-steps of 0.0005My appear to plot along the same line and are not resolvable at this resolution. These results therefore suggest 0.0005My would be an appropriate time-step.

to section 3.4.4.1), a larger dataset (and therefore larger number of transitions from one facies to another) usually yields much higher χ^2 test values. A greater number of transitions mean it is more likely the data will show an ordered, and not random, distribution as the likelihood of transitioning from one facies to another increases. It would therefore be an unfair test to compare runs of 1My with runs of 10My. For this reason, simulations are grouped into a 'run-plan' with runs of equal durations, usually with the aim of addressing a specific problem, or investigating a range of variables.

A distinguishing feature of the numerical forward model presented here is its ability to efficiently conduct thousands of runs, thereby quantitatively assessing the effects of a range of variables. Because of this, a single run-plan usually consists of a set of runs where only two or three variables are changed. This allows an investigation into the effect of parameters where the nature of all interactions must be considered. This can quickly result in very large numbers of runs needing to be conducted. For example, sea-level parameters being investigated by changing their amplitudes at 5m increments between 5m and 100m will necessitate 100 runs. However, investigating three sea-level parameters and a production function with 10 variables requires 10,000 runs.

The length of a run depends on the issue under investigation. Within TED, glacio-eustatic oscillations are usually the variable requiring the most time to operate. Therefore, as a general rule when conducting simulations involving glacio-eustatic sea-level oscillations, the simulation should run for a length of time an order of magnitude greater than the period of the oscillation. As glacio-eustatic sea-level oscillations are envisaged to occur on a 10-100ky scale, a run-time of 3-6My is generally sufficient, although if longer frequency (low-order) oscillations are the object of investigation then a longer run-time may be required. For each set of runs the run-time will be constant and clearly stated.

In this numerical forward model each variable and measured value in a run starts with a value zero. This is not the case in a real-world scenario, where values exist in a continuum and each value has a 'history'. This is simulated in some two- and three-dimensional models where underlying topography is a consideration for carbonate accumulation (e.g. Paterson *et al.*, 2006). However, in terms of a one-dimensional model, this issue is largely irrelevant, as the only issue is if carbonate accumulation is occurring, not occurring, or the platform is being denuded or altered. Therefore if, at the start of the simulation sea-level begins by exceeding the platform top, it is treated by the model as a normal occurrence. The one-dimensional model therefore incorporates some of the 'history' of the sedimentary system in its initial conditions.

3.3.3 Accumulation

There is extensive literature on the subject of carbonate sedimentation on carbonate platforms and the rates at which this occurs (e.g. Bosscher & Schlager, 1993; Tipper, 1997; 2000; Pomar, 2001a; Schlager, 2003; Pomar *et al.*, 2004; Rankey, 2004; Wright & Cherns, 2004). There have also been broad attempts at determining the best way to incorporate this data into forward models as numerical functions (e.g. Bosence & Waltham, 1990; Enos, 1991; Goldhammer *et al.*, 1991; Watney *et al.*, 1991; Tipper, 1997; Spence & Tucker, 1999; Burgess *et al.*, 2001; Boylan *et al.*, 2002; Demicco & Hardie, 2002; Burgess & Wright, 2003; Burgess, 2006).

There exists a distinct difference between carbonate production rates and carbonate accumulation rates. Production rate may be considered as the rate at which calcium carbonate sediment is produced by organisms and abiogenic processes. Yet, between the time an organism dies, leaving a calcium carbonate test as its legacy, and the time it accumulates as lithified sediment, there are a multitude of processes which may act for or against its potential for lithification. In recent years, transport, early dissolution of aragonite and decreased dependence on framework building sediment producers in the Palaeozoic are all issues which have been shown to have control on sediment accumulation rates (Cherns & Wright, 2000; Pomar, 2001a; Burgess & Emery, 2004). The difficulties in extracting data from the stratigraphic record can lead to widely different estimates of sedimentation rate. For instance, compare the rate of 1000m/My used in many contemporary estimates and based on the work of Bosscher & Schlager (1992; 1993), with the 6000m/My estimated by Strasser & Samankassou (2003).

For the purposes of a numerical forward model, it is the rate of calcium carbonate accumulation which is important. Accumulation rate refers to the rate at which calcium carbonate accumulates as lithified sediment (Wilkinson *et al.*, 1999). Accumulation rate, however, is a difficult property to extract from the sedimentary record due to post-depositional processes (compaction and early diagenesis to give two examples; Steckler, 1999; Cherns & Wright, 2000), and modern sedimentation rates must therefore be used to infer values on rates of carbonate deposition and accumulation.

TED incorporates the ability to simulate both a 'Pomar' and a 'Bosscher & Schlager' production curve (Figure 3.7). The Bosscher & Schlager curve is based on data for the main Caribbean reef-building coral (*Montastrea annularis*) and assumes that carbonate production is a function of water depth, such that

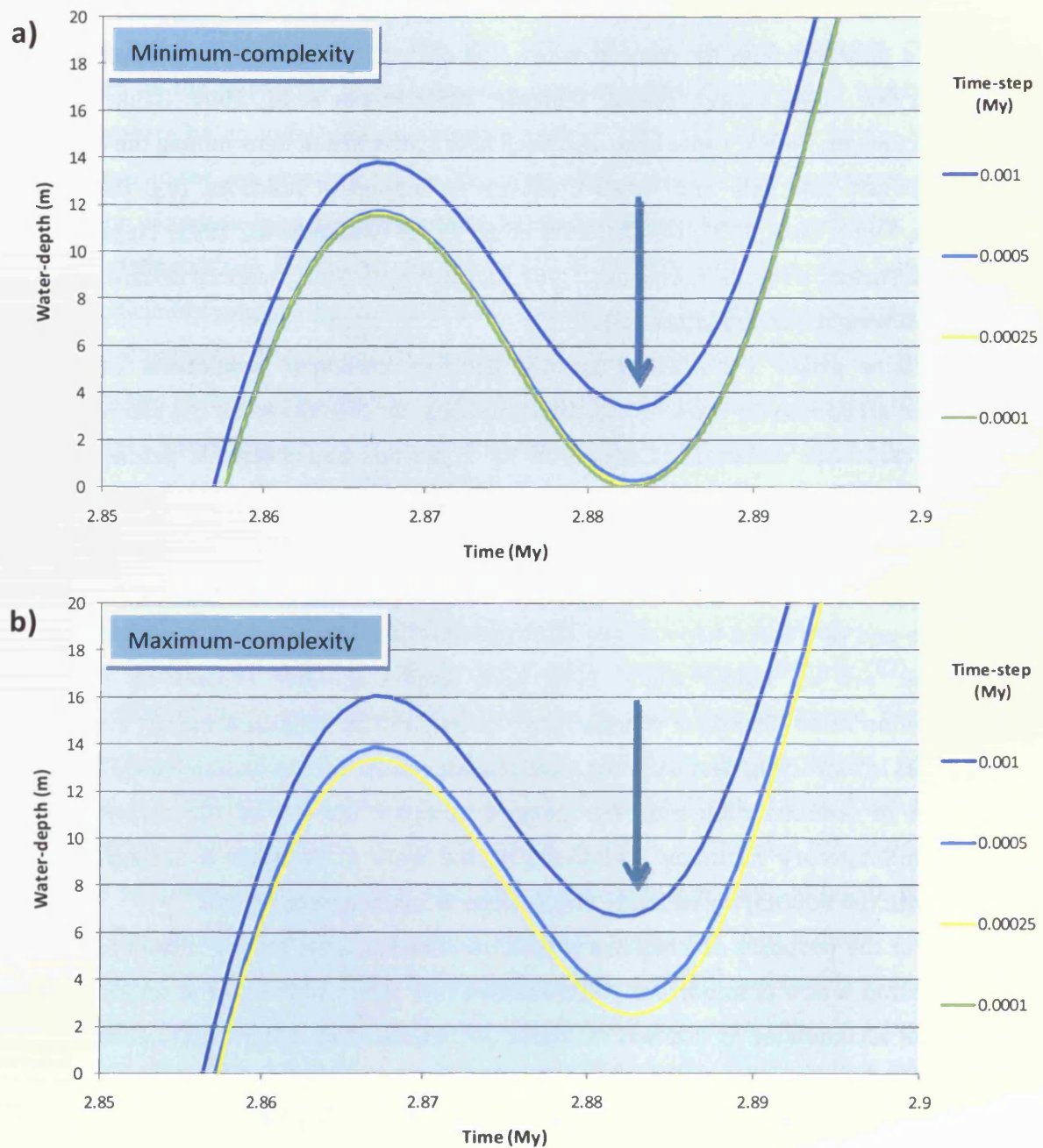


Figure 3.7: a) Graph plotting water-depth against time as an indicator of numerical stability in minimum complexity situations (minimum number of modules loaded). This situation does not include non-essential algorithms such as diagenesis and sub-aerial dissolution. The chart focuses on potentially 'good' time-steps as identified by previous analyses. In this scenario 0.0005My is suggested to be a somewhat-appropriate time-step, as it creates less than 10cm of approximation error at the arrowed time (2.883My). b) Graph plotting water-depth against time as an indicator of numerical stability in maximum complexity situations (maximum number of modules loaded). This scenario shows 0.0005My to be an inappropriate time-step, constituting approximately 90cm of approximation error at the arrowed location. A time-step of 0.00025My however represents less than 1cm of approximation error after 2.883My compared with shorter time-steps, therefore identifying itself as an appropriate time-step for use in simulations.

$$g_{(z)} = g_{(m)} \tanh\left(\frac{I_0 e^{-kz}}{I_k}\right)$$

3.2

where z is water depth, $g_{(m)}$ is a maximum rate of growth, I_0 is surface light intensity, I_k is saturation light intensity and k is extinction coefficient. This, essentially, can be expressed as a hyperbolic curve away from a maximum, and is applied in the model as

$$e_{(t)} = e_{(m)} \cdot \tanh(k \cdot \exp(d \cdot w_{(t)}))$$

3.3

where w is water depth, t is the current timestep, e is carbonate accumulation, d is a decay constant, m is maximum production rate, and k is a rate constant. However, the Bosscher & Schlager curve has well documented problems with regard to its application to ancient systems (for a critique refer to Demicco & Hardie, 2002). The fundamental argument is that a curve of this nature alone, based on modern framework-building organisms, could not replicate what is seen in much of the stratigraphic record (e.g. Goldhammer *et al.*, 1990; Riley, 1993; Horbury & Adams, 1996; Della Porta *et al.*, 2002) where sedimentation is seen to take place at much deeper locations, by distinctly different organisms. This curve, although programmed into the model, is not used in simulations unless otherwise stated.

An alternative to the work of Bosscher & Schlager was presented by Pomar (2001a). By this method, carbonate accumulation is qualitatively subdivided into three 'factories' which can be represented by individual curves based upon their affinity to light (Figure 3.7). The 'Pomar-style' curve is expressed in the model by three functions representing the individual curves, which are described independently in sections 3.3.3.3, 3.3.3.4 and 3.3.3.5. The Bosscher & Schlager curve is still present as a euphotic production curve, but only as an element of the overall production regime (Figure 3.8). This approach leads to a much better ability to simulate the stratigraphy of ancient successions as the segregation groups according to light-dependence allows characterisation of facies according to the relative proportions of biota within them (refer to Horbury & Adams, 1996). An important point to note about this segregation of production is that all three trophic processes can operate at the same time; they are not mutually exclusive (Figure 3.9). Therefore, while one regime may dominate (e.g. euphotic at shallow-water depths) the biota belonging to the other trophic regimes may still be present. Evidence for this is

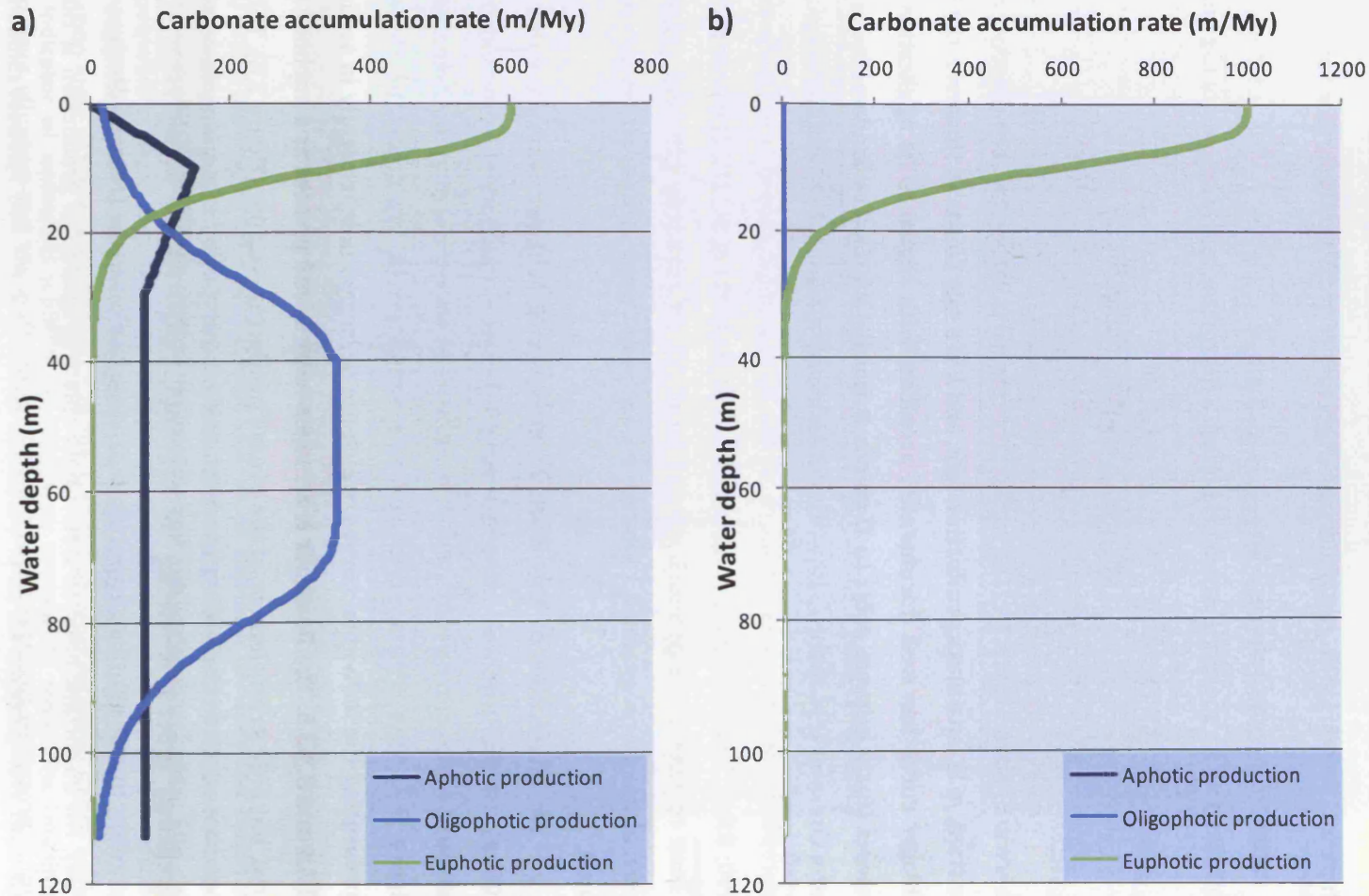


Figure 3.8: Plots comparing a 'Pomar-style' production curve (a) with a 'Bosscher & Schlager-style' curve (b). The Bosscher & Schlager curve is based on sedimentation rates observed at modern tropical reefs (Bosscher & Schlager, 1993). The Pomar curve is based upon empirical grain accumulations in carbonate sediment (Pomar, 2001b), and is preferred to the Bosscher & Schlager curve in TED simulations due to its non-reliance on framework-producing biota, which are not abundant during the Upper Palaeozoic (Pomar, 2001b). The segregation according to light-affinity is useful to classify sediment accumulations into facies.

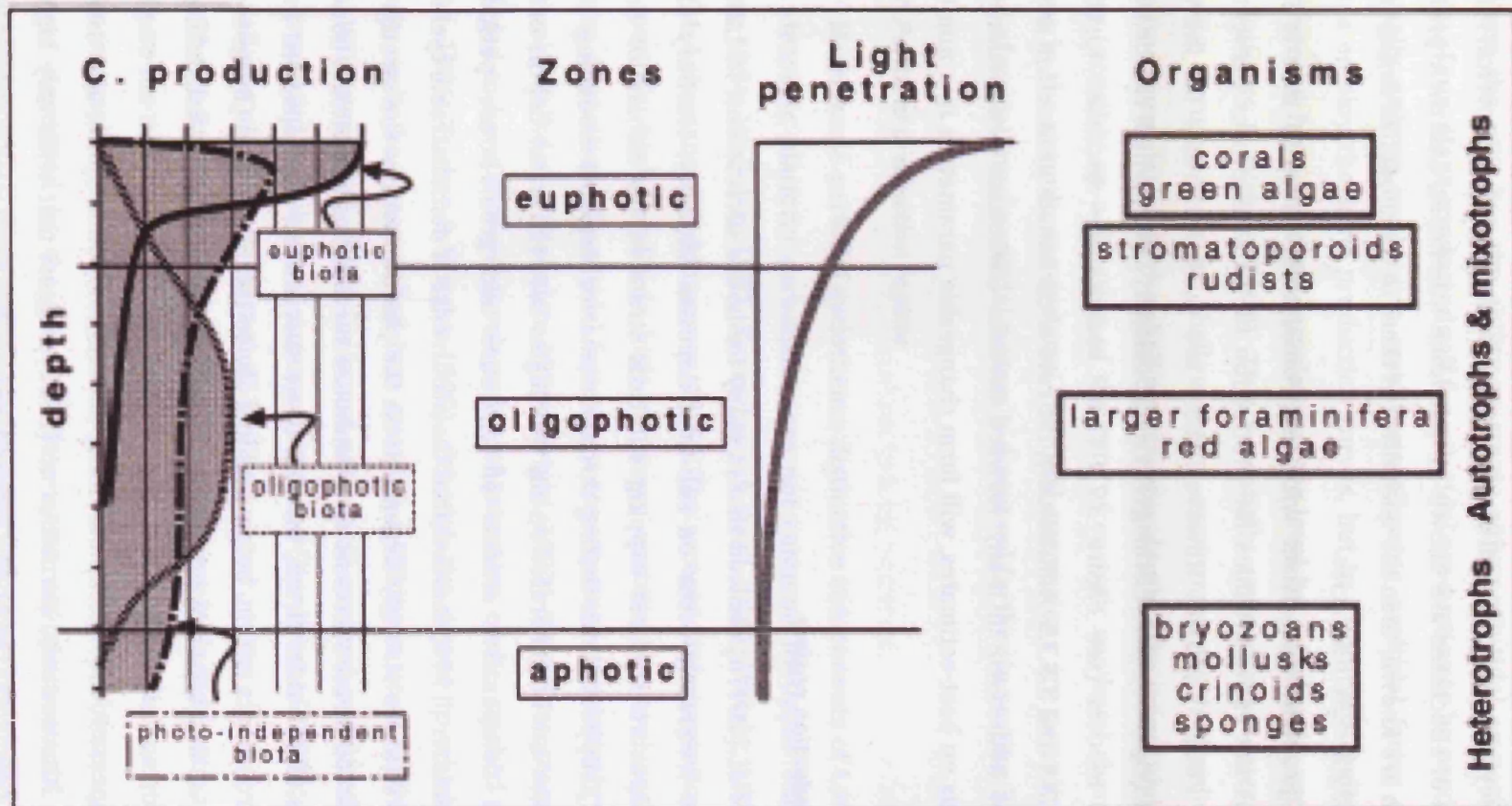


Figure 3.9: Conceptual diagram from Pomar (2001b) segregating calcium carbonate production based upon an organism's affinity to light. This allows classification of lithofacies depending upon the proportion of a given production regime responsible for its composition. Compare this diagram with the implementation of the 'Pomar' curve in TED (Figure 3.29).

provided by Horbury & Adams (1996), who show that while certain allochems may be dominant in portions of the water column, other organisms co-habit these areas in lesser numbers. This is a key observation when characterising facies from the numerical forward model. If quantities of allochems are known in individual lithofacies, and their preferred depths of habitation are known, then the quantities of them in the modelled sediment can be used to confidently assign lithofacies.

The major problem that exists with the Pomar-style curve is that it is not quantitative; it does not contain values for production or water depth as presented in Pomar (2001a) or Pomar (2001b). However, there are published rates for individual aspects of the curve (e.g. Bosscher & Schlager, 1992; Schlager, 2003) which can be used in numerical forward models (see Figure 3.7). These sources are discussed further in sections 3.3.3.3, 3.3.3.4 and 3.3.3.5. Additionally, the rate of carbonate production is one of the major variables addressed in many forward models. Carbonate production rates, whilst having a basis on best-estimates, will form changeable parameters in a number of run-plans.

3.3.3.1 Sub-tidal production regime

Wilkinson *et al.* (1997a) showed that in many ice-house successions, instances of sub-aerial exposure frequently occur on sub-tidal deposits. Similarly, Horbury (1989) noted sub-aerial exposure surfaces capping sub-tidal strata in the Asbian of Britain. Barnett *et al.* (2002) supported this finding through numerical forward modelling, stating that exposure surfaces can be generated on any lithologies between water depths of 0m to greater than 20m. Comparative studies of ice-house and green-house periods by Lehrmann & Goldhammer (1999) indicate that the occurrence of demonstrable cyclicity in platform carbonate strata is strongly dependent on the position within the stratigraphic record. In contrast to ice-house successions, greenhouse successions exhibit less abnormal sub-aerial exposure of sub-tidal strata. Instead, these successions are deposited in very shallow-water environments within, below and just above the tidal range (Burgess *et al.*, 2001). Successions of this type are notable by their absence during ice-house intervals (Wright, 1992).

This may represent the incomplete filling of accommodation space, and therefore 'incomplete cycles'. Alternatively, Barnett *et al.* (2002) suggest that with very high sub-aerial erosion rates (30m/My) the upper, more shallow-water lithofacies may be stripped. Barnett *et al.* also demonstrated that, in their models, many externally-forced cycles are shown to deepen-upwards before being truncated by sub-aerial exposure. The taphonomic aspect of facies preservation is discussed further in section 3.1.1.

The ability to discriminate between sub-tidal and peritidal production was included in TED to investigate the controls on the contrasting style of cyclicity. In any model run the user has the ability to create either sub-tidal or peritidal deposits. The majority of run-plans conducted call for sub-tidal production to be used, and peritidal runs are usually only to investigate conditions allowing peritidal facies development. Both methods employ the same production curves, but in a sub-tidal regime carbonate facies are prevented from building complete to sea-level by a hydraulic scour effect (Osleger, 1991; Burgess & Wright, 2003). This essentially replicates an interpretative model of carbonate accumulation in shallow-water environments; hydraulic action prevents carbonate accumulation in the shallowest water-depths (the inter-tidal zone) in ice-house systems (possibly as a function of the rate of eustatic sea-level change; Osleger, 1991) whereas in the greenhouse systems, peritidal successions are permitted to develop. The method of modelling a peritidal system is discussed further in section 3.3.3.2.

3.3.3.2 Peritidal production regime

Metre-scale peritidal cyclothem; distinctive components of Lower Palaeozoic and many Mesozoic platform carbonates, are not common in Upper Palaeozoic sequences (Davies, 1984; Walkden, 1987; Koerschner & Read, 1989; Wright, 1992; Goldhammer *et al.*, 1994; Lehrmann & Goldhammer, 1999). The accepted interpretation is that during ice-house periods, high-amplitude high-frequency eustatic sea-level oscillations precluded extensive deposition of peritidal facies as a consequence of relatively rapid variations in base level (Walkden & Walkden, 1990; Wright, 1992). Therefore greenhouse periods are considered to have allowed development of extensive, cyclic, stacked peritidal sequences (Wright, 1986; Tucker & Wright, 1990), although the degree to which these successions are truly cyclic has been called into question (Wilkinson *et al.*, 1996; Wilkinson *et al.*, 1997b; Wilkinson *et al.*, 1998). Ice-house periods, in contrast, produced irregular sub-tidal cycles, truncated by sub-aerial exposure surfaces (Hardie *et al.*, 1986; Goldhammer *et al.*, 1990; Saller *et al.*, 1994; Barnett *et al.*, 2002).

The ability to model peritidal cyclothem was included in the numerical model to investigate the reasons for this disparity in occurrence. Modelling peritidal production in a one-dimensional world is relatively simple. In one-dimensional terms, peritidal sediments are those deposited in the most shallow-water environments of the water-column (Burgess *et al.*, 2001), regardless of the reasons why they may or may not occur there. A user-defined switch therefore determines whether peritidal or sub-tidal production operates in a given simulation. If peritidal production is selected, no hydraulic erosional scour takes place within the inter-tidal zone, allowing sediment to be deposited.

3.3.3.3 Euphotic calcium carbonate production

Benthic skeletal components are the most conspicuous constituents of carbonate platforms, whilst open-ocean settings receive a significant quantity of sediment from planktonic production (Pomar, 2001b). Platform carbonate production depends on photosynthesis, either directly via autotrophic and autoheterotrophic organisms, or indirectly through heterotrophic organisms. These organisms are therefore reliant on light saturation of the water column (Bosscher & Schlager, 1993; Demicco & Hardie, 2002). In very shallow-water conditions (above fair-weather wave-base) non-skeletal carbonate production (faecal pellets and ooids) is also a significant contributor to sediment supply. The overall dependence of carbonate producing organisms on light saturation permits the segregation (see Figure 3.9) of carbonate producers into three main groups; euphotic, oligophotic and aphotic biota (Pomar, 2001b).

Euphotic biota refers to autotrophic and autoheterotrophic organisms that rely upon significant light-levels in the water column, and as such exist at relatively shallow depths (in the euphotic zone). The lower limit of the euphotic zone may be defined as the maximum depth of prolific hermatypic coral growth, and as such can be said to have a maximum extent of 40-50m in very clear water, but more typically a depth of 20-30m (Pomar, 2001b after Milliman, 1974 and Hallock & Schlager, 1986). Green algae and corals are the most characteristic modern examples of euphotic biota. During ice-house successions green algae, such as *Koninckopora*, has been shown to be an important component of shallow-water lithofacies (Horbury & Adams, 1996).

Previous estimates of sedimentation rates for the euphotic zone based on interpreting the sedimentary record have varied widely (e.g. Demicco & Hardie, 2002; Strasser & Samankassou, 2003) and are likely to be incorrect given the uncertainties present (e.g. Cherns & Wright, 2000; Burgess & Wright, 2003). Numerical forward models are therefore reliant on observations of analogous modern rates to applied definitive values to production and accumulation rates in ancient systems.

Fortunately, the euphotic zone has well documented modern rates of sedimentation provided by Bosscher & Schlager (1993). Maximum rates of production based on this work are usually cited as around 1000m/My based on Bosscher & Schlager (1992). More realistic rates taking into account the usually limited extent of framework-building organisms around platform margins suggest inner platform rates of sedimentation may be 400-600m/My (Smith & Kinsey, 1976; Bosence & Waltham, 1990). Where euphotic accumulation is not a variable, it is the rate of 600m/My that is preferred in TED (to take account of framework-building and non-framework building organisms). The light-dependent euphotic curve has been employed by numerous studies where sedimentation rate is a control or variable under investigation (e.g. Goldhammer *et al.*,

1991; Bowman & Vail, 1999; Burgess *et al.*, 2001). It is therefore utilised here as the euphotic component of the Pomar-style production regime, and is represented by the same function as the Bosscher & Schlager-curve; equation 3.3.

3.3.3.4 Oligophotic calcium carbonate production

Oligophotic biota refers to organisms (autotrophic and autoheterotrophic) that can inhabit environments with reduced levels of light. The oligophotic zone is characterised by a decrease in light and sometimes temperature (Milliman, 1974; Pomar, 2001b). The upper and lower limits of this zone depend on the light-penetration coefficient of seawater, with the lower boundary typically lying within the depth range of 50-100m (Pomar, 2001b). The zone, lying below fair-weather wave-base, will receive significantly higher quantities of micritic material being deposited as sediment, and so is not envisaged to produce 'clean' grainstones, but rather packstones and wackestones.

The existence of these lithofacies at water depths approximately corresponding to that of the oligophotic zone is supported by semi-quantitative studies of allochem distribution in microfacies of the Dinantian of the UK by Horbury & Adams (1996). In addition to the using analogous modern biota to assign water-depths to facies units, they infer associations between the position of allochems within a HfS and the water depth they inhabited. The middle of HfSs, comprising micritic wackestones and packstones, therefore display an abundance of oligophotic allochems: algae such as *Epistacheoides*, the palaeoberesellids *Kamaena* and *Kamaenella* and the microproblematicum *Ungdarella*. Furthermore, foraminifera can make up a significant component of lithofacies. Rates of sedimentation are not necessarily significantly lower than the euphotic factory depending on the depositional context (Della Porta *et al.*, 2004). Workers are notably reluctant to put definite values on rates of deposition within deeper-water carbonate factories (Pomar, 2001b; Schlager, 2003), however Pomar estimates it to be between 30-60% of the rate of the euphotic factory. The oligophotic component of the Bosscher & Schlager curve is implemented in TED differently to the euphotic curve, necessitated by its different shape, and is represented by the function

$$o_{(t)} = o_{(m)} \cdot w_{(t)} < o_{(a)} \Rightarrow \tanh(o_{(k)} \cdot \exp(o_{(d)} \cdot (o_{(a)} - w_{(t)}))) \vee \tanh(o_{(a)} \cdot \exp(o_{(d)} \cdot (w_{(t)} - o_{(a)})))$$

3.4

where w is water depth, t is the current timestep, o is carbonate accumulation, a is a turn-around depth constant, d is a decay constant, m is maximum production rate, and k is a rate constant. Rates are in metres per million years. This gives the curve shown in (b).

3.3.3.5 Aphotic calcium carbonate production

Aphotic biota refers to heterotrophic organisms that do not require light. They may live in any environment and depend only on limiting factors such as substrate requirements, nutrient supply, competitive displacement, temperature, salinity or hydraulic energy (Pomar, 2001b). The faunal assemblage within this group includes bryozoans, crinoids, molluscs, brachiopods and sponges. In terms of distribution through a HfS, Adams & Horbury (1996) note that certain bioclasts (such as ostracods, bivalves, small gastropods, the alga *Coelosporrella* and *Saccamminopsis*) are only present at the base of a cyclothem. Because of this zones independence with respect to light, the aphotic realm is not incorporated into the numerical model using the same algorithm as euphotic or oligophotic production. It is therefore modelled according to the function

$$a_{(t)} = a_{(m)} \cdot w_{(t)} < a_{(w)} \Rightarrow w_{(t)} \cdot a_{(w)} \vee w_{(t)} < a_{(p)} \Rightarrow 1 - \left(\frac{(a_{(w)} - w_{(x)})}{(a_{(w)} - a_{(p)})} \right) \cdot a_{(r)} \vee a_{(r)}$$

3.5

where w is water depth, t is the current timestep, a is carbonate accumulation, p is a turn-around depth constant, r is a rate constant. Rates are in metres per million years.

Production rates for aphotic sedimentation at shallow water depths is poorly constrained and is often categorised along with euphotic sedimentation rates (Pomar, 2001b). Aphotic sedimentation in deeper water is constrained much better, with evidence from Pleistocene and Holocene data suggesting pelagic sedimentation to occur at a rate of 52-66m/My (Vollbrecht & Kudrass, 1990).

3.3.3.6 Marine Erosion

Marine erosion within TED aims to simulate two distinct concepts, the first being hydraulic action by standing waves, and the second being wave scour. Wave scour is addressed in section 3.3.3.7. Hydraulic action above fair-weather wave-base is commonly simulated in forward models as a transport function. This is usually achieved by a function which subtracts sediment from the locus production and deposits it elsewhere (e.g. Bosence & Waltham, 1990; Burgess *et al.*, 2001). This is not possible in a one-dimensional model, where the sediment cannot be moved as it exists only at a given point in time. It is therefore subtracted directly from the sedimentation functions according to the function

$$m_{(t)} = m_{(a)} \cdot \tanh(k \cdot \exp(d \cdot w_{(t)}))$$

3.6

where w is water depth, t is the current timestep, m is marine erosion, d is a decay constant, a is maximum erosion rate, and k is a rate constant. Rates are in metres per million years. This creates a hyperbolic tangent, similar to that of equation 3.3, where erosion decreases after a certain depth (in this case fair-weather wave-base). Hydraulic action is therefore used simply to attenuate marine carbonate production above wave-base.

3.3.3.7 Lag-depth

Lag-depth, or lag-time in some cases, is used to refer to the minimum water-depth which must be achieved before carbonate sedimentation will take place after a marine transgression. In the case of lag-time, it is usually used as a proxy for the time taken to colonise a given geographic location by carbonate producing organisms. Lag-time is a common tool within numerical forward models (e.g. Grotzinger, 1986; Read *et al.*, 1986; Koerschner & Read, 1989; Elrick & Read, 1991; Osleger & Read, 1991; Drummond & Wilkinson, 1993a) to force a simulation to generate shoaling-upwards cycles; if relative sea-level rise has a head start on sedimentation, but sedimentation can outpace the rise once initiated, then a shoaling-upwards cycle will be created (e.g. Read *et al.*, 1986). While this may not necessarily be the correct approach, it is not sufficient to exclude a lag time or depth parameter from a forward model simply because the model in question creates 'natural' shoaling-upwards sequences (e.g. Paterson *et al.*, 2006). A forward model should attempt to faithfully recreate the systems it is attempting to simulate. A shoaling-upwards succession usually simply means that water-depth decreased over time, which could have a number of causes, with or without lag-depths.

Tipper (1997) argues that the lag between sea-level change and change in carbonate production occurs naturally when platforms are colonised by carbonate producing organisms. This is undoubtedly true and is a principle reason why an arbitrary lag time should not be used in forward models. Lag-depth, however, does not infer a period of time with which to associate rates of colonisation (e.g. Goldhammer *et al.*, 1987; 1990). Rather, it relates to a portion of the water column and the physics of sedimentation and hydraulic action operating in that interval. If no sedimentation takes place in this portion of the water column in reality, then it should be included in a numerical simulation. This process would not only occur during a transgression, but also during regression, and so may be more appropriately termed erosional scour, rather than lag-depth.

Furthermore, Tipper (1997) uses the theory of island biogeography (MacArthur & Wilson, 1967) to support his assertions that "setting values for special lag parameters can never show the true nature of the lag phenomenon: it can only hide it". However, even the

extreme rates of sea-level change seen during ice-house periods provide ample opportunity for the most remote isolated platform settings to be re-colonised according to island biogeography, before the lag-depth is exceeded. It should also be remembered that inner-platform carbonates never 'start from scratch'; facies belts are only moved during transgressions or regression. To use an example (with values from Paterson *et al.*, 2006) with moderate rates of sea-level change; 45m/My and 75% asymmetry, sea-level would rise 45cm every 250 years. If lag-depth prevented sedimentation within the top 1m of the water-column, organisms would therefore have to relocate 90cm shallower or deeper within 500y (or 0.18cm/y); a not unrealistic period of time according to biogeographical colonization theory (MacArthur & Wilson, 1967).

Tipper's decree that models of platform sedimentation do not need lag parameters and those that do "should be used with care" is wrong. Unfortunately, Tipper failed to take into account the problems in including a cellular automaton model in a one-dimensional world. Paramount among these is the fact that such a model would only contain one cell at any given point; an insufficient number to conduct a simulation of colonisation. Some models of carbonate accumulation do need to include a lag-depth (better defined as erosional scour), not to generate shoaling-upwards cyclicity, but to accurately reflect the processes thought to be occurring on carbonate platforms.

Erosional scour is not used as a proxy for time or for colonisation in TED. It is a reflection of the suppression of carbonate accumulation by hydraulic action (Osleger, 1991), and is representative of the lateral transport process detracting from sediment accumulation at very shallow water depths (e.g. long-shore drift). The existence of these processes, coupled with high wave-energy and little opportunity for cementation and lithification, lowers the preservation potential for sediment within this zone and necessitates representation in a the numerical forward model presented here. Rate of colonisation by euphotic organisms (e.g. algae) within this zone are likely to significantly outpace relative sea-level change.

3.3.3.8 Compaction

Compaction is a relatively unknown quantity in carbonate sedimentary systems and is not included as a parameter within the numerical model presented here. The effects of compaction are not well understood as preserved sedimentary sections in the subsurface and at outcrop are likely to represent best-case scenarios of minimum compaction. Therefore, there is significant difficulty in incorporating such an unknown factor into a numerical model. Any such incorporation would be founded upon limited data, and would introduce significant uncertainty into simulations. In addition to this,

algorithms for compaction are computationally slow, and would be of significant detriment to the versatility of the model in producing large numbers of simulations.

The degree to which differential compaction, in particular, effects diverse sedimentary facies is difficult to quantify. Disregarding this uncertainty for a moment, were differential compaction incorporated into the model, in one-dimension it could essentially be represented as a modifier on carbonate accumulation. For example, facies with less micrite content (i.e. those produced primarily from the oligophotic and aphotic curves) would presumably compact more than grain-dominated facies. Yet in this example, this could only be represented as a modifier to accumulation rates of highly-compacted facies which would have the effect of reducing thickness. As production rates are derived primarily from empirical evidence of sedimentary thickness, they effectively already include compaction. For these reasons, it was not felt necessary to include a separate compaction parameter as it would constitute a significant source of uncertainty. It is therefore prudent to consider the caveat that significant differential compaction may impact simulated lithofacies proportions.

3.3.4 Sub-aerial exposure

Exposure surfaces on carbonate strata are well known from late Palaeozoic sequences, envisaged to reflect sea-level falls caused by ice sheet growth (Horbury, 1989; Goldhammer *et al.*, 1991). This ice-house period is thought to have begun in the late-Mississippian (Smith & Read, 2000; Wright & Vanstone, 2001) and continued into the Permian, with many workers providing detailed description of the associated exposure features, for example in the Mississippian (e.g. Walkden, 1974; Somerville, 1979; Wright, 1982b; 1982a; Davies, 1991; Adams & Cossey, 2004; Haas, 2004). Wright (1994), in a review of palaeosol occurrence on carbonate platforms, argues that it is vital to realise that a range of exposure surface types can be generated depending on the prevailing climate. A four-component gradient is envisaged, ranging from humid to arid (Figure 3.10), with a critical consideration being the seasonality of the climate.

Within peritidal systems, many exposure surfaces have been described which exhibit evaporites or replaced evaporites, and are associated with sabkha development (Figure 3.10; A). This type of exposure produce a characteristic range of features, usually related to artesian groundwater and repeated wetting and drying of the sediment, such as tepees, vadose pisoids, brecciation and marine (typically aragonitic) cements (Wright, 1994). Modern analogues to these semi-arid to arid climates are also conducive to the precipitation of carbonates, sulphates and other salts from groundwaters as the result of evaporative conditions. Pedogenic calcrete profiles are rarely associated with such surfaces, reflecting the lack of sufficient moisture from the limited rainfall to mobilise

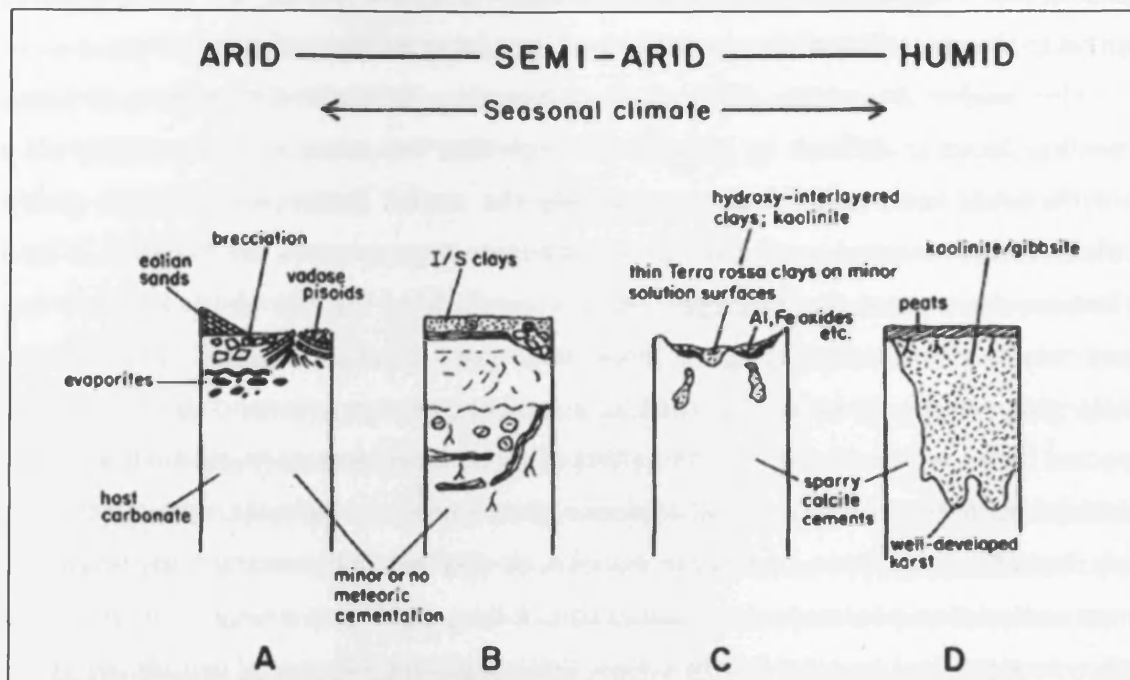


Figure 3.10: Effects of sub-aerial exposure on carbonate surfaces under different climatic regimes (from Wright, 1994). A) Exposure under arid conditions creates evaporite deposits, tepees, brecciation and vadose pisoids. Typically associated with supra-tidal vadose caps of peritidal cycles; soils with calcretes do not develop under such arid conditions. B) Calcrete profile, including illite-smectite clay horizons. Secondary vertic features and carbonate horizons may develop beneath the clay-rich horizons if wetting-drying cycles comprise a significant portion of time. C) A more humid, seasonal climate may generate Al-rich terra rossa soils on low-relief karstic surfaces. Under these conditions sparry calcite cementation occurs in the top of the sedimentary column. Thicker bauxitic deposits may accumulate in larger karstic depressions. D) Under a predominantly wet, humid climate (possibly monsoonal) extensive karstification occurs, along with the development of leached, organic-rich soils. In low relief platform settings extensive march carbonates may develop.

carbonates, and it is the evidence of peritidal conditions that prevails in the sedimentary record. TED does not aim to model this type of environment explicitly. Instead, it is considered that the features indicative of this type of facies are inherent in peritidal facies development, and are considered to be present along with this facies.

Under climates which promote seasonally wetter conditions (Figure 3.10; B), but are semi-arid overall, carbonate can be mobilised in the wet phases and fixed during drier periods to produce calcrete (Wright, 1994). The increased moisture in the soil is likely to support a more extensive vegetation cover, resulting in a range of biologically-influenced microfabrics (e.g. Košir, 2004). Dominant features under such climates are therefore likely to be biologically-influenced fabrics with mottled, massive, laminar and pisolitic features. TED models features produced under this type of climate through a combination of pedogenesis (to simulate the likelihood of soil-cover development) and diagenesis of the underlying bedrock (addressed in sections 3.3.4.2 and 3.3.4.3).

With increased precipitation carbonate will no longer accumulate in the soil zone and dissolution will dominate. Karstic surfaces commonly develop and, as a consequence of dissolution of aragonite and calcite, cementation takes place lower in the vadose or in the phreatic zones. The karst features which develop are typically small-scale karren, with small solution hollows or root pipes (Foos, 1991). Under these wetter conditions platform carbonates usually lack calcretes but show evidence of extensive dissolution. If the exposure period is sufficient, prominent lateritic or bauxitic horizons may develop, associated with extensively karsted surfaces (Wright, 1994). As pedogenesis is usually insignificant in terms of the quantity of sediment it generates under these conditions, TED does not use the pedogenesis function to model this climate-type. It does, however, invoke platform denudation to represent the dissolution of the platform through karstification.

In increasingly humid conditions, specifically climates which lack a significant dry season, a more extensive vegetation cover is likely to develop (Figure 3.10; D). This, in combination with more precipitation will result in more leached soils and more extensive karstification, which again is modelled using the denudation function (see section 3.3.4.1).

The climate under which palaeo-exposure surfaces developed has wider significance, as the climatic regime can control diagenesis and porosity evolution of the whole carbonate sequence. The knowledge of where, and which type, of exposure surface occurs potentially allows prediction of porosity distribution in cyclic carbonates. Climate change throughout the Mississippian and Pennsylvanian has been demonstrated by Vanstone (1993) and by Cecil (1990), who showed that the climate in North America during the latest Mississippian and Pennsylvanian fluctuated between semi-arid and humid. In general terms, humid phases are characterized by extensive dissolution and cementation of the carbonate whilst more arid phases are distinguished by less

dissolution and the formation of calcrete features such as rhizoliths. While the rates of such change may be open to debate (a factor which TED is able to investigate), it is essential to try and model these processes in simulations of stratigraphy.

In TED the four-component climate-dependent gradient can be represented by three distinct parameters; denudation of the platform by sub-aerial processes, pedogenesis and diagenesis of platform-top facies. The comparatively simple one-dimensional system means that diagenesis can be expressed by the straightforward function

$$d_{(t)} = e_{(t)} + p_{(t)} + a_{(t)}$$

3.7

where t is time, e is rate of platform denudation, p is rate of pedogenesis and a is rate of diagenesis of bedrock. Rates are in metres per million years. By using a combination of these parameters, the effects of each climate shown in Figure 3.10 can be simulated on an exposed platform.

3.3.4.1 Sub-aerial platform denudation

Carbonate platforms, under the correct conditions, are denuded by erosional processes over time. The evidence for this exists throughout the sedimentary record (Baars & Stevenson, 1981; Walkden & Davies, 1983; Hardie *et al.*, 1986; Davies, 1991; Budd *et al.*, 2002). Platform denudation has previously been incorporated into both one-dimensional and more sophisticated models (Bosence & Waltham, 1990; Quinn & Matthews, 1990; Goldhammer *et al.*, 1991; Paterson *et al.*, 2006), with varying degrees of success. Goldhammer *et al.*, for example, in their seminal examination of a sedimentary hierarchy in Pennsylvanian strata of the Paradox Basin, use a denudation rate, or 'caliche formation', of 10m/My (Goldhammer *et al.*, 1991; p401). However, this clearly contradicts information given in their Figure 25 (p403), which shows platform denudation of 35m from 170 to 390ky, giving a total rate of approximately 140m/My platform denudation. Disregarding this discrepancy in values, the minor cycles produced when the '5th-order' (*sensu* Goldhammer *et al.*, 1991) curve floods the platform top, should be denuded when the platform is subsequently exposed, even by the stated 10m/My (given their thin nature). They should therefore not be recorded in the strata. This does not happen in the model of Goldhammer *et al.*, and consequently a sedimentary hierarchy is able to be generated. It is therefore critical, that platform denudation parameters are implemented correctly.

The durations of time 'missed' at hiatal surfaces in ancient successions is not well known (Wright, 1994). Estimates from modelling studies indicate between 15% and 60%

of strata are preserved (Burgess & Wright, 2003). Modern exposure surfaces on carbonate platforms experience relatively rapid rates of denudation in conducive climates (James & Choquette, 1988). Rates of denudation have received attention from various workers (cf. Trudgill, 1985; Bosence & Waltham, 1990; Paulay & McEdward, 1990; Goldhammer *et al.*, 1991; Paterson *et al.*, 2006). Rates for platform denudation are, however, dependent on climate, are therefore poorly constrained and investigations necessarily span a wide range of variables (e.g. Paterson *et al.*, 2006).

3.3.4.2 *Sub-aerial pedogenesis*

In any studies of cyclic carbonates it is necessary to carefully evaluate the relative degree of pedogenesis as an aid in defining major boundaries and for detecting trends. Series of soils which differ from one another because of their relative durations of formation are referred to as chronosequences (Birkeland, 1984). They not only indicate the occurrence of sequence boundaries related to sea-level falls but their accurate interpretation is essential if the time significance of boundaries is to be determined. In theory, distinguishing between low- and intermediate- or high-order sequence boundaries should depend as much on the identification of major exposure intervals as on the styles of sedimentation (Tucker, 1993). However, this is often not the case in practice (e.g. Vanstone, 1998).

Rates of pedogenesis are dependent upon climate. Considering this, TED employs user-defined linear rates of pedogenesis as accumulation on the platform surface while exposed, in order to simulate different climates (see Figure 3.10).

3.3.4.3 *Sub-aerial diagenesis*

The effects of diagenesis cannot be accurately modelled within a one-dimensional environment, as diagenesis invariably has complex three-dimensional controls, usually related to fluid flow (e.g. Patterson & Walter, 1994). However, diagenesis has shown to be important, particularly with regard to vertical partitioning of reservoir-prone facies within sequences (Kenter *et al.*, 2007).

Diagenesis can, however, be simulated in terms of residence time. If it is accepted that in one-dimensional terms, a zone of diagenesis at a given point in space is represented by a depth-range beneath the platform surface (regardless of the three-dimensional configuration of the zone; e.g. Gischler, 2002), it becomes very easy to emulate diagenesis. This cannot be done in terms of assessing the effects diagenesis will have on a given lithofacies, but it is enough to determine the period of time a portion of rock spends in a zone of diagenesis (a vadose, phreatic or mixing zone for example).



TED models diagenesis in terms of diagenetic penetration below the platform top, according to a user-defined linear rate. This 'diagenetic-front' is lowered with respect to the sediment column over time; therefore the longer the period of sub-aerial exposure, the deeper the diagenetic-front will penetrate into the lithology from the sub-aerial exposure surface. As with the rates of platform denudation, this function can be used in isolation or with combinations of the other parameters to simulate climatic conditions shown in Figure 3.10.

3.3.5 Accommodation

3.3.5.1 Subsidence

Subsidence has been shown to be the fundamental creator of accommodation in carbonate HfS development (Burgess, 2001). As such, it typically forms a major variable in simulations conducted in this study; usually with rates comparable to passive margins and foreland basins (10-160m/My; Allen & Allen, 2005).

Subsidence can be modelled either as a user-defined constant rate applied uniformly throughout a simulation, or as pulses of subsidence, greater than or less than an average, for a certain duration. The majority of numerical forward models employ a fixed rate of subsidence (e.g. Bosence & Waltham, 1990; Walkden & Walkden, 1990; Burgess *et al.*, 2001; Paterson *et al.*, 2006), with very few employing differential subsidence (e.g. Goldhammer *et al.*, 1987; Goldhammer *et al.*, 1991). For models attempting to simulate ice-house environments, subsidence ostensibly changes on a scale deemed to be greater than changes of accommodation due to glacio-eustatic oscillations. Differential subsidence is therefore usually not considered as a major control on high-frequency sequence development in these simulations (e.g. Goldhammer *et al.*, 1991).

While this is likely to hold true for relatively quiescent settings (Guidish *et al.*, 1984; Bosence & Waltham, 1990), in tectonically active settings pulsed subsidence may operate in the 10ky- to 100ky-scale commonly attributed to Milankovitch-band allocyclic forcing of sea level (Cisne, 1986; Hardie *et al.*, 1991; de Benedictis *et al.*, 2007; refer to section 2.2.2). Given this, a function to simulate pulsed-subsidence was included in TED. At user-defined points during a simulation subsidence rate can be increased or decreased for a specific time, or periodically throughout a simulation. The application of pulsed subsidence in simulations should be used with care, however. Given the assumed periodicity of ice-house eustatic fluctuations (e.g. de Boer & Smith, 1994), the use of largely arbitrary-timings of pulsed subsidence, as a result of poorly constrained data, could produce unrealistic results.

3.3.5.2 *Symmetric sea-level oscillations*

Early one-dimensional models of carbonate accumulation employed symmetric sinusoidal sea-level oscillations (Walkden & Walkden, 1990; Allen & Allen, 2005). The current consensus is that an asymmetric curve should be used to reflect the asymmetric build-up and melting of ice sheets (Clark *et al.*, 1999). Low-order eustatic sea-level may not necessarily be forced by glaciations; an alternative is forcing on a My-scale caused by tectonism (Kendall & Lerche, 1988; de Boer & Smith, 1994; Barnett *et al.*, 2002; Artyushkov *et al.*, 2003). If this is the case then an asymmetric sea-level curve is not necessary, and a symmetric sea-level curve should be used.

In addition, during greenhouse periods, global climate prohibited large volumes of water being stored as continental ice (Wright, 1992). During these periods, minor changes in insolation, envisaged to force ice-formation or melting, would not have a significant effect on the quantity of water stored as continental ice, and therefore would not dictate sea-level. Relative sea-level oscillations during these periods may be best simulated using symmetric sinusoids (e.g. Warrlich *et al.*, 2002).

For these reasons, the same functions that are used to model asymmetric sea-level variations retain the ability to simulate symmetric sea-level oscillations.

3.3.5.3 *Asymmetric sea-level oscillations*

Eustatic fluctuations in sea-level are envisaged to occur by many authors as a result of a 'hierarchy' of forcing (e.g. Goldhammer *et al.*, 1991), and based on temporal durations of eustatic 'cycles' (Vail *et al.*, 1977). Proponents of allocyclic control of cyclic sequences have based their arguments primarily on the assumption that the periodicity of individual cycles (as calculated from numbers of cycles and sequence duration) commonly falls within the same range as that of Milankovitch-band parameters (20-400ka; Berger, 1978). There are well documented problems with this, and other, inferences made by some workers, which are discussed in sections 2.1.2 and 2.5.

Despite these problems, advocates of a glacio-eustatic control are uncritical in application of simplistic Milankovitch models to complex sedimentary systems (e.g. Paterson *et al.*, 2006). In general it is envisaged that allocyclic control operated within the Milankovitch-band, with intermediate-order oscillations having an amplitude of 45-75m (Crowley & Baum, 1991; although amplitudes of up to 95m have been suggested; Heckel, 1986; Wright & Vanstone, 2001). High-order oscillations are typically envisaged to have a slightly smaller amplitude of up to 35m (e.g. Paterson *et al.*, 2006).

With TED, allocyclic eustatic fluctuations forced by glacial build-up and melting are modelled using an asymmetrically-modified sinusoidal oscillation (Emery, 2006, pers. comm. 05-05-2006), according to the function

$$f(x) = \begin{cases} \sin\left(\frac{\pi x}{\alpha}\right) & \text{for } -\alpha/2 < x < \alpha/2 \text{ and} \\ \sin\left(\frac{\pi}{2} + \frac{\pi}{\beta} \cdot \left(x - \alpha/2\right)\right) = \cos\left(\frac{\pi}{\beta} \cdot \left(x - \alpha/2\right)\right) & \text{for } \alpha/2 < x \leq \alpha/2 + \beta \end{cases}$$

3.8

where α is the relative proportion of the period represented by the positive gradient limb, and β is the relative proportion of the period represented by the negative gradient limb. Outside this range $f(x)$ is defined to be periodic with period $\alpha + \beta$. Since this function is odd (i.e. $f(-x) = -f(x)$) its Fourier series consists of sines, therefore

$$f(x) = \sum b_n \cdot \sin\left(\frac{2\pi n x}{\alpha + \beta}\right)$$

3.9

where

$$b_n = \left(\frac{2}{\pi}\right) \cdot \left\{ \frac{1}{1 + \frac{\beta}{\alpha} - 2n} - \frac{1}{1 + \frac{\beta}{\alpha} + 2n} + \frac{1}{1 + \frac{\alpha}{\beta} + 2n} - \frac{1}{1 + \frac{\alpha}{\beta} - 2n} \right\} \cdot \cos\left(\frac{\pi n}{1 + \frac{\beta}{\alpha}}\right)$$

3.10

3.4 OUTPUT FROM TED

TED outputs data in several forms, all intended to facilitate the quantitative analysis of accumulations of carbonate sediment and the stacking patterns which they may form.

3.4.1 Visualisation

TED provides four main ways to visualise data in addition to the other plotting methods, HfS analysis and statistical analysis. The first three methods (integrated plots, simulated stratigraphic sections and chronostratigraphic plots) provide the user with a visual representation of the style of cyclicity but are not used for every model as they significantly decrease program performance (by a factor of 10; caused by the inability of Microsoft Excel to construct charts from very long arrays). They are therefore used to qualitatively compare sedimentary sections, very much in the same way as looking at actual sedimentary logs. The visual plots are qualitative representations of the same data that is used in each run as part of the quantitative numerical and statistical analyses.

The integrated plot (Figure 3.11) is a plot of time against amplitude, with superimposed eustatic and relative sea-level, thickness of carbonate strata (i.e. the platform surface in one-dimension) and grain-type (lithofacies). TED also outputs a plot of time against magnitude of sedimentation and sea-level change; essentially a chronostratigraphic diagram (Figure 3.12). This is a particularly useful tool for visually identifying short-term 'cycles' and periods of sedimentation, which do not appear physically separate from adjacent periods of sedimentation in the stratigraphic column.

Perhaps the most useful plot for qualitative visualisation is the simulated stratigraphic column (Figure 3.13). This provides an analogue to real-world lithologies and is useful in determining the 'style' of cyclicity, which may not be evident from the numerical output.

The final method involves plotting all the variables in a given run-plan against each other, allowing analysis of a variable against its parameters (parameter-space plotting; Figure 3.14). This technique involves using a sufficiently large dataset to study a range of parameters in depth (typically more than 1000 runs are required), which would take an unfeasibly long period of time with more complex models (in excess of 20,000hrs with rates published for CARB3D+; Paterson *et al.*, 2006). TED lends itself well to this kind of

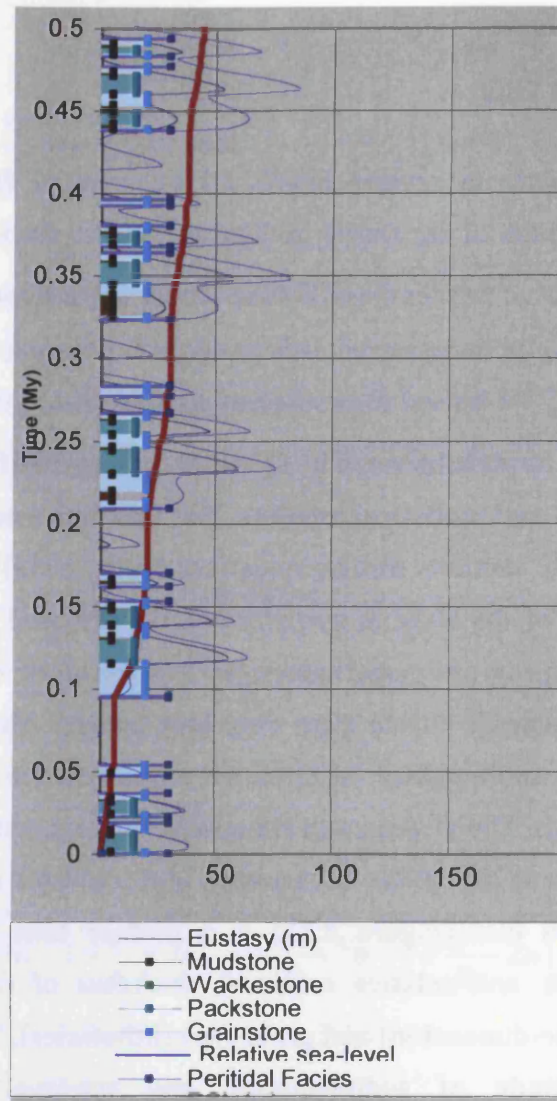


Figure 3.11: Example of an 'integrated' diagram from TED. The x-axis is plotted as amplitude (metres; only positive amplitudes shown). Facies are assigned an arbitrary metre value to plot on the graph like a sedimentary column, although, as the y-axis represents time, they are positioned according to when they were deposited; as such this is a chronostratigraphic diagram.

The brown line represents the top of the sediment surface (a carbonate accumulation represented in one-dimension). When relative sea-level is greater than the top sediment surface (i.e. passes the brown line to the right) sedimentation is occurring in the simulation, and a lithofacies is also plotted on the diagram.

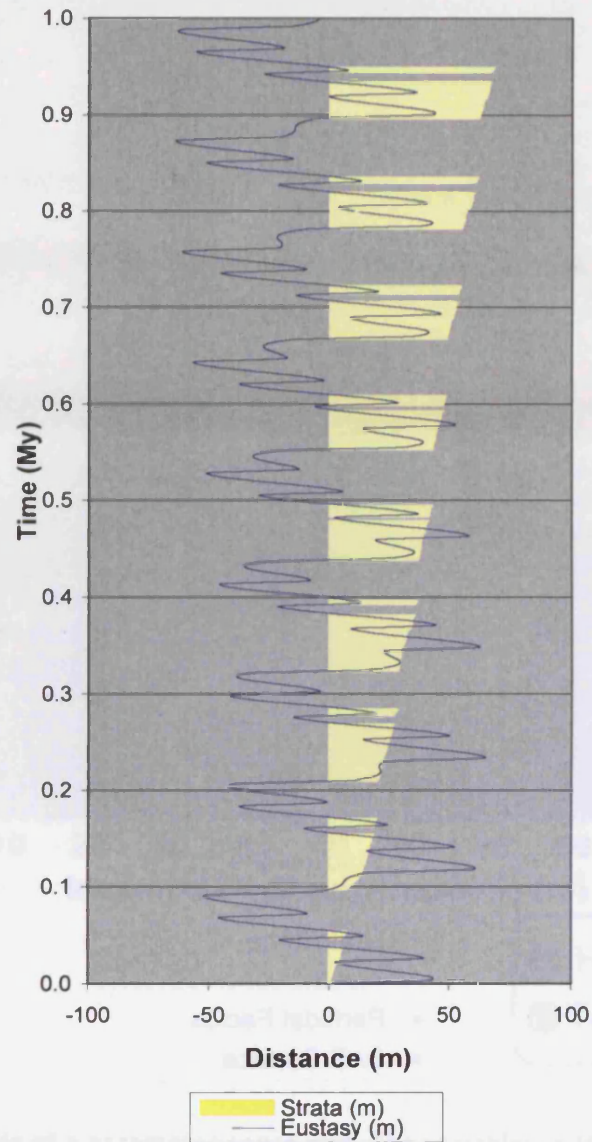


Figure 3.12: Example of a chronostratigraphic diagram from TED. The solid blue line represents eustatic sea-level in metres. The cream-coloured bars represent periods during which sediment is deposited. The amount of sediment deposited is represented by the degree to which the cream-coloured bars extend to the right. This type of plot is useful to constrain during which sea-level oscillations sedimentation occurs.

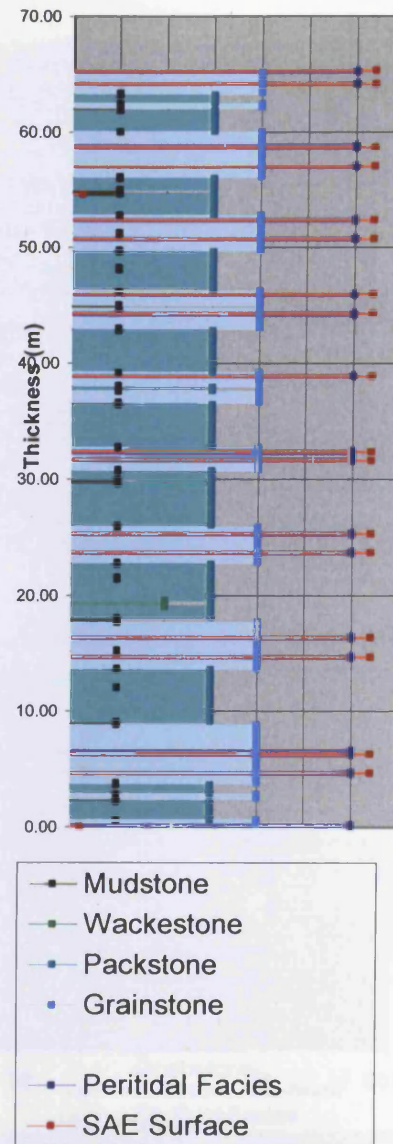


Figure 3.13: Example of a simulated stratigraphic column from TED. Not all keyed lithofacies are displayed in the column.

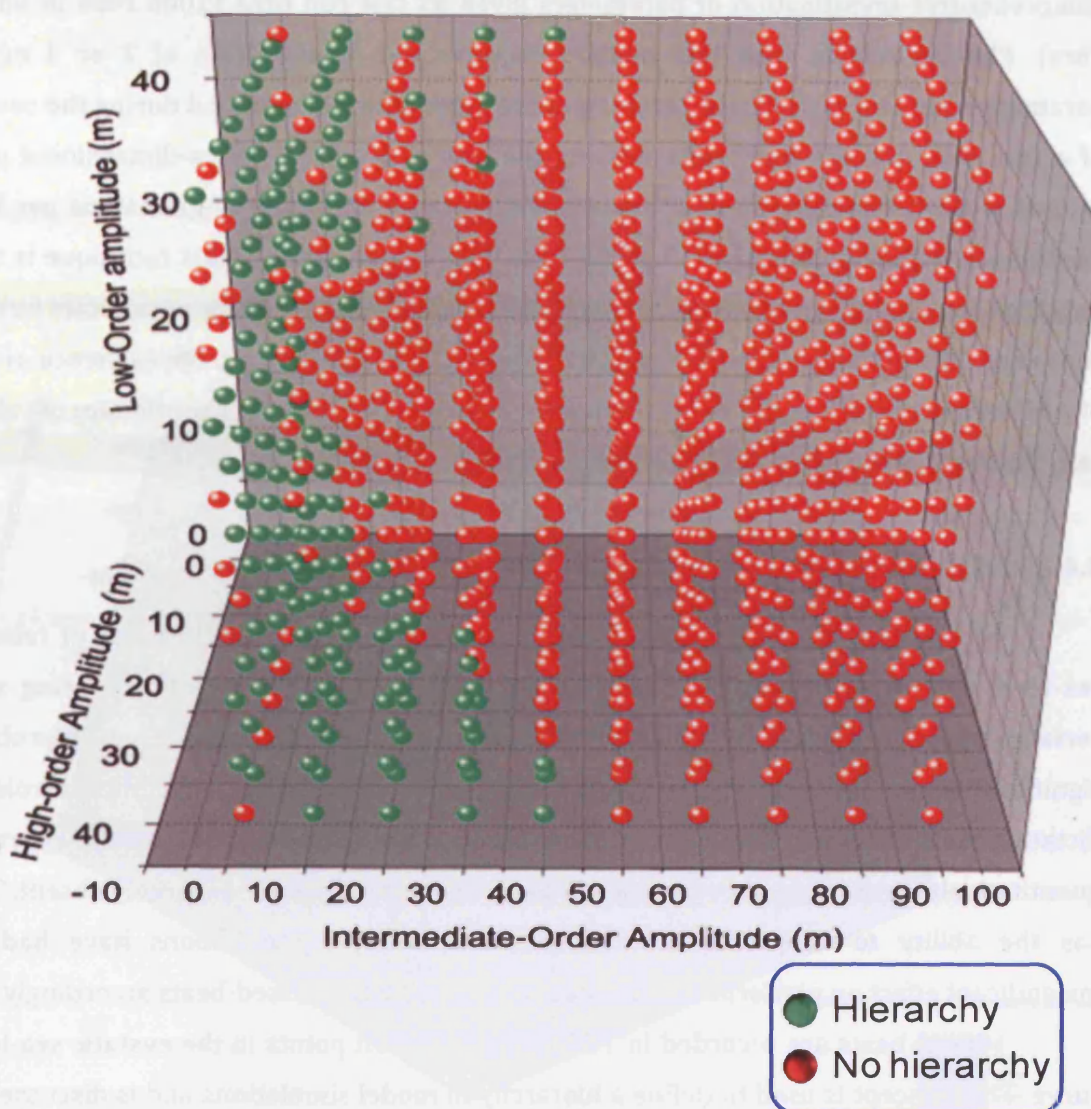


Figure 3.14: Example of a parameter-space plot. The variables in this run-plan were the three eustatic parameters; low-, intermediate- and high-order amplitudes of oscillation. These are plotted along the axis of a three-dimensional plot. 1000 runs are plotted. The criterion being evaluated is the existence of a hierarchy in each run. In this case the plot compares runs which show a sedimentary hierarchy in terms of cycle thickness and those which do not. (The definition of a sedimentary hierarchy is discussed further in Chapter 4.) Individual two-dimensional slices can be taken at any point through the plot.

comprehensive investigation of parameters given its fast run time (1000 runs in under 7hrs). Plotting results with this method requires the identification of 2 or 3 major parameters per run plan. These parameters are systematically modified during the course of a run plan, and are then plotted along the axis of a two- or three-dimensional plot, against which a variable can be compared (for instance, thickness of grainstone per Hfs; examples are given in Figure 3.15 and Figure 3.16). A condition of this technique is that only 2 or 3 variables can be investigated per set of runs; more variables necessitate further run-plans. The variable under investigation can either be bipolar (e.g. the existence or not of a hierarchy of stacked cycles in a given run; Figure 3.14) or form a continuum of values (e.g. the average thickness of grainstones per run; Figure 3.15).

3.4.2 Missed-beats

'Missed-beats' (*sensu* Goldhammer et al., 1987) refers to oscillations of relative sea-level not recorded as platform top sedimentation due to the platform being sub-aerially exposed, or submerged beneath a significant volume of water such as to prohibit significant sedimentation. To date, while acknowledged to play a significant role in dictating the style of platform top sedimentation (e.g. Goldhammer *et al.*, 1991), efforts to quantitatively assess the degree to which missed-beats occur have been largely absent. TED has the ability to objectively determine which sea-level oscillations have had an insignificant effect on platform top sedimentation and assign missed-beats accordingly.

Missed-beats are recorded in TED using inflection points in the eustatic sea-level curve. This concept is used to define a hierarchy in model simulations and is discussed in detail in section 4.2.2. Missed-beats in the context of a sedimentary hierarchy are also discussed in Chapter 4. In identifying missed-beats inflection points are used to determine portions of time attributable to a given eustatic order of forcing. Once this period of time is known, TED checks if sedimentation (in terms of facies type) has been altered by a relative shallowing or deepening. If no change has occurred then a missed-beat is assigned. In this manner, for each run, the number of intermediate-order and high-order beats that are missed can be found. The model further subdivides the missed-beats into those missed above the platform surface, and those missed below. Theoretically, generating a missed-beat above the platform surface is much more difficult than generating one below; during submergence the platform is nearly always accumulating sediment, so the missed-beat must usually occur in sufficiently deep water not to alter the proportion of oligophotic production.

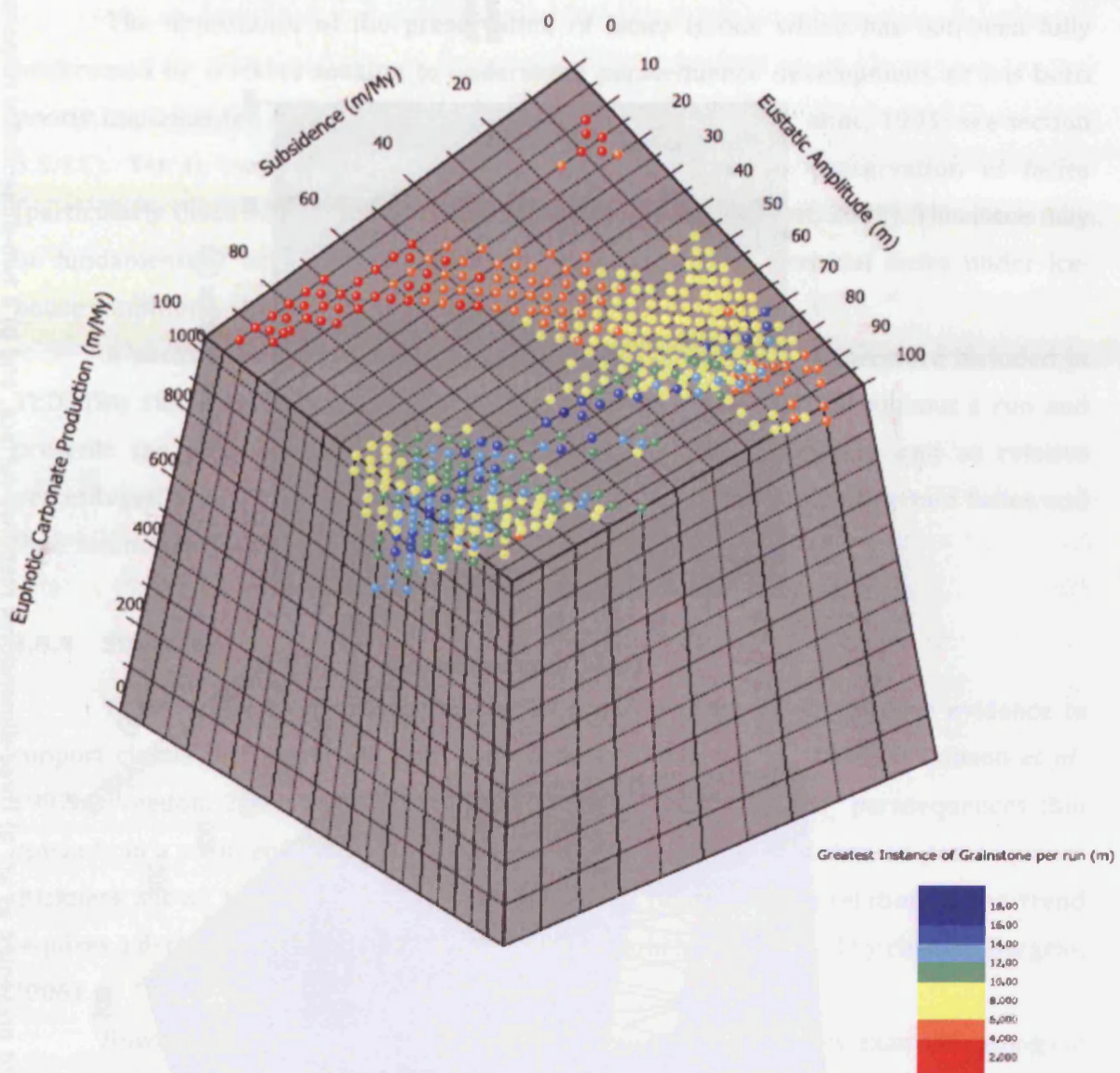


Figure 3.15: Example of a parameter-space plot plotting eustatic amplitude against carbonate production and subsidence. The criterion under investigation is the thickest instance of grainstone facies per run. Two-dimensional slices can be made through the plot.

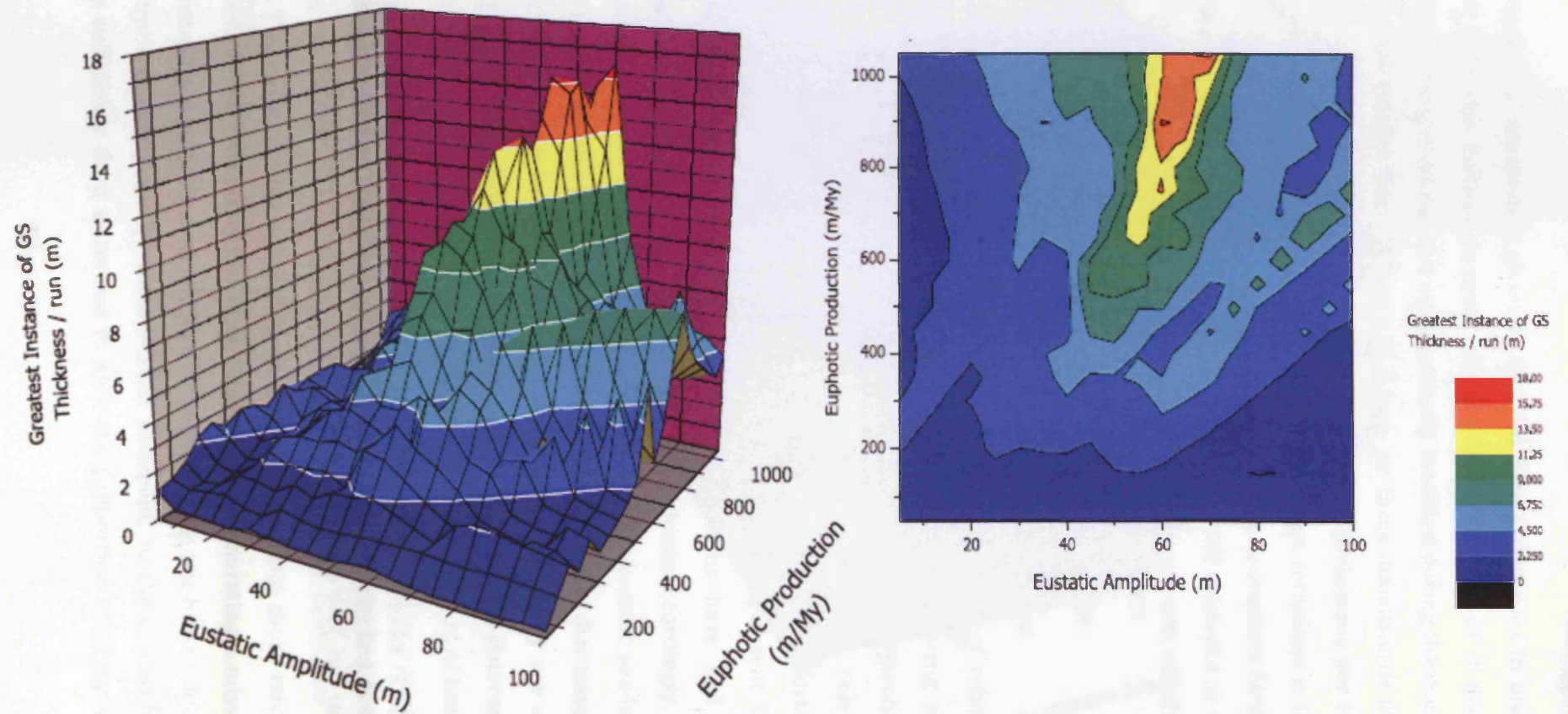


Figure 3.16: Example parameter-space plot presented as an: a) three-dimensional response-surface, and b) a two-dimensional response-surface. GS = grainstone.

3.4.3 Facies taphonomy

The importance of the preservation of facies is one which has not been fully understood by workers seeking to understand parasequence development, or has been poorly implemented in numerical forward models (Goldhammer *et al.*, 1991; see section 3.3.4.1). Yet it may hold critical importance for the likely preservation of facies (particularly those occurring at the tops of parasequences; Barnett, 2002). This issue may be fundamentally important when assessing the absence of peritidal facies under ice-house conditions, a concept addressed in section 7.4.2.

A package to analyse the taphonomy of individual facies is therefore included in TED. This suite records the thickness of each facies in a HfS and throughout a run and presents the data both per HfS and per run, in actual thicknesses and as relative percentages. This allows a quantitative assessment on the controls of certain facies and their relative quantities in HfSs.

3.4.4 Statistics

There exists an increasing burden of proof in terms of quantitative evidence to support claims that strata are inherently ordered (Sadler *et al.*, 1993; Wilkinson *et al.*, 1997b; Weedon, 2003; Burgess, 2006). Qualitative claims such as “parasequences thin upwards in a sedimentary succession” can only be substantiated if data on parasequence thickness shows a definable thinning trend, and a realistic interpretation of the trend requires a determination of the probability that it could have occurred by chance (Burgess, 2006).

However, a major problem when attempting to quantitatively examine geological problems stems from the nature of the data geologists are forced to deal with. For example, when considering a stratigraphic sequence of lithologies a geologist may be interested in the significance of the succession, but lacks a meaningful scale to apply to the sequence. The lithologies represent deposition of sediment over time, but estimates of time are rarely accurate enough to be applied confidently. Thickness is used in the absence of time, but thickness of components of the sequence can vary geographically, even if the sequence itself does not. If considering thickness, the fact that the third bed in the succession is the same as the sixth, for example, has no significance that can be expressed numerically; the sixth position is not ‘twice’ the third position. Similarly, the lithologic states of the units cannot be expressed numerically beyond arbitrarily assigning them a number (e.g. 1-2-3-4-1-2-3-4). This poses particular problems when trying to quantitatively assess sections of the stratigraphic record.

Forward-modelling offers a method of working around this problem as models are not constrained by limited data like real-world scenarios; every variable and value is known in a model-world. One-dimensional forward models lend themselves to statistical analysis well, as they essentially comprise a linear continuum (or series) of data-points. The data itself is characterised by its position along the line and this facilitates analysis of the data in a quantitative manner. Furthermore, techniques can be applied according to the nature of the measured variables (nominal or interval data).

The importance of quantifying statements cannot be underestimated. Qualitative methods can be so abstruse as to provide little insight into an issue, and can even serve to cloud understanding of it. For example - consider the quantitative discussion of a sedimentary hierarchy provided by Goldhammer *et al.* (1990) and the contradictory qualitative method provided by Anderson (2004). Such methods often provide little evidence beyond the ideas of the author to support the subjective claims made (e.g. Anderson, 2004). The salient problem of the qualitative approach adopted by Anderson (2004) is inadvertently highlighted in the conclusions of that work: that the "interpretation of the cyclic structure of [a sedimentary section] is strongly influenced by models adopted by the observer." This may be avoided if quantitative techniques are applied without prejudice.

The statistical methods described in this section aim to quantify the output from the forward model in ways which are difficult or inappropriate for 'real-world' scenarios. They can provide answers to the following broad questions (Davis & Herzfeld, 1993): Are the observations random, or do they contain evidence of a trend or pattern? If a trend exists, what is its form? Can cycles or repetitions be detected and measured? Can predictions or estimations be made from the data? Can variables be related or their effectiveness measured? These questions are particularly valuable in order to assess the style of sedimentation in platform carbonates, and the controls on this sedimentation.

3.4.4.1 Embedded Markov chain analysis

In mathematical terms, a Markov chain is a series of states of a system that can be said to have the Markov property. The Markov property itself can be said to be present in a system if the conditional probability distribution of future states of the process, given the present states and all future states, depends only on the present state and not on any past states (i.e. it is memoryless, or conditionally independent of past states given the present state). Essentially, a Markov chain is a sequence of random values whose probabilities at a given time interval depend upon the value of the number at the previous time. In a geological context, this means a sequence of data that consist of ordered or disordered successions of mutually exclusive states.

Markov chains rely on analysis of the transitions from one facies to another within a given sequence. The underpinning null-hypothesis of Markov chain analysis is that a given state is completely independent of the immediately previous state. A sequence having the Markov property is intermediate between deterministic sequences and completely random sequences (Davis, 2002). It is possible for a system to exhibit different Markov properties; first-order Markov properties, for example, are present if a statistical dependency exists between the current state and the immediately preceding state; second-order Markov properties exhibit a significant conditional relationship between points that are two steps apart.

Embedded Markov chains are sequences in which transitions from a state to itself are prohibited. Either Markov chains or embedded Markov chains are appropriate for use in analysis of sedimentary successions; however embedded Markov chains are more suitable for examining carbonate shoaling-upwards sequences. Although in a sedimentary succession a state is not prohibited from following itself (for example, a sharp-based channel sandstone can be overlain by another sharp-based channel sandstone, comprising one facies but two beds), states are excluded from following themselves within embedded Markov chains. This stems from the fact that a Markov chain is measured using nominal data – only the condition of the state being measured is recorded at a given point. In other words, the Markov chain does not remember how a state arrived at its current condition, only that it is what it is. In the sandstone-sandstone example, although separated by a bedding plane, a Markov chain would recognise no transition and class the two beds as one state.

Disregarding thickness and only taking into account instances where a transition is made makes embedded Markov chains, as opposed to non-embedded Markov chains, attractive to investigate thick sequences of strata, and it has been employed to good effect in quantitatively assessing the orderedness of Carboniferous carbonate platform successions in the south-western U.S. by Lehrmann & Goldhammer (1999). Due to the suitability of this technique in any investigation of ordering, and to make our analysis comparable with previous studies, embedded Markov chain analysis is used in this study to provide a quantitative measure of the degree of ordering in simulated sections.

Embedded Markov chains provide us with the ability to examine, in terms of facies (the building blocks of shoaling-upwards cycles), the nature of carbonate successions, and to make statements based on statistical evidence rather than qualitative assertions, as to their basis and form. Davis (2002) documented how embedded Markov chains can be applied to geological problems, however, to understand the results of this statistical method it is necessary to discuss how the mathematics of the approach is implemented within the forward model.

The iterative method for embedded Markov chain analysis lends itself well to conversion for use in TED (Figure 3.17). The first step in the process is to analyse every transition from one state (facies) in the simulation to another. This gives the observed frequency transitions for a simulation, which can be compiled into a transition frequency matrix (Figure 3.18; a). The benefit of compiling this information into a matrix lies in the model being able to easily manipulate the data in multi-dimensional arrays (which themselves can be thought of as multiple matrices), conferring a significant performance increase (discussed in section 3.2.1). Even in the deterministic model environment, the matrix tends to be asymmetric (as a need not necessarily follow b , even if b followed a), and in general $a_{i,j} \neq a_{j,i}$ (Davis, 2002).

The tendency for one state to succeed another can be emphasised in the matrix by converting the frequencies to decimal fractions. Probabilistically, these are estimates of the conditional probability, $p(j|i)$, or the probability that state j will be the next to occur, given that the present state is i (Figure 3.18; Figure 3.39; b).

The χ^2 test used to analyse embedded Markov chains relies on comparing these observed frequencies of transitions with *expected* transitions using a marginal probability vector (the relative proportion of each state in the system, or, in a geological context, each lithology in the section). This is derived from the observed frequency transition matrix, but requires observations from one state to itself – a situation that can occur in standard Markov chains, but is not permitted in embedded Markov chains. Instead, the frequencies of transitions from a state to itself are estimated. The diagonal elements of the observed transition frequency matrix can be considered to be a censored sample from an ordinary succession in which transitions from a state to itself can occur (Norris, 1997). It would therefore be expected that the diagonal elements (representing transitions from a state to itself; see Figure 3.18) would be values other than zero. If a transition probability matrix were to be computed from this example observed frequency transition matrix and raised to an appropriately high power, it would estimate the transition probability matrix of a sequence in which successive states were independent. The assumed diagonals could then be removed and the other non-diagonal probabilities recalculated leaving the expected transition probability matrix for an embedded sequence whose states are independent.

A numerical forward model deals with this process extremely efficiently. The process is effectively trial and error by searching for inserted diagonal values that do not

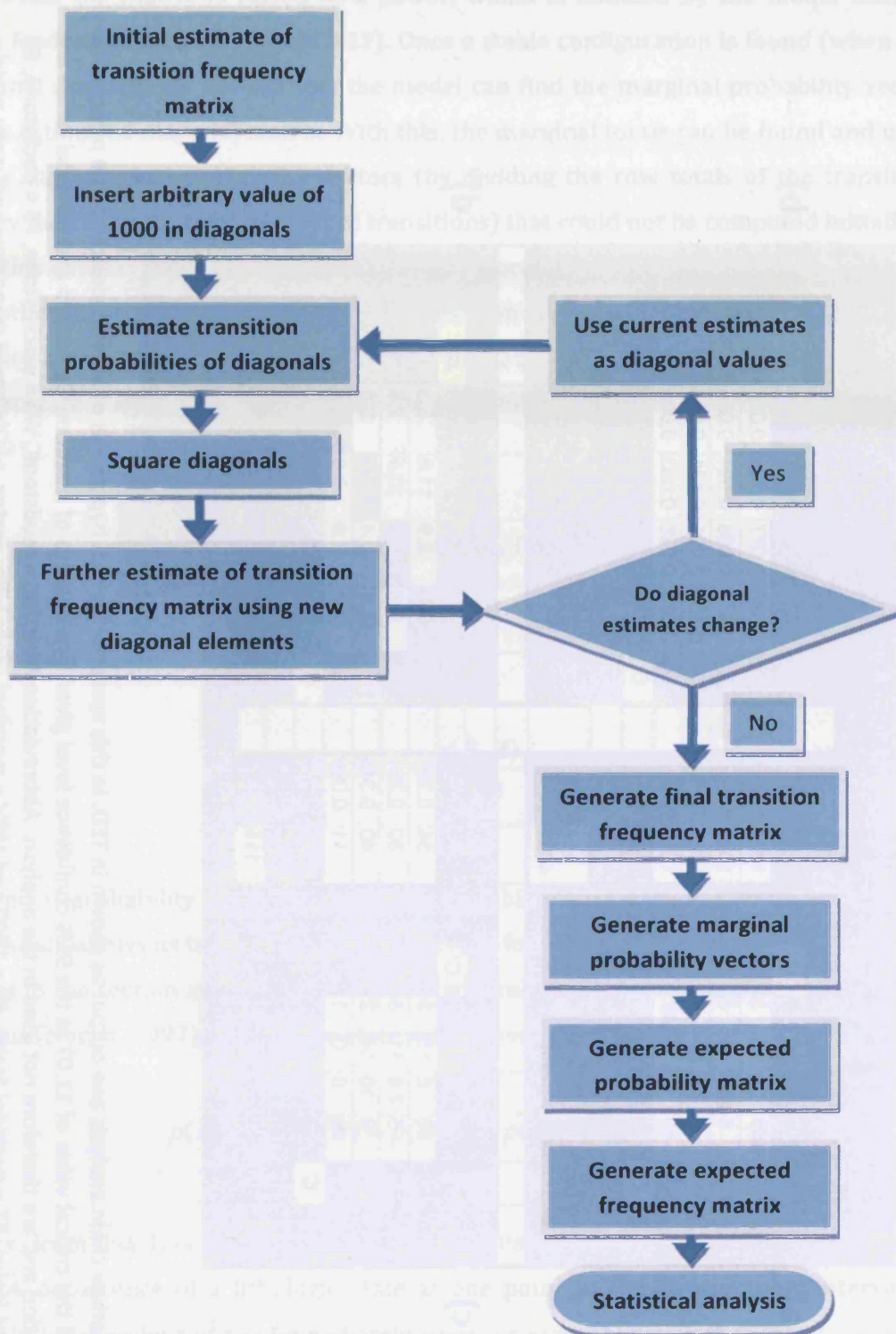


Figure 3.17: Process for embedded Markov chain analysis in TED. The decision-loop for estimation of diagonal elements represents the bulk of computational time, commonly taking 5-20 iterations. The fixed probability vector is found, by summing each row and dividing by the total number of transitions, and is then used to estimate diagonal transition probabilities. These are powered by squaring and multiplied by the grand total to obtain new diagonal frequency transition estimates, which can be used in the process again if the diagonals are found not to be stable. (Process modified from Davis, 2002).

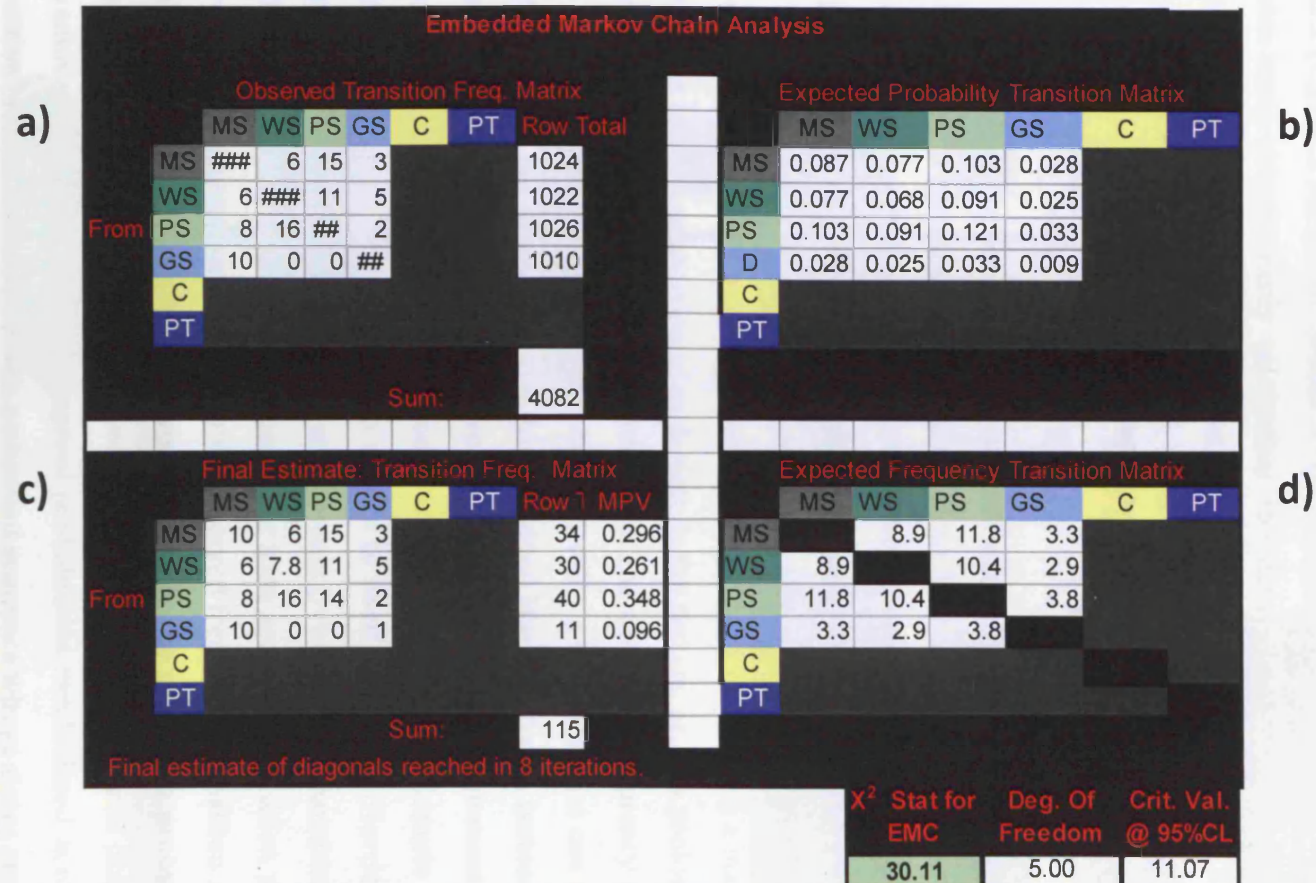


Figure 3.18: Embedded Markov chain analysis and output as shown in TED. In this scenario the null hypothesis of independence can be rejected as the χ^2 test statistic exceeded the critical value of 11.07 at the 95% confidence level given five degrees of freedom. Cemented and peritidal facies are not invoked in this simulation and are therefore not used in the analysis. Abbreviations are: MS = mudstone, WS = wackestone, PS = packstone, GS = grainstone, C = cemented facies, PT = peritidal facies, ## = 1000 and MPV = marginal probability vector. a) Observed transition frequency matrix. The matrix is read from rows to columns. For example, there are 6 transitions from mudstone to wackestone, 15 from mudstone to packstone, and 3 from mudstone to grainstone. The transition frequency matrix is a concise way of expressing the incidence of one state following another. b) Expected probability transition matrix. The probability that a given facies will be succeeded by another, including itself (using derived diagonals from the arbitrary starting point of 1000; see Figure 3.38 for explanation). c) The final estimate of the transition frequency matrix using calculated diagonals (note original observed transitions do not change). d) The expected frequency transition matrix if the succession was indistinguishable from random; this is compared against c) in the χ^2 or Fisher's exact test.

change when the matrix is raised to a power, which is handled by the model using a negative feedback approach (Figure 3.17). Once a stable configuration is found (when the off-diagonal elements do not change) the model can find the marginal probability vector from this estimated-diagonal matrix. With this, the marginal totals can be found and used to derive the marginal probability vectors (by dividing the row totals of the transition frequency matrix by the total number of transitions) that could not be computed initially.

This enables the calculation of the expected probabilities and expected frequencies of a hypothetical sequence of independent states from the marginal probability vector. The probability of two joint events A and B , is the probability that state B will follow state A given that state A and B occur, divided by the probability that state A occurs. (Grinstead & Snell, 1997). This can be expressed as

$$p(A, B) = p(B|A)p(A)$$

3.11

or, rearranged,

$$p(B|A) = \frac{p(B, A)}{p(A)}$$

3.12

The marginal probability vectors give us the probability that state B would occur in the section, which allows us to determine if it is likely to follow state A . If the occurrences of all the states in the section are independent, the same relationship holds true for all possible transitions (Norris, 1997), so in a four-state world as in Figure 3.18:

$$p(B|A) = p(B|B) = p(B|C) = p(B|D) = p(B)$$

3.13

Therefore, from this, it is possible to predict the transition probability matrix of a section where the occurrence of a lithologic state at one point in the stratigraphic interval is completely independent of the immediately previous state. Through the use of a χ^2 test, the expected frequency transition matrix can be compared to the transition probability matrix to test the null hypothesis; that all states are independent of immediately previous states. Expected frequencies of transitions can be found by multiplying each element of the expected transition probability matrix by the total number of transitions (Figure 3.18). The χ^2 test can be expressed as

$$\chi^2 = \sum \frac{(O - E)^2}{E}$$

3.14

where O is the observed number of transitions from one state to another and E is the expected number of transitions from one state to another if the states are independent. The test has $(m - 1)^2$ degrees of freedom, where m is the number of states (method from Davis, 2002). The test is conducted for each element in the matrix. If the χ^2 value exceeds the critical value provided by the degrees of freedom, then we can conclude that the null hypothesis of independence of successive states is not correct, and there is a statistically significant relationship between states.

In most situations the χ^2 test works well, however there are cases where this method of analysis is not appropriate. Specifically, these cases encompass situations where there may exist a scarcity of data or data is particularly skewed (favouring transitions from wackestone to grainstone above all others, for example). This contingency problem is created if there aren't enough observations to reliably estimate the expected frequency transitions. Essentially this means that if any of the elements of the expected frequency transition matrix have a value less than five, only a conservative test of independence may be made, as analysis of data by χ^2 test may produce unreliable values (Davis, 2002).

This problem is apparent in work presented in Lehrmann & Goldhammer (1999). Lehrmann & Goldhammer (1999) present an illustration of Markov chain analysis using an example sedimentary section from the Silurian Barn Hills Formation, Utah (their Figure 13, presented here as Figure 3.19). This example shows the expected frequency transition matrix for this section, where, of 100 possible transitions, only 6 elements show an expected frequency above the critical value of five. This introduces significant uncertainty into the result of the χ^2 test Lehrmann & Goldhammer (1999) performed on this Markov chain analysis. The result, in this example, yielded a χ^2 statistic of 126.6 which proved non-randomness by exceeding the critical value at the 95% confidence interval of 91.67. The contingency problem means that, in this case, the result could be called into question, given the small difference between the two values. The solution to this contingency problem would be to run a longer run, thereby obtaining more observed transitions and increasing the values in the expected frequency transition matrix. This is not possible when dealing with stratigraphic sections, and an alternative is to group the categories (in this case facies) into bins of larger size, decreasing the ratio of bins to transitions.

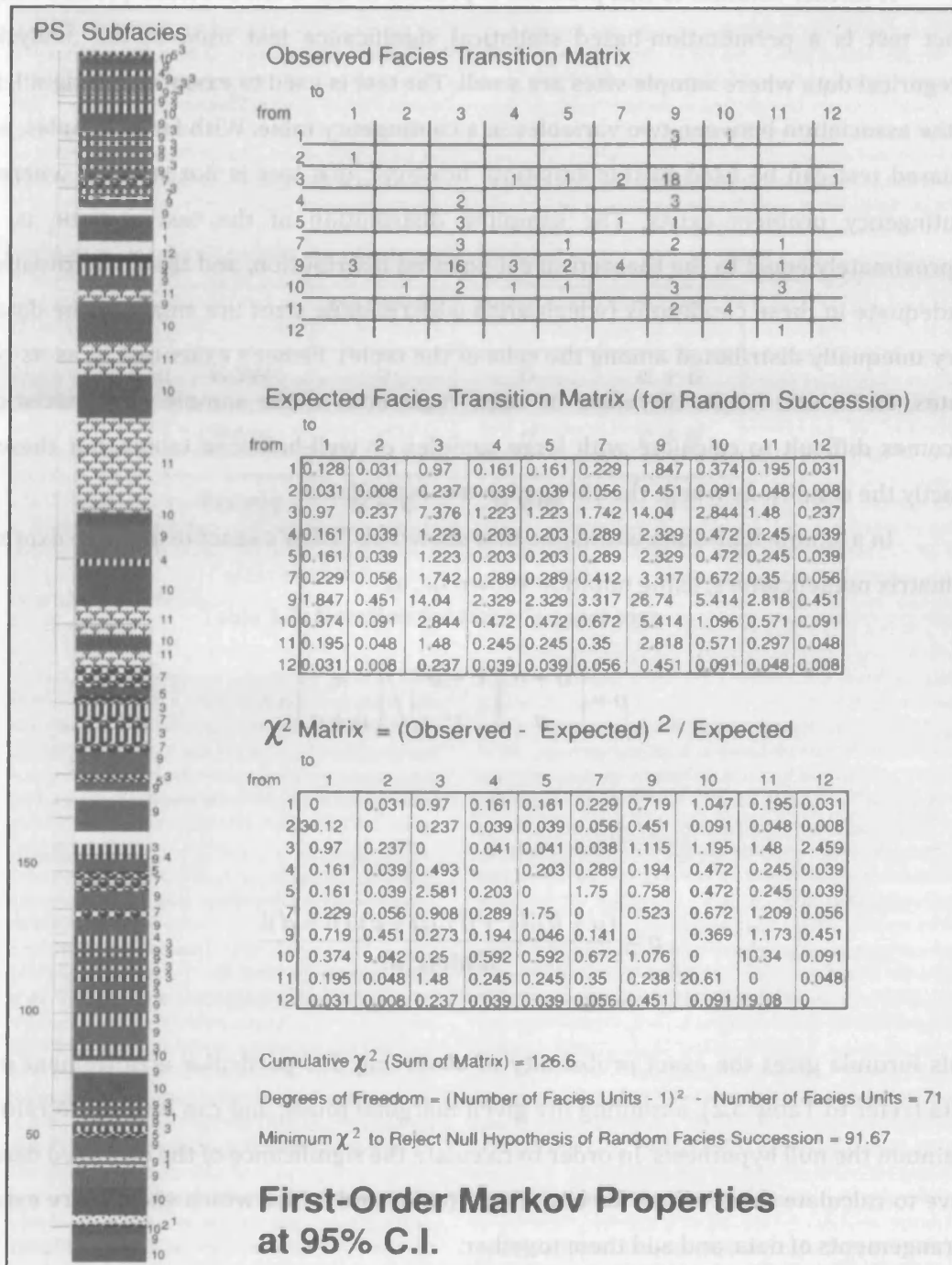


Figure 3.19: Illustration of Markov chain analysis used in Lehrmann & Goldhammer (1999, Figure 13), with data from the Silurian Barn Hills Formation. The assertion that the succession displays first-order Markovian properties (i.e. is non-random) contains considerable uncertainty due to a contingency problem. The expected facies transition matrix should have a minimum value of 5 in each element, but only 6 elements of 100 exceed a value of 5. This lowers the confidence in the expected frequencies predicted for a completely random succession, and renders the result unreliable.

A further solution to this problem is present in the work of Fisher (1922). Fisher's exact test is a permutation-based statistical significance test used in the analysis of categorical data where sample sizes are small. The test is used to examine the significance of the association between two variables in a contingency table. With large samples, a chi-squared test can be used in this situation; however, this test is not suitable where the contingency problem exists. The sampling distribution of the test statistic is only approximately equal to the theoretical chi-squared distribution, and the approximation is inadequate in these conditions (which arise when sample sizes are small, or the data are very unequally distributed among the cells of the table). Fisher's exact test is, as its name states, exact, and it can therefore be used regardless of the sample characteristics. It becomes difficult to calculate with large samples or well-balanced tables, but these are exactly the conditions where the chi-square test is available.

In a simple four-state world like that shown in, Fisher's exact test can be expressed in matrix nomenclature, using notation shown in , as

$$p = \frac{\binom{a+b}{a} \binom{c+d}{c}}{\binom{n}{a+c}}$$

3.15

or

$$p = \frac{(a+b)!(c+d)!(a+c)!(b+d)!}{n!a!b!c!d!}$$

3.16

This formula gives the exact probability of observing this particular arrangement of the data (refer to Table 3.2), assuming the given marginal totals, and can be used to refute or maintain the null hypothesis. In order to calculate the significance of the observed data, we have to calculate the p values for both these tables and tables which show more extreme arrangements of data, and add them together.

The disadvantage of calculating significance values for Fisher's exact test lies in the computational time required to conduct it. The factorial terms involved quickly become very large, and with larger sample sizes, the number of possible tables more extreme than that observed quickly becomes substantial. Even for small samples (which is where the test is usually needed), the calculations involved can be significant. Therefore, within TED, Fisher's exact test is only employed where the χ^2 test cannot be, and in these situations it is explicitly stated that analysis is by Fisher's exact test.

	Column	Column	Total
Row	a	b	$a + b$
Row	c	d	$c + d$
Totals	$a + c$	$b + d$	n

Table 3.2: Notation for Fisher's exact test.

3.4.4.2 Facies & system entropy analysis

Entropy may be most easily defined as the number of possible configurations of a system. Randomness in a given succession can also be evaluated of entropies of both facies and the system, and can be calculated from the matrices involved in Markov chain analysis. Entropy analysis is also useful in assessing the degree of symmetry and asymmetry present in sedimentary cycles.

To calculate entropy in a given sedimentary section the observed frequency transition matrix (Figure 3.18, a) and the expected probability transition matrix (Figure 3.18, b) of a succession are used. Entropy of one facies transition to the next (i.e. across rows in the matrix) with respect to i can be calculated by the function

$$E_i^{facies} = - \sum_{j=1}^n p_{ij} \cdot \log p_{ij}$$

where n is the number of possible transitions ij , i is the current state of the system, and j is the next state of the system. If $E_i^{facies} = 0.0$, one of p_{ij} ($j = 1,2,3,4$) is unity (i.e. all others are 0.0), and it can be said that I exerts a decisive influence upon the selection of states of its successors. Consequently, i is overlain by a certain lithology. Large E_i^{facies} signifies that the memory effect is poor and the system has random tendencies. If the transition probabilities for facies i are equally spread amongst all possible alternatives, $E_{faciesi(normalised)} = 1$. Like Markov chains, the size of entropy is likely to increase with the number of states. Thus, the entropy must be corrected by a certain reference standard in response to the number (n) of state variables, according to

$$R = \frac{E}{E_{\max}}$$

3.17

where

$$E_{\max} = -\log 1/(n-1)$$

3.18

Entropy of the entire succession (E_{system}) can also be calculated, essentially by summing entropies of all possible transitions from the facies matrix

$$E_{system} = -\sum_{i=1}^n \sum_{j=1}^n r_{ij} \cdot \log r_{ij}$$

3.19

where

$$r_{ij} = c_{ij} F$$

3.20

and

$$F = \sum_{i=1}^n \sum_{j=1}^n c_{ij}$$

3.21

This technique was used by Lehrmann & Goldhammer (1999) as it imparts the possibility to detect levels of facies ordering, and is particularly good for gauging vertical changes in the level of facies ordering within non-stationary systems. However, Lehrmann & Goldhammer note that because E_{system} is particularly sensitive to changes in HfS symmetry. Only a strictly deterministic system with asymmetric HfSs (1, 2, 3, 4, 1, 2, 3, 4) will yield an $E_{system} = 0$. They also note that E_{system} varies based upon cycle truncation and autocyclicity. However, the calculations presented as an example in Lehrmann & Goldhammer (their Figure 16) do not match the function presented by Hattori (Hattori, 1976) or by (which are presented the same in Lehrmann & Goldhammer, 1999). The results presented in their Figure 16 require $2n$ to be used in the function in place of $x \cdot \log(x)$. This error in calculation is likely to distort results and is likely to account for some of the sensitivity of the analysis described by Lehrmann & Goldhammer.

3.4.4.3 Runs tests

Runs tests, as opposed to the previous two statistical methods described, are performed on HfSs as a unit rather than the facies that comprise them. Runs are defined as uninterrupted sequences of the same state, or in a geological context; contiguous sets of HfSs that are either greater than or less than the average HfS thickness (Drummond & Wilkinson, 1993b; Lehrmann & Goldhammer, 1999; Davis, 2002; Burgess, 2006). As both variants of the non-parametric runs test are based on HfS thickness they usually contain a relatively small number of observations and, combined with the simplicity of the equations, this makes them computationally straightforward. The method is a statistical evaluation of the probability that the number of runs, and the length of the longest run, could be generated by a random-walk process (Drummond & Wilkinson, 1993b). The runs test is based on a null hypothesis that cycle thicknesses are indistinguishable from random (or, rather, indistinguishable from thickness series produced by a random walk) and by rejecting this hypothesis it is possible to say that the sequence displays a sequence of runs beyond that expected for a random walk. The test is measured using a standard confidence interval z -statistic to compare the number of runs in the test section with a number of runs produced by a random walk process (Sadler *et al.*, 1993; Burgess, 2006).

TED employs two types of runs test which provide different tests for orderedness within the forward model, the first being an about-the-mean runs test and the second being an up-down test. An about-the-mean test uses the average HfS thickness to calculate the probability that a given sequence of runs was created by the random occurrence of two states; greater-than average or less-than average. If a randomly generated sequence were comprised of n_1 instances of state 1 and n_2 instances of state 2, then the mean number of runs can be expressed as

$$U = \frac{2n_1n_2}{n_1 + n_2} + 1$$

3.22

with the expected variance in the mean number of runs as

$$\sigma \frac{2}{U} = \frac{2n_1n_2(2n_1n_2 - n_1 - n_2)}{(n_1 + n_2)^2(n_1 + n_2 - 1)}$$

3.23

It is therefore possible to determine the mean number of runs and the standard error of the mean number of runs in all possible arrangements of n_1 and n_2 states (Davis, 2002). A z -test statistic can now be calculated, where U is the observed number of runs:

$$z = \frac{U - \bar{U}}{\sigma_{\bar{U}}}$$

3.24

A two-tailed test of randomness can then be applied, rejecting non-randomness in the presence of either too few or too many runs. A two-tailed test has the hypotheses

$$H_0 : U = \bar{U}$$

$$H_1 : U \neq \bar{U}$$

3.25

with the null hypothesis stating that there is no difference between the observed number of runs and the mean number of runs from random sequences of the same size. By this two-tailed test, the z-statistic value can discriminate between runs which lie in a zone of randomness (i.e. those indistinguishable from random sequences) and those which lie in an ordered field (Figure 3.20). At the 95% confidence level, a value of $-2.4 < z < 2.4$ delineates the zone of randomness (Burgess, 2006).

The second variation of runs test applied in TED is an up-down test, which disregards the polar states used in the about-the-mean test and instead concentrates on whether an observation (HfS thickness in this case) is larger or smaller than the preceding observation (Figure 3.21). As the observations are expressions of magnitude, the result is a series of runs of 'up' or 'down'. In this manner we can generate the two states necessary to create a randomly generated sequence of runs and the z-statistic. This is accomplished with the same method as an about-the-mean test; using equations 3.22 to 3.24. The up-down runs test is generally regarded to be the most robust of the runs tests because it utilises changes in magnitude of every point with regard to adjacent points (Davis, 2002), whilst other dichotomising schemes, like the about-the-mean test, only reflect changes with respect to a single value (see Figure 3.20).

Runs tests check for the existence of non-randomness expressed by the presence of too few or too many runs, and are therefore appropriate when the cause of the non-randomness is the issue under investigation. They do not identify overall trends and cannot determine the existence of randomness itself as the condition of random occurrence forms the null hypothesis. They can, however, demonstrate that the null hypothesis is incorrect and the sequence is therefore not random or that the sequence does not exhibit any non-randomness. They therefore provide a useful tool in studying real and modelled sedimentary successions.

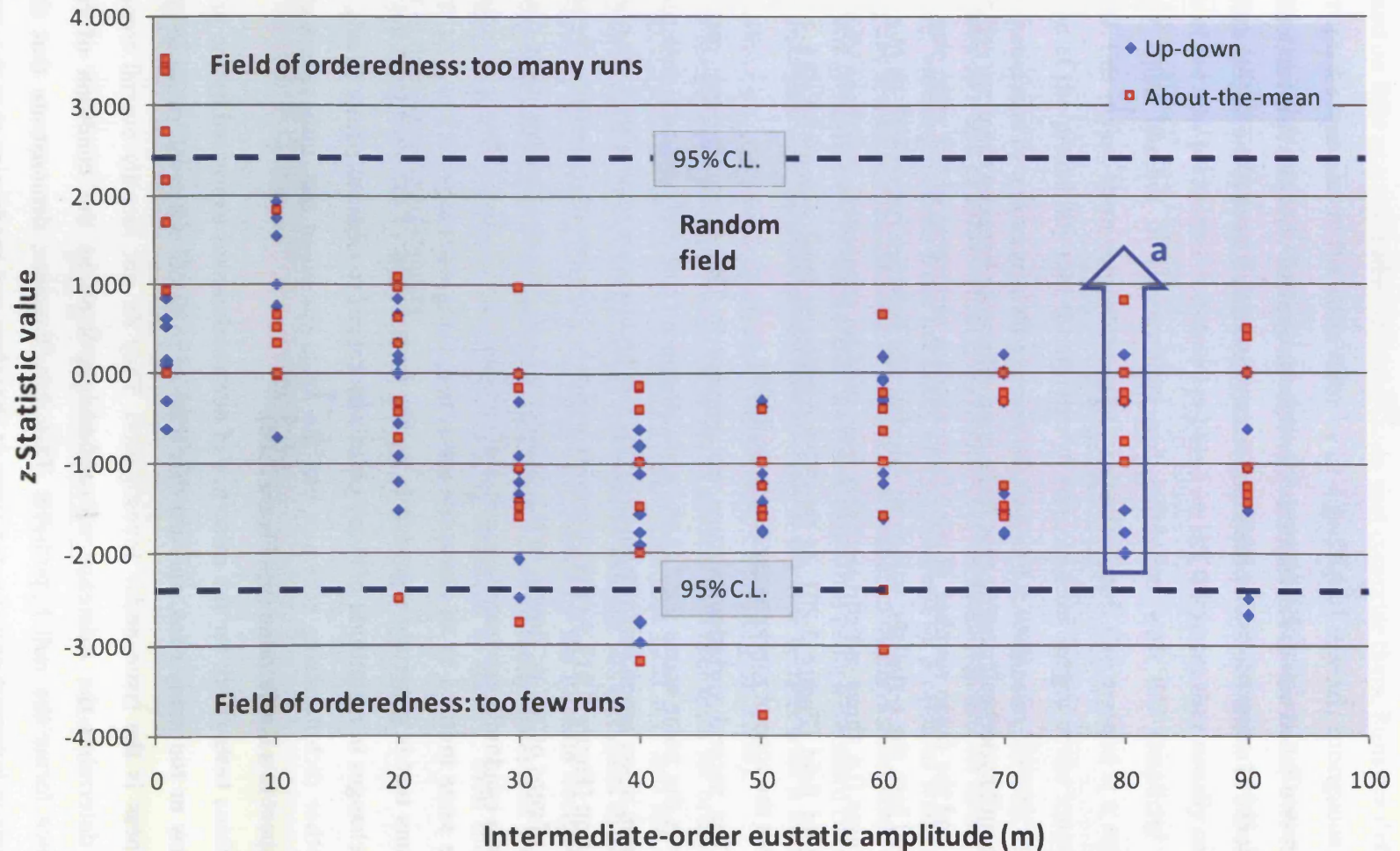


Figure 3.20: Comparison of about-the-mean and up-down runs tests conducted upon an example set of runs from TED. Each method was run on the same dataset where the variables were amplitude of intermediate-order sea-level changes and amplitude of high-order sea-level changes. The z-statistic is plotted here against intermediate-order amplitude change. The effects of high order amplitude change are shown by arrow (a) and act to increase the z-statistic with increasing amplitude of high-order change. The up-down runs test is marginally more robust and is seen to constrain variables to a tighter degree, although the general trend of the two statistics is, in this case, similar.

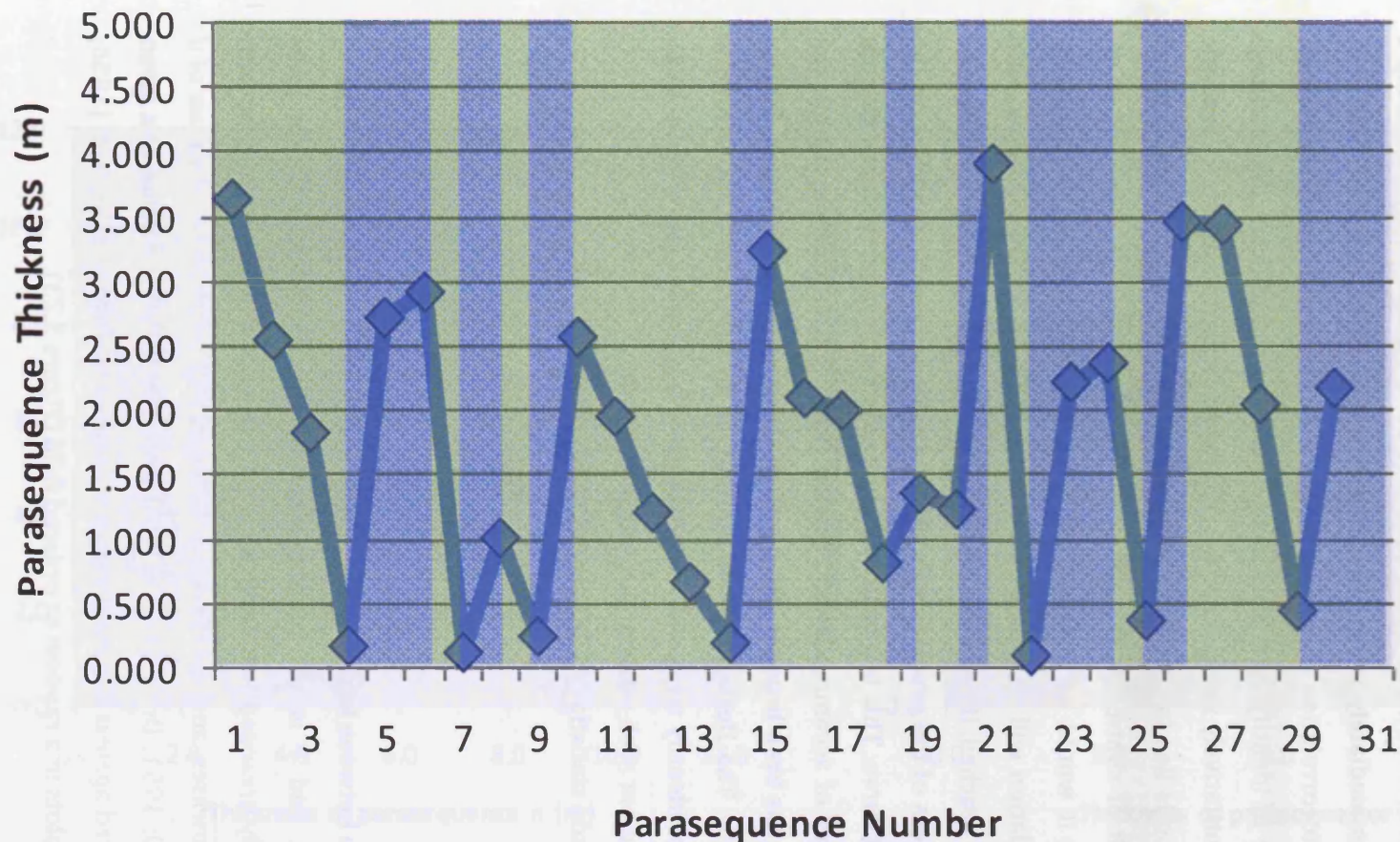


Figure 3.21: Example of runs up and runs down. Blue shading indicates a run up and green shading a run down. The longest run in the sequence is a run down of 4 between parasequence 10 and 14, and the shortest run is 1 (numerous instances). There are a total of 18 runs in this sequence. As the observations are recording a magnitude (parasequence thickness) it is unlikely that there will be a 'tie' (two consecutive runs of the same value), if, however, there should be, the tied value could belong to either the previous or next run.

3.4.4.4 Durbin-Watson test

The Durbin-Watson method is a one-offset autocorrelation technique (Durbin & Watson, 1950; 1951; Davis, 2002). One-offset autocorrelation refers to the relationship a given HfS has with the immediately prior HfS (Lehrmann & Goldhammer, 1999; Burgess, 2006; an example of autocorrelation is shown in Figure 3.22). As previously mentioned, runs tests are incapable of identifying trends, which presents a significant disadvantage when attempting to quantitatively study stacking-patterns in carbonate strata. An example of the importance of trends lies in the thickness distribution that would be expected of HfSs forming as a result of sinusoidal eustatic sea-level oscillations (e.g. Barnett *et al.*, 2002). In this example, it would be expected that on the rising limb of an oscillation slightly more accommodation will be created for a given HfS than for the previous, until the top of the sinusoid is reached. If this is the case, the thickness of a given HfS will appear to depend on the thickness of the previous HfS, being greater or lesser depending on the position on the sea-level curve. This is a basic principle of using 'Fischer' plots to identify long-term change in rates of accommodation creation (Read & Goldhammer, 1988); the objective basis of which has been brought into question (Drummond & Wilkinson, 1993b; Boss & Rasmussen, 1995). The Durbin-Watson method, as an autocorrelation technique with a one-offset lag, can identify trends in a way the runs test cannot (see Figure 3.22), and as such they complement each other in their implementation.

The Durbin-Watson statistic can be calculated by

$$d = \frac{\sum_2^T (e_t - e_{t-1})^2}{\sum e_t^2}$$

3.26

where e_t is the difference between log thickness and the mean of log thicknesses, t is the individual HfS number, and T is the total number of HfSs. Sequences where cycle thicknesses are randomly arranged will result in large values of d , while sequences with gradually changing thicknesses, and are therefore ordered, will result in small values of d (Durbin & Watson, 1950; 1951; Drummond & Wilkinson, 1993b). The d value of a given sequence can be compared against d -critical values published by Durbin & Watson (1950; 1951) to determine if it plots in a random or ordered field (Figure 3.23).

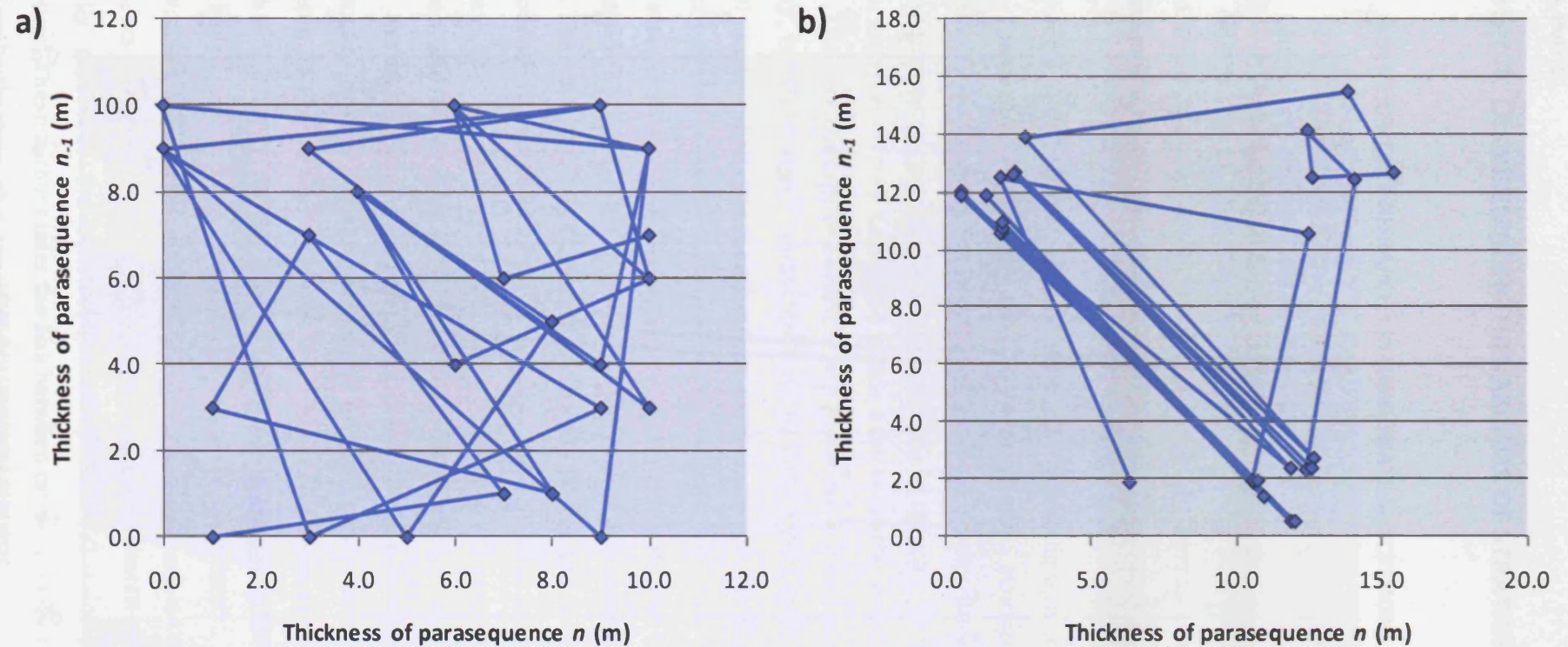


Figure 3.22: Example of a one-offset autocorrelation technique and its application in identifying trends. The one-offset refers to the comparison of the thickness of a given parasequence (n) and the immediately previous parasequence (n_{-1}). This is the same principle used in the Durbin-Watson test. a) Autocorrelation of a sequence of 30 pseudo-random (as generated by Microsoft Excel's random number generator) numbers in place of parasequence thickness. b) Autocorrelation of an example TED model run of 30 parasequences. There is a visible relationship, with a thicker parasequence tending to follow a thinner one.

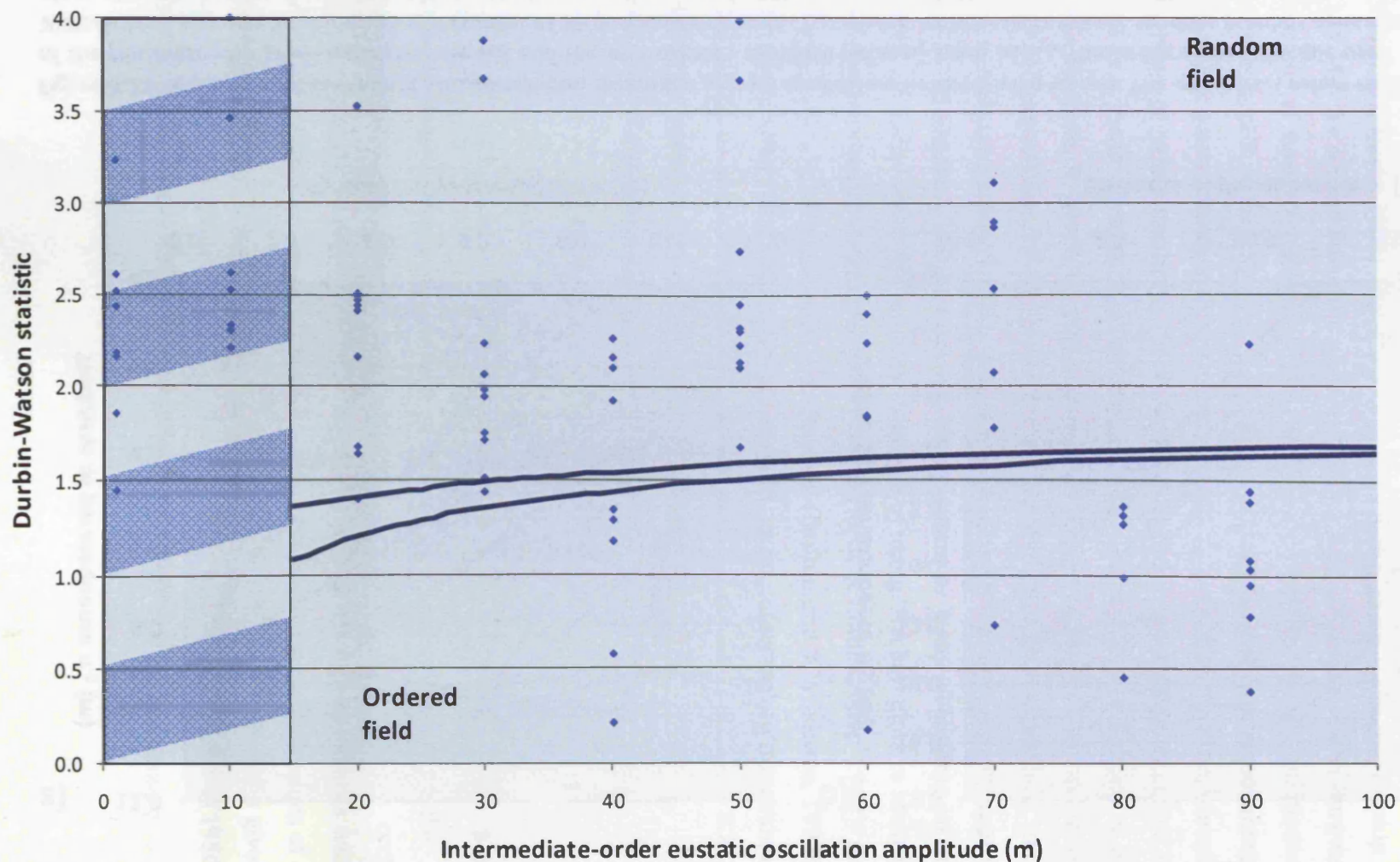


Figure 3.23: A plot of the Durbin-Watson statistic against the amplitude of intermediate-order eustatic sea-level oscillation from an example model run of TED. The striped area represents the area without critical values for d ($n < 15$), which were not calculated by Durbin & Watson (1950; 1951). Critical values for d can be found by extrapolating this line, however. The majority of points plot in the random field.

Chapter 4: DISASSEMBLING HIERARCHIES OF STRATIGRAPHIC CYCLICITY

4.1 A SEDIMENTARY HIERARCHY IN CARBONATE SUCCESSIONS

4.1.1 Lack of a formal definition of a hierarchy

“Hierarchy” is a term that is widely used in stratigraphic studies but is not well defined. Many modern investigations into stacking patterns of carbonate strata address the concept of a hierarchy using only qualitative statements (e.g. Goldhammer *et al.*, 1987; Dunn *et al.*, 1991; Tinker, 1998; Lerat *et al.*, 2000). An example of such a statement comes from Osleger & Read (1991), who state that; “shallowing-upward, meter-scale carbonate cycles (parasequences) tend to be systematically arranged within larger scale successions”, and that “trends in cycle thickness and composition” can be used to identify larger sequences (Osleger & Read, 1991; p1225). In this case a hierarchy is implied to be a stack of metre-scale cycles arranged within a thicker cycle, or sequence.

The core concept of a sedimentary hierarchy is based on “composite stratigraphic cyclicity, in which small depositional cycles build into larger sequences” according to vertical stacking patterns (Goldhammer *et al.*, 1994; p267). Thus the identification of a hierarchy in this manner relies on accurate recognition of cycle boundaries. Many studies which identify a hierarchy infer evidence of deepening as cycle boundaries, and therefore as evidence of eustatic sea-level oscillations (e.g. Goldhammer *et al.*, 1991; Lerat *et al.*, 2000). The usefulness of inferring cycle boundaries on the basis of facies-associations is questionable (discussed below). A hierarchy should therefore be defined in terms of thickness, and only infer cycle boundaries where there is very clear evidence of change in relative sea-level, which, in most cases means sub-aerial exposure of cycles.

Examples of more rigorous attempts to address the concept of a hierarchy come from studies critical of interpretations of order in carbonate successions (Drummond & Wilkinson, 1993b; 1993a; Wilkinson *et al.*, 1997a). Drummond & Wilkinson (1993b; p688) state that “...many cyclic sequences exhibit a distinct stacking hierarchy wherein a pattern of thickness is repeated throughout an individual sequence” . Drummond & Wilkinson (1993a; p369) expand upon this: “Explicit in this argument is that each meter-scale cycle represents a single excursion of sea-level and that repeated patterns in cycle thickness faithfully represent the constructive interference of forcing functions of different frequency”. These authors infer the link between cause and effect in their descriptions, but do not explicitly state what constitutes a hierarchy.

The implication is that an ordered forcing-mechanism causes an ordered pattern to be recorded in sedimentary strata by influencing accommodation. This is usually

attributed to climate-variations resulting from Milankovitch-scale orbital variations, which vary global sea-level by dictating the amount of water stored as continental ice (refer to section 2.1.1 for a full review). The accommodation changes are therefore inferred to be periodic, and to create a sedimentary hierarchy by virtue of overlapping of the differing wavelengths of Milankovitch oscillations.

Given the ambiguous nature of a sedimentary hierarchy and the likelihood of misinterpretation, coupled with the importance of a hierarchy in terms of its potentially predictive power, there exists a need to formally define the term. Even a simple, qualitative definition of a hierarchy could differentiate orders of the hierarchy by the measuring criterion; in this case, parasequence or high-frequency sequence thickness.

A qualitative definition would then state that cycle thicknesses are directly proportional to the amplitude and duration of sea-level change. In an environment where sea-level changes according to parameters with differing temporal frequencies, cycle thicknesses would be expected to correspond to the hierarchical parameter believed to have forced them. This qualitative definition would therefore dictate that 'fourth'-order cycles would be consistently thicker than 'fifth'-order cycles, reflecting an oscillation of longer duration and a potentially greater opportunity for accumulation.

The absence of a more precise quantitative definition is perhaps a consequence of the fact that a lack of clarification of the term 'hierarchy' does not preclude its use. Strata can be interpreted to be hierarchical without a clear definition, although only in a subjective and qualitative way. Most importantly, different qualitative definitions implied by various authors (cf. Goldhammer *et al.*, 1991; Drummond & Wilkinson, 1993a; Lerat *et al.*, 2000) prevent consensus, decrease reproducibility and inhibit testing for presence of hierarchical strata. For example, the sedimentary hierarchy described by Lerat *et al.* (2000) differs in its diagnostic criteria to the concept of a hierarchy most explicitly described by Goldhammer *et al.* (1991). In order to establish a "cycle hierarchy", Lerat *et al.* state that the criteria rest not on thickness but on the "extent of changes in the depositional environments recorded within a cycle" and "the importance of the cycle bounding surfaces in regional correlations" (Lerat *et al.*, 2000; p78). Furthermore, they state that a '5th-order cycle' or 'genetic unit' is defined by a "cyclic but minor change in bathymetry or accommodation as deduced from facies", and are "the expression of a short term cyclic variation of relative sea-level". '4th-order sequences', in contrast, are said to represent "major changes in bathymetry or accommodation". The subjective nature of the distinctions between major and minor are clear; especially as the majority of sedimentation in contemporaneous ice-house platforms has been interpreted as occurring in very shallow water-depths (Horbury & Adams, 1996). By attributing '5th-order cycles' (or 'genetic units') to a cyclic excursion of relative sea-level, Lerat *et al.* necessarily invoke

this same causal mechanism for their larger hierarchical units. This implies that there is a hierarchical forcing mechanism in place.

The major problem with the hierarchy as defined by Lerat *et al.* (and utilised by other contemporary works on cyclicity in the Paradox Basin; Grammer *et al.*, 2000; Van Buchem *et al.*, 2000), is that the sedimentary hierarchy, defined in this way, depends on accurate identification of bounding surfaces. Lerat *et al.* utilise evidence of deepening as the criteria for these boundaries, however the fundamental basis of identifying a hierarchy on these grounds must be called into question given recent work on the complexity and completeness of carbonate strata (Burgess & Wright, 2003; Rankey, 2004; Burgess, 2006). Moreover, vertical facies associations have repeatedly been shown to be statistically indistinguishable from disordered or random models (Drummond & Wilkinson, 1996; Wilkinson *et al.*, 1996; Wilkinson *et al.*, 1997b; Wilkinson *et al.*, 1998). For example, from work presented here (refer to sections 5.3.10 and 5.3.11), hardgrounds recognised within individual beds may or may not be interpreted as evidence of deepening; a conservative interpretation is that hardgrounds are only evidence of non-deposition, which may or may not be linked to a deepening event. Certainly it is possible to imagine various other controls, other than water depth, that could cause a temporary decrease in carbonate accumulation and generation of a hardground.

Thus the use of “minor bathymetric changes” appears extremely tenuous as the basis for a cycle boundary. Furthermore, recent work has shown that very shallow-water carbonate-producing organisms do not necessarily organise themselves into well-defined depth zones, and that “variables other than bathymetry may significantly influence the ecological and sedimentologic attributes of depositional surfaces” (Rankey, 2004). Fundamentally, therefore, the genetic facies units may not represent “minor” bathymetric changes, but ecological processes poorly recorded as sedimentary facies.

4.1.2 Comparison of a new qualitative definition with that of Goldhammer *et al.* (1991)

Goldhammer *et al.* (1991; 1994) used thickness trends within a sedimentary section to define a sedimentary hierarchy; providing one of the clearest examples of what a hierarchy is interpreted to constitute (Figure 4.1). Based on observations of variations in cycle thickness throughout a sequence, a hierarchy was classified based on the relative position of thicker and thinner ‘fifth-order’ high-frequency sequences within a “lower-order” sequence (Goldhammer *et al.*, 1991). Fifth-order cycles were interpreted to thin-upwards within a succession and, when a thicker fifth-order cycle was seen, it was considered to be the end of that particular sequence and the start of a new lower-order sequence (‘fourth-order’). This provides the basis for the ‘cycle-bundling’ now commonly

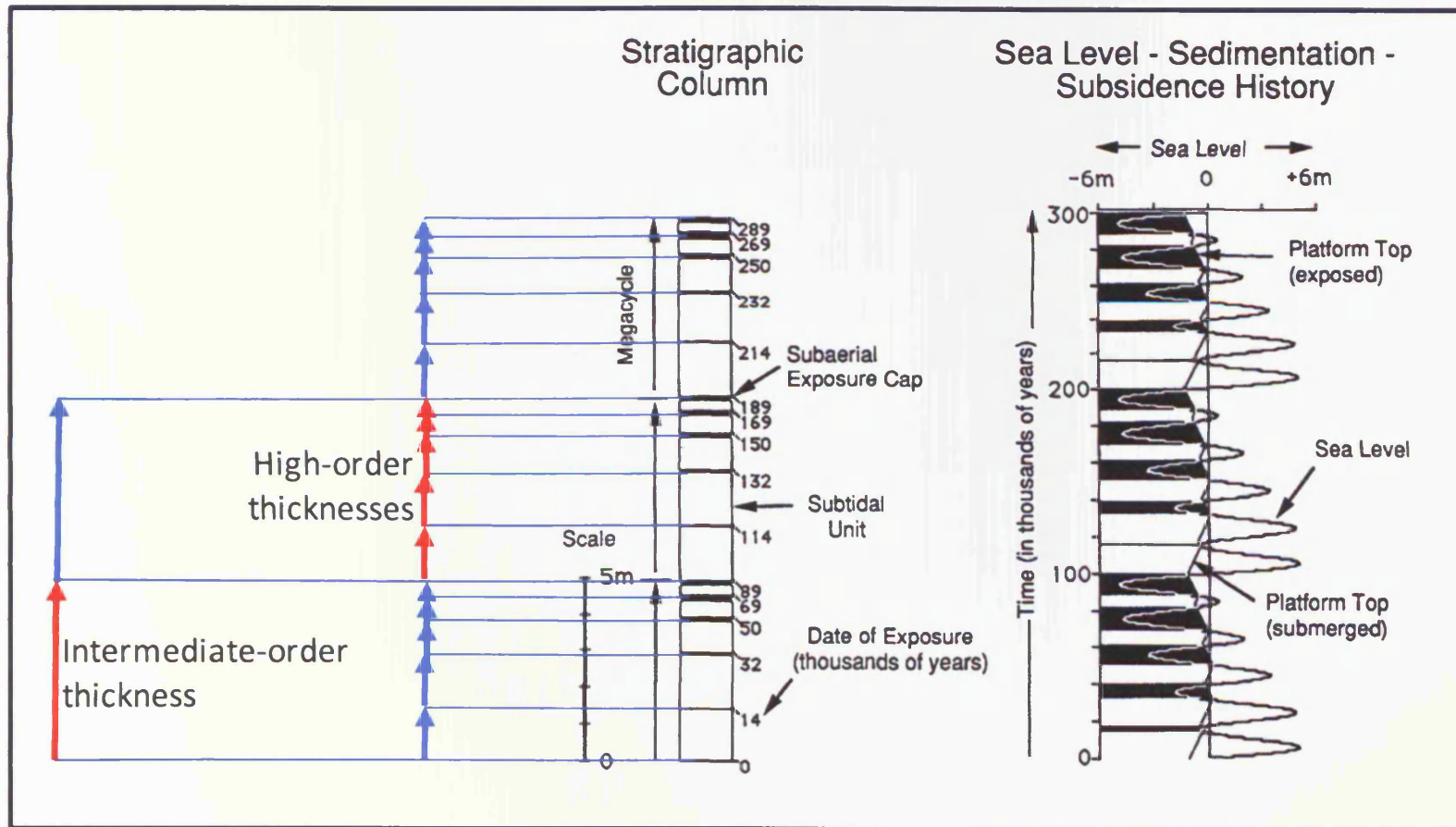


Figure 4.1: Figure from Goldhammer *et al.* (1990; with subsequent modification in colour) showing the organisation of high-frequency sequences (here labelled high-order thicknesses) into sequences. The hierarchical classification is based on the upwards-thinning arrangement of high-order thicknesses. If a thicker higher-order sequence than the previous one is recorded, a new intermediate order thickness is started.

advocated by workers as evidence for the operation of glacio-eustasy according to Milankovitch forcing (e.g. Cozzi *et al.*, 2005; Schwarzacher, 2005; Algeo & Hinnov, 2006). In the case of the Honaker Trail cycle-bundling is manifest at a maximum ratio of 9:1 (with a minimum of 3:1), contrasting with the usual 5:1 ratio quoted for many successions (e.g. Goldhammer *et al.*, 1987). Conveniently, a shortfall in the number of high-frequency sequences per sequence is usually accounted for by citing missed beats as a cause (Goldhammer *et al.*, 1994; p262). This explanation has rather more difficulty demonstrating how nine precession or obliquity ~20ky beats fit into the ~100ky framework afforded by the 'short' eccentricity Milankovitch parameter, which is claimed to be responsible for the 5:1 ratio.

A problem created by the qualitative approach used by Goldhammer *et al.* (1991) is apparent in the thickness of the differing orders, which are not indicative of a hierarchy even according to the definition of Goldhammer *et al.* (1991; 1994). Goldhammer *et al.* interpret fourth-order cycles as having a range of 10-40m, and fifth-order cycles; a range of 2.5-11m (Goldhammer *et al.*, 1994; p249 and p266). Yet, if the thickness distribution of the different orders are considered throughout a sequence, then they would be seen to exist in a continuum; that is, there would be no separation between the fourth- and fifth-orders. If the thinnest fourth-order sequence is thinner than the thickest fifth-order high-frequency sequence, it is not possible at outcrop to distinguish between the two. This is particularly true considering the uncertainties arising as a result of an incomplete stratigraphic record.

It may be argued that a fifth-order cycle can be identified as such if it contains no cycles of higher-frequency units, as the boundaries are based on vertical facies associations. However, this does not hold true; firstly in light of the already mentioned complexity inherent in carbonate strata, and also because Goldhammer *et al.* (1991; 1994; their sedimentary section HT#8) document deepening events which are not counted as cycle boundaries. The subjective answer to the question; "how deep is deep enough?" - is therefore based upon lithofacies interpretations. The composition of these lithofacies, at best, is only affected by non-depth dependent accumulation (Rankey, 2004), and at worst suffers from incomplete recording of facies (Burgess & Wright, 2003), dissolution of major biotic components – skewing the perceived habitat and depth regime (Cherns & Wright, 2000), and major diagenetic overprinting (Saller *et al.*, 1994).

In contrast to the difficulties described above, model-space is a simple place. The critical limitations of investigating a sedimentary hierarchy using outcrops are removed within a model environment; since every parameter is known, and the link between parameter and model output can also be known. This allows an objective evaluation of conditions under which a hierarchy will be generated. Studies by Goldhammer *et al.*

(1991; 1994) represent the only attempts to quantify the existence of a hierarchy of stacked cycles through numerical forward modelling. This innovative study attempted to express numerically stacking patterns which had previously only been described qualitatively (e.g. Schwarzacher, 1975). The model of Goldhammer *et al.* recreates the observed cycles boundaries of these workers, however these boundaries are based on potentially tenuous facies-depth associations. The numerical model presented by Goldhammer *et al.* (1991) is also reliant upon accommodation created during periods of sub-aerial exposure to generate hierarchical stacking patterns, and this may not be realistic.

The rate of 'caliche formation' quoted by Goldhammer *et al.* (1994) is 10m/My, which is accreted to the platform surface rather than being denuded from it. This calcrete formation essentially protects the platform surface, whereas evidence from modern and ancient examples suggest that under most conditions the platform surface would be lowered rather than significantly raised (Wright, 1994). Estimates of rates of dissolution from modern analogues are roughly in line (10m/My; Plan, 2005) with the rate of caliche formation presented by Goldhammer *et al.* (1994). However, in humid climates the rate is likely to be up to an order of magnitude greater (Wright, 1994; Vanstone, 1996). The net result being that significant numbers (i.e. >85%) of high-order beats which are recorded on the platform top would be removed; therefore not recording any hierarchy that may be present in the forcing mechanism.

If this model employed parameters more likely to be realistic, the very thin cycles present at the tops of larger cycles (the 'thinning-upwards' cycles) may be completely removed even by low rates of sub-aerial erosion (<10m/My), disassembling the hierarchy. The importance of this problem cannot be under-estimated: it is the main reason a hierarchy is recorded by the Goldhammer *et al.* model. This is not to say that with super-imposed orders of periodic forcing and an absence of dissolution a hierarchy will certainly develop; this study aims to show that generation of a hierarchy requires very specific and potentially unrealistic conditions (4.3.1.1).

The model of Goldhammer *et al.* does not create a truly objective, definable hierarchy with discrete groups of cycle thicknesses. Instead, a qualitative hierarchy is created which cannot correctly be designated as hierarchical because cycle thicknesses exist within a continuum. This problem has skewed understanding of the conditions under which a hierarchy is likely to exist, and how likely it is that a hierarchy will be generated in ice-house successions.

4.1.3 A quantitative definition of a sedimentary hierarchy

Building upon the previously discussed qualitative definition, a more rigorous quantitative definition of a hierarchy is proposed as follows; “a hierarchy consists of a series of sedimentary cycles, either parasequences or high-frequency sequences, each bounded by sub-aerial unconformities, in which there exist at least two discrete groups in terms of thicknesses”. Discrete here means that the thickness groups either do not overlap, so that the thinnest of one group is thicker than the thickest in another group, or that the thickness distributions do not overlap beyond a chosen quantile of the distribution, as determined by the range of thicknesses in the succession. The opposite case, where overlap does occur, would be a continuum of cycles, with no grouping apparent in the thicknesses. This may be regarded as a prototype definition, the veracity of which will be assessed by numerical forward modelling of sedimentary sequence generation in an environment containing a truly hierarchical forcing mechanism.

A hierarchy refers to the thickness of cycles; the composition of cycles in terms of facies is only an issue when considering boundary placement. It is therefore the boundaries (the flooding surfaces and discontinuity surfaces) that define the cycles, and the resulting thicknesses should define the sedimentary hierarchy, if one is present. For reasons previously mentioned, cycle boundaries should only be interpreted where there is unequivocal evidence of sub-aerial exposure. Vertical facies associations are not enough to distinguish orders of the hierarchy from outcrop given the complicated controls on and limited completeness of carbonate strata. A distinction made according to vertical facies associations is fundamentally qualitative. This method, however, limits the uncertainty involved in characterising a hierarchy.

A hierarchy further implies that levels are ranked according to some measure (in this case; thickness). If levels cannot be distinguished from one another, then the hierarchy is not a relevant method of differentiation. Therefore, there must be a separation in thicknesses in order to distinguish between levels. In practice, this is likely to take the form of a ‘cut-off’ below which lies one order, and above, the superior order, with a gap of time or thickness in between (otherwise a continuum could be arbitrarily subdivided).

Therefore, a hierarchy may be objectively and quantitatively said to exist when the following criteria are met:

1. Orders are assigned to sedimentary sequences objectively (refer to section 4.2.1).
2. There should be a differentiation in terms of thickness between different orders.

3. There should be only acceptable levels of overlap of thicknesses between orders, allowing an objective differentiation of cycles into different orders on the basis of their thicknesses.

4.2 ONE-DIMENSIONAL FORWARD MODELLING OF SEDIMENTARY HIERARCHIES

4.2.1 The objective basis of TED

While outcrop studies of hierarchy should be limited to consideration of thickness, in forward modelling two aspects of hierarchy can be considered; the thickness of the cycles, and the length of missing time represented by the bounding surfaces. For example, given superimposed third-, fourth- and fifth-order eustatic sea-level changes, theoretically the third-order lowstand would represent more missing time than the fourth-order, and the fourth-order more than the fifth-order. If so, you could define a hierarchy on the basis of these durations in the strata, and infer from that a hierarchical forcing in the driving sea-level curve.

The role of hiatal durations in diagnosing hierarchies has been largely overlooked, mainly due to the extreme uncertainties in interpreting the length of exposure recorded in these surfaces (Wright, 1996; Vanstone, 1998; Budd *et al.*, 2002; Sattler *et al.*, 2005). This limitation is removed in numerical forward models, where the exact length of exposure is known. This criterion can therefore be used to evaluate the presence of a hierarchy in simulated stratigraphic sections.

A similar method can be employed with thicknesses of cycles. Critically however, the entire thickness between each class of surface must be taken. For example, for a third-order sequence the entire thickness between the third-order initial flooding surface and final sub-aerial exposure during the subsequent third-order falling stage. Third-order thickness will therefore encompass fourth-order thicknesses, and fourth-order thickness will include fifth-order thicknesses. This method is in keeping with the concept of a hierarchy from Goldhammer *et al.* (1991).

Where this scheme, as it is used in TED, differs from its incorporation in the work of Goldhammer *et al.* is its objective application. The process of identification of a hierarchy by Goldhammer *et al.* (1991; 1994), in contrast, is founded on subjective sequence stratigraphic interpretations which are *subsequently* applied to the sedimentary section or synthetic section. The flaws inherent in this method of hierarchy recognition are exposed when attempting to encode it in a deterministic and strictly literal computer model.

Essentially, what is occurring in the model of Goldhammer *et al.* is an assignment of two orders of forcing to a high-frequency sequence. The first is the fundamental source of the cycle; the fifth-order oscillation, and the second is the 'parent' fourth-order oscillation to which it belongs. This does not seem problematic until there is cause to consider it objectively. It is easiest to illustrate these points with an example of trying to

integrate the system of Goldhammer *et al.* into a forward model (refer to Figure 4.2 and Figure 4.3).

Within TED, inflection points on the sea-level curve are used to attribute an order of forcing to a period of sedimentation. Inflection points (defined as the point on a curve at which the curve changes sine) are assigned according to several simple rules:

1. Flooding surfaces are attributed to an order using HST inflection points during the period of sedimentation subsequent to the flooding surface.
2. Discontinuity surfaces are attributed to an order using LST inflection points during the hiatus subsequent to the discontinuity surface.
3. When attributing orders, the lowest-order takes precedence.
4. A given surface cannot be forced by more than one order.

This method makes assigning two orders of forcing to the initiation or termination of one period of sedimentation impossible, thereby objectively assigns orders of forcing to flooding surfaces and discontinuity surfaces, and bounding periods of sedimentation. From this thicknesses of sediment associated with a given order can be known, as can the durations of hiatuses between periods of sedimentation. This allows identification of a hierarchy using two different criteria.

4.2.2 Methodology

Several run-plans were created in order to address, through numerical modelling, the occurrence of a sedimentary hierarchy against a number of interacting independent variables (Table 4.1). The run-plans investigate the role of eustatic sea-level oscillation amplitude, subsidence, carbonate accumulation and sub-aerial exposure. These independent variables were used as they represent the primary controls on the creation of accommodation, and the potential to fill this accommodation with sediment. They are therefore the most likely to have an effect on the creation and preservation of a hierarchy.

The ranges of values for variables are selected from published studies. A range is used to observe how variables interact, and to bound the large margin of error associated with many of the variables. Each run-plan contains three variables, all other values are held as controlled variables. Each variable is varied within its range by 10 steps according to a preset increment. Simulations of every possible combination of increments therefore results in 1000runs per run-plan. For each run, the existence of a hierarchy in terms of both hiatal duration and thickness is evaluated. The runtime for all simulations is set to

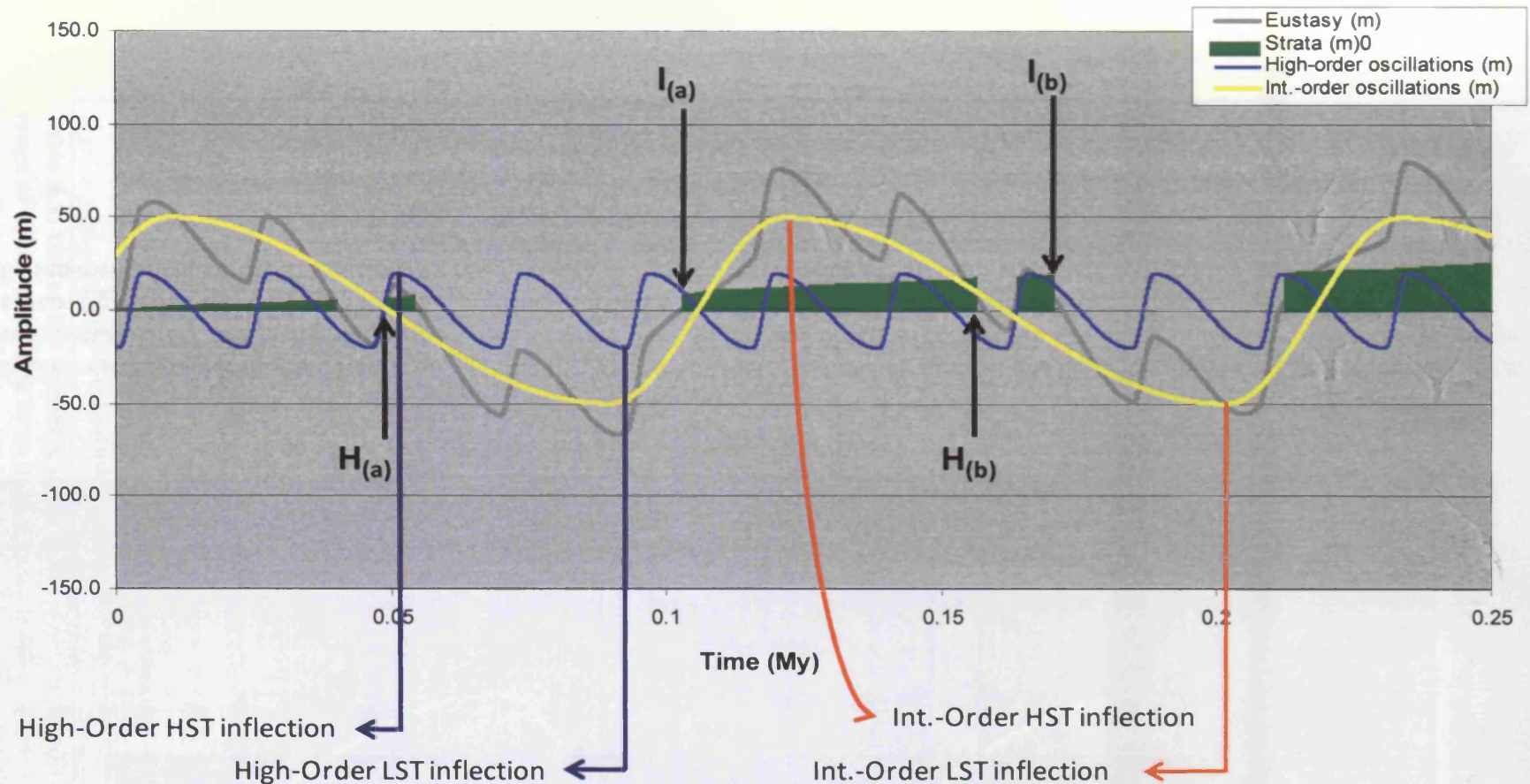


Figure 4.2: Chronostratigraphic diagram illustrating the inflection point concept used to attribute periods of sedimentation to a forcing order in TED. 0m amplitude can be considered the platform surface, above which, sedimentation can potentially take place. TED uses inflection points on the individual sea-level curves to objectively assign orders of forcing to cycles (i.e. periods of sedimentation). Examples of a HST and LST inflection for both high- and intermediate-order forcing are shown. $I_{(a)}$ and $I_{(b)}$ are a flooding surface and discontinuity surface, respectively, determined using inflection points to be forced by intermediate-order. Although two high-order HST inflection points also exist during this period, the lower order takes precedence – a fundamental concept of a hierarchy. $H_{(a)}$ and $H_{(b)}$ are a flooding surface and discontinuity surface, respectively, determined using inflection points to be forced by high-order. By this method a hierarchy in terms of thickness can be found objectively, as lower orders should contain greater thicknesses. The complete run (3My – only 0.25My depicted) of this example is non-hierarchical: periods of sedimentation attributed to high-order forcing are of similar thickness to those deposited by intermediate-order, and so cannot be distinguished from each other. This would not be the case in a hierarchical system (see Figure 4.2).

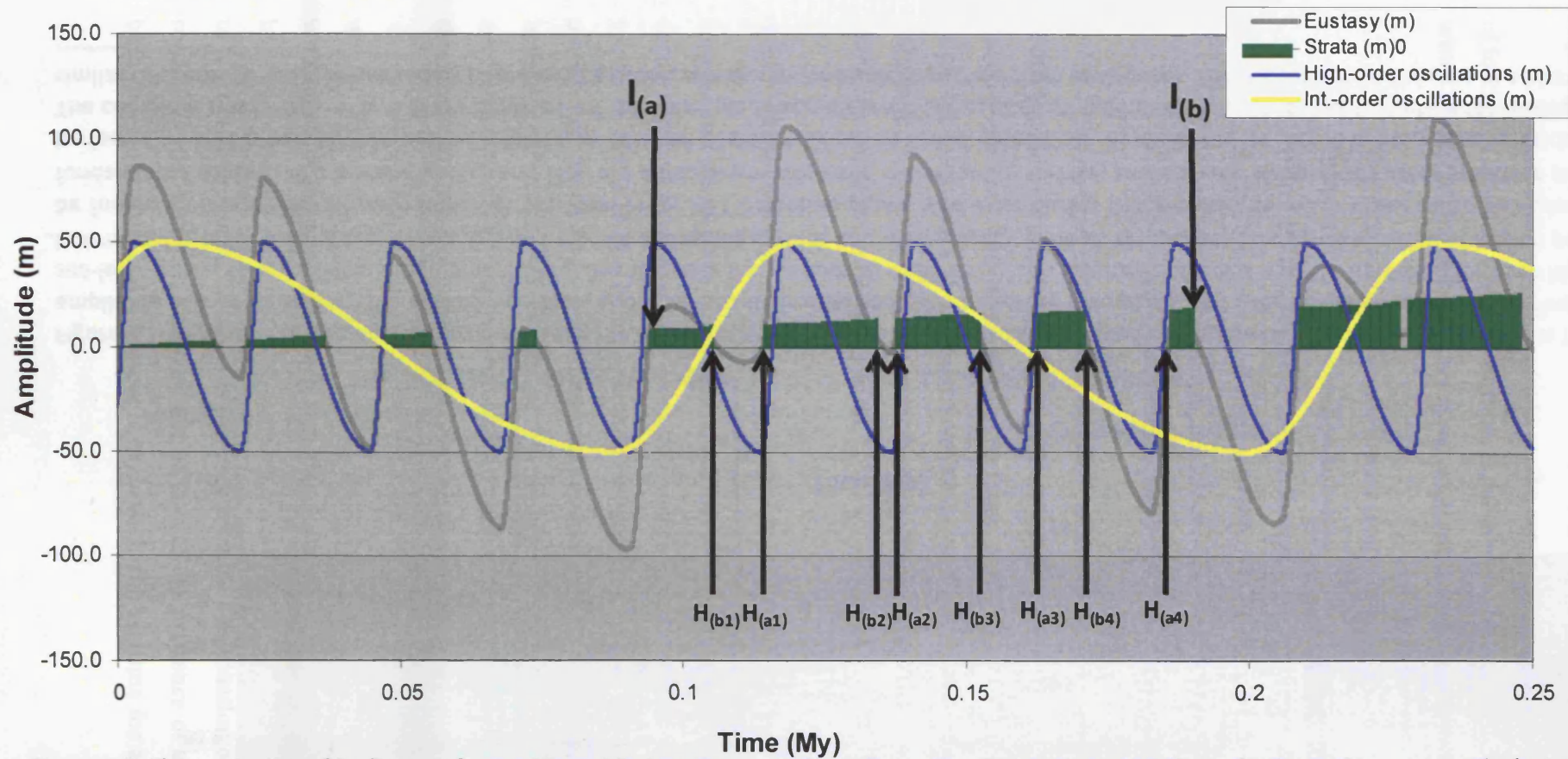


Figure 4.3: Chronostratigraphic diagram from a hierarchical section. (a) and (b) refer to flooding surfaces and discontinuity surfaces, respectively. I and H refer to intermediate-order and high-order, respectively. Diagram displays the way orders of forcing are attributed using inflection points. Note the difference from Figure 4.2: this diagram shows a hierarchical section with five high-order periods of forcing attributed during one intermediate-order period. The sedimentary hierarchy in this case is a result of high-order oscillations being of sufficient amplitude to flood the platform top on a regular basis.

Runs investigating:	Variables	Min. value	Max. value	Increment	Source
Eustatic amplitude	High-order amplitude	0m	40m	5m	Paterson <i>et al.</i> , 2006
	Intermediate-order amplitude	0m	90m	10m	Heckel, 1986; Wright & Vanstone, 2001
	Low-order amplitude	0m	40m	5m	Goldhammer <i>et al.</i> , 1994
Subsidence	Subsidence rate	20m/My	200m/My	20m/my	Allen & Allen, 1990
	High-order amplitude	5m	45m	5m	See above
	Intermediate-order amplitude	10m	100m	10m	See above
Carbonate accumulation	Euphotic accumulation rate	100m/My	1000m/My	100m/My	Smith & Kinsey, 1976; Bosence & Waltham, 1990
	High-order amplitude	5m	45m	5m	See above
	Intermediate-order amplitude	10m	100m	10m	See above
Sub-aerial exposure	Platform denudation rate	0m/My	100m/My	10m/My	Goldhammer <i>et al.</i> , 1991; Plan, 2005
	High-order amplitude	5m	45m	5m	See above
	Intermediate-order amplitude	10m	100m	10m	See above

Table 4.1: List of the variables used in runs investigating a hierarchy. Variables address a range of values according to an increment. For each run plan, the variables are modified one per run according to the increment, until each combination has been addressed.

3My, a time which gives the long-frequency eustatic components time to operate but does not represent an unacceptable runtime.

4.3 RESULTS OF MODELLING STUDIES

4.3.1 Runs investigating eustatic amplitude

4.3.1.1 *A hierarchy of sedimentary thickness*

The amplitude of eustatic oscillations represents the critical component in the development of a sedimentary hierarchy. It represents the ordered forcing mechanism necessary for the generation of a hierarchy. Therefore, in this first set of simulations the amplitudes of the three eustatic components form the independent variables. The dataset from these runs is evaluated in terms of evidence for both a hierarchy in terms of thickness of high-frequency sequences and in terms of time (i.e. the durations of hiatal periods recorded as exposure surfaces).

Of the 1000 runs conducted, 18.4% displayed a hierarchy in terms of terms of thickness (Figure 4.4). This relatively low percentage is a result of a very specific relationship between amplitudes of different orders of forcing and the potential creation of a sedimentary hierarchy. A stacking hierarchy in the sedimentary record is fundamentally dependent on the amplitude and frequency of sea-level curve components as it is these that apply the forcing mechanism order to the sediment. This is an important principle; stacking of cycles according to Milankovitch-ratios necessitates that it is the orbitally-forced oscillations which contain the order. In addition, note that the ordered periodic nature of any earth system oscillations in response to Milankovitch forcing as merely an assumption for most of Earth history. The sedimentary hierarchy is dependent on recognising, in some way, the order inherent in the forcing mechanism in terms of amplitude and frequency. Sedimentation, however, bears a non-linear relationship with time. Two periods of sedimentation of equal length may produce different thicknesses of strata depending on the depositional conditions during, and subsequent to, that period.

Figure 4.5 illustrates the importance of amplitude on the generation of a hierarchical section. The reason this specific amplitude relationship exists is due to the number of times a sea-level oscillation of a given order must cause sedimentation on the platform top during the lower-order oscillation on which it 'rides'. Minor variations in amplitude may cause high-order oscillations to be missed. If this occurs the hierarchy inherent in the forcing example begins to break down. Not only are there less 'beats' attributable to high-order oscillations, but the proportion of time (and potentially thickness) attributed to high-order oscillations is skewed closer to that of intermediate

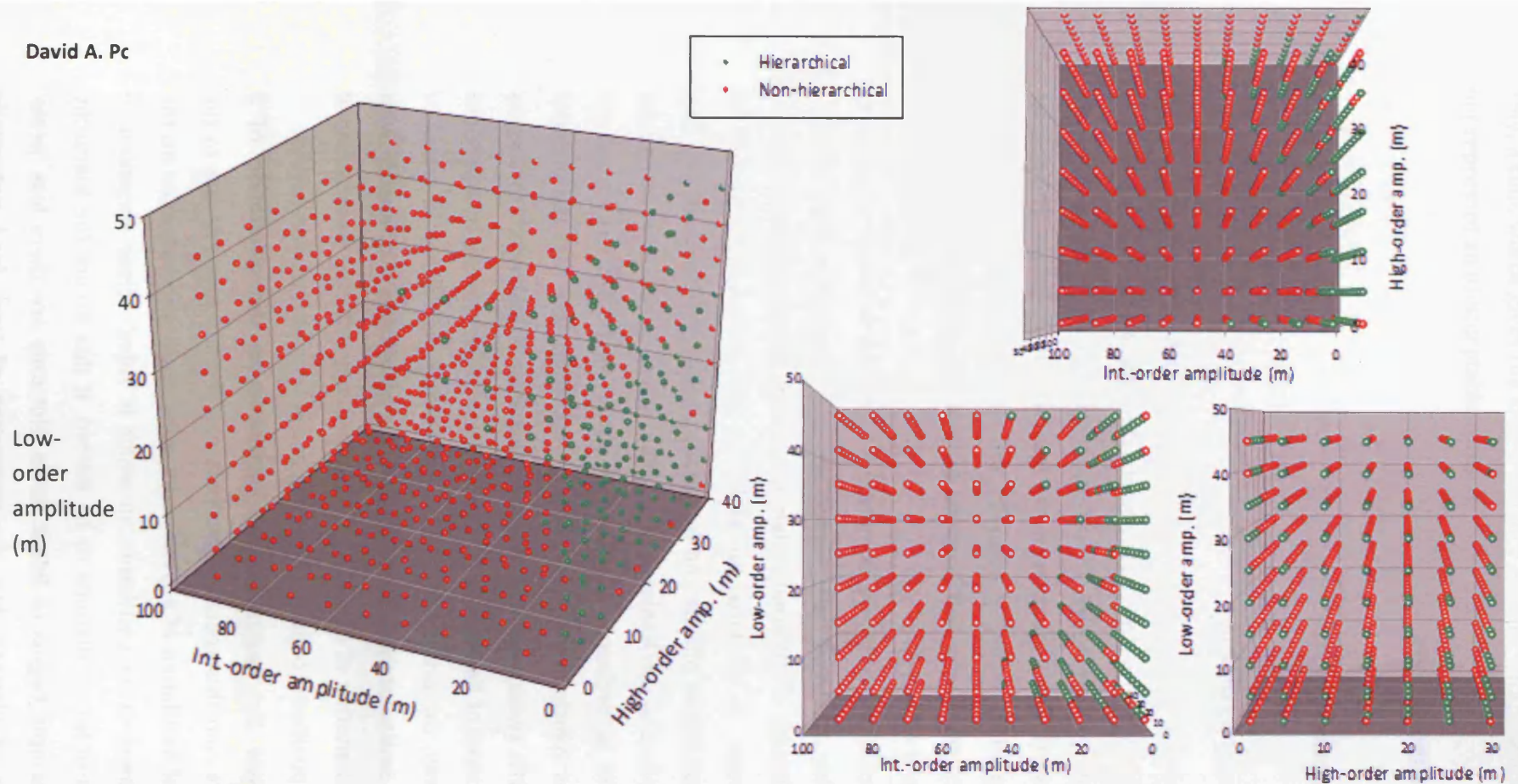


Figure 4.4: Parameter space plot comparing runs which contain hierarchical sections and those which do not. Axes are the variables used in each run; amplitudes of low-, intermediate- and high-order eustatic sea-level oscillations. The hierarchical sections show a very specific relationship between the amplitudes which give rise to the sedimentary hierarchy. To generate a hierarchy it is necessary for high-order sea-level oscillations to have an amplitude equal to, or greater than, 0.75 the amplitude of intermediate-order oscillations. If the high-order oscillations are less than this ratio they fail to submerge the platform sufficiently during the course of an intermediate-order oscillation to generate a hierarchy. Low-order oscillations compound this effect through the introduction of a third-frequency. This reduces the likelihood of high-order beats submerging the platform top on sufficient occasions to produce a recognisable hierarchy. This principle holds true if more orders of oscillation are also present; the more orders, the greater the degree of complexity, and the less likelihood of a hierarchy being recorded in the sedimentary record.

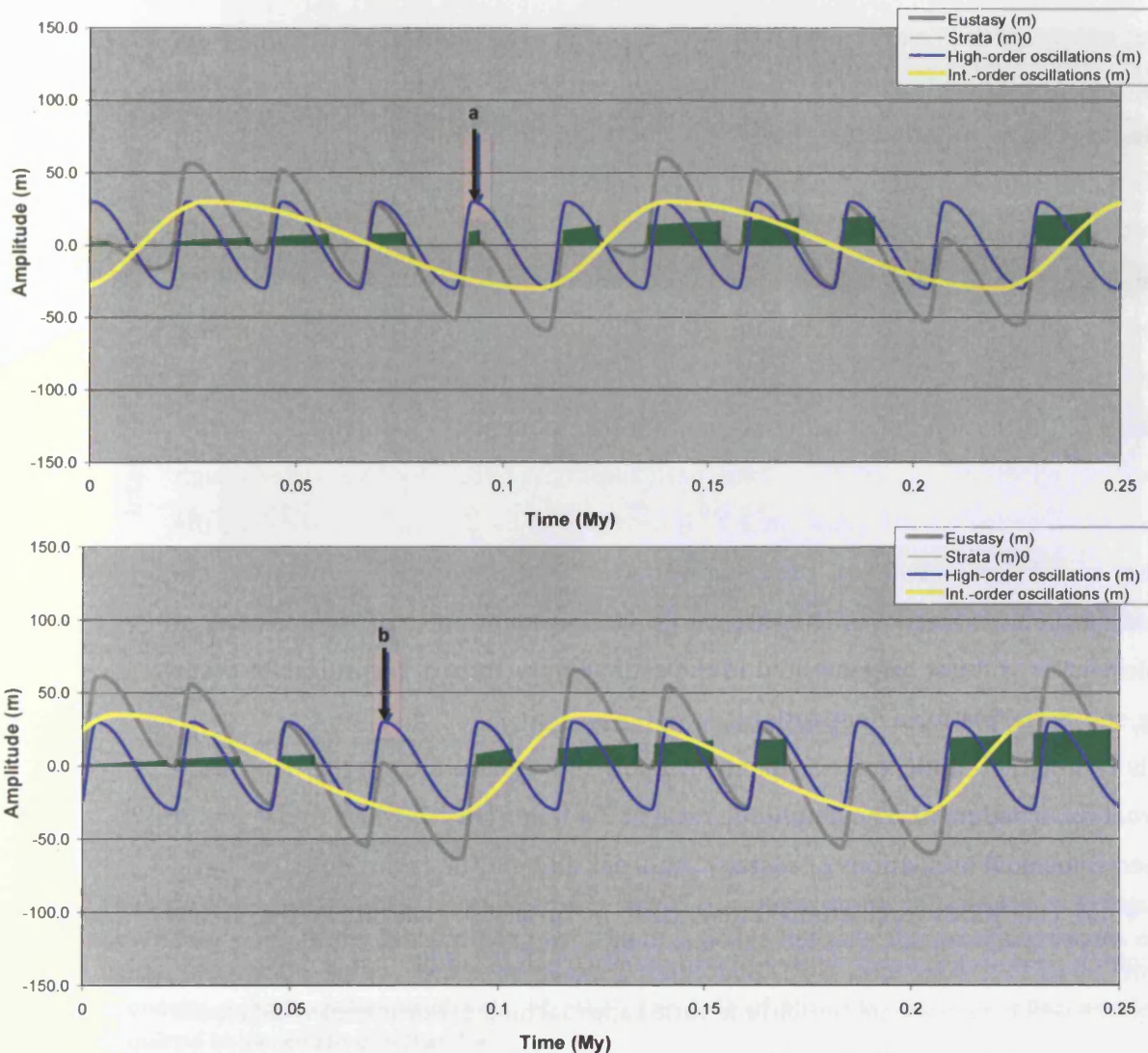


Figure 4.5: Chronostratigraphic diagram from a hierarchical section (top) and a non-hierarchical section (bottom). The hierarchical section has an amplitude ratio between the high-order and intermediate order components of 1:1 (both have amplitudes of 30m) whilst the non-hierarchical section has an amplitude ratio of 0.7:1 (the high-order component has 30m amplitude and the intermediate-order component 35m amplitude). The resulting difference is the absence of a hierarchy. The amplitude change causes high-order beats to be 'missed' (compare points a and b) and not recorded as sedimentation. This increases the proportion of time (and therefore thickness) attributed to high-order forcing, and as a result the periods of sedimentation attributed to different orders are no longer distinguishable from each other. In this example (at the beginning of a run), the lower plot still appears hierarchical, however over the full run of 3My (only 0.25My depicted) there are sufficient examples of high-order thicknesses exceeding those of intermediate-order to rule out a hierarchical structure in terms of thickness.

order. In the example of Figure 4.4, the increased numbers of missed beats (i.e. Figure 4.4; b) ultimately results in the breakdown of the hierarchy. Enough periods of sedimentation need to be recorded on the platform top, consistently, in order to generate the hierarchy. This is a relationship which holds true for all levels of the hierarchy.

The link between amplitude of opposing orders can be further refined by contrasting ratios at which a hierarchy does and does not occur. Figure 4.5 suggests that for a simple case of two summed eustatic components, the minor component must have an amplitude ratio of 3:4 (or 0.75) to generate a hierarchy. This figure is stable for this simple scenario but is broken down as more complexity is introduced. By solely examining high- and intermediate-orders of forcing, without interference from any other forcing orders, we can see the basic nature of the relationship (Figure 4.6). Essentially, the inferior component (i.e. the higher-order oscillation) must have amplitude that is equal to, or greater than, 75% of that of the immediately superior component of the forcing hierarchy. This ratio of 3:4 represents the inferior-component amplitude necessary to ensure enough oscillations are recorded on the platform if a hierarchy is to be generated. Therefore the inferior forcing order must have an amplitude ratio of greater than 3:4 compared to the forcing order at the next level of the hierarchy. If this ratio is not met, then a hierarchy of stacked thicknesses will not be generated in the sedimentary record, regardless of other factors (e.g. sub-aerial platform denudation).

This ratio is not static and is dependent upon all factors affecting the deposition and preservation of sediment. The amplitude ratio of 3:4 holds true for the simple case of two summed sinusoidal oscillations of eustatic sea-level, and may be regarded as the basic amplitude ratio conditions oscillations must meet in order to generate a hierarchy. Scenarios which contain a greater degree of complexity, such as additional orders of sea-level oscillation, will have a greater amplitude ratio (approaching 1:1 or more) which must be met to generate a hierarchy (Figure 4.6).

Longer-term eustatic oscillations still conform to this ratio. However, as low-order oscillations are usually of less amplitude than higher-order oscillations the ratio is often superseded. This is primarily due to the order of magnitude difference in frequencies between Milankovitch-scale oscillations and low-order oscillations (1-3My; Read & Goldhammer, 1988) coupled with comparatively low amplitudes (less than 50m; Saller *et al.*, 1994; Barnett *et al.*, 2002). Therefore, a hierarchy between long-term low-order oscillations and Milankovitch-scale oscillations is generated more often than not. This reflects what occurs in the sedimentary record, where low-order stratal thicknesses are usually measured in hundreds of metres rather than the few tens attributed to intermediate-order. An example of this is the Honaker Trail section, which is considered to

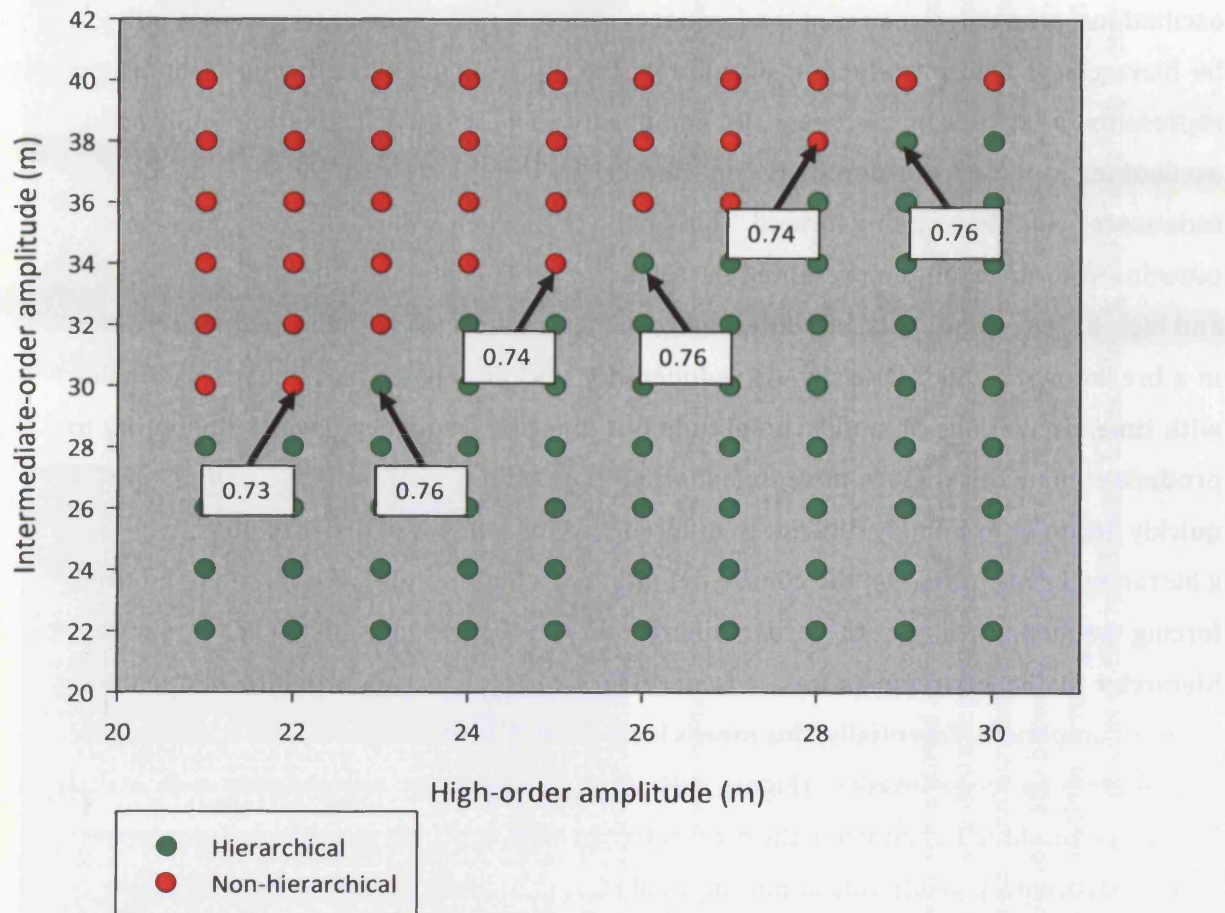


Figure 4.6: High-resolution cross-plot from model runs using same parameters as in Figure 4.5. Low-order oscillations are switched off. Caption boxes indicate the amplitude ratio of high-order oscillations to low-order oscillations (expressed as a decimal fraction). In this basic scenario, a high order amplitude of >0.75 (or 3:4) of the intermediate-order amplitude is required to generate a hierarchy.

be one low-order sequence of 151m, comprising multiple ten-metre scale intermediate-order cycles (Goldhammer *et al.*, 1991; refer to section 5.1).

Despite a hierarchy being present between Milankovitch-scale and low-order oscillations, primarily because of the frequency difference, the overall section may still not be hierarchical. The introduction of multiple (i.e. more than two) eustatic components represents a significant increase in complexity. The result of multiple interacting oscillations can be considered as 'interference' which decreases the likelihood of a sedimentary hierarchy being formed. This can be seen when a third eustatic component is introduced to the example presented in (Figure 4.7). The similar amplitudes of the low- and high-order components, but differing frequencies, causing 'missed beats' and resulting in a breakdown of the hierarchy. As sedimentary thickness has a non-linear relationship with time, oscillations of similar amplitude but differing frequency have the potential to produce similar thicknesses of sediment when they interact with further components. It quickly becomes extremely difficult to differentiate thicknesses in order to objectively say a hierarchy exists (based on the clinical definition of a hierarchy). The addition of multiple forcing frequencies masks the order inherent in the forcing mechanism. To generate a hierarchy in these circumstances it is necessary for one forcing-order to dominate in terms of amplitude. Essentially, this means increasing the amplitude ratio to a point where that order is no longer masked (Figure 4.8). With three eustatic components, even with a low-order amplitude of only 6m, the ratio between high- and intermediate-order increases to 1:1 (Figure 4.9). While this is not impossible, it is unlikely given modern estimates of rates of sea-level rise and fall (e.g. Heckel, 1986). It therefore seems improbable that even a small number of glacio-eustatic components can generate a sedimentary hierarchy (while up to seven have been advocated; e.g. Maynard & Leeder, 1992).

For this reason, in subsequent model runs, intermediate- and high-order oscillations are kept as independent variables along with a third interacting component (subsidence, carbonate production and sub-aerial platform denudation). The difficulty in generating a sedimentary section with three eustatic components suggests it is more appropriate to use only two eustatic oscillations as a control with which to assess the effect of the third independent variable.

Perhaps surprisingly, accommodation generation, and degree of stratigraphic completeness, has little bearing on the generation and preservation of a sedimentary hierarchy. Figure 4.10 shows that hierarchical sections occur over a range of stratigraphic completeness values. This is caused by runs with large eustatic amplitudes, which may result in long periods of exposure, and limited filling of accommodation (and therefore low recorded-time values) but still be hierarchical. This has important implications for the

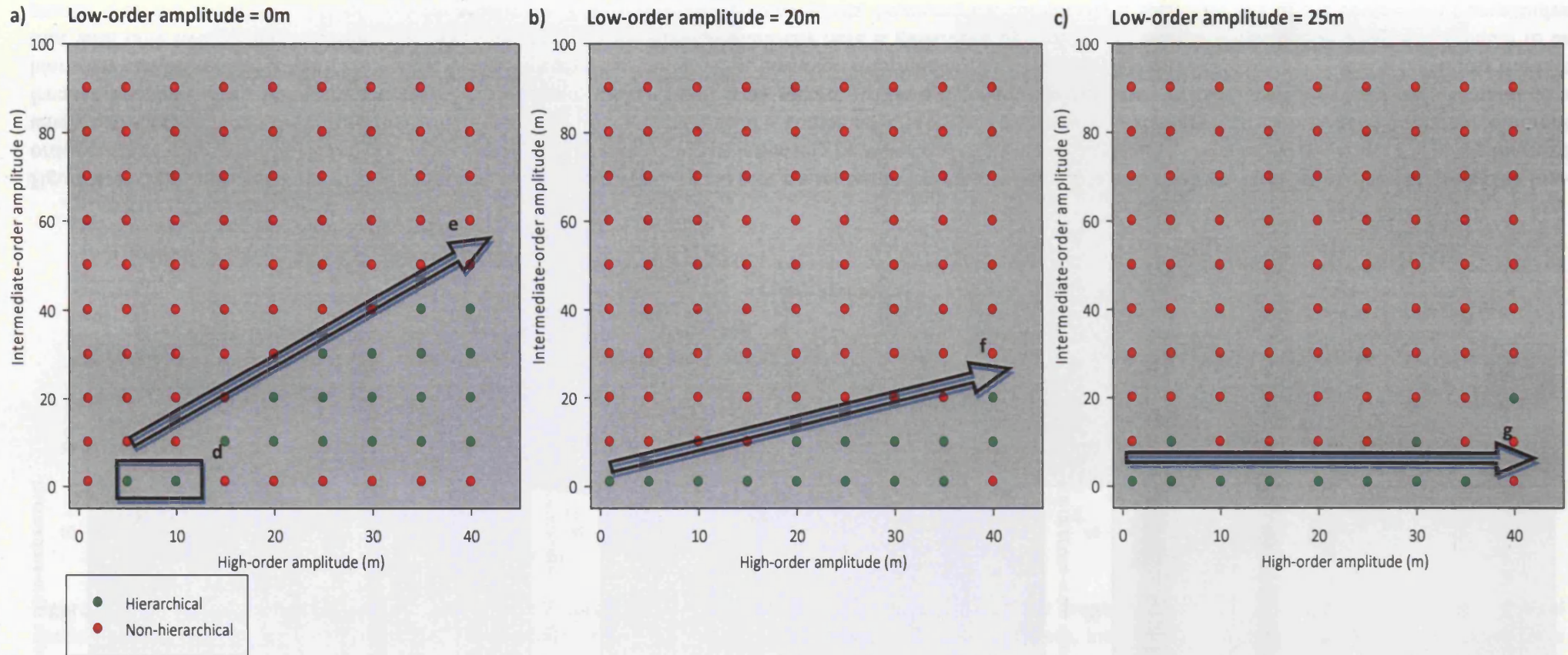


Figure 4.7: Cross-plots taken from the three-dimensional parameter-space plot presented in Figure 4.4. Plots a, b and c vary in terms of the amplitude of the low-order eustatic component. Box d shows runs which generate a hierarchy when all three eustatic components are of relatively similar size. A hierarchy is not maintained above 10m high-order amplitude as a result of this component becoming dominant, and masking lower order forcing signals. Arrow e shows the relationship between high- and intermediate order forcing: in order to generate a hierarchy the amplitude ratio between high- and intermediate order must be 3:4 or greater. Arrow f shows the breakdown of this relationship as a result of interference from low-order oscillations. Arrow g shows that as the 'interference'-order (low-order) in this case equals or exceeds the amplitude of the order responsible for the sedimentary hierarchy (high-order), this relationship breaks down, and a hierarchy is only constructed where two orders are dominant (i.e. intermediate-order amplitude is very low).

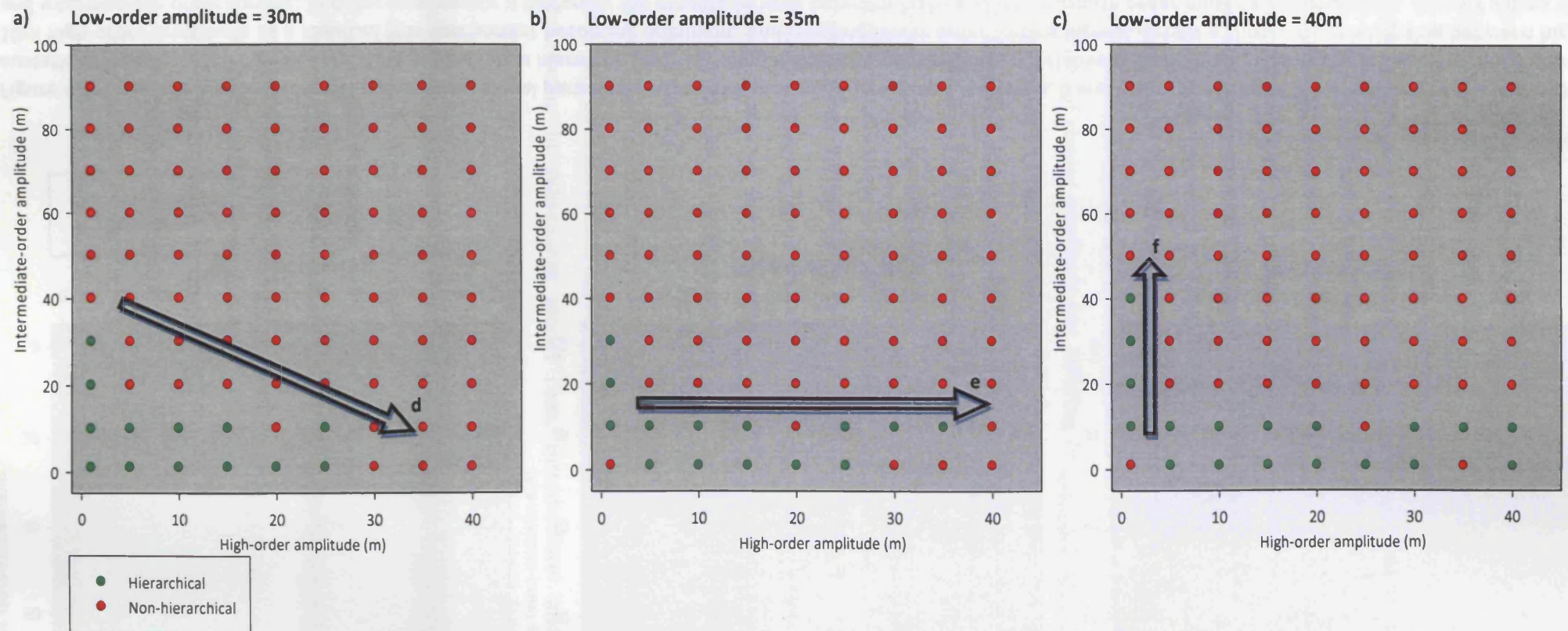


Figure 4.8: Cross-plots taken from the three-dimensional parameter-space plot presented in Figure 4.4. Plots a, b and c vary in terms of the amplitude of the low-order eustatic component. Arrow d shows breakdown of the hierarchical relationship between orders at higher high-order amplitudes. A hierarchy is only generated when high-order amplitude is less than low-order amplitude; otherwise the combined effects of two orders of forcing with similar amplitudes but different frequencies serve to mask the forcing signal represented in the sedimentary record. Arrow e highlights this effect; with an increase in third order amplitude a hierarchy can be generated within a greater range of high order amplitudes, however, intermediate-order amplitudes must remain low. Arrow f illustrates the fact that with only two forcing frequencies a hierarchy may be generated. A hierarchy here is generated by intermediate-order amplitude as long as it is equal to or greater than the amplitude of the low-order amplitude. With three forcing components, however, the complexity is such that one of the component's amplitudes must be very low (to be of negligible effect) for a hierarchy to be generated.

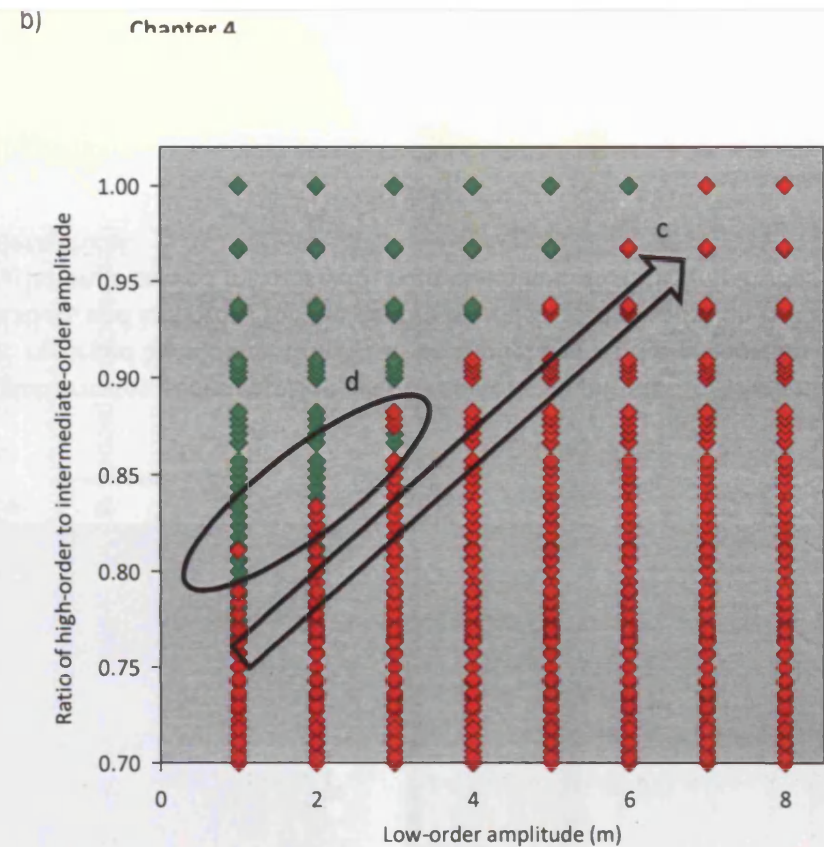
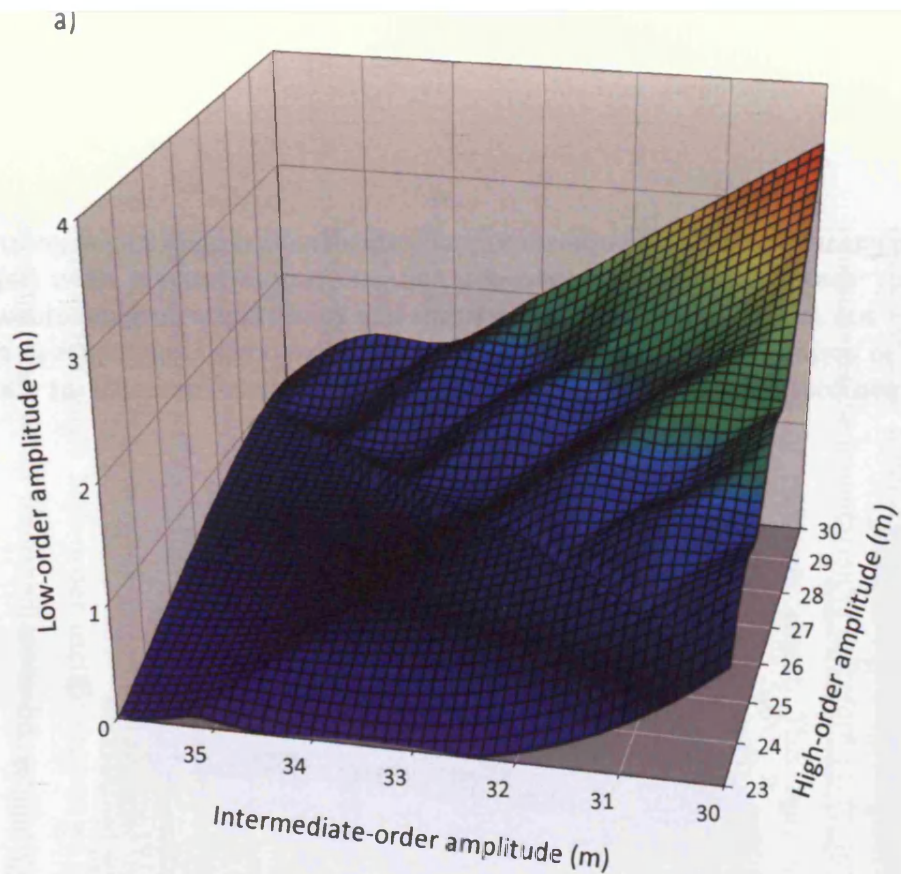


Figure 4.9: a) Three-dimensional contour plot of hierarchical model runs. The plot is representative of the greatest low-order amplitude at which a hierarchical section will be created, for given high- and intermediate order amplitudes. As low-order amplitude increases, intermediate-order amplitude must decrease for a section to be hierarchical. b) Comparison of the high- to intermediate-order amplitude ratio required to generate a hierarchical section (green points) and the ratio in those runs which do not generate a hierarchy (red points). As low order amplitude increases, the amplitude of high-order oscillations (and therefore the ratio against intermediate order beats) must increase to generate a sedimentary hierarchy (c). Ellipse d shows that this amplitude relationship has a 'fuzzy' boundary. Around the ratio transition from hierarchical to non-hierarchical, there may exist occasions at which specific amplitudes give rise to combined oscillations of sea-level which still produce non-hierarchical sections, despite having a sufficiently large amplitude ratio. This does not occur in simulations with only two eustatic components, and represents 'interference' from additional eustatic components. At sufficiently large ratios, this does not occur.

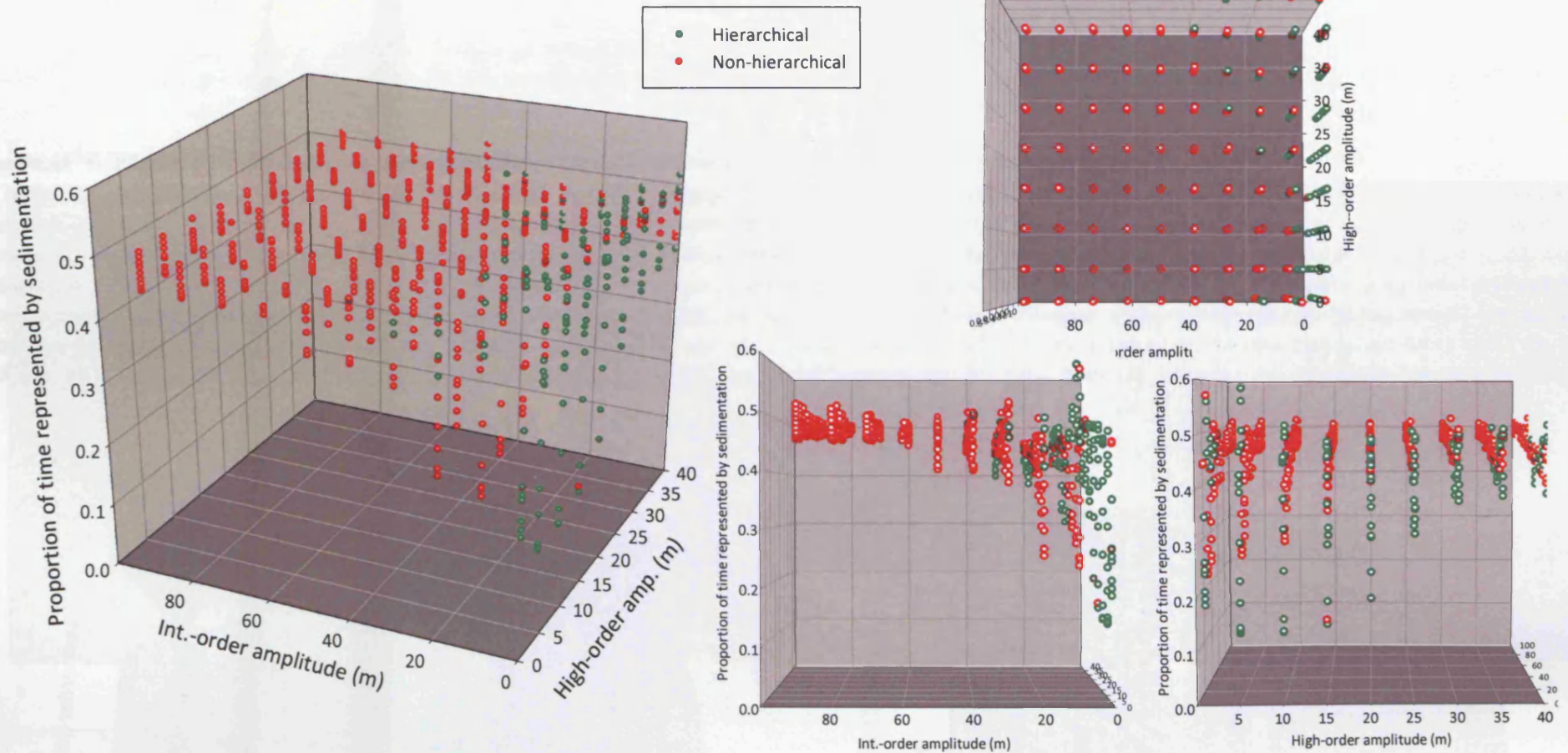


Figure 4.10: Parameter-space plots comparing the proportion of time recorded as platform-top sedimentation against eustatic amplitudes for hierarchical (in terms of sedimentary thickness) and non-hierarchical runs. The proportion of time recorded by sedimentation can be thought of as the proportion of time sedimentation is occurring during one eustatic oscillation, averaged over one simulation, and is a proxy for the degree to which accommodation is filled. The greatest range in terms of time-recorded is evidenced by hierarchical runs. The variation is caused by runs with high combined eustatic amplitudes, which may result in long periods of exposure (and low recorded-time values) but still be hierarchical.

hierarchical potential of subtidal sections as compared with peritidal sections. It may be intuitively expected that peritidal successions, representative of a more complete filling of accommodation, may more accurately record excursions of relative sea-level. However, modelling suggests this not to be the case. The fact that hierarchical runs occur over a greater range of stratigraphic completeness values than non-hierarchical runs, suggests that the generation of a hierarchy in a sedimentary succession is independent of the degree to which accommodation is filled. Peritidal successions, which fill accommodation to sea-level, are therefore no-more likely to contain a sedimentary hierarchy than subtidal successions.

Attempting to model hierarchical sections also brings into question the use of vertical stacking patterns to identify a sedimentary hierarchy. Figure 4.11 shows a model run of a hierarchical section that does not show the thinning-upwards parasequences advocated by many workers. Instead, the high-frequency sequence with the greatest thickness can be said to exist during the highstand of the intermediate-order oscillation. Prior to this, during the intermediate-order transgressive systems tract, a thinner high-frequency sequence is developed (if a high-order oscillation results in sedimentation at all). The greatest accommodation exists as a result of the combined peaks of intermediate- and high-order oscillations. Furthermore, this particular combination of oscillations results in the longest duration of platform submergence possible from two eustatic components. Sedimentation is therefore more likely to take place for longer and greater accumulations of sediment result. This may not be the case for particularly high amplitudes of oscillation, which may result in production occurring only very slowly from the oligophotic and aphotic factories. During these types of oscillation, however, the falling-stage systems tract will still be extended and substantial thicknesses of sediment are deposited when the oligophotic and euphotic factories dominate production.

All hierarchy-generating scenarios based on varying amplitudes of eustatic oscillation result in high-frequency sequences being deposited during the transgressive systems tract of an intermediate-order oscillation. The frequencies of the Milankovitch parameters, the estimated amplitudes of sea-level change, and the very nature of a hierarchy dictate that this is so. Based on the way eustatic parameters interact, and when periods of sedimentation occur during an intermediate-order oscillation, it does not seem realistic to expect the thickest high-frequency sequence to be at the base of every sequence (e.g. Goldhammer *et al.*, 1987).

The asymmetry of intermediate-order oscillations would affect this stacking pattern if a single high-order oscillation was of greater duration than the transgressive systems tract of an intermediate-order oscillation. However, as both intermediate- and high-order oscillations are considered to be fixed Milankovitch parameters, this could only

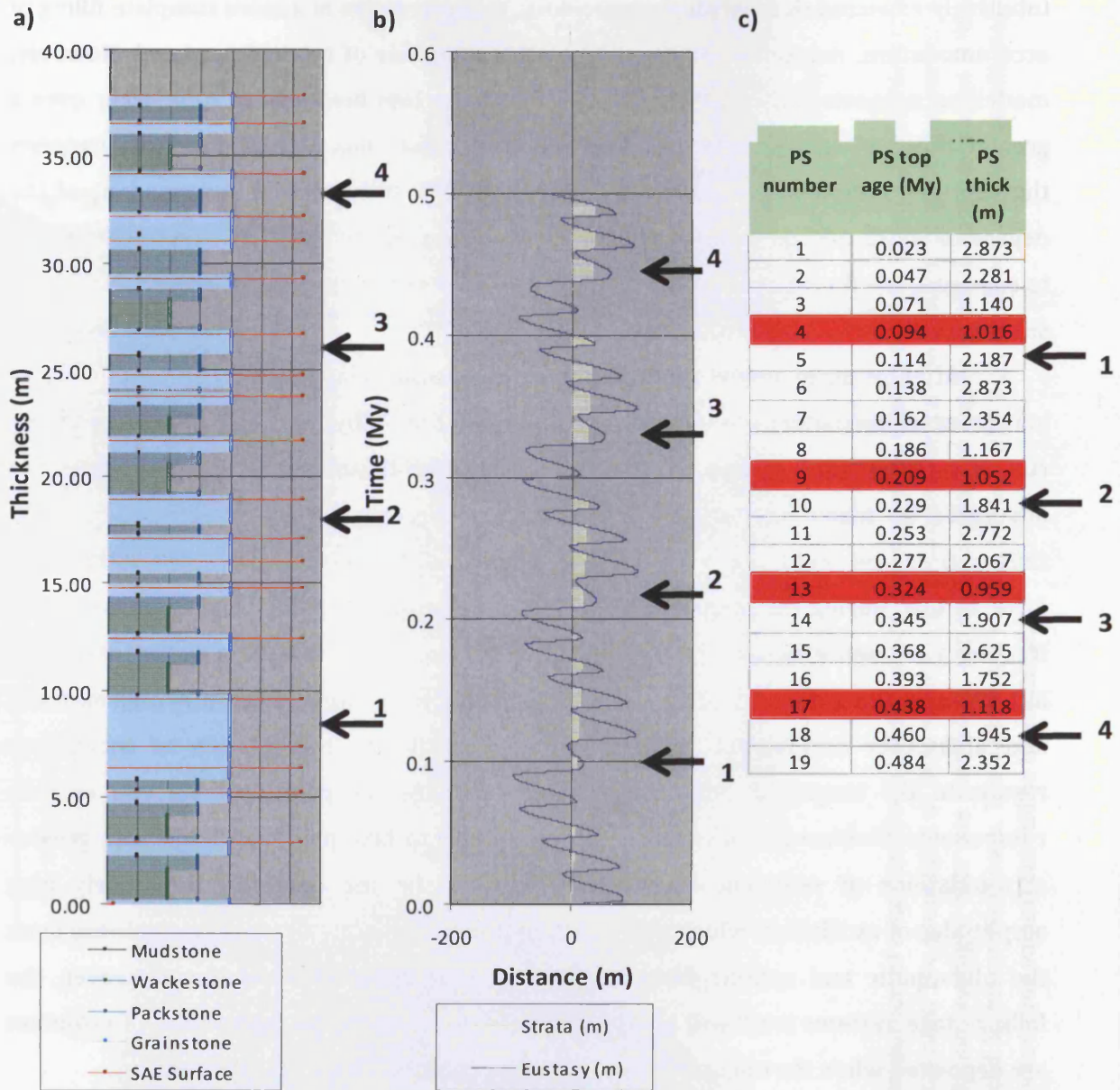


Figure 4.11: Thicknesses of parasequences from a hierarchical section. a) Synthetic stratigraphic column. b) Chronostratigraphic diagram. c) Parasequence number, age and thickness (red sections mark the last parasequence of a parasequence-set). Arrows denote thinner parasequences at the start of every parasequence set. N.B. The first parasequence begins at the base of the plots.

be achieved through increasing the asymmetric aspect of the oscillation (which itself is relatively well constrained; Crowley & Baum, 1991). As they have the same control, if the asymmetric aspect is increased (from the 95% asymmetry used in these simulations), then the high-order oscillation asymmetry would also increase. Thus little difference would be made to the occurrence of high-frequency sequences during intermediate-order transgressive systems tracts. In addition, high-order oscillations are not considered to correspond to an exact ratio with those of intermediate order; the occurrence of high-order oscillations is not fixed relative to lower-order oscillations. They will therefore vary in terms of their relative position, and the thickest high-frequency sequence may not necessarily always be at the base of a sequence.

4.3.1.2 A hierarchy of hiatal duration

A hierarchy in terms of hiatal duration may be considered a more accurate indicator of a hierarchical and ordered forcing mechanism. If high-frequency ice-house sea-level excursions result from glaciation forced by changes of insolation due to variations in the Earth's orbit, the durations of hiatuses should bear a direct relationship to the periodicity of the forcing mechanism. Unlike sedimentation, which is dependent on numerous other factors, the duration of a hiatus is not subject to modification by factors such as sedimentation rate and is a comparatively direct effect of changes in relative sea-level. While tectonics may affect this, it is unlikely to have as great an effect as Milankovitch parameters are considered to, especially over short time-scales. Reliably and accurately dating the duration of a hiatus at outcrop, is however, impossible at the current time. For this reason, hiatal durations, despite the likelihood of being able to accurately record a hierarchical forcing mechanism, have been appropriately ignored. Forward modelling, however, allows knowledge of the precise duration that a hiatus on a platform surface exists for. If the model is able to produce realistic packages of strata as the result of reasonable inputs, then there is no reason to mistrust the durations of hiatuses that are a component of these packages.

A hiatus hierarchy is much more prevalent than a sedimentary hierarchy, occurring in 62.4% of model simulations (Figure 4.12). This is a result of the direct time-based relationship between hiatus-duration and the wavelength of the eustatic components. A hiatus hierarchy is not subject to autocyclic processes and has only allocyclic controls. Lower-order oscillations have longer lowstand system tracts, and are more likely to expose the platform for a longer period of time than those of a higher-order. Unlike sedimentary thicknesses, this period of time is not subject to syn-depositional or post-depositional modification and is therefore the simplest and most accurate record of a sedimentary hierarchy.

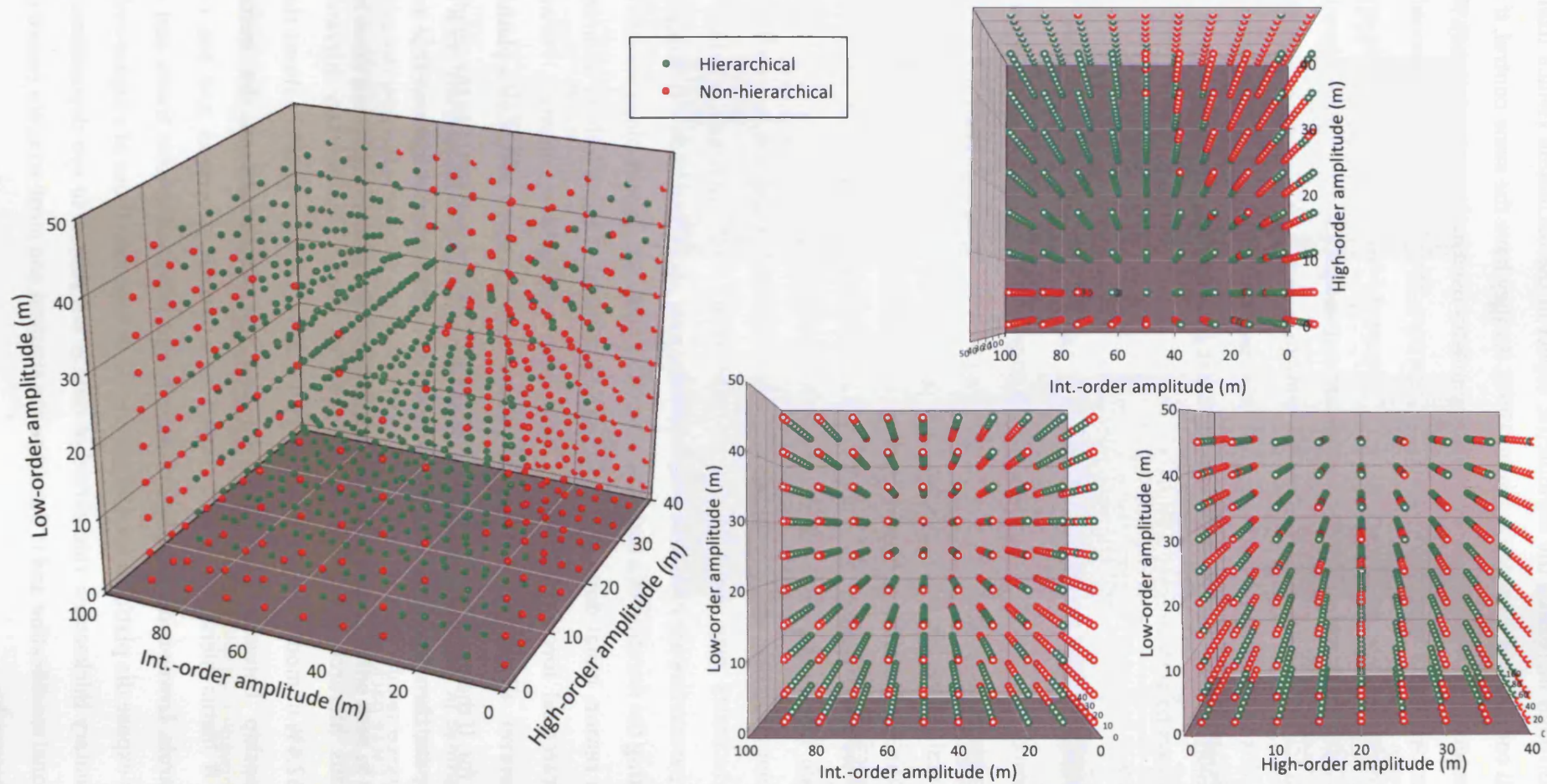


Figure 4.12: Parameter-space plots comparing simulations where a hierarchy in terms of hiatus duration is generated, and those where it is not. A much greater number of simulations show a hiatus hierarchy than a sedimentary hierarchy (62.4% to 18.4% respectively). Hiatus duration is only dependent on the amplitude and wavelength of eustatic sea-level oscillations and so is a much more accurate recorder of an ordered forcing mechanism than sedimentary thickness (which is subject to autocyclic processes).

Figure 4.13 shows that as a result of this direct relationship with the forcing mechanism the generation of a hiatal hierarchy is much more robust in recording the forcing. The introduction of a third eustatic component (low-order) has less of an effect on hiatal hierarchy, than thickness hierarchy because the duration of a hiatus is dependent on only the combined effects of eustacy during a lowstand period. If the durations of lowstands forced by different orders are still distinguishable from one another, then it is possible to assess the existence of a hierarchy.

Interestingly, Figure 4.13 (d) shows that for all low-order amplitudes a hierarchy is not generated when high-order amplitudes do not consistently cause sedimentation on the platform top. As intermediate-order amplitude increases a hierarchy is less likely to be developed, yet as low-order amplitude increases a hierarchy may be developed at higher intermediate-order amplitudes. This shows the replacement of high-order oscillations as the cause of the primary 'beat' of a hierarchy. In this case the hierarchy is consistently generated by low- and intermediate-order oscillations. This reiterates the fact that a hierarchy may be generated between any two orders of the hierarchy, regardless of wavelength and amplitude, at least in terms of hiatal duration. This is not necessarily the case for a thickness hierarchy, where because of a lead-dependent relationship between time and the sedimentary system, eustatic wavelength and thickness may not necessarily fall into a hierarchical relationship (see section 4.3.1.1). This is reiterated in Figure 4.13 (g), where high low-order amplitude substitutes for intermediate-order amplitude, and a hierarchy is generated with high-order amplitude.

Figure 4.13 (e) illustrates the amplitude dependence between orders of forcing further. When intermediate-order amplitudes are low, high-order amplitudes must also remain relatively low to generate a hierarchy. Comparatively Figure 4.13 (f) indicates that with increasing low-order amplitude, greater intermediate-order amplitudes are required to generate a hierarchy. Again the cause behind this is the necessity of recording enough beats on the platform top to generate a hierarchy. If this does not take place, then hiatal durations for the higher-order lowstands become longer, and cannot be distinguished from hiatuses belonging to a lowstand of a lower-order.

In terms of accommodation, as with a thickness hierarchy, there is no relationship between the degree of accommodation filled and the generation of a hiatal hierarchy (Figure 4.14). Both non-hierarchical and hierarchical simulations record an average of approximately 45% of the total time during the simulation with preserved deposition. There is no indication that simulations where a greater proportion of time is recorded by sedimentation equates to a greater likelihood of generating a hierarchy.

It may be noted by comparing Figure 4.14 and Figure 4.10 that simulations generating a sedimentary hierarchy often do not generate a hiatal hierarchy (Figure 4.15).

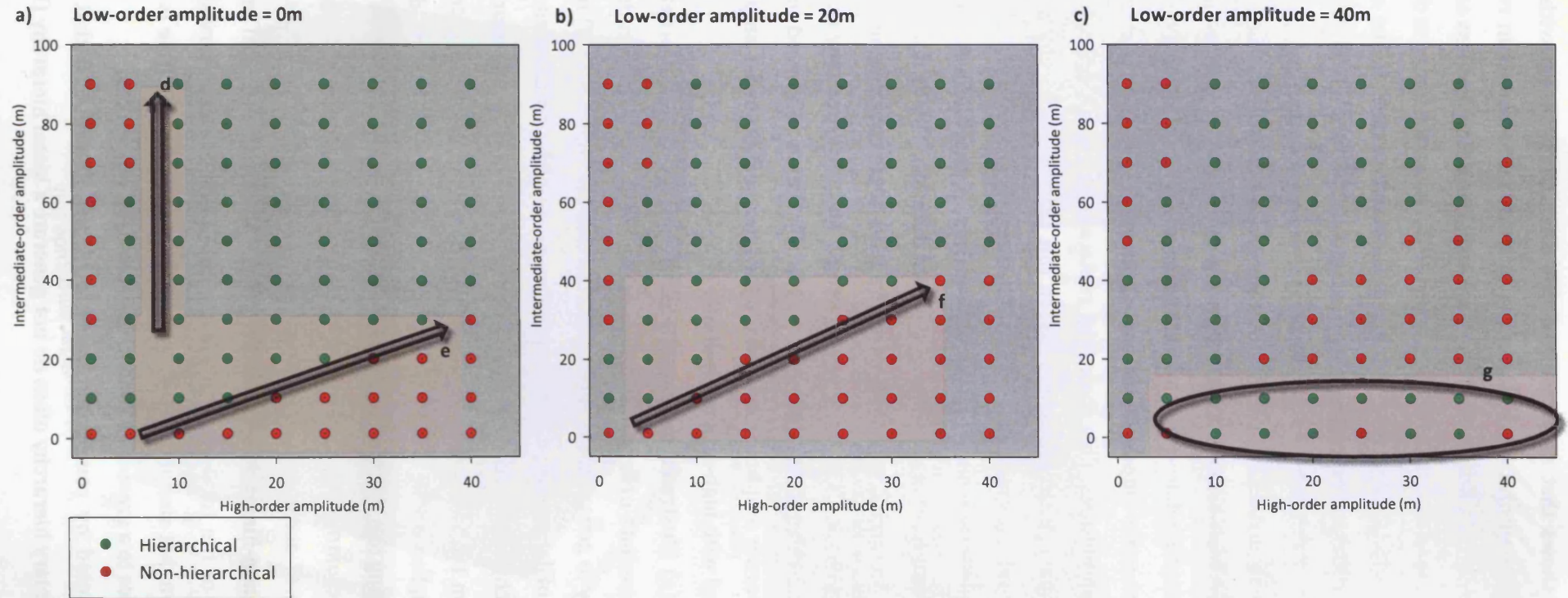


Figure 4.13: Cross-plots taken from the three-dimensional parameter-space plot presented in Figure 4.10. Plots a, b and c vary in terms of the amplitude of the low-order eustatic component. Trends in terms of a hiatal hierarchy are affected less by the introduction of more eustatic components compared to trends in terms of a sedimentary hierarchy. Arrow d identifies a trend that is present in all three plots. For all low-order amplitudes a hierarchy is not generated when high-order amplitudes do not consistently cause sedimentation on the platform top. Arrow e shows that when intermediate-order amplitudes are low, high-order amplitudes must also remain relatively low to generate a hierarchy. Arrow f indicates that with increasing low-order amplitude, greater intermediate-order amplitudes are required to generate a hierarchy. A hiatal hierarchy may be generated if low-order amplitudes are relatively high enough to effectively act as a substitute for intermediate-order amplitudes, yet because of their long wavelength, still allow high-order oscillations to regularly cause sedimentation on the platform top (Ellipse g).

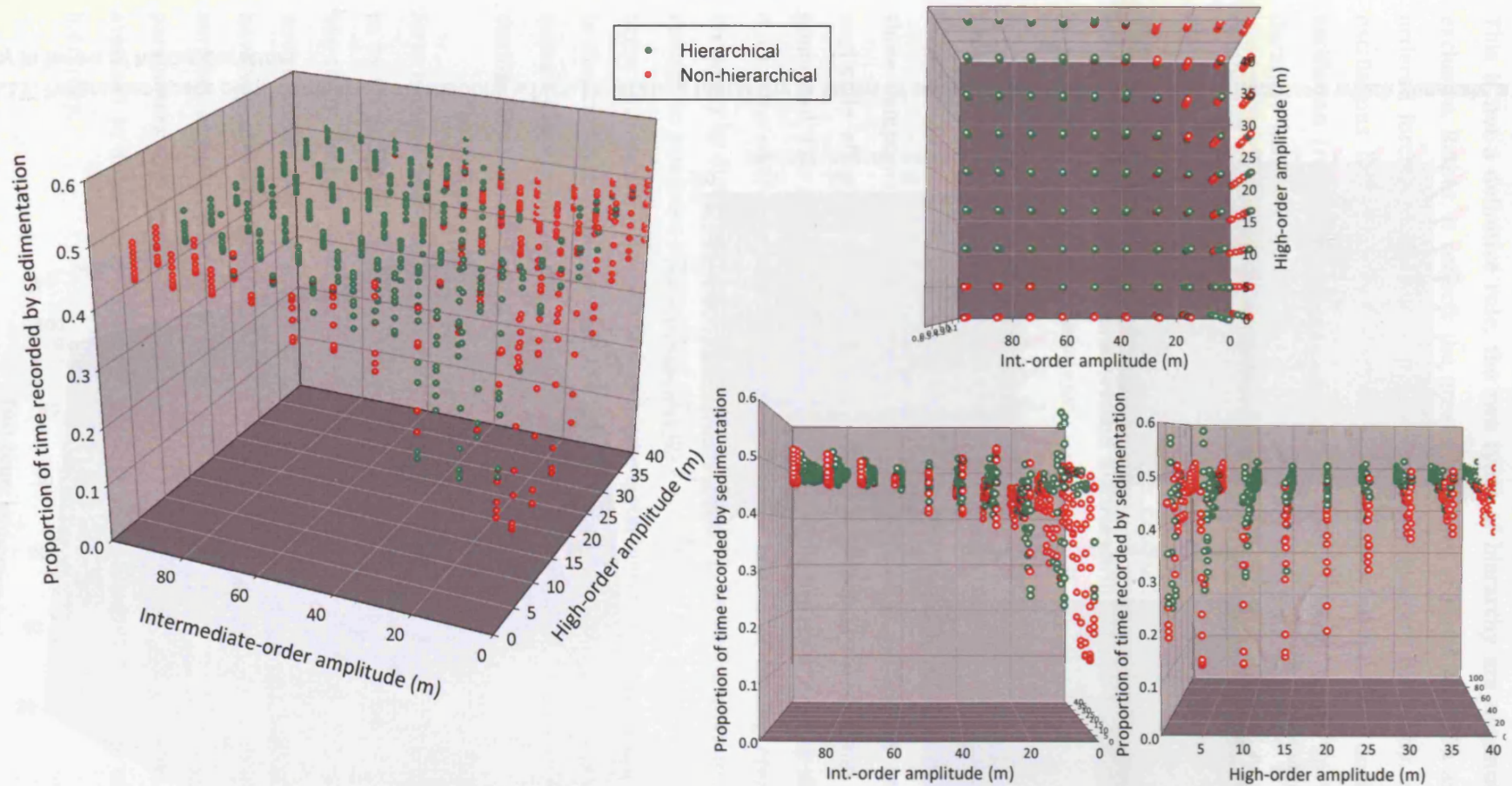


Figure 4.14: Parameter-space plots comparing the proportion of time recorded as platform-top sedimentation against eustatic amplitudes for hierarchical (in terms of hiatal duration) and non-hierarchical runs. The proportion of time recorded by sedimentation can be thought of as the proportion of time sedimentation is occurring during one eustatic oscillation, averaged over one simulation. There is no significant trend to differentiate between hierarchical and non-hierarchical simulations.

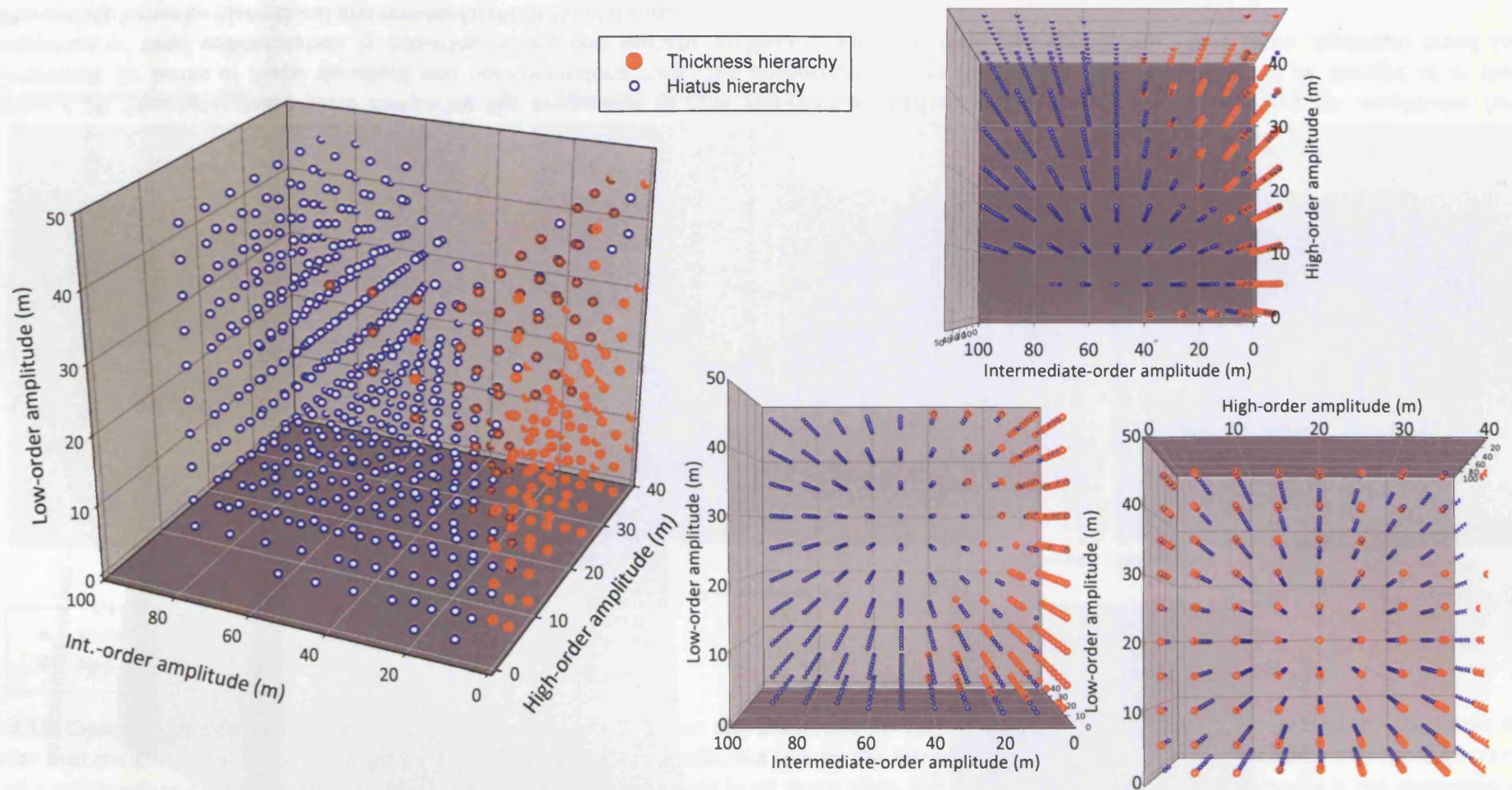


Figure 4.15: Parameter-space plots comparing simulations which generate a hierarchy in terms of sedimentary thicknesses and simulations which generate a hierarchy in terms of hiatus duration.

This is not a definitive rule; the two types of hierarchy are not mutually inclusive or exclusive. Rather, it reflects the greater accuracy of hiatal duration as a recorder of an ordered forcing mechanism. To generate a sedimentary hierarchy, one set of higher-oscillations have to submerge the platform most of the time during a lower-order oscillation (regardless of the mechanism) which usually break up the effect of long duration hiatuses at the lower-order lowstands. This principle is illustrated when comparing Figure 4.2 and Figure 4.3; longer lowstands exist in the simulation not displaying a sedimentary hierarchy. This effect does not always necessarily occur, but it usually does; as if the platform surface is exposed during lowstands of higher-order oscillations, then lower-order lowstand hiatuses will also usually be interrupted by the higher-order oscillations.

There are situations where both forms of hierarchy can be generated (denoted by overlapping points in Figure 4.15). These scenarios exist where two eustatic components dominate in terms of amplitude, suppressing the influence of the third component. In a three component system, if one of the amplitudes is sufficiently small as to have a negligible effect on overall eustacy, both a sedimentary and hiatal hierarchy can be generated. This reflects the interference of multiple orders of eustacy discussed in section 4.3.1.1. In such a scenario, the two dominant orders of forcing create a sedimentary hierarchy by dictating the length of periods available for sedimentation (which occur often enough to comprise a hierarchy), but do not truncate the hiatal durations of the lower-order with regularly enough to disrupt the hiatal hierarchy. In practical terms, this equates to the amplitude ratio between the two orders existing in a 'sweet-spot', where beats are missed slightly below the platform in the lowstand, but are not missed as frequently during a lower-order highstand.

The different prevalence of the two forms of hierarchy raises the question of which form is more relevant; a topic discussed in section 4.4.3. A hiatal hierarchy is more likely to be recorded in a modelled environment, and best reflects the forcing mechanism. A hierarchy derived from sediment thickness, is much harder to detect in a modelled environment, but potentially will be better detected at outcrop. Hiatal hierarchies, however, are not detectable to any degree in the development of sub-aerial exposure surfaces at outcrop or in the sub-surface. It is only in a model environment, where all parameters are known, that their effect can be quantified. For this reason, variables assessed in subsequent sections are primarily evaluated in terms of the sedimentary hierarchy.

4.3.2 Runs investigating subsidence

Subsidence represents the fundamental control on accommodation. Even with an ordered forcing mechanism, a hierarchical section would not be generated without some form of subsidence. Broad trends in the relationship between subsidence, an ordered forcing mechanism and the likelihood of generating a sedimentary hierarchy can be identified by examining parameter-space plots of model runs which use subsidence as a variable (Figure 4.16).

With increasing subsidence a sedimentary hierarchy is less likely to be generated with larger intermediate-order amplitudes. It can be said that a cut-off exists at 40m intermediate-order amplitude, above which a hierarchy will not be generated under these conditions. Clearly, this is not true for all scenarios; higher carbonate production rates may still influence the development of a hierarchical section, for instance. However, with two eustatic components and subsidence as the main independent variables a hierarchy will not develop above this cut-off. In addition, as previously mentioned, a specific amplitude ratio is necessary to develop a sedimentary hierarchy in the first instance. In a very simple model environment (and with 70m/My subsidence rate), this can be said to be 0.75 (or 3:4; discussed in section 4.3.1.1). Therefore, once intermediate-order amplitude exceeds the point at which high-order amplitude can meet this ration (i.e. above 50m and above) a hierarchy will not be developed.

With increasing intermediate-order amplitudes and increasing subsidence rates the platform is more likely to drown entirely and cease significant carbonate sedimentation. Above 120m/My a significant number of high-order beats are missed above the platform surface (i.e. they do not cause sub-aerial exposure, and may not influence sedimentation depending on the depth). As the number of missed beats increases, the hierarchy ceases to be generated. Consequently, hierarchical sections cease to be generated entirely above 120m/My subsidence rate. With large high-order amplitudes, a hierarchy is consistently generated up to 120m/My subsidence rate. These scenarios reflect runs where sedimentation is recorded regularly enough for a hierarchy to be generated. There therefore exists a set of rules under which a hierarchy can be generated: the basic amplitude ratio of 3:4 between forcing orders must be met, subsidence must be less than 120m/My and intermediate-order amplitude must be less than 40m (Figure 4.16; a).

At very low subsidence rates (<40m/My) a hierarchy is able to be generated, albeit in a restricted range of scenarios due to the limited accommodation available (Figure 4.17). A hierarchy is not generated above 40m intermediate-order amplitude (Figure 4.17; d) as the amplitude of the oscillation is sufficient to exceed the depth of maximum carbonate production. Once this occurs, little sediment is deposited during highstands,

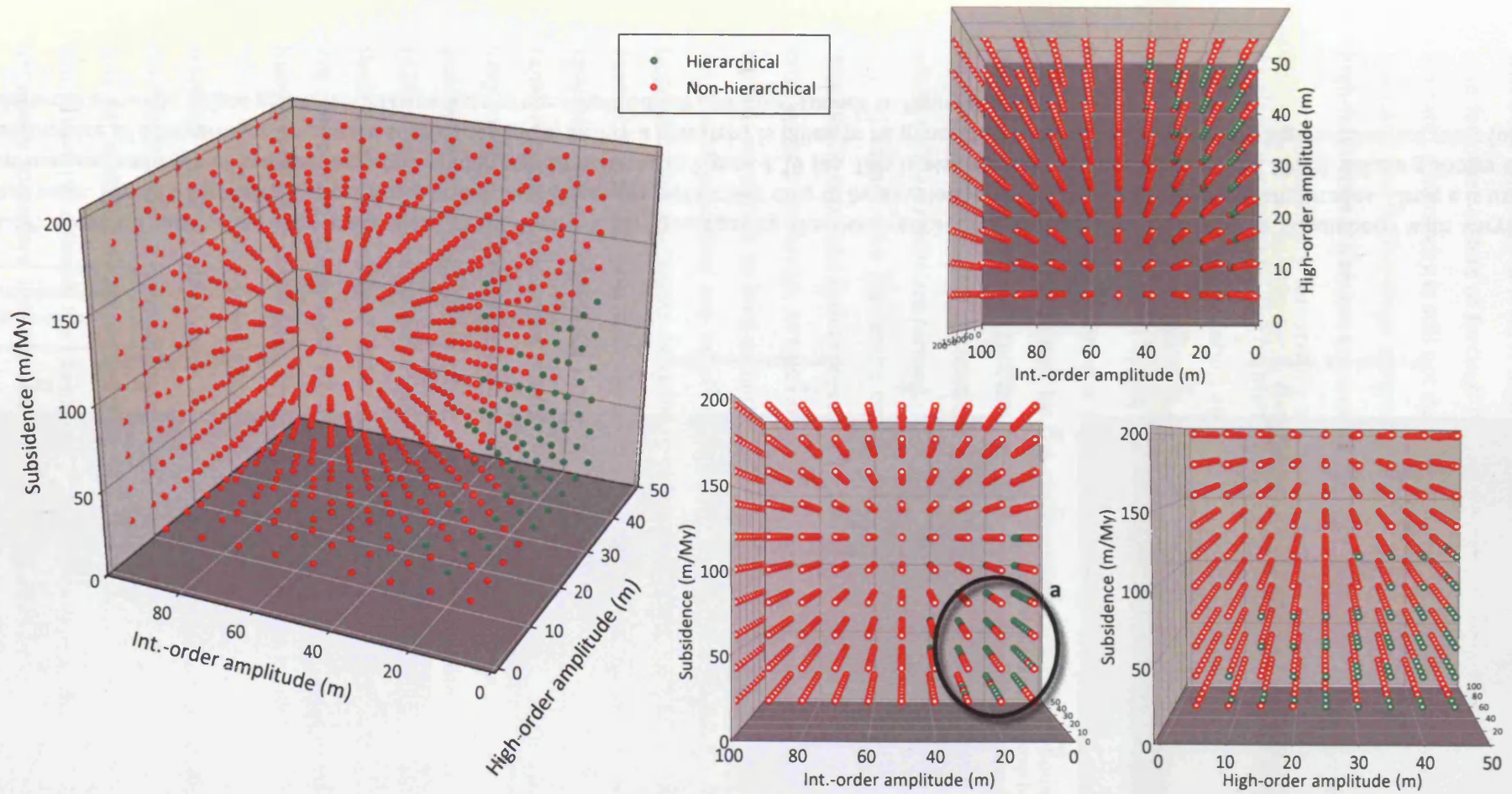


Figure 4.16: Parameter-space plots comparing those simulations which generate a sedimentary hierarchy and those which do not, using two eustatic components and subsidence as variables. Ellipse a denotes the main parameter-space area of hierarchy generation.

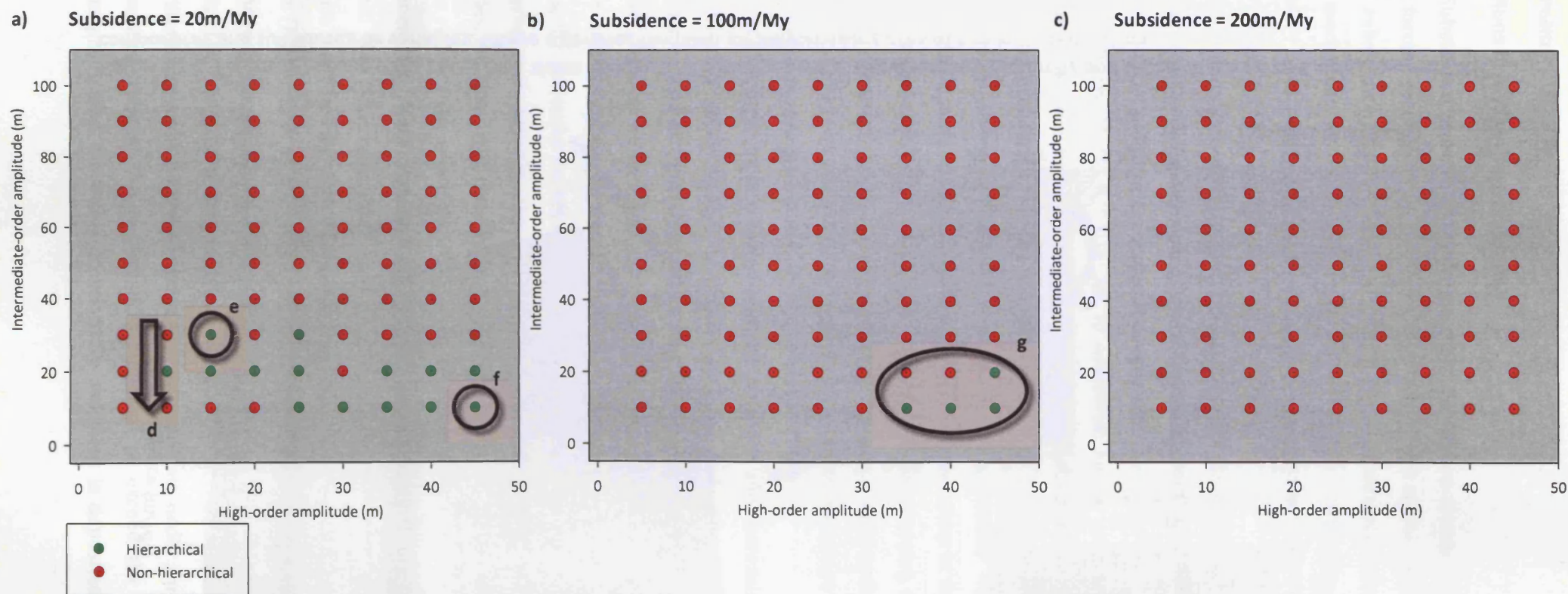


Figure 4.17: Slices through parameter-space plots (from Figure 4.16) investigating the occurrence of a sedimentary hierarchy in simulations with varying subsidence rates. Arrow d highlights the tendency at low subsidence for hierarchies only to be developed at low intermediate-order amplitudes. Circle e is used as an end-member example of sedimentary style in hierarchical sections in Figure 4.19 (a). This is also the case for circle f (Figure 4.19; b). Ellipse g shows the limited occurrence of a hierarchy at increased subsidence rates, before a hierarchy is failed to be generated in any simulation at very high subsidence rates (plot c). The hierarchical run (in ellipse g) with an intermediate-order amplitude of 20m corresponds to Figure 4.19 (c).

when the relative sea-level is high enough to suppress euphotic sedimentation. This is also true for other orders of forcing. Therefore even at amplitude-relationships exceeding the 3:4 ratio, a hierarchy is still not developed, as the majority of sediment is deposited during lowstand and falling-stage systems tracts. As a result, similar thicknesses sequence and high-frequency sequences are created, ruling out a hierarchy.

Sedimentary hierarchies are most likely to be generated at low subsidence rates. As already mentioned, the number of hierarchies forming below $<40\text{m/My}$ is restricted as a result of low accommodation and high-amplitude eustatic oscillations. The peak rate of subsidence for the generation of a sedimentary hierarchy is in the range of $40\text{--}80\text{m/My}$ (Figure 4.16). In practical terms, this equates to the subsidence rates which are most conducive to the formation of a hierarchy at the greatest number of eustatic variables. Below this rate, while limited by the constraining factors mentioned above, significant numbers of hierarchical sections are still able to be generated. Above 70m/My , the number of hierarchical simulations decreases to the cut-off point of 120m/My , above which no hierarchies are formed.

Figure 4.16 (a) can be considered to exist as the part of this continuum; where 70m/My subsidence rate represents peak subsidence conditions for the generation of a sedimentary hierarchy. At this rate, a hierarchy can be generated in the most number of eustatic scenarios, as long as both the amplitude ratio condition, and intermediate-order amplitude condition are met. Comparing Figure 4.16 (a) to Figure 4.17 (b and c) highlights the transition away from peak conditions, to high subsidence rates which severely limit the potential for creating a sedimentary hierarchy. (Figure 4.18) These severely limiting subsidence rates exist above 80m/My . Beyond this rate subsidence is rapid enough to drown the platform (at the given rates of carbonate production) above very small amplitudes of eustatic oscillation. At these rates a sedimentary hierarchy is only generated at very specific eustatic conditions: very small intermediate-order amplitude ($<20\text{m}$) and very large intermediate order amplitude ($>40\text{m}$). Given that Milankovitch-theory, and the geological literature relating to it, implies that the amplitudes of forcing are not inverted, there must be significant doubt cast on the existence of a sedimentary hierarchy at rates above 80m/My (and even at all rates of subsidence).

Up until this point, this study has not focussed on the sedimentary style (or stacking patterns) developed in hierarchical successions. However, this is a critical consideration in assessing the possibility of hierarchies existing in the sedimentary record. It is not sufficient to simply test for the existence of categorically hierarchical sections in simulations; to quantify the likelihood of the existence of a sedimentary hierarchy it is also necessary to ensure that simulations display a style of cyclicity (or stacking patterns) which are similar to that seen in the sedimentary record. The majority of various

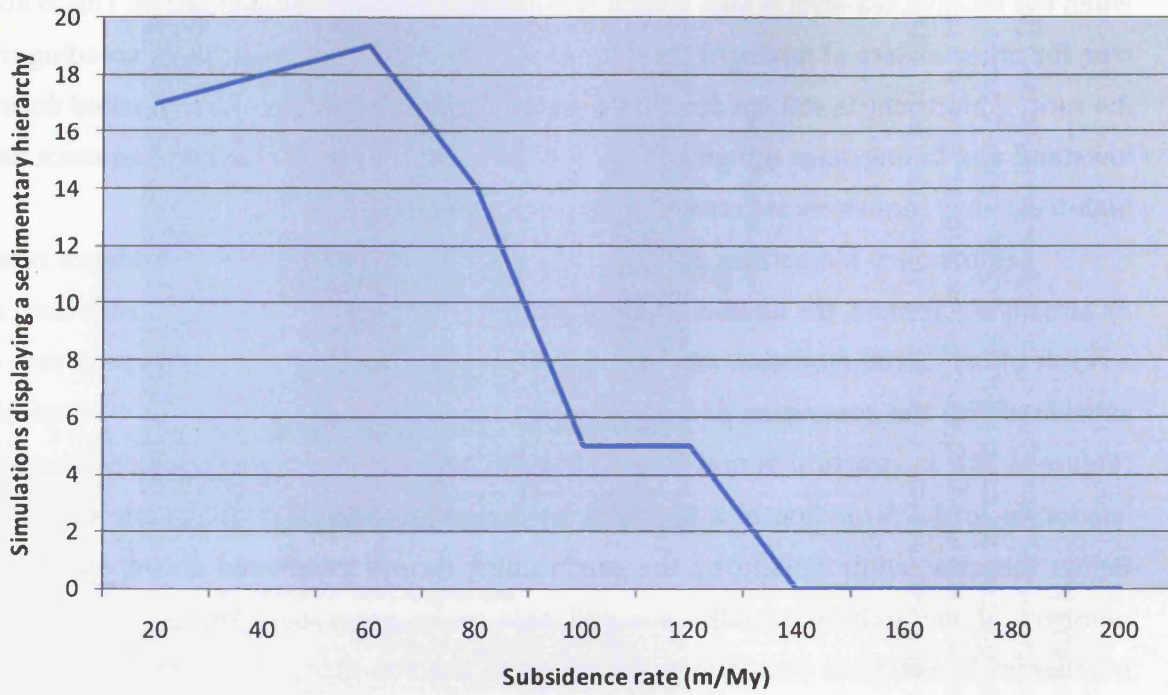


Figure 4.18: Plot displaying the number of hierarchical simulations (of a maximum of 100) per subsidence rate.

subsidence values examined here create strata with stacking patterns which do not resemble what is seen at outcrop or in the subsurface (Figure 4.19). This is not an artefact failure of the model, but a demonstration of the objectivity of the program in finding order in successions which a less rigorous set of criteria would not find to be hierarchical. Not all hierarchical sections are composed of strata exhibiting obvious shallowing-upwards cycles.

The hierarchical sections generated at very low subsidence rates (<20m/My) bear little resemblance to actual ice-house sections identified in the sedimentary record (Figure 4.19; a). As a result of the very low accommodation, cycle thicknesses correspond to the length of the forcing eustatic component; meaning thicker cycles correspond directly to longer wavelength oscillations. Additionally, the cycles are almost exclusively composed of shallow-water lithofacies, as water depth never exits the euphotic zone. This is something which is not observed in the stratigraphic record. Figure 4.19 (b) shows a more realistic section as a result of increased accommodation from higher subsidence rates. Cycle thicknesses no longer directly equate to wavelength, and because of this, very thin cycles are created. The consistently thin cycles in modelled sections is again uncommon in the sedimentary record. The prevalence of thin cycles at outcrop is a topic discussed in section 6.5.1. The most realistic stacking patterns from a hierarchical simulation are presented in Figure 4.19 (c); which shows shallowing-upwards cycles composed of shallow-water lithologies, with stacking feasible for low-accommodation settings. The critical problem for hierarchies generated at the upper range of high-order amplitudes (e.g. Figure 4.17; g), such as the hierarchy shown in Figure 4.19 (c), is that they require an inversion of the amplitudes of forcing orders to operate (i.e. high-order amplitude greater than intermediate-order amplitude). Although this may be true for the Carboniferous, it does not seem likely given current assumptions about orbitally-forced eustatic parameters (refer to section 2.1.1).

The numerical simulations in this section suggest that a sedimentary hierarchy could be generated under a range of subsidence conditions. However, given the unusual style of cyclicity generated in regimes where subsidence is less than 40m/My, the potential for development of hierarchies in these situations must be questioned. Similarly, above 80m/My, hierarchical sections become rarer as the result of a greater number of missed beats. This remains true up to 120m/My subsidence rate, beyond which the simulations presented here do not generate hierarchal sections, essentially due to the platform being deeply submerged (although not terminally drowned). Between these boundaries there exists a 'sweet-spot' for the generation of a sedimentary hierarchy (40-80m/My). This is broadly in the range of passive margin subsidence (Allen & Allen, 2005), but is too low for higher subsidence regimes (e.g. foreland basins; cf. section 5.2.1).

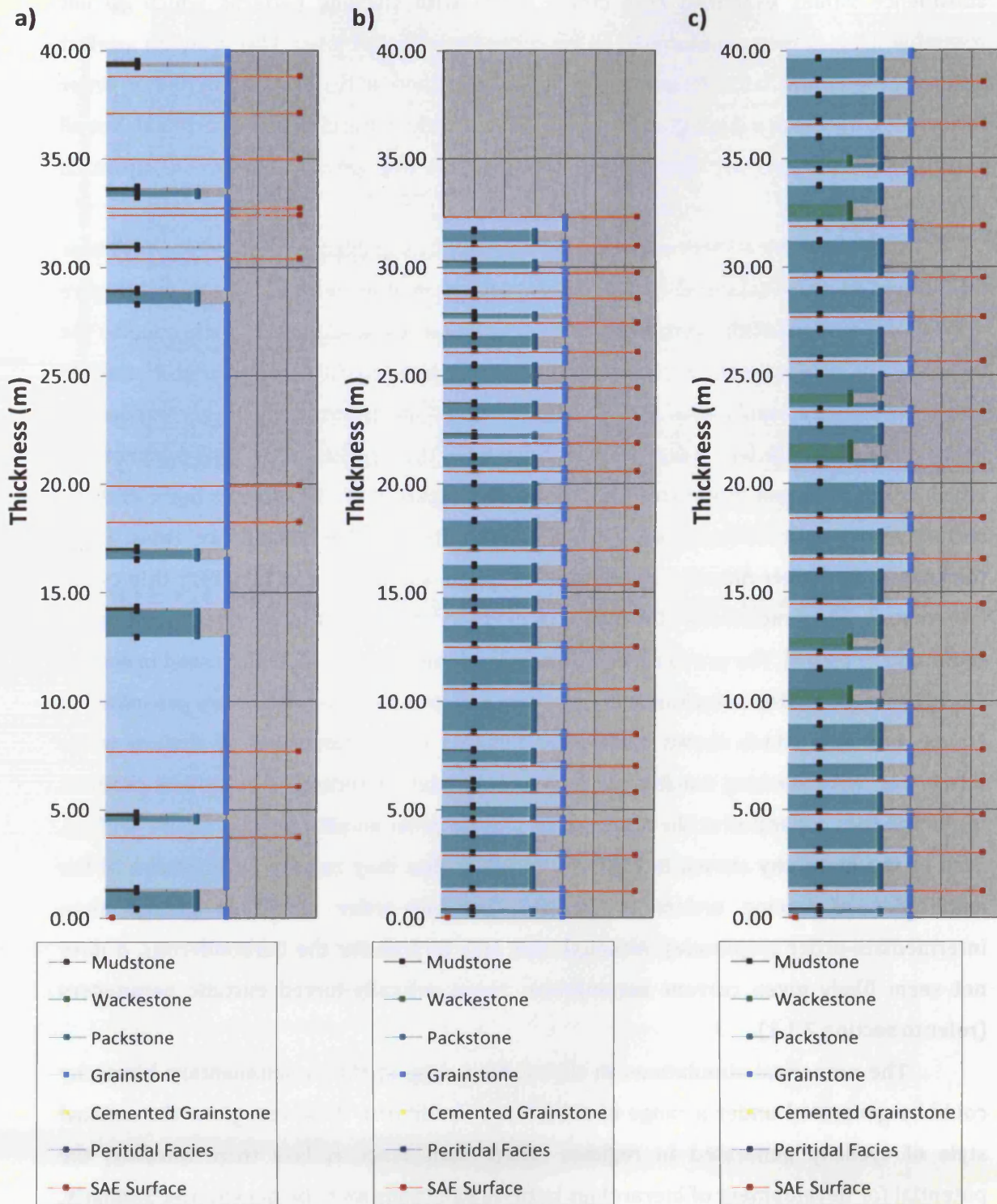


Figure 4.19: Synthetic lithology examples of hierarchical sections from simulations presented in Figure 4.17. Plots (only show 40m thickness). Plots a and b represent a subsidence rate of 20m/My, but plot b has a larger high-order amplitude. Plot c has a subsidence rate of 100m/My. In all cases sedimentation occurs in very shallow water, resulting in an abundance of grainstone lithologies.

Importantly, however, subsidence rate is not a critical limiting factor on the generation of a sedimentary hierarchy.

4.3.3 Runs investigating carbonate accumulation

The nature of the relationship between sedimentary hierarchy-generation and carbonate accumulation can be considered to be relatively simple (Figure 4.20). Carbonate production and accumulation is the process that dictates the way in which the ordered forcing mechanism is recorded in the sedimentary record. As such, if sedimentation is occurring at a very low rate then it is unlikely to create hierarchical patterns of thickness, as it will not show much variation in response to excursions of relative sea-level. For this reason, euphotic carbonate production has the greatest impact on the formation of a sedimentary hierarchy. The euphotic regime is considered to be the system with the potential for producing the greatest amount of sediment, and is therefore the most likely to record order conferred by eustatic oscillations.

Figure 4.21 reflects the logical way in which this principle impacts upon the development of a hierarchy. At very low euphotic production rates a hierarchy is predictably hard to generate (Figure 4.21; a). Very low rates represent an extreme example of decoupling from the wavelength of the ordered forcing mechanism (previously discussed in section 4.3.1.2). The low euphotic values effectively mean that production is no longer depth-dependent, and therefore responds only very slightly to changes in water depth (Figure 4.22). As a result the decoupling of sedimentation from the time-based ordered forcing mechanism is much more pronounced, and it becomes extremely difficult to produce a hierarchical section.

Logically, as the euphotic production rate increases the effect of the decoupling is less pronounced, and a hierarchy is generated in more situations. The similarity of plots b and c from Figure 4.21, suggests that this decoupling effect can be mitigated only up to a point; beyond which increasing rates of carbonate production have little effect on the generation of a sedimentary hierarchy. From Figure 4.21, this point can be said to be at a rate lower than 500m/My. Above this rate a sedimentary is not dependent on the rate of euphotic carbonate production, but is still primarily dependent on the interaction of the eustatic components, and specifically the ratio of amplitudes between the components.

The number of simulations displaying a sedimentary hierarchy steadily increases up to the cut-off point of 500m/My (Figure 4.23). Between 500m/My and 900m/My the number of simulations remains relatively stable. It is in this zone that the generation of a hierarchy is most likely, and is dependent on factors other than production rate. Within this zone, the degree of depth-dependence of production is not as significant as the fact that production *is* depth-dependent. Similar numbers of hierarchical sequences are

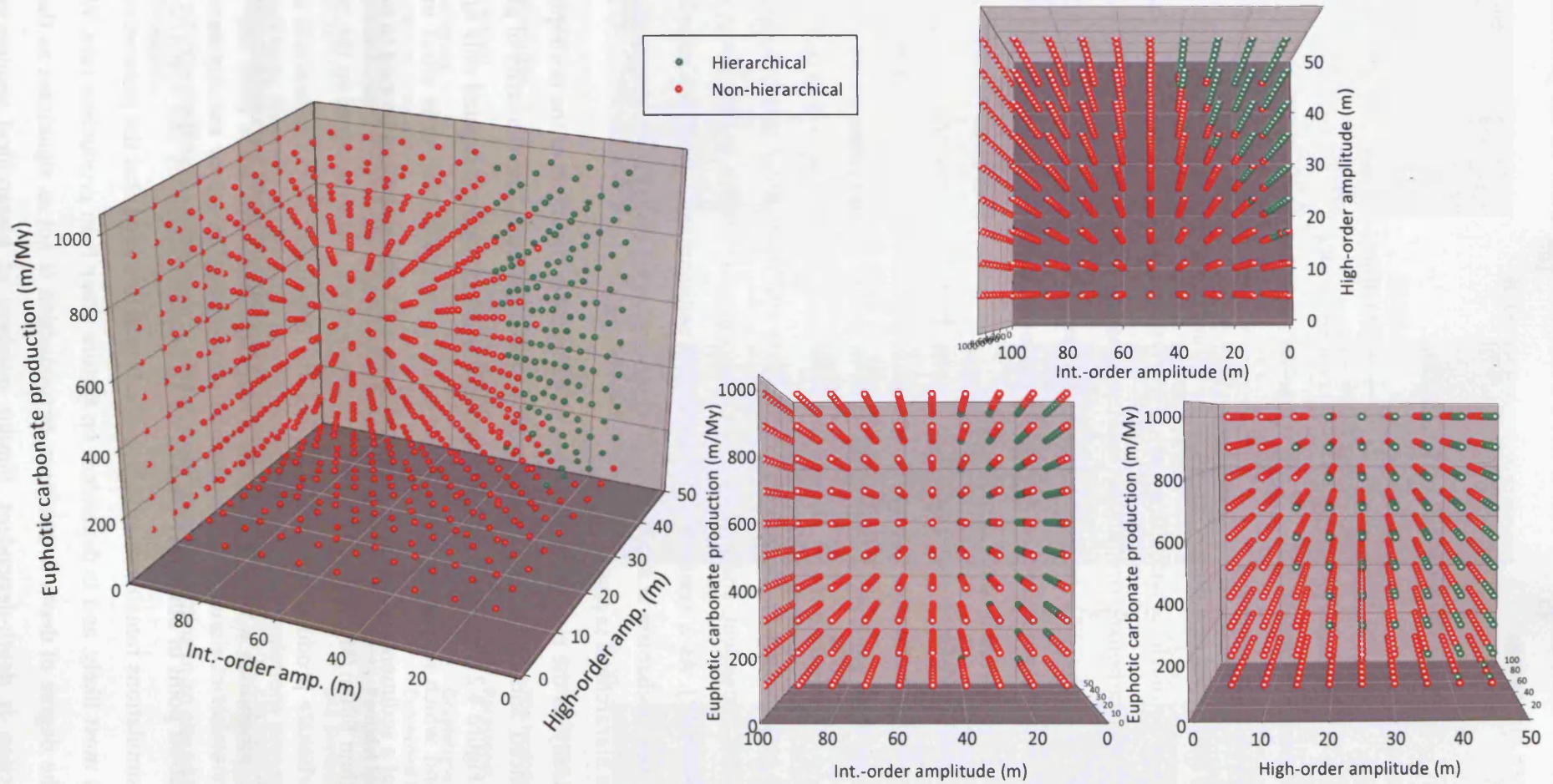


Figure 4.20: Parameter space plots comparing those simulations which generate a sedimentary hierarchy and those which do not, using two eustatic components and euphotic carbonate production rate as variables. At higher rates of euphotic production hierarchical sections occur at a wider range of scenarios.

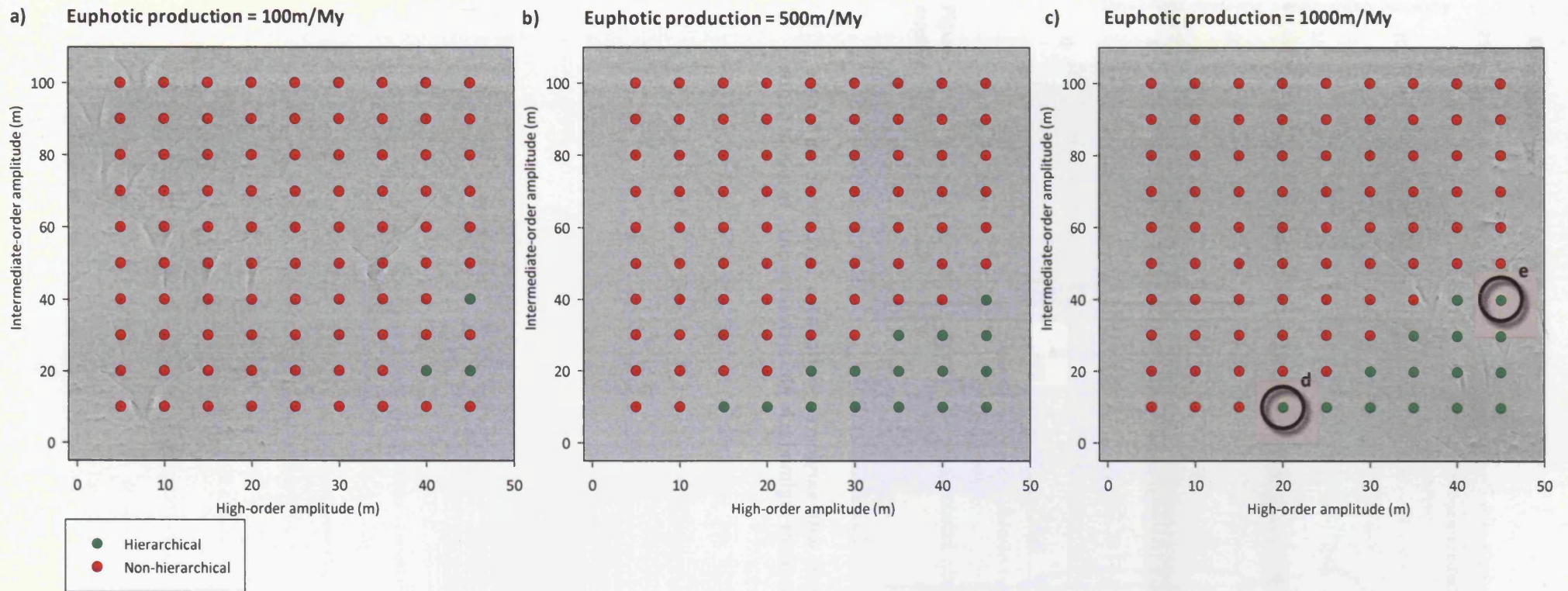


Figure 4.21: Slices through parameter space plots presented in Figure 4.20. Plot a represents the minimum rate of euphotic carbonate production, b the median and c the maximum. At low rates (a) hierarchical sections are extremely rare. Plots b and c bear a strong similarity to each other, and suggest that euphotic production increases the likelihood of generating a sedimentary hierarchy up to a point (see Figure 4.23). This point occurs at a rate lower than 500m/My. Circles d and e correspond to the synthetic sections presented in Figure 4.24.

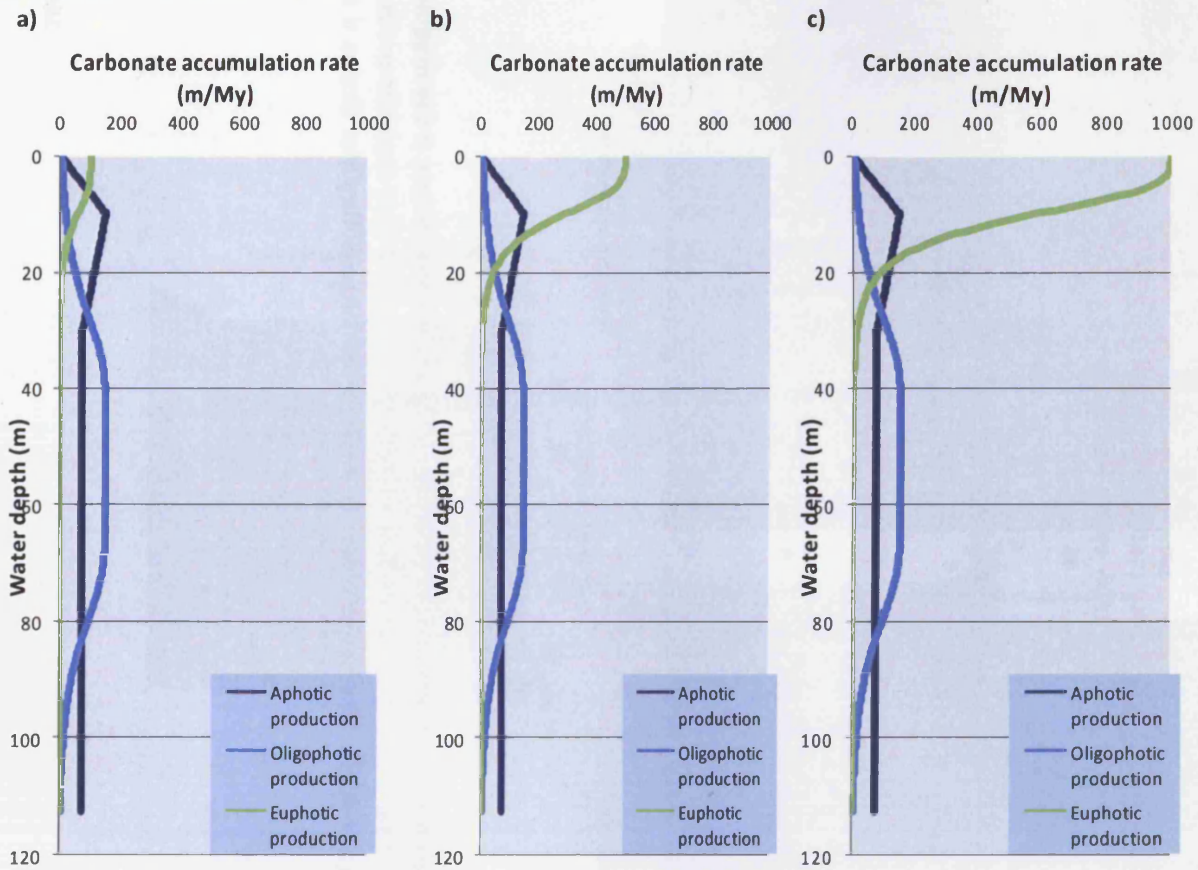


Figure 4.22: Examples of production regimes with varying euphotic rates of euphotic carbonate production, ranging from a non-depth-dependent regime (a; in hierarchical terms), to highly depth dependent (c).

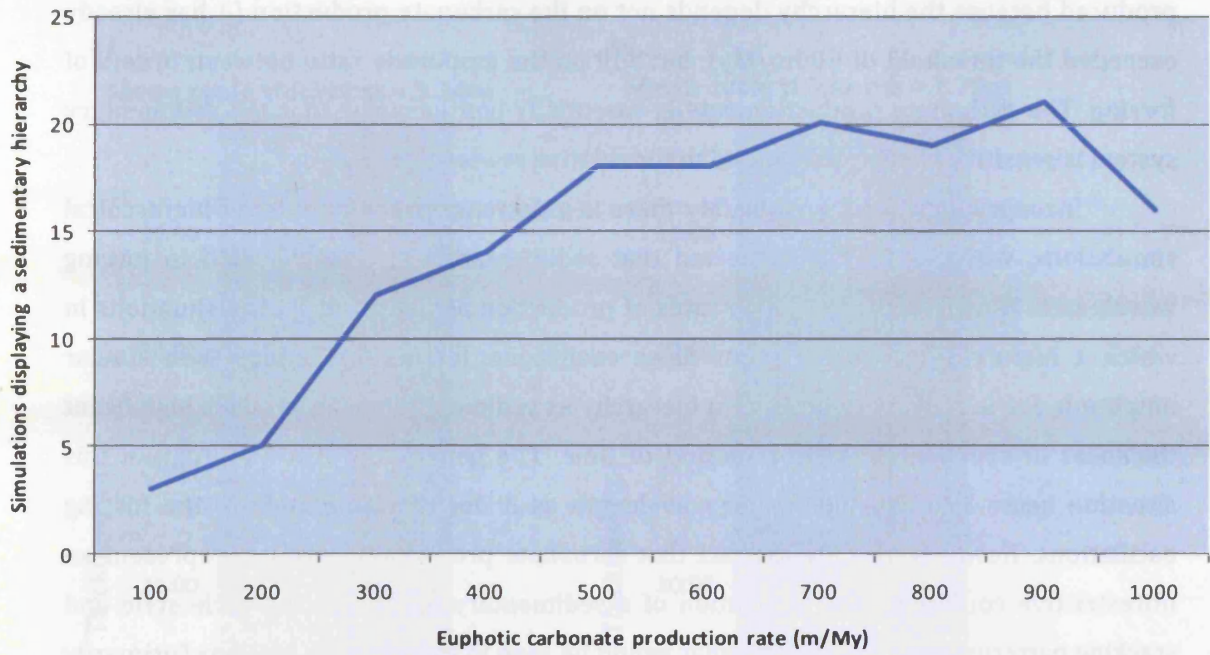


Figure 4.23: Plot displaying the number of hierarchical simulations (of a maximum of 100) per euphotic carbonate production rate.

produced because the hierarchy depends not on the carbonate production (it has already exceeded the threshold of 500m/My), but still on the amplitude ratio between orders of forcing. The carbonate production rate is essentially just ensuring that the sedimentary system is sensitive enough to respond to the relative sea-level changes.

Incongruously, above 900m/My there is a decrease in the number of hierarchical simulations, where it may be expected that sedimentation is closely linked to forcing wavelength. However, the very high rates of production actually restrict the situations in which a hierarchy can form. Under these conditions, forcing-oscillations with similar amplitude are less likely to produce a hierarchy as sedimentation can produce significant thickness of sediment in a short period of time. The generation of a hierarchy in this situation bears less dependence on wavelength as it does on amplitude of the forcing oscillations. However, despite the fact that carbonate production seems to represent an unrestrictive control on the generation of a sedimentary hierarchy, the cycle style and stacking patterns are not typical of what would be seen in sedimentary sections (primarily because cycles are too thin; Figure 4.24).

The way the euphotic carbonate production influences sedimentation culminates in the pattern of hierarchy development seen in Figure 4.20. This can be summarised by stating that with increasing rates of euphotic carbonate production there is increasing likelihood of hierarchy generation. Euphotic carbonate production is not a limiting factor for the generation of a sedimentary hierarchy. By virtue of the magnitude of production rate from the euphotic regime, this can also be said to be true for the other production regimes. A sedimentary hierarchy can be generated at all realistic estimates of euphotic carbonate production (approximately above 300m/My). 500m/My to 900m/My represents the production rates most conducive to the creation of a sedimentary hierarchy; rates which are broadly in-line with modern estimates of carbonate production from organisms dwelling in the euphotic zone.

4.3.4 Runs investigating sub-aerial platform denudation

The role of the rate of sub-aerial platform denudation has been largely ignored in previous efforts to quantify a sedimentary hierarchy (e.g. Goldhammer *et al.*, 1991). However, there is considerable evidence to suggest that rates of sub-aerial erosion (and therefore platform denudation) are significant, both in modern examples (Plan, 2005), and throughout the past (Vanstone, 1996).

Increasing rates of sub-aerial erosion show a very direct relationship with the potential of recording a sedimentary hierarchy (Figure 4.25): the greater the rate of sub-aerial platform denudation, the less likely it is that a sedimentary hierarchy will be preserved. This is the result of the simple fact that the removal of strata from the top of the

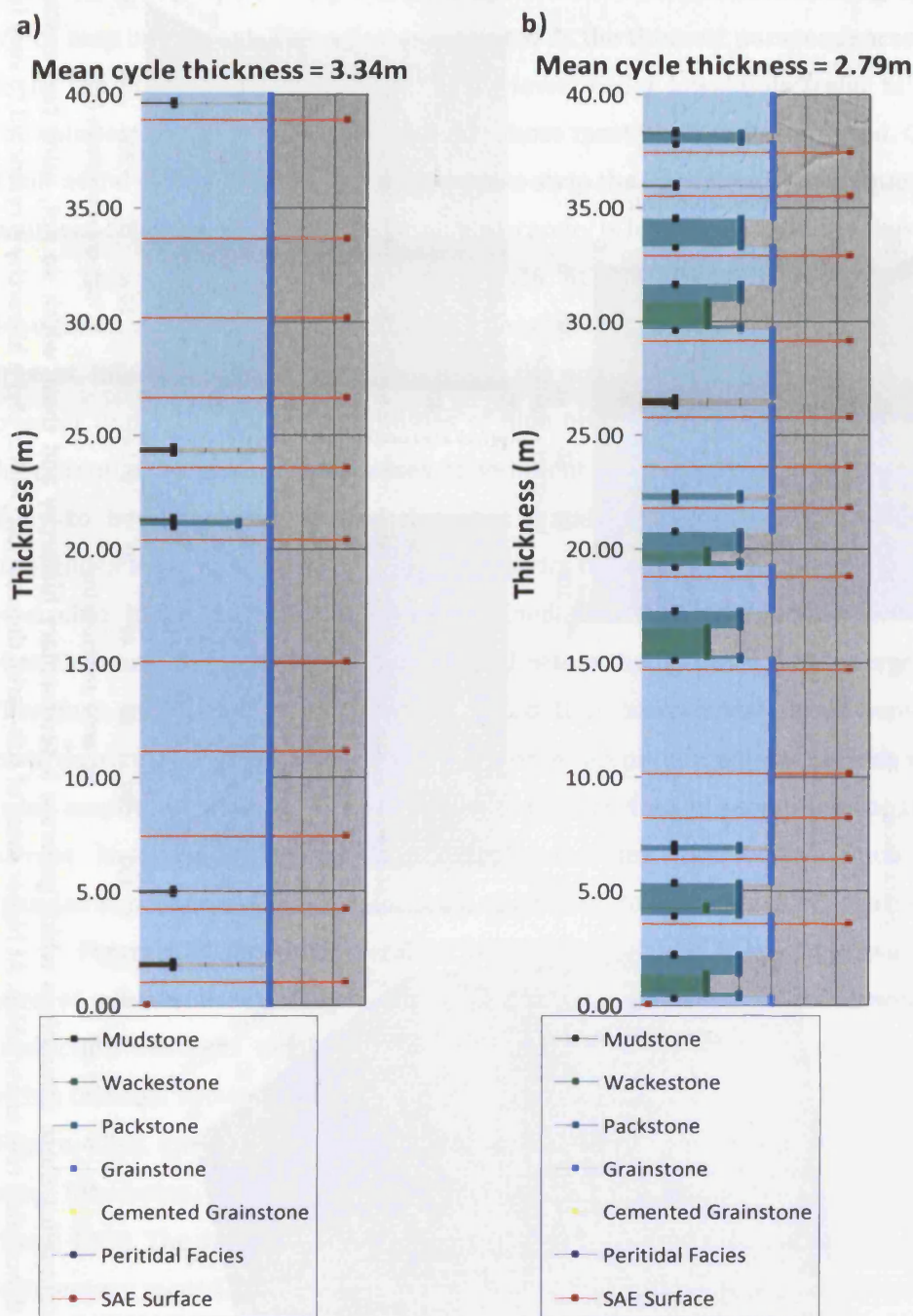


Figure 4.24: Synthetic lithologies from runs with varying rates of carbonate production (section a corresponds to Figure 4.21; d, and b to Figure 4.21; e). Plots only show 40m thickness. a) The limited amplitude of eustatic oscillations produces very thin cycles comprised of very shallow-water facies. b) Larger amplitude oscillations create more recognisable shallowing-upwards motifs, but cycles remain anomalously thin.

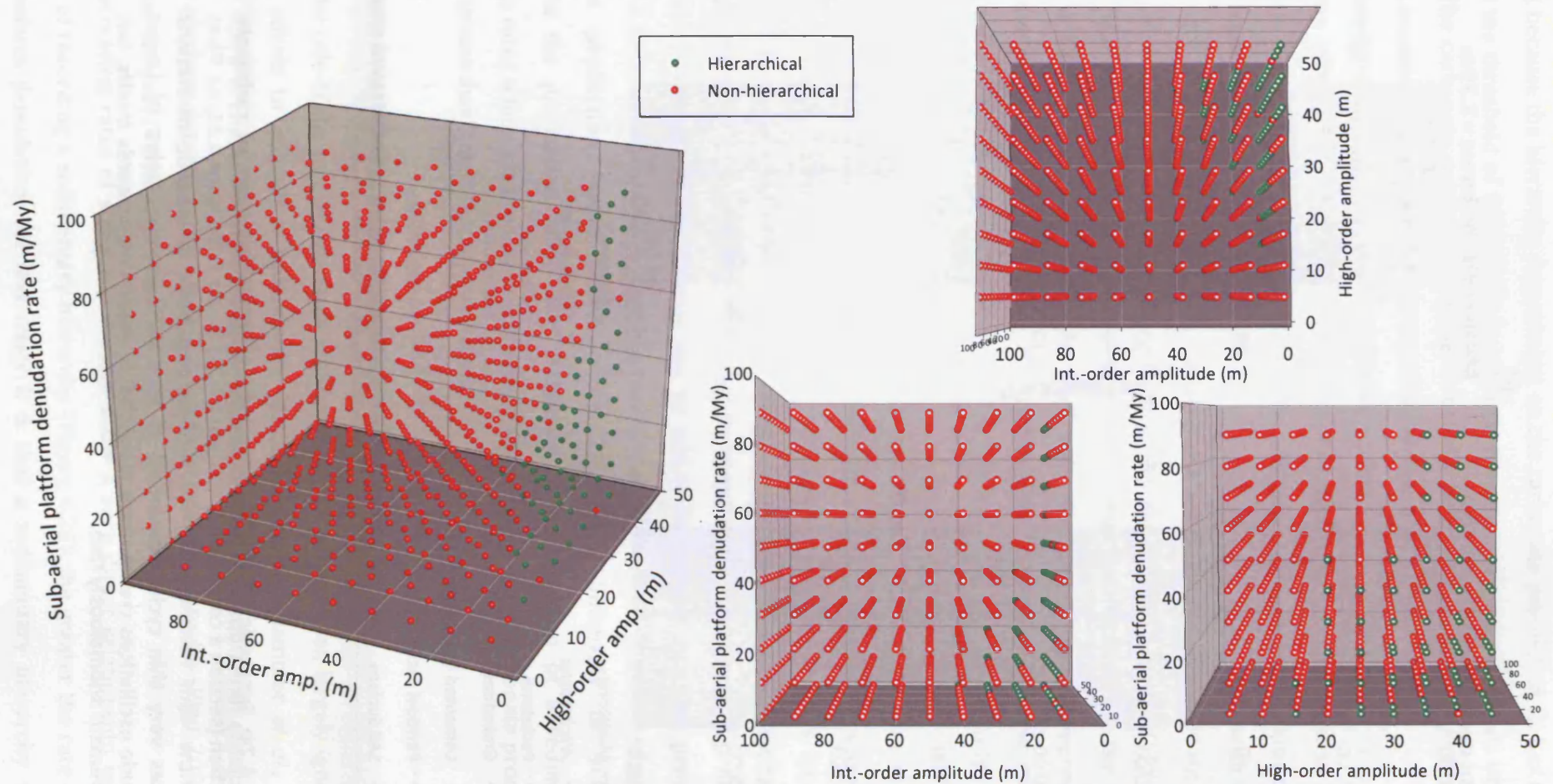


Figure 4.25: Parameter space plots comparing those simulations which generate a sedimentary hierarchy and those which do not, using two eustatic components and sub-aerial platform denudation rate as variables. At higher rates of sub-aerial denudation ($>40\text{m/My}$) a hierarchy is restricted to very few unrealistic scenarios where the amplitudes of forcing orders are inverted.

sediment column potentially removes cycle boundaries, deconstructing any hierarchy which may be present. This effect is catalysed as the thinnest parasequences usually exist at the top of the sediment column during lower-order lowstands (refer to Figure 4.11). The thinnest parasequences are therefore those most likely to be removed. Consequently, if sub-aerial erosion rates are high enough to strip the uppermost parasequences from the sediment column during hiatuses, then a hierarchy is less likely to be developed.

This process is evident in Figure 4.26. At increasing rates of sub-aerial platform denudation a hierarchy is progressively less likely to be preserved; if it was originally present. Effectively, under these conditions, the potential for a hierarchy to be preserved is greatest under the highest amplitudes of high-order eustatic oscillations. This increases the potential for greater thicknesses of sediment to be deposited, meaning they are less likely to be completely eroded during a hiatal period. Similarly, intermediate-order amplitudes will preferentially be low, to restrict the amount of strata that can potentially be eroded. If, for instance, during an intermediate-order lowstand sea-level only falls by 10m, then only 10m of strata can be eroded before the platform is submerged once more. Therefore, at high rates of sub-aerial denudation, hierarchical simulations are skewed towards occurring in scenarios where high-order amplitude greatly exceeds intermediate-order amplitude. This, as has been mentioned previously, seems improbable based on current knowledge of eustatic sea-level behaviour. Hierarchical sections in high-denudation scenarios (Figure 4.26; b and c) conform to this pattern of occurrence.

Figure 4.27 shows the trend for hierarchical sections to be less prevalent at greater rates of sub-aerial denudation. A rate of 40m/My marks the point at which hierarchy production becomes negligible. The hierarchical sections still occurring at scenarios within this rate show a stacking pattern which is significantly altered by sub-aerial erosion (Figure 4.28). Parasequences are significantly thinned by stripping of the upper, shallow-water lithofacies. Total sedimentary thickness is consequently much thinner as well (cf. Figure 4.19). The degree to which this significant sub-aerial erosion would be visible in the sedimentary record is not clear, and is a factor which is unable to be addressed by forward modelling. However, from studies of exposure surface development, the length of time strata are exposed and the degree of karstification experienced are not directly equivalent (Vanstone, 1996; Budd *et al.*, 2002). What is clear is that sub-aerial exposure rates well within the range of predicted values are able to significantly inhibit the preservation of a hierarchy in the sedimentary record.

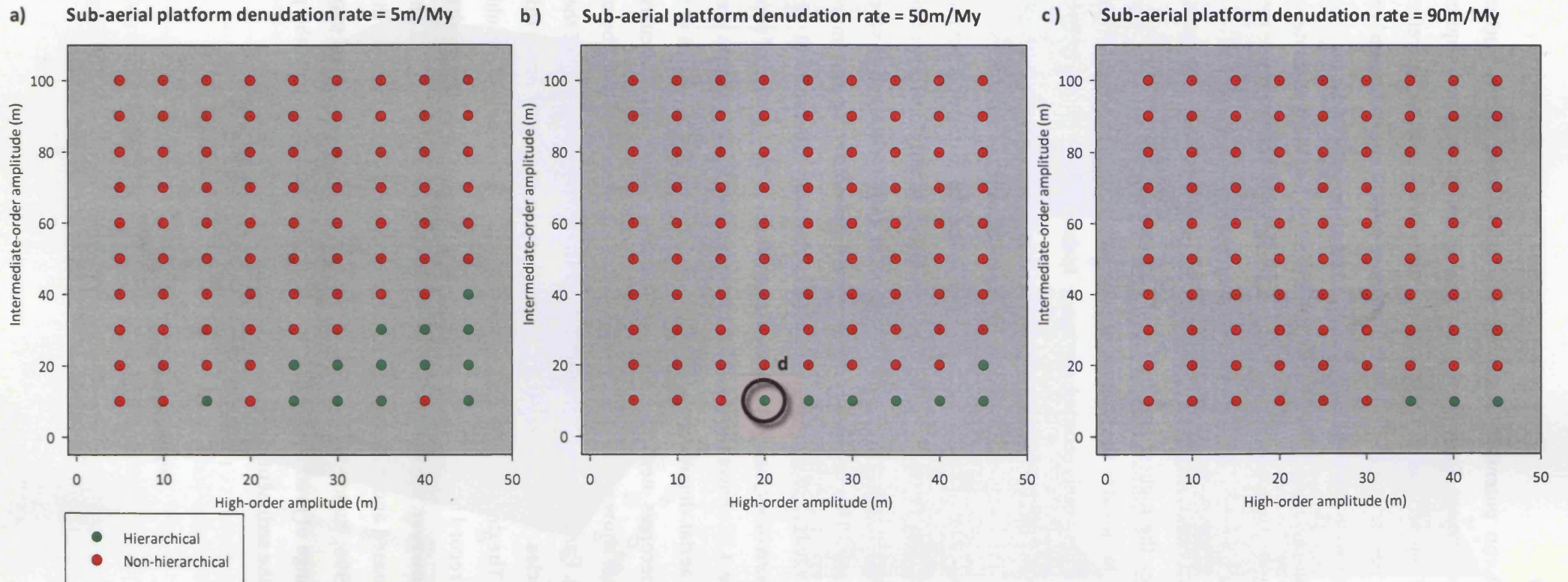


Figure 4.26: Slices through the parameter-space plots presented in Figure 4.25. Increasing rates of sub-aerial platform denudation (from plot a to plot c) increasingly limit the potential for hierarchy generation.

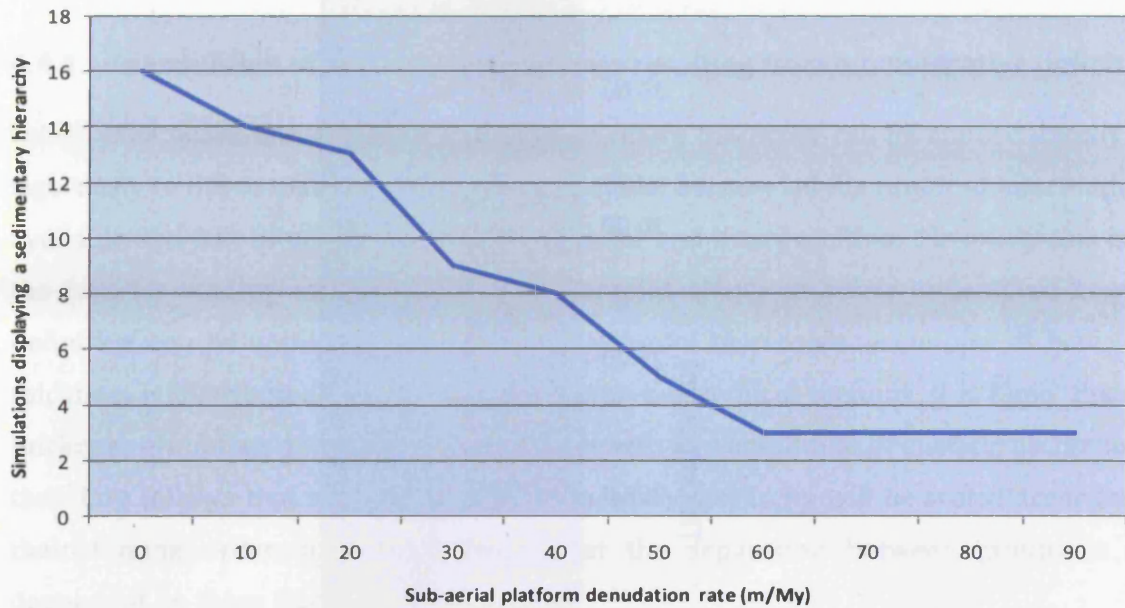


Figure 4.27: Plot displaying the number of hierarchical simulations (of a maximum of 100) per sub-aerial platform denudation rate.

Mean cycle thickness = 1.73m

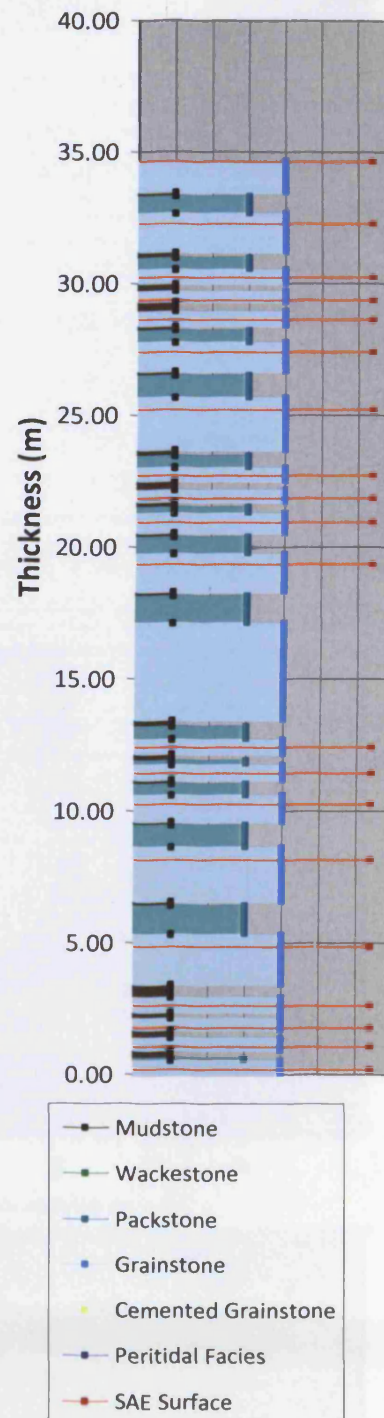


Figure 4.28: Synthetic lithology from Figure 4.26 (d). High rates of sub-aerial erosion strip the tops of cycles, resulting in very thin cycles.

4.4 INTERPRETATION

4.4.1 Examination of hierarchical groupings resulting from a quantitative definition

The quantitative definition of a sedimentary hierarchy can be applied exactly and rigorously to the output from the numerical model because all the required information is available and free of uncertainty related to error and interpretation. Obviously this is not the case for outcrop or subsurface data examples. Hence to better understand how the definition can be applied to real strata, it is useful to consider examples of how cycle thickness is distributed in hierarchical and non-hierarchical sections. It is likely that any thickness groupings are related to the wavelength and amplitude of eustatic oscillation. It therefore follows that the groups of a sedimentary hierarchy will be scaled according to their forcing order, and furthermore, that the separation between groups is also dependent on these factors.

Figure 4.29 shows the distribution of thickness groups in a hierarchical and non-hierarchical section. Two plots of HfS thicknesses are displayed for simulations where the only difference is a variation of 20m in intermediate-order eustatic amplitude (Figure 4.29; x & y). This sample is taken as a 'typical' representative of the differentiation in terms of groupings between hierarchical and non-hierarchical sections. The difference is a result of the precise application of the quantitative definition of a sedimentary hierarchy described in section 4.1.3. What is important is that despite a relatively small parameter change (of 20m), the difference between groups is distinct. This is a result of more high-order beats being recorded as sedimentation on the platform because of a greater amplitude ratio between oscillations.

The hierarchical section displays well-defined groups with a separation in terms of thickness between them. Figure 4.29 and Figure 4.30, suggest approximately 15-30% of intermediate-order thickness; equating to a 1-4m separation in cycle thicknesses. Note also that high-order thicknesses are less than intermediate-order thicknesses in this hierarchical section, a consequence of the direct dependence of cycle thickness on the amplitude and wavelength of sea-level oscillation in a true hierarchy.

Correspondingly the thickness separation between groupings is also dependent on the relative durations of sea-level oscillations. The magnitude of separation is less important than the fact that in hierarchical sections defined quantitatively, there should always be a separation. Although the separation between groupings may be comparatively small, in a hierarchical section the groupings are be tightly-constrained (dictated by

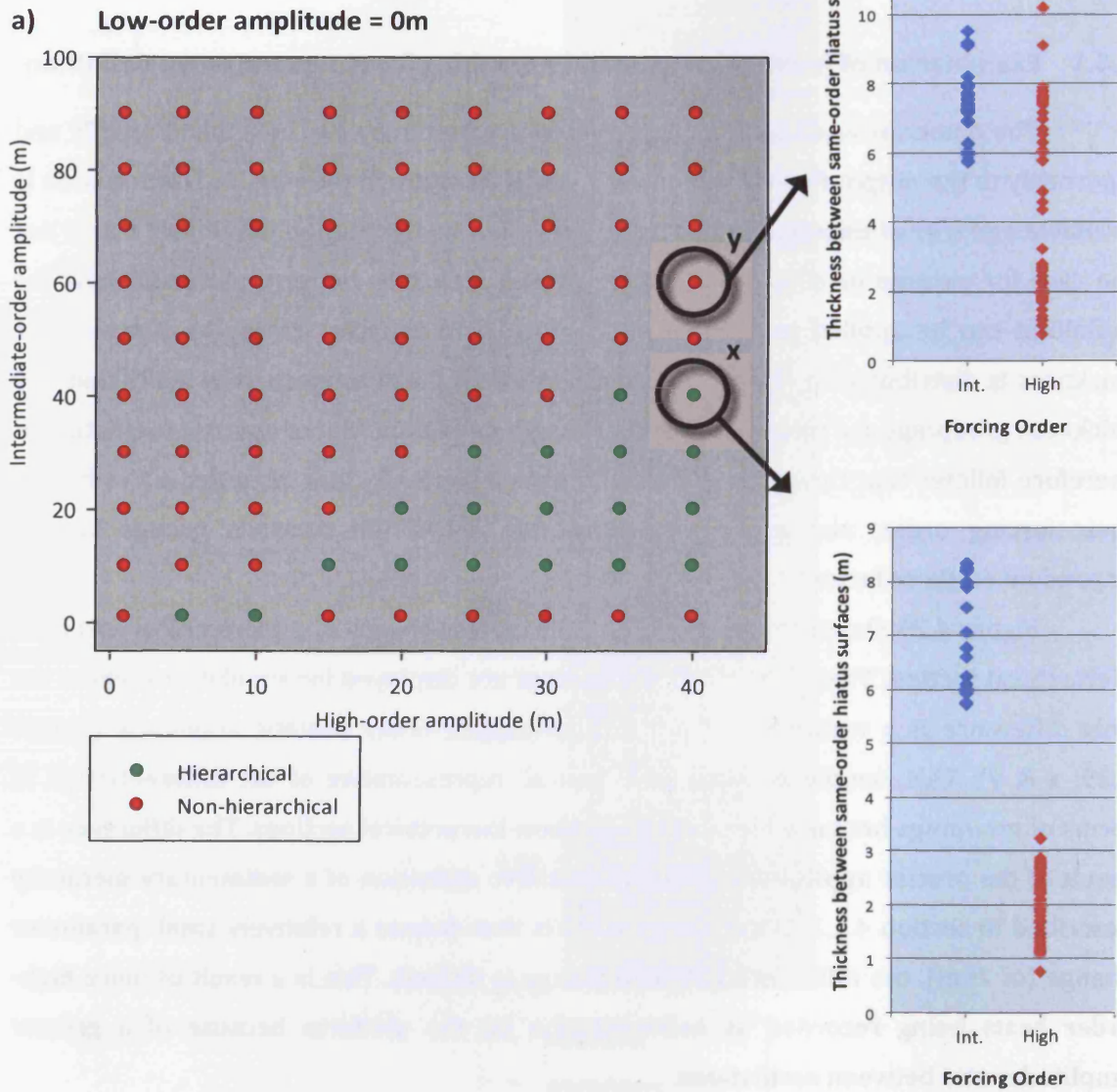


Figure 4.29: a) Parameter-space plot from Figure 4.25, with plots showing the thickness of intermediate-order and high-order cycles for a hierarchical section (x) and a non-hierarchical section (y). A hierarchy is identified by a lack of overlap of thicknesses, as opposed to the continuum of thicknesses observed in the non-hierarchical section.

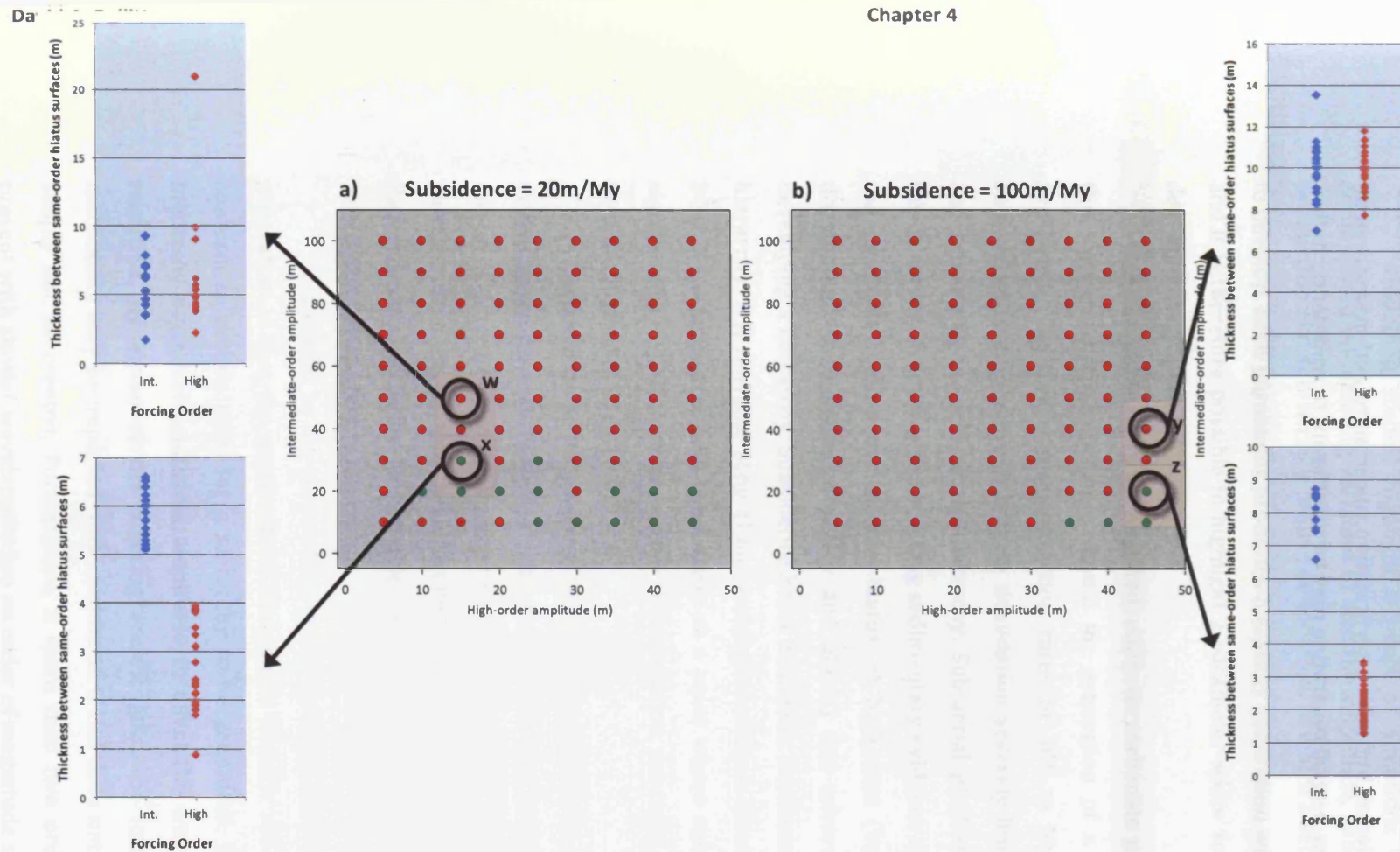


Figure 4.30: a & b) Parameter-space plots from Figure 4.17, with plots showing the thickness of intermediate-order and high-order cycles for hierarchical sections (x & z) and non-hierarchical sections (w & y). The difference is that hierarchical sections always result in cycles of different orders arranged into discrete groups whilst non-hierarchical sections display a continuum of thicknesses. This is not surprising behaviour from the model – it represents the strict application of the quantitative definition. It is important to note however the stark contrast caused by a minor parameter change. Given this, it is not likely that some sections are rejected for being ‘marginally’ hierarchical. These section would exist in a very narrow zone and are rejected by the strict criteria of the definition as not displaying a distinct separation of thicknesses. The salient point of this diagram is that if a sedimentary hierarchy could quantitatively be said to exist in the sedimentary record it is likely that it would display a marked separation of thicknesses.

wavelength) and a separation should be visible. Whether this would be visible at outcrop is debateable, and seems unlikely. In a model environment this separation, and definition, is more than sufficient to distinguish between hierarchical and non-hierarchical sections with a high degree of confidence, but with interpretation uncertainty and measurement error in a real outcrop section, a small separation may be insufficient to confidently define a hierarchy.

4.4.2 Scenarios where a hierarchy may exist

Modelling studies highlight a range of situations with respect to the major accommodation-affecting variables of eustatic amplitude, subsidence, euphotic carbonate production and sub-aerial platform denudation, in which a sedimentary hierarchy is likely to develop. Each parameter promotes hierarchy generation within a given range of values, and it is therefore possible to highlight a parameter-space zone of preferential hierarchy development (Figure 4.31).

Of the parameters investigated, euphotic carbonate production can be said to be the least restrictive on the potential for generation of a hierarchy. Hierarchies are generated consistently for production rates of 500 m My^{-1} and above. In contrast, subsidence and sub-aerial platform denudation severely limit the potential for creating and preserving a sedimentary hierarchy. Sub-aerial platform denudation accomplishes this in a very direct way, by removing sedimentary evidence of a hierarchy from the top of the sediment column during each hiatus. At high-rates (but well within the range of documented possibilities; 40 m/My and above) this adversely affects the chances of developing a hierarchy. Subsidence has a less linear relationship with the generation of a hierarchy. A favourable zone of hierarchy generation is identified between 40 m/My and 80 m/My subsidence. This zone exists at a point where subsidence is not too great to significantly impact upon periods of sedimentation, yet rapid enough to create significant accommodation.

It should be noted however, that even in hierarchical sections the style of cyclicity evident is not necessarily that which has been identified in the sedimentary record. This is not an artefact of the model, since its ability to produce realistic lithologies and stacking patterns from reasonable, well-documented parameters is demonstrated in section 5.4. Rather, it reflects the fact that an objectively-defined sedimentary hierarchy often requires unrealistic parameters to generate.

The caveat to the above statements regarding conditions conducive to hierarchy generation is that the amplitude of component eustatic sea-level oscillations must also conform to certain rules for a hierarchy to be generated. Each element of the forcing hierarchy must have sufficient amplitude to effect the way sediment is produced and recorded. By virtue of the differing wavelengths, the intrinsic order of the forcing mechanism may be imparted to the sediment. If this does not occur, then a hierarchy will simply not be created. Furthermore, if more than two orders of eustatic forcing are present with similar wavelengths (on an order of magnitude scale; i.e. Milankovitch scale) then this effect is exacerbated. Each order of forcing must be sufficiently distinct in terms of amplitude from the next to cause differing amounts of sedimentation; otherwise a

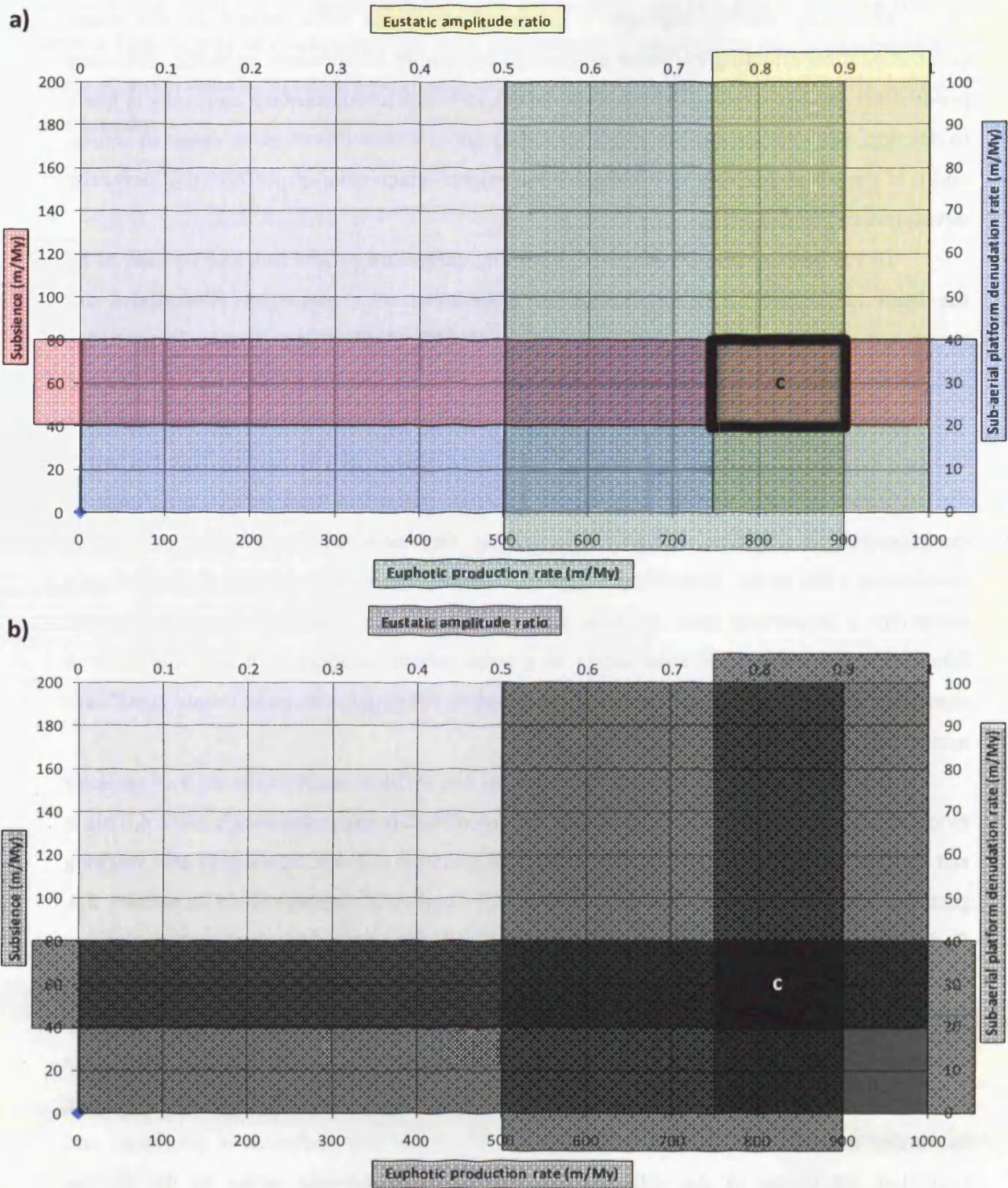


Figure 4.31: a) Schematic parameter-space plot showing zones for each variable where conditions are conducive to the formation of a sedimentary hierarchy. b) Darker areas depict zones with greater potential for generating a hierarchy. Rectangle c shows the zone of parameters most conducive to the formation of a sedimentary hierarchy.

hierarchy will not be developed. With only three orders of hierarchical forcing the complexity quickly becomes significant, and unrealistic amplitudes (i.e. amplitude inversion) are required to generate a hierarchy – which is limited to very few situations. This effect is not infinitely extendable, however. With more than three eustatic components, the combined effect would be to increase complexity to a point where, even with individually distinctive amplitudes, sedimentation no longer bears good relation to the ordered forcing mechanism.

It may be expected that if accommodation is filled to a greater degree, sedimentation may have a greater likelihood of forming a sedimentary hierarchy (as a result of closer interactions with relative sea-level). Even though high-amplitude high-frequency glacio-eustatic oscillations were thought not to be occurring during greenhouse periods, peritidal successions have been interpreted as the most likely places to detect order in strata (cf. Wilkinson *et al.*, 1997b). Greenhouse peritidal carbonate successions show shallowing-upwards lithologies without the characteristic sub-tidal truncation of carbonate cycles characteristic of ice-house inner platforms. It is reasonable to expect that if an ordered forcing mechanism existed, it may be more likely to display a sedimentary hierarchy in these situations. Contrary to what may be expected, however, one-dimensional forward modelling shows no link, between accommodation and the preferential development of hierarchical sections (refer to section 4.3.1.1 and Figure 4.8). Therefore, it is probable that hierarchical successions are no more likely in peritidal sequences than they are in sub-tidal sequences.

4.4.3 The likelihood of the existence of a hierarchy in the sedimentary record

The conditions under which a sedimentary hierarchy is most likely to develop have been discussed in the previous section (section 4.4.1), yet this is distinct from considering if a hierarchy is likely to be manifest in the sedimentary record. Previous studies have limited themselves to describing strata interpreted to be hierarchical, but based on a very loose definition of what a hierarchy is. These results indicate that a more objectively defined hierarchy is likely to be developed only in very specific circumstances usually requiring one or more unrealistic parameter values. These circumstances (most fundamentally, the amplitude ratio between orders of eustatic sea-level oscillation) result in only 13.8% of simulations recording a sedimentary hierarchy. Furthermore, all of these hierarchies are generated by unreasonable parameter interactions, and are not likely to be recognisable in the rock record were they to exist.

An ordered (and hierarchical) forcing mechanism is recorded better in terms of hiatus duration than it is in terms of sedimentary thickness: 67.8% of simulations recorded a hierarchy in terms of hiatus duration. Hiatus duration is recorded in time and

bears a direct linear relationship to the wavelength of eustatic oscillations. Thickness, in comparison, is not directly proportional to time and so this link is not maintained. This decoupling effect results in the ordered forcing mechanism being more difficult to record in terms of sedimentary thickness than hiatal duration. A hierarchy of forcing is therefore better recorded by a hiatal hierarchy. It must also be kept in mind that a sedimentary hierarchy is rarely manifested in a sedimentary section that displays a characteristic shallowing-upwards cycle motif. Usually, the cycles are too thin and may not shallow-upwards, and therefore do not exhibit a similar sedimentary style to successions from the sedimentary record.

Of the two hierarchical forms, it is most probable that a hierarchy in terms of hiatal duration would be recorded. The sedimentary hierarchy is more likely to be preserved in the sedimentary record, but the hiatus hierarchy is more likely to be created in the first instance and reflects the forcing better. Unfortunately, given the imprecise nature of dating the durations of sub-aerial exposure surfaces in the sedimentary record, a hiatal hierarchy is nearly impossible to detect from outcrop at the current time.

Disregarding the disordered vertical associations of facies, and the likelihood of non-depth-dependent shallow-water calcium carbonate producers (e.g. Rankey, 2004; discussed previously), hierarchical sections can also be shown to be developed in simulations which are statistically disordered. This reflects the fact that a hierarchy is not dependent upon facies, only thicknesses between bounding surfaces. Facies are used by some workers to identify bounding surfaces, however this identification must be objective or there is a risk hierarchical sections could be falsely identified. Figure 4.32 shows two examples where hierarchical sections are as often as not developed in situations where the stacking pattern is indistinguishable from random. Figure 4.33 also shows that trends in parasequence thickness (such as thinning-upwards) are not robust enough to statistically disprove that the section is disordered. If facies transitions are disordered (as other authors have argued) and modelling shows that stacking-patterns do not equate directly with hierarchical sections, then the presence of order as interpreted from the sedimentary record is questionable.

The different prevalence of the two forms of hierarchy raises the question of which form is more relevant. There can be no doubt that the hiatal hierarchy, being directly derived from the wavelength and amplitude of eustatic oscillations, best records the order inherent to the forcing mechanism. A hiatal hierarchy is more likely, too, to be recorded within the sediment of a modelled world. A forcing hierarchy, derived from sediment thickness, is much harder to detect in both a modelled and physical environment, as it depends on a multitude of factors not directly dependent on the wavelength and amplitude of the ordered forcing mechanism. This is the fundamental flaw of any

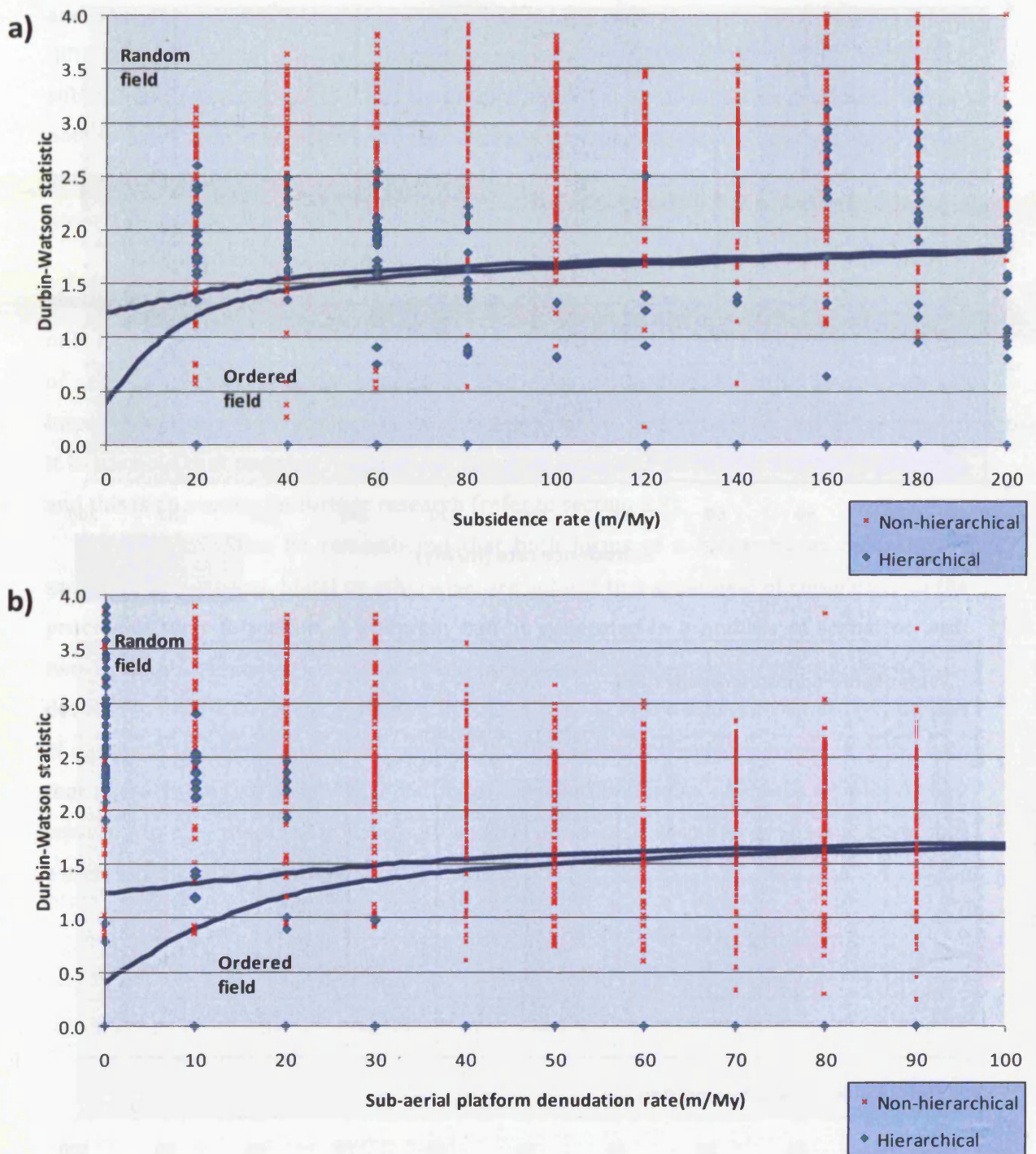


Figure 4.32: Durbin-Watson statistics for simulations where subsidence rate (a) and sub-aerial platform denudation rate (b) are the main variables. In each case, the majority of hierarchical sections occur in the field of randomness. Therefore, each parasequence has no relationship with its predecessor and the stacking of the section is indistinguishable from random.

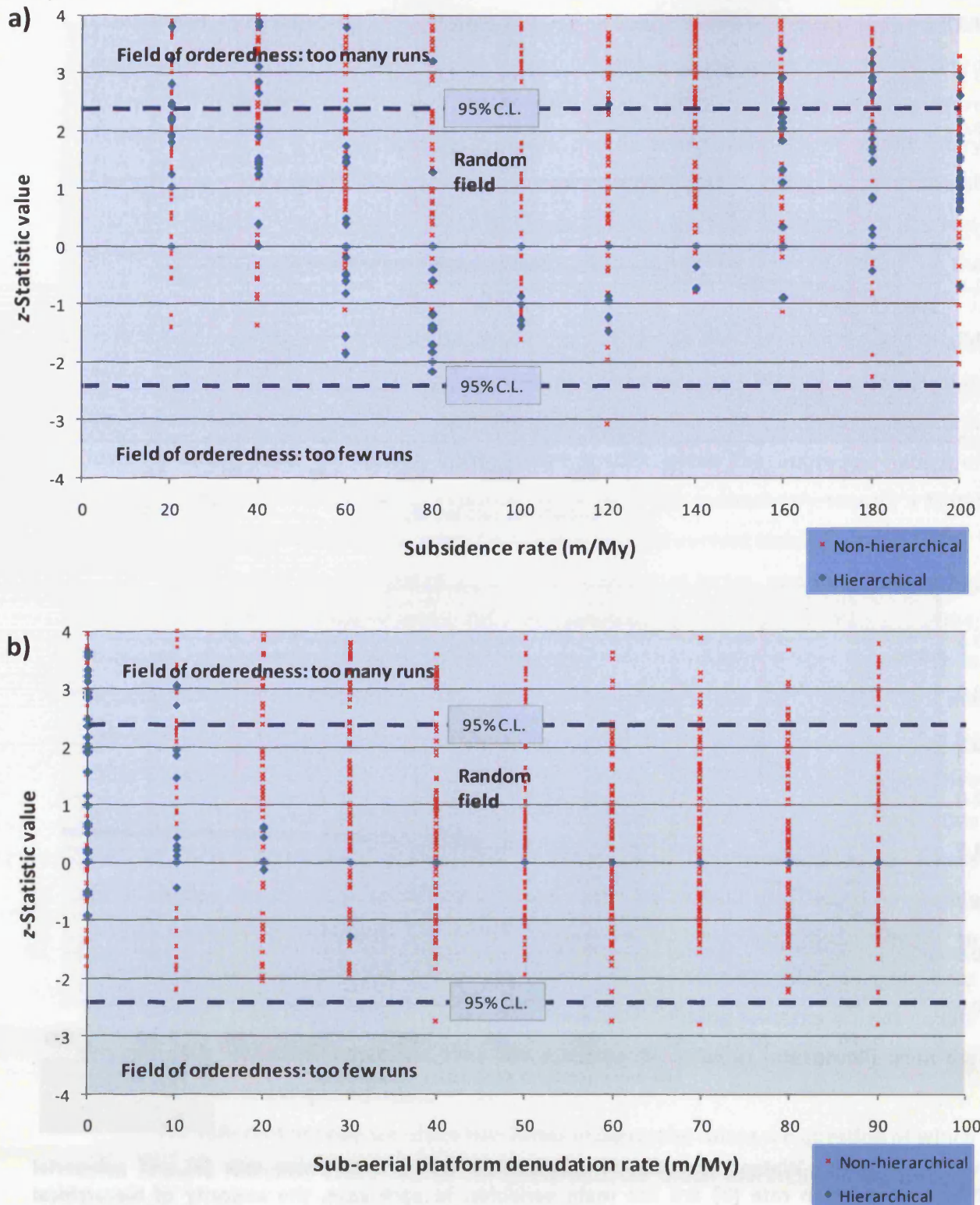


Figure 4.33: z-Statistic values from up-down runs tests on simulations where subsidence rate (a) and sub-aerial platform denudation rate (b) are the main variables. In each case the majority of hierarchical sections plot in the random field. The non-randomness check is failed as runs of significant length are not developed.

hierarchy based on sedimentary thicknesses or stacking patterns – they are modified syn- and post-depositionally by disordered processes (or at least, processes conforming to a different form of order). They therefore represent the order of the forcing mechanism subsequent to modification. Hiatal hierarchies are not subject to this problem, yet they are not detectable to any degree in the development of sub-aerial exposure surfaces at outcrop or in the sub-surface. It is only in a model environment, where all parameters are known, that their effect can be quantified.

Whilst addressing the likelihood of different forms of a sedimentary hierarchy it should be taken into account that the quantitative definition presented here represents only one definition of a hierarchy – albeit one which is based on the objective application of sequence stratigraphy. It is proposed that this quantitative definition is a significant improvement over previous conceptual and qualitative models and definitions. However, it is possible that ongoing research can improve upon this definition and its application, and this is an avenue for further research (refer to section 8.3).

It should also be remembered that both forms of a hierarchy as recorded by sedimentary patterns, hiatal or otherwise, are subject to a great deal of complexity in the process of their formation. A hierarchy can be generated in a number of scenarios with two eustatic components, but three or more eustatic components severely restrict the development of a hierarchical section. This also does not take into account the interaction of autocyclic elements and more complex, local tectonics. It therefore seems very unlikely that in the geological past, where multiple eustatic components of similar amplitude and wavelength are envisaged to have operated in conjunction with autocyclic processes, that a hierarchical section would be created.

4.5 CONCLUSIONS

- Attempts to quantify the existence of a sedimentary hierarchy have been hampered by qualitative, subjective, unclear and often conflicting definitions of the form of such a hierarchy. To determine when a hierarchy can objectively be said to exist, a robust set of simple criteria must be rigorously applied to sedimentary successions. The criteria presented here (in section 4.1.3) are used to quantitatively test for the existence of hierarchies in modelled successions.
- A quantitative definition of a sedimentary hierarchy is presented: a hierarchy consists of a series of sedimentary cycles, either parasequences or high-frequency sequences, each bounded by sub-aerial unconformities, in which there exist at least two discrete groups in terms of thicknesses.
- Hierarchies of hiatal duration would be a more accurate recorder of the forcing mechanism but are undetectable in the sedimentary record at this time, and therefore not of practical use.
- Hierarchies of hiatal duration and sedimentary thickness are not mutually exclusive, but often do not occur in the same section. A well-developed thickness hierarchy (indicative of few missed beats) will have high-order oscillations necessarily disrupting the longer duration lowstands of a lower-order. Similarly, a hiatal hierarchy will have uninterrupted long-duration hiatuses during lower-order lowstands, meaning more missed beats, and lower likelihood of a sedimentary hierarchy. This raises the question of which form of hierarchy is more informative or relevant to understanding the forcing mechanism. In terms of fidelity, it is undoubtedly the hiatal hierarchy. However due to the inability to extract high-resolution information of hiatal duration from the sedimentary record, the sedimentary hierarchy has to be said to be more likely to be detected and have more relevance.
- In the first instance a sedimentary hierarchy can only be said to form when there is an amplitude ratio of 3:4 between high-order and intermediate-order oscillations. This is true for simple simulations where eustatic amplitude is the only independent variable. In more complex scenarios (with an additional variable) a sedimentary hierarchy is only created when sea-level amplitudes are inverted (i.e. high-order is larger than intermediate-order). Although not contradictory to Milankovitch-forcing doctrine, this seems unlikely given what is known regarding sea-level behaviour.

- There are certain subsidence, euphotic production, and sub-aerial denudation scenarios where a sedimentary hierarchy can be said to be most commonly developed. However, this is only true if sea-level amplitudes are inverted, or approximately equal.
- The addition of multiple orders of forcing significantly increases complexity. With just three orders of forcing unrealistic amplitudes of sea-level oscillation are required to generate a sedimentary hierarchy. For this reason, it is unlikely that an ordered forcing mechanism would be apparent in the sedimentary record if more than two orders of high-frequency oscillation are combined.
- The degree to which accommodation is filled does not appear to have a bearing on the generation of a sedimentary hierarchy. Peritidal carbonate successions may therefore be no more likely to exhibit a hierarchical section than sub-tidal successions unless an alternate autocyclic mechanism can invoke a thickness hierarchy.
- A sedimentary hierarchy is fundamentally unrealistic as very high amplitudes of high-order oscillation (in excess of intermediate-order oscillation amplitudes) are often needed to generate the differential thicknesses of sediment. This does not seem congruous with what we know about rates of sea-level change during ice-house conditions. Furthermore, the style of cyclicity inherent to ice-house successions is not characteristic of ice-house cycles. Most important, however, is the level of complexity introduced by multiple orders of eustatic sea-level oscillation, which renders the creation of a sedimentary hierarchy extremely improbable.
- The extreme improbability of a sedimentary hierarchy existing means 'bundled' stacking patterns should not be used as a predictive element to determine stacking patterns of inner-platform ice-house successions in the subsurface.

Chapter 5: SUBSIDENCE-MODULATED GLACIO-EUSTASY: AN EXAMPLE FROM MIDDLE PENNSYLVANIAN SHELF CARBONATES OF THE PARADOX BASIN, USA

5.1 INTRODUCTION

Cyclic sedimentation has been documented in a number of sedimentary basins of Pennsylvanian age. The Pennsylvanian was a time of extensive glaciation on southern hemisphere land masses (Smith & Read, 2000) and the cyclicity of strata has often been attributed to high-frequency large-amplitude glacio-eustatic oscillations (e.g. Heckel, 1986; Veevers & Powell, 1987; Goldhammer *et al.*, 1991; Lerat *et al.*, 2000). Paradox Shelf strata are interpreted to display this prominent cyclicity in a mixed system of carbonate and siliciclastic lithologies, which are also laterally correlative with evaporites in the basin (Peterson & Hite, 1969; Baars, 1988; Stevenson & Baars, 1988).

The Desmoinesian succession of the Paradox Shelf was interpreted by Goldhammer *et al.* (1991) to display a distinctive, hierarchical style of cyclicity; where 'fifth-order' shallowing-upward cycles stack vertically into 'fourth-order' sequences, which themselves are embedded in third-order accommodation trends (Figure 5.1). The fundamental assumption behind this sedimentary hierarchy is that fourth- and fifth-order patterns represent individual excursions of eustatic sea-level; interpreted to be forced by periodic and cyclic continental glaciation. The longer-term third-order trends were considered as probably driven by long-term variations in subsidence. Quantifying the temporal duration of inferred high-frequency cycles is difficult not only because of the complexity and likely incompleteness of the strata, but also because high-resolution biostratigraphic data is lacking for the Desmoinesian of the Paradox Basin. This is important because it means no independent line of evidence exists to test the hypothesis of high-frequency 'Milankovitch' climatic forcing.

Within the Paradox Shelf succession, more recent studies have further identified 6th-order cyclicity (Grammer *et al.*, 2000). Grammer *et al.* assert that their use of 5th- and 6th-order does not bear relationship to the duration taken to deposit such cycles, but rather merely indicates their location embedded within 3rd- and 4th-order sequences. This fundamentally imposes a duration upon the higher-order cycles, however, as they must be of shorter duration than a cycle of lower-order to be embedded within it.

It should be noted that in this study discussions concerning excursions of relative sea-level do not use 5th-, 4th- and 3rd-order terminology, therefore not ascribing a particular hierarchical forcing-mechanism to the oscillations. Instead, oscillations are

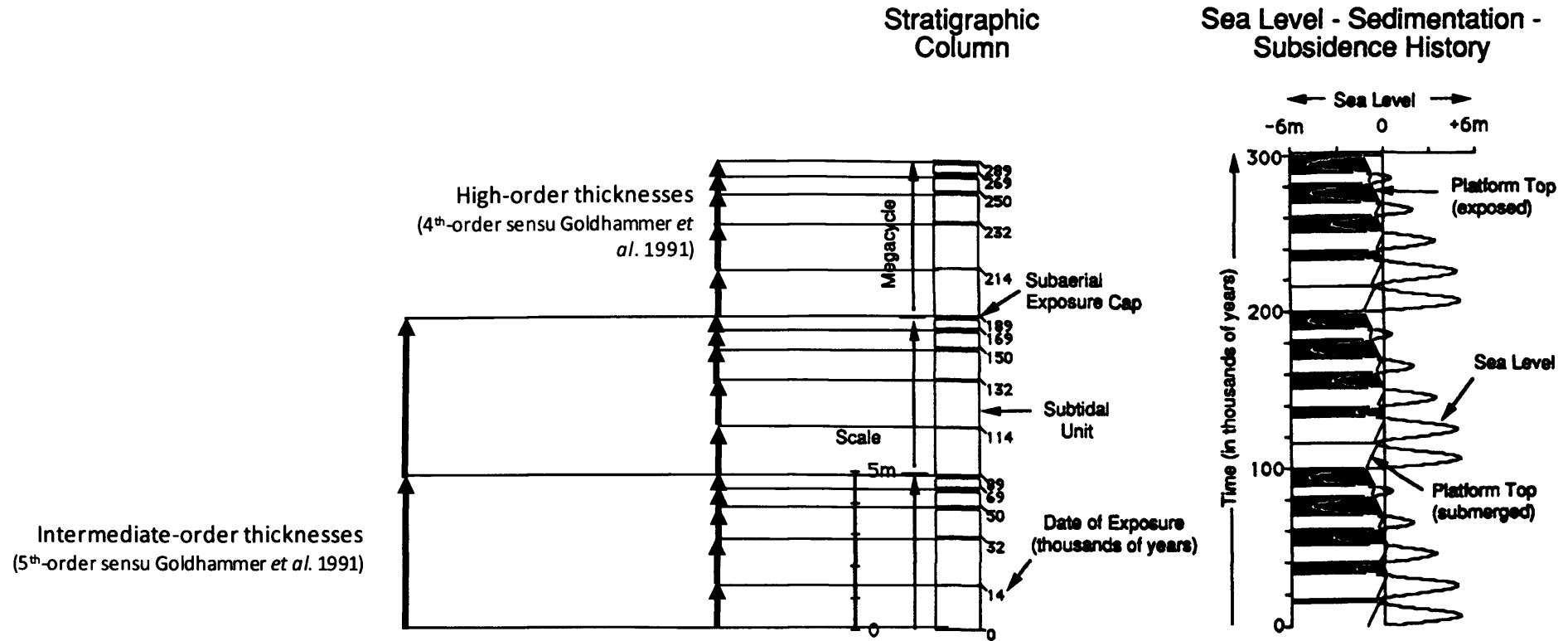


Figure 5.1: Diagram showing the concept of a sedimentary hierarchy from Goldhammer *et al.* (1991). High-order high-frequency sequences are bundled into intermediate-order sequences based upon their thickness relative to the immediately adjacent high-frequency sequence. When a thicker sequence occurs, a new intermediate order sequence begins.

categorised in terms of their wavelength and are referred to in terms of high-order, intermediate-order and low-order (refer to section 1.4).

The Paradox Basin is particularly well known for extensive Pennsylvanian algal mound development (Roylance, 1990; Eberli *et al.*, 2000). These algal mounds created palaeotopographic highs and lows and significantly affected the lateral distribution and continuity of facies where they were present (Lerat *et al.*, 2000). The topographic variations created by algal mounds are a fundamental autocyclic control on accommodation generation, and introduce significant uncertainty when trying to attribute relative sea-level oscillations to a given cause. Algal mounds can be said to have little influence of the style of the section at the Honaker Trail, it being outside the main locus of mound development (developed primarily away from the proximal Paradox Shelf; Figure 5.2). One mound (as interpreted by previous workers, but more accurately described as a biostrome) does outcrop at the Honaker Trail; however it has lateral continuity on the kilometre-scale and shows little variation in thickness. Furthermore many of the beds at the HTS have kilometre-scale lateral continuity and show little evidence of pinching out. Smaller cycles identified in the section have been noted to be of limited lateral extent ('5th-order'; Grammer *et al.*, 2000); it therefore follows that these cycles must be controlled by more than just relative sea-level oscillations, otherwise they would be more laterally extensive.

The method of Goldhammer *et al.* (Goldhammer *et al.*, 1991) in using vertical facies analysis assumes significant lateral continuity of facies. Although significant problems have subsequently come to light regarding vertical facies analysis as a method of quantifying cyclicity (cf. Wilkinson *et al.*, 2003), the Honaker Trail section (HTS) presents an ideal place to study cyclicity in one-dimension, both at outcrop and using one-dimensional forward modelling because it has demonstrable lateral continuity of facies at this locality (Van Buchem *et al.*, 2000).

In light of previous research focussed on the Pennsylvanian of the Paradox Basin, this study aims to quantify, through outcrop studies and numerical forward modelling, the fundamental controls on any apparent cyclicity in the carbonate strata. The primary objectives of this study were to quantify the fundamental controls on the stacking patterns of the section, objectively assess the presence of a sedimentary hierarchy in a section of the Hermosa Group; and based on this, to contribute to the debate on the presence or absence of Milankovitch forcing in this case.

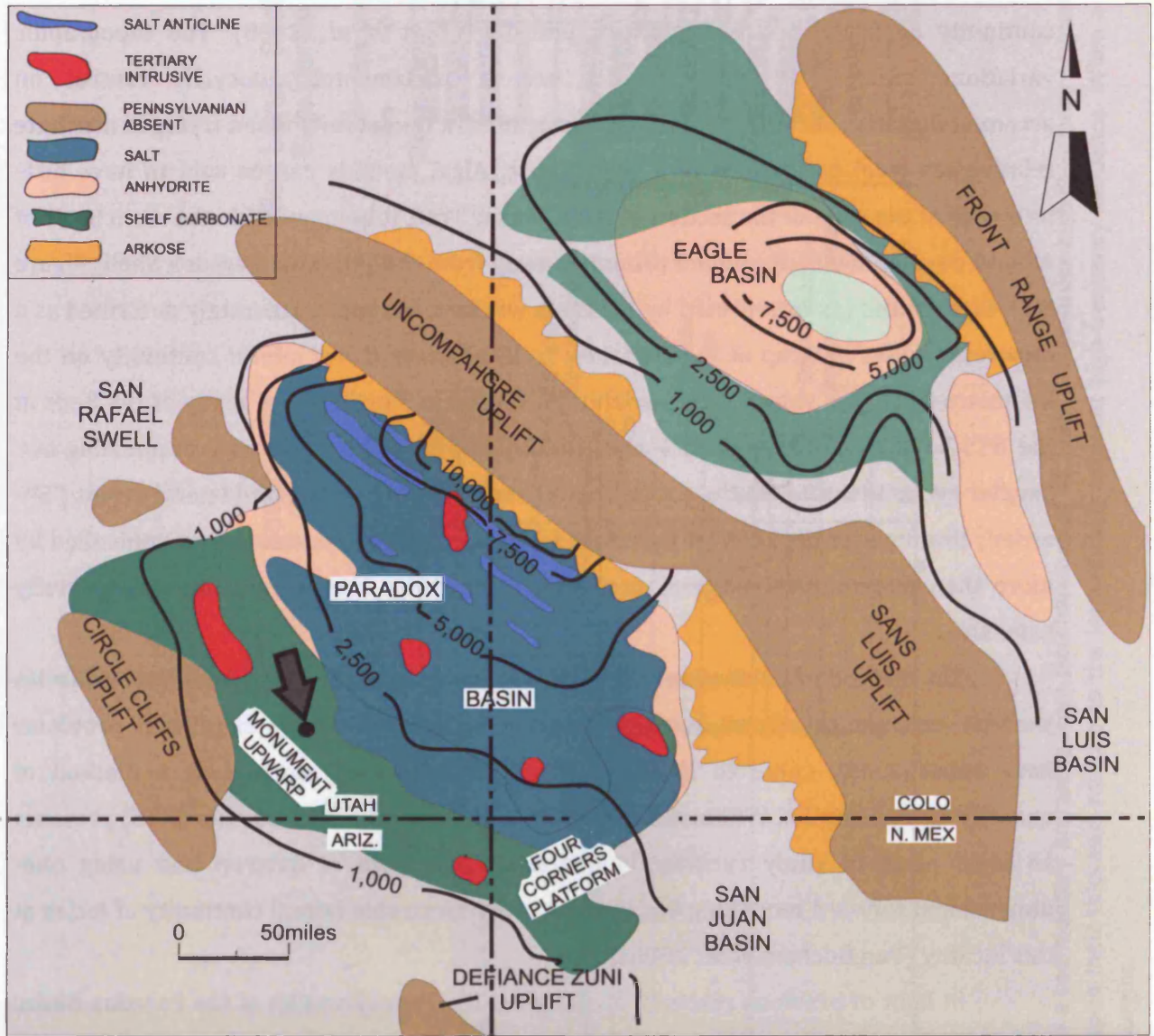


Figure 5.2: Isopach and facies map of the Pennsylvanian succession of the Four Corners region. Isopach units are feet. Also shows major areas of uplift during the Pennsylvanian. Honaker Trail section is arrowed. Line of cross section is shown in Figure 5.3. Modified after Peterson & Hite, 1969 and Goldhammer *et al.*, 1991.

5.2 GEOLOGICAL SETTING

5.2.1 Tectonic setting

The Paradox Basin is a $\sim 5 \times 10^4$ km² structurally asymmetric basin that developed along the south-western flank of the Uncompahgre Uplift during the mid-Pennsylvanian to early Permian (Figure 5.3; Wengard, 1962; Stevenson & Baars, 1986). The basin is bounded to the northeast by the Uncompahgre Uplift; a 200-300km long, 50km wide, NW-SE trending, basement-cored arch, itself bounded by fault zones in the southwest and northeast. The Paradox Basin has traditionally been interpreted as a transtensional strike-slip basin of Pennsylvanian age (Stevenson & Baars, 1986). The structural style and depositional fabric of the Paradox Basin strongly indicate that the overall morphology of the basin was dictated by pull-apart tectonics. Yet other factors, including kinematics, geometry and subsidence history, are not easily interpreted using a pull-apart model, and point to a complex, polyphase tectonic history.

Stevenson & Baars (1986) proposed that the Paradox Basin developed through a transtensional (releasing-bend) mechanism in the distal foreland of the Ouachita-Marathon orogenic belt, thereby accommodating the earlier escape-tectonic model for the Ancestral Rocky Mountains (ARM) proposed by Kluth & Coney (1981). The Uncompahgre Uplift was considered by Stevenson & Baars to be part of a continental-scale wrench fault system that was active throughout the Phanerozoic. They identify both a northwest-trending basement fault system and a northeast-trending fracture system. The fault system in particular may represent a significant control on the distribution of facies within the Paradox Basin. These contrasting tectonic fabrics are indicative of a polyphase tectonic history, through which Stevenson & Baars considered the basin to evolve from a sag basin, to an interior fracture basin to a wrench basin in the late Pennsylvanian.

The Pennsylvanian Paradox Basin has a complex, polyphase tectonic history. Recently, the Paradox Basin was reinterpreted in its ARM context as an intra-foreland flexural basin, based upon its tectonic kinematics, geometry and subsidence history (Barbeau, 2003). ARM basin development is considered to be coeval with northeast to southwest suturing between northern Gondwana and southern North America along the Appalachian-Ouachita-Marathon fold belt (Dickinson & Lawton, 2003). In response to the development of this convergent orogenic front to the south, the Desmoinesian Paradox Shelf experienced increased rates of subsidence subsequent to a pre-Pennsylvanian phase of relative stability (Ross, 1979; Pindell & Dewey, 1982; Ross, 1986).

Barbeau (2003) proposes that the Paradox Basin fits the geometric profile of a foreland basin more comfortably than that of a dominantly extensional regime.

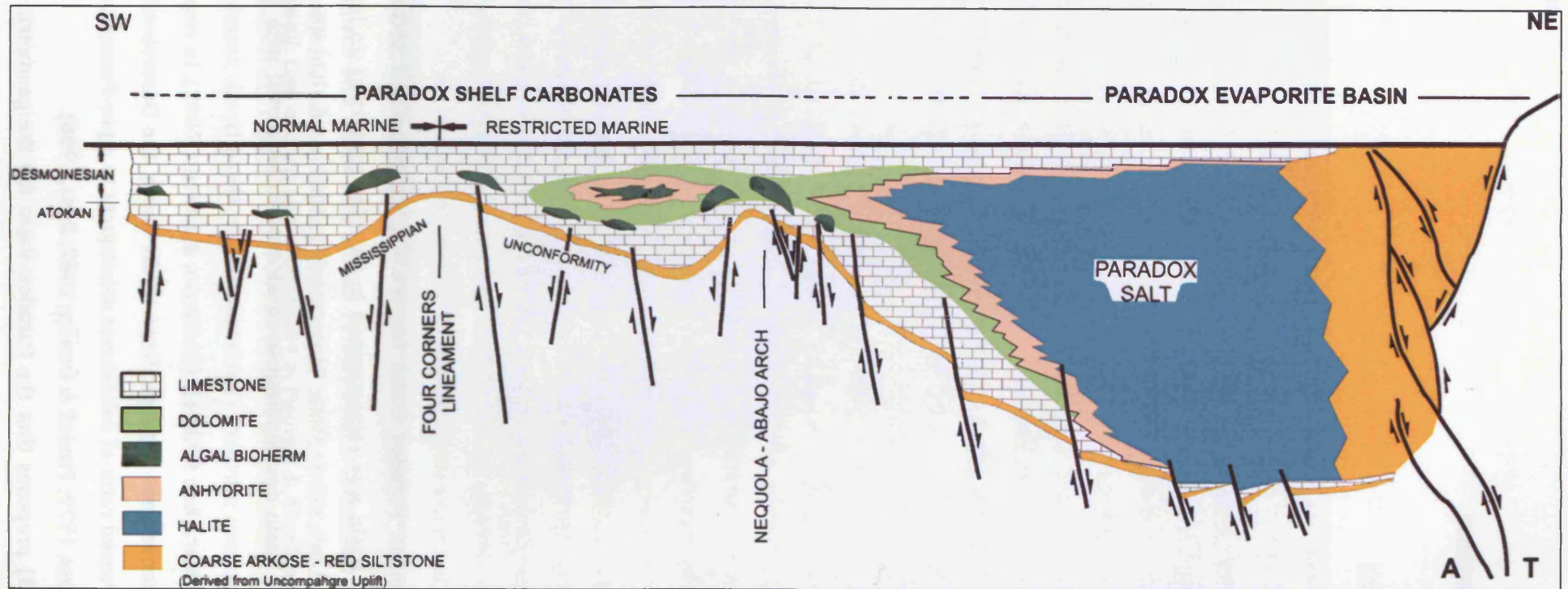


Figure 5.3: Schematic palinspastic cross-section across the Paradox Basin during the Desmoinesian, showing relationship of shelf carbonates to basinal facies. Modified after Baars & Stevenson (1982).

Furthermore, if the Paradox were an extensional basin, the dominant subsidence component would be thermo-tectonic, and would be accompanied by extension-related magmatism; something which is absent in ARM basins. Subsidence rates were high throughout the basin, but there is a differential between the proximal basin, where rates were too rapid to be explained by thermal subsidence alone, and parts of the distal basin. A model of subsidence induced by flexure of the lithosphere by supra-crustal loading of the Uncompahgre Uplift is in line with this model. While subsidence rates and basin geometry during the Pennsylvanian indicate a foreland-basin style tectonic regime, the polygenetic tectonic history of the basin suggests that there is an additional component of transtensional displacement (Baars & Stevenson, 1981; Stevenson & Baars, 1986; Barbeau, 2003). The implications of this are discussed in section 5.5.

5.2.2 The Middle Pennsylvanian carbonate succession

The pre-Pennsylvanian succession across the Colorado Plateau records relatively stable flat-topped, attached-platform conditions (Baars, 1988). At the end of the Mississippian regional uplift exposed the shelf, leading to widespread karstification and development of palaeosols above Mississippian carbonate strata. A marine transgression is recorded in the Pennsylvanian in the form of reworked terrestrial material in the Atokan Molas Formation, which forms the first unit of the Hermosa Group (Figure 5.4). The Hermosa Group is between 900 and 1200m thick on the Paradox shelf, and in addition to the Molas Formation comprises the Desmoinesian Paradox Formation and the Desmoinesian-Virgilian Honaker Trail Formation (Ohlen & McIntyre, 1965).

The Middle Pennsylvanian Paradox system is typified by cyclic shelf carbonates and coeval basinal evaporites interpreted to represent cyclic, reciprocal patterns of accommodation and accumulation. Strata on the shelf have very gentle dips to the northeast, towards the basin; depositional strike being northwest-southeast. The Honaker Trail Formation, which this study focuses upon, is composed largely of bioclastic packstones and grainstones inter-bedded with quartzose siltstones and sandstones as well as calcareous mudstones. Beds are generally laterally extensive, but thinner units are sometimes seen to be lenticular in nature (Lerat *et al.*, 2000). Cross stratification is abundant in calc-arenitic sandstones and grainstone beds. Bioclasts present in massive packstones and grainstones (including crinoids, brachiopods, fusulinids and bryozoans) suggest an open marine environment.

The Honaker Trail Formation on the Paradox Shelf has been interpreted as representing a coastal channel system comprised of inter-fingering carbonate shoals and marine channels on a shallow flat-topped platform (Lerat *et al.*, 2000). In the proximal basin alluvial fans dominated throughout the Late Pennsylvanian (Barbeau, 2003).

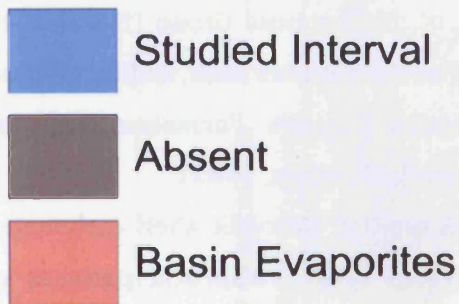
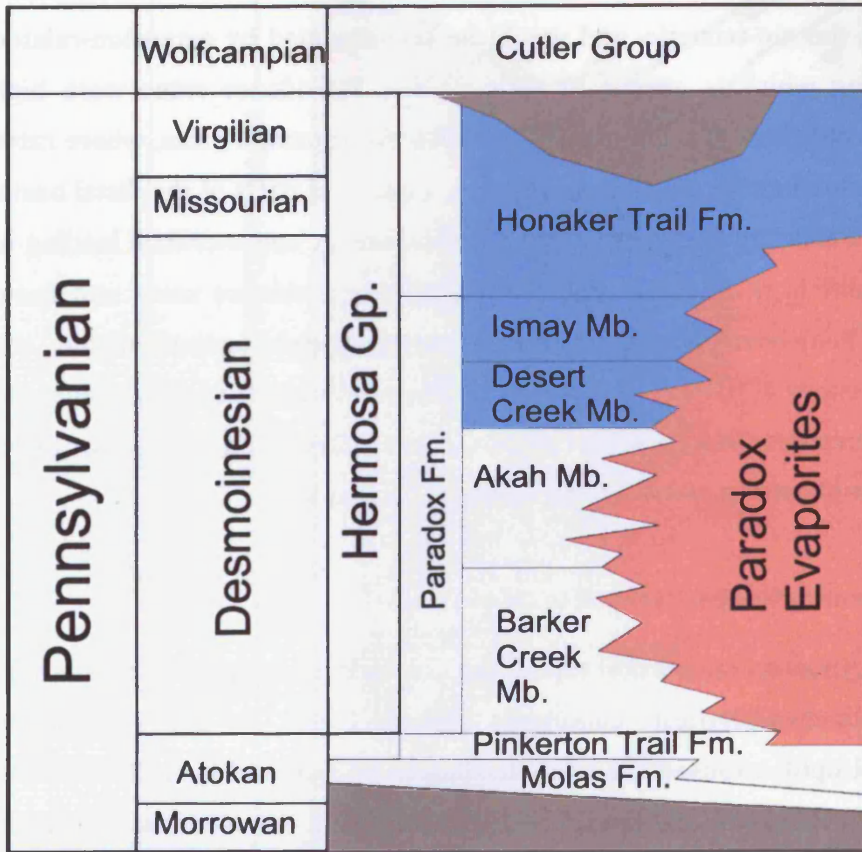


Figure 5.4: Pennsylvanian chronostratigraphy of the Paradox Basin. Modified after Baars & Stevenson (1982).

Siliciclastic influx onto the shelf only occurred during relative sea-level lowstands (Goldhammer *et al.*, 1991; Lerat *et al.*, 2000). The proportion of thick, lenticularly-bedded, cross-bedded siliciclastics increases upwards (particularly in the Upper Honaker Trail Formation), however previous studies have not cited a cause of this change in sedimentation. The Paradox Shelf itself is judged to have acted as a baffle to open-ocean circulation; restricting the basin during periods of low eustatic sea-level (Figure 5.3). Periodically, strata of a restricted marine assemblage were deposited on the shelf along with extensive evaporite deposition in the proximal basin (Peterson & Hite, 1969).

The age model for the Pennsylvanian succession in the Paradox Basin is poorly constrained. Previous attempts to date cyclicity have focussed on deriving temporal durations of sedimentation from cycle thicknesses and inferred forcing mechanisms (Goldhammer *et al.*, 1991). The problems with this method are numerous, not least because of the importance of 'missed beats' and the degree of completeness of the sedimentary record (e.g. Burgess & Wright, 2003). Recent attempts to attribute temporal durations to high-frequency cycles have been made on the basis of conodont biozonation (Ritter *et al.*, 2002). However, given that the Virgilian in the U.S. mid-continent can be divided into 6 conodont zones, and the Missourian into 4, resolution in these zones can only give a maximum resolution of 250Ky (Barrick & Heckel, 2000). Furthermore, this division is inadequate even for longer term 100Ky-magnitude '4th-order' cycles. At the moment therefore, there is not a clear age model for cyclicity in the Paradox Basin accurate enough to attribute temporal durations to sedimentary cycles.

5.3 FACIES ANALYSIS

5.3.1 Aims

The aim of logging this section was a revised measured section; presented in condensed form as Figure 5.5, and in full in Appendix 2. There were three objectives of logging this section in detail:

1. To quantitatively address the level of facies ordering in a section deemed to be hierarchically stacked;
2. To objectively examine cycle boundaries, particularly the existence of exposure surfaces;
3. To use the measured section in comparison with synthetic sections generated by the stratigraphic forward model TED to identify the controlling factors of stacking patterns.

5.3.2 Method

The facies, strata and palaeontology of the Paradox Basin have been documented by numerous authors (e.g. Wengard & Matheny, 1958; Wengard, 1963; Peterson & Hite, 1969; Goldhammer *et al.*, 1990). This study follows the facies classification scheme of Goldhammer *et al.* (1991). Where possible this facies scheme is adhered to, however these facies are re-assessed in order to quantitatively examine the stacking patterns of the HTS. In the log of the section, particular attention was paid to the vertical contacts between facies, and the nature of exposure surfaces, which are critical in defining cyclicity (Figure 5.5).

The Middle Pennsylvanian shelf succession of the Paradox Basin is exposed along canyon sections of the San Juan River. The entire Desmoinesian succession is accessible along the Honaker Trail located in the Goosenecks area of southeast Utah (Figure 5.2). The section described here begins at the base of the Desert Creek Member of the Paradox Formation, and ends at the top of the Upper Honaker Trail Member of the Honaker Trail Formation. This section and its facies have been discussed previously by Wengard (1963), Hite & Buckner (1981), Goldhammer *et al.* (1991) and Lerat *et al.* (2000). The section was measured, logged, and sampled for analysis using thin sections. This section employs the facies scheme outlined in section 5.3; a revised form of the facies scheme proposed by Goldhammer *et al.* (1991). The major difference adopted in the scheme presented here



SECTION: Honaker Trail
LOCATION: Utah, USA
DATA TYPE: Stratigraphic log
DATA DEPTHS: 0-154.11m
LOGGED BY: David Pollitt
DATE: December, 2006

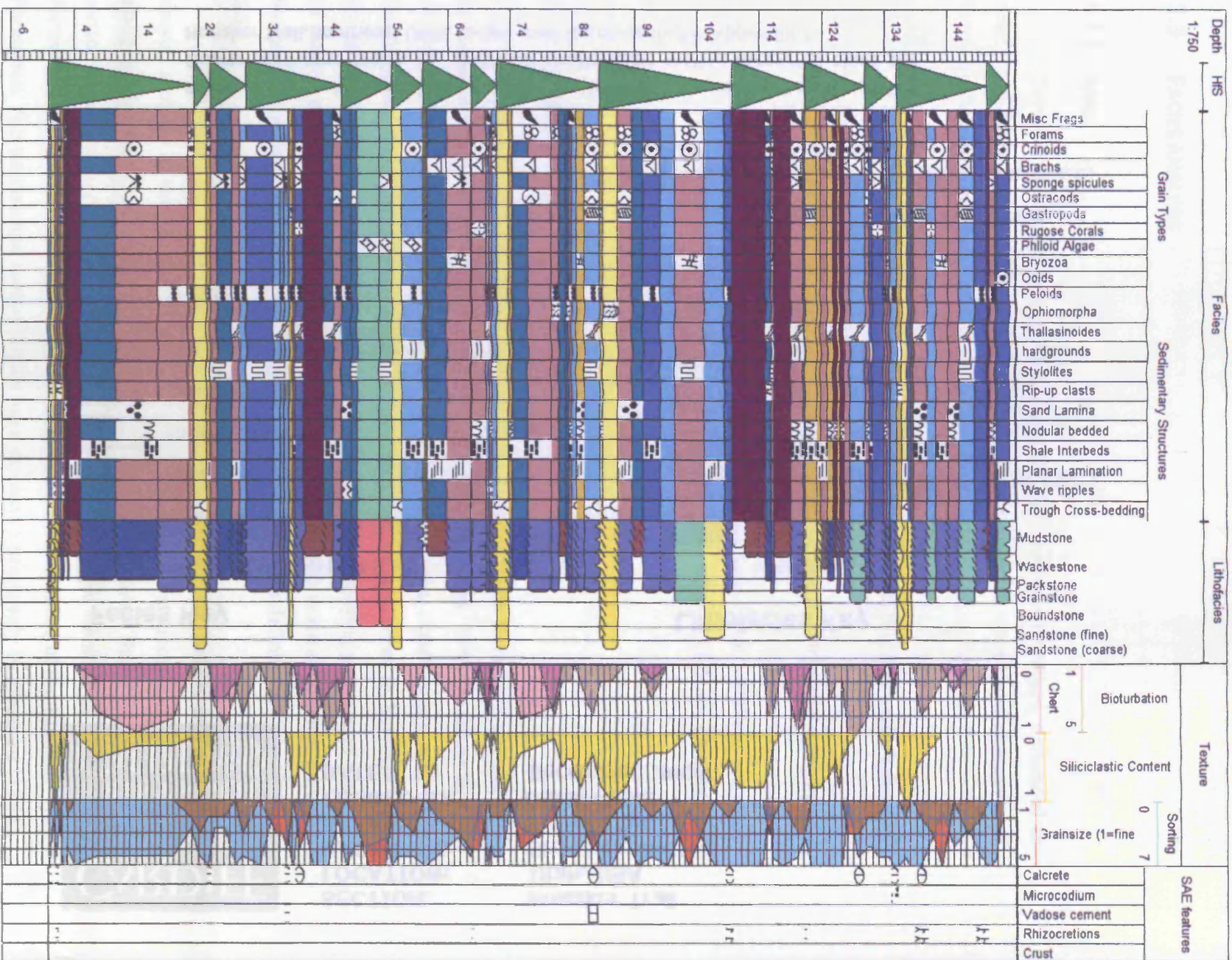
Facies Key

	Black Laminated Mudstone
	Sponge Facies
	Algal Facies
	Skeletal-silt facies
	Skeletal Facies
	Non-skeletal Facies
	QSF1
	QSF2

Lithofacies Key

	Missing
	Mudstone
	Silty carbonate shale (50% silt grains)
	Wackstone
	Packstone
	Diagenetic Crust
	Grainstone
	Boundstone
	Siltstone (20-63um grain size)
	Sandstone (very fine to granule size)

Figure 5.5: a) Facies and lithology key for the Honaker Trail measured section. QSF = Quartz sandstone facies. b) Overleaf: stratigraphic section measured along the Honaker Trail, southeast Utah. Larger scale log presented in Appendix 2.



compared with previous works is the definition of high-frequency sequence (Hfs) boundaries, which are only inferred when there is clear evidence of sub-aerial exposure (refer to the definition of a Hfs; section 1.4.3, and section 5.3.11).

5.3.3 Black laminated mudstone

Comprising 8.29% of the HTS, the black laminated mudstone (BLM) facies forms the basis for the division of the Paradox Fm. into several of its members, notably the Desert Creek and Lower Ismay Members. These stratigraphic boundaries are placed at intervals where the BLM facies is several metres thick (refer to Figure 5.5). This facies is seen to have its greatest vertical thickness towards the base of the Paradox Formation, higher-up the stratigraphic column thicknesses are notably less. Typically, the BLM facies forms recessive slopes in the HTS, and smaller covered intervals are likely caused by this unit, which is the most easily weathered of the facies discussed here (Figure 5.6).

At outcrop the facies is seen to be well-laminated with alternating layers of darker, black, more organic-rich sediment and slightly-lighter very dark-grey layers with a higher quartz component (Figure 5.7, a). This planar lamination is ubiquitous on a millimetre- and centimetre-scale. The basal contact of this facies is sharp, and usually overlies massive units of skeletal facies, non-skeletal facies or quartz-sandstone facies. Upwards, this facies is usually seen to grade into a coarser-grained bioturbated carbonate unit (commonly, but not exclusively, sponge facies; Figure 5.7, b).

This facies is mainly composed of organic-rich mudstone comprising a significant clay or silt component. The major siliciclastic mineral component of this facies is quartz (<70%) alongwith clay minerals (<20%). Carbonate content is usually in the form of amorphous micritic material, occasionally distinct as peloids; the majority of which may be dolomitized (Hite & Buckner, 1981). A sparse faunal assemblage (predominantly conodonts and phosphatic thin-shelled brachiopods) has been reported by Hite & Buckner (Hite & Buckner, 1981). Goldhammer *et al.* (1991) also noted the presence of disseminated iron sulphides within this facies.

5.3.3.1 Interpretation

The BLM facies is interpreted here (and previously by others; Peterson & Hite, 1969; Goldhammer *et al.*, 1991) as representative of deeper-water deposition under anaerobic marine conditions, based on the limited faunal assemblage, high silt and clay content, planar lamination and organic-rich composition. The existence of planar lamination, in particular, is indicative of deposition taking place with a minimum of water turbulence (Byers, 1977). Deposition primarily occurred by sediment settling out of suspension. The limited marine fauna and, in particular, the presence of phosphatic thin-



Figure 5.6: Example of a recessive slope formed primarily by erosion of BLM facies (beneath the figure) at the base of the Desert Creek Member. This is the most well-developed slope of this type in the section. Vertical cliffs are restored when as the BLM facies gradationally changes vertically into another facies unit.



Figure 5.7: a) Example of planar lamination in the BLM facies at the base of the Desert Creek Member (5m from base of section). Lamination can be seen in the cut-section below and to the right of the hammer. b) The BLM facies has a gradational contact on a metre-scale with the overlying facies (sponge facies), which is also marked by the appearance of nodular cherts (which probably follows the morphology of some burrows).

shelled brachiopods, suggests a highly-restricted, euxinic depositional environment (Elias, 1963). Estimations of water-depth based on cross-section correlations have led previous workers to estimate water depths of greater than 30m (Peterson & Hite, 1969; Goldhammer *et al.*, 1991).

Typically, euxinic or anoxic basin conditions are associated with very deep water depths, below the pycnocline (>150m; Byers, 1977). Previous studies have noted, however, that anaerobic conditions can be maintained at much shallower depths within an evaporite basin as a result of super-saturation below the halocline (Byers, 1977). The barred-basin model (Stevenson & Baars, 1986) for the Paradox Basin supports this interpretation. The periodic alternation of restricted conditions resulting from lowering of relative sea-level results in a restricted basin and hypersaline conditions. Goldhammer *et al.* (1991) propose that during relative sea-level rise the dense, anoxic brines developed in the restricted basin would have opportunity to reflux onto the shelf, establishing anoxic conditions there. The reflux layer of saline water would produce euxinic conditions on the shelf due to its low dissolved oxygen content, but in relative shallow water. The BLM facies is therefore interpreted as representing the transgressive phase after a relative sea-level lowstand. Depth of deposition is believed to be not more than 30-40m (Goldhammer *et al.*, 1991). The relative abundance of quartz grains as silt particles suggests deposition a significant distance from any source of sedimentation. This reiterates the interpretation of the Uncompahgre Uplift as a siliciclastic source (to which the Paradox Shelf is distally located), and has important implications regarding the relative timing of sedimentation (refer to section 5.5.4).

5.3.4 Sponge facies

Sponge facies (SF) comprises 13.96% of the HTS, and is evenly distributed, with occurrences in each of the stratigraphic members (refer to Figure 5.4 & Figure 5.5). It was originally defined by Pray & Wray (1963) on the basis of the relative abundance of sponge spicules. At outcrop this facies usually forms grey-to-pink-weathering cliffs, commonly above BLM facies (Figure 5.8). Where this facies does overlie BLM facies, the contact is gradational (Figure 5.7, b). Basal contacts with other facies are always gradational, but may appear sharp due to the presence of nodular or lenticular chert. The SF has previously been interpreted to display sharp basal contacts where it overlies a more massively bedded unit (i.e. quartz-sandstone facies, non-skeletal facies or skeletal facies; Goldhammer *et al.*, 1991), however there is little sedimentary evidence for this. The SF has limited occurrence throughout the section, and this interpretation was largely inferred at, or near, covered intervals (such as at 92m; Appendix 2). In some instances the facies is more accurately interpreted as a marl (refer to quartz-sandstone

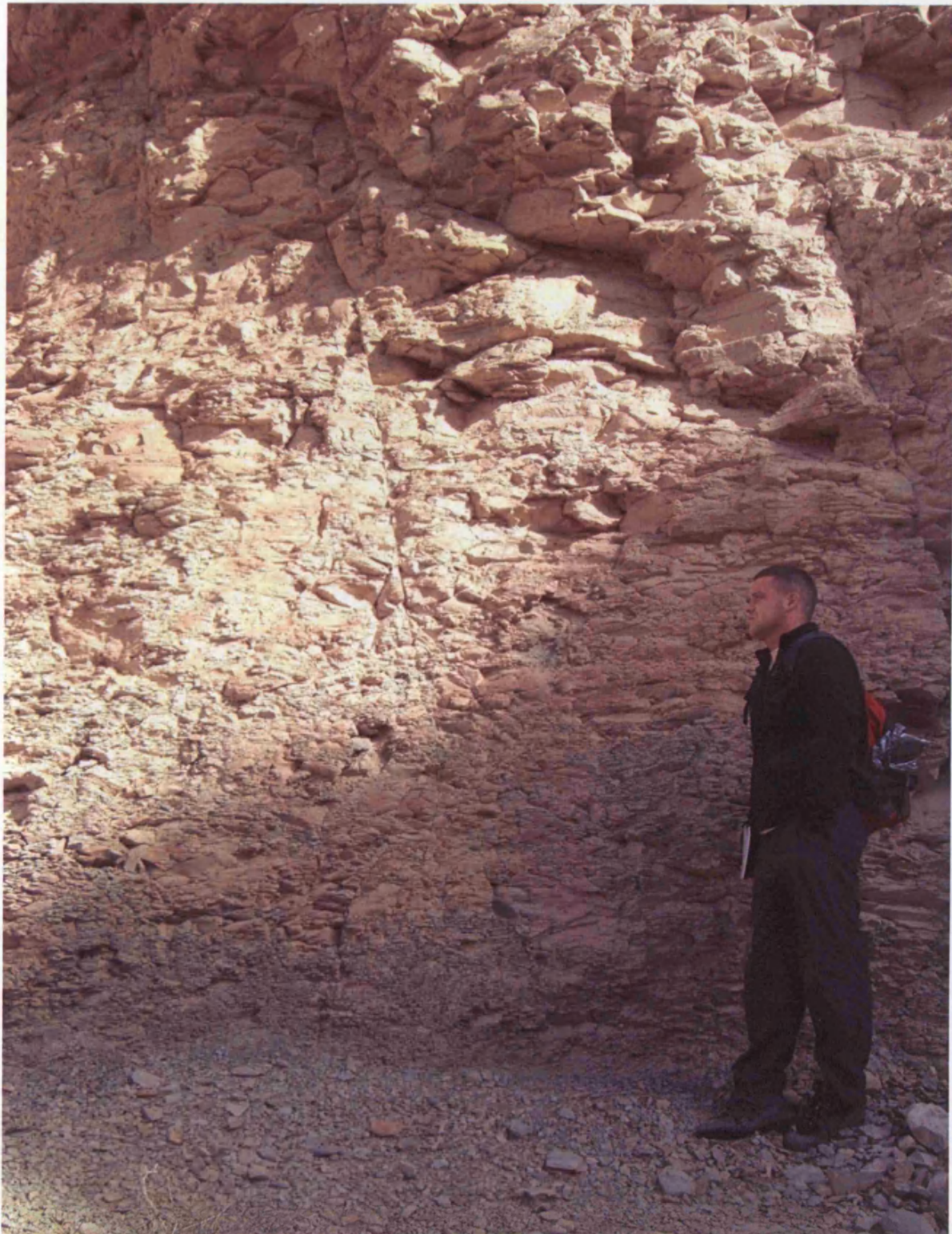


Figure 5.8: Sponge facies near the base of the Desert Creek Member (~17m from base of section); prominent nodular bedding is displayed.

facies; section 5.3.9). Similarly, upper contacts are also gradational over a tens-of-centimetre scale.

Chert, occurring as nodules, lenticular-beds, or nodular beds, is ubiquitous, and increases upwards throughout a bed (Figure 5.9). Bioturbation is present throughout this facies, and the morphology of smaller chert nodules suggests burrows may form preferential areas for chert development. Mechanical compaction during deposition resulted in a parallel-to-sub-parallel orientation of sponge spicules and consequently the facies displays sub-parallel lamination.

SF is composed primarily of siliceous sponge spicules, admixed quartz silt and carbonate peloids (Figure 5.10). Sponge spicules are well-sorted, aligned sub-parallel and generally less than 70µm in diameter. The quartz content can comprise up to approximately 40% of the facies in the form of coarse sub-angular grains. Minor components include disseminated pyrite, minor phosphatic shells (mainly thin-shelled brachiopods and conodonts), and rare silt-sized dolomite rhombs (Goldhammer *et al.*, 1991).

5.3.4.1 Interpretation

The limited marine fauna, presence of sponge spicules, and parallel lamination indicate deposition in a deep, restricted environment. The presence of significant quantities of bedded chert in a facies which is commonly found at the base of the sedimentary cycles, which has a significant siliciclastic content, suggests its origin may be linked to the quantities of silica in the sediment (Cecil, 2004). The dominance of sponge spicules suggests hypersaline conditions given the ability of sponges to tolerate extremely briny conditions (Elias, 1963; Pray & Wray, 1963). The presence of pyrite indicates a reducing, anaerobic environment (Elias, 1963), however the it may be more appropriate to consider the environment as being dysaerobic due to the presence of bioturbation and burrowing. It is speculated that SF represents continued restricted conditions of the shelf after a transgression (Goldhammer *et al.*, 1991). Although less restricted than the BLM facies (which often underlies the SF), it is envisaged that the Paradox Shelf still acted as a bar. Gradually, the marine transgression promoted more mixing and normal marine conditions resumed. It should be noted that the often high proportion of well-sorted, coarse, sub-angular quartz implies that a source of siliciclastic sediment was more active (and possibly nearer) than earlier in the transgressive phase (when BLM facies was being deposited).



Figure 5.9: Nodular-bedded and lenticular-bedded chert in sponge facies (45m from base of section).

Skeletal size facies was proposed in the facies scheme of Goldammer et al. (1991). It replaces "intermediate facies" of Goldammer and is both re-interpreted and renamed here. It was included for consistency with the other larger units that are primarily

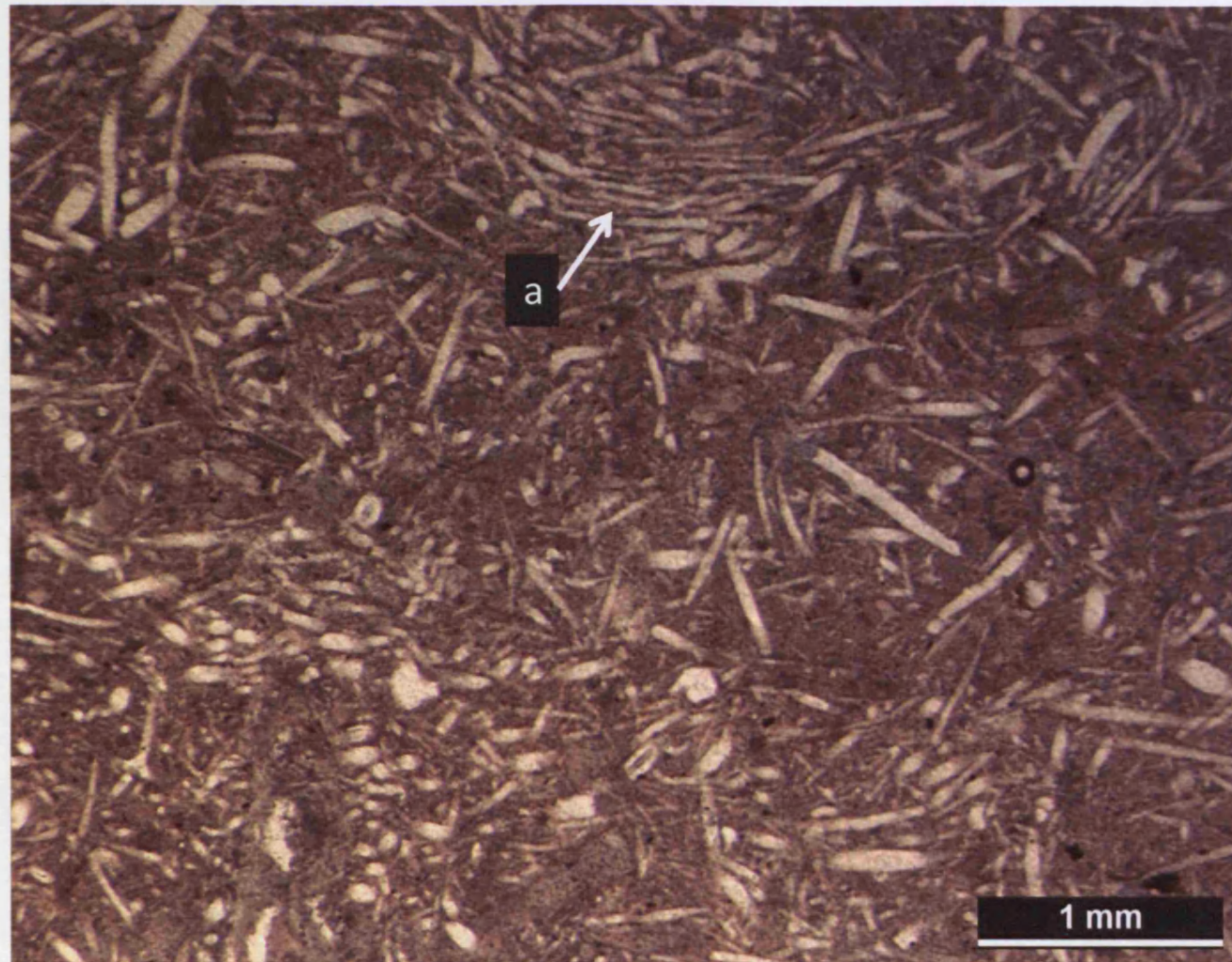


Figure 5.10: Photomicrograph from bed 17 of the HTS. Sponge spicules are abundant, as is fine-grained disseminated peloidal material. a) denotes an area of burrow fill.

5.3.5 Algal facies

This facies is present in the HTS as a single bed (53m; Appendix 2). The morphology of the algal facies (AF) at this locality may be more accurately described as a biostrome rather than a mound, being laterally continuous over a distance of >18.5km towards the basin (Van Buchem *et al.*, 2000). In this respect, the facies differs from true mounds in more proximal parts of the basin (relative to the Uncompahgre Uplift). The absence of mounds is particularly important for one-dimensional modelling, as it means that there was no mound-created depositional topography at the HTS, which may influence interpretations of cyclicity. This largely negates one of the fundamental criticisms levelled at the use of one-dimensional models (refer to section 3.1). The model is applied in a dominantly aggradational setting, with no evidence for significant lateral variability created by palaeotopography.

Given the limited prevalence of this facies (comprising 3.69% of the section), it is not described in full here. For a thorough description refer to Pray & Wray (1963) or Goldhammer *et al.* (1991). The AF at outcrop has a sharp basal contact, and a sharp, erosional upper contact with evidence of sub-aerial exposure. The bed is massive, very-light grey and display prominent mouldic porosity associated with abundant algal plates (Figure 5.11). The lithology is predominantly bafflestone. The dominant component is phylloid-algal plates (*Ivanovia*) cemented by sparry calcite (Figure 5.12). Minor amounts of peloidal material are restricted to areas of primary inter-particle and shelter porosity (Figure 5.12).

5.3.5.1 Interpretation

Algal facies is interpreted as undergoing deposition in a shallow, unrestricted, marine environment. Furthermore a sub-fair-weather wave-base setting (but still within the euphotic zone) is advocated by Pray & Wray (1963); on the basis that the morphology of the algal plates suggest that they would not have resisted significant hydraulic action. The overall lack of micrite supports this interpretation. The sub-aerial exposure surface at the top of this unit, along with vadose meteoric cement (Pray & Wray, 1963), suggest that this unit was deposited prior to a relative sea-level fall.

5.3.6 Skeletal-silt facies

Skeletal-silt facies is not present in the facies scheme of Goldhammer *et al.* (1991). It replaces "Intermediate facies" in that scheme and is both re-interpreted and renamed here. It was renamed for consistency with the other facies names that are primarily



Figure 5.11: Hand-specimen of algal facies from near the top of the Lower Ismay Member. Facies is predominantly a well-cemented bafflestone. Phylloid-algal plates are ubiquitous and visible as darker crescent-shapes (53m from base of section).

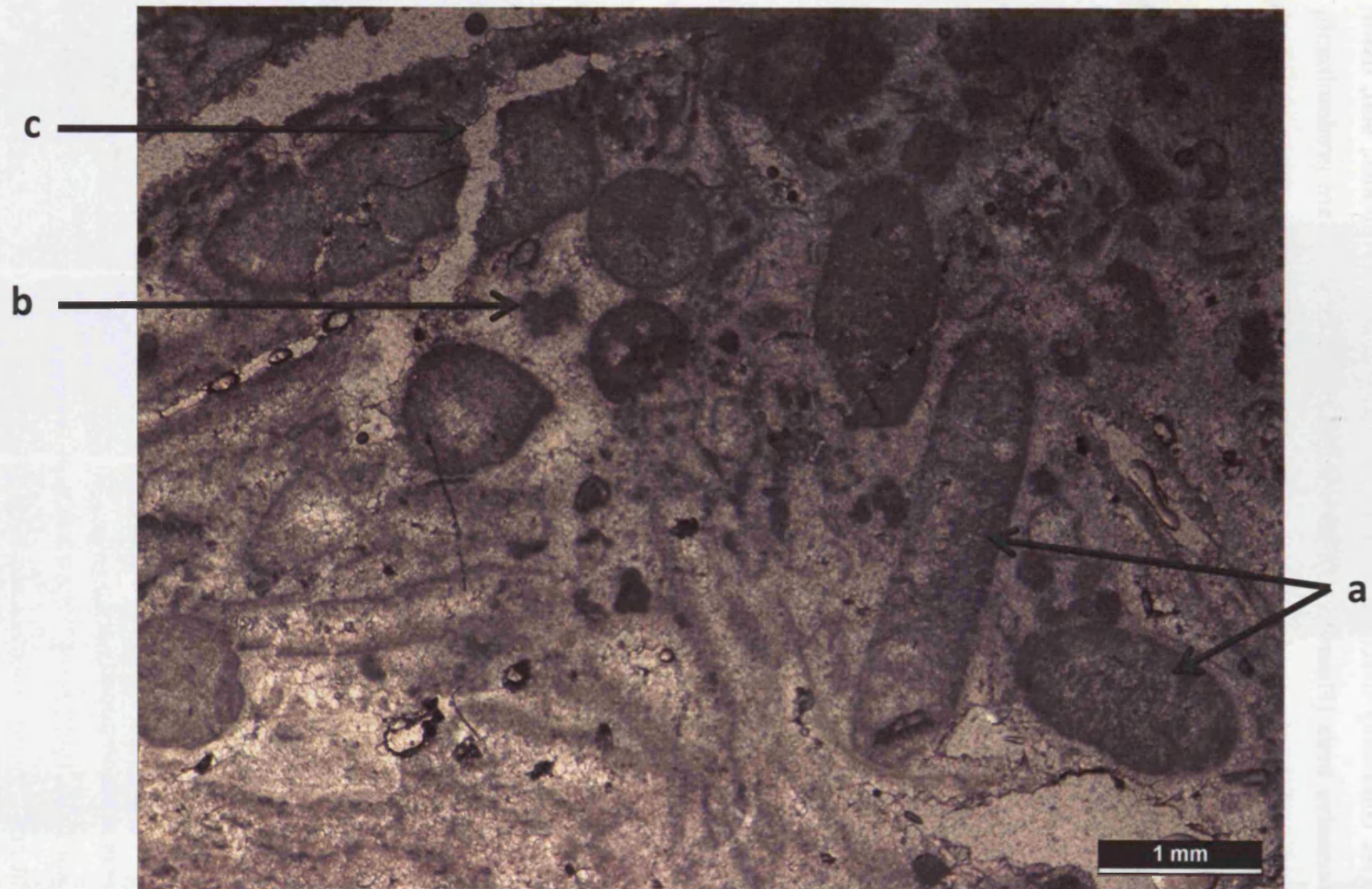


Figure 5.12: Photomicrograph from bed 22 of the HTS. a) Phylloid-algal plates from the major grain component. b) Fine-grained peloidal material occurs mainly in inter-granular and shelter porosity. c) Calcite veining subsequent to primary marine cementation.

descriptive in nature; “Intermediate facies” was not considered appropriate as it has little descriptive value.

Sedimentary units interpreted as skeletal-silt facies (SSF) comprise 32.83% of the HTS. This facies commonly outcrops as thin, lenticular-to-nodular bedded, soft, fissile, green-grey recessive beds (Figure 5.13). Lower and upper contacts are predominantly gradational, although hardgrounds and sub-marine erosional surfaces are common both within beds, and forming contacts between facies (Figure 5.13, b). Chert is also abundant, and may be nodular or lenticular-bedded, commonly overprinting bedding planes. This facies displays an open marine fauna including brachiopods (spiriferids), bryozoa, coral fragments, large echinoderm fragments, occasional phylloid algal plates, and foraminifera including fusulinids (Figure 5.14). Large fragments, particularly of crinoids and brachiopods, are common (Figure 5.13, c). In this respect, sorting is poor and grain-size is predominantly medium-grained silt. There is a significant amount of micrite, and the rock fabric is predominantly mud-wackestone, although very localised grain-rich (commonly burrow fills) are packstone. Quartz content is also significant (as silt-very fine sand), comprising 20-40% of the unit (Figure 5.14), and the facies is notably sandy at outcrop.

5.3.6.1 Interpretation

Skeletal-silt facies are interpreted as deposits of a relatively deep offshore environment below fair-weather wave-base, based primarily on the abundance of micritic material, normal marine assemblage and lack of sedimentary structures. The poor sorting of the facies lends support to this. Salinity was normal marine, reflecting less restricted conditions in the basin subsequent to a marine transgression (Pray & Wray, 1963; Goldhammer *et al.*, 1991).

5.3.7 Skeletal facies

Skeletal facies and non-skeletal facies (refer to section 5.3.8) correspond to skeletal cap facies and non-skeletal cap facies defined by Goldhammer *et al.* (1991). “Cap”, however, has been omitted from the title of these facies as it implies a stratigraphic position at the top of cycles. This is not always necessarily the case, and so this nomenclature is not maintained here.

Skeletal facies (SkF) constitutes 16.98% of the HTS, and is apparent at outcrop as massive, light-grey, jointed metre-scale beds (Figure 5.15, a). Lower contacts may be gradational or sharp-based whilst upper boundaries are usually sharp. This facies is commonly burrowed, may occasionally display trough cross-bedding, and, rarely, cross-lamination. Particularly distinctive burrow mottling is present in numerous beds (Figure 5.16). Chert may also be present.

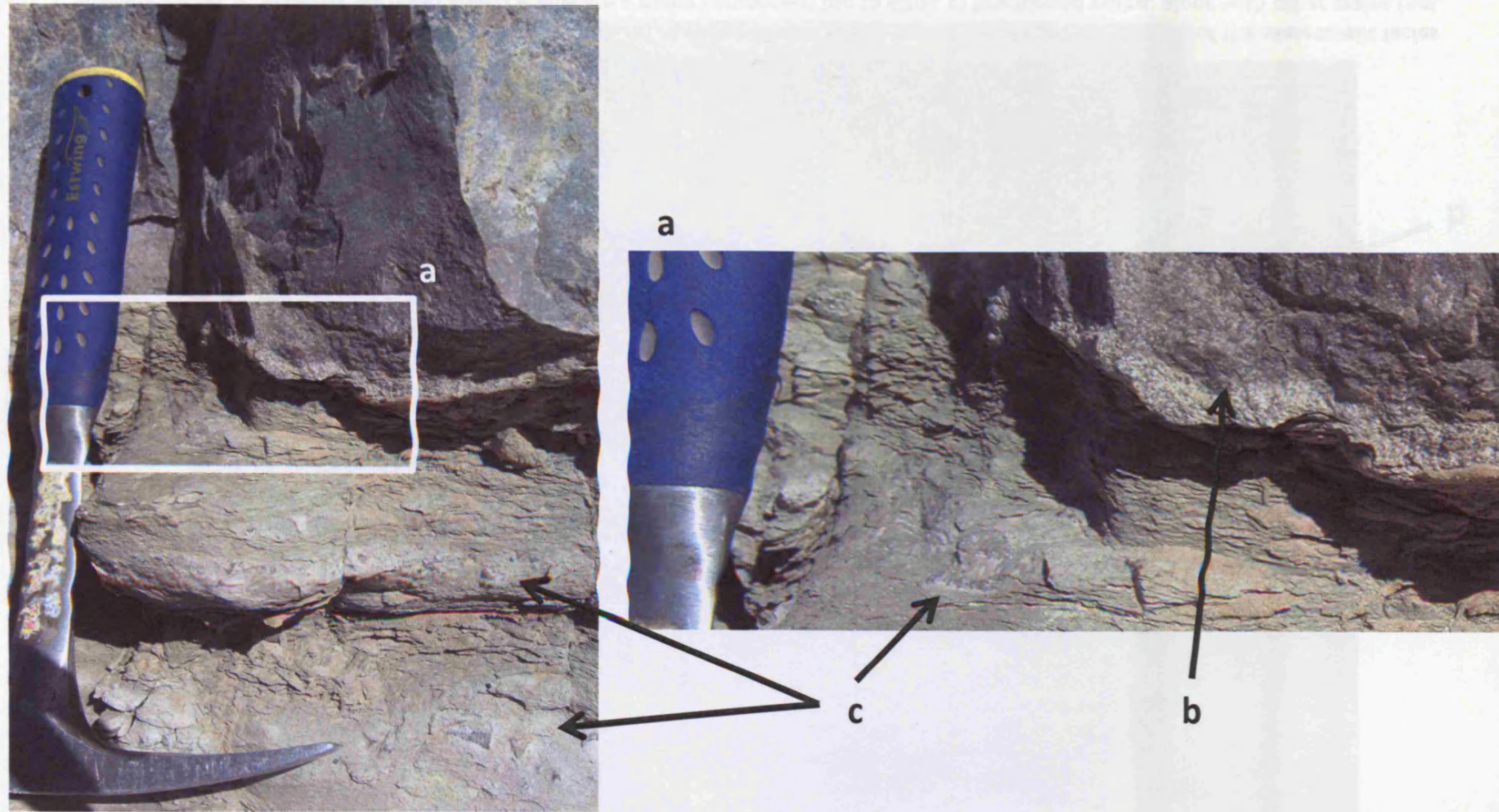


Figure 5.13: Example of skeletal-silt facies. SSF appears at outcrop to be green-grey weathering, recessive, lenticular-to-nodular bedded, silty with predominantly gradational upper and lower contacts. In this case, the upper contact is a marine erosional surface (b). Large fossil fragments (brachiopods, echinoderms) are abundant (c). 70m from base of section.



Figure 5.15: a) Massive beds of skeletal facies from the base of the Upper Honaker Trail Member. b) Massive beds of non-skeletal facies from the top of the Lower Honaker Trail Member. Both facies appear very similar at outcrop.



Figure 5.16: Distinctive burrow mottling in skeletal facies. This bioturbation overprints primary mechanical sedimentary structures where it is present. 88m from base of section.

This facies is primarily composed of packstone fabrics; however grainstone fabrics also occur. Within packstones, micritic disseminated material and peloids may comprise up to 20% of the facies (Figure 5.17). A normal marine fauna dominates, primarily composed of echinoderm and brachiopod fragments. Minor faunal components include rugose corals, bryozoa, foraminifera, including fusulinids, and molluscs. Notably, siliciclastic material is mostly absent in this facies.

5.3.7.1 Interpretation

The grain-supported fabric, abundance of a normal marine fauna and numerous euphotic organisms (including coralline material) suggest an unrestricted and very shallow environment of deposition. Sedimentary structures suggest that this was above fair-weather wave-base in a zone of constant agitation by hydraulic energy. This is supported by the fact that grains are mainly detrital (skeletal grain fragments are abundant). Cross-stratification in some grainstone beds also suggests that this facies migrated as dunes or bars under this dynamic regime. Deposition of packstone beds of the same facies is possibly a consequence of deposition in a marginally deeper environment.

5.3.8 Non-skeletal facies

Non-skeletal facies comprise 10.93% of the HTS. At outcrop the facies looks very similar to skeletal facies (Figure 5.15, b), occurring as massive, and jointed, light-grey metre-scale beds (Figure 5.18). Like those of skeletal facies, beds of non-skeletal facies (NSF) may display sharp or gradational lower boundaries although upper boundaries are usually sharp (and may display evidence of sub-aerial exposure). Sets of relatively large (~0.5m thick) trough cross-bedding are common, and easier to identify than in skeletal facies due to the absence of bioturbation. Planar lamination is also common (Figure 5.18). Large, high-amplitude stylolites are common, as are hardground surfaces (refer to section 5.3.10).

Rock texture is predominantly grainstone (although packstones also occur). This facies often displays moderately well-sorted medium- to coarse-sand-size grains. Major grains are primarily non-skeletal, including; ooids, peloids and intraclasts, but foraminifera can form a significant component (Figure 5.19). Other skeletal grains are present as a relatively minor component and comprise a normal marine fauna (brachiopods and echinoderm fragments dominate). Siliciclastic material is usually rare, but is more prevalent in some beds in the Honaker Trail Formation. Quartz sand can be seen to delineate sedimentary structures where it is present. Primary porosity included interparticle, intraparticle and mouldic porosity; however, this is usually totally filled with

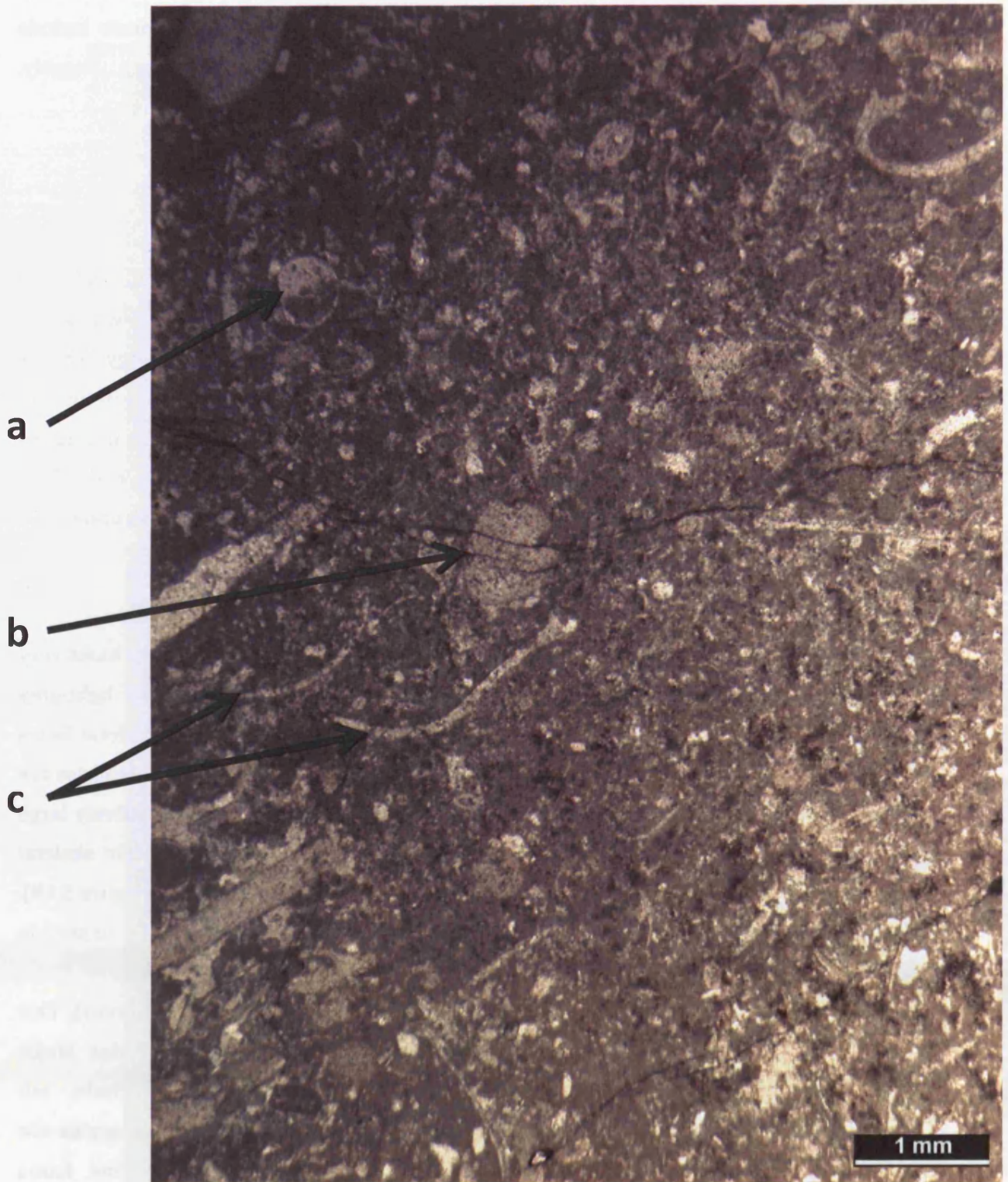


Figure 5.17: caption overleaf

Figure 5.17: Example of skeletal facies from the HTS (Bed 46). a) Gastropod with geopetal infill. b) Abraded crinoid plates are common. c) Brachiopod shell fragments. Overall fabric is a wacke/packstone.

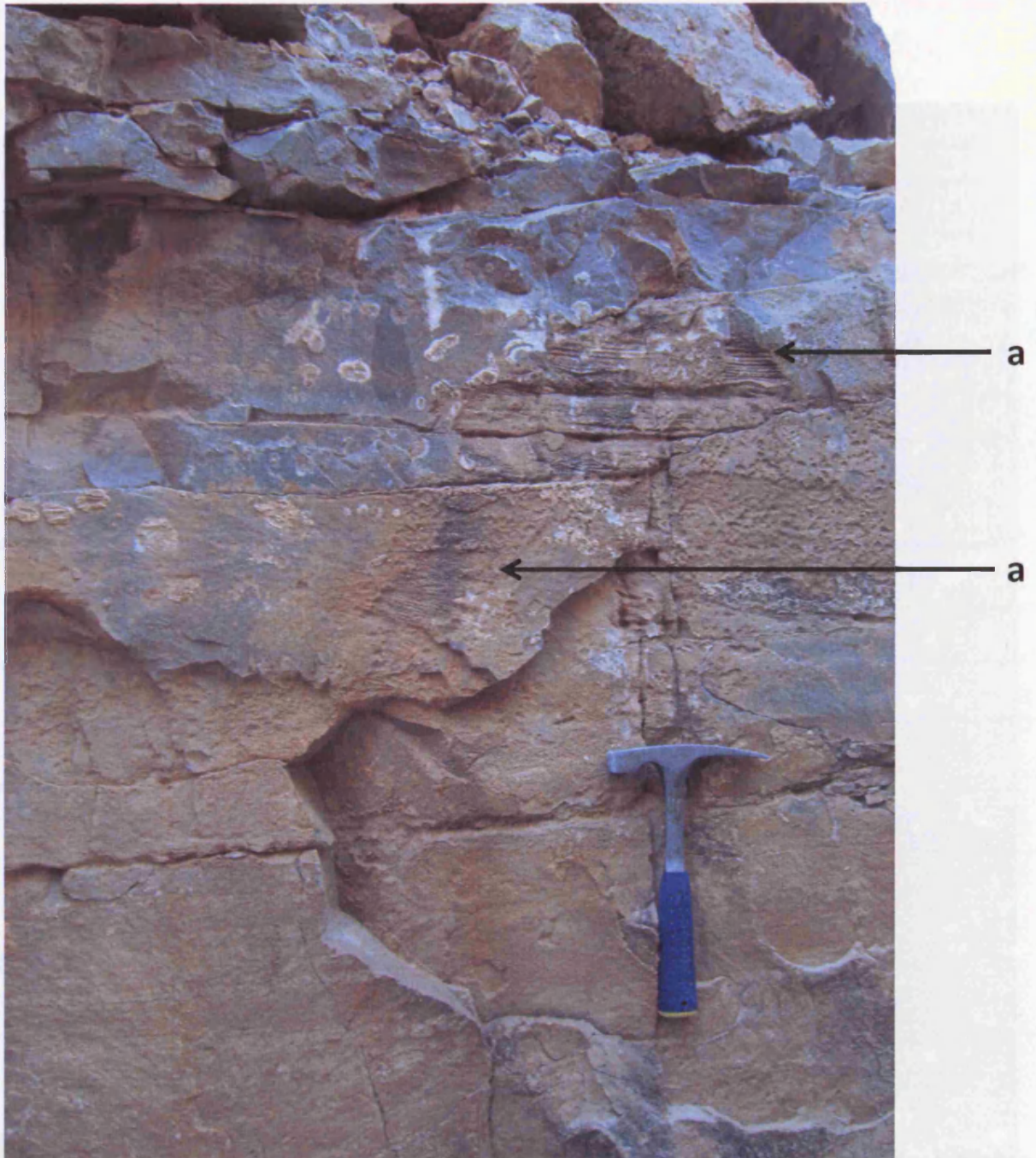


Figure 5.18: a) Planar lamination in non-skeletal facies delineated by sorting of siliciclastic quartz grains and coarser material. 25m from base of section.

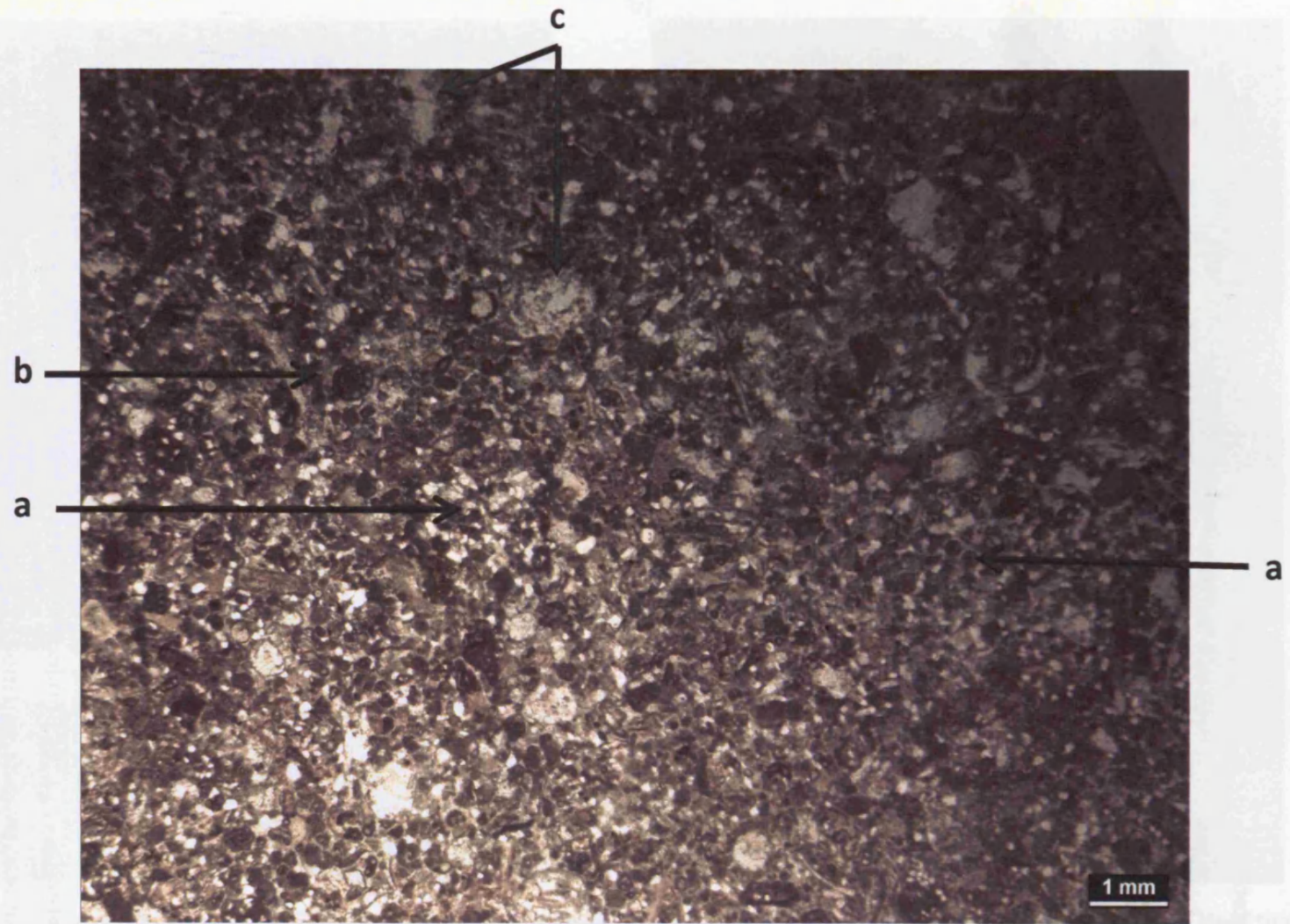


Figure 5.19: Example of packstone non-skeletal facies from bed 31 of the HTS. a) Principle grains are small peloids. b) Forams represent the major bioclastic component. c) Equant calcite cement filling mouldic porosity.

medium- to coarsely-crystalline, equant sparry non-ferroan calcite. There is also evidence of leaching as a result of sub-aerial exposure.

5.3.8.1 Interpretation

The light-colour, grain-supported fabric, abundance of non-skeletal grains (especially well-rounded ooids), fragments of fossil skeletal material, and the prevalence of cross-bedding suggest that this facies was deposited in a high-energy sub-tidal environment. This is envisaged to have been at or around fair-weather wave-base in a zone of relatively intermittent agitation by hydraulic action, based on the fossil assemblage and the sedimentary structures present (principally trough cross-bedding and planar lamination). This interpretation is similar to skeletal facies (refer to section 5.3.7.1).

Goldhammer *et al.* (1991) note that cementation occurred in multiple phases; cementation both preserves the form of mouldic pores subsequent to dissolution, and then fills them during a second phase. Cement morphology (and evidence of dissolution in the form of mouldic porosity) indicates that much of the cementation occurred within the phreatic zone (Peterson & Hite, 1969; Goldhammer *et al.*, 1991). However, given that the distance between exposure surfaces is often less than 15m, and that phreatic diagenesis can pervade significant distances beneath the platform surface this should not be considered a definitive proxy for proximity to a sub-aerial exposure surface.

5.3.9 Quartz-sandstone facies

Quartz-sandstone facies (QSF) comprises 13.32% of the HTS. At outcrop, it varies in form significantly from tan-pink massive silt- and sandstones to grey-green units which may be best described as calcareous sandstones. To account for the two end-member forms of this facies, two sub-facies are used; QSF1 and QSF2 to account for the massive silt- and sandstones and the more calcarenitic units, respectively. This follows the nomenclature proposed by Goldhammer *et al.* (1991), although the distinction was by these workers on sedimentary structure alone. This is maintained here, but there is significant differential in terms of mineralogy (specifically carbonate content) and other components that warrant differentiation in terms of facies designation (Figure 5.20).

Both facies are laterally continuous on a kilometre scale. Basal contacts of this facies are usually sharp against carbonate units, whilst contacts between sub-facies are usually gradational. Basal contacts where QSF1 overlies carbonate facies are often accompanied by lithoclasts (Figure 5.21). The upper contacts of both sub-facies are usually gradational; where a sharp boundary exists; there is no evidence of erosion.

a)



b)

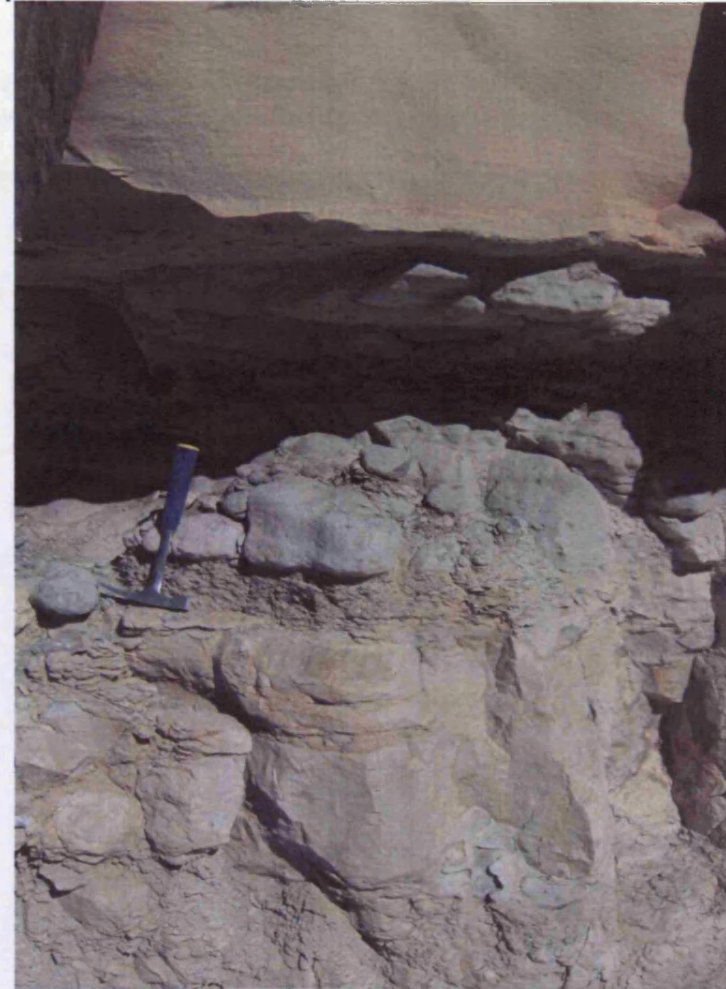


Figure 5.20: Comparison between QSF1 (a, next to hand, overlying QSF2) and QSF2 (b, next to hammer, QSF1 overlies it). Note that these are photographs of beds at different stratigraphic intervals within the Lower Honaker Trail Member. QSF1 is massive, with prominent trough cross-bedding, whilst QSF2 forms nodular, recessive units as a result of increased fine-grained carbonate content. Note that in both cases QSF2 has a gradational contact with QSF1. 85m from base of section.

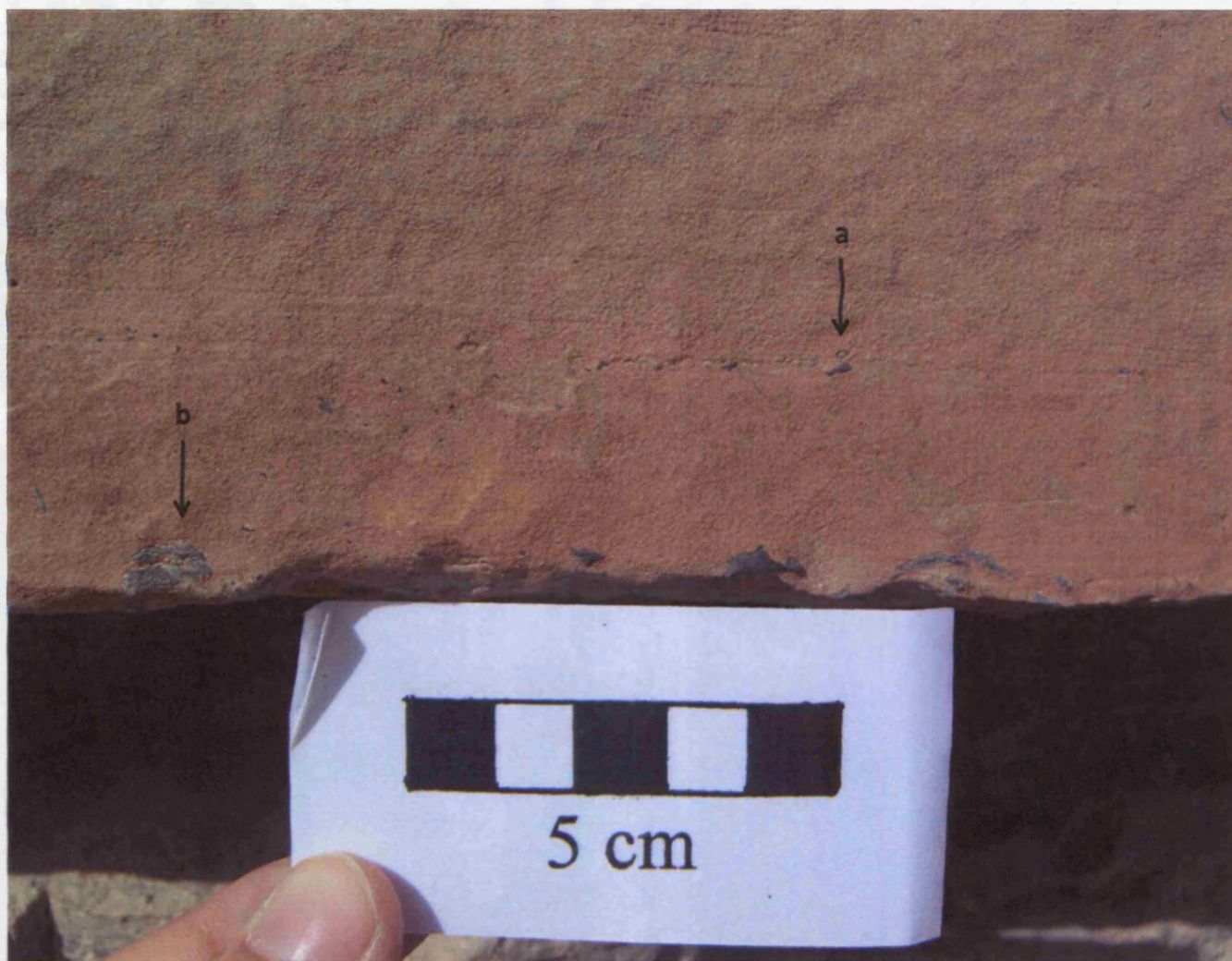


Figure 5.21: Carbonate grains from the underlying facies (skeletal facies) incorporated into QSF1 as individual grains deposited along foresets (a) and large lithoclasts at the base of the section (b). 72.1m from base of section.

The siliciclastic content is similar in both facies; grains are very well-sorted, sub-angular to sub-rounded fine quartz with little or no clay material (Figure 5.22). Grain-size varies from fine sand in QSF1 to coarse silt in QSF2. Both sub-facies may contain carbonate material. In the case of QSF1 this is usually in the form of grains including large fossil fragments (Figure 5.21), which are particularly prevalent at the base of a bed, and constitutes <10% of the total content of the rock. QSF2 contains more calcareous material as well as admixed well-sorted peloids which can comprise up between 10% and 40% of the unit (Figure 5.22). Consequently QSF2 is usually of packstone or wackestone texture, in contrast to QSF1. The increased carbonate content is the cause of the variation in terms of colour, fissility and outcrop appearance between this sub-facies and QSF1 (Figure 5.20). Both facies are therefore composed of well-sorted, fine-grained siliciclastic sediment and marine sedimentary structures and admixed grains.

Sedimentary structures in QSF1 consist of trough cross-bedding (0.5m thick). Bi-directional planar cross-lamination is present in some beds, although is rare overall. This facies displays prominent (although not abundant) *Ophiomorpha* burrows; which are distinctly visible due to their nodular, pelleted exterior (*O. nodosa*; Driese & Dott, 1984; de Gibert *et al.*, 2006; Figure 5.23). Burrowing is most visible in the upper 0.5m of beds.

QSF2 is distinct in that it lacks large scale cross-bedding, and appears more fissile, nodular, with muddy lenses, and is characterised by small-scale sedimentary structures: bedding is much thinner than in QSF1, and beds occasionally display sub-parallel lamination. Lenticular beds are also common and fine-grained inter-layers are wavy bedded (Goldhammer *et al.*, 1991; Figure 5.20, b).

5.3.9.1 Interpretation

Both QSF1 and QSF2 are interpreted to have been emplaced as unlithified aeolian sediment during lowstands before being reworked and finally deposited by marine processes during the subsequent transgression. Goldhammer *et al.* (1991) invoke very specific models for deposition for both sub-facies, and while that of QSF1 is maintained here, the environment interpretation for QSF2 has been modified based on observations.

QSF1 is interpreted as marine in origin, based upon the presence of carbonate grains indicative of a normal marine fauna, sedimentary structures and *Ophiomorpha* burrows. The trough-cross-bedding and planar cross-lamination in particular suggests lateral migration as bars within a zone of hydraulic turbulence (i.e. above fair-weather wave-base). There is a conspicuous lack of aeolian sedimentary structures (e.g. large-scale, high-angle cross-bedding), however, the very high degree of sorting, relatively small grain-size, distinct lack of clay and sub-angular grain shape indicates that primary transport and

a)



b)

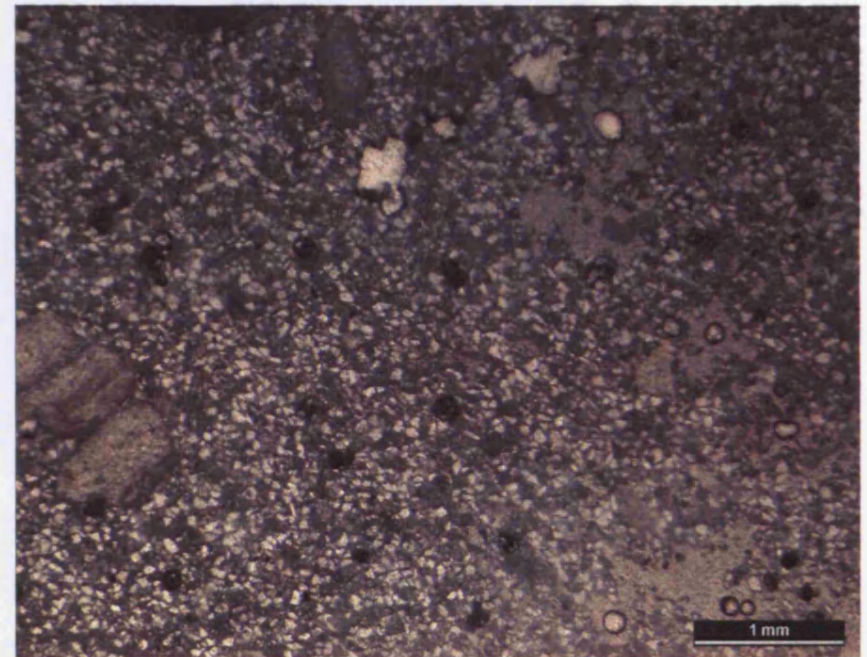


Figure 5.22: Example of QSF1 (a) and QSF2 (b) facies from the HTS (beds 33 and 32, respectively). QSF1 has very well-sorted silt-sized quartz grains. QSF2 has the same quartz silt grains, but a much higher percentage of large, abraded, admixed carbonate grains (principally crinoid fragments). There is also a much larger micrite content.

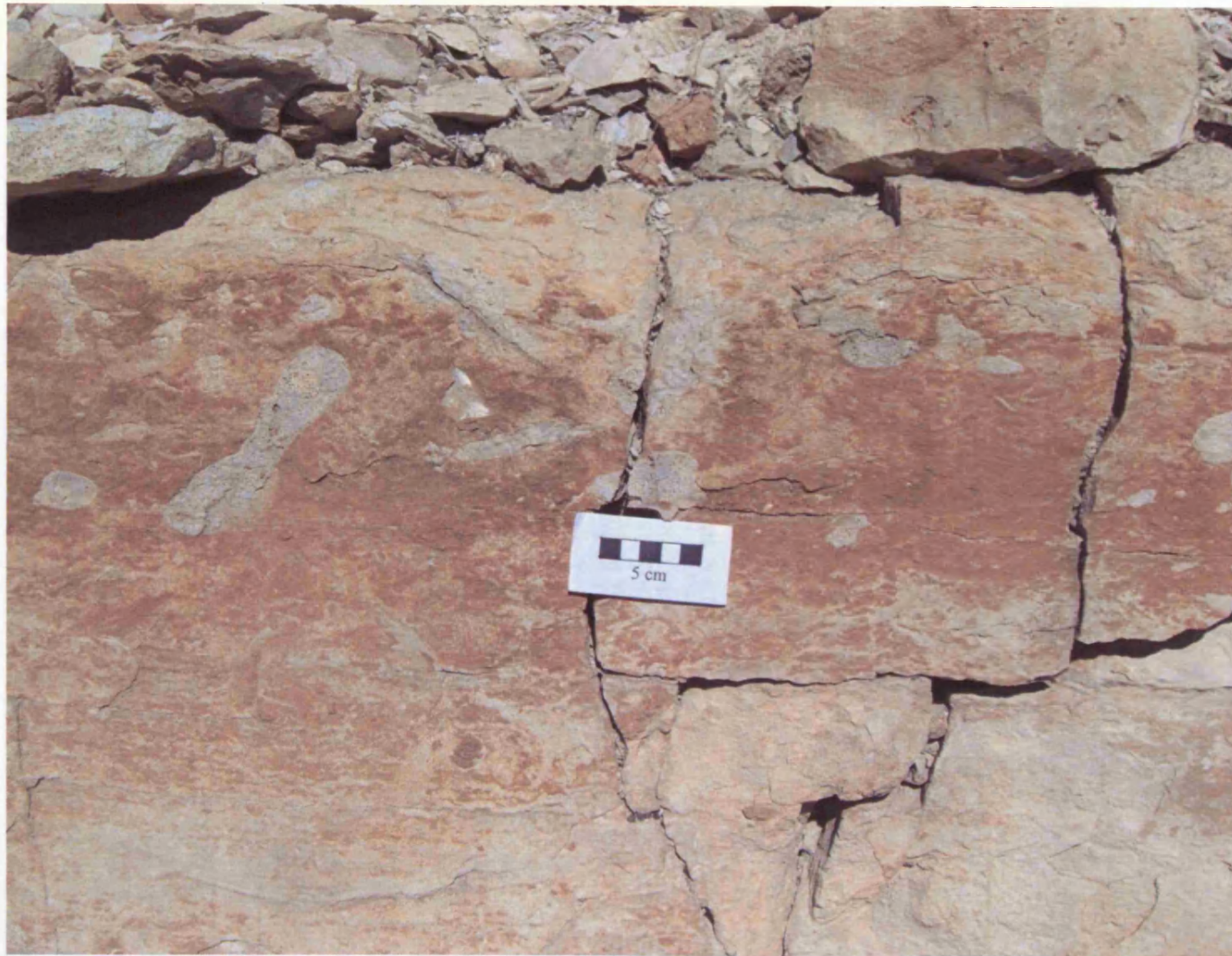


Figure 5.23: *O. nodosa* burrows (heavily weathered and visible due to differential fill) in QSF1 facies. Burrows are anastomosing and independent of bedding orientation. 81.6m from base of section.

deposition was probably not achieved by a fluvial or marine medium. Borer & Harris (1989) proposed a mechanism of formation whereby siliciclastic sediment is transported across an exposed shelf during lowstands of relative sea-level and subsequently reworked during a transgression of relative sea-level. This is supported by the nature of stratigraphically adjacent units. Surfaces immediately below QSF may show evidence of sub-aerial exposure (particularly calcrete and rhizcretions), implying that relative a sea-level fall exposed the platform top. In contrast, the upper contacts of QSF facies are commonly gradational into carbonate facies interpreted to represent relatively deep-marine conditions. QSF facies has therefore been previously interpreted as a lowstand to transgressive deposit (Goldhammer *et al.*, 1991). This interpretation was abandoned by Grammer *et al.* (2000) among others (Eberli *et al.*, 2000; Lerat *et al.*, 2000; Van Buchem *et al.*, 2000), who adopted “double cycles” to explain the stratigraphic position of siliciclastic units. This invokes two oscillations of relative sea-level separated by exposure of the platform at the top the siliciclastic unit. This is not supported by sedimentary evidence; siliciclastic units do not show erosive or diagenetic features attributable to direct sub-aerial exposure at the top of QSF beds. The source of the siliciclastic material of QSF facies is not well constrained. This and the relative timing of intervals of sedimentation in relation to sea-level change are discussed in section 5.5.4.

QSF2 was interpreted by Goldhammer *et al.* (1991) to represent shallow sub-tidal to inter-tidal deposits based on the evidence of mud-cracks which were not found in this study. There was also little supporting evidence of a tidal flat interpretation (e.g. ripples indicative of oscillatory flow, distinct flaser bedding, adhesion structures; refer to Hardie & Shinn, 1986). Critically, there are no salt pseudomorphs associated with the QSF facies which may be expected, as, during lowstands the Paradox Shelf was an arid setting. This study maintains that QSF2 represents shallow sub-tidal deposition, but interprets its environment of deposition as restricted lagoon. This fits the observed fabric, limited presence of marine fossils and sedimentary structures (fine-grained, variably wackestone-packstone, significant quantities of disseminated micrite and peloids, inter-layers) more appropriately than an inter-tidal interpretation. Additionally, given the shallow nature of the environment, it does not preclude inter-tidal deposits from being present. The creation of lagoonal conditions is attributable to the presence of QSF1, which is closely associated in terms of occurrence with QSF2. It is envisaged that away from the direct locus of re-sedimentation of QSF1, lagoonal conditions were created in the sheltered back-barrier of the prograding bars of QSF1. Finer sediment in suspension and the restricted hypersaline basin water prevented extensive carbonate sedimentation. The relative timing of sedimentation and the creation of prograding bars during the transgressive phase is discussed in section 5.5.4.

5.3.10 Discontinuity and sub-aerial exposure surfaces

The HTS displays 16 surfaces indicative of direct sub-aerial exposure. Facies showing evidence of sub-aerial exposure may display evidence of significant diagenesis as a result of exposure (such as multiple diagnostic features), or they may show poorly developed diagenetic markers. Meteoric diagenesis is visible in terms of microfacies though mouldic porosity, vuggy porosity and recrystallisation within existing textures. However this is not attributable to a specific exposure surface and the zones of meteoric and phreatic diagenesis may penetrate the platform to depths greater than cycle thicknesses (refer to section 5.3.8 and Vanstone, 1998; Saller *et al.*, 1999), negating their use in locating actual sub-aerial exposure surfaces.

Direct evidence of sub-aerial exposure is restricted to karstification, solution horizons, calcrete, rhizcretions and the microproblematica *Microcodium*. Karstic relief associated with exposure surfaces is not large, and rarely exceed approximately 15cm, and may locally be filled with lithoclast breccia (Figure 5.24). Calcretes are interpreted only to be developed at regionally correlative sequence boundaries (Goldhammer *et al.*, 1991), however there is evidence of minor calcrete development several metres stratigraphically above and below these surfaces. Well developed calcretes are present in the HTS as laterally discontinuous (on a tens-of-metres-scale), irregular laminated horizons, that commonly encrust solutional surfaces with relief of up to 15cm (Figure 5.25). Internally, the horizons consist of micritic peloids in a diagenetic mud-matrix (Goldhammer *et al.*, 1991). Within the micritic crust, eroded sand-sized skeletal grains and quartz grains are visible and vuggy-type pores are filled with micritic sediment. In addition calcrete is associated with a discrete light-grey coloured mottling on weathered surfaces, interpreted to represent microbial alteration of root structures to calcite (Figure 5.26). Poorly developed calcretes, however, may only show one of these features.

Microcodium is present in the HTS as brown-weathering millimetre-sized calcite aggregates (Figure 5.25). The presence of *Microcodium* in shallow-marine limestones has been interpreted to indicate that formation took place during early stages of palaeosol development, and reflects specific types of vascular plants of a pioneer community that were able to colonize carbonate substrates during the early phases of sub-aerial exposure (Košir, 2004).

Rhizcretions are an abundant indicator of exposure surface development at the HTS, occurring at almost all exposure surfaces. They range from 30cm-long (2cm diameter), to less than 2cm long and millimetre-scale diameter (Figure 5.27). Rhizcretions extending approximately 0.5-1m below an exposure surface are common. They commonly have a branching form, and display a darker micritised alteration 'halo' representing microbial alteration of the original root (Davies, 1991). The abundance of



Figure 5.24: Erosion surface (relief ~15cm) with very thin laminar calcrete (mm-scale) and lithoclast breccia fill. 1.5m from base of section.



Figure 5.25: Irregular laminar calcrete horizon coating a solutional surface of $\sim 0.05\text{m}$ relief. Below the profile *Microcodium* is present (appears as $\sim 1\text{mm}$ -sized brown-weathering calcite crystals between scale bar and laminar crust). 121.46m from base of section.

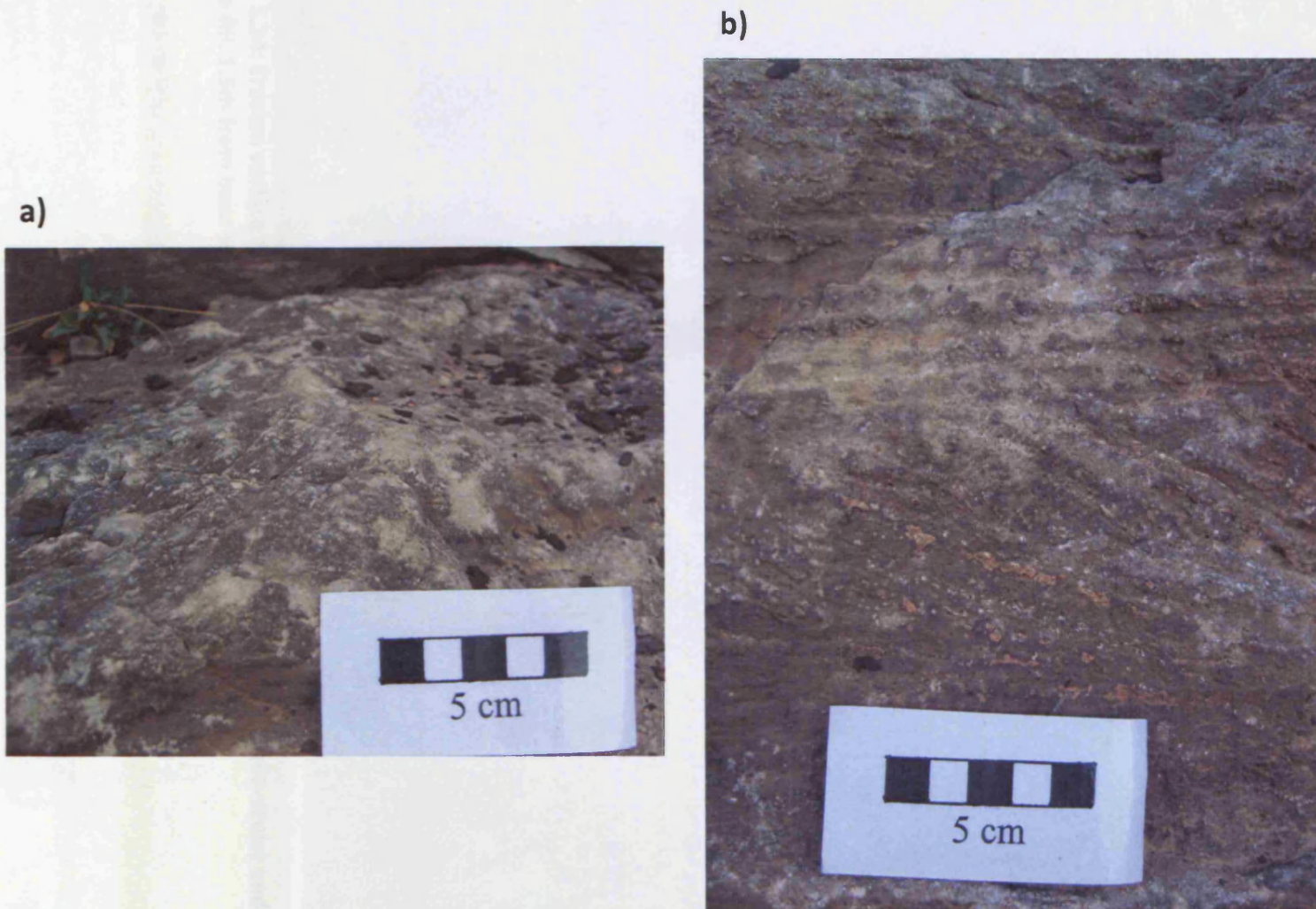


Figure 5.26: a) Light-coloured weathering developed up to ~1m below an exposure surface; which probably represent calcite concentration around root structures. b) Similar weathering patterns displayed on trough cross-bedded non-skeletal facies. 0m and 0.5m above base of section, respectively.

a)



b)

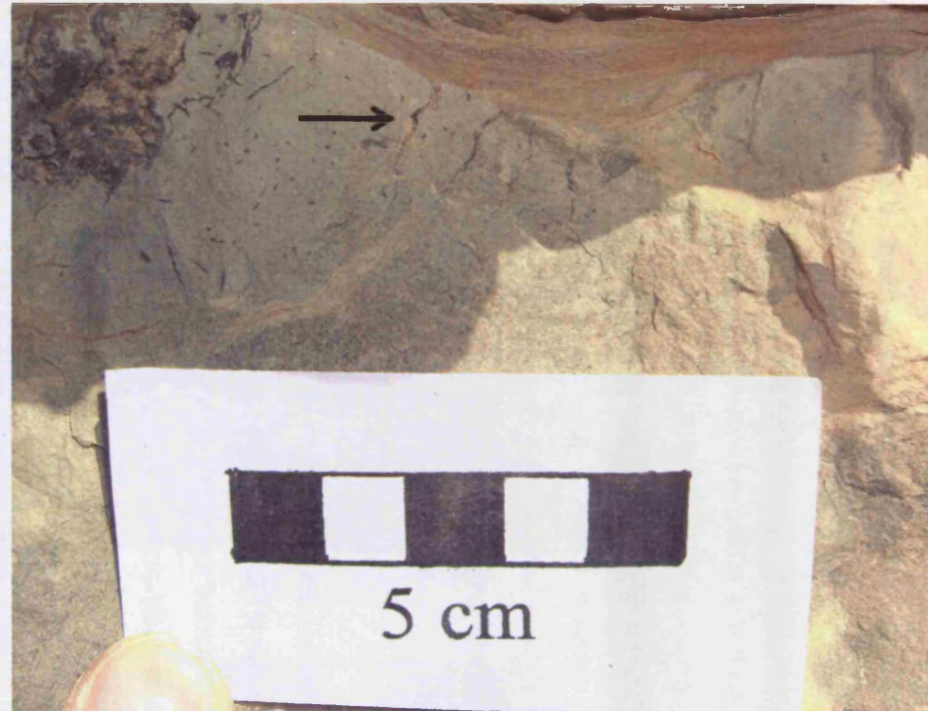


Figure 5.27: Examples of rhizocretions from different stratigraphic layers. a) Tap-root. b) Minor branching roots extending <10cm from an exposure surface. 1.6m and 140.8m from base of section, respectively.

roots in association with exposure surfaces, and the length to which they penetrate below an exposure surface, makes diagnosing an exposure surface in the absence of root development very tenuous.

In addition, hardgrounds occur as centimetre-sized, discontinuous surfaces representing syn-sedimentary lithification, and are abundant in the HTS (but are not visible in muddier beds; BLM, SF, and usually SSF). They are primarily identified at outcrop by differential cementation, with a well-cemented layer typically overlain by a less well-cemented, micrite-rich lithology (Figure 5.28). Encrusting organisms characteristic of hardgrounds are present (primarily echinoderms and bryozoans) but are rarely in life position, and provide little direct evidence of hardground formation. The presence of hardgrounds in the HTS (and therefore missing time) provides reason not to use facies-depth relationships as evidence of cycle boundaries.

5.3.11 Cycle boundaries

HfS sequence boundaries used in this study differ from those employed by previous authors working on the HTS. The differentiation stems from the use of deepening events as indicated by vertical facies association as cycle boundaries; a convention which is not maintained here. This study argues that the identification and interpretation of deepening events is fundamentally subjective and should not be utilised as a proxy for excursions of relative sea-level. The underlying problem with this method is that there is significant empirical and numerical evidence to suggest lithofacies changes are not forced by depth-changes alone (e.g. Tedesco & Wanless, 1991; Kindler, 1992; Wilkinson *et al.*, 1996; Wilkinson *et al.*, 1997; Wilkinson *et al.*, 1998; Wilkinson *et al.*, 1999; Burgess, 2001; Burgess & Wright, 2003; Rankey, 2004).

A more appropriate method of identifying sequence boundaries is to infer relative sea-level changes only where there is clear evidence of direct sub-aerial exposure (e.g. Foos, 1996). Evidence of relative sea-level change is only proven where abnormal sub-aerial exposure of sub-tidal strata is identified, otherwise sub-aerial exposure at the top of a cycle may be due to normal autocyclic shoreline or tidal-flat progradation processes (e.g. Burgess, 2001). Where sub-aerial exposure of sub-tidal facies occurs there is therefore unambiguous evidence of relative sea-level change and a HfS boundary can be objectively defined.

5.3.12 Statistical analysis of vertical facies transitions

Quantifying the level of facies ordering in the HTS was a primary aim of this study (refer to objectives; section 5.3.1). Statistical analysis was conducted using embedded Markov chains and analysed with chi-square test and Fisher's exact test. Embedded



Figure 5.28: Hardground surface developed in skeletal facies, separating a packstone lens (lighter area; well-cemented with early marine cement) from the dominantly darker wackestone fabric. 60m from base of section.

Markov chains quantify the degree to which discrete states are independent of one another (refer to section 3.4.4.1 for a full description). The chi-square statistic allows the construction of an approximate and conservative estimate of the probability that the vertical lithofacies transitions will occur by chance under the null hypothesis. Fisher's exact test is a more powerful significance test than chi-square because it is based on direct application of the laws of probability whereas chi-square is an approximation. It is used here because it works well in situations of sparse data, where chi-square test can be unreliable (refer to section 3.4.4.1).

Statistical analysis of embedded Markov chains indicates that vertical facies transitions are probably ordered in the HTS. This conclusion is made based on the results of both chi-square and Fisher's exact tests; which both indicate that there is a very small probability of the observed facies transition being random (Table 5.1). This means that there is a statistically significant relationship between one facies, and its transition to the next. This finding is in agreement with previous statistical analysis of the HTS conducted by Lehrmann & Goldhammer (Lehrmann & Goldhammer, 1999; although this study relied upon the potentially unreliable chi-square test). The implications of this are discussed in section 5.5.1.

a) X_2

	BLM	SF&A	SSF	SkF	NSF	QSF
BLM	4	3	2	0	0	1
SF&A	0	3	9	0	1	1
SSF	1	4	6	13	2	2
SkF	0	1	6	7	0	8
NSF	1	1	1	2	1	2
QSF	4	2	5	2	1	6

	BLM	SF&A	SSF	SkF	NSF	QSF
BLM	0.99	1.39	2.77	2.08	0.79	1.98
SF&A	1.39	1.94	3.88	2.91	1.11	2.77
SSF	2.77	3.88	7.76	5.82	2.22	5.54
SkF	2.08	2.91	5.82	4.37	1.66	4.16
NSF	0.79	1.11	2.22	1.66	0.63	1.58
QSF	1.98	2.77	5.54	4.16	1.58	3.96

Degrees of freedom = 25

Critical value = 37.7

 $X_2 = 54$

Probability = 0.001

b) Fisher's Exact Test

	BLM	SF&A	SSF	SkF	NSF	QSF
BLM	4	3	2	0	0	1
SF&A	0	3	9	0	1	1
SSF	1	4	6	13	2	2
SkF	0	1	6	7	0	8
NSF	1	1	1	2	1	2
QSF	4	2	5	2	1	6

	BLM	SF&A	SSF	SkF	NSF	QSF
BLM	0.98	1.37	2.84	2.35	0.49	1.96
SF&A	1.37	1.92	3.98	3.29	0.69	2.75
SSF	2.75	3.84	7.96	6.59	1.37	5.49
SkF	2.16	3.02	6.25	5.18	1.08	4.31
NSF	0.78	1.1	2.27	1.88	0.39	1.57
QSF	1.96	2.75	5.69	4.71	0.98	3.92

Probability = 0.001

Table 5.1: Observed frequency transition matrix and expected frequency transition matrix from a) chi-squared test and b) Fisher's exact test for embedded Markov chain analysis conducted on the HTS. Both tests result in rejection of the null hypothesis that states are independent of one another and that facies transitions are not ordered. Fisher's exact test was conducted as the results of chi-square are not reliable given that most of the elements in the expected frequency transition matrix are less than 5 (creating a contingency problem). Fisher's exact test is a direct measure of probability and is not subject to this problem, although in this case produces a very similar result to chi-square. There is therefore a high degree of confidence that these results are accurate. Note that given the rarity of algal facies in the HTS it is binned with sponge facies.

5.4 STRATIGRAPHIC SIMULATIONS

5.4.1 Aims

The overall aim of employing numerical modelling in this study was to compare synthetic sections with the measured Honaker Trail section in order to identify the controlling factors of stacking patterns. This aim builds upon the stratigraphic study (section 5.3) by quantitatively examining two fundamental characteristics of sedimentary sections:

1. Lithofacies distributions. Lithofacies distributions are examined as they present the HfS and parasequence boundaries used by previous workers, and therefore are the fundamental basis of a hierarchy as identified in the HTS. Investigation of lithofacies thicknesses are also important in this respect as they can help quantify the level of facies ordering in a simulated section.
2. High-frequency sequences. Evaluation of the HfSs produced by simulations, and comparison with those in the HTS, is a way of assessing the degree to which simulations can replicate the stratigraphic section at the HTS. In turn, this comparison is used to provide insight into the controls on stacking patterns of HfSs.

This precise method by which simulated lithofacies and HfSs are compared to those in the HTS is documented in section 5.4.2.

5.4.2 Method

Two methods of computer simulation were employed using TED in order to investigate the controls on stacking patterns of the Honaker Trail sedimentary section. TED employs parameters considered to be fundamental to the creation of rhythmic carbonate successions. These parameters are based on a range of values currently thought to be realistic (refer to section 3.3 for a full explanation).

A number of the facies identified in section 5.3 can be said to have potentially non-depth-dependent controls. Therefore, the facies scheme was simplified for forward modelling according to the predominant lithofacies type for each facies (Table 5.2). A lithofacies scheme represents the simplest way of representing the facies seen at outcrop within a numerical forward model. It is the most likely to be modelled successfully as the

Lithofacies	Facies
Mudstone	Black Laminated Mudstone
Wackestone	Sponge Facies
Packstone	Skeletal-Silt Facies Skeletal Facies QSF2 Facies
Grainstone	Algal Facies Non-Skeletal Facies QSF1 Facies

Table 5.2: Division of the facies characterisation scheme used for the HTS into a simpler lithofacies scheme.

complexity is significantly less than with the full facies scheme. If facies are depth-controlled and forced by parameters thought to be fundamental in dictating accommodation creation and sediment supply, then it may be expected that the arrangement of lithofacies displayed in the HTS can be simulated accurately.

In the first instance, lithofacies thicknesses of individual simulated sections are compared to lithofacies thicknesses of the HTS (section 5.4.3). Comparison is made between total summed lithofacies thickness in a given simulation and total summed lithofacies thickness in the HTS. This method is an effective first-order method of assessing how parameters affect lithofacies proportions. In sections which have lithofacies thicknesses similar to those observed in the sedimentary section, further analysis can take place by observing the stacking patterns and lithofacies proportions in individual HfSs.

The second aspect of stratigraphic simulation of the HTS is HfS matching (section 5.4.4). The thickness of HTS HfSs is derived from exposure surfaces identified in the HTS (refer to section 5.3). A HfS is therefore the relatively conformable succession of genetically-related strata bounded by unconformities (*sensu* Lehrmann & Goldhammer, 1999). This definition eliminates any ambiguity associated with defining sequence boundaries according to interpreted deepening events. As such, the cycle boundaries used in this study are only those which display clear evidence of sub-aerial exposure and differ from previous studies which document this section (e.g. Goldhammer *et al.*, 1991; Lerat *et al.*, 2000). HfS matching is accomplished in two ways.

Firstly, the cumulative thickness of a simulated section comprising 16 HfSs (as there are 16 HfSs at the HTS) is compared against the cumulative thickness of the measured section (154m). The two values are then compared. The difference between the two values is referred to in this study as the "cumulative deviation", and is a measure of the ability of parameters to produce thicknesses of sediment comparable to the HTS.

Secondly, the deviation in thickness between a given HfS in a simulated section and the correspondingly numbered HfS in the HTS is observed. For example, the thickness of the 1st HfS in a simulated section would be compared to the thickness of the 1st HfS at the HTS (23.3m); the 2nd simulated HfS thickness compared to the 2nd HTS HfS. This process would be repeated for all 16 HfSs in the measured HTS. This method provides a more detailed way of isolating parameters which can potentially replicate the stacking pattern observed at the HTS.

Both aspects of HfS matching are evaluated using parameter-space plots; a method of plotting and visualising data in terms of the generative parameters used. Therefore in parameter-space plots the axes are usually values input into the numerical model (e.g. maximum euphotic production rate). The results are therefore plotted according to the independent variables used and usually depict the dependent variable by colour.

Parameter-space plots are used as they represent the most convenient way of evaluating results in terms of their parameters, and in addition can be viewed in three dimensions, allowing the relationships between three sets of parameters to be observed.

Response surface methodology is another technique used to visualise the relationship between parameter and result. Specifically the response surface allows visualisation of two independent variables with a dependent variable plotted as a contour surface. The variation in the surface is the 'response' of the dependent variable. This method is particularly useful for visualising cumulative deviation between individual HfSs or stacked HfSs.

5.4.3 Lithofacies-matching of the Honaker Trail sedimentary section

Initially, simulations were conducted to assess the degree to which the facies succession of the HTS could be successfully forward modelled. The independent variables in these simulations were parameters which are thought to have the greatest control on cyclothem stacking patterns. These are eustatic sea-level oscillation amplitude, subsidence rate, euphotic carbonate production and sub-aerial platform denudation rate. They are interpreted to represent the most significant control on stacking patterns as these parameters most directly affect the generation of accommodation and the quantity of sediment deposited and preserved as simulated strata. Static parameters used in the simulations are best-fit estimates derived from contemporary empirical data and are described in detail in section 3.3.

5.4.3.1 Simulations investigating amplitude of eustatic oscillation

Simulations investigating the effect of the three major eustatic parameters only show lithofacies thicknesses similar to the Honaker Trail in very few isolated instances (Figure 5.29, a; b). Overall, variation of the eustatic parameters does not result in good correlation with observed lithofacies thicknesses of the HTS. Generally, the existence of two or more high-frequency large-amplitude eustatic components reduces the probability of simulations bearing significant similarity to the HTS (in terms of cumulative lithofacies thickness). This observation is made from two broad trends.

Firstly, runs with less than 20m high-order eustatic amplitude have a tendency to produce significantly thicker sequences of grainstone lithofacies than those observed in the HTS (Figure 5.29). This is a direct result of limited accommodation created by the small-amplitude high-frequency oscillations. Sedimentation under these conditions occurs while water depth is shallow, leading to abundance of grainstone lithofacies. Increasing

Figure 29: Schematic plot comparing the cumulative deviation of lithofacies thickness from the HTS for each simulation. This run plan varies the amplitudes of three eustatic components. The dependent variable is plotted on the y-axis. The dependent variable (deviation from HTS lithofacies thickness) is plotted as a cumulative histogram. The independent variable plotted is plotted along the x-axis and in this case is the run number (i.e. 1 to 1000).

The eustatic amplitude independent variables vary according to run number. Precisely how they vary is shown above the plot. High-order amplitude increases from 0m to 50m over 10 runs. Low-order amplitude increases from 0m to 40m over 100 runs, varying one increment every 10 runs. Intermediate-order eustatic amplitude varies from 0 to 100m over 1000 runs, varying one increment every 100 runs. Dashed-lines represent repetition of this sequence. This addresses every combination of parameter increments in the run plan. Plotting by run number is the most convenient way to show trends as the parameter values change.

- a) Run with significant deviation of grainstone lithofacies represents 0m high-order amplitude, 0m intermediate-order amplitude and 40m low-order amplitude.**
- b) Run with the least deviation (0m high-order, 70m intermediate-order, 10m low-order).**
- c) Trend of decreasing grainstone lithofacies and increasing wackestone lithofacies as a result of increasing accommodation effected by increased intermediate-order amplitude.**

intermediate-order amplitude creates more accommodation and consequently grainstone thicknesses decrease; matching those observed in the HTS (Figure 5.29, c). However, this also causes an increase in the cumulative thickness of wackestone lithofacies, as production begins to take place from deeper water-depths. This mutually-exclusive state prevents accurate matching of lithofacies quantities of the HTS through variation of eustatic components alone.

The second trend is that mudstone and wackestone lithofacies are always under-represented in simulations, and is most visible where simulated lithofacies bear closest resemblance to the HTS (i.e. Figure 5.29, b). There are a number of possible reasons for this, which are investigated by looking at subsidence and carbonate production rate variables and discussed below. This means, however, that lithofacies thickness bears greatest similarity to the HTS when high-order eustatic amplitude is small. Under these conditions, accommodation is relatively limited and best-fit sections to the HTS can be generated at points where grainstone and wackestone lithofacies both show a good match. At larger high-order amplitudes, accommodation and degree of sea-level oscillation is sufficient to create significant deviations in lithofacies thickness, such that the average margin of error is greater than +/-50m. Interactions of three eustatic parameters therefore suggest similar lithofacies thicknesses to the HTS are only attained when one high-frequency eustatic component is of negligible amplitude to influence relative sea-level.

5.4.3.2 Simulations investigating rate of platform denudation

Rates of sub-aerial platform denudation show a close and well-defined relationship with simulated lithofacies thickness, particularly grainstone thicknesses. This is due to the deterministic nature of the model: grainstone lithofacies form the uppermost units in HfSs, and as such are the first unit to be exposed. If strata are denuded from the platform surface, then grainstones are the most likely to be stripped. This is reflected in thickness patterns displayed in Figure 5.30. Overall correlation between runs varying rate of sub-aerial platform denudation and observed lithofacies thickness in the HTS is poor. The best thickness-matches are observed with only one high-frequency large-amplitude eustatic component in operation and low rates of sub-aerial platform denudation (10m/My; Figure Figure 5.30, a). Increasing rates of sub-aerial platform denudation result in grainstone thicknesses being reduced and bearing less of a resemblance to those of the HTS (Figure 5.30, b).

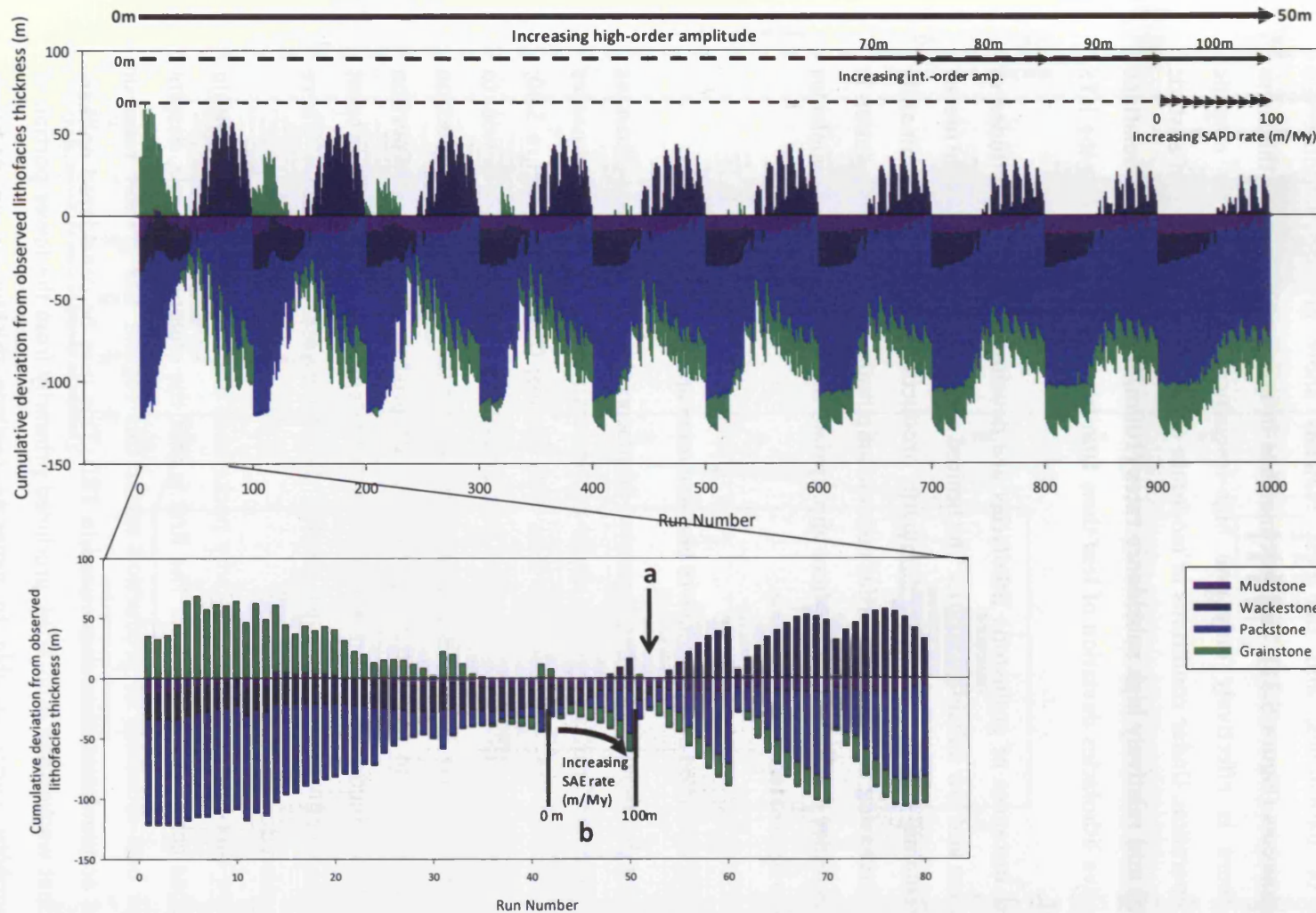


Figure 5.30: Schematic plot comparing the cumulative deviation of lithofacies thickness from the HTS for each simulation in a run-plan comparing varying amplitudes of two eustatic components and sub-aerial platform denudation rate (SAPD). a) Shows the run with the least deviation (high-order amplitude 0m, intermediate-order amplitude 10m, sub-aerial platform denudation rate 10m/My). b) Grainstone deviation increases as grainstone lithofacies are removed as a result of SAPD.

5.4.3.3 Simulations investigating rate of subsidence

Runs which vary subsidence rate result in the best correlation with observed lithofacies thicknesses in the HTS. These runs, however, are still commonly under-representative of packstones, and the best matches show greater-than-observed grainstone thicknesses (Figure 5.31). The best matches in terms of lithofacies thickness occur where there is effectively only one high-frequency large-amplitude eustatic component in operation. Under conditions of moderate amplitude oscillations of eustatic sea-level (50m) and relatively high subsidence rates (100m/My), numerical simulations show a cumulative lithofacies deviation of less than 10m from that observed at the HTS (Figure 5.31, b).

Greatest instances of grainstone lithofacies are developed at low amplitudes of eustatic oscillation and low subsidence rates. The limited accommodation available means water-depth remains shallow and the dominant production regime is dominantly euphotic. With increasing intermediate-order eustatic amplitude, more accommodation is created, and it is under these conditions where appropriate thicknesses of each lithofacies are most likely to be created.

5.4.3.4 Reasons for deviation between the HTS and simulated lithofacies

The largest discrepancy between simulated lithofacies thicknesses and thicknesses observed in the Honaker Trail is caused by under-representation of packstone thicknesses (which are thinner than the HTS in greater than 99% of runs; (Figure 5.29; Figure 5.30; Figure 5.31). This is in contrast with the other lithofacies, which all have the potential to show good correlation given the correct parameters. Under the Pomar-style production regime used in TED (refer to section 3.3.3) packstones are produced by the upper portion of the oligophotic production curve (i.e. up to the plateau depth). As such they represent relatively high production in a zone just outside the shallowest water depths where euphotic production dominates.

There are three probable reasons why packstones are relatively thinner within simulated sections compared to the HTS. The first is that the oligophotic curve, despite being based on best-estimates of production under this regime, has greater rates of production and accumulation than those used in TED. This may be considered unlikely given the fact that wackestone lithofacies, produced primarily from the lower portion of the same oligophotic curve, is able to generate realistic thicknesses on occasion. Furthermore, there are a minority of occasions where packstone thicknesses show good correlation (Figure 5.29, a). A comparison of varying rates of production for the euphotic, oligophotic and aphotic regimes reveals that there is a well-defined set of rates which

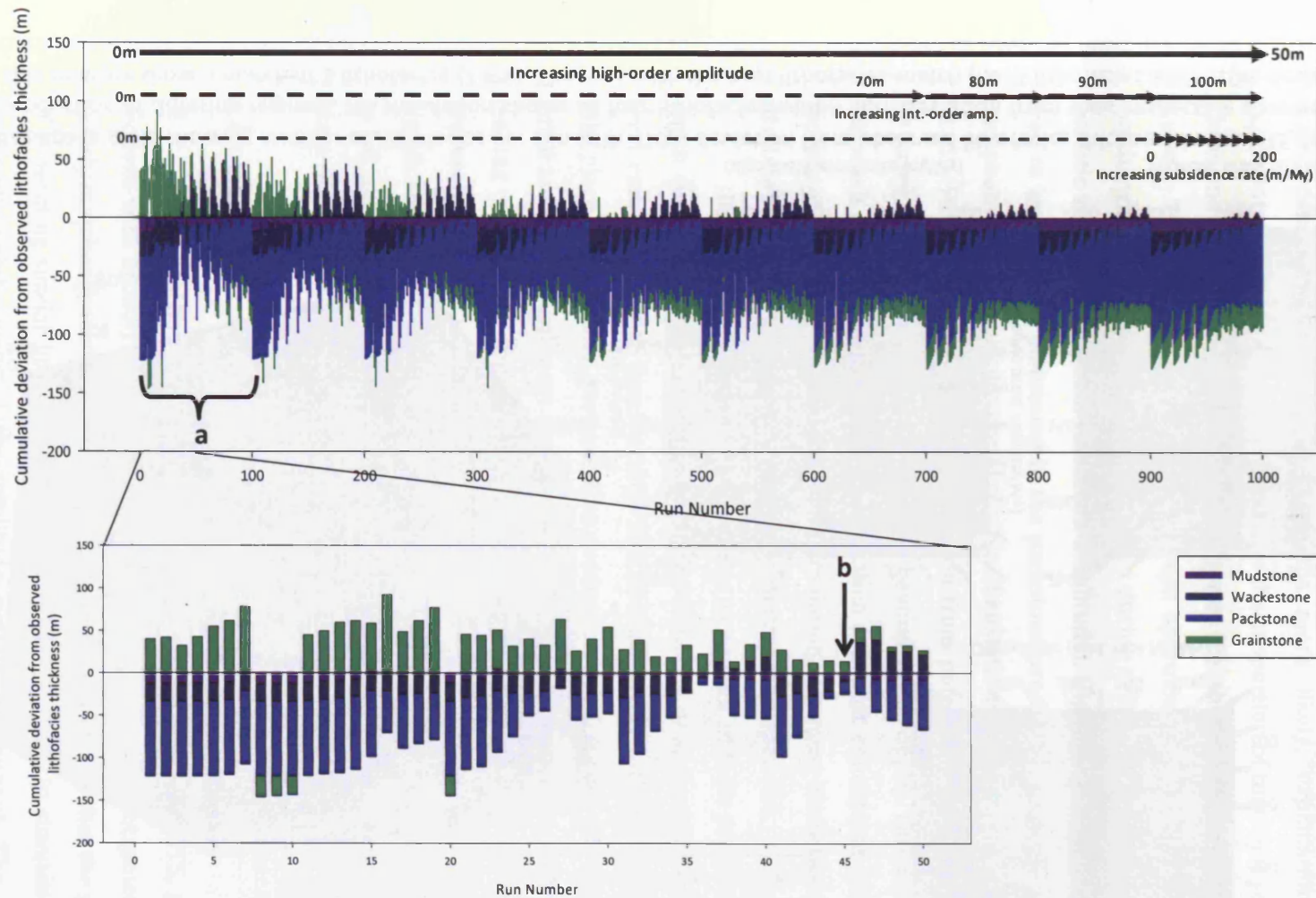


Figure 5.31: Schematic plot comparing the cumulative deviation of lithofacies thickness from the HTS for each simulation in a run-plan comparing varying amplitudes of two eustatic components and subsidence rate. a) 'Spiking' being created as an artefact of visualisation; reflecting runs varying subsidence rate in a sub-set of 100 runs with similar intermediate-order eustatic amplitude. b) Shows the run with the least deviation (high-order amplitude 0m, intermediate-order amplitude 10m, subsidence rate 100m/My). Deviation is <10m in this case.

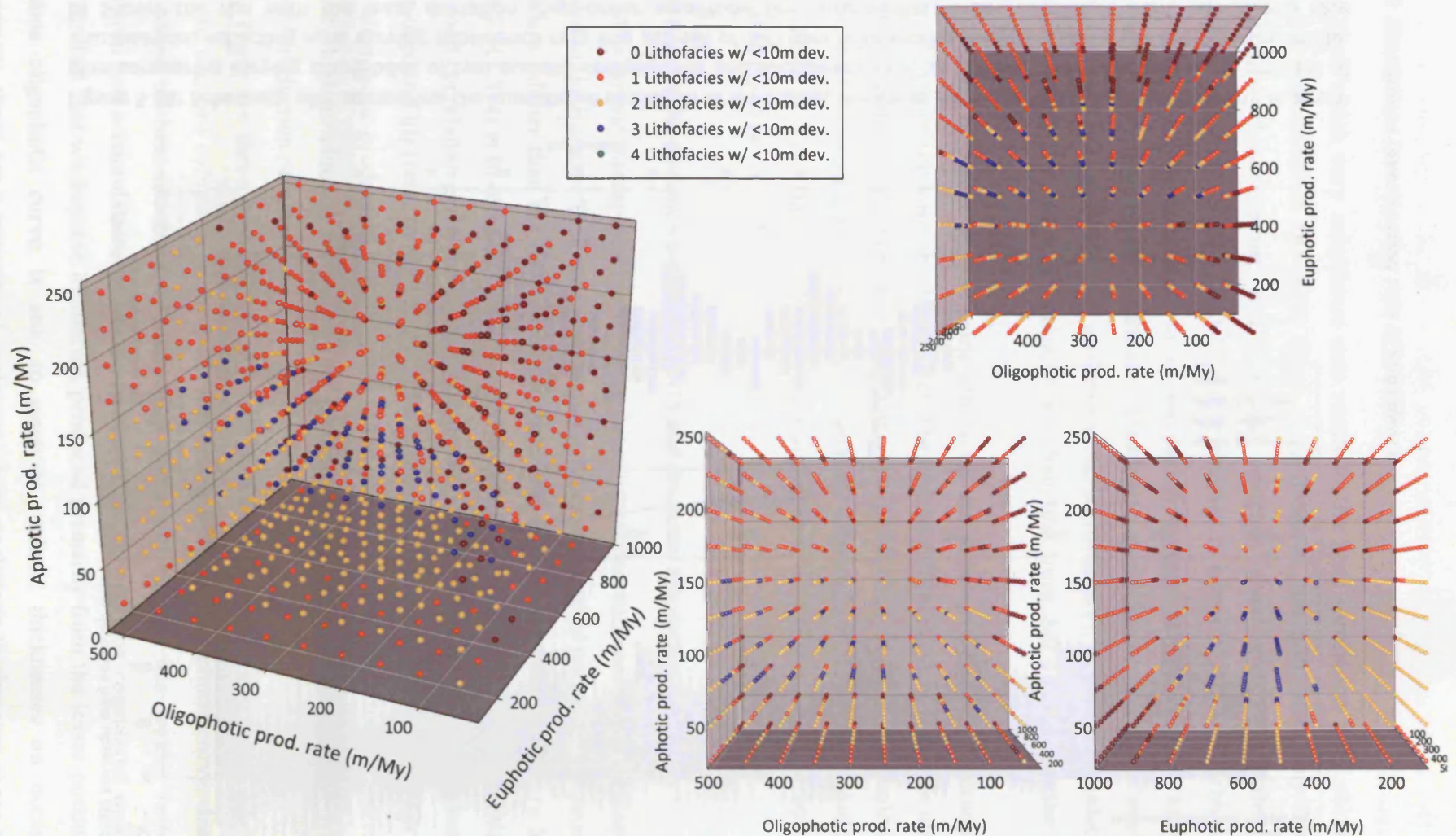


Figure 5.32: Parameter-space plots showing number of lithofacies per run with <10m deviation from observed lithofacies thickness in the HTS, for simulations comparing rates of production of differing regimes. No simulation shows all four lithofacies within 10m deviation from their respective observed lithofacies, although a considerable number show a match of 3 lithofacies (7.8%). The runs with the best lithofacies-match (i.e. 3 lithofacies with <10m deviation) suggest oligophotic and euphotic production rates need to be slightly higher than the average used in TED simulations to have the most likelihood of matching the HTS (250m/My compared to 150m/My and 75m/My compared to 50m/My, respectively), although the average euphotic rate used in TED simulations (500m/My) creates the most number of lithofacies matches.

show the best match with lithofacies observed in the HTS, and that these closely match the average rates derived from empirical data and used in most TED simulations (Figure 5.32).

Given this, another and perhaps more likely, explanation for the under-representation of packstone thicknesses is the proportion of time that sedimentation takes place under conditions producing packstones (i.e. the upper portion of the oligophotic curve). This curve segment exists between approximately 20m and 50m water depth; depths which are usually rapidly exceeded during average large-amplitude oscillations of eustatic sea-level (i.e. >60m combined amplitude). Highstands of relative sea-level rarely lead to water depth plateauing in the packstone-producing part of the oligophotic curve except at very small amplitudes of combined eustatic oscillation (<50m).

Finally, this discrepancy may result from potentially non-depth dependent facies or facies which have significant controls beyond water depth. This means the modelling approach is probably inaccurate, but so then are most conceptual and non-quantitative models of carbonate production and accumulation. It is most likely that some combination of all three reasons is responsible for the observed discrepancies.

Under-representation of packstones as a result of their position on a production-depth curve allows important observations of timing of sedimentation on a relative sea-level curve. Modelling demonstrates that comparatively little sedimentation is likely to take place in the median portion of the production-depth curve (~20-50m). Comparatively small amounts of sediment are deposited during the transgressive part of an oscillation, leading to the under-representation of packstone lithofacies. HST periods are also under-represented as the platform is usually relatively deeply submerged and not experiencing significant amounts of sedimentation. Sediment supply again peaks when sea-level begins to fall, allowing production to catch up. The vast majority of sedimentation therefore takes place during the TST and to a lesser extent, during the FSST.

5.4.3.5 Summary

Numerical investigations of lithofacies quantities in the HTS, generate synthetic sections with broadly similar quantities of lithofacies, but cannot generate a section that exactly matches that of the HTS. Generally, modelling suggests that the greatest likelihood of generating similar lithofacies thicknesses to the HTS are in simulations that have one dominant high-frequency large-amplitude eustatic component. The introduction of a greater number of high-frequency components results in significant deviation from HTS quantities of lithofacies.

Subsidence and sub-aerial erosion, the other accommodation-controlling parameters, are less restrictive in promoting sections of similar lithofacies thickness to the

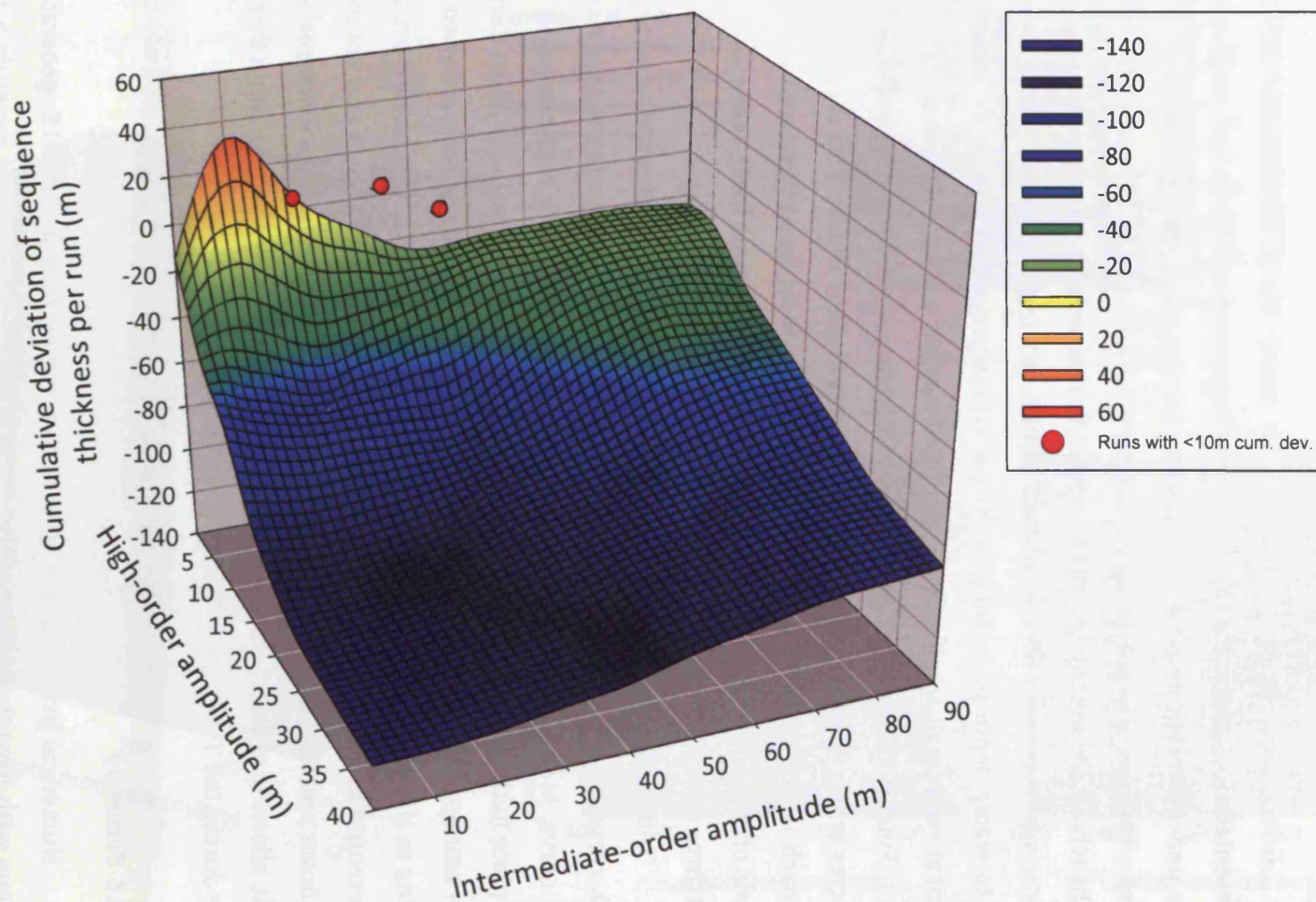


Figure 5.33: Parameter-space plot showing the cumulative deviation response surface of three eustatic components (low-order amplitude not plotted). Runs with <10m cumulative deviation only occur at 0m high-order amplitude.

HTS and generate closest matches at realistic rates (100m/My and 10m/My, respectively). Similarly, carbonate production generates sections with minimal deviation at 'realistic' rates. It is notable however, that in any given run all four lithofacies are unable to be matched to with less than 10m total deviation from the equivalent lithofacies in the HTS. It is also important to note that these parameters are most conducive to the formation of HTS-style lithofacies stacking if there is only one high-frequency large-amplitude eustatic component in operation. The probability of creating a run showing a small amount of deviation *and* the correct lithofacies proportions has not been addressed here; however the likelihood of generating similar HfS stacking-patterns is assessed in section 5.4.4.

Due to the large overall cumulative deviation of lithofacies in the majority of runs, and the fact that no combination of parameters produced four lithofacies of similar thickness to the HTS, it seems unlikely that the lithofacies (and facies) are forced by the modelled controls alone. These results therefore reemphasise the probability that facies units in the HTS and elsewhere have a significant non-depth-dependent control, suggesting that current sequence stratigraphic conceptual models are a poor representation of real-world carbonate deposystems.

5.4.4 High-frequency sequence matching

5.4.4.1 Simulations investigating amplitude of eustatic oscillation

High-frequency sequence matching was initially conducted for 1000 simulations evaluating the effect of varying amplitude of eustatic oscillation on the ability to simulate similar stratigraphic sections to the HTS (Figure 5.33). Overall, there is a relatively poor correlation with the HTS; with greater than 99% of runs showing greater than 10m cumulative deviation (i.e. summed HfS thickness) for the entire simulated section. Furthermore, over half show deviation of greater than 50m.

It is notable that the simulated section is usually thinner than the HTS, and therefore represents negative cumulative deviation from observed thickness of the HTS. This results from total subsidence precluding significant accommodation and production being unable to keep up with eustatic rise, therefore producing thinner sections. The fact that very few runs show a positive deviation from HTS thicknesses suggests that variation of other factors is required to generate a HTS-similar simulated section.

The greatest positive deviation occurs at very small amplitude interactions of intermediate- and high-order sea-level. Despite the relatively limited accommodation available with these limited amplitudes, the small variations in sea-level ensure production always occurs in the upper-most, and most productive, portion of the water

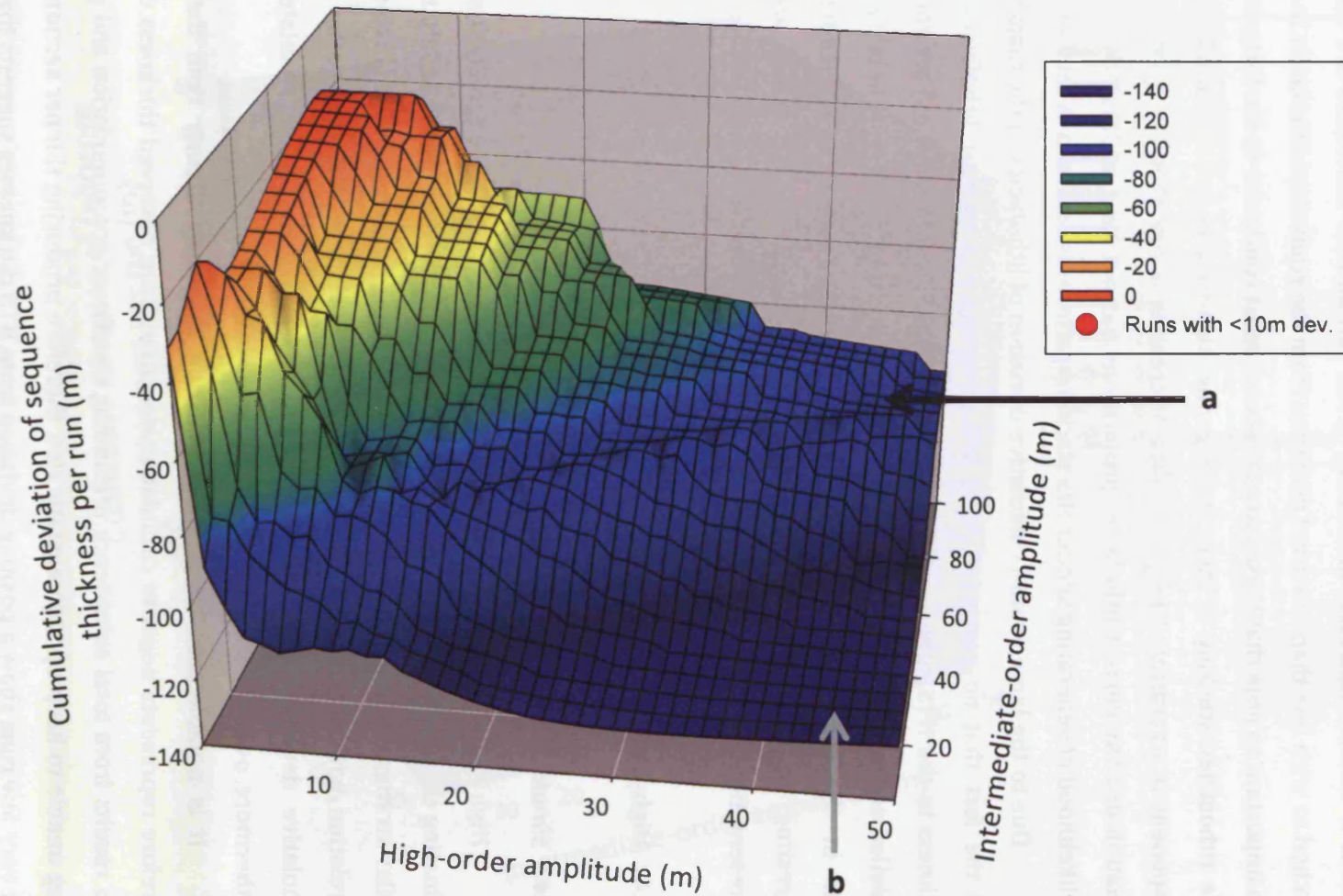


Figure 5.34: High-resolution parameter-space plot showing the cumulative deviation response surface of two variable eustatic components. The low-order eustatic component is fixed at 10m amplitude. No runs occur with <10m cumulative deviation, as a result of no low-order oscillation (compare with Figure 5.33). (a) and (b) show the difference in negative deviation caused by increasing intermediate-order amplitude.

column. Available accommodation is therefore filled to a greater degree, and thick sedimentary sections can be created.

At greater amplitudes of high-order oscillation, and therefore greater accommodation, cumulative deviation from the HTS rapidly increases to a maximum of -130m (at 40m amplitude; Figure 5.33). Contrary to what may be expected, increasing intermediate-order amplitude negates this effect: at very large intermediate- and high-order amplitudes the deviation from total HTS thickness is not as great as at small intermediate-, large high-order amplitudes (Figure 5.34). At these ratios, despite more available accommodation greater amounts of sediment can be deposited during the longer-term intermediate-order TST which have a slower rate of sea-level rise than that associated with high-order rises. The overall effect of increasing eustatic amplitude is, however, to increase deviation from observed thicknesses of the HTS. At any combination of amplitudes, the interaction of two high-frequency oscillations of eustatic sea-level serves to increase deviation of HfS thickness.

This effect is not maintained at small high-order amplitudes (<20m), where increasing intermediate-order amplitude has limited effect. Deviation between 30m and 100m intermediate-order amplitude only varies by 10m. The distinction between this small deviation and the prominent positive deviation seen in Figure 5.33 is caused by low-order amplitude. It is low-order amplitude (combined with intermediate-order amplitude) that is responsible for generating runs with less than 10m cumulative deviation from the HTS. This is determined from Figure 5.33 where these runs plot above the response surface, and always at 0m high-order amplitude. Given this, and the fact that Figure 5.34 shows that high-intermediate interactions produces runs of greater than 18m in all simulations, the interaction of low- and intermediate-order are determined to be responsible for the close resemblance HTS and simulated thicknesses.

By conducting simulations with no high-order eustatic variation (fixed at 20m amplitude) it is possible to isolate the interactions of low-order and intermediate-order amplitudes which give rise to HTS-matching sections. Figure 5.35 is a high-resolution response surface of the low-order and intermediate-order variables that produce simulations with minimum cumulative deviation to the HTS. The difference between this response surface and that shown in Figure 5.34 is marked. The interaction of low- and intermediate-order eustatic parameters creates cumulative deviation which varies from -140m to greater than 150m. Low-order amplitude is therefore demonstrable to have a much greater effect when varied in conjunction with intermediate-order amplitude, than high-order amplitude does.

In Figure 5.35, at small intermediate-order and large high-order amplitudes, positive deviation is at its maximum. This reflects the slow rate of rise of a low-order

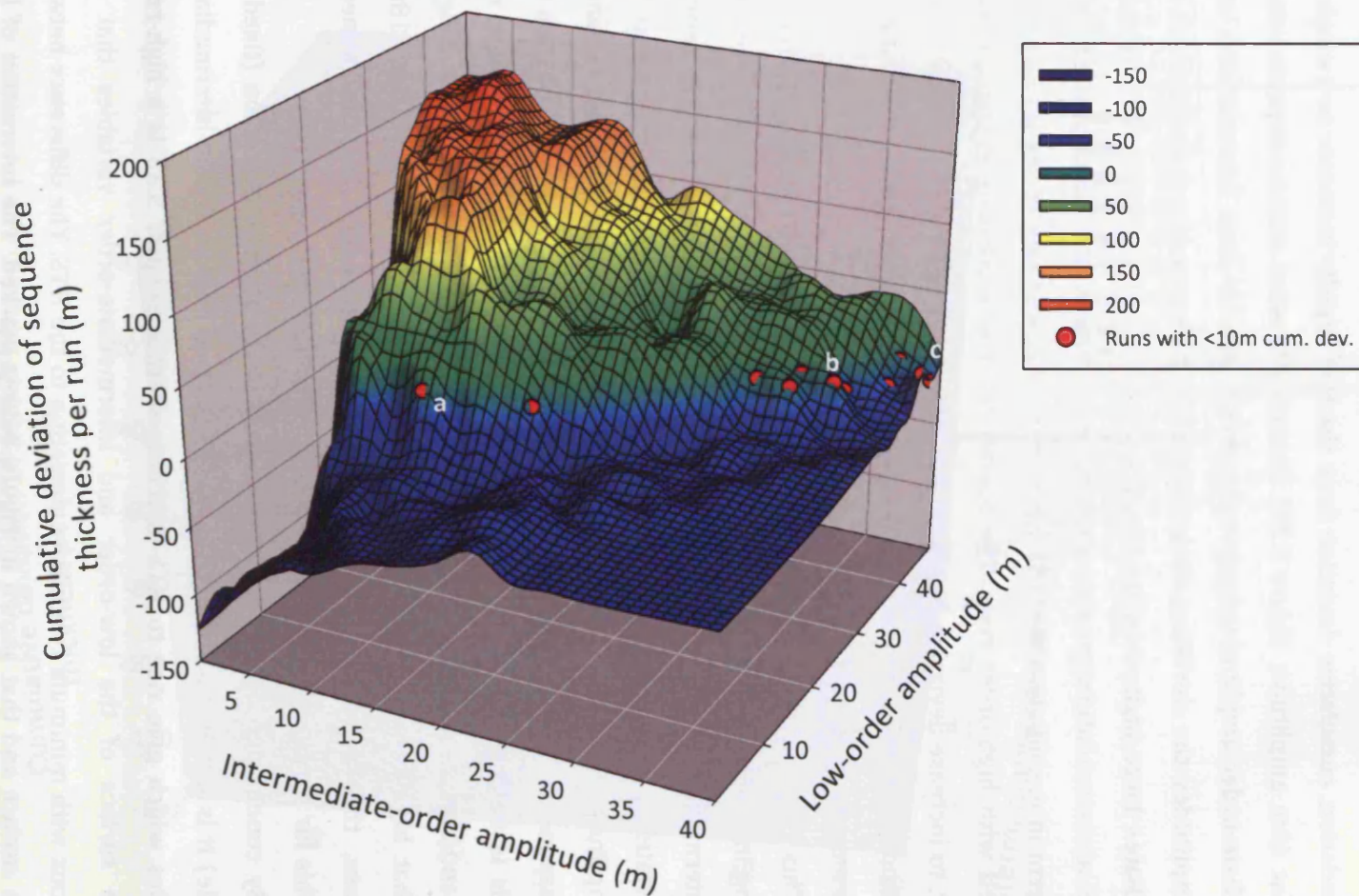


Figure 5.35: High-resolution parameter-space plot showing the cumulative deviation response surface of two eustatic components. High-order amplitude is fixed at 20m. The plot shows the precise parameter space location of the three <10m deviation runs shown in Figure 5.33. Interaction of low-order and intermediate-order eustasy is responsible for the creation of these runs. (a) is evaluated in terms of deviation of individual high frequency sequences and stacking pattern in Figure 5.36, and (b) and (c) in Figure 5.37.

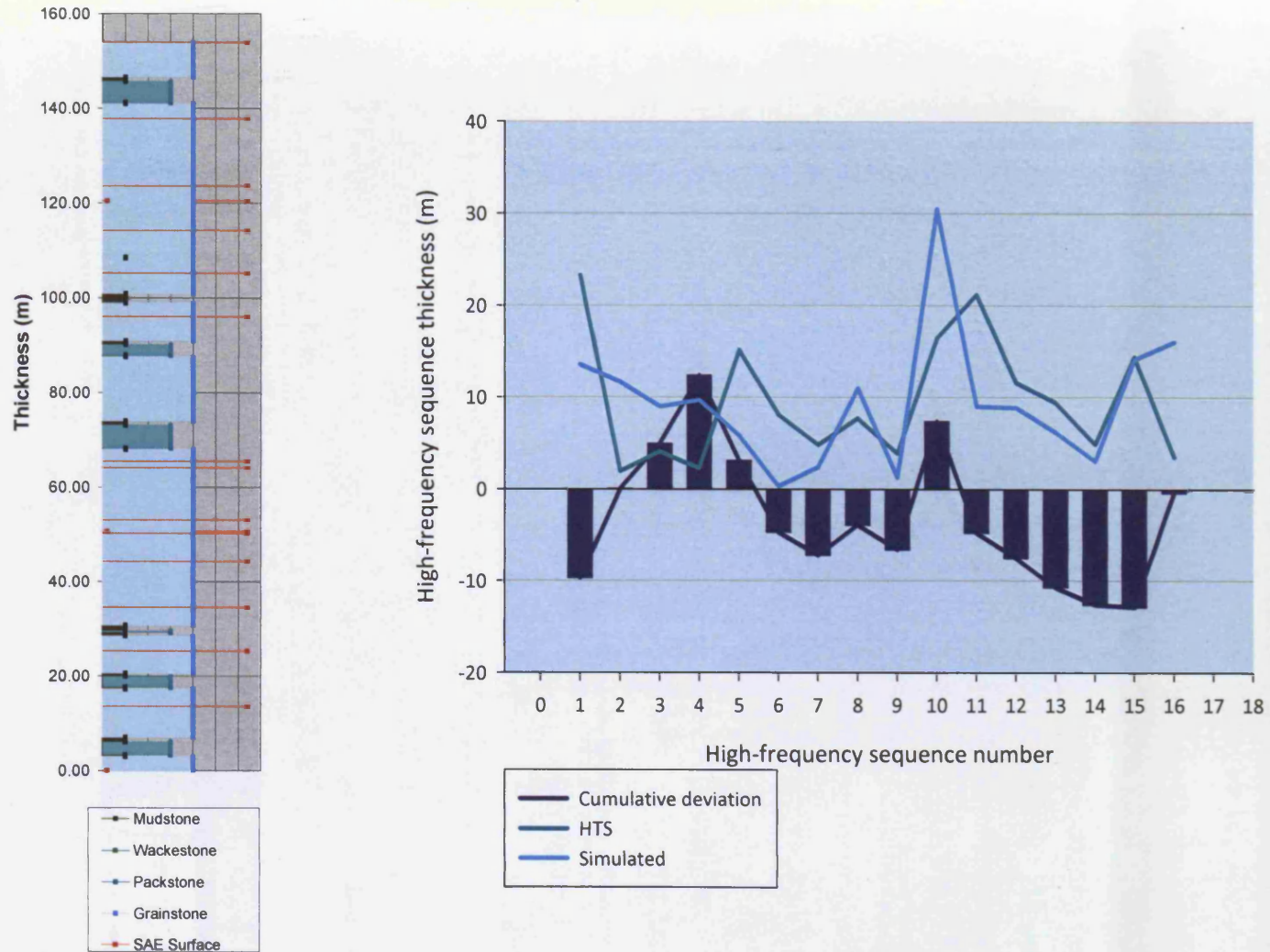


Figure 5.36: Plots showing the facies stacking pattern (left) and individual HfS deviation from corresponding observed HfSs in the HTS (right), for a run with <10m cumulative deviation (Figure 5.35; a). HfS numbers correspond to the simulated stratigraphic column, with cumulative deviation measured from the same 'number' sequence in the HTS.

oscillation allowing production to keep up with sea-level rise and deposit significant volumes of sediment. As intermediate-order amplitude increases, higher-frequency rise exceeds production to a greater degree and positive deviation decreases. The three instances of minimum cumulative deviation in Figure 5.33 exist along this continuum. With only one large-amplitude eustatic component the distribution and relationship of minimum deviation runs can be seen (Figure 5.35). This high-resolution example identifies a greater number of instances of minimum (i.e. less than 10m) cumulative deviation compared with Figure 5.33 not because of greater resolution, but due to the lack of a variable high-order parameter.

A comparison between Figure 5.34 and Figure 5.35 illustrates that with two variable high-frequency large-amplitude eustatic components; there is significant difficulty in generating a simulated section comparable to the HTS. However, with one static eustatic component and a low-order oscillation, a HTS-equivalent section can be generated with a range of parameter values. A crucial point is that runs with minimum cumulative deviation only occur when low-order amplitude is greater than 20m (Figure 5.35). This is not the case in Figure 5.34, where low order amplitude is fixed at 10m.

It seems improbable based on results of numerical forward modelling, that two combined high-frequency large-amplitude eustatic components alone can generate a good approximation of the HTS, at least in terms of thickness (and constrained by the same number of HfSs). What is needed to achieve realistic thicknesses is the inclusion of a low-order component at least 20m in amplitude.

5.4.4.2 Evaluation of stacking patterns

So far, only the total thickness of a simulated section and the extent to which it deviates from the total HTS thickness has been considered. Whilst this is indicative of conditions that could produce a section similar in scale to the HTS, it does not provide information on stacking patterns and their resemblance to the HTS. This is a crucial consideration in evaluation of forcing of cyclic successions. By evaluating the deviation in terms of thickness of individual HfSs within single simulations the degree to which a simulation matches the HTS can be assessed. Ideally, there should be a minimum of deviation between the simulated and observed sections for each HfS. Assessing sections in this way is a second-stage method of comparing simulations with the HTS section, and is not conducted for simulations with a cumulative deviation of 10m or greater. These sections are likely to show too much deviation to show good correlation with the HTS.

While a section may show good correlation in terms of cumulative deviation (i.e. less than 10m) it may display poor correlation of individual HfS thicknesses. Figure 5.36 shows the simulated sedimentary stacking patterns and individual deviation of HfSs, and

is an example of poor individual correlation resulting in a good overall match. The relatively limited accommodation as a result of small amplitude eustatic oscillations means production is usually able to keep pace with sea-level change. Consequently, production is mainly from within the euphotic zone, and the simulated stratigraphy is dominated by grainstone lithologies. Analysis of deviation of individual HfSs reveals a relatively poor overall correlation between simulated sequences and HTS sequences. There is a tendency for HfSs to be too thin, and it is only through the occurrence of two anomalously thick sequences that the section shows a good cumulative deviation match.

Further comparison of runs with small amounts of cumulative deviation also reveals large deviation of individual HfSs. Analysis of the deviation of individual HfSs within the parameter-space zone of minimum cumulative deviation (Figure 5.35; a, b & c), shows that individual HfSs rarely show good correlation with their HTS counterpart (Figure 5.37). Furthermore, in cases of good correlation the small amount of deviation is rarely maintained for more than one HfS. The occurrence of a section with little cumulative deviation is therefore usually coincidental, rather than a result of a combination of parameters producing a stacking pattern similar to that of the HTS.

Despite the improbability of creating a run of HfSs that replicate the HTS, a hierarchy of eustatic oscillations should not be ruled out as a mechanism for generating similar sedimentary sections. Figure 5.37 (b) demonstrates that whilst sections may display significant deviation of individual HfSs, the facies stacking patterns do not show a great deal of differentiation from the HTS. Given that minimum cumulative deviation sections cluster in a parameter-space zone, it could be envisaged that a certain combination of parameters would give rise to similar stacking patterns *and* sedimentary style. This was not, however, the case for runs which had amplitudes of eustatic parameters as their major variable.

5.4.4.3 Simulations investigating rate of subsidence

As HTS-equivalent simulations only exist at very specific values of the eustatic components, it is also necessary to assess the effect of subsidence on the creation of HTS-similar simulated successions. Subsidence, as the major accommodation-creating parameter, is the most likely to have significant impact on the likelihood of matching simulations to the HTS.

Simulations employing subsidence as the major independent variable show a significant tendency to develop runs with less than 10m cumulative deviation at very high rates of subsidence (Figure 5.38). At high subsidence rates (greater than 170m/My) there is remarkable uniformity of simulations showing minimal cumulative deviation, largely regardless of intermediate-order amplitude. This is not seen in other simulations where

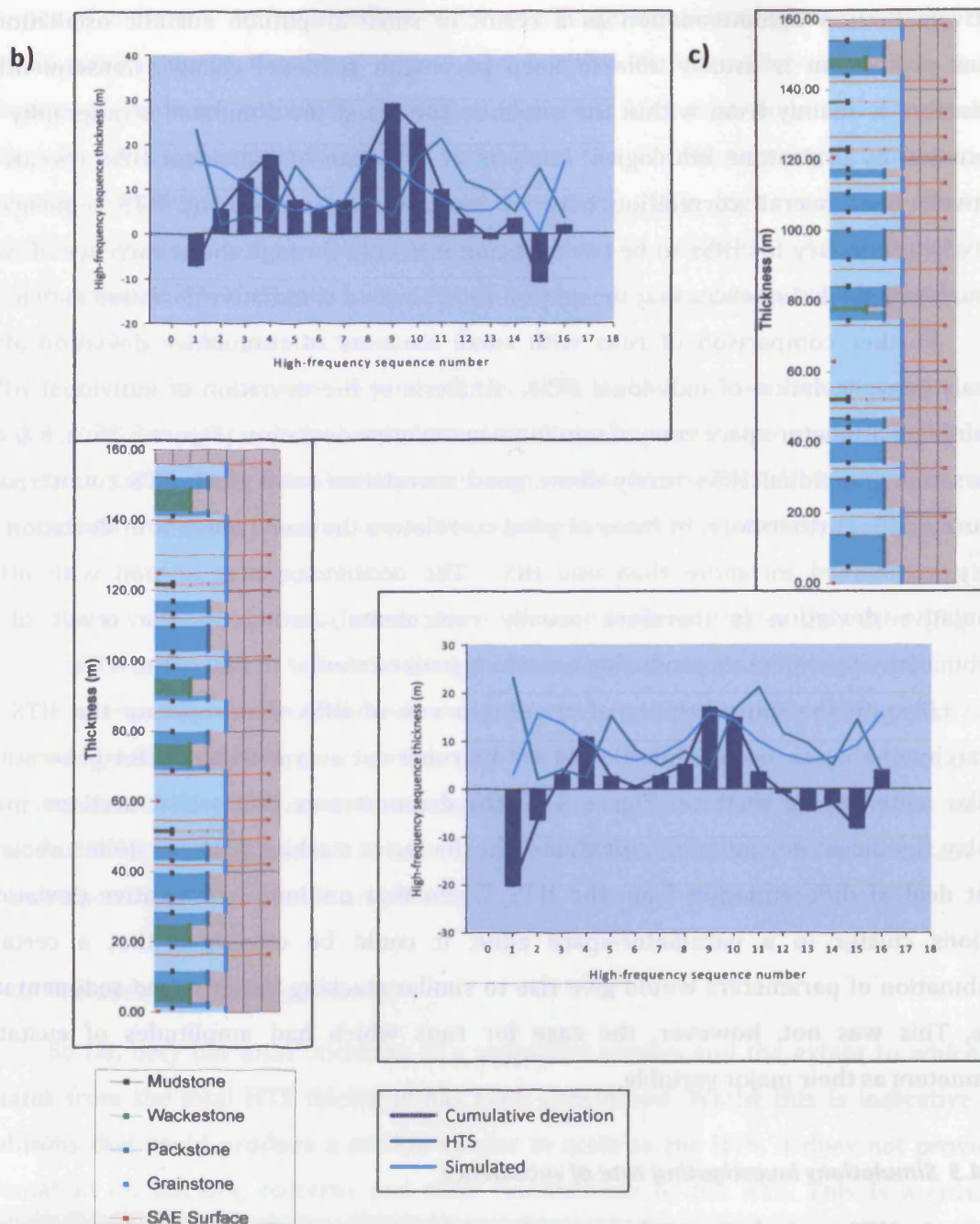


Figure 5.37: Plots showing the facies stacking pattern and individual HfS deviation from corresponding observed HfS in the HTS, for runs with <10m cumulative deviation (Figure 5.35; b and c).

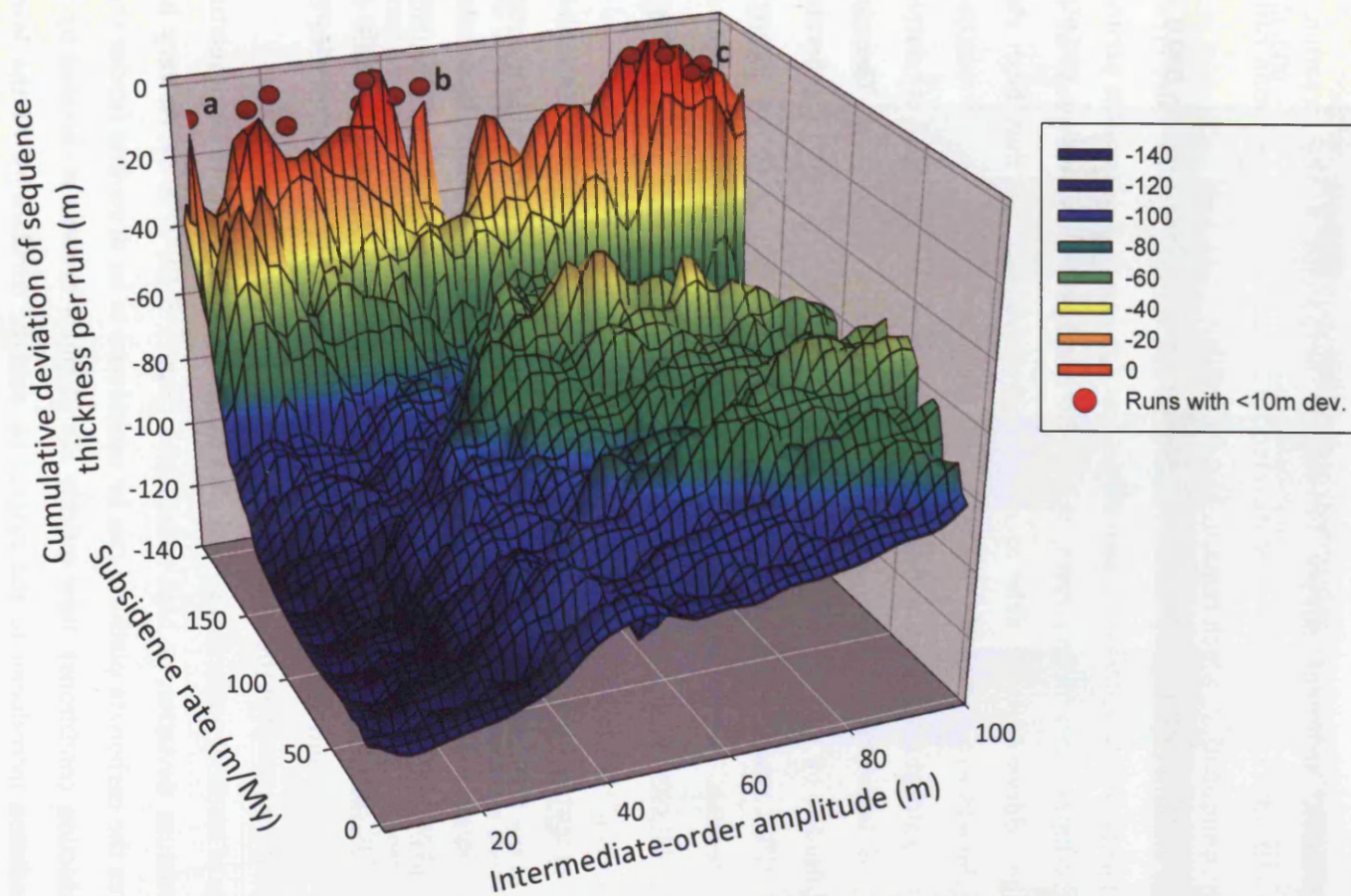


Figure 5.38: High-resolution parameter-space plot showing the cumulative deviation response surface of subsidence rate against the intermediate-order eustatic component. Subsidence rates of $<160\text{m/My}$ show the least deviation from observed HTS thicknesses. These subsidence rates are comparable with rates observed in the Paradox Basin. Runs with $<10\text{m}$ are separated into two groups a small-medium eustatic amplitude group (a, b) and a group associated with large eustatic amplitudes (c). These groups are examined in terms of their individual HfS deviation and stacking patterns in Figure 5.40.

intermediate-order amplitude is used as an independent variable; changing intermediate-order amplitude usually significantly affects the likelihood of generating HTS-similar sections. The fact that it does not significantly vary at very high subsidence rates suggests that the rate of accommodation-creation significantly exceeds that of sediment production rate before further modification from eustatic oscillations. As amplitude of eustatic oscillations increases, sediment supply is already outpaced by the creation of accommodation. HfS thickness is therefore dictated by the rate of sedimentation rather than available accommodation, which remains largely unfilled.

The large amount of accommodation created at high subsidence rates also creates the potential for very thick sequences of sediment to be deposited. Whether this occurs is dependent on sediment production rates, which, at average values (in terms of the parameter range addressed), are able to create simulated sections that bear close resemblance to the HTS in terms of cumulative HfS thickness.

It is very significant that similar-thickness sections are best developed at relatively small amplitudes of intermediate-order oscillation (less than 50m; Figure 5.38). Therefore, significant amplitudes of eustatic sea-level oscillation are not required to generate a succession of HfSs, which cumulatively show minor deviation from an observed sedimentary succession. The implication of this is that eustatic sea-level oscillations are not the fundamental control in generating HfSs that bear resemblance to the HTS (Figure 5.39).

This statement is supported by observations of individual deviation of simulated HfS from those of the HTS, although analysis of the style of sedimentary stacking identifies scenarios which do not exhibit realistic stacking patterns (Figure 5.40). Simulations with very high subsidence but very low amplitudes of intermediate-order eustatic oscillation (less than 20m) fall into this category (Figure 5.40; a). Under these conditions HfSs are predominantly too thin, and show an abundance of grainstone facies; representative of a style of cyclicity not apparent at the HTS.

Analysis of stacking patterns also reveals a trend that is apparent in all simulations generating minimum deviation at high-subsidence (Figure 5.40; a, b, c). At very high subsidence rates the carbonate platform can be considered to be drowning (under these carbonate production conditions). How quickly the platform drowns is dictated by the extra accommodation introduced to the system by eustatic oscillations. At the lowest amplitude of eustatic oscillation exposure surfaces (and therefore HfSs) stop being created after 130m of section. By this time accumulation has failed to keep up with accommodation created by subsidence to the extent that eustatic oscillations no longer expose the platform surface. Conversely, at the highest eustatic amplitudes addressed in

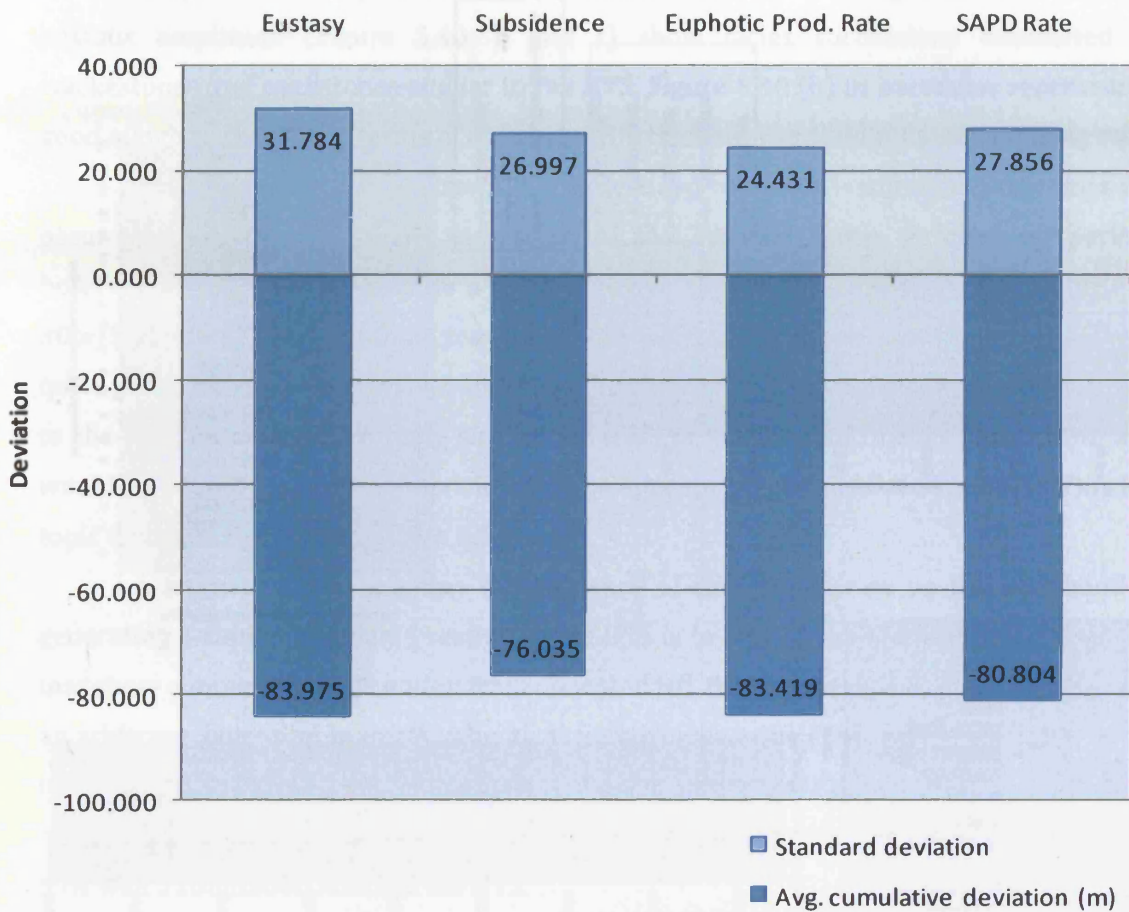


Figure 5.39: Histogram showing standard deviation of all simulations per parameter and average cumulative deviation of model runs from the HTS thickness (for all simulations) per parameter. Eustasy shows the greatest cumulative deviation, suggesting that modification of eustatic parameters results in the worst match to the HTS. It also has the highest standard deviation value illustrating that modification of this parameter causes the greatest spread of modelled section thicknesses.

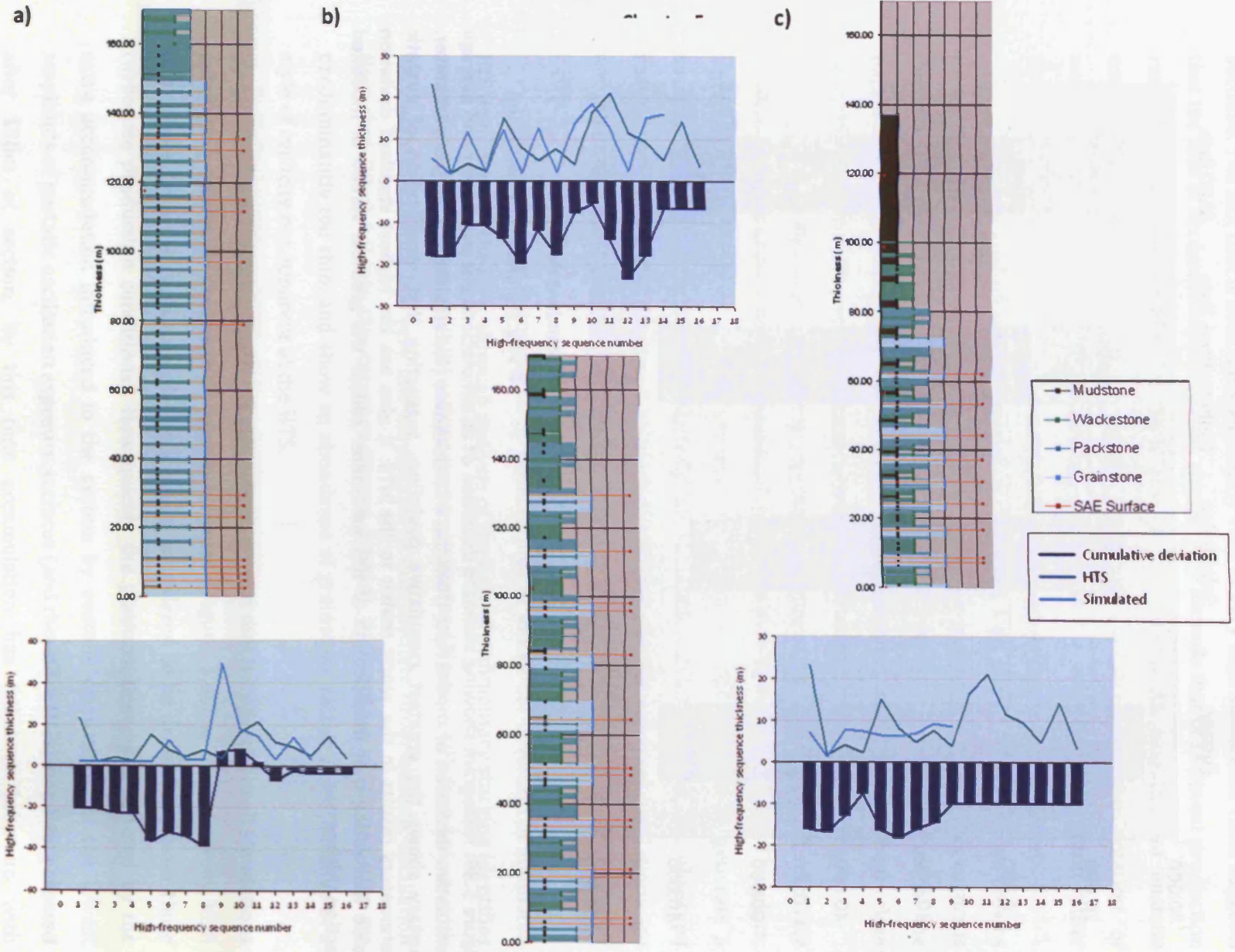


Figure 5.40: Plots showing the facies stacking pattern and individual HfS deviation from corresponding observed HfSs in the HTS, for runs with <10m cumulative deviation (Figure 5.38; a, b and c). All three simulations show a tendency to drown the platform due to very high subsidence rates.

this study (100m) this occurs after only 65m of section. This does not detract from the fact that until the system drowns, the sections show small cumulative deviation from the HTS.

Despite eventually drowning, simulated sections resulting from an increased eustatic amplitude (Figure 5.40; b and c) show facies successions dominated by wackestones and packstones similar to the HTS. Figure 5.40 (b) in particular represents a good match to the HTS in terms of individual HfS thickness and sedimentary stacking style.

This still represents a system that is destined to drown – something that does not occur with the Desmoinesian succession of the Paradox Basin. A ‘catch-up period’, however, would only necessitate a minor relative slowing of subsidence (by as little as 30m/My) after several million years. Given the complex tectonics in this region this is quite possible. The end-result would be a stratigraphic section, which, while not identical to the HTS, would be extremely similar in terms of stacking and facies proportion; and would be produced by parameters likely to be appropriate for the Paradox Basin. This is a topic discussed further in section 5.5.1.

A further way to examine the influence of subsidence rate on the likelihood of generating a similar simulated section to the HTS is to look at the number of HfSs per run that show a minimum of deviation from observed HfS thickness (Figure 5.41). By assigning an arbitrary, but suitably small, value to acceptable deviation (2m represents 1.3% of the total section and approximately 20% of average HfS thickness) the number of simulations ‘matched’ by a run can be known. A quantitative assessment can therefore be made as to how well a simulation matches the HTS.

Whilst Figure 5.41 does not show any systematic variation it is possible to identify a general trend of simulations that display a better match to the HTS. Sea-level amplitudes between 0m and 60m tend to create a greater number of HfSs than higher amplitudes of eustatic sea-level oscillation. It should be noted however, that although some parameters create a closer match to the HTS than others, no simulation matches even half of the observed HfS thickness. Whilst this does not unequivocally suggest a range of possible amplitudes of eustatic oscillation, it suggests that amplitudes in this range are more likely to be capable of generating HfSs that are of similar thickness to the HTS. Further analysis of response surfaces showing the number of ‘accurate’ HfS thicknesses per run suggests individual parameter-space areas are able to match at least 50% of observed HfSs per sequence to within this small amount of deviation (Figure 5.42).

5.4.4.4 Simulations investigating production rate and platform denudation rate

There are specific rates at which carbonate production and sub-aerial platform denudation are most likely to show minimum deviation from HTS HfS thickness (Figure 5.43). This does not preclude simulations from exhibiting negligible deviation from the

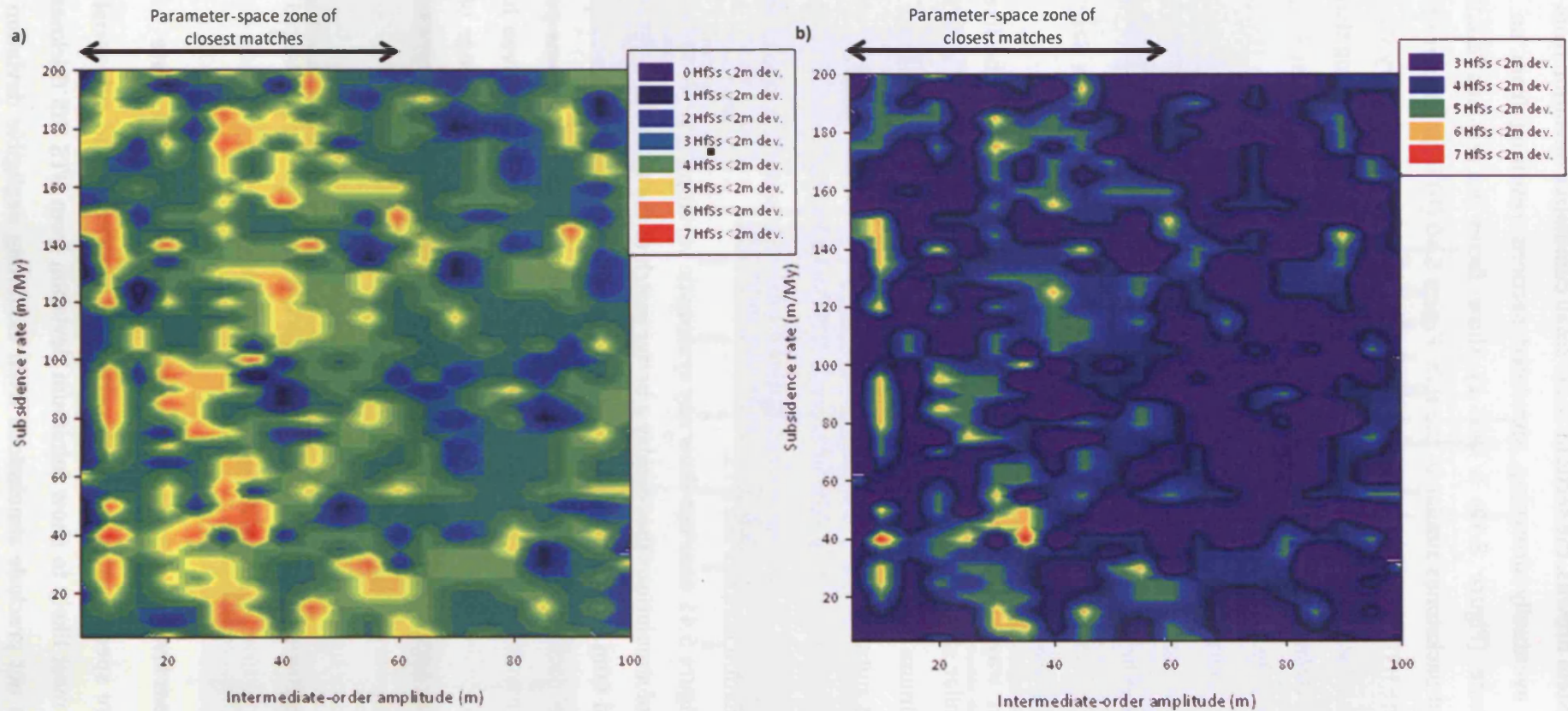


Figure 5.41: Parameter-space response surfaces of cumulative HfS deviation for subsidence rate. (b) is the same image as (a) with a lower threshold applied to highlight the preferential development of runs with a greater number of HfS thickness matches at eustatic amplitude of less than 60m.

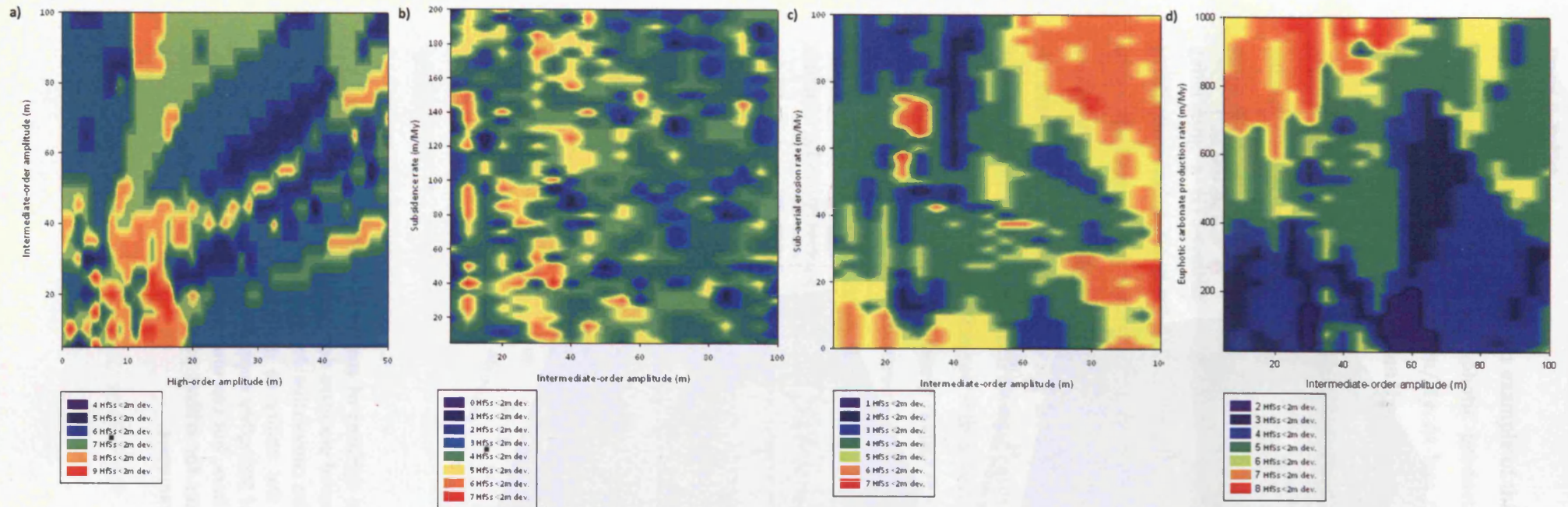


Figure 5.42: Parameter-space response surfaces of cumulative HfS deviation for eustatic amplitude (a), subsidence rate (b), sub-aerial platform denudation rate (c) and euphotic carbonate production rate (d). Note the slightly different scales. Only at very specific interactions of sea-level is it possible to generate >50% of HfSs with less than 2m deviation from their respective HTS sequence (a). The poor ability of all parameter interactions to correlate well with the HTS is indicative of the difficulty in accurately modelling the HTS.

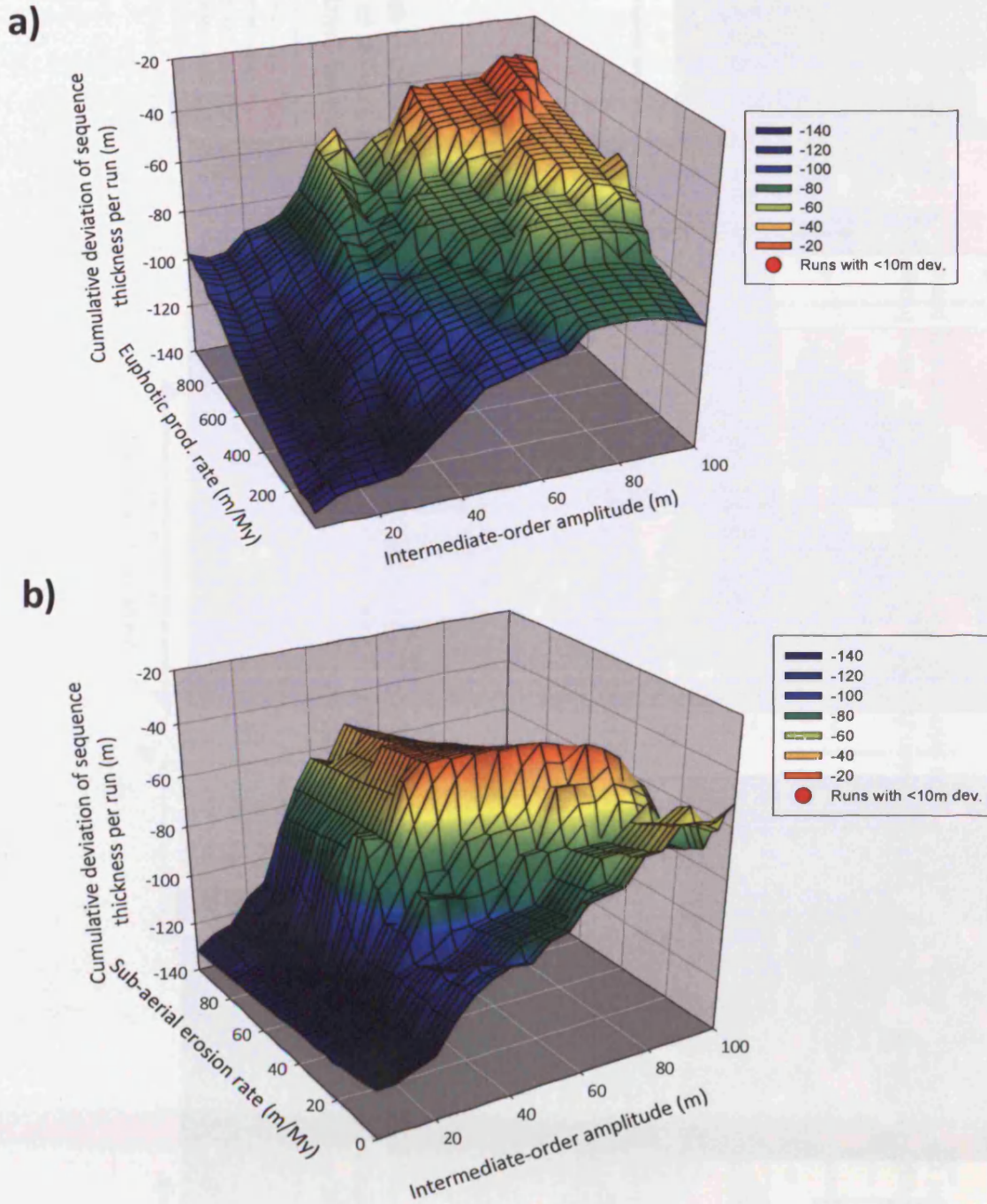


Figure 5.43: Parameter-space response surfaces of cumulative HfS deviation for euphotic production rate (a) and sub-aerial platform denudation rate (b). Neither set of runs shows simulations with <10m cumulative deviation. These parameters may be considered as modifiers to the ability to generate realistic stacking patterns of HfSs. For instance, a rate of 500m/My euphotic carbonate production does not produce realistic thicknesses here, but can under appropriate conditions (e.g. Figure 5.34). This would not occur for critical parameters which generate realistic thicknesses only at specific parameters.

HTS, however. Figure 5.34 is an example of this; where simulations show less than 10m deviation despite having a euphotic production rate of 500m/My, and a sub-aerial platform denudation rate of 0m/My. At less than ideal scenarios, it is still possible to create a HTS-similar section, given the right circumstances.

These observations show that these controls are subordinate in importance to others in creating a good match to the HTS (principally eustatic amplitude and subsidence). It is possible to summarise other parameters, apparently integral to the generation of sedimentary sections, as essentially being 'modifiers' to the ability of generating a HTS-similar simulated section. These parameters, primarily carbonate production regimes and sub-aerial platform denudation, are integral to the development of the stacking pattern but do not represent a critical control on the ability to create HTS-similar thicknesses and stacking.

On the whole, this is not the case for 'critical' independent variables such as eustatic amplitude and subsidence, which in most cases will not result in a minimum of deviation from observed thicknesses except with a very specific combination of parameters. It is difficult to assess and appropriately realise the effect of combined independent variables in a complex system, even constrained within a simple one-dimensional model, without the use of more sophisticated mathematical methods. However, it is possible to visualise a scenario where this does not hold true, and an extreme of euphotic carbonate production rate (for instance) will generate a comparable section to the HTS, despite improbable combinations of other parameters, but these situations are relatively unlikely compared with the probability of generating realistic simulated sections with critical variables. Consequently, it is most appropriate to consider these parameters as non-critical modifiers to the likelihood of generating HTS-similar simulations.

5.5 INTERPRETATION

5.5.1 Evaluation of an ordered forcing-mechanism

One of the primary aims of this study was to quantify the level of facies ordering in the HTS (documented in section 5.3.1). Statistical analysis shows the HTS to have ordered stacking patterns. Embedded Markov chain analysis suggests that there is little probability of facies being randomly ordered. It is therefore logical to conclude that the forcing mechanism responsible for dictating stacking patterns is also somewhat ordered. Ordered lithofacies transitions reinforce what is currently thought to be true regarding sea-level oscillation and resulting sedimentation during ice-house periods: namely that an ordered or semi-ordered mechanism is responsible for fluctuating eustatic sea-level.

It may therefore be expected that by incorporating these parameters into a numerical forward model, the HTS section could be reasonably simulated. However, modelling of processes often stated to be responsible for controlling stacking patterns has great difficulty in replicating the HTS. Given the correct range of parameters, individual components of the sedimentary stacking pattern (vertical facies associations, HfS thickness and overall sequence thickness) may show good correlation with empirical data from the HTS. However, all three of these criteria are rarely satisfied in the same simulation. It is more common for simulations to display results that bear an overall resemblance to the HTS in one or more aspects. Furthermore, there is additional evidence to suggest that significant proportions of the HTS can be modelled relatively accurately (over 50% of HfSs can be matched to within 2m deviation; Figure 5.30).

The improbability of successfully forward modelling the HTS raises important points about the complexity of the section, given that facies transitions in the HTS are demonstrably ordered. TED, based on empirical published data incorporated into a computer simulation by proven methods, can successfully create similar stratigraphic sections to the HTS. However, it consistently does not create thicknesses and stacking patterns that exactly match the HTS. There is no theoretical reason why TED should not be able to model the HTS when it is capable of producing similar modelled lithologic successions in terms of stacking pattern. The cause of deviation therefore exists in the parameters employed to model the HTS; either in terms of inappropriate values, processes that are not included in the model, or a combination of both. The negative results of this process-based approach to modelling provide important indicators as to the relative complexity of the section.

Vertical facies associations are an important example of a component of sedimentary style not reproduced satisfactorily. If HfSs truly shallow-upwards then the

facies associations within them should reflect this fact. However, lithofacies proportions in simulations never match those in the HTS precisely. It is therefore likely that there is a significant controlling parameter not represented in the model which acts as a fundamental control on lithofacies stacking.

Matching of modelled lithofacies associations in comparison with the HTS supports the argument that more than the parameters represented in the model act as a control on facies stacking. As TED incorporates fundamentally depth-dependent carbonate production the lithofacies generated in simulated successions display highly-ordered vertical facies associations. Comparison of Embedded Markov chain analysis for the HTS and simulations reveal that both are highly ordered in terms of facies transitions (Table 5.3). Yet despite this, modelled sections consistently fail to accurately represent the HTS section in terms of both stacking *and* lithofacies proportions.

The probable reason for this deviation is that although HTS facies transitions are ordered, they may not be solely depth dependent – a factor which causes deviation between the very highly-ordered model runs and the ordered HTS. An alternative hypothesis is that the HTS has ordered facies transitions as a result of major changes in water depth; those likely to significantly shift facies belts. Whilst at very shallow water depths, facies distributions are non-depth dependent – a theory in keeping with the findings of Rankey (2004). The true answer may well be a combination of both factors. In either case, given the divergence between modelled and physical section caution should be used when using vertical facies associations to identify cycle boundaries as previous workers have.

What numerical forward modelling of lithofacies ultimately tells us is that there is significant complexity in the sedimentary section that is not represented in the numerical model. Were this not the case, then under certain parameters the HTS could be simulated exactly. Importantly, since TED is only a quantitative representation of typical sequence stratigraphic conceptual models for cyclic carbonate accumulation, failure to reproduce the observed section suggests that these conceptual sequence models may also be too simplistic.

The nature of this complexity in the HTS strata is unknown. It is likely that both autocyclic and allocyclic elements play a significant role in the distribution of lithofacies on a carbonate platform (e.g. Burgess, 2001; 2006). Autocyclic mechanisms are prominent on the Paradox Shelf in several forms, most notably the siliciclastic sediments which are discussed in detail in section 5.5.4. Algal mounds are present in shelf-distal sections which create significant palaeotopography commonly infilled with resedimented carbonates (Roylance, 1990). Algal mounds do not extend into proximal sections of the shelf however (with only one biostromal form at the HTS) and therefore are not thought to be a

Run set	Average χ^2 score
Int.-order amp.	156.139
Subsidence	110.428
Euphotic production rate	146.405
Sub-aerial platform denudation rate	127.328
HTS (single score)	54 ($p = 0.05$)

Table 5.3: Average χ^2 score for each run set of 1000 runs and for the HTS. A run can be considered to have a non-random vertical facies association with a 95% confidence level if it exceeds the critical value of 11.070 (with 5 degrees of freedom). The very large values displayed here display first-order Markovian properties; that is each facies is directly dependent on the preceding facies. There is a high level of ordering in the facies associations.

Analysis for the HTS results in rejection of the null hypothesis that the facies succession is not ordered (in contrast to the simulated successions). The critical value for the HTS is 37.65 at the 95% confidence interval.

significant autocyclic factor during the Desmoinesian HTS. An indicator of a potentially greater source of autocyclic variation is the cross-bedding prominent in a number of shallow-water bioclastic pack/grainstones (Figure 5.26, b). These facies are interpreted to have formed as migratory bars of coarser-grained sediment. Consequently, they represent slight palaeotopographic highs between which finer-grained sediment accumulated. Despite this, there is no evidence of lateral variation of facies at the HTS at less than a kilometre scale. There is therefore clear evidence of depositional facies change over a very small water depth range which is not adequately recorded in the stratigraphic record. It is likely that this and other unquantified allocyclic parameters assert significant influence over the distribution of lithofacies on the platform top, and could be responsible in part for the deviation of ordered simulated lithofacies successions from observed HTS facies associations.

5.5.2 Controlling parameters on sedimentation and stacking

Simulations addressing interactions of the three major eustatic components (low-, intermediate- and high-order amplitude) generate very few 'best-fit' sections comparable to the HTS. In contrast, simulations that address the intermediate-order eustatic parameter and subsidence alone show the most realistic stacking patterns, and the HfS thicknesses which most resemble the HTS.

These 'best-fit' simulations are developed at relatively high rates of subsidence (greater than 150m/My) - in line with rates cited for the Paradox Basin (Goldhammer *et al.*, 1991). Given that eustatic oscillations alone create relative poor matches for the HTS, and subsidence rate provides the basis for better correlations, it is probable that the complex tectonic setting of the HTS and encompassing Paradox Basin plays a prominent role in dictating the nature of the sedimentary succession.

The complex subsidence history of the Paradox Shelf does not fit easily into a single tectonic model. Following a pre-Pennsylvanian phase of general stability, the Desmoinesian Paradox Shelf experienced increased rates of subsidence in response to the development of the Marathon-Ouachita convergent orogenic front to the south (Figure 5.44). These rates place the Desmoinesian within the zone of maximum subsidence for the shelf; a zone which is likely to represent similar subsidence rates to optimal rates of HTS-sequence generation in TED. Under very high rates of subsidence, deviation from observed HTS HfS thicknesses is at a minimum (Figure 5.38). In addition, sedimentary style under these conditions, while not identical to the HTS, is similar in terms of dominant lithofacies components (wackestone and packstone) and lithofacies proportions (Figure 5.40). It also represents the closest match to the HTS section seen in simulated sections.

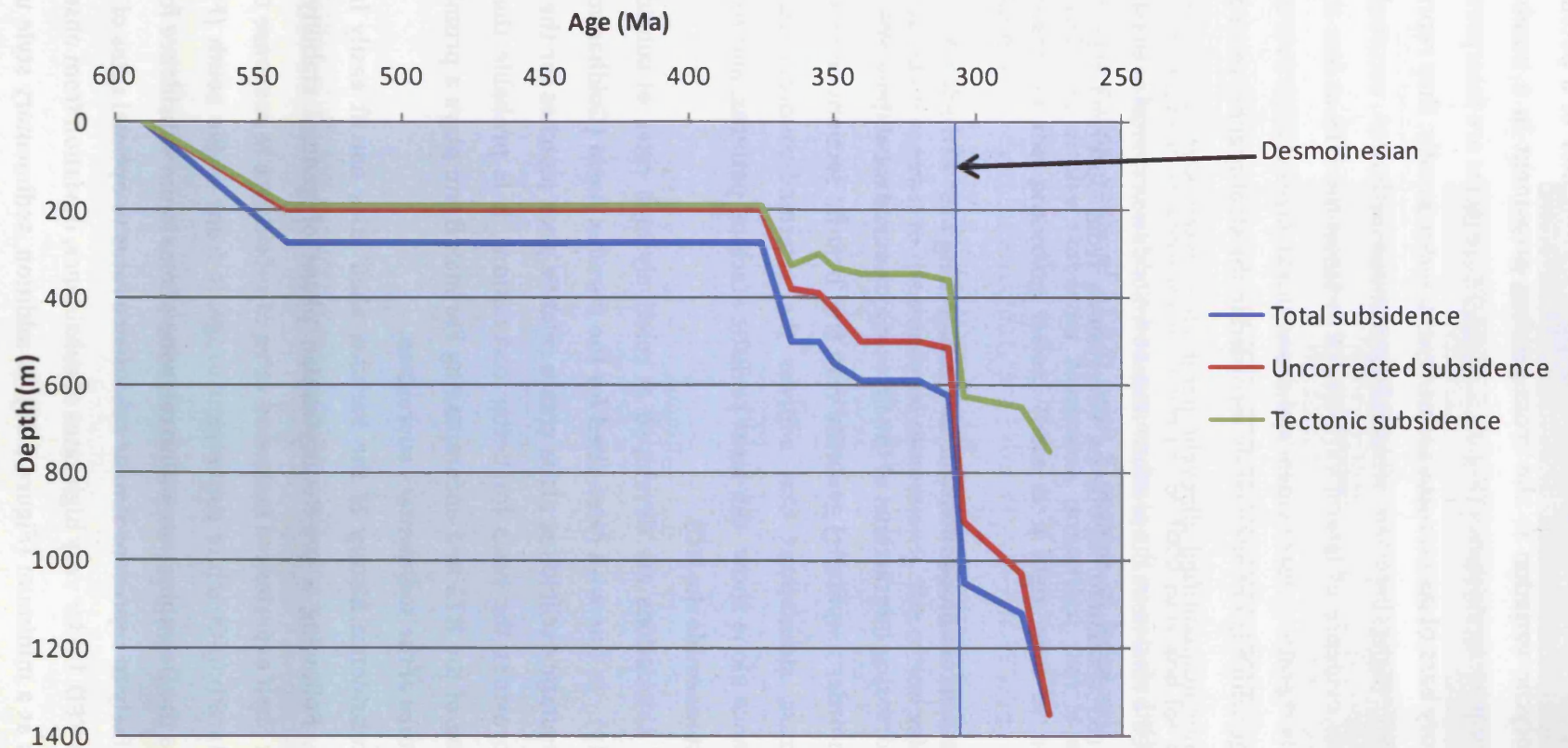


Figure 5.44: Subsidence profiles for the Paradox Shelf based on age-depth pairs from the Texaco Johns Canyon No. 1 well located in San Juan County, Utah (R. 18 E, T. 41 S.; sec. 6). Palaeozoic time scale is that of Gradstein *et al.* (2004). Tectonic subsidence refers to non-isostatic basement subsidence. Uncorrected subsidence is derived from total rock thickness versus time. Total subsidence includes the effects of sediment loading, compaction, inferred palaeobathymetry and basement subsidence. Modified after Goldhammer *et al.*, 1991.

The major problem with the simulations presented in Figure 5.38 is that each of the high-subsidence scenarios causes the platform to eventually drown; accommodation creation outpaces sediment supply, either gradually or very rapidly. This reflects a pattern of sedimentation not seen in the HTS. In fact, the opposite is more likely to be true on the Paradox Shelf where the Honaker Trail Formation contains a greater proportion of shallower-water facies (principally; QSF1, QSF2, non-skeletal facies, skeletal facies) than the underlying Paradox Formation.

Very high-subsidence rates associated with the Desmoinesian are interpreted to have assumed a more sedate pace by (and possibly even before) the Missourian. As divergent strike-slip movement waned, basin collapse processes and associated subsidence rates slowed considerably (Stevenson & Baars, 1986). After the high-rates of the Desmoinesian, this allowed sediment supply to fill the available accommodation and maintain shallow-water conditions. The change from extremely rapid to comparatively very slow rates of subsidence occurred on a timescale of 2-3My. It is therefore possible that a simulated section could produce similar lithofacies thicknesses, HfS stacking patterns and overall sequence thickness to the HTS, if a gradual reduction in subsidence rate occurred which prevented the platform from drowning.

It is therefore possible to envisage a scenario where very high subsidence rates were in operation during deposition of the Atokan/Derryan-Desmoinesian (representing 311.7 to 306.5Ma +/- 1My; Gradstein *et al.*, 2004) sequence on the Paradox Shelf. Near the end of the Desmoinesian, subsidence rates slowed, preventing drowning and maintaining the development of shallow-water facies units. Such a scenario would bear close resemblance to simulations of the HTS without causing distinct deepening or drowning of the platform (e.g. the sedimentary style of Figure 5.40, b, with no deepening event after 120m). The implication is therefore that subsidence is highly variable on a million-year timescale. It seems likely, given the high subsidence rates experienced by the Paradox Shelf in the Desmoinesian, along with results of modelling studies, that this is a plausible mechanism for the development of the HTS.

This interpretation still does not adequately explain why simulations fail to accurately model the HTS, although the complex tectonics operating in the Paradox Basin do provide a plausible mechanism for the difficulty in modelling of the HTS. The palaeostructural interpretation of the Paradox Basin is that of an extensional rhombochasm bounded by dextral master faults originating in Atokan time. The tectonic setting may be further complicated by the possible presence of horst- and graben-like structures arising from the transpressional collision of Gondwana and Euramerica during the late Palaeozoic, similar to structures seen in the Permian Basin (Pindell & Dewey, 1982; Ross, 1986). Baars & Stevenson (1982) suggest that 'small-scale oscillating vertical

movements recurred along fault blocks throughout the Upper Palaeozoic across the Four Corners Plateau. These authors suggest that in the Pennsylvanian the same 'small-scale basement structures actively controlled the distribution of middle Pennsylvanian carbonate lithofacies' in the Paradox Basin by providing positive fault blocks favourable to shallow water carbonate production. This primarily applies to shelf-distal sections, where fault blocks create palaeotopographic highs that significantly influence algal mound development. Evidence from well data taken from the Paradox Shelf, however, also suggests that these inverted basement structures occur across the width of the Paradox Shelf (Figure 5.3). The effect of that these small-scale basement structures had was to subtly vary palaeobathymetry across the Paradox Shelf, likely creating localised facies variations (Baars & Stevenson, 1982). The fact that these facies variations are not quantifiable as lateral variation at outcrop is indicative of the unseen complexity within the stratigraphic record. Even very minor depth and facies changes would result in dissimilar stacking patterns at different points on the shelf. Localised tectonics may therefore have had significant impact on the way in which stacking patterns developed, and on their overall style; even if they are not detectable in the stratigraphic record.

Previous authors have dismissed the notion of significant tectonic influence on the stacking patterns of the HTS. For instance, although Goldhammer *et al.* (1991) noted that "it is more likely that localized tectonics, in the form of gentle uplifts acted to influence the distribution of major algal mound development", he dismissed it as a significant influence on cycle development. This judgement was based on the improbability of repeated pulses of subsidence being of sufficient regularity and ordered magnitude to consistently generate HfSs. This was an appropriate conclusion to make but it does not allow for a more subtle influence to be exerted over HfSs by fault-related differential subsidence. Tectonically-influenced cyclicity need not be forced by extreme events such as periods of pulsed subsidence, or even periodic inversion, it is only necessary for subsidence rates to differ slightly to significantly varying styles of sedimentation (refer simulations conducted in section 4.3.2).

Furthermore, more recent work has suggested that both thrust and extensional faulting could be directly responsible for creating the accommodation necessary to generate sedimentary cycles (Kamola & Huntoon, 1995; de Benedictis *et al.*, 2007). These scenarios are particularly relevant for an active, complex tectonic system. This is something which has been suggested previously and dismissed (cf. Cisne, 1986 and de Boer & Smith, 1994). Sinclair (1997) suggests that subsidence rates would always be outpaced by high-frequency sea-level oscillations. However, even though this may be true, it would only take a variation in subsidence rate on the order of tens of metres per million years to affect stacking patterns significantly. Wedge-shaped geometries commonly

associated with fault-block movement (e.g. Nagy *et al.*, 2005) may not necessarily be noticeable if the movement occurred over a sufficiently large area and did not have a large throw (de Benedictis *et al.*, 2007).

Even if this was not the exclusive method of accommodation creation active in the Paradox Basin, the fact that extensional faulting of the same nature to those faults seen on the Paradox Shelf can generate cycles as a result of small amounts of instantaneous throw on faults, should not be underestimated. If this type of faulting and cycle generation occurred only several times per million years, the extra accommodation created would significantly affect attempts to link HfSs to orbitally-forced eustatic sea-level change.

There is also significant supporting evidence to suggest that subsidence plays a significant role in dictating the sedimentary style of the HTS. The tectonic history is complex, but during the Desmoinesian rapid subsidence dominates as a result of extensional faulting. This compares well with modelled scenarios most likely to represent realistic stacking patterns and sedimentary style. These factors combine to represent significant probability that subsidence plays a significant role in defining stacking patterns on the Paradox Shelf. However, this is not to say that glacio-eustasy is not occurring, as the repeated sub-aerial exposure suggests. Many of the facies documented in section 5.3, require sub-million-year eustatic oscillations to force restricted or normal conditions within the basin, for instance.

In conclusion, it is probable that the sedimentary cyclicity apparent in the HTS is the result of glacio-eustatic oscillations. However, it is very likely that the glacio-eustatic signal is significantly modulated by long- and short-term allocyclic variations in subsidence, as well as important autocyclic variations influencing depositional topography; both tending to mask any glacio-eustatic signal that might be present. It is likely that this variation in subsidence is the cause of variation between observed characteristic of the HTS and numerical simulations. Furthermore, it is worth remembering that the glacio-eustatic signal in the Pennsylvanian may have produced more complex patterns of sea-level oscillation (refer to section 2.5).

5.5.3 Hierarchical stacking-patterns

That the HTS can be said to have statistically ordered vertical facies transitions is not itself indicative of a hierarchy. As a hierarchy is defined based on thickness of HfSs, the vertical facies transitions, while potentially indicative of an ordered forcing mechanism, are not evidence of a hierarchical section. Indeed, it is possible to envisage a sedimentary section with ordered facies transitions produced by a non-hierarchical mechanism (e.g. Burgess, 2001).

The implication from numerical forward modelling of eustatic parameters is that stacked eustatic components fail to replicate the stacking pattern of the HTS (section 5.4.4). Furthermore, modelling suggests that the assumed presence of an intermediate- to high-frequency ordered forcing mechanism (i.e. large-amplitude eustatic components) is not enough to infer order in sedimentary successions. Simulations where eustasy is a dominant component rarely show a hierarchy, and in cases where a hierarchy is generated, sections do not show a close correlation in terms of HfS thickness or stacking patterns with the HTS (Figure 5.34; Table 5.4).

Two high-frequency large-amplitude eustatic components experience significant difficulty in generating a simulated section comparable to the HTS. However, with one static eustatic component and a low-order oscillation, a HTS-equivalent section can be generated at a range of parameters, although crucially only where low-order amplitude is large enough to have significant effect on accommodation (i.e. greater than 20m; see section 5.4.4).

Modelling suggests that it is improbable that two combined sub-My large-amplitude eustatic parameters alone can generate a good approximation of the HTS. However, modelling conducted in section 4.3.1 indicate that to generate a sedimentary hierarchy high-order oscillations need to be of similar amplitude to, or greater than, that of intermediate-order oscillations. This would seem to preclude a hierarchy generation *and* the generation of realistic HTS thickness.

The reinterpretation of cycle boundaries made by previous workers calls into question the existence of a hierarchy in the HTS. A reinterpretation of the HTS, only identifying cycle boundaries where there is unambiguous evidence of direct abnormal sub-aerial exposure of sub-tidal strata therefore represents a much more objective way of characterising HfSs. This method is also more satisfactory in comparison with the definition of a HfS. Only interpreting HfSs where there is unambiguous evidence of sub-aerial exposure results in a breakdown of the sedimentary hierarchy identified by previous workers; one based on potentially compromised facies-depth associations (e.g. Goldhammer *et al.*, 1991; Lerat *et al.*, 2000).

HfSs in the HTS do not lend themselves well to being categorised into arbitrary thickness groupings (Table 5.5). HfS thicknesses are more suggestive of a continuum in cycle thicknesses (*sensu* Drummond & Wilkinson, 1996). These workers suggest that the “hierarchical compartmentalization of the stratigraphic record is little more than a scheme of stratigraphic classification”. The results of modelling and facies studies of the HTS would tend to support this statement: HfS thicknesses display a range of values that do not easily allow segregation or grouping into distinct units. Indeed, it is notable that two high-frequency sequence thicknesses are greater than the thickness of the Lower Ismay

Run set	Simulations displaying a sedimentary hierarchy (%)
Int.-order amp.	18.5
Subsidence	10.8
Euphotic production rate	9.2
Sub-aerial platform denudation rate	5.7

Table 5.4: Percentage of simulations per run set (1000 runs) which display a sedimentary hierarchy. Runs displaying a hierarchy are not those which display a good correlation in terms of HfS thickness or sedimentary style to the HTS.

High-frequency sequence number	Thickness (m)
1	23.3172
2	2.0066
3	4.1148
4	2.3368
5	15.24
6	8.2042
7	4.9276
8	7.8232
9	3.9878
10	16.5354
11	21.2598
12	11.7094
13	9.525
14	5.0038
15	14.5034
16	3.6068

Table 5.5: High-frequency sequences thickness from the HTS. Max is 23.32m. Min is 2.00m. Range is 21.31m. Median is 8.01m. Mean is 9.63m. This data does not lend itself well to inclusion in arbitrary bin sizes of a hierarchical thickness distribution.

Member (16.74m; interpreted as a 'fourth'-order sequence by previous workers; Goldhammer *et al.*, 1991).

Given the already documented impact of subsidence on the HTS, it is likely that this also has significant impact on the generation of a sedimentary hierarchy. It is envisaged that the most likely mechanism of formation for this continuum was variable rates of tectonic subsidence combined with glacio-eustatic sea-level oscillations (see section 5.5.2).

The existence of a sedimentary hierarchy in the HTS also appears tenuous based on the ability of the HTS to be modelled. The extreme improbability of generating a sedimentary hierarchy under normal conditions is illustrated in section 4.4.3. This remains true, and in the case of the HTS high-rates of subsidence decrease the probability of generating a hierarchy (refer to section 5.5.2). The explanation for this is straightforward; the identification of a sedimentary hierarchy requires a recording mechanism of sufficient fidelity to record the order of the forcing mechanism. In the case of sedimentary cycles, this refers to glacio-eustatic sea-level oscillation hierarchically stacked on a sub-million-year scale. Introduction of controlling elements that are not dependent on this forcing-hierarchy acts as interference; and in the case of the HTS, subsidence is the major interfering factor.

Simulations consistently do not generate a hierarchy in the majority of cases, even with the presence of an ordered forcing mechanism suggesting that a hierarchy is unlikely. The effect of increasing subsidence rate within numerical simulations serves to decrease the already low probability that the ordered forcing mechanism has a recognisable effect. Furthermore, given that simulations using realistic, and even non-realistic parameters, cannot replicate the HTS, it is likely that there is significant complexity in the sedimentary environment which is not represented in the model.

Statistical evidence resulting from numerical forward modelling also suggests that a hierarchy is unlikely. Simulations determined by TED to be hierarchical are predominantly shown to have a succession of HfSs that are indistinguishable from random (Figure 5.45). The implication of this is that if, as previous workers have suggested, a hierarchy can be based upon stacking of HfSs, which should thin-upwards throughout a lower-order sequence, then a section should display ordered 'runs' of HfSs. As this is not the case, HfS thickness cannot be used to infer a sedimentary hierarchy. Although some hierarchical runs do plot in the ordered field of 'too many runs', they are greatly outnumbered by non-hierarchical sections. It is difficult, therefore, to distinguish between an ordered hierarchical and non-hierarchical run outside of the modelled environment. The majority of the evidence from the HTS (e.g., statistical independence of HfSs and significant problems in accurately modelling) strongly suggest that a hierarchy in Paradox

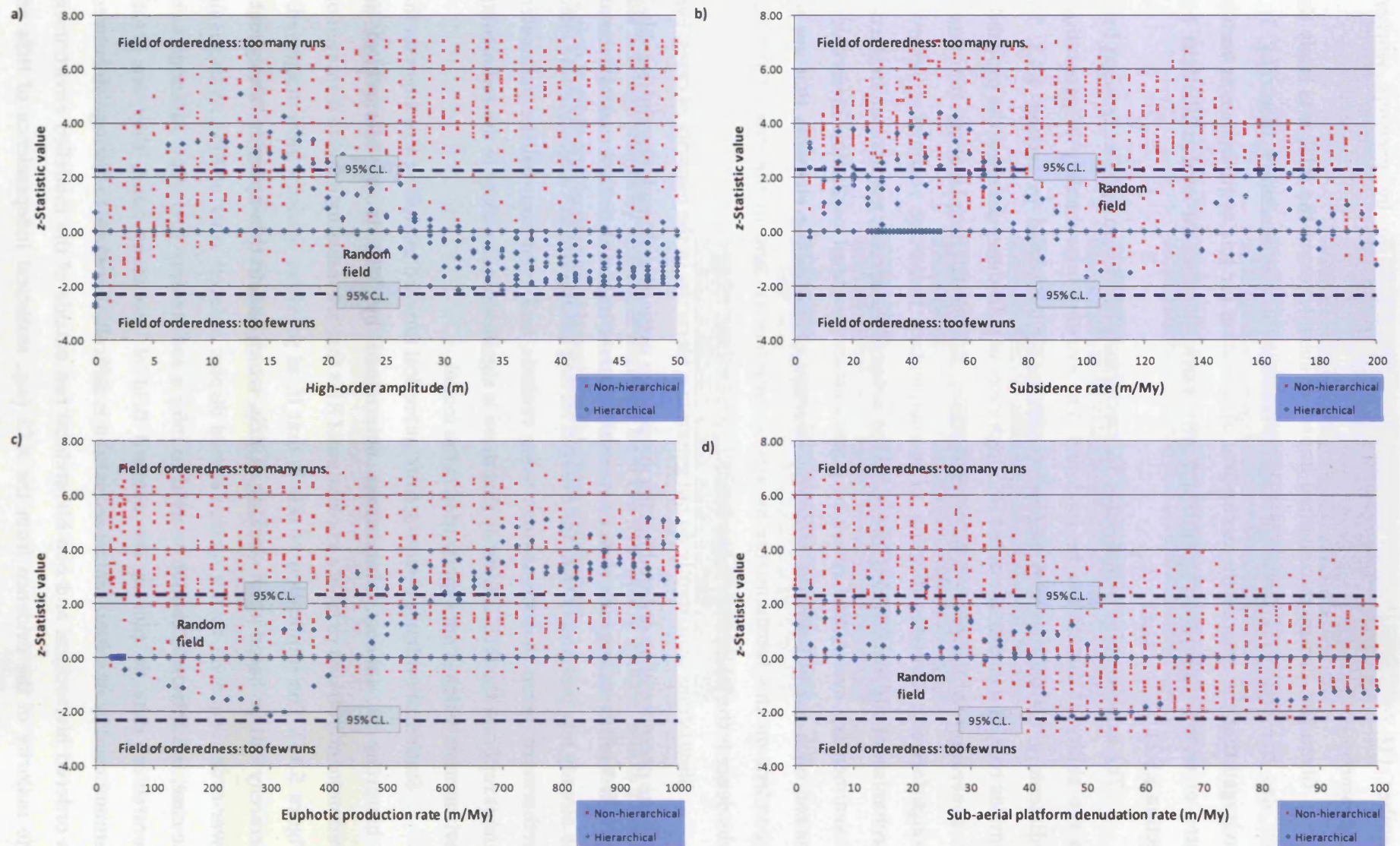


Figure 5.45: Durbin-Watson statistics for simulations where high-order eustatic amplitude (a), subsidence rate (b), euphotic production rate (c) and sub-aerial platform denudation rate (d) are the main variables. The non-randomness check is failed as runs of significant length are not developed. In each case, the majority of hierarchical sections occur in the field of randomness, suggesting that runs which may be identified as hierarchical are statistically dis-ordered. Hierarchical points along 0 on the y-axis are artefacts of plotting.

Shelf strata is unlikely. Evidence in fact suggests that a continuum of sedimentary thicknesses is the more appropriate interpretation of this section.

5.5.4 Revised genetic stratigraphy

The relative timing of sedimentation has received very little attention from previous workers studying the Desmoinesian Paradox Shelf succession. It has however, important implications for facies interpretations and how sediment behaves under oscillations of relative sea-level. Given what is currently thought to be most probable regarding vertical facies associations, it is likely that previous works have misinterpreted the timing of some of the most important aspects of the HTS facies stacking. A revision of the sequence stratigraphic model for the Desmoinesian succession of the Paradox Shelf therefore seems prudent.

Lowstands of relative sea-level on the Paradox Shelf are particularly important, given that they are most likely to represent periods of sub-aerial exposure, and therefore HfS boundaries. Goldhammer *et al.* (1991) interpreted QSF as lowstand sediment, redeposited during a subsequent transgression. More recently, two oscillations of relative sea-level have been invoked to explain the sequence-stratigraphic positions of siliciclastic beds. Under this scheme, the deposition of QSF is envisaged to be deposited during one oscillation, and after a period of exposure, carbonate deposition occurs during another oscillation of relative sea-level. This was defined as a “double cycle” (Grammer *et al.*, 2000; their Figure 24).

There are two major problems with the definition of double cycles in the Paradox Shelf succession, primarily evidenced by stratigraphy and supported by modelling. Double cycles assert that there exists evidence for sub-aerial exposure at both the base and top of QSF beds; such evidence is absent both here and in earlier studies (Goldhammer *et al.*, 1991). QSF facies commonly display an erosive or scoured basal contact, both at the HTS and elsewhere on the Paradox Shelf (Stevenson, 2007, pers. comm., 3 August). However, this study maintains the findings of previous work on the HTS (Goldhammer *et al.*, 1991) in finding that top contacts of QSF are commonly gradational, and occasionally sharp, but with no evidence of sub-aerial exposure. This lack of evidence for direct sub-aerial exposure of QSF beds calls into question the assertion by Grammer *et al.* (2000) that double cycles represent an individual oscillation of relative sea-level. Furthermore, significant ambiguity surrounds the forcing mechanism for double cycles that does not explain why one cycle is occupied entirely by siliciclastic sediment, and one by purely carbonate facies. Were glacio-eustasy to be the mechanism, as implied by Grammer *et al.*, it would be expected that these cycles would at least bear resemblance in their facies successions, rather than be segregated according to content. Furthermore modelling has

shown that there is no evidence for the “5th and 6th order” (Grammer *et al.*, 2000; p. 55) cyclicity characterised by double cycles, either in terms of lithofacies distribution, HFS thickness distribution or statistically.

It is therefore likely that siliciclastic and carbonate sediments were deposited during one oscillation of relative sea-level. The palaeoenvironmental interpretation of QSF facies can also offer relatively precise refinement of the timing of sedimentation subsequent to sea-level lowstands. The interpretation of QSF2 differs here from the initial analysis by Goldhammer *et al.* (1991), who advocate a sub-tidal to predominantly intertidal setting (refer to section 5.3.9.1). This study maintains that QSF2 represents shallow sub-tidal deposition, but interprets its environment of deposition as restricted lagoon. The creation of lagoonal conditions is attributable to the presence of QSF1, which is closely associated in terms of occurrence with QSF2. It is envisaged that away from the direct locus of resedimentation of QSF1, lagoonal conditions were created in the sheltered back-barrier of the prograding bars of QSF1. Finer sediment in suspension and the restricted hyper-saline basin water prevented extensive carbonate sedimentation.

During lowstands widespread aeolian dunes were present directly on or near the exposed Paradox Shelf. There is also significant evidence for aeolian sedimentation in, and around, the Paradox Basin (Driese & Dott, 1984; Loope & Haverland, 1988; Soreghan, 1992; Soreghan *et al.*, 2002; Evans & Reed, 2007). The high-degree of sorting and fine grain size of QSF suggests an aeolian origin beyond reasonable doubt, but the source terrain for the siliciclastic sediment is very poorly constrained. Throughout the Desmoinesian there is evidence for several upland areas on the periphery of the Paradox Basin (Figure 5.2). However, data on the extent and the magnitude of these exposed areas is poor, largely due to a lack of research and proprietary data as a result of petroleum exploration.

It is known that the Uncompahgre Uplift and the Zuni-Defiance uplifts represented topographic highs throughout the late-Pennsylvanian, and are likely sources for the siliciclastic sediment. The Uncompahgre Uplift is also likely to have been of significant relief and extent and represents a major potential source of sediment (Soreghan, 2002). Cross-sections through the Paradox Basin do not show siliciclastic sediment shed from the Uncompahgre as reaching the Paradox Shelf from the other side of the basin (Figure 5.3). It is possible however, that, during lowstands the sediment reached the shelf via a more indirect route, possible from the west if sea-level fall was sufficient to close the seaway there (Wengerd, 1959). The distance sediment was transported and by what mechanism, before final deposition occurred, is hard to gauge. The maturity of the sediment, its composition and lack of coarser coeval siliciclastics suggests a significant transport distance from the nearest upland terrain. In this aspect, the Uncompahgre Uplift, with

documented aeolian sediment shed elsewhere (e.g. Soreghan *et al.*, 2002) is a major potential source. The Zuni-Defiance uplift presents an alternative source for sediment, but it was only a “barely emergent positive area” during the late Pennsylvanian (Soreghan, 1992). Nevertheless, there is evidence from the Hermosa Group that dune systems can be maintained on unlithified, minor topographic features (Atchley & Loope, 1993). There is however a lack of consensus (and data) on the origin of aeolian sediment at this time, and the possibility remains that the siliciclastic sediment had multiple sources at different times (Stevenson, 2007, pers. comm., 29 July).

The mode of sandstone formation strongly resembles that documented for similar carbonate-siliciclastic cycles in northern Utah and Colorado, with one major difference (Driese & Dott, 1984). These sandstones bear many similar characteristics: very-fine grained aeolian sediments prograde over an exposed shelf resulting in cross-bedded units with comparable structures, including *Ophiomorpha nodosa* burrows. Erosive contacts are interpreted to have been caused by a relative sea-level oscillation; exposing, and subsequently resubmerging the platform. This would equate with the double cycle proposed by Grammer *et al.* (2000), albeit on a more reasonable scale when compared with probable amplitudes of intermediate-order oscillations (25m average cycle as opposed to less than 5m). However, the upper contacts are always erosive in this section, and not comparable with the sometimes gradational upper contacts of QSF. The difference, as interpreted here, is that the siliciclastic beds of the HTS do not represent one single oscillation of relative sea-level, but only the initial transgression.

The upper-contact of the siliciclastic beds is evidence of continuous sedimentation between siliciclastic and predominantly relatively deep-water carbonate sedimentation. Double cycles and multiple high-frequency oscillations of relative sea-level do not reconcile well with either the sedimentary structures seen in these facies or models of sea-level behaviour. However, a feasible mechanism for the formation of this sedimentary sequence is suggested by sedimentary evidence. Goldhammer *et al.* (1991) established that QSF represents lowstand deposits reworked during a transgression. If this is the case then the majority of sediment must be physically generated during lowstands. As the platform is submerged the source of this sediment is essentially prevented from generating more sediment. At the point of subsequent transgression there therefore exists a surplus of sediment stored on the shelf, which is then reworked. This implies therefore that there is a finite amount of sediment available to be re-sedimented; or, restated, sediment supply is the major limiting factor on deposition during a transgression. Modelling suggests that there is a significant period of time available during each lowstand of relative sea-level for the generation of aeolian sediment (Table 5.6). Once this sediment is reworked and finally lithified then there is little siliciclastic material to replace it. There

Run set	Average maximum exposure duration (ky)	Average mean exposure duration (ky)	Max. % time represented	Mean % time represented
Int.-order amp.	40.26	33.64	88.22	45.96
Subsidence	48.29	28.05	95.49	52.41
Euphotic production rate	47.99	33.49	93.03	43.82
Sub-aerial platform denudation rate	42.45	42.57	90.52	44.31

Table 5.6: Exposure duration data for simulations investigation major accommodation and sedimentation controls. Maximum and mean percentage of time represented is the time when sedimentation is occurring.

may be residual aeolian activity on the submerging upland source, which could contribute to some of the siliciclastic-rich carbonate facies, but not sufficient to deposit thick beds of siltstone and sandstone.

It is therefore probable that the very early TST, when the flat-topped platform is initially submerged, represents a period of very rapid sedimentation. There is also evidence of alpine glaciation in the Uncompahgre Uplift; recorded by proglacial strata and glacially-carved topography (Soreghan, 2002; Soreghan *et al.*, 2007b). If this is correct, then autochthonous ice-melting may have had an impact on transport rates, increasing sedimentation due to global climate change. This may have significantly increased sediment movement (and increased the discharge – and therefore transport - distance of rivers) during the early TST. There is no data available on sediment-shedding as a result of platform submergence. However evidence from modern analogues suggest it could be very rapid. A modern alpine glacier has been recorded to output 95% of its proglacial sediment via fluvial mechanisms during meltwater flooding over 3 days each year (Warburton, 1990). While not an ideal analogue, appropriately upscaled it gives an impression of the potential output from alpine glaciers during melt. There is also evidence from the ARM that aeolian sediment flux was at its maximum during glacial to incipient interglacial (lowstand to very early transgression), and rapidly waned during interglacials (Soreghan *et al.*, 2007a).

QSF2 is envisaged to be coeval with QSF1, albeit in a slightly different depositional environment. As documented in section 5.3.9.1, it is envisaged that QSF2 was deposited away from the major locus of sedimentation. Most models for the deposition of the siliciclastic material of the HTS are vague on the subject, usually categorising it as “middle to upper shoreface” (Grammer *et al.*, 2000; p35) or similar. However, the large-scale trough cross-bedding implies that deposition occurred specifically as the result of down-flow migration of lunate dunes, probably from a point-source. There would exist, therefore, loci of sedimentation where reworked sediment was discharged from a probable fluvial source onto the shelf. If the locus were to migrate with time then it is probable that this resulted in a beach-barrier system, consequently creating lagoon conditions behind the barrier (Scholle & Spearing, 1982). Where sedimentation was not occurring, in the lagoon, there would be relative restricted conditions given the salinity of the overall basin at this point. It is therefore interpreted that QSF represent resedimented lowstand aeolian sediment, but in more restricted, sheltered environment (Figure 5.46). The sedimentary structures and faunal assemblage of QSF2 support this interpretation. This model also allows for the gradational upper contact of QSF1, usually into QSF2, and the usually sharp-based contact of QSF (as a consequence of dune migration).

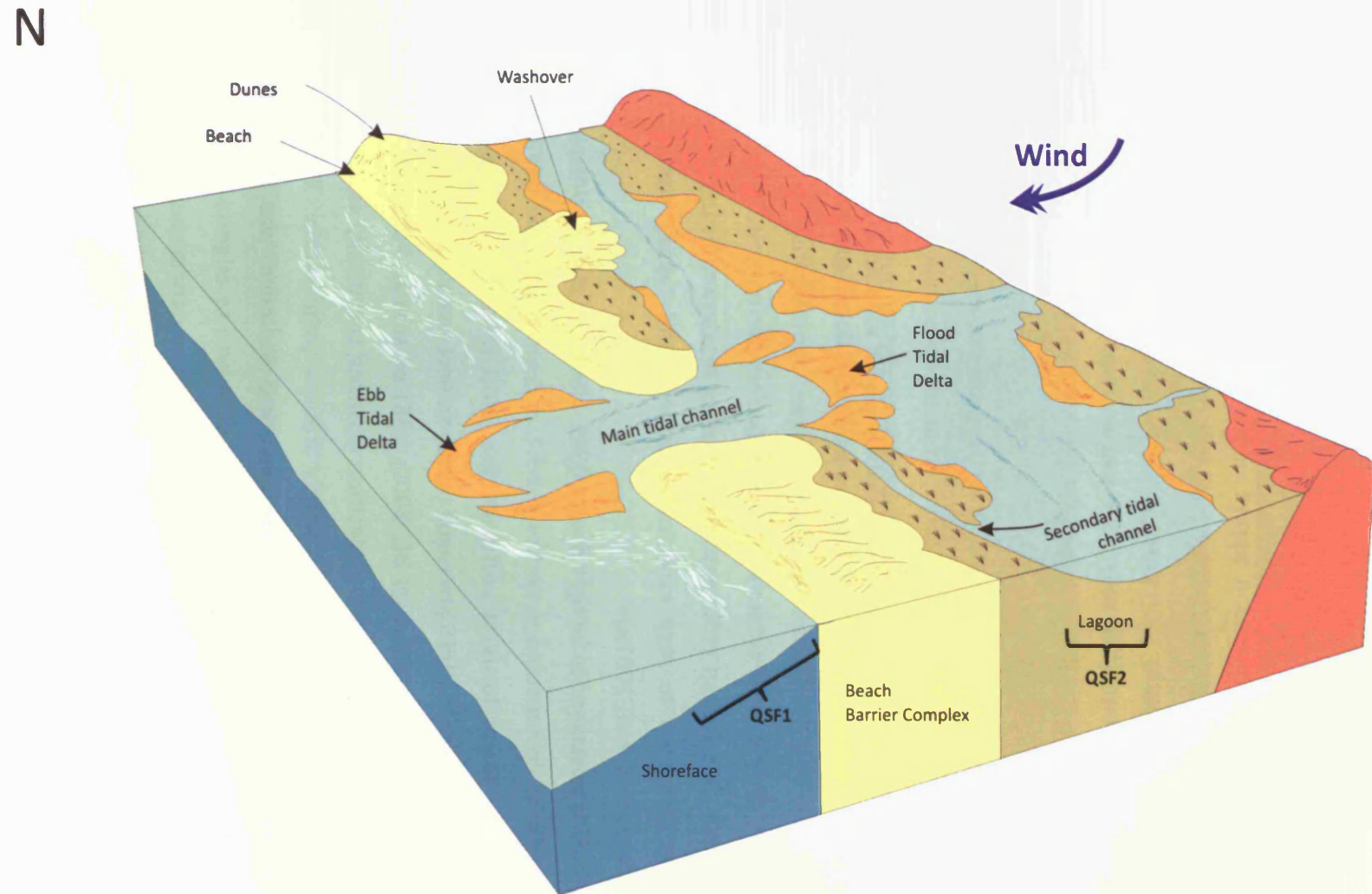


Figure 5.46: Schematic facies model for the Honaker Trail section during very early TST. Positions for QSF facies are shown. Modified from Walker & James, 1992.

Despite the initially readily available sediment, transport rates to the basin and sediment deposition were not sufficient to keep up with sea-level rise. Evidence for this is provided by the gradational contact of QSF into usually deeper-water carbonate facies (i.e. black laminated mudstone, sponge facies or intermediate-facies). By the time the siliciclastic source was depleted (either by transport or submergence and redeposition) water-depth was sufficient to prevent colonisation by biota preferring shallower-water conditions. Instead, deeper water fauna established themselves as the siliclastic sediment was switched off. Residual siliciclastic sediment remaining in the system or being output at a reduced rate may also restrict the diversity of carbonate-producing organisms. This sediment is preserved as admixed siliclastic grains in some facies. During this phase of sedimentation, modelling suggests comparatively little sediment is deposited, compared to the large amounts deposited during a short period during shallower periods (Figure 5.47). Modelling also suggests that sedimentation usually terminates during the early to middle FSST.

It therefore seems probable that although sedimentation is relatively evenly distributed throughout a relative sea-level oscillation. The short periods where water depth is shallowest; at the beginning and end (very early TST and early-mid FSST) are the period where sedimentation occurs at its greatest rate.

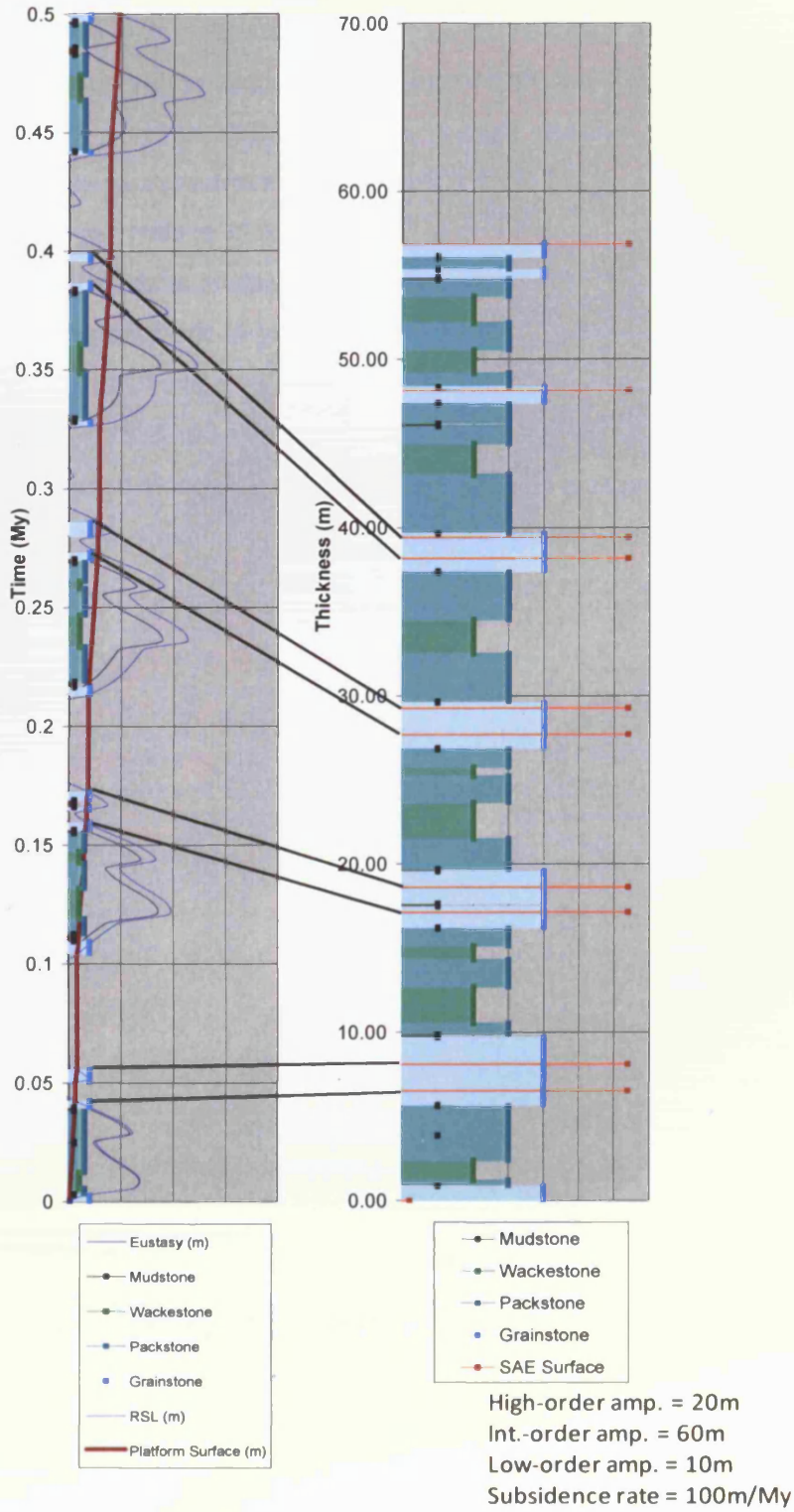


Figure 5.47: Correlation of exposure surfaces between an integrated chronostratigraphic diagram and a simulated sedimentary column. Higher sedimentation rates at shallow depths result in a significant proportion of the sediment being deposited in a small fraction of total time.

5.6 CONCLUSIONS

- The reinterpretation of cycle boundaries made by previous workers calls into question the existence of a hierarchy in the HTS. Vertical facies associations reflecting deepening are not fundamentally indicative of an excursion of relative sea-level and, moreover, may be caused by factors other than an increase of base-level. Furthermore, the identification and interpretation of these deepening events is fundamentally qualitative. Combined, these factors introduce significant uncertainty into the interpretation of apparent deepening events as HfS boundaries. A reinterpretation of the HTS, only identifying cycle boundaries where there is unambiguous evidence of abnormal sub-aerial exposure of sub-tidal strata offers a more objective way of characterising HfSs.
- The reinterpretation of cycle boundaries in the Honaker Trail Section (HTS) based upon unambiguous evidence of sub-aerial exposure leads to the definition of 16 High-frequency Sequences (HfSs).
- Based on this, and modelling studies (see below), it is unlikely that a sedimentary hierarchy exists in the HTS.
- Embedded Markov chain analysis of lithofacies suggests that facies show a first-order Markovian property. However, simulations investigating lithofacies proportions in the HTS show a large overall cumulative deviation of lithofacies in almost all runs. Given this, and the fact that no combination of production rates produced four lithofacies of similar thickness to the HTS, it seems unlikely that the controls of lithofacies (and facies) are forced only by controls of eustatic amplitude. Other possibilities are rates of subsidence, production and sub-aerial platform denudation. This reiterates the probability that facies units in the HTS and elsewhere have a significant non-depth-dependent control.
- Lithofacies modelling suggests that best fits with the Honaker Trail section in terms of lithofacies proportions if only one high-frequency large-amplitude eustatic component has significant amplitude. Lithofacies modelling further suggests that it is the interaction of the low-order eustatic component and a single dominant glacio-eustatic component that produces the best match with the observed HTS. This implies that a single dominant eustatic component (i.e. intermediate-order) generates the closest match to the HTS.
- High-frequency sequence matching supports this. Modelling HfS thickness in response to varying eustatic amplitude indicates that the overall effect of increasing eustatic amplitude is to increase deviation from observed thicknesses of

the HTS. At any combination of amplitudes, the interaction of two high-frequency large-amplitude eustatic components serves to increase deviation of HfS thickness.

- Simulations using two or more high-frequency large-amplitude eustatic components cannot create a comparable section to the HTS. However, simulations which evaluate a low-order oscillation and single dominant high-frequency eustatic component can. Therefore, modelling suggests that two high-frequency glacio-eustatic components can only generate a good approximation of the HTS in terms of thickness if one component (i.e. high-order) is of negligible amplitude (so as not to significantly affect accommodation).
- An important implication of this is that a sedimentary hierarchy is unlikely to be manifest in the HTS. Modelling conducted in section 4.4.2 indicates that to generate a sedimentary hierarchy high-order oscillations need to be of similar amplitude to, or greater than, that of intermediate-order oscillations. This would seem to preclude of realistic HTS thicknesses as a hierarchy.
- Furthermore, a sedimentary hierarchy is shown to be unlikely by statistical analysis, which suggests that runs of HfS thickness are not of sufficient length to reject randomness. This is borne out by observations of simulations displaying an ordered succession of HfS thicknesses, but which do not show a good correlation for consecutive HfS thicknesses in the HTS.
- Simulations of HTS HfSs did not create realistic representations of HTS lithofacies, HfS stacking patterns and cumulative sediment thicknesses. This is likely to have a number of causes, not least of which is a significant complexity in the sedimentary environment that is not incorporated in the one-dimensional model. This should prompt a re-evaluation of the controlling parameters on the stacking of carbonate sequences and significant modification of simplistic sequence stratigraphic conceptual models (e.g. Spence & Tucker, 2007).
- Simulations addressing interactions of the three major eustatic components (low-, intermediate- and high-order amplitude) generate fewer sections that resemble the HTS than simulations that emphasise the intermediate-order eustatic parameter and subsidence alone. These simulations show that the most realistic stacking patterns, and the thicknesses which most resemble the HTS, are developed at relatively high rates of subsidence (greater than 150m/My). These subsidence rates are in line with rates cited for the Paradox Basin (Goldhammer *et al.*, 1991). Given that eustatic oscillations alone create relative poor matches for the HTS, and subsidence rate provides the basis for better model fits, it is probable that the complex tectonic setting of the HTS and encompassing Paradox Basin

plays a prominent role in dictating the nature of cyclicity in the sedimentary succession.

- Rapid subsidence during the Desmoinesian as a result of extensional faulting compares well with modelled scenarios most likely to represent realistic stacking patterns and sedimentary style. Inverted basement faults, known to provide significant local topography as a result of differential sedimentation, and which force different subsidence rates, are likely to have significantly affected HTS stacking patterns. Furthermore, there is the possibility of subsidence-driven accommodation created as a result of near-instantaneous fault block movement. These factors combine to represent significant probability that subsidence plays a significant role in defining stacking patterns on the Paradox Shelf.
- It is probable that the sedimentary cyclicity apparent in the HTS is the result of glacio-eustatic oscillations. However, it also seems very likely, given the tectonic setting of the HTS, that the glacio-eustatic signal is significantly modulated by long- and short-term allocyclic variations in subsidence, complicating the glacio-eustatic signal and representing the greatest source of variation between the observed HTS and numerical simulations.
- “Double cycles” as proposed by Grammer *et al.* (2000) are not supported by sedimentary evidence. A more appropriate interpretation for HTS HfSs necessitates only one oscillation of relative sea-level to deposit both siliciclastic and carbonate sediment.
- The interpretation of QSF as transgressively reworked lowstand deposits suggests that sediment supply for this facies was limited to that eroded during significant-duration sub-aerial exposure at lowstands of relative sea-level. This was resedimented very quickly during the early transgressive systems-tract. Carbonate sedimentation was limited during siliciclastic influx and gradually resumed as the stored reworked aeolian sediment became depleted.
- QSF2 represents deposition in a relatively shallow-water, sheltered environment; probably a back-barrier lagoon away from the main locus of siliciclastic sedimentation. QSF2 is contemporaneous with QSF1 facies.
- Modelling suggests that significant quantities of sediment are likely to have been deposited during the shallowest-water phases of a relative sea-level oscillation; the very-early TST and the early-mid FSST.

Chapter 6: TECTONICALLY-MODULATED GLACIO-EUSTATIC FORCING OF CARBONATE SUCCESSIONS: EXAMPLES FROM THE PENNSYLVANIAN OF NEW MEXICO (USA) AND ARKHANGEL'SK OBLAST (RUSSIA)

6.1 INTRODUCTION

To evaluate the relative importance of eustatic and tectonic controls on the stacking patterns of ice-house platform carbonates two contrasting sections of Pennsylvanian age were studied: the Gobbler Formation of southern New Mexico, and the Moscovian of Arkhangel'sk Oblast in northern Russia. These represent sections which are broadly contemporaneous, but are from disparate tectonic settings.

The Pennsylvanian Gobbler Formation is apparently cyclic, yet has received relatively little attention, particularly with respect to controls on stacking patterns of the ostensibly highly cyclic platform (e.g. Algeo et al., 1991; Algeo et al., 1992; Algeo, 1996; Lapeter & Holterhoff, 2007). This is surprising given the quality of outcrop in the Sacramento Mountains and the zeal with which similar cyclic Mid-Continent successions are continually studied and interpreted (e.g. Mazzullo, 1999).

Work by Algeo and co-workers represents the most explicit attempt to quantify stacking patterns within the Gobbler Formation (Algeo *et al.*, 1991). This study attributes cyclicity in the Sacramento Mountains to a purely glacio-eustatic cause albeit with interpreted cycle periods which do not conform to commonly accepted 'Milankovitch' periodicities. Furthermore, Algeo *et al.* (1992) document "two orders of cyclicity" in the Gobbler Formation; thereby invoking a sedimentary hierarchy of stacked shoaling-upwards cycles and groups of cycle sets. This hierarchy is based on 3-20m thick "shoaling cycles" and 20-80m thick "cycle sets" based on "overall upward coarsening and reduction in shale content". If these are truly eustatic oscillations, and the major control on sedimentary stacking patterns, their effect would be present in other sedimentary sequences.

The Moscovian succession of Arkhangel'sk Oblast in northern Russia represents such a succession, and was deposited as a carbonate shelf in an intra-cratonic basin. However, there has been comparatively little modern research conducted on this succession. The presentation of new sections here allows comparison of two contemporaneous platforms in terms of their sedimentary cycle stacking patterns.

The goals of this study are (1) to identify exposure surfaces in both study areas, with an aim to objectively define cycle thicknesses and stacking patterns; (2) to discuss the relative importance of eustatic versus tectonic controls on stacking patterns by

comparing the studied sections; and (3) to assess the degree to which the two studied sections can be said to be hierarchical.

6.2 METHOD

6.2.1 Facies analysis

The studied sections were chosen both because they are contemporaneous with respect to each other, and because they are geographically-distant from one another. As such, if sea-level oscillations are truly eustatic then the two sections may be expected to display a similar sedimentary response to variations in base level. Fieldwork was conducted in both study areas with the aim of identifying cycle boundaries and stacking patterns. In New Mexico a continuous section of the Bug Scuffle Limestone Member (BSLM) of the Gobbler Formation was logged at Fresnal Canyon (FC; Figure 6.1). At this locality, approximately 120m of Gobbler Formation is affected significantly by deformation associated with the Fresnal Fault (and is mostly covered by drift). The remaining ~120m, logged here (Figure 6.2; displayed in full in Appendix 3), is consistent with logged thicknesses reported by previous workers (Pray, 1961). Microfacies analysis was based on field logs combined with 30 representative thin sections, and over 200 acetate peels. Facies are examined here in order to appropriately identify exposure surfaces and place them in context within the framework of stacked cycles. Comprehensive facies analysis also ensures that no exposure surfaces are missed during logging.

The Arkhangel'sk Oblast section represents the best exposure of Pennsylvanian strata in the region, but is only 34m thick. This section does however contain a comparable number of high-frequency sequences (HfSs) to that of the BSLM (8 HfSs, compared to 11 in New Mexico). The succession was logged in two sections, both in the Severnaya Dvina – Pinega (SDP) area; the Orletsy Quarry and riverside outcrops along the northern bank of the River Pinega between the villages of Rozhevo and Nizhnyaya Palenga (Figure 6.3). Correlation between the two sections can be reliably anchored by the presence of a top-Myachkovskian unconformity and a marker mudstone bed above it (Figure 6.4). Microfacies were studied using 115 thin sections with areas of at least 10cm². As with New Mexico, facies are described here (section 6.4.2.1) in order to provide context to the stacking patterns and sedimentary style of the succession, and are examined in more detail elsewhere (Kabanov *et al.*, in prep.).

The sequences ORL1 through ORL3 (Figure 6.4), have been linked, correspondingly, to the Korobcheevo, Domodedovo, and Peski Fms. of the type Moscovian section by Kabanov & Baranova (2007). Contrastingly, the River Pinega sections are reported here for the first time. Below the base of the Orletsy section, extensive non-

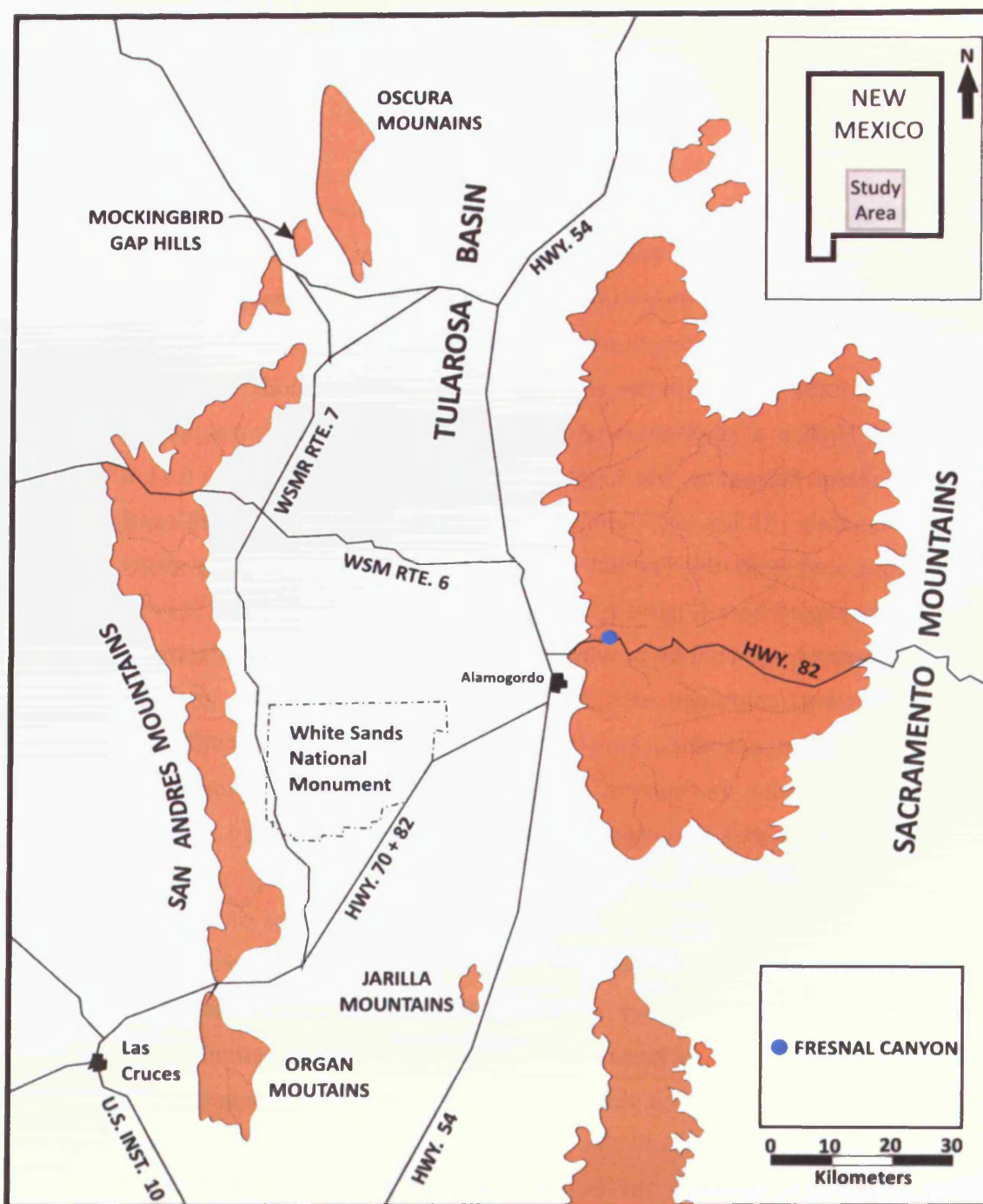


Figure 6.1: Location map of the Gobble Formation measured section. The Fresnal Canyon section is located along the fault-bounded eastern flank of the Orogrande basin, which also forms the margin of the modern Tularosa Basin.



SECTION: Fresno Canyon
LOCATION: New Mexico, USA
DATA TYPE: Stratigraphic log
DATA DEPTHS: 0-124m
LOGGED BY: David Pollitt
DATE: November, 2005

Lithofacies Key

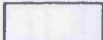
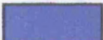
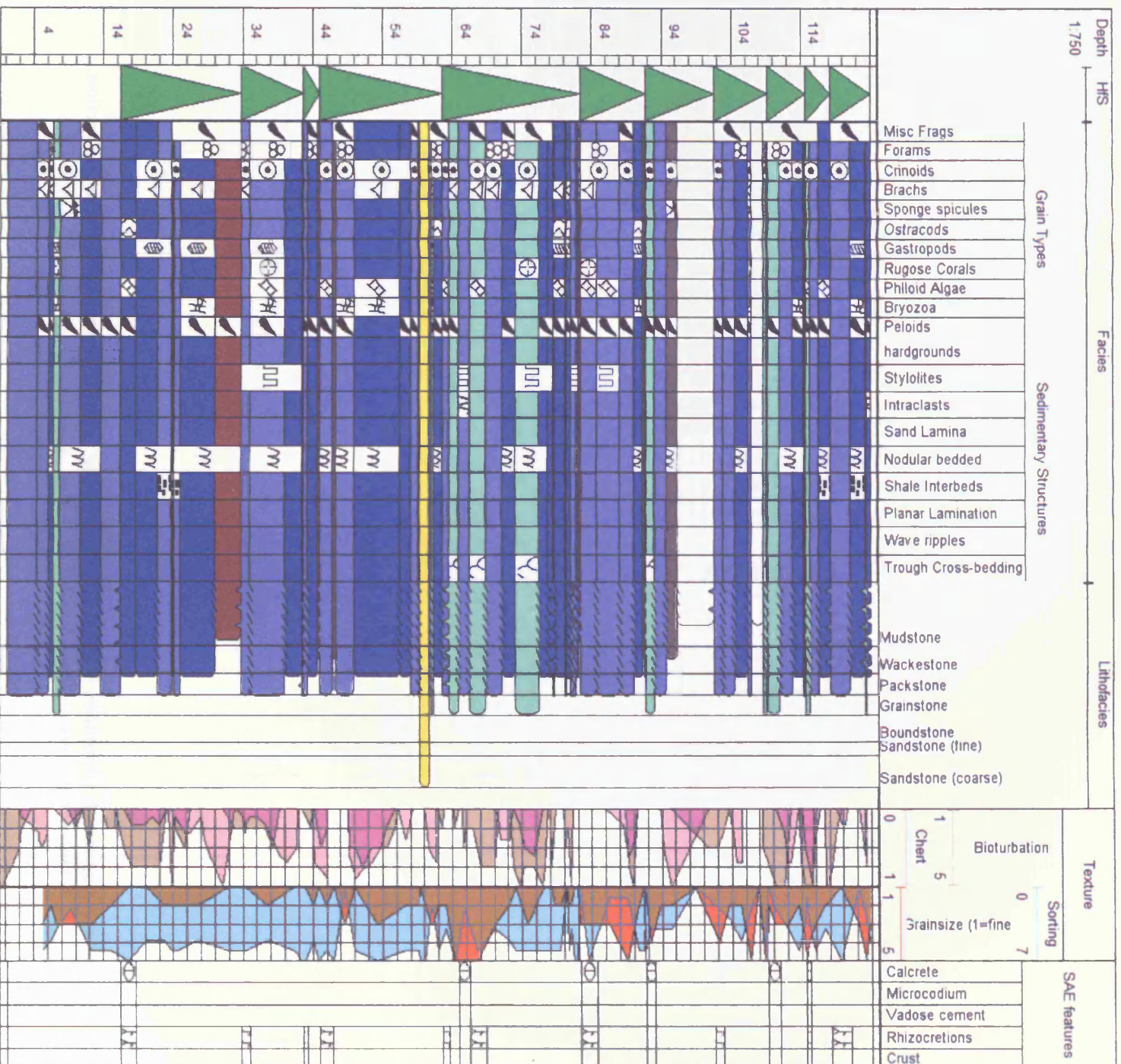
	Missing
	Mudstone
	Silty carbonate shale (50% silt grains)
	Wackstone
	Packstone
	Grainstone
	Sandstone (very fine to granule size)

Figure 6.2: Lithofacies key and stratigraphic log (overleaf) of the Fresno Canyon section. A larger scale version of the log can be seen in Appendix 3.



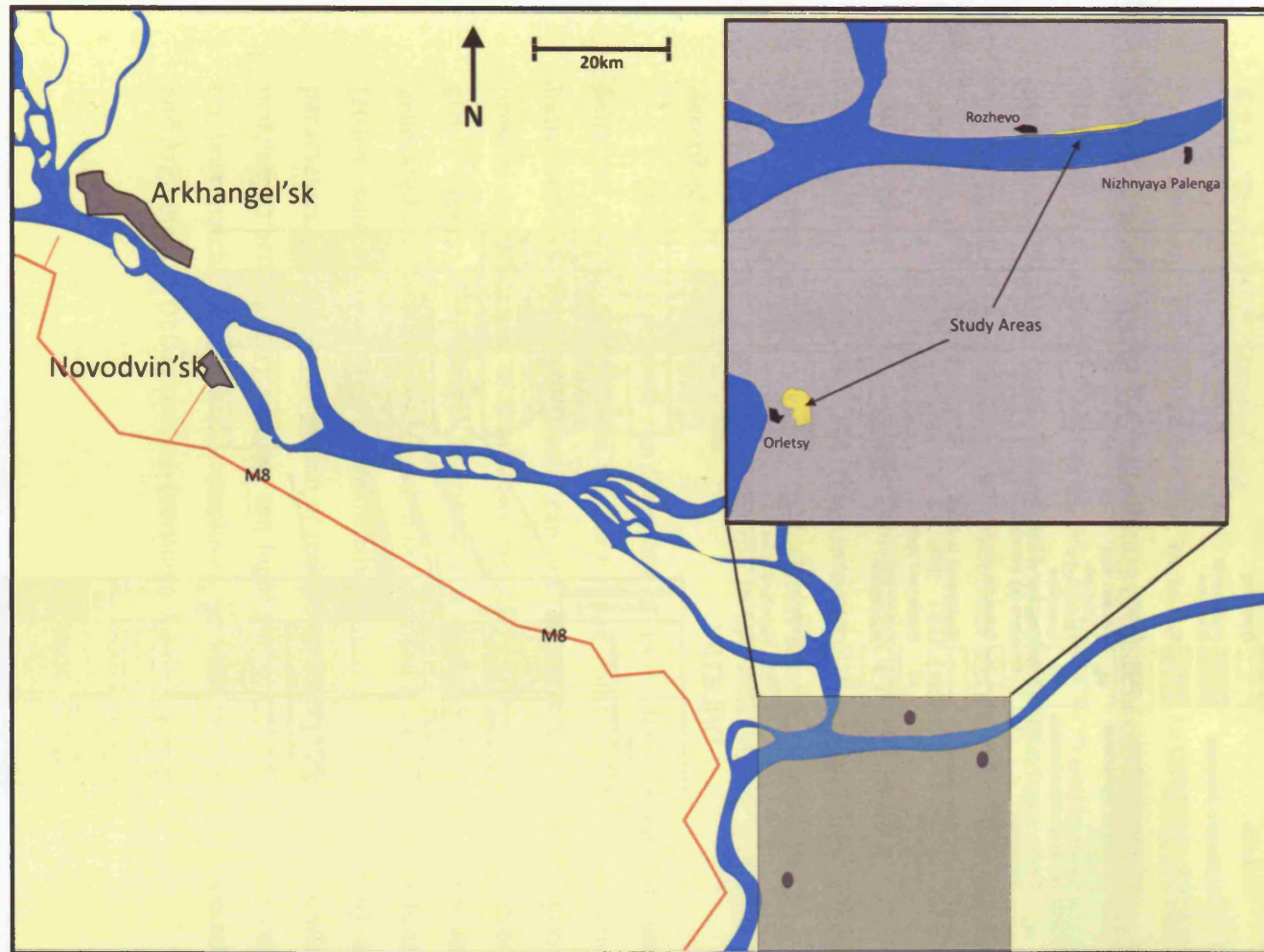


Figure 6.3: Location map of the measured sections (yellow portions of inset map) from Arkhangel'sk Oblast, Russia. Exposure occurs in Orletsy Quarry and as river outcrops between the villages of Rozhevo and Nizhnyaya Palenga.

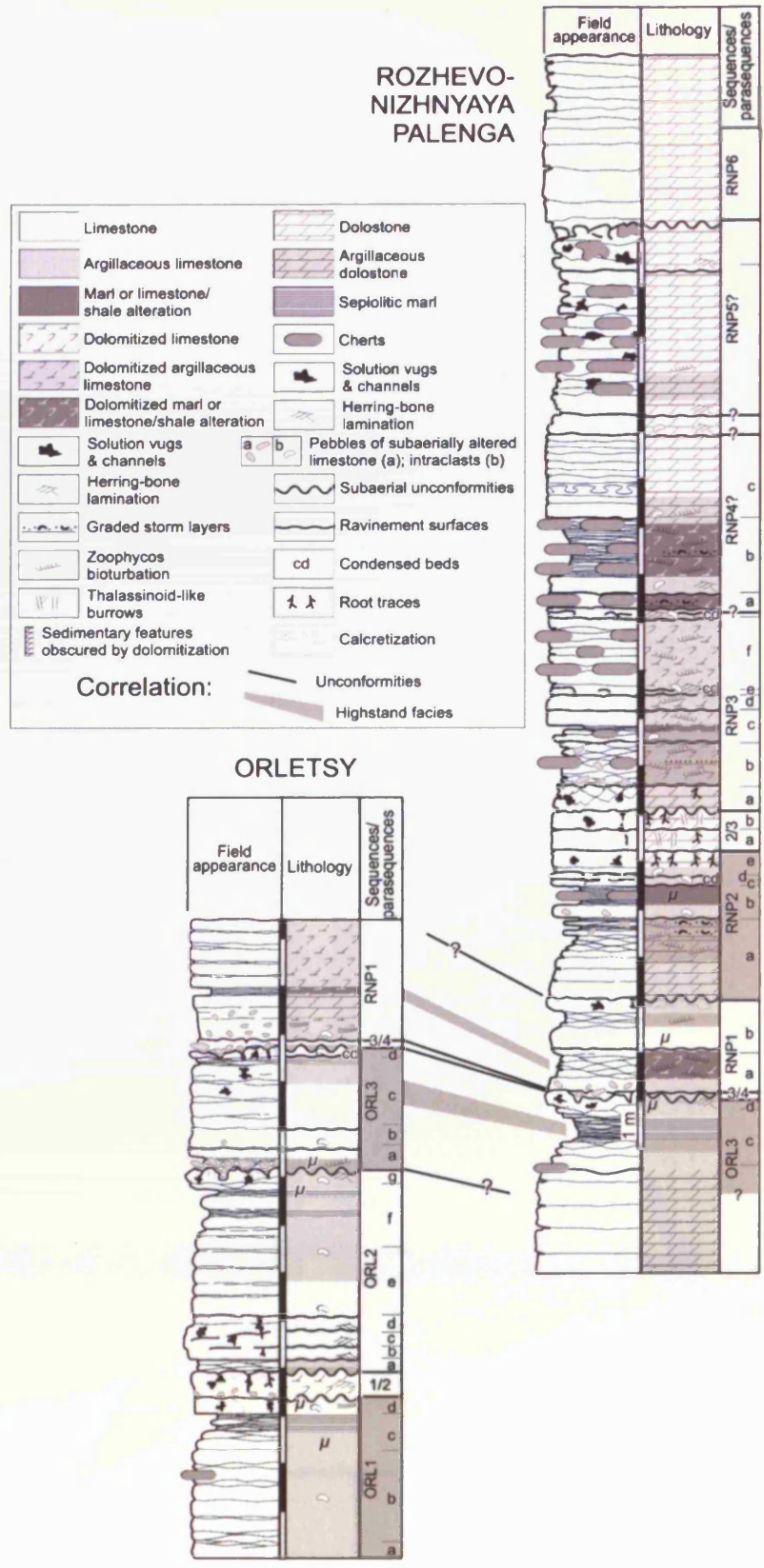


Figure 6.4: Stratigraphic log from the SDP sections. From Kabanov *et al.* (in prep.).

selective dolomitization conceals the lower part of the ORL1 HfS as well as Kashirian-Podolskian sequences below. This constrains the base of the section, whilst extensive and complete replacing dolomitization (destroying all primary texture) also bounds the studied interval above HfS RNP5.

6.2.2 Stratigraphic simulations

Numerical forward modelling was employed in this study with two aims; firstly, to establish the controls on the sedimentary cyclicity of contemporaneous but geographically disparate sedimentary successions, and secondly to evaluate the degree to which these sedimentary sections show evidence of hierarchical ordering.

To accomplish these goals simulations were conducted using the one-dimensional stratigraphic numerical forward model; TED (refer to section 3.2). Simulations were conducted according to published parameters believed to be the major controls on HfS stacking (Table 6.1), and the results of simulations compared by HfS matching. This method compares the deviation in thickness between a given HfS in a simulated section and the correspondingly numbered HfS in the sedimentary section. This process is also described in section 5.4.2.

Simulated sections can therefore be evaluated in terms of cumulative deviation from the sedimentary section they are being compared to, or in terms of deviation of individual HfS thickness. Results can subsequently be plotted in parameter-space, and provide an indication of conditions required to replicate the sedimentary section to a given degree of accuracy. Specifically a parameter-space response surface can be generated which allows visualisation of deviation from observed sedimentary thicknesses (either singular per HfS or cumulative for a complete section) against all varied parameters. Further investigation of individual HfSs within runs showing close-thickness matches to sedimentary sections can highlight ranges of parameter values that generate the best match. This method is employed for both the Gobbler Formation (section 6.3.3) and Arkhangel'sk Oblast sections (section 6.4.3).

Runs investigating:	Variables	Min. value	Max. value	Increment	Source
Eustatic amplitude	High-order amplitude	0m	50m	2.5m	Paterson <i>et al.</i> , 2006
	Intermediate-order amplitude	0m	90m	5m	Heckel, 1986; Wright & Vanstone, 2001
Subsidence	Subsidence rate	20m/My	200m/My	10m/my	Allen & Allen, 2005
	Intermediate-order amplitude	10m	100m	5m	See above
Carbonate accumulation	Euphotic accumulation rate	100m/My	1000m/My	100m/My	Smith & Kinsey, 1976; Bosence & Waltham, 1990
	Intermediate-order amplitude	10m	100m	5m	See above
Sub-aerial exposure	Platform denudation rate	0m/My	100m/My	5m/My	Goldhammer <i>et al.</i> , 1991; Plan, 2005
	Intermediate-order amplitude	10m	100m	5m	See above

Table 6.1: List of the variables used in numerical simulations. Variables address a range of values according to an increment. For each run plan, the variables are modified one per run according to the increment, until each combination has been addressed. Each run-plan was investigated once for both the FC and SDP sections. 15000 runs were conducted in total.

6.3 THE ATOKAN/DERRYAN-DESMOINESIAN (MOSCOVIAN) GOBLER FORMATION, NEW MEXICO, USA

6.3.1 Geological setting

6.3.1.1 Tectonic setting

During the Early Carboniferous, south-central New Mexico was a southward-tilted region, bordered on the north by the Transcontinental Arch and interspersed with intra-cratonic basins (Figure 6.5). This included the embryonic Orogrande Basin, which borders the current Sacramento Mountains to the east. The Orogrande Basin is a north-trending extensional basin resulting from craton-ward overstep of the Ouachita-Marathon orogenic front; a broad dextral strike-slip zone transecting the south-western margin of North America (Kottlowski, 1965; Greenwood *et al.*, 1977; Dickinson & Lawton, 2003). By the mid-Mississippian the Orogrande Basin was more extensive and included the Pedernal Uplift on its eastern margin (Figure 6.5).

The Orogrande Basin was bounded asymmetrically by a high-relief, faulted eastern shelf and a low-relief flexural western ramp (Algeo *et al.*, 1991). Basin asymmetry is reflected in greater lateral continuity of cycles and facies belts on the broad, stable western shelf relative to the narrow eastern shelf (possibly as narrow as 6km; Wilson, 1972), which exhibits variable cycle thickness, syn-sedimentary slumping and a fault-bounded clastic-filled intra-shelf trough (Algeo *et al.*, 1991).

The Orogrande Basin exhibited two phases of subsidence with the Gobbler Formation being deposited during the initial phase of subsidence. The first was an Early-Middle Palaeozoic phase characterised by passive-margin subsidence along the entire south-western margin of the North American craton. The second phase spanned the Middle Pennsylvanian-Middle Permian interval, during which the geothermal gradient and subsidence history suggests the development of an intra-cratonic tectonic style characterised by relatively low subsidence (Kottlowski, 1963; Algeo *et al.*, 1992; Figure 6.6).

Total subsidence during the first phase was comparatively small compared with the subsequent intra-cratonic phase (0.5km compared to 2km; Algeo *et al.*, 1992). Algeo *et al.* (1992) note that although basin subsidence appears to have occurred at a uniform rate of 50m/My over 50My, it is likely that over shorter timescales subsidence rates varied to a greater degree. These workers also note that uncertain dating of Pennsylvanian stages

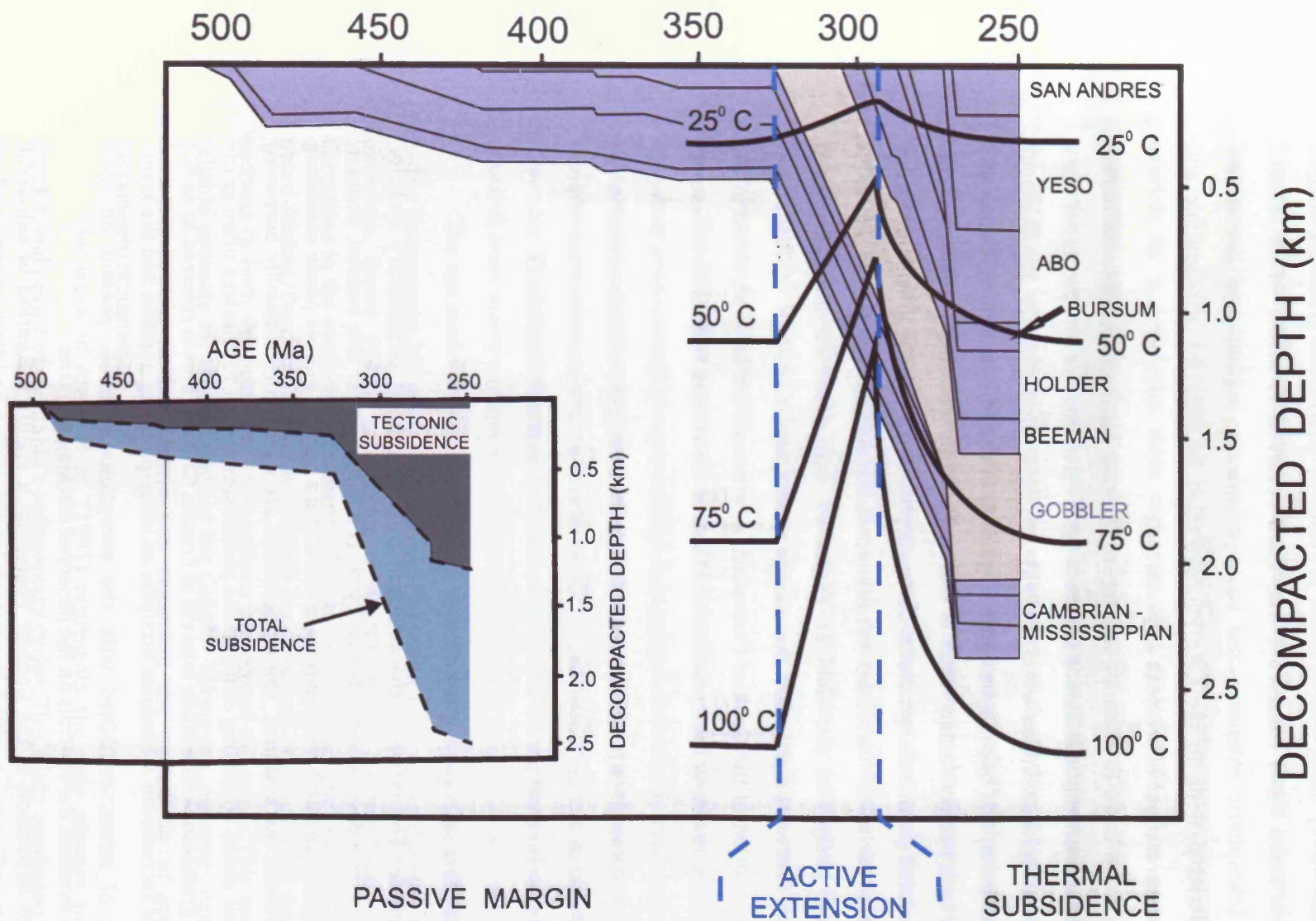


Figure 6.6: Burial history plot for the central Orogrande Basin. Stratigraphic thicknesses were sequentially backstripped and decompactified. Tectonic subsidence was calculated based on methods described in Allen & Allen (1990). Redrawn from Algeo *et al.* (1992).

combine to make these rates tentative estimates. Evidence of significant basin deepening and sediment starvation of the basin centre from the Virgilian Panther Seep Formation (Kottowski *et al.*, 1956), along with evidence provided by geothermal gradients, suggest that episodes of more rapid subsidence may have occurred. A model which invokes simultaneous lithospheric extension and basin subsidence beginning in the Middle Pennsylvanian and peaking in the Late Pennsylvanian satisfies the stratigraphic and geochemical interpretations of previous workers.

Furthermore, there is evidence to suggest elevated geothermal gradients during burial stabilisation of the Gobbler Formation as representative of increased Late Pennsylvanian subsidence. Algeo *et al.* (1992) invoke a model where simultaneous lithospheric extension and basin subsidence beginning in the Middle Pennsylvanian and peaking in the Late Pennsylvanian result in elevated subsidence rates. Evidence for this comes from elevated geothermal gradients during deposition of Gobbler Formation strata, which suggest a period of increased rift-related subsidence (Algeo *et al.*, 1992). It therefore seems likely that the Gobbler Formation was deposited during elevated subsidence rates that were higher than the average of 50m/My.

After deposition of the Gobbler Formation, a carbonate platform persisted in the Late Pennsylvanian, resulting in deposition of 275 m of the Holder Formation limestone. Subsequently, the Sacramento Mountains escarpment was subjected to a complex depositional and tectonic history that included Early Permian deformation, deposition of the overlying Permian section (about 762 m), deposition of an unknown thickness of post-Paleozoic strata, and several phases of post-Paleozoic deformation (Pray, 1961).

6.3.1.2 The carbonate succession of the Gobbler Formation

The Gobbler Formation is characterised by a prominent sedimentary cyclicity. Previous studies have described the typical cycle as having a lower thin bedded, nodular, argillaceous wackestone unit which passes upward into a normal-marine phase consisting of dark fossiliferous wackestones. The wackestones are overlain by a heavily burrowed wackestone unit phase consisting of bioclastic packstones, which themselves often grade into bioclastic grainstones. The study interval in Fresnal Canyon (herein referred to as FC) in the northern Sacramento Mountains occupies an inner-platform position and the layer-cake stacking of strata, combined with the exceptional outcrop, present an ideal opportunity to evaluate the controls on the observed stacking patterns.

Prior to deposition of the Gobbler Formation a significant period of sub-aerial exposure resulted in extensive karsting and erosion of Mississippian strata (Scholle & Goldstein, 1991). Sub-marine sedimentation resumed during the Pennsylvanian, with best estimates indicating a Morrowan/Derryan age for the onset of Gobbler Formation

deposition in the Sacramento Mountains (Algeo *et al.*, 1991). Sedimentation of Gobbler beds continued until the end of the Desmoinesian when beds of the Beeman Formation were deposited (Figure 6.7). In the northern Sacramento Mountains, the Beeman Formation is distinguished from underlying units by red marls interbedded with grey limestones (Pray, 1961).

The Gobbler Formation is divisible into a 50-125m thick basal siliciclastic unit overlain by a 175-325m thick carbonate unit (Pray, 1961). The upper, carbonate-dominated section is designated the Bug Scuffle Limestone Member (BSLM), and comprises the study interval here. The associated shales, siltstones and sandstones within the BSLM are interpreted to mark the emergence of the Pedernal Uplift (a local source-area for siliciclastics) which rearranged the north-south shelf-to-basin transition of the Mississippian to an east-west shelf-to-basin transition in the Pennsylvanian (Scholle & Goldstein, 1991). Due to its proximity and extent the Pedernal Uplift remained the dominant terrigenous source for the south-central New Mexico area throughout the Pennsylvanian (Kottlowski, 1965; Benne, 1975). The study interval in FC represents an inner platform location which was probably less than ten kilometres from the coeval platform margin (Figure 6.5).

The BSLM has previously been interpreted as containing between 25 and 11 high-frequency sequences (Algeo *et al.*, 1991 & Lapeter & Holterhoff, 2007, respectively). This study, which identifies high-frequency sequences (HfS) only where there is evidence of sub-aerial exposure, identifies 13 HfS in the FC section (Figure 6.2; displayed in full in Appendix 3). Individual shoaling cycles are 3-17m in thickness and generally grade upwards from shaley and spiculitic deep-water marls to clean shallow-water limestones.

The age model for Gobbler Formation sedimentary cyclicity is poorly constrained. In the Sacramento Mountains age estimates for the base of the Gobbler Formation are uncertain. Benne (1975) interpreted a Morrowan age for the base of the Gobbler Formation in the southern Sacramento Mountains. More recently however, Wilson (1989) noted Atokan/Derryan fusulinids (notably *Beedeina* and *Profusulinella*) near the base of sections in both the northern and southern sections of the range. This seems the more reliable estimate for the base-age of the Gobbler Formation, however, constraining this does not convey further information regarding the periodicity of cyclicity in the Sacramento Mountains.

The work of Algeo *et al.* (1991) represents the only attempt to quantify the depositional period of the BSLM's sedimentary cycles. This study concluded that cycles on the Sacramento shelf had a depositional duration of 140ky \pm 30ky. This study, however, was contemporaneous with increasing awareness of 'missed beats' as representing a significant proportion of cycle period (e.g. Goldhammer *et al.*, 1991), and so does not take

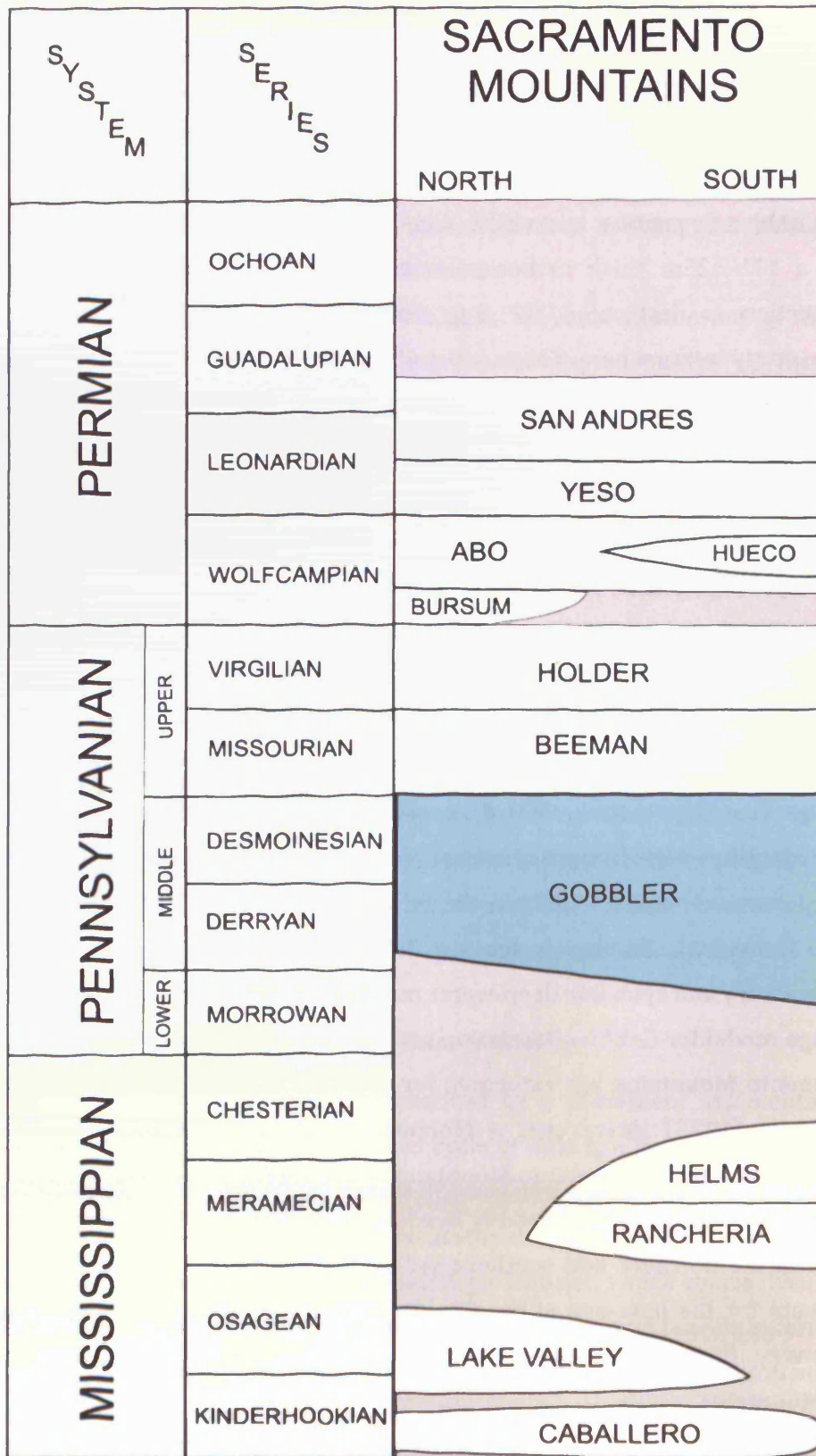


Figure 6.7: Permo-Carboniferous stratigraphy of the Sacramento Mountains of New Mexico (after Kottlowski *et al.*, 1956; Pray, 1961; Kottlowski, 1963).

this 'missing' time into account. The figure of 140ky is also based on two factors which each comprise significant sources of error; the duration of the Desmoinesian Stage (4My \pm 1My) and long-term accumulation rates which may be inaccurate, as some workers suggested, a significant amount of sediment is re-mobilised by dissolution during early diagenesis (cf. Cherns & Wright, 2000). Accurate constraints on the precise age and periodicity of the cycles evident in the Sacramento Mountains are therefore not able to be derived from the sedimentary record at present.

6.3.2 Depositional facies

6.3.2.1 Lithofacies

Shallow marine units of the BSLM consist mainly of bioclastic wackestones and packstones with an open-marine fossil assemblage. Principle grains include echinoderms, brachiopods, bryozoans, fusulinids, endothyrids, rugose and tabulate corals, phylloid algae, *Komia* and *Chaetetes*. Many of the muddy fossiliferous units are thick-bedded to massive, owing to pervasive bioturbation. Terrigenous detritus is either absent or present in very minor quantities, predominantly as clay, and is concentrated in the lower sections of cycles. The shoaling-upwards nature of the sedimentary cycles present in the Sacramento Mountains allows cycles to be broadly divided into four lithofacies, not all of which may be present in a given cycle (Figure 6.8). This may be interpreted as an indicator that the cyclicity evident in some successions is more apparent than a physical reality.

The bases of cyclothems commonly show a well developed lag, comprising reworked lithoclasts and detrital grains derived from the underlying unit (Figure 6.8; a). Above this, argillaceous mudstones and wackestones dominate basal sections of cyclothems, and have been interpreted by previous workers to represent the deepest environment during deposition (Algeo *et al.*, 1991). Abundant burrow-mottling along with shale inter-layers gives this facies a characteristically nodular-bedded appearance at outcrop (Figure 6.8; e). These basal facies are usually dominated by a fauna of brachiopods (commonly in life-position) and sponges (Figure 6.8; d).

Basal units commonly grade-upwards into a more well-bedded bioclastic wackestone (Figure 6.8; e). This facies is characterised by abundant nodular and lenticular-bedded chert. The chert is likely to be related to diagenetic re-mobilisation of silica derived from abundant sponge spicules as chert is rarely associated with other facies in the succession, and certainly not in the same quantities (15-20% of the rock). This facies is also heavily bioturbated and it is likely that the morphology of chert nodules reflects the differential sediment infill of some of the larger burrow systems. The majority of the visible burrow systems probably belonged to the ichnoguild *Thalassinoides*, based

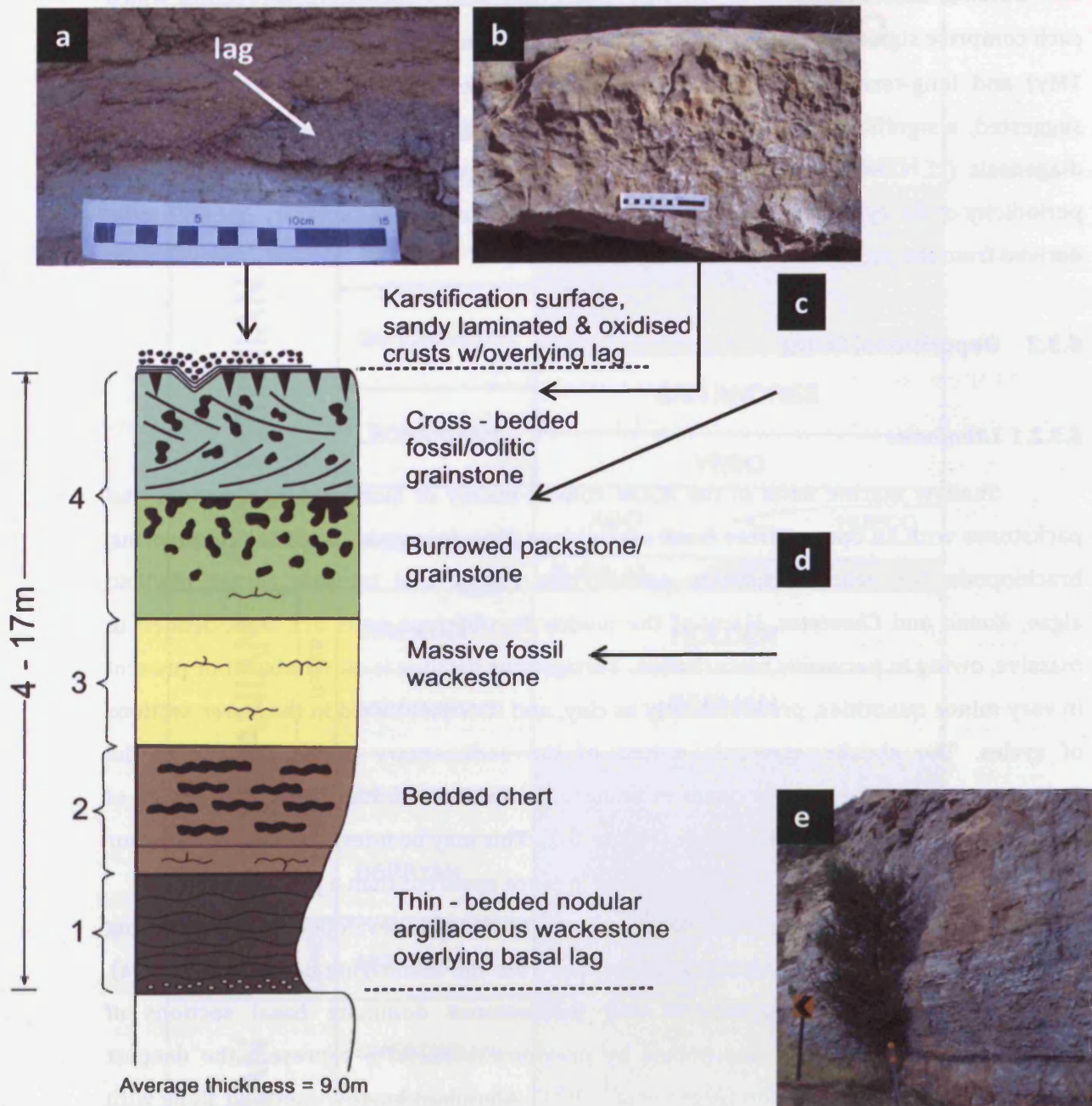


Figure 6.8: Schematic representation of a typical BSLM HfS, displaying general shoaling-upwards motif with weak to strong development of sub-aerial exposure features at cycle tops. **a)** Palaeotopographic depression on palaeokarstic surface infilled by silicified fossil lag. **b)** Diagenetically-enhanced burrow fabrics, where unsilicified burrows are encased in a silicified matrix. Palaeokarstic surface at top. **c)** Coarse-grained echinoderm-rich skeletal packstone from a cycle top. **d)** Argillaceous wackestone with abundant sponge spicules. **e)** Base of a cycle (adjacent to sign); nodular- to wavy-bedded wackestone at base grading up into more massive wackestone with chert (not pictured). Cyclothem terminates approximately at top of tree. Sign is 2m for scale. (Log modified from Algeo *et al.*, 1992).

on the horizontal to slightly inclined large diameter burrows (Figure 6.8; b). This facies always exhibits a gradational transition with the above facies, which may often only be distinguished at outcrop by the absence of chert nodules. It is commonly present as a massive bioclastic wackestone which contains fewer sponge spicules than the equivalent facies with chert (although they may still be common) and has a more diverse, open-marine fauna composed primarily of echinoderm and brachiopod fragments; prompting the interpretation of shoaling during this period of deposition.

The capping facies of cyclothem is usually a massive bioclastic grainstone with trough cross-bedding, although in some cycles this may be a packstone. The basal contact may occasionally be scoured, although this is usually obscured by significant bioturbation, particularly in packstone beds. Bioturbation is particularly prominent as a distinct grey-brown colour-mottling at outcrop, caused by diagenetic-enhanced of burrow fabrics whereby unsilicified burrows are encased in a silicified matrix (Figure 6.8; b). This preferential silicification is likely to be the result of early meteoric cementation of burrows, which were consequently less-permeable than the inter-burrow matrix. The matrix was silicified by later flux of silica-rich burial fluids, derived from spiculitic overlying facies, through the more permeable matrix (Algeo *et al.*, 1991).

The primary grain type is usually echinoderm fragments (Figure 6.8; c). The lack (or presence of minimal amounts) of micrite is interpreted as evidence of deposition in a shallow, high-energy environment. The abundance of moderately-sorted, abraded, sub-angular to sub-rounded skeletal fragments lends support to this interpretation. The upper boundary of this facies is always sharp and, where identified as a cycle boundary, show evidence of sub-aerial exposure.

6.3.2.2 Cycle boundaries

Previous studies have identified cycle bounding surfaces in the BSLM based upon vertical facies associations (e.g. Algeo *et al.*, 1991). This technique relies upon facies-depth associations which may not accurately reflect the controls on facies distribution in ancient successions (cf. Rankey, 2004). The problems inherent to this method have previously been discussed in this study and are not repeated here (refer to section 5.3.12). Interpretations here of cycle boundaries in the BSLM are thus solely based upon evidence of direct sub-aerial exposure.

Cycles are separated by sharp, disconformable surfaces that are primarily identified at outcrop by palaeokarstic surfaces, rhizocretions and overlying basal lag (Figure 6.9). Palaeokarstic surfaces are commonly of low relief (<10cm), display karstic solution pits and occasionally, solution-enlarged joints. These surfaces are commonly associated with platy oxidised crusts and very rarely, small (<2mm) pyrite nodules.

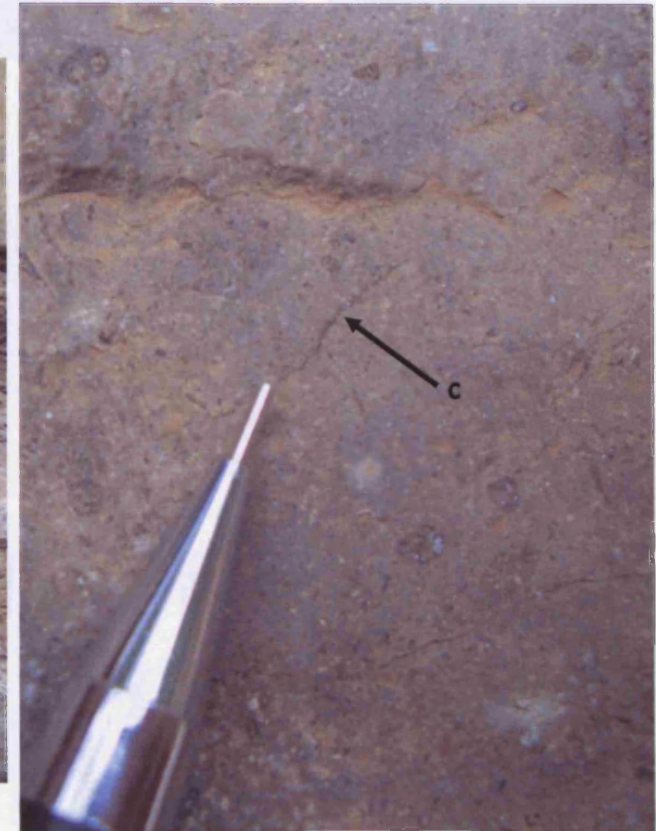
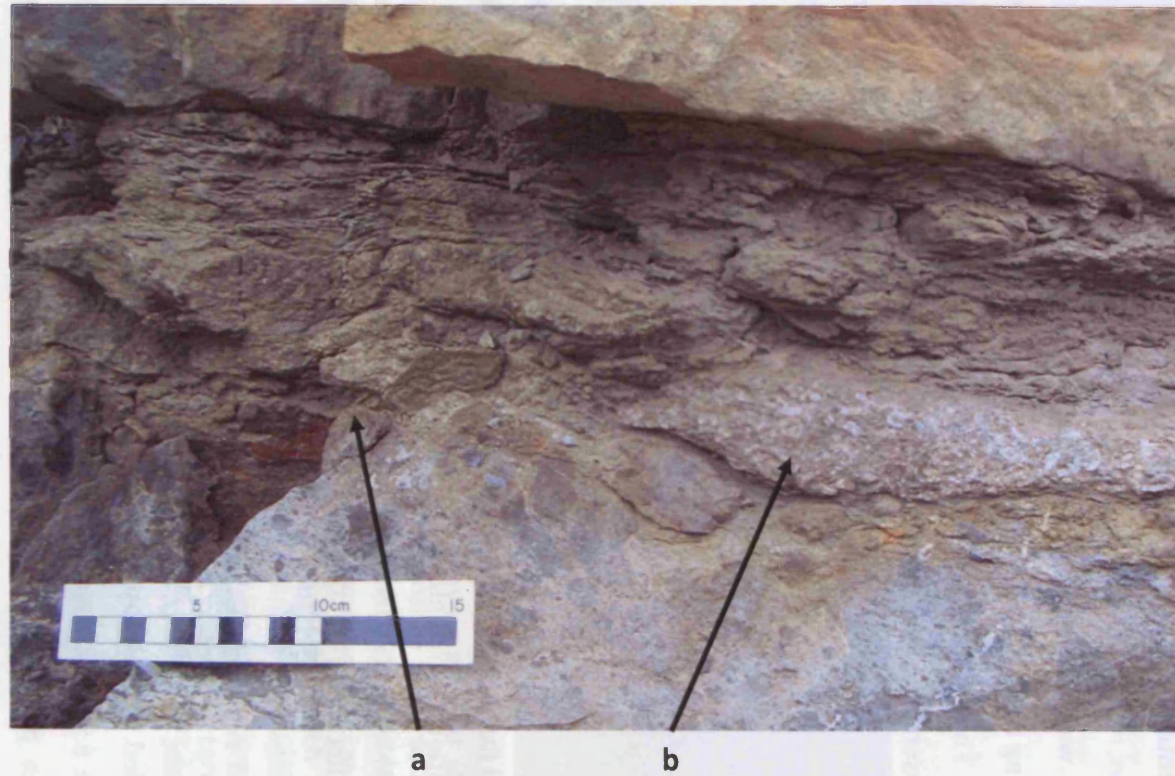


Figure 6.9: Palaeokarstic surface at the top of HfS 1 (5.8m above base of section). a) Low-relief (10cm) palaeokarstic surface. b) Coarse-grained echinoderm-rich fossil lag (thickness 5-15cm) overlying platy oxidation crust on underlying cycle top.

Rhizocretions are present and, although small (<1mm diameter) are relatively easily identified by the presence of alteration halos around them (cf. Davies, 1991).

The basal lag, which overlies most cycle boundaries, is dominated by echinoderm fragments. These are predominantly coarse-grained, but very poorly sorted (ranging from <1mm to >2cm). Skeletal grains are severely abraded and typically admixed with phosphatic grains, glauconite pellets and quartz sand (>20%). It has been interpreted by previous authors as a transgressive deposit on a hiatal surface (Algeo *et al.*, 1991).

Crucially, the three primary indicators of exposure outlined above, are restricted to within a few centimetres below the exposure surfaces providing a good constraint on cycle thicknesses. They therefore collectively demonstrate a recurrent genetic relationship between cycle tops and sub-aerial exposure.

Previous work has also identified diagenetic features diagnostic of proximal sub-aerial exposure (Algeo *et al.*, 1991). Calcrete is present at some sub-aerial exposure surfaces, but not all, and so cannot be relied upon to give unequivocal evidence of exposure. One of the most ubiquitous features of sub-aerial exposure noted by previous workers are diagenetically-enhanced burrow fabrics, where unsilicified burrows are encased in a silicified matrix (Figure 6.10). As noted, these fabrics have previously been interpreted as the product of early meteoric cementation of burrows; yet the preferential silicification can permeate several metres below the disconformity. As such this feature is not inferred to represent a physical boundary; it was only used at outcrop to infer proximity to individual exposure surfaces.

6.3.3 Stratigraphic simulation of high-frequency sequences

Numerical forward modelling was conducted in order to investigate the likely controls on stratal stacking patterns. In total, 7500 simulations were conducted with individual sets of runs investigating a range of parameters (Table 6.1). These parameters were chosen based upon their identification as those most likely to effect the thickness and cycle stacking pattern of a sedimentary succession and span a range of values derived from primarily empirical evidence (refer to section 3.3).

The runs were analysed in terms of the parameter-space response surface generated by measuring a variable against two parameters. Specifically, the measured variable is the number of HfSs that match the corresponding sedimentary HfS within a certain margin of error. For example, the 5th HfS in the FC section is 9.8m thick (Figure 6.2) – the 5th HfS recorded in a simulation would therefore have to match the thickness of this observed HfS to within a certain range to be judged a ‘good’ equivalent. The number of HfSs that provide a good match per run provide the measured criterion in these response surfaces. For simulations addressing the studied section at FC, two response surfaces were

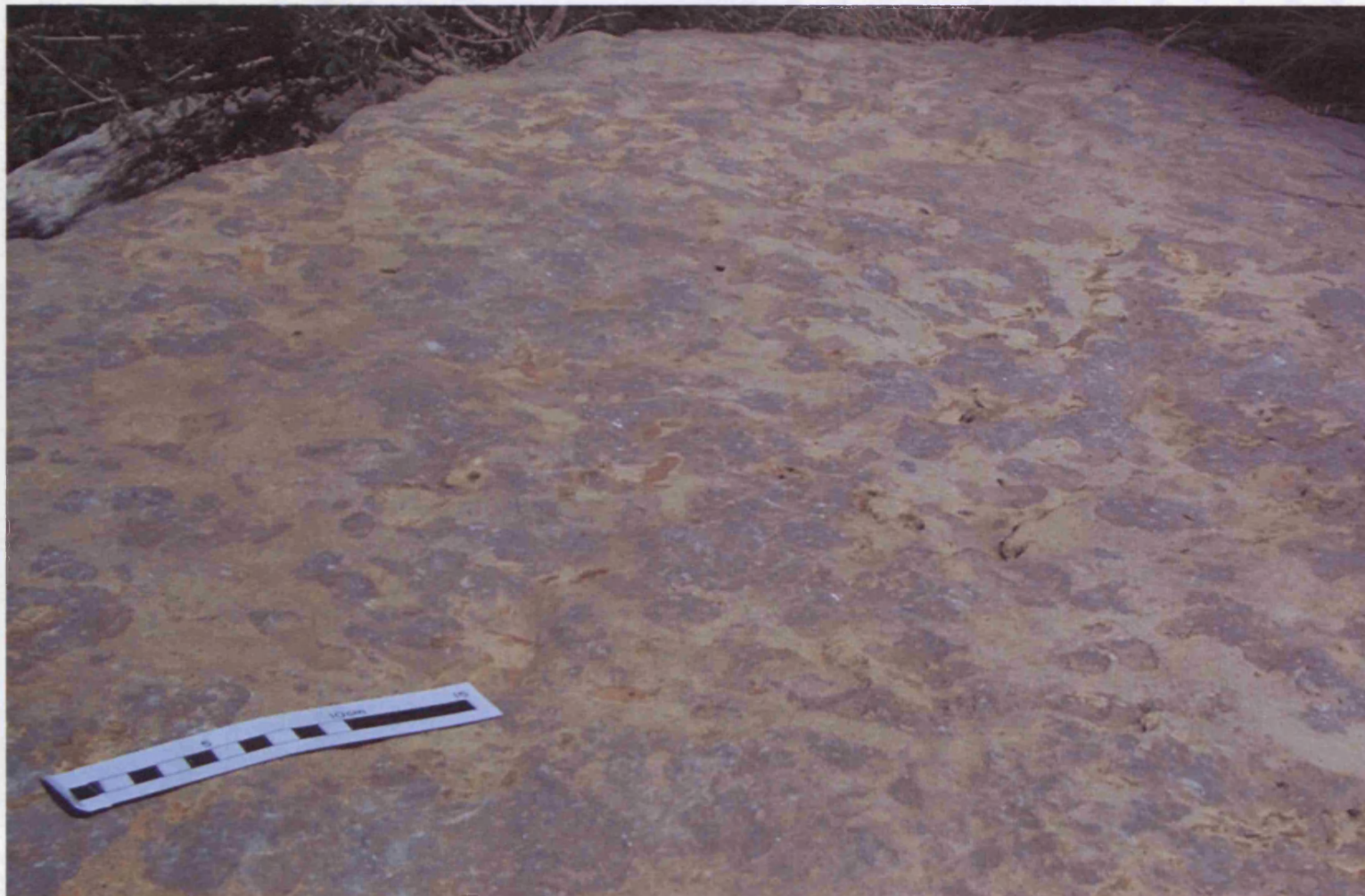


Figure 6.10: Palaeokarstic surface at the top of HfS 8. Surface has low-relief (5cm) and displays evidence of rhizocretions (not depicted). The most prominent structure is the diagenetically-enhanced burrows set in a silicified matrix (grey/brown mottling).

generated for each run-set, each with a different range of error. Firstly, a 2m error catchment was used, representing a margin of slightly over 20% of the average cycle thickness (22.2%). Secondly, a more precise margin of error was used: 1m (11.1%). The coarser margin of error allows trends to be identified, while the smaller margin allows precise identification of zones representing good matches.

Runs that vary the oscillation amplitude of two sea-level components show a reasonable ability to replicate the observed FC section, as up to 7 of 13 HfSs (54%) can be simulated to within a 11% margin of error (Figure 6.11). Simulations displaying the best section-matching potential occur in a very specific parameter-space. Broadly, this can be said to be above 40m intermediate-order amplitude and below 10m high-order amplitude. More specifically, the best section matches are developed above 70m high-order amplitude. This distribution is due to the number of high-order beats recorded on the platform top as intervals of sedimentation; with increasing high-order amplitude there is a greater probability that high-order cycles will be recorded. As these oscillations are of short duration they tend to be relatively thin (less than 2m); a source of deviation from the consistently thicker (average 9m) cycles observed at FC (average approximately 10m thick). If high order amplitude is greater than 10m, high-order beats are recorded more consistently, and cause a sharp drop-off in the number of good matches beyond 10m high-order amplitude. Modification of only two eustatic parameters achieves a maximum of 8 good-matches (61%), however; suggesting that modification of eustatic amplitude alone is not capable of replicating the FC section.

The stacking patterns generated by large intermediate-order amplitude and small high-order amplitude are consistent in terms of overall sedimentary style, thickness and lithofacies proportions to stacking patterns observed in FC (Figure 6.12). Simulated cycles display a consistently similar thickness to observed HfSs and lithofacies distribution is also broadly in-line; with a significant wackestone component at the base, prominent packstone interval, and thinner grainstone bed. Although the observation and comparison of lithofacies is, in this case, a qualitative affair, it is useful in assessing if a simulation has a reasonable lithofacies distribution in comparison with the measured section.

The identification of a parameter-space zone of good matches with large intermediate-order amplitude and negligible high-order amplitude is in line with values obtained by other studies. Numerous workers have asserted that intermediate-order oscillations must be of considerable amplitude during ice-house periods (e.g. Heckel, 1986; Lehrmann & Goldhammer, 1999). Furthermore, the observation that a simulation bears most resemblance to the observed sedimentary succession at very-small high-order amplitudes supports the findings of section 4.5: the Honaker Trail section in south-eastern Utah is best replicated with small-amplitude high-order oscillations.

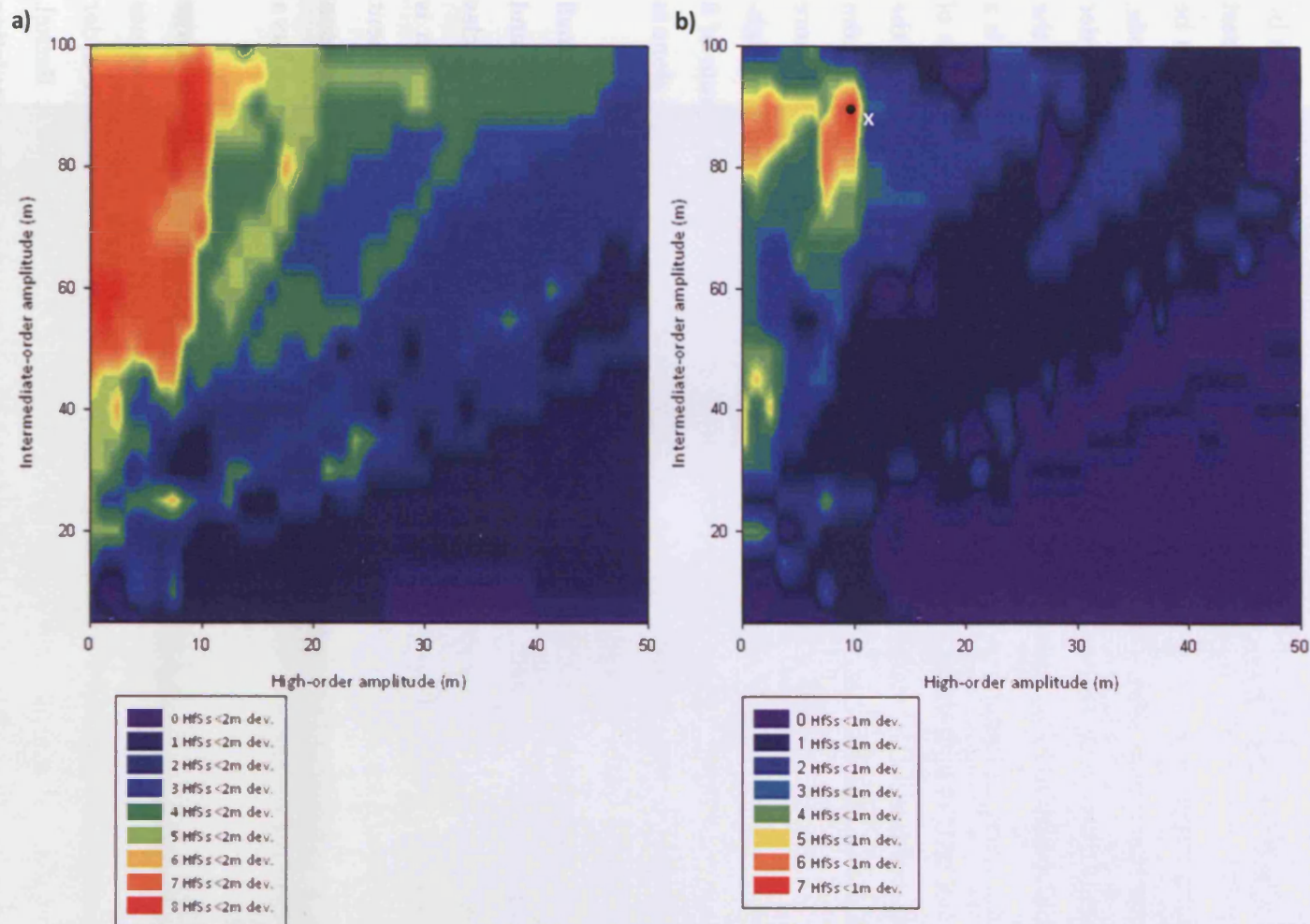


Figure 6.11: Parameter-space response surface plot comparing HfSs generated by simulations, with HfSs in the observed FC section. The plot shows the number of HfSs per simulation which fall within a specified margin of error (in terms of thickness). Eustatic amplitude is the major variable. Note the different scales. a) Response surface with a 2m margin of error. b) Response surface with a 1m margin of error. Simulations displaying the best section-matching potential occur above 40m intermediate-order amplitude and below 10m high-order amplitude. More specifically, the best section matches are developed above 70m high-order amplitude. x) Refers to the parameters of the simulation used in Figure 6.12.

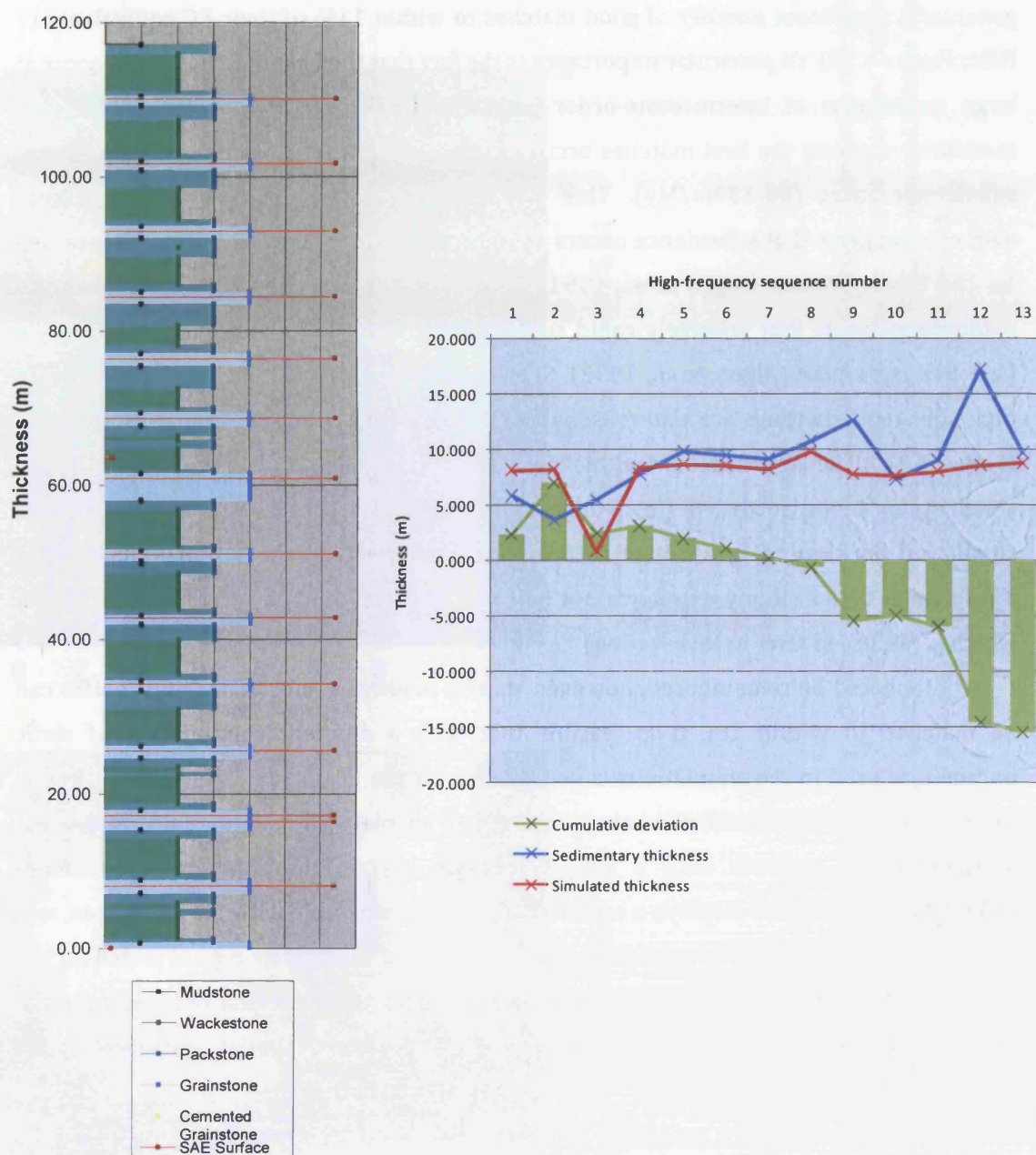


Figure 6.12: Simulated lithologic section (left) and thickness plot for HfSs (right) generated at point x in Figure 6.11. Qualitatively it can be said that simulated cycles display a consistently similar thickness to observed HfSs and that lithofacies distribution is also broadly in-line; with a significant wackestone component at the base, prominent packstone interval, and thinner grainstone bed. Cumulative deviation in thickness is largely due to 2 major thickness deviations in HfS 3 and 12.

In terms of subsidence, simulations incorporating this variable were also able to generate a significant number of good matches to within 11% of their FC equivalents (7 HfSs; Figure 6.13). Of particular importance is the fact that the best matches again occur at large amplitudes of intermediate-order oscillation (40-80m). It is also notable that modelling suggests the best matches occur at relative rapid (for an intra-cratonic basin) subsidence rates (80-130m/My). This is certainly possible given that geochemical evidence suggests that subsidence occurs at an increased rate above the 50m/My average for the Pennsylvanian (Algeo *et al.*, 1991). As mentioned in section 6.3.1.1, geochemical evidence suggests that relatively rapid subsidence is likely to have occurred during the Late Pennsylvanian (Algeo *et al.*, 1992). Stacking patterns and lithofacies distribution in high-subsidence settings are also reasonable in comparison with the observed succession (Figure 6.14). The large cumulative thickness deviation in Figure 6.14 is the result of very small cycles being recorded (from high-order oscillations); the result of a computer simulation performing as a better recording mechanism than the sedimentary record. These small cycles (if any exist) are not likely to be recognised at outcrop (the effect of which is discussed later in this section).

It should be remembered, however, that by modifying subsidence only 7 HfSs can be matched to within 1m. It is feasible that with a different combination of static parameters used in the simulations, a good match for the FC section could potentially be developed at lower subsidence rates. Figure 6.15 displays the simulated stratigraphic section from a scenario with a subsidence rate beyond the zone of best-matches (80m/My). This section displays a sedimentary style comparable with the FC section, and suggests that a lower rate of subsidence has the potential to generate a good match for the FC section – if other parameters could potentially compensate for that reduced rate. For instance, a lower production rate could feasibly produce similar thickness cycles combined with slower subsidence.

Numerical forward modelling generates the most appropriate matches for the FC section at relatively rapid subsidence rates. This evidence suggests that the Orogrande Basin may have been subsiding at a rate of 80-130m/My, however lower rates may have been supported given the right circumstances. It is also likely that subsidence varied over the Pennsylvanian Epoch, and this is likely to be a significant source of error.

Evidence from modelling of the euphotic calcium carbonate production parameter supports results from the other simulations as the best matches are generated at large intermediate-order oscillation amplitudes (Figure 6.16). It also suggests slightly higher rates than the average used in simulations (500m/My) generate the best matches for the FC section. This rate is slightly below the rate suggested for modern euphotic framework-building organisms (e.g. Bosscher & Schlager, 1993), but broadly appropriate for the

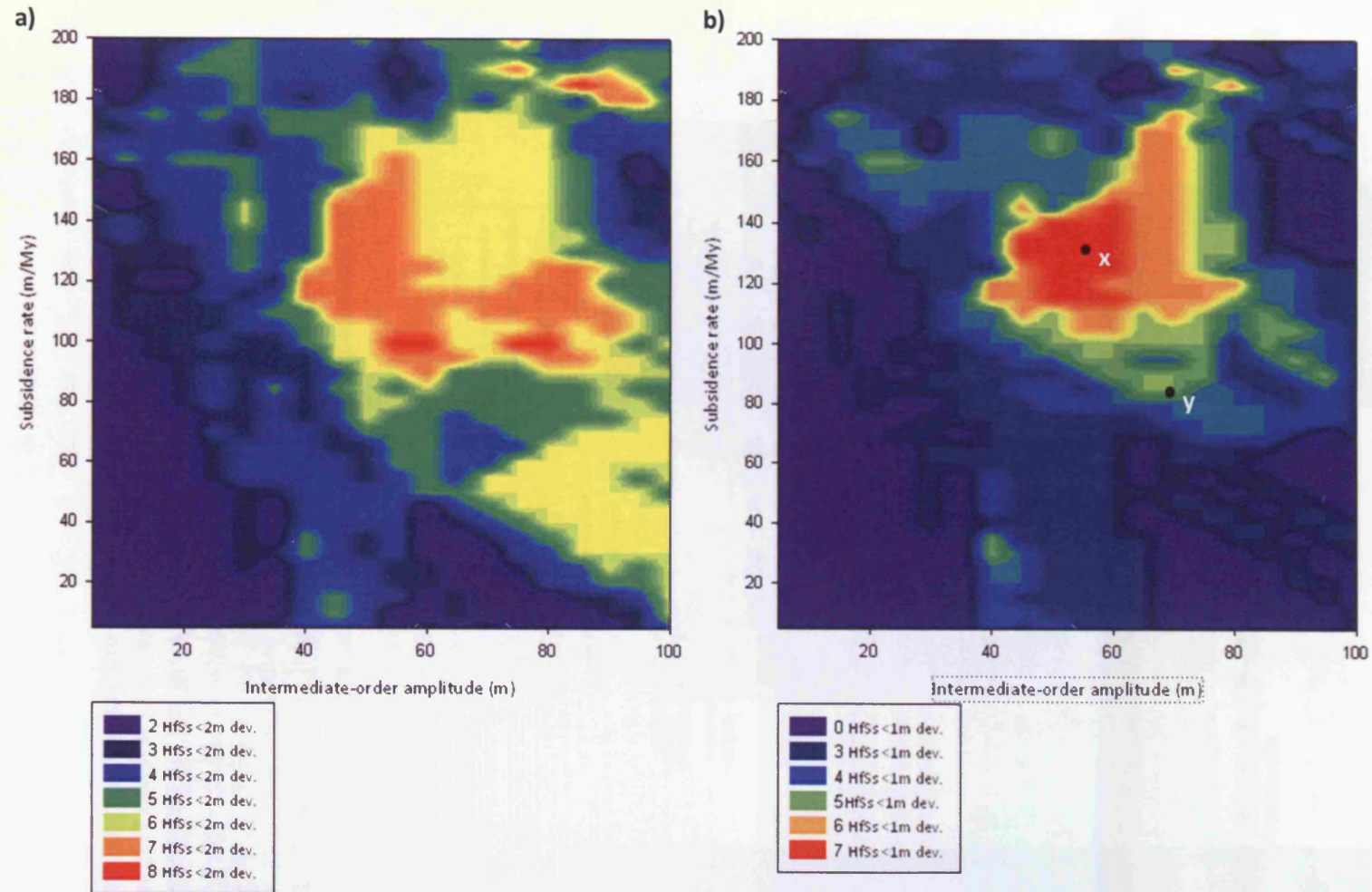


Figure 6.13: Parameter-space response surface plot comparing HfSs generated by simulations with HfSs in the observed FC section. Subsidence rate is the major variable. Note the different scales. **a)** Response surface with a 2m margin of error. **b)** Response surface with a 1m margin of error. The best matches occur at large amplitudes of intermediate-order oscillation (40-80m). It is also notable that modelling suggests the best matches occur at relative rapid (for an intra-cratonic basin) subsidence rates (80-130m/My). x and y) Refer to the parameters of the simulations used in Figure 6.14.

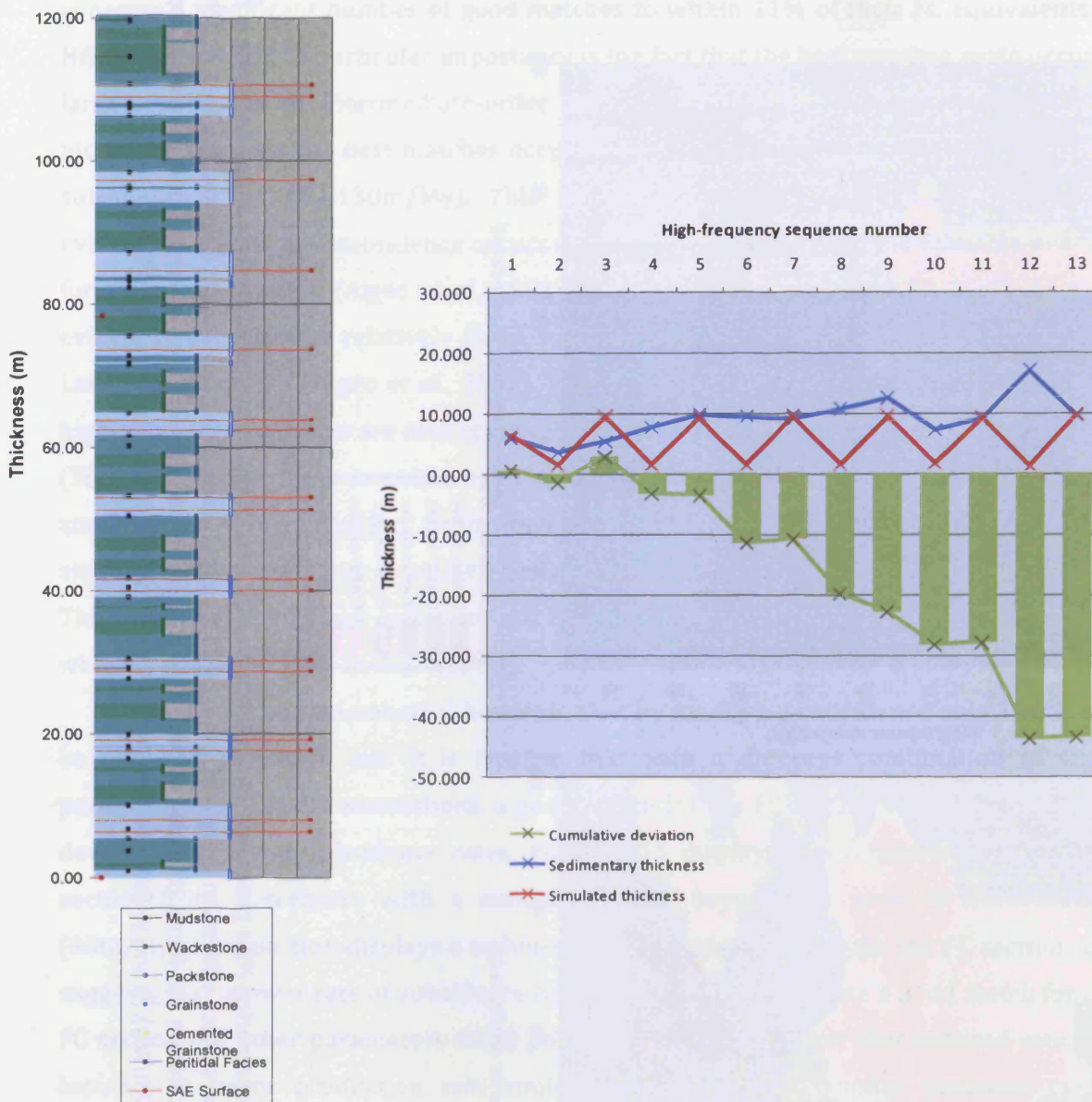


Figure 6.14: Simulated lithologic section (left) and thickness plot for HfSs (right) generated at point x in Figure 6.13. The large cumulative thickness deviations are the result of very small cycles being recorded (as a result of the effect of a high-order oscillation); the result of a computer simulation performing as a better recording mechanism than the sedimentary record. These small cycles (if any exist) are not likely to be recognised at outcrop. At outcrop they may be apparent as discontinuity surfaces in a grainstone bed; as a result of short-duration sub-aerial exposure few diagenetic features are likely to be well-developed.

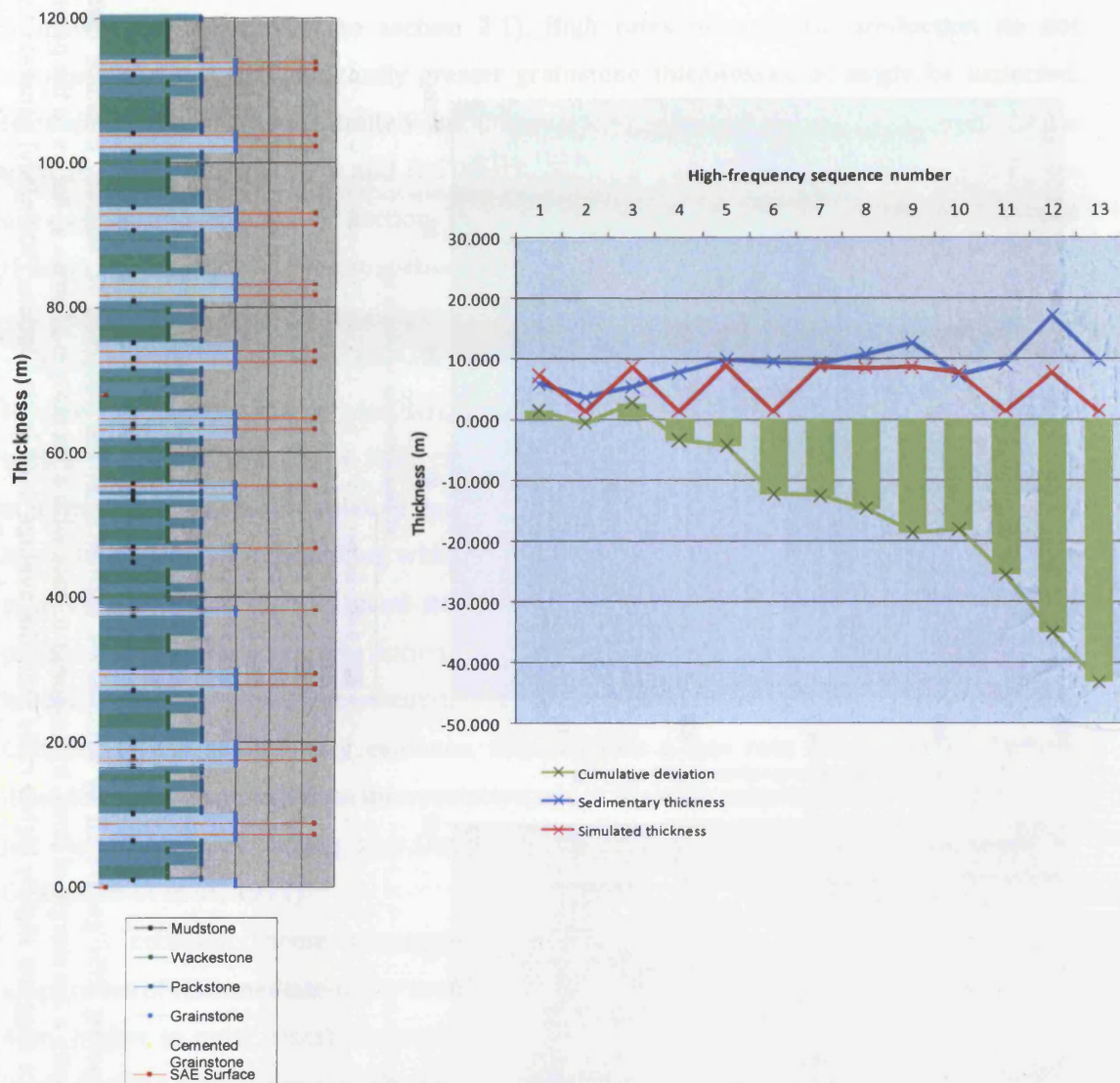


Figure 6.15: Simulated lithologic section (left) and thickness plot for HfSs (right) generated at point y in Figure 6.13. The thickness plot shows a similar pattern to Figure 6.14, but some cycles and the lithological facies association are similar to the FC section. Those which differ in terms of thickness are very thin cycles caused by high-order oscillations (e.g. HfSs 2, 4, 6, 11, 13). These create significant cumulative deviation from the observed section. The thickness of the remaining parasequences (excluding HfS 12) fall within 11% deviation from the corresponding FC thickness.

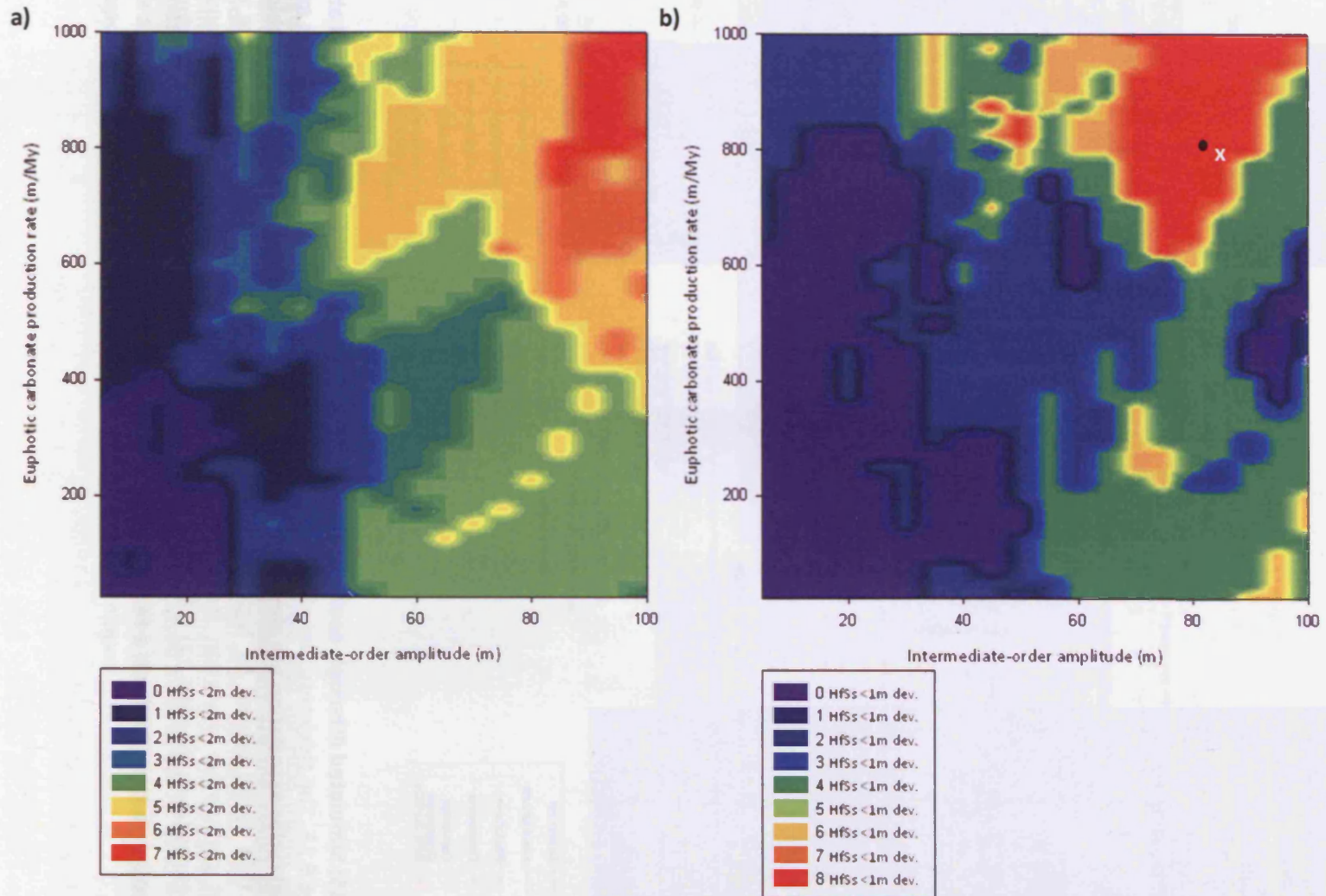


Figure 6.16: Parameter-space response surface plot comparing HfSs generated by simulations with HfSs in the observed FC section. Euphotic carbonate production rate is the major variable. a) Response surface with a 2m margin of error. b) Response surface with a 1m margin of error. x) Refers to the parameters of the simulation used in Figure 6.17. The response surface suggests slightly higher rates than the average used in simulations (500m/My) generate the best matches for the FC Section. This rate is slightly below the rate suggest for modern euphotic framework-building organisms (e.g. Bosscher & Schlager, 1993), but broadly appropriate for the Pennsylvanian inner-platform setting of the study area (which is not dominated by framework-builders; refer to Chapter 3).

Pennsylvanian inner-platform setting of the study area (which is not dominated by framework-builders; refer to section 2.1). High rates of euphotic production do not necessarily result in significantly greater grainstone thicknesses, as might be expected, because of the relatively limited amount of time the platform surface spends in the euphotic zone (during TSTs and FSSTs; refer to section 5.5.2). Instead stacking patterns are comparable with the FC section, both in terms of consistently generating appropriate thicknesses, and lithofacies proportion (Figure 6.17).

Simulations which investigate sub-aerial platform denudation show that the best section-matches occur at relatively high rates of platform denudation (Figure 6.18). However, it is important to note that in simulations with sub-aerial exposure, the nearest match is only possible to 4 HfSs compared with 7-8 in other situations. In addition, stacking patterns show a relative depletion of grainstones (Figure 6.19), which are most likely to be removed; something which is not reflected in the FC section. Given that only a relatively small number of good-matches can be generated in runs where sub-aerial platform denudation actually occurs (in comparison with runs where it is turned off); modelling suggests it was not occurring at significant rates during formation of the BSLM. Combined with sedimentary evidence, this suggests a low rate of sub-aerial platform denudation was operative; an interpretation which fits with palaeoclimatic interpretations for North America during the Desmoinesian (a rate of 10m/My is suggested by Goldhammer *et al.*, 1991).

A common theme amongst all simulations is that they require significant amplitudes of intermediate-order oscillation to generate the best section matches (at least 40m, higher in most cases); something that confirms many of the statements regarding likely eustatic amplitudes made by previous workers.

Crucially however no simulation manages to replicate the thickness of more than 70% of HfSs. Only 4.76% of simulations show a cumulative deviation for the simulated section (measured to the 13th HfS to correspond to the FC section) of less than 10m. The inability to model entire section to similar thickness in 13 HfSs *and* generate minimal deviation at each individual HfS potentially reveals a lot about the complexity of the succession. It is encouraging however that HfS-matching is able to replicate a significant number of high-frequency sequences, using realistic parameters, to within 10% deviation (61% of HfSs). The large cumulative deviation experienced by most simulations is partially due to the model recording very thin (centimetre-scale) high-frequency sequences, forced by high-order sea-level oscillations, which are likely not to be recognized at outcrop. These would be present at outcrop as grainstone beds vertically adjacent to each other but separated by a disconformity representing a short period (<10ky) of sub-aerial exposure. An example of this occurs in Figure 6.14. Another, and perhaps more important reason is

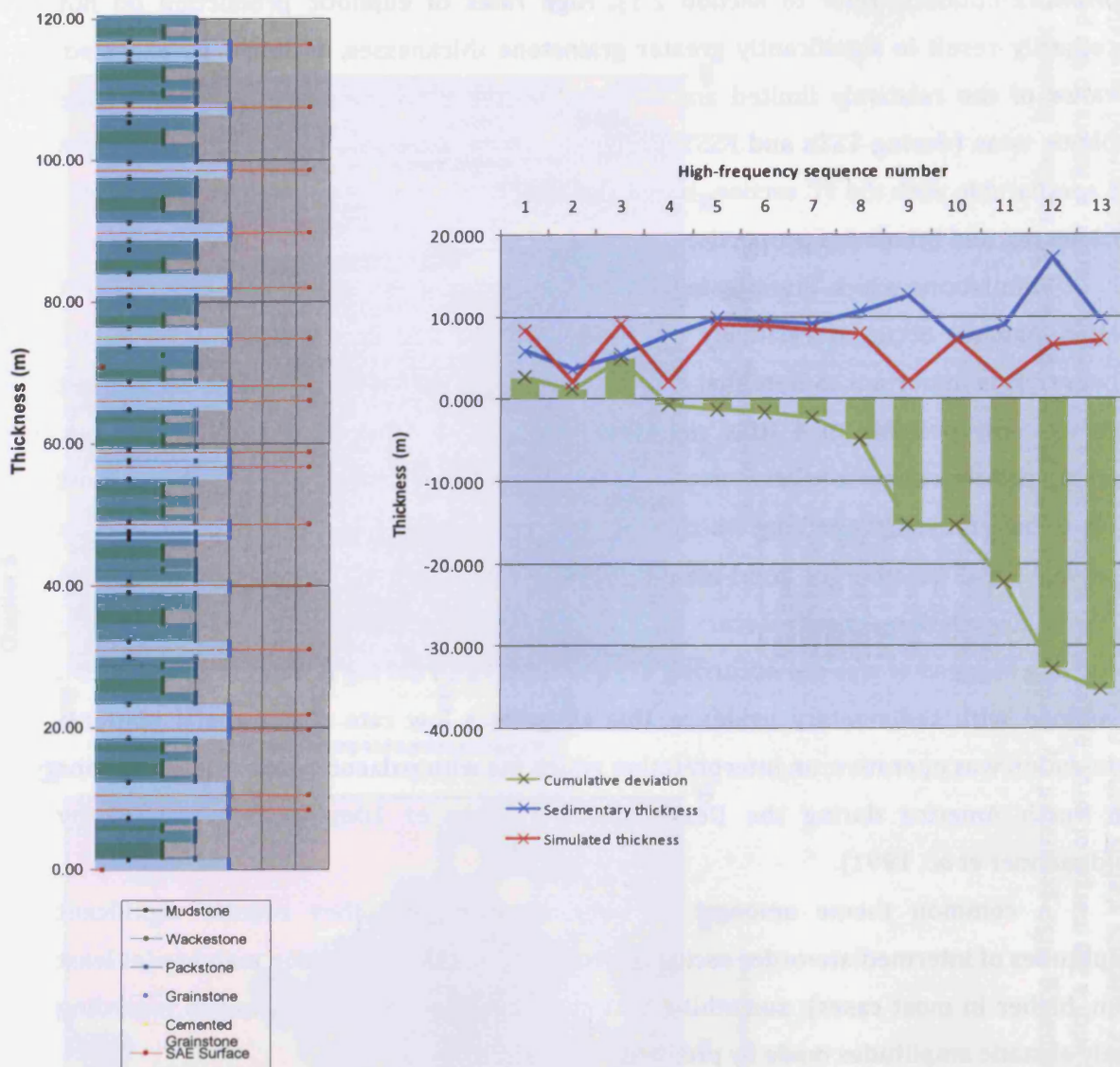


Figure 6.17: Simulated lithologic section (left) and thickness plot for HfSs (right) generated at point x in Figure 6.16. High rates of euphotic production do not necessarily result significantly greater grainstone thicknesses, as might be expected, because of the relatively limited amount of time the platform surface spends in the euphotic zone (during TSTs and FSSTs; refer to Chapter 4).

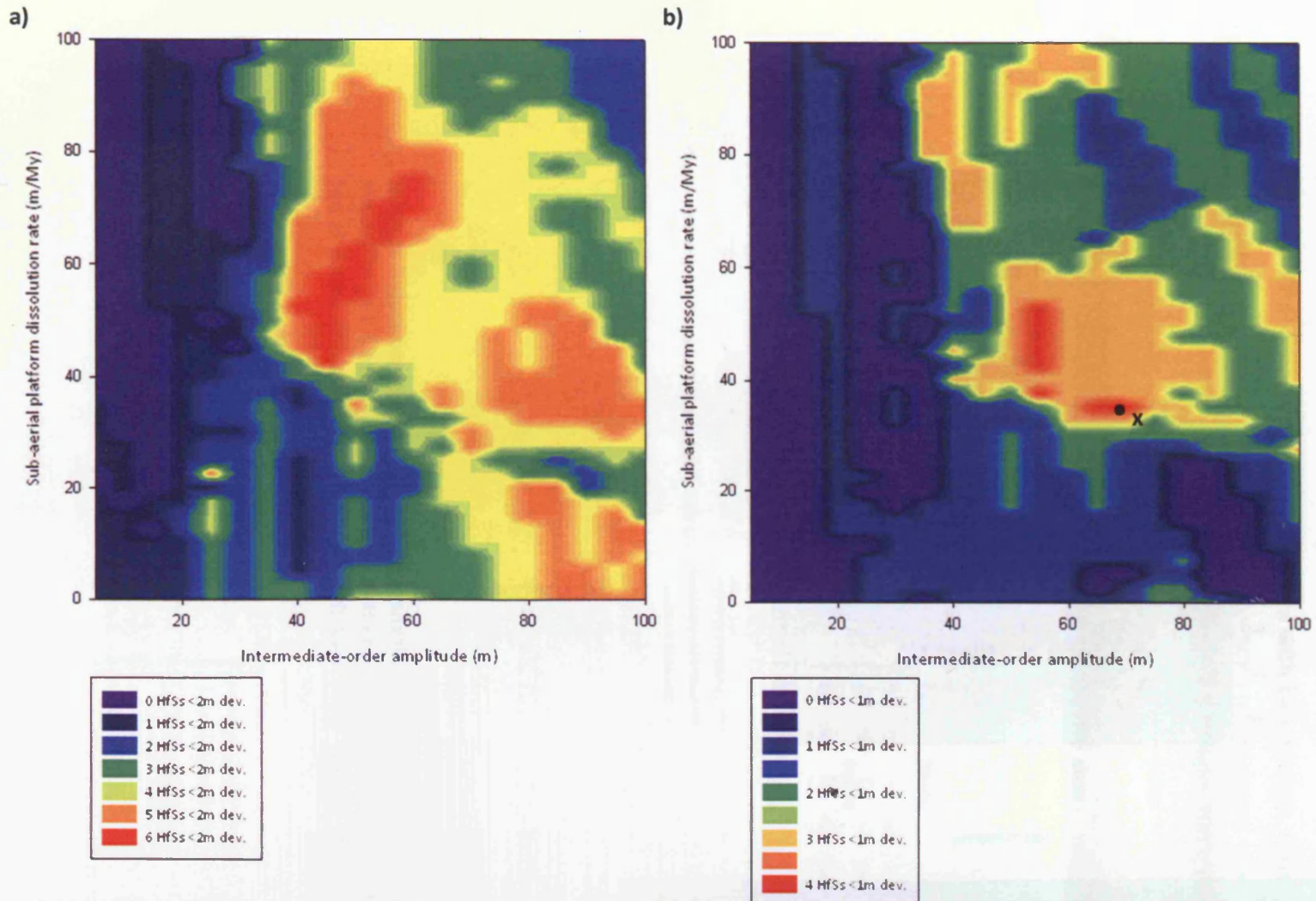


Figure 6.18: Parameter-space response surface plot comparing HfSs generated by simulations with HfSs in the observed FC section. Sub-aerial platform denudation rate is the major variable. Note the different scales. a) Response surface with a 2m margin of error. b) Response surface with a 1m margin of error. x) Refers to the parameters of the simulation used in Figure 6.19. The best section-matches occur at relatively high rates of platform denudation, however the nearest match is only possible to 4 HfSs compared with 7-8 in other situations.

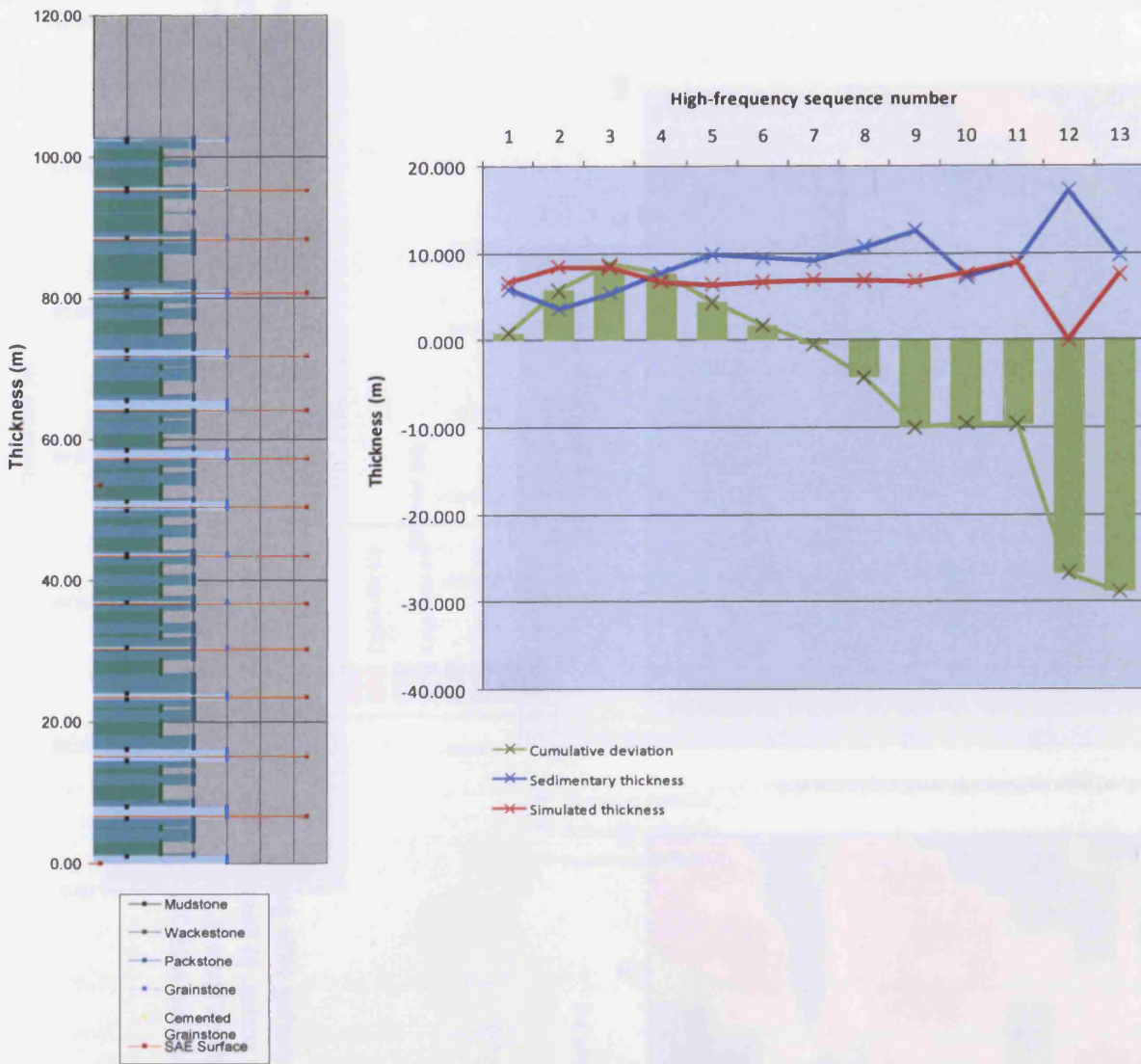


Figure 6.19: Simulated lithologic section (left) and thickness plot for HfSs (right) generated at point x in Figure 6.18. Stacking patterns show a relative depletion of grainstones (Figure 6.19), which are most likely to be removed as they usually exist near the top of a HfS; something which is not reflected in the FC section.

firstly the quality of the sedimentary record as a recording mechanism but also the quality of the outcrop. In the case of FC the outcrop quality is excellent, however very thin cycles may still not be identified, particularly if they are embedded in units of similar lithofacies. The chance of observational error increases with bad outcrop. Observer bias is likely to play a significant role in skewing the frequency and thickness of recognised beds, and potentially, HfSs (cf. Schwarzacher, 2005 & Burgess & Wright, 2003; Burgess, 2007).

6.4 THE MOSCOVIAN SUCCESSION OF ARKHANGEL'SK OBLAST, RUSSIA

6.4.1 Geological setting

6.4.1.1 Tectonic setting

The study localities are situated in the south-central (Precambrian) East European Craton as part of the Baltica sub-plate, within the intra-cratonic Mezen Syncline (Figure 6.20). The Mezen Syncline is poorly documented as a stand-alone entity as it is adjoined to the larger Moscow Syncline, and these basins are usually grouped together as the Moscow-Mezen Basin (e.g. Nikishin *et al.*, 1996). This nomenclature is maintained here. The Moscow-Mezen Basin represents the largest Late Palaeozoic area of moderate tectonic subsidence of the East European Craton (Nikishin *et al.*, 1996). During the Late Carboniferous, this area of Laurussia was situated in equatorial to northern sub-tropical latitudes (Jurdy *et al.*, 1995) and covered by a predominantly carbonate epicontinental sea.

Throughout the Carboniferous, fundamental changes in lithospheric plate interaction had major repercussions for the evolution of the Baltica sub-plate, which borders the Moscow-Mezen Basin to the west. Modification in plate configurations were primarily a result of the evolution of the Variscan and Uralian orogens and account for the major palaeogeographic changes during Late Carboniferous and Early Permian; these changes to stress systems were responsible for controlling the subsidence of intra-cratonic basins on the East European Craton (Nikishin *et al.*, 1996).

The Moscow-Mezen Basin was characterised by several phases of accelerated and decelerated subsidence, punctuated by phases of uplift (Nikishin *et al.*, 1996). Comparison with rates observed in other intra-cratonic basin settings suggest a rate of subsidence well below 50m/My (cf. Allen & Allen, 2005). This is supported by tectonic subsidence values derived from a number of wells in the northern Moscow-Mezen Basin (Figure 6.21). This well data suggests that although there were periods of relatively rapid subsidence during the Late Pennsylvanian, these were still less than 50m/My. These Middle and Late Carboniferous rapid subsidence events on the East European Craton may be related to stresses exerted on the East European Craton from the Uralian collision front (Nikishin *et al.*, 1996). During the Moscovian, however, a period of quiescence prevailed. This prompted Izart *et al.* (2003) to model the Moscow-Mezen Basin with a lithospheric heating phase from Devonian to Bashkirian times and a subsequent cooling phase generating thermal subsidence from the Moscovian to Asselian. As such, the subsidence rate in the

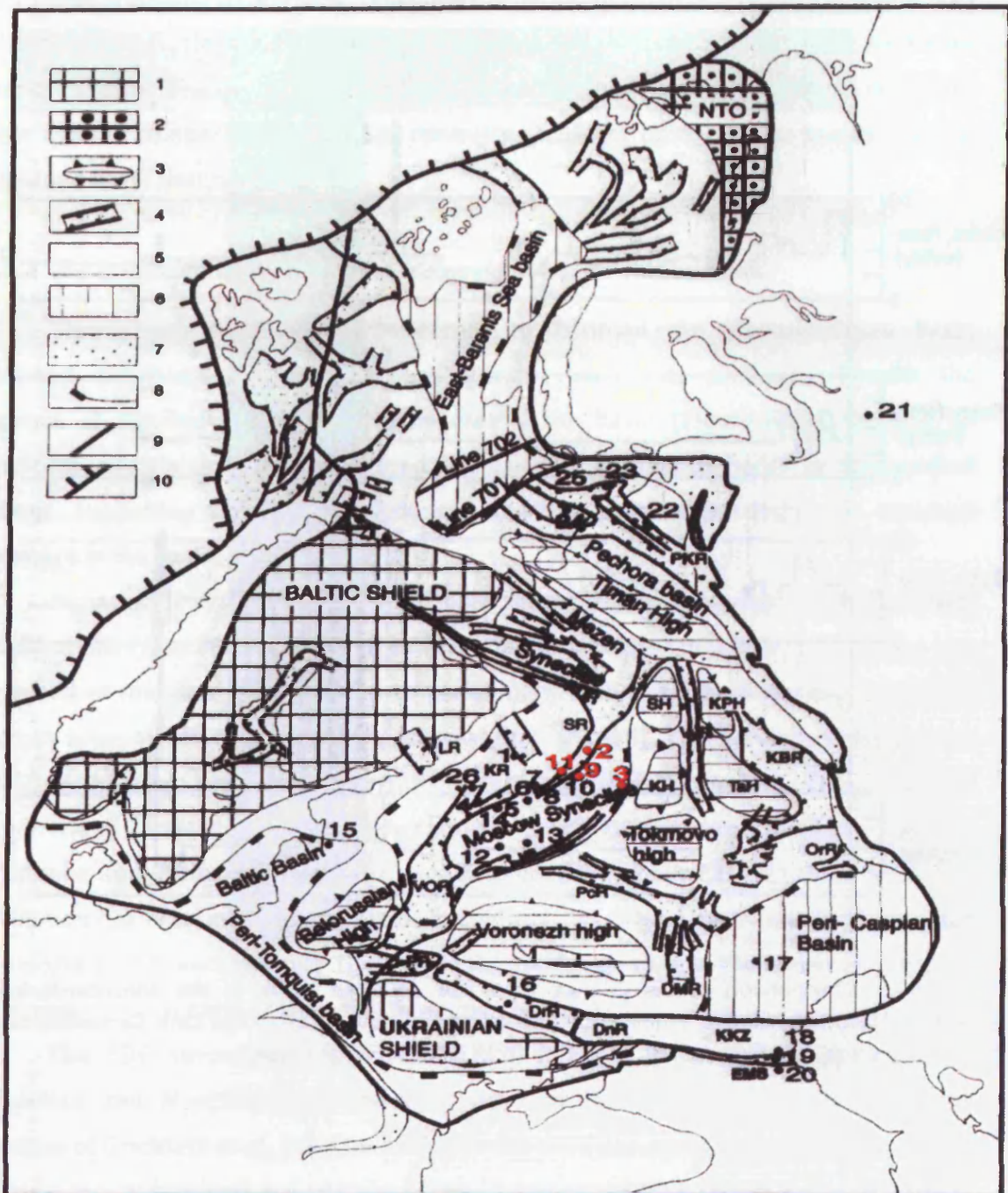


Figure 6.20: Sedimentary basins of the East European Craton which surround the Moscow-Mezen Syncline. Numbers in red correspond to the wells shown in Figure 6.21. Modified from Nikishin *et al.* (1996). 1 = Early Precambrian basement (shield); 2 = Late Precambrian basement (0.8-0.55 Ga); 3 = intraplateau highs; 4 = intra-cratonic rift basins; 5 = platform areas; 6 = very deep sedimentary basin (up to 20-23 km); 7 = foreland basins (Fore-Ural basin, Fore-Timan basin, Fore-Carpathian basin); 8 = outlines of some sedimentary basins; 9 = boundary of EEC; 10 = passive margin of the Atlantic-Arctic Ocean. Names of structures: *DMR* = Don-Medveditsa rift basin; *DnR* = Donets rift basin; *DrR* = Dniepr rift basin; *EMB* = East-Manych basin; *KBR* = Kama-Belaya rift basin; *KDR* = Kandalaksha-Dvina rift basin; *KH* = Kotelnich High; *KKZ* = Karpinsky Kryazh zone; *KPH* = Komi-Permyak High; *KR* = Krestets rift basin; *LR* = Ladoga rift basin; *MR* = Moscow rift basin; *NTO* = North-Taymyr orogen; *OrR* = Orenburg rift basin; *PcR* = Pachelma rift basin; *PKR* = Peehora-Kolva rift basin; *PR* = Pripyat rift basin; *SH* = Sysola High; *SR* = Soligalich rift basin; *Tall* = Tatarian High; *VOR* = Volyn-Orsha rift basin; *VyR* = Vyatka rift basin.

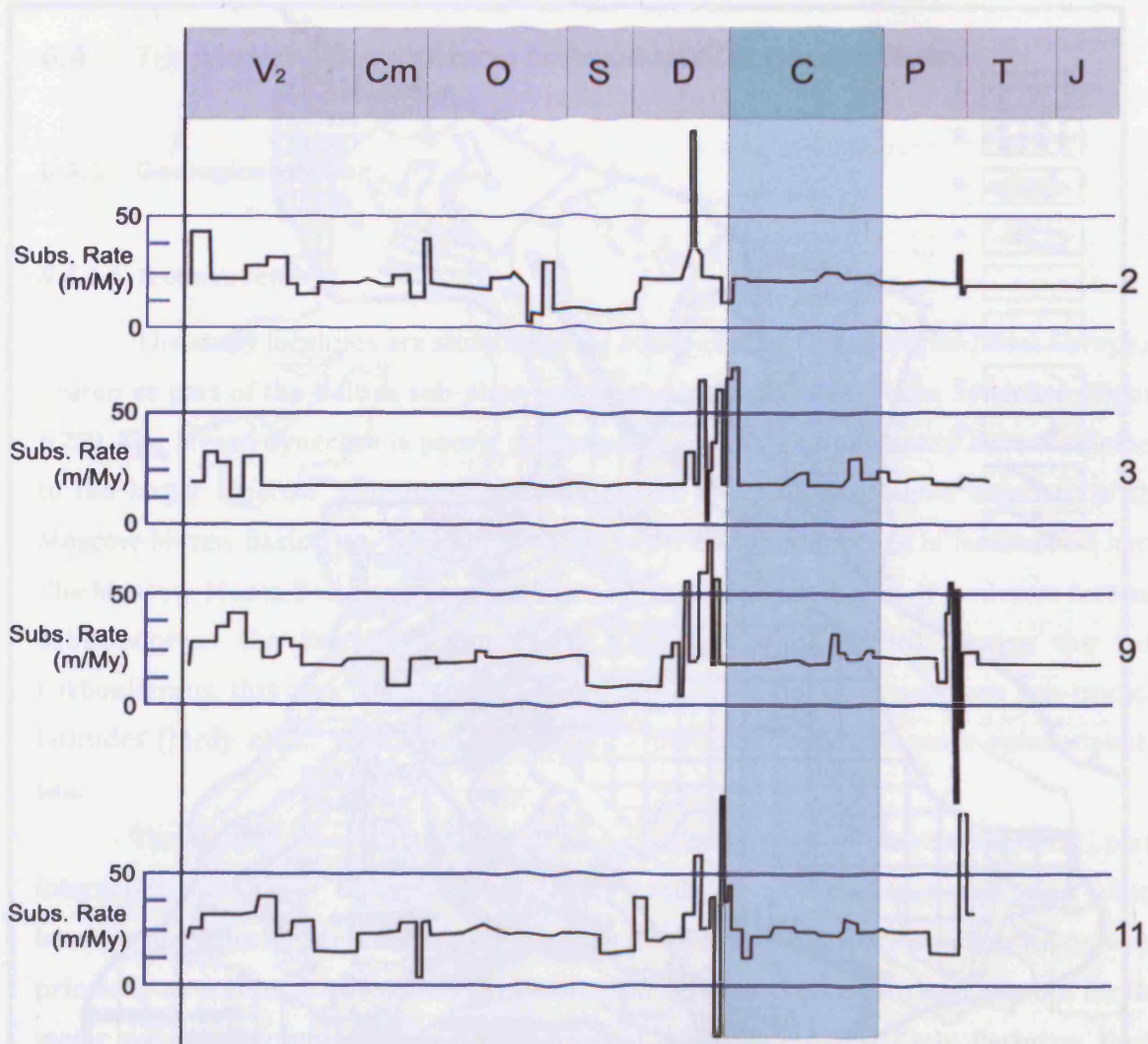


Figure 6.21: Comparison of subsidence rates for selected wells in the Moscow-Mezen Syncline. Note the relative quiescence and extremely low rates in the Late Carboniferous. For well locations see Figure 6.20. Modified from Nikishin *et al.* (1996).

latter phase is comparatively slow, reflecting the period of relative quiescence. Figure 6.21 highlights the very slow rate of tectonic subsidence experienced by the Moscow-Mezen Basin during the Moscovian. The figure of 10-30m/My suggested by Nikishin *et al.* (1996) is low even in comparison with other relatively quiescent intra-cratonic basins (e.g. the Orogrande Basin described here).

6.4.1.2 The carbonate succession of the Moscovian Moscow-Mezen Basin

Throughout the Early Carboniferous to Permian the Moscow-Mezen Basin contained significant expanses of shallow-water carbonate platforms. Despite the presence of significant highlands to the east of the basin (Figure 6.20), there is no significant siliciclastic content (beyond argillaceous carbonate beds) in the studied sections, suggesting the locus of sediment shedding from these highlands occurred elsewhere in the basin.

Eight major cyclothems are recognized in the upper Moscovian (Podolskian and Myachkovskian) interval (Figure 6.4). The basal sections of these cyclothems are composed of muddier lithologies up to packstones, with occasional storm-graded beds (seen in areas which are devoid of pervasive bioturbation), *Zoophycos*-dominated trace fossil assemblages and a predominantly heterozoan skeletal content. These inferred deeper-water facies grade up over relatively small thicknesses (<5m) to sub-tidal packstones and grainstones that are usually capped by abnormal sub-aerial exposure. Correlation has been made of two major unconformities (Podolskian and Myachkovskian unconformities) to sections over 1000 km to the south, attesting to the co-joined nature of the Moscow-Mezen Basin (Kabanov & Baranova, 2007).

The SDP succession comprises 8 HfSs in 34m of strata; representing the Podolskian and Myachkovskian Russian Stages of the Moscovian Stage (using the timescale of Gradstein *et al.*, 2004), which have not been described before. Age constraints are provided by fusulinid and conodont data (Kabanov, 2003b). Whilst these cyclothems do display evidence of shoaling-upwards, their 'thin' nature distinguishes them from 'classic' decimetre scale cyclothems of Mid-Continent successions (e.g. Heckel, 1986). Given the comparable tectonic setting to New Mexico, and the global nature of eustatic behavior, it may be expected that the cycles would display a similar style of cyclicity. This is an issue which has not been addressed for this undocumented succession. As noted in section 6.1, one of the aims of this study is therefore to establish the controls on the sedimentary stacking patterns.

6.4.2 Depositional facies

6.4.2.1 Lithofacies

Due to the limited thickness of cycles in the Moscow-Mezen Basin, commonly on the order of 1-2m in thickness, distinction of a large variety of facies was problematic. In many cycles distinction was only possible between a deeper and shallower unit on the basis of micrite content and diversity of fossil assemblage (Figure 6.22). Due to the difficulty in differentiating facies over a very small thickness range, particular emphasis was placed during logging on the accurate identification of discrete sub-aerial exposure surfaces rather than a rigid facies classification scheme.

Units interpreted to represent highstand deposits are primarily bioclastic packstones. Also common are wacke/packstones with normal-marine brachiopod and fusulinid-dominated benthic fossil assemblages (Figure 6.23). These facies are characteristically depleted in micritised grains and phylloid algal fragments. In the Kasimovian, these intervals sometimes contain tempestite features with storm graded beds (Figure 6.24).

Beds at the base of cycles are usually thin (<20cm) and are dominated by peloidal wackestones. Basal lags may be present immediately above sub-aerial exposure surfaces and contain abundant rip-up lithoclasts derived from the eroded crusts of sub-aerial cementation (Figure 6.23). Where not truncated, these interpreted early transgressive grainstones grade up to sub-tidal packstones and wackestones.

Bioturbation, particularly Zoophycos traces, are most common towards the base of cyclothems and are interpreted to be indicative of deeper water given the micritic nature of the facies they occur in. Apparent absence of Zoophycos and abundance of grains interpreted to represent shallow-water deposition (principally abraded, poorly sorted brachiopod and echinoderm fragments) reinforces the interpretation that the basin generally had limited accommodation.

Cycles ORL2-a-d are distinct from the general style of cyclicity. These cycles contain shallow-water bioclastic wackestone to grainstone lithofacies with large quantities of early (possibly syn-depositional) lithification and extensive development of micritic to micro-peloidal cements (Figure 6.23). Hardgrounds are abundant in these cycles and it has been interpreted that several cycles may be merged into composite hardgrounds correlated to the Panshino Member of the Moscow Syncline (Kabanov, 2003a; Kabanov & Baranova, 2007). Many Kasimovian shoal grainstones (RNP2-c,d, RNP3-e, and RNP3-g to RNP4-a) are distinct by highly worn grains which are rounded, micritized, cemented by micrite and reworked as lithoclasts (Figure 6.24). Such condensed layers show one or more internal erosional surfaces and intraclasts of similar grainstone.

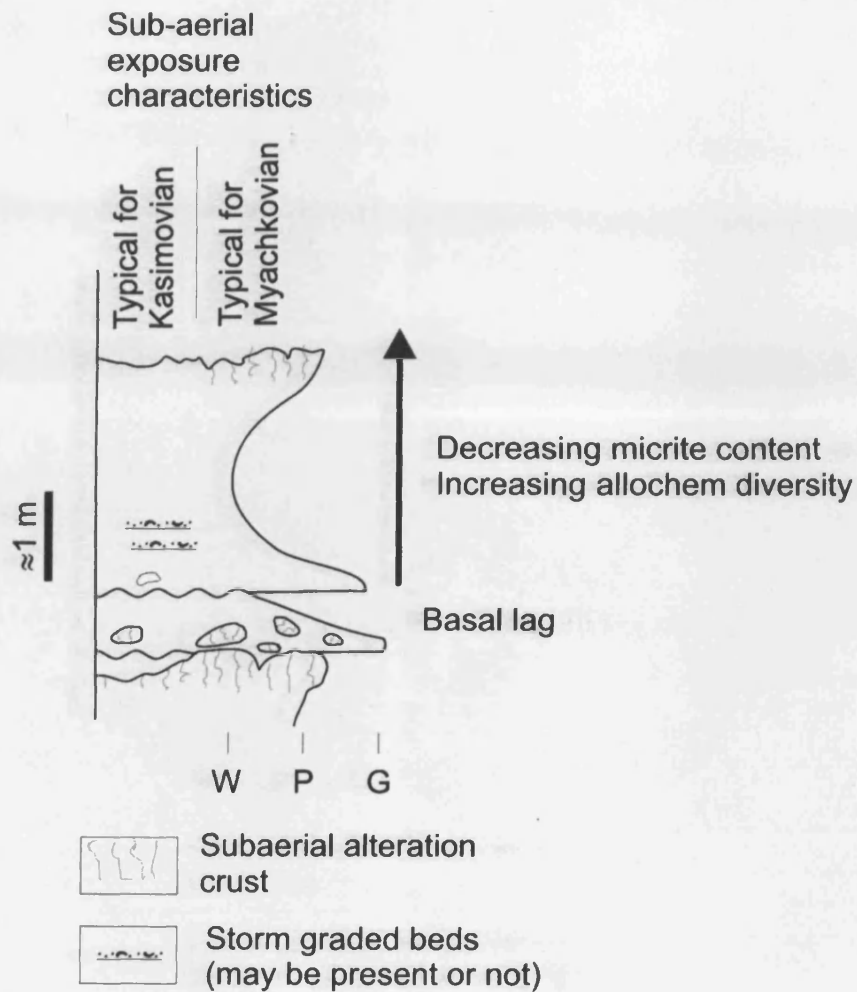


Figure 6.22: Typical cyclothem for the SDP sections. Due to the thin nature of individual cycles a facies characterisation scheme was not developed. Shallower lithofacies are distinguished from deeper lithofacies on the basis of decreased micrite content and increased diversity of biotic allochems.

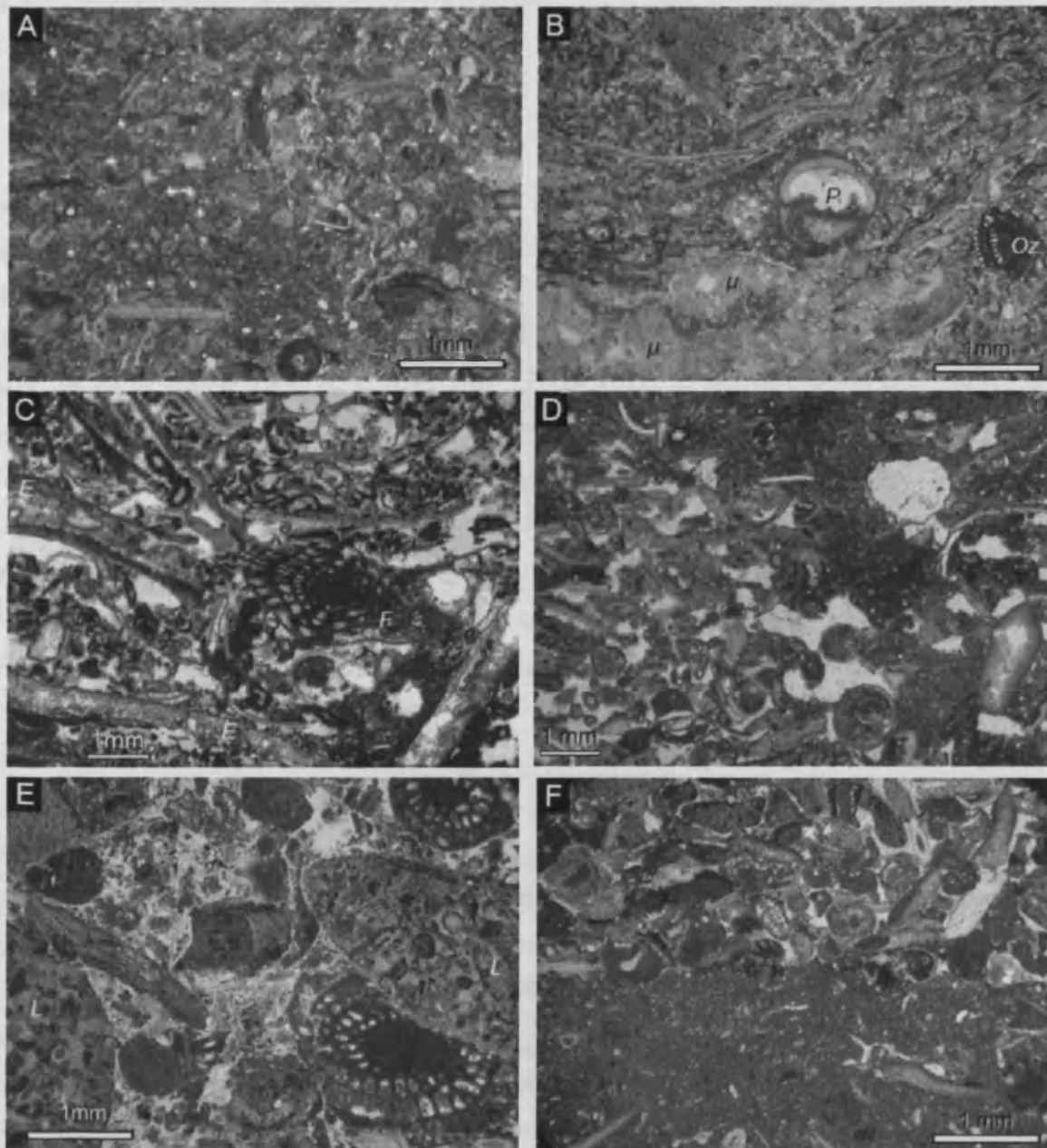


Figure 6.23: Moscovian lithofacies (sequences ORL1-3), Orletsy. A-B) interpreted offshore relatively deep-water lithofacies: A) skeletal wacke/packstone, 2.7 m below top of sequence ORL1; B) brachiopod-debris (possibly storm-sedimented) in wackestone-packstone fabric with Palaeotextulariid (*P*) and Ozawainellid (*Oz*) foraminifer, 1.3 m below top of sequence ORL3, (μ) *Microcodium* penetrations from overlying unconformity. C-E) interpreted shallow sub-tidal lithofacies: E) phylloid algal rudstone-boundstone with preservation of the thalli of *Eugonophyllum johnsoni* (*E*) and rhombic fusulinoid *Fusulinella famula* (*F*). D) typical example of interpreted shallow lithofacies of cycles ORL2-b to ORL2-d: grainstone-packstone with extensive micritic cement forming hardground; E) coarse, rounded, bioclastic grainstone with numerous sub-aerially cemented lithoclasts (*L*), base of sequence ORL-2; matrix is entirely replaced by sepiolite. F) – Contact of cycles truncated by a hardground surface: wackestone of ORL3-a is truncated by the lag grainstone of the base of ORL3-b. Modified from Kabanov *et al.* (In prep.).

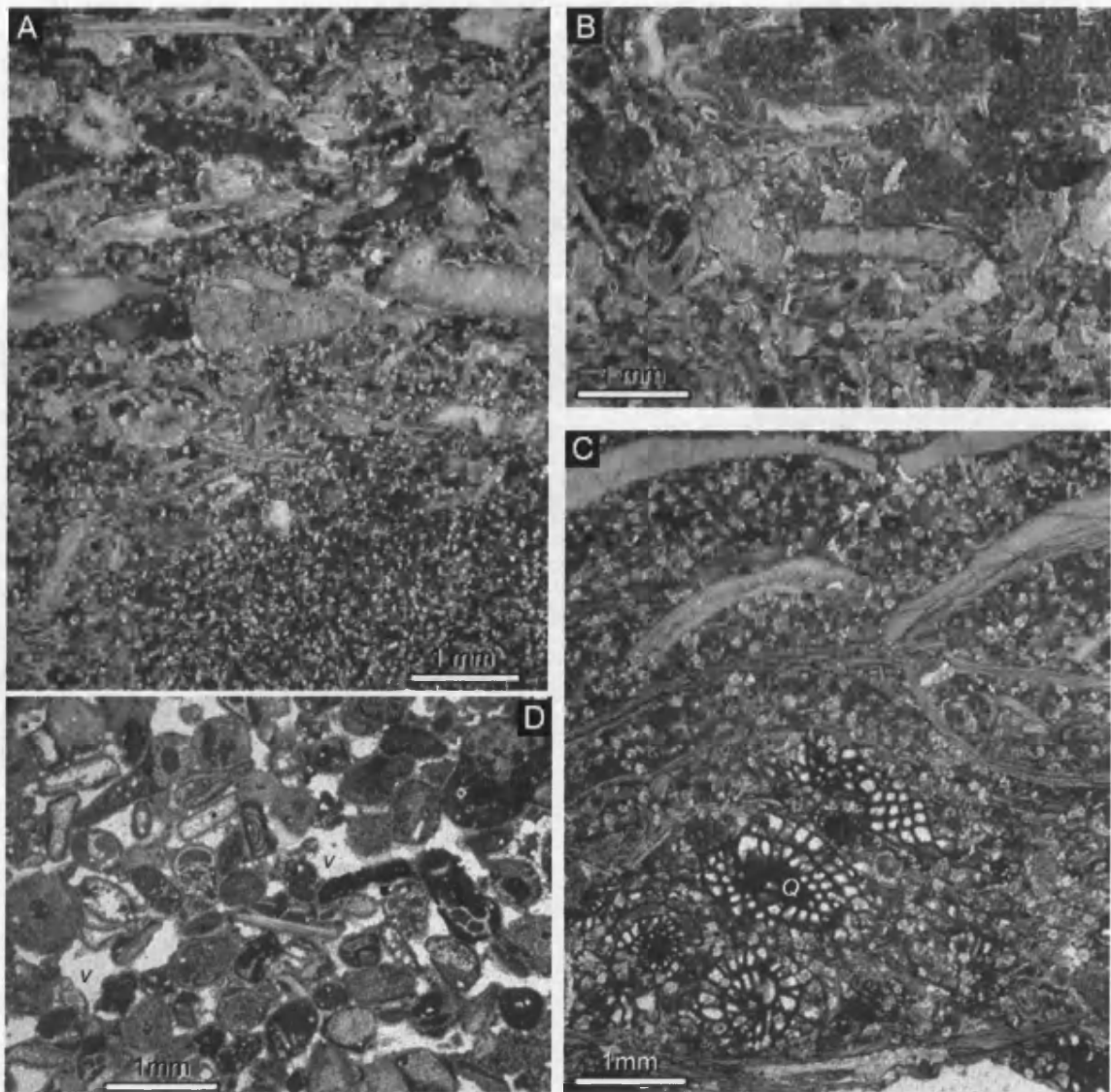


Figure 6.24: Kasimovian lithofacies (sequences RNP2-3), Rozhevo-Nizhnyaya Palenga. A-C) offshore lithofacies: A) moderately dolomitized tempestite with storm lag on marly wackestone, uppermost part of cycle RNP2-a; B) marly wacke/packstone, ORL2-b; note that interpreted deeper-water facies on A) and B) are still rich in shallow-water material (bored and micritized grains, rounded fragments of phylloid algae). C) brachiopod fragments in wackestones dominated by the ichnofossil *Zoophycos* RNP3-f. *Quasifusulinoides* tests (Q) indicating terminal Moscovian to early Kasimovian age. D) condensed grainstone RNP2-d interpreted as undergoing deposition in very shallow water. Contains highly worn (micritized and rounded) grains indicating relatively mature sediment prior to lithification; enlarged inter-particle pores and vugs (v) are attributed to sub-aerial exposure events. Modified from Kabanov *et al.* (In prep.).

Although palaeosol features in these layers have not been observed, solution vugs (Figure 6.24) point to sub-aerial exposure events in grainstone accumulation.

6.4.2.2 Cycle boundaries

The meter-scale shoaling-upwards cyclothems are separated by extensive sub-aerial unconformities with and without evidences of soil forming processes (Kabanov, 2003b; Kabanov & Baranova, 2007). These sub-aerial exposure surfaces are used here as boundaries for high-frequency sequences.

The sub-aerial unconformities of Severnaya Dvina - Pinega area lack micritic pedogenic calcrete structures and clay-layers seen to overlie unconformities in the southern part of the Moscow Basin (Kabanov, 2003a). While the latter may be truncated, absence of the former criterion suggests that true soils categorically did not form. Diagenesis in these sub-aerial exposure surfaces is expressed only as layers of vadose cementation, low-relief karstification, and *Microcodium* development (Figure 6.25; a, d, e).

Karstic surfaces are mostly devoid of biogenic features and may be present only as a low-relief disconformity surfaces (<10cm; Figure 6.25; a, b, c). This is in contrast to more southerly locations in the Moscow-Mezen Basin; where Podolskian and Myachkovskian sub-aerial profiles become prominently rooted (Kabanov, 2003a). A notable feature which commonly immediately overlies exposure surfaces are conglomeratic basal lags consisting of very poorly sorted, angular to sub-angular lithoclasts. Grain-size ranges from coarse sand to large cobbles (greater than 10cm diameter), although the thickness of the bed rarely exceeds 20cm. These lags directly overlie, and therefore fill depressions in, karstic surfaces.

In certain beds diagenetically altered facies also exhibit solution channels and vugs. *Microcodium* occurs in the form of clumps and continuous lenses (coalesced clumps) and is particularly conspicuous in less dolomitized units that retain their primary textures (Figure 6.25; a). *Microcodium* horizons and lenses occur most prominently less than half a metre below unconformities, but may be present up to one metre below in some instances. Sub-aerial unconformities within the studied sections are mainly manifest as karstic surfaces. True palaeosols are typically lacking and sub-aerial unconformities are usually characterized by the presence, and typically abundance, of rhizocretions and associated biogenic structures including *Microcodium*.

Evidence of sub-aerial diagenesis commonly disappears within a few centimetres of the unconformity, confirming proximity to an exposure surface where these features are recognised. Only vadose cementation pervades a significant distance below the exposure surface, and so this is not used as a primary indicator of a sub-aerial unconformity. In addition large sections of the succession are inter-layered with sepiolite

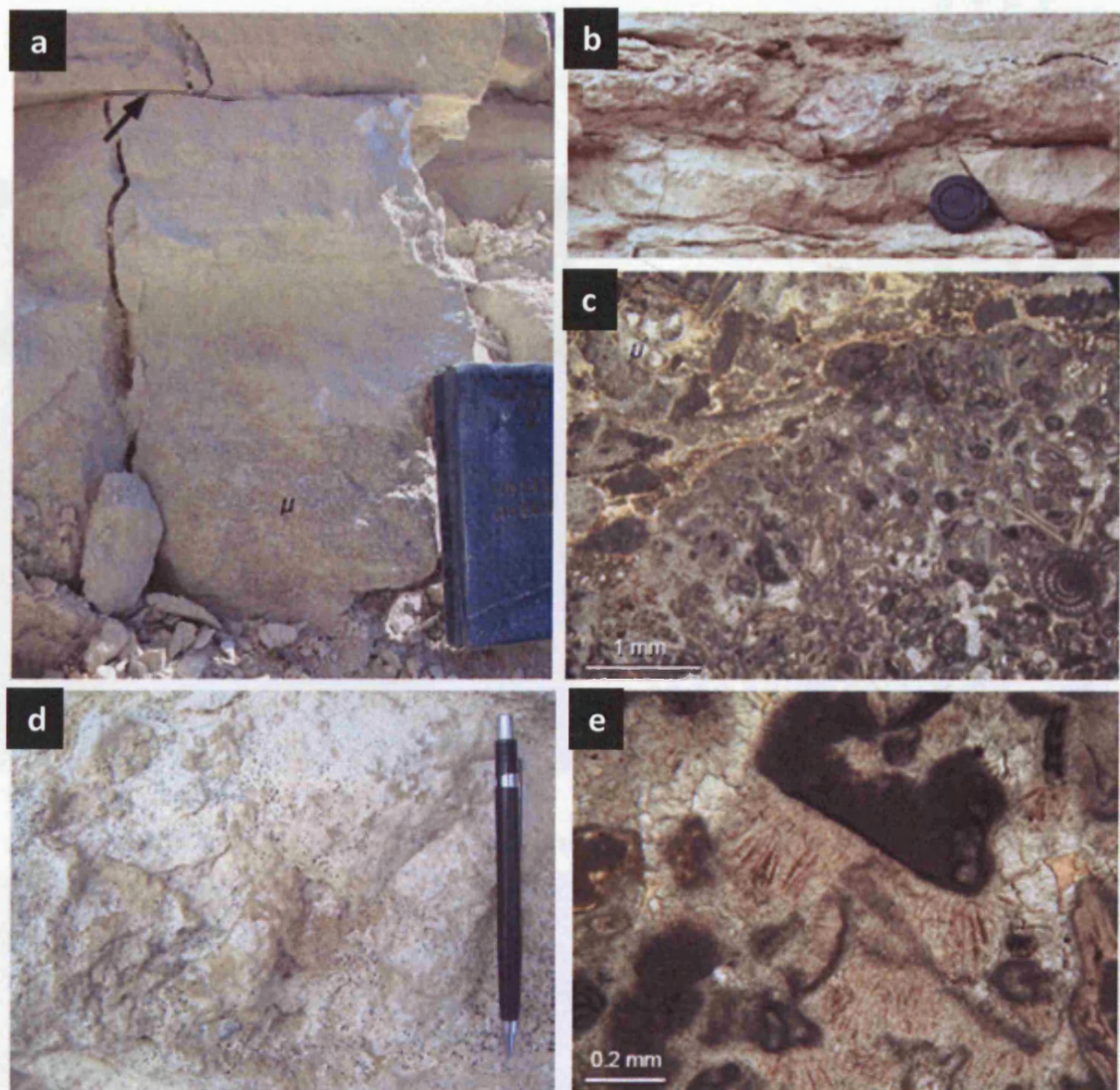


Figure 6.25: Sub-aerial exposure features of the SDP section. surfaces of S Dvina-Pinega: a) - Unconformity above Hfs 2 with planar low-relief karstic surface (arrowed) and no macro-scale alteration other than subsurface *Microcodium* (μ) layer; unconformity is overlain by lithoclastic calcarenite with blackened lithoclasts. Notebook is 15 cm tall. b, c) From Hfs 2 sub-aerial exposure surface: (b) outcrop appearance of basal lag composed of angular, abraded lithoclasts; lens cap 6cm in diameter; (c) micritic crust of vadose cementation from the unconformity surface in thin section, overlain by a compacted grainstone with an absence of root or other pedogenic calcrete structures in the underlying sub-aerially cemented grainstone; d, e) Hfs 7 unconformity; (d) brown vadose cement, plan view, pencil 15 cm long. e) extensive gravitational pendant cement forming brown rinds on d; the yellow colour possibly represents by inclusions of Fe^{3+} .

clay that primarily occurs as thick (~2cm) seams. These horizons occur at up to one metre below each unconformity. These clays have previously been interpreted as having a non-sedimentary, weathering-crust origin (Kabanov, 2005).

6.4.3 Stratigraphic simulation of high-frequency sequences

The margin of error for simulations addressing the SDP sections was modified to reflect the lower average cycle thickness. Margins of 2m (55% deviation from average cycle thickness), 1m (27%) and 0.5m (14%) were used. Numerical forward modelling of eustatic oscillation amplitude parameters resulted in development of a number of simulations that show an excellent match with the SDP section (12.5% error; Figure 6.26). However this occurs at a range of parameters which are dichotomously opposed to findings presented here (compare with Figure 6.11). Specifically, the best section matches occur at very small high- and intermediate-order amplitudes (approximately 10m for both). These values are also unrealistic given sedimentary evidence of amplitudes of intermediate-order oscillation in ice-house periods (e.g. Heckel, 1986).

Although modelling suggests that with increasing high-order amplitude more good matches can be generated, this only reflects the fact that with larger high-order oscillations fewer high-order missed beats are recorded. These oscillations are more likely to only briefly submerge the platform, consequently accumulating a relatively small thickness of sediment. There is therefore a large chance that one of these high-order oscillations will match a thin cycle from the sedimentary section.

Although this mechanism of brief flooding should not be rejected as a method of generating cyclicity on a slowly subsiding platform, it does not correspond with either estimates of sea-level amplitudes in contemporary studies (e.g. Lehrmann & Goldhammer, 1999) or those presented here. Specifically, modelling studies suggest that high-order oscillations are best interpreted as a relatively minor component in dictating sedimentary style and stacking patterns (section 5.6). Furthermore, these simulations, although displaying good matches are characterised by a style of cyclicity comparable to Figure 6.15 where very thin cycles are separated by much thicker cycles. This stacking pattern is not comparable with the SDP section, where cycles are consistently very thin. The good matches are therefore the result of these thin cycles skewing the results, but they exist in sections display a consistently dissimilar style of cyclicity to the SDP section. In light of this, it is likely that the trend in Figure 6.26 of increasingly good matches with increasing high-order amplitude is more likely to be an artefact of the modelling technique than a viable method of producing cyclicity.

Model runs incorporating subsidence as the major variable also have significant difficulty replicating the SDP section, except at very small amplitudes of inter-mediate-

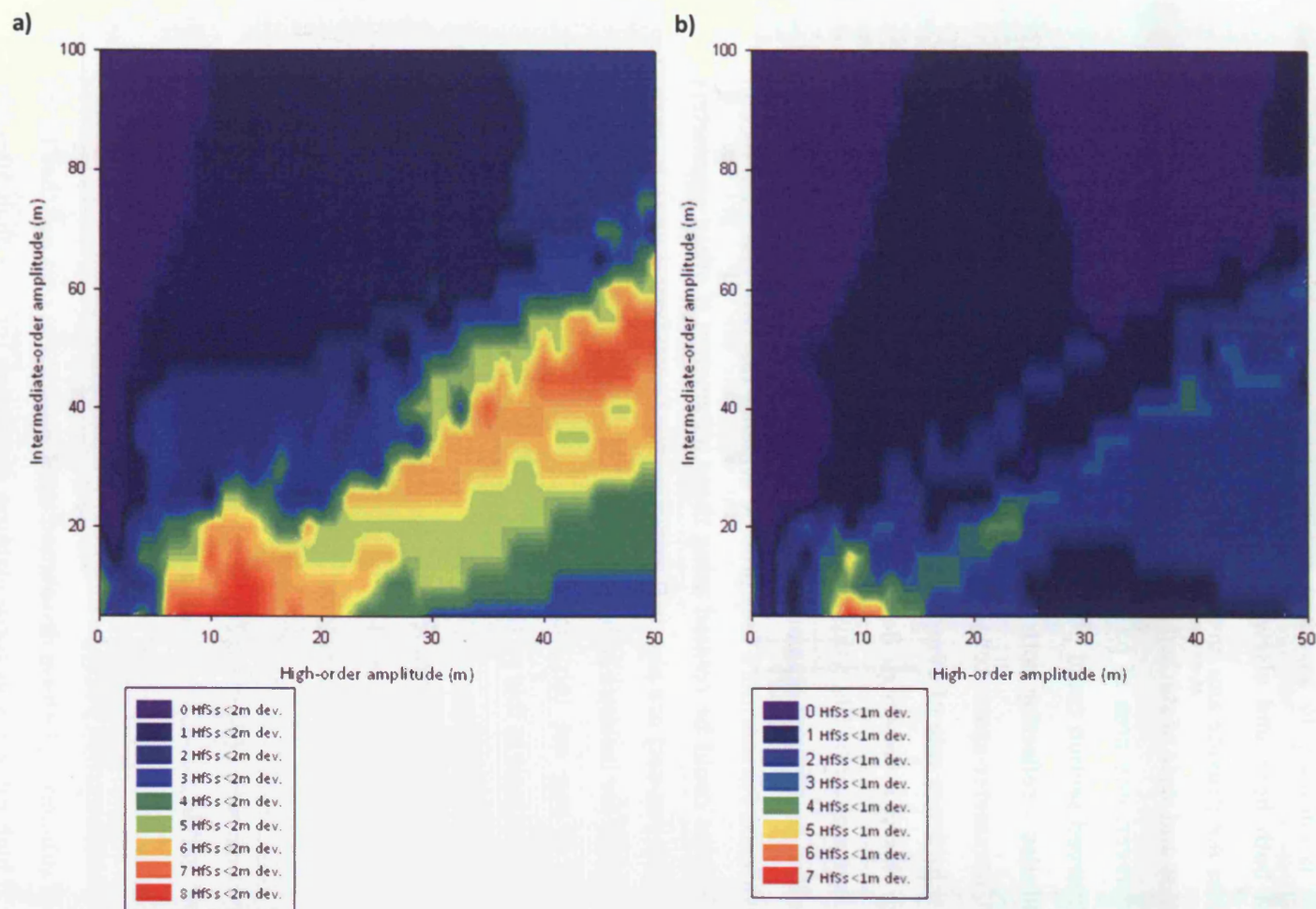


Figure 6.26: Parameter-space response surface plot comparing HfSs generated by simulations with HfSs in the observed SDP section. Eustatic amplitude is the major variable. Note the different scales. a) Response surface with a 2m margin of error. b) Response surface with a 1m margin of error. Simulations show excellent correlation with the SDP section (87.5% correlation). The best section matches occur at very small high- and intermediate-order amplitudes. These values are unrealistic given sedimentary evidence of amplitudes of intermediate-order oscillation in ice-house periods (e.g. Heckel, 1986). They reflect an artifact caused by the recording of short-wavelength high-amplitude high-order oscillations; an effect which increases the greater high-order amplitude becomes.

order oscillation (less than 40m; Figure 6.27). The cause of this trend lies in the limited accommodation generated at small amplitudes of sea-level oscillation; at higher amplitudes thicker sequences of sediment are deposited per cycle, thus increasing the deviation from observed thickness at SDP. This, however, does not reflect sedimentary evidence and again is contrary to assumed eustatic sea-level behaviour in ice-house periods, as argued both here and elsewhere. In this context, modelling of different subsidence rates does not provide any further information as to the role of subsidence in dictating the thickness and style of stacked cycles.

There is however, one area of parameter-space which does indicate that good-matches for the observed section could potentially develop at low subsidence rates and high eustatic amplitudes – reflecting both forward modelling and sedimentary evidence (Figure 6.27; x). A parameter-space zone centred on an intermediate-order amplitude value of 60m and subsidence rate of 20m/My shows a 80% error of HfSs to within 14% deviation. Although this is a very high degree of error, comparison with a 27% error-boundary shows a match of 50%. While this does not compare to the 50% match at 14% of error shown by the best matches, these parameter values are in line with other modelling and sedimentary evidence. Furthermore they provide evidence that SDP-matching section in terms of HfS thickness could be created using these parameters if other parameters (which are static in this run-set) are also varied. Lower production rates, or higher sub-aerial erosion rates, could for instance reduced HfS thickness and could potentially create more good matches. A run set incorporating these low-subsidence high-amplitude parameters is investigated later in this section.

Results of runs investigating euphotic calcium carbonate production also suggest that with increasing high-order amplitude more good matches can be generated. Again, this does not compare with how sea-level oscillations are thought to operate, and is not thought to be a viable mechanism for generating cyclicity. Results are skewed by this to low-amplitudes of intermediate-order oscillation; a parameter-space zone that promotes the development of thin cycles (Figure 6.28). What these results do indicate, however, is that there is preferential development of good matches at production rates above 700m/My. This is in-line with modelling studies of the FC section, and comparable with estimates of production in ancient platform interiors.

Modelling of sub-aerial platform dissolution rates suggest the best matches to the SDP section occur at high rates of sub-aerial platform dissolution (greater than 40m/My; Figure 6.29). The sedimentary evidence does not wholly support these high rates of sub-aerial erosion. Such a high rate of denudation is likely to result in extensive high-relief karstic surfaces and well-developed soil profiles developed in a very humid (possibly monsoonal climate; Wright, 1994), which are not present at the SDP section. In the

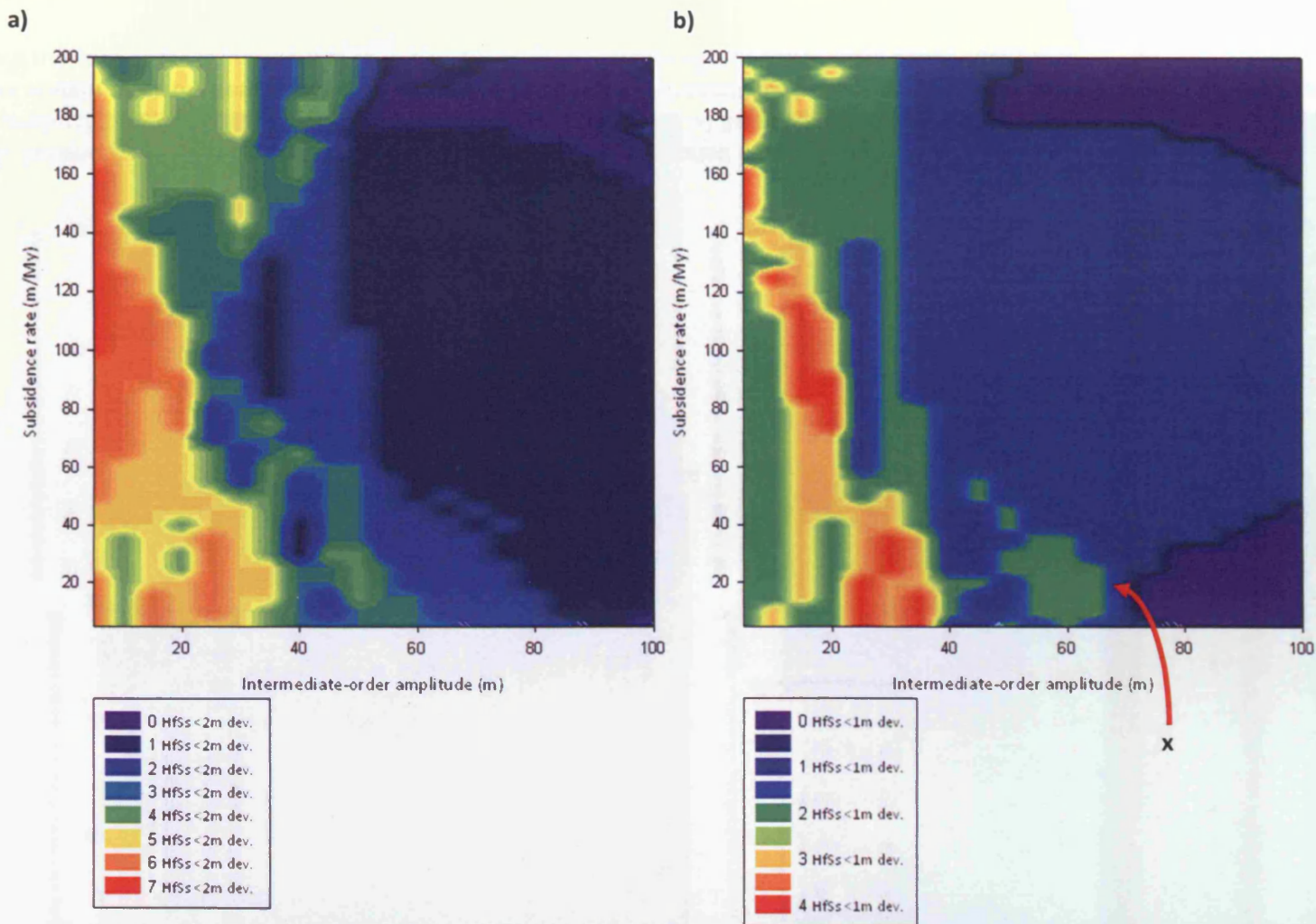


Figure 6.27: Parameter-space response surface plot comparing HfSs generated by simulations with HfSs in the observed SDP section. Subsidence rate is the major variable. Note the different scales. a) Response surface with a 2m margin of error. b) Response surface with a 1m margin of error. Model runs incorporating subsidence as the major variable also have significant difficulty replicating the SDP section, except at very small amplitudes of inter-mediate-order oscillation (less than 40m). This is a result of the limited accommodation generated at small amplitudes of sea-level oscillation; higher amplitudes result in thicker sequences of sediment being deposited per cycle; increasing the deviation from observed thickness at SDP. x) Shows a zone of relative good matches around which the simulations in Figure 6.30 focus.

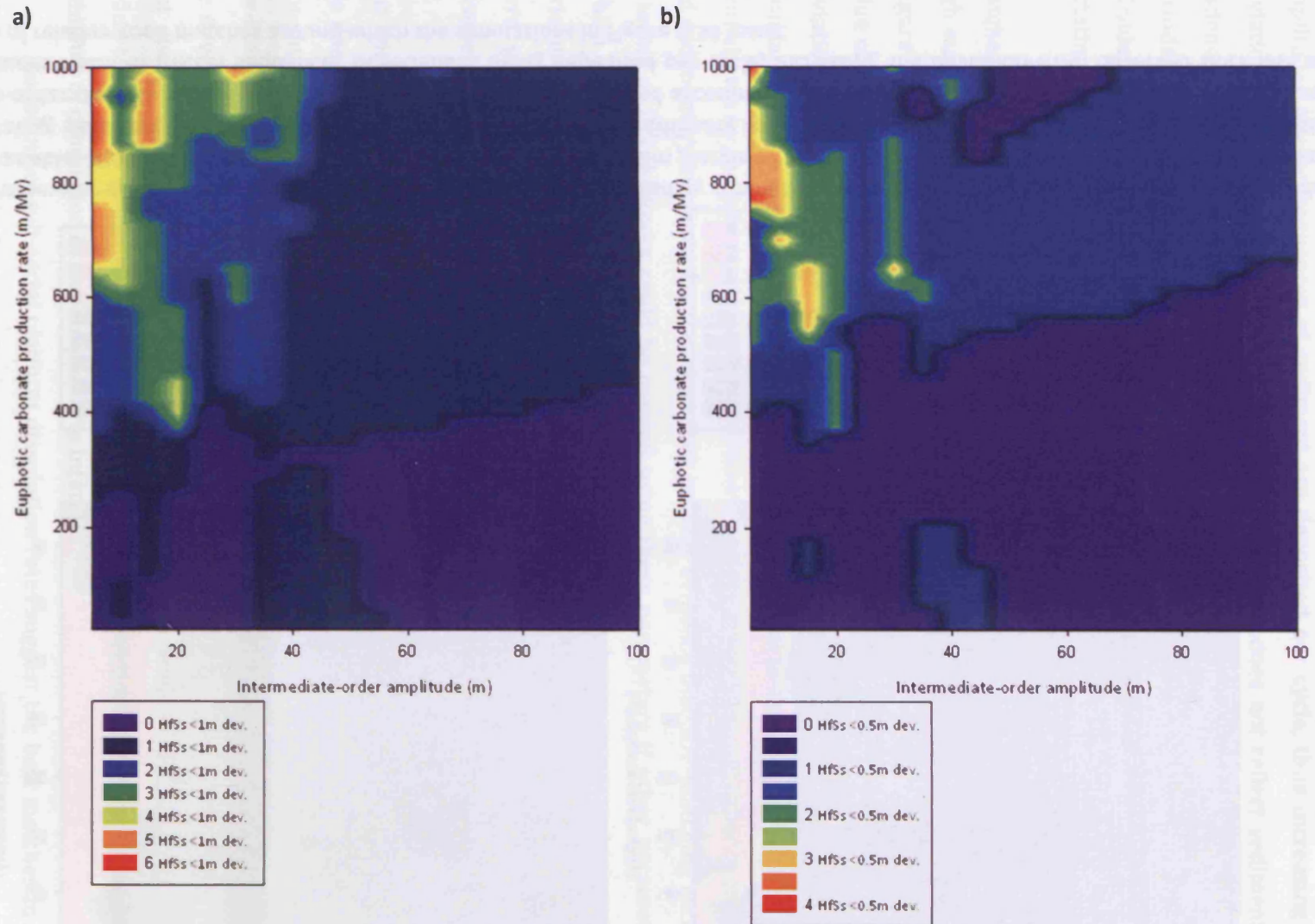


Figure 6.28: Parameter-space response surface plot comparing HfSs generated by simulations with HfSs in the observed SDP section. Euphotic carbonate production rate is the major variable. Note the different scales. a) Response surface with a 1m margin of error. b) Response surface with a 0.5m margin of error. Results are skewed to low-amplitudes of intermediate-order oscillation by the same artefact which affects the previous two run-sets. There is preferential development of good matches at production rates above 700m/My.

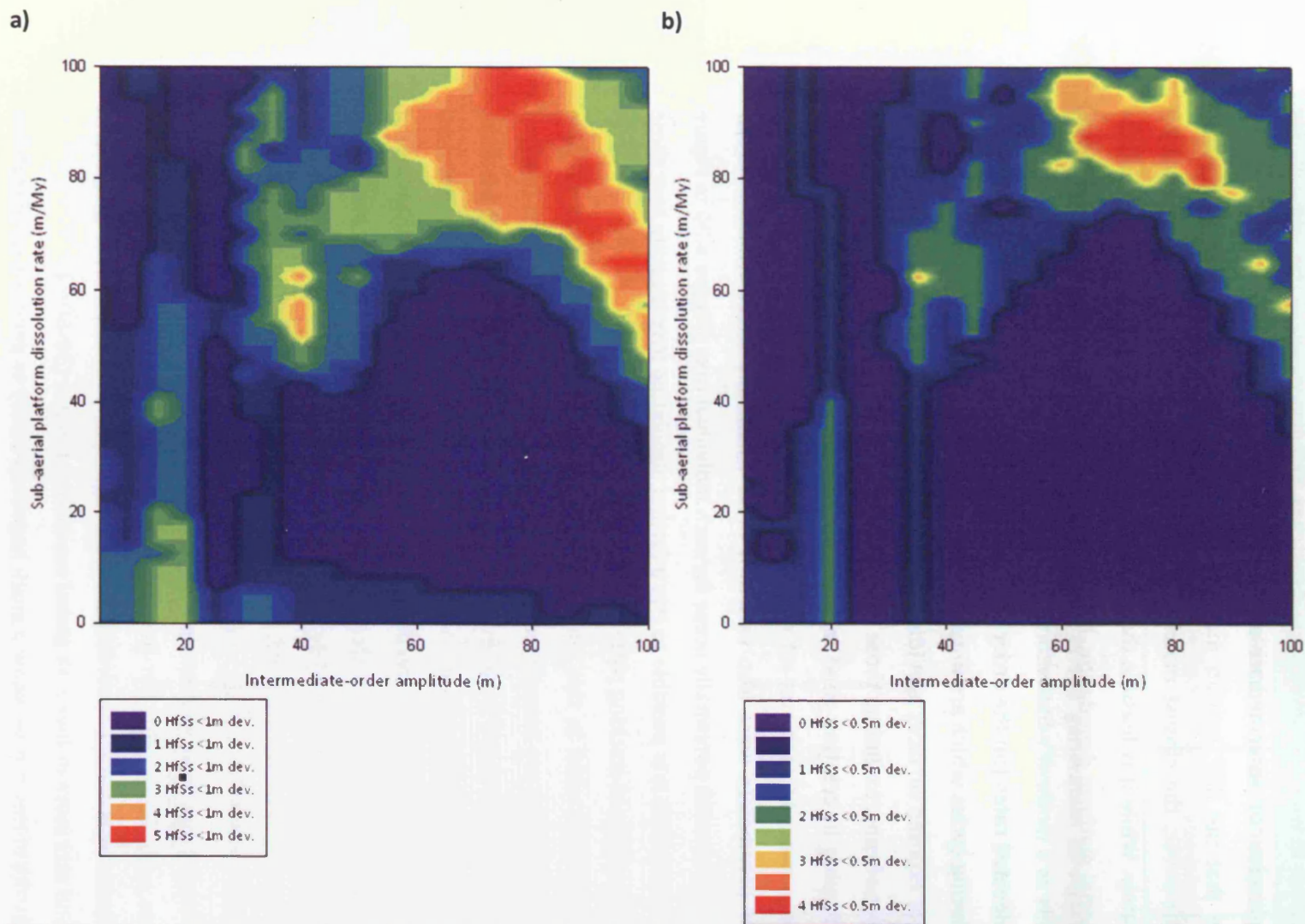


Figure 6.29: Parameter-space response surface plot comparing HfSs generated by simulations with HfSs in the observed SDP section. Sub-aerial platform denudation rate is the major variable. Note the different scales. a) Response surface with a 1m margin of error. b) Response surface with a 0.5m margin of error. Modelling of sub-aerial platform dissolution rates suggest the best matches to the SDP section occur at high rates of sub-aerial platform dissolution (greater than 40m/My).

simulated sections, good matches are prevalent at high rates of denudation as they trim the thick cycles produced by large-amplitude oscillations. There is consequently a greater amplitude window in which to develop good matches. The occurrence of the best matches at high amplitudes of intermediate-order oscillation would seem to support an interpretation that the SDP section may have resulted from an interaction of these parameters. However, the closest match only represents 50% of the HfSs in the SDP section accurately. While it is feasible that the SDP section could be generated with high-rates of sub-aerial platform denudation, lack of extensive meteoric diagenesis would seem to preclude this as a mode of genesis for the stacking patterns. Nevertheless, it is feasible that slightly elevated rates (on the order of 20m/My) of dissolution could potentially be a factor in producing cycles which are unusually thin; the unequivocal evidence of low-relief karstification of exposed surfaces is evidence of at least some platform lowering.

Each set-of runs, excluding those that address euphotic carbonate production, has significant difficulty in creating good matches for the SDP section. There are, however, parameter space zones in each run-set which may have the potential to provide a good match if other parameters were also varied. If these conditions under which a similar sedimentary section could potentially occur for each individual case (Figure 6.26 to Figure 6.29) are combined, then it is possible to run a further simulation investigating how these factors interact in terms of stacking patterns.

The parameters used in this run set are shown in Table 6.2. The non-variable parameters are those that are interpreted as comparatively well constrained as a result of numerical modelling presented here: euphotic production rate and sub-aerial platform denudation rate. These have been modified from the rates used in the standard simulations (500m/My and 0m/My respectively, to 700m/My and 20m/My. In the case of euphotic production rate there is a clear preferential development of good matches at rates of 700-800m/My. For sub-aerial denudation the rate was raised slightly to reflect the fact that erosion undoubtedly occurred, but at an unquantifiable rate. The two variables used are intermediate-order eustatic oscillation amplitude and subsidence rate; the two parameters that are the least well constrained after simulations. Subsidence parameters were varied in accordance with the tectonic setting of the basin (10-50m/My), whilst eustatic amplitude was varied according to the range which could potentially create a good match, and was more in-line with global sea-level estimates (30-60m).

The results of this run set show a much improved ability to generate good matches with the sedimentary section (up to 87.5% correlation at 27% deviation). There are two main loci of good matches within parameter space; a low-subsidence group and a 'high'-subsidence group (Figure 6.30; a and b respectively).

Static Parameter	Value	Variable	Value range	Increment
Euphotic production rate	700m/My	Intermediate-order amp.	30-60m	2.5m
Sub-aerial platform denudation rate	20m/My	Subsidence rate	10-50m/my	2.5m/my

Table 6.2: Static parameters and variables used in the generation of Figure 6.30. Static parameters noted are only those changed from the standard values.

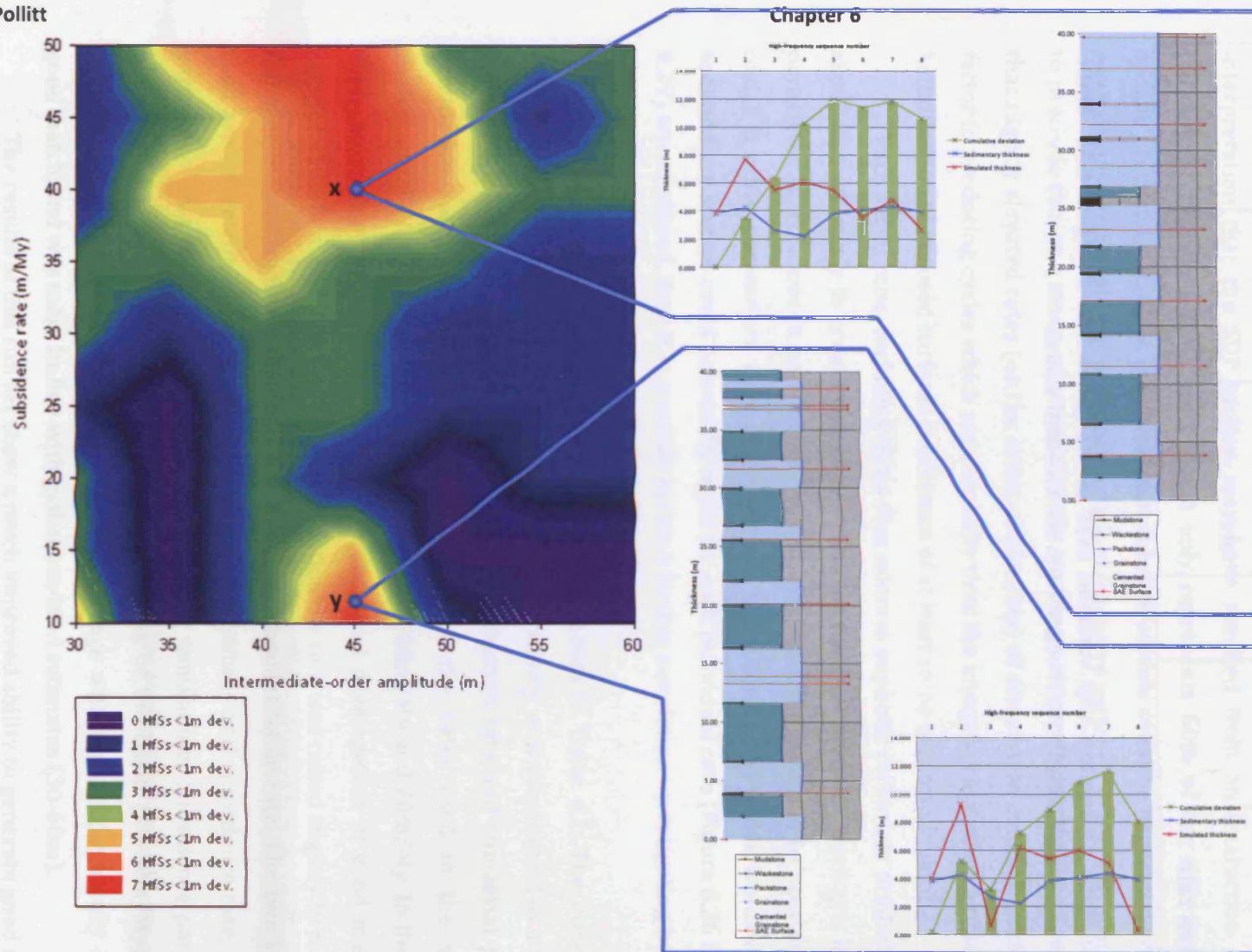


Figure 6.30: Parameter-space response surface plot comparing HfSs generated by simulations with HfSs in the observed SDP section. Subsidence rate is the major variable. Surface has a 1m error catchment. In addition to the variables, these runs employ a static euphotic production (700m/My) and sub-aerial erosion (20m/My) parameter. The modification of these two variables allows very good matches with the SDP section to be created (points x and y; 87.5% correlation). Simulated sections developed at these low subsidence scenarios are similar to those observed in the SDP section.

Both groups show HfS thicknesses broadly comparable with those observed in the SDP section. Counter-intuitively, the high-subsidence group shows better correlation in terms of lithofacies thickness, generating slightly thinner cycles. In addition, the lithofacies distribution in both groups is comparable with the SDP section; but again, the high-subsidence group shows the better match with the observed succession. The lithofacies association is mainly shallow-water packstones and grainstones, but is punctuated by intervals in which deeper-water existed, leading to the deposition of mudstones. It is feasible to expect that a combination of these two zones could operate at different times to create one composite section.

As it stands, numerical modelling suggests that it is possible to generate a similar section to the SDP at subsidence rates that are supported by sedimentary evidence. A slightly elevated rate of sub-aerial platform dissolution also seems likely. Furthermore, the extremely high-amplitude eustatic oscillations, characteristic of ice-house periods, are not precluded by this model (as the thin cycle thickness may suggest) but are ultimately necessary to create the cyclicity.

These simulations do not recreate the SDP section perfectly; they are founded on simple assumptions, and to expect them to do so would be unrealistic. However, they do show that broadly comparable HfS thicknesses, stacking patterns and lithofacies distributions can be reproduced with a 1D model. The ability of the model to produce the demonstrated level of match by changing the values of only two parameters is an important result because it suggests that despite the apparent complexity of the outcrop section, basically simple processes might account for a high proportion of the observed complexity. Although the sections produced in Figure 6.30 are probably not developed at sea-level amplitudes appropriate for ice-house periods, it is an important point that relatively simple changes in parameters can result in combinations which result in good matches for the observed sedimentary section. It is feasible that further refinements to variables not addressed here (e.g. oligophotic carbonate production, sub-marine erosion, eustatic oscillation asymmetry) could result in better matches to the observed section.

The potential permutations of parameters are significant, and may change substantially over the million-year timeframe it takes to deposit a sedimentary section. Given the vast numbers of potential variables, in this case it has not been possible to constrain them further. It is also highly likely that the uncertainties shown to be endemic in the interpretation of the sedimentary record (e.g. Burgess, 2006) could serve to deviate the observed section from the deterministic numerical model.

6.5 INTERPRETATION

6.5.1 Evaluation of controlling parameters on stacking patterns

There are several conclusions which can be drawn from the numerical forward modelling of the FC and SDP sections. The first, and perhaps most important, finding is that there must be some level of repetitive behaviour in terms of relative sea-level to induce the repetitive sub-aerial exposure, and therefore cyclicity, seen in these sections. Furthermore, this is most likely to be derived from eustatic oscillations of sea-level; there is no other mechanism operative in either setting which could generate the sub-aerial exposure which defines the cycles. The peritidal facies which typify greenhouse cycles and conceivably create repetitive sedimentary successions through autocyclicity (e.g. Ginsburg, 1971) are notably absent. Although a solely tectonic mechanism has recently been advocated as a means of forcing cyclicity (de Benedictis *et al.*, 2007), the relatively quiescent intra-cratonic setting and lack of normal faults with the necessary displacement would in both cases rule this out. This would suggest that the only known mechanism capable of generating these cycles is high-frequency, climatically-controlled glacio-eustasy.

In addition, numerical forward modelling of both the FC and SDP sections indicates that a high amplitude of intermediate-order eustatic oscillation is the most likely to have generated a section of similar style to the observed successions. Modelling comparisons with the FC section constrain this parameter best, and indicate that an amplitude of 60-80m and a period of 112ky creates the most appropriate matches to the FC section. This range of values is in-line with contemporary estimates of intermediate-order oscillation amplitudes, derived from both modelling and sedimentary evidence (Heckel, 1986; Lehrmann & Goldhammer, 1999; Barnett *et al.*, 2002). It is also supported by findings presented here (section 4.5).

Through comparison of the simulations of the two studied sections it is apparent that whilst glacio-eustasy is probably fundamentally responsible for the creation of the sedimentary cyclicity it does not represent the only control on cycle style. Were this to be the case, then the two successions would show more similarity than they actually do. A cursory comparison of cumulative thickness and also mean parasequence thickness highlights the difference between the two sections. If eustatic sea-level dictated cycle style, the two sections would be noticeably more similar. Stacking patterns, in this case at least, must also be determined by other, non-eustatic controls.

Modelling suggests that euphotic carbonate production occurred at similar rates in each succession and is not thought to be a major source of differentiation between the two sections. Sub-aerial platform denudation, although likely to have occurred at slightly different rates in the two areas, is expected not to have enough effect to cause the thickness, and therefore stacking, differences in the two sections. Of the investigated parameters, only subsidence remains and it is feasible that this is the source of the dissimilarity between FC and SDP.

Simulations suggest that the FC section is best modelled using relatively high rates of subsidence for an intra-cratonic basin. Under these conditions the simulations show the best matches to the studied section. This is supported by sedimentary evidence, which suggests that during deposition of the Gobbler Formation subsidence occurred at a significantly elevated rate above the average Pennsylvanian-Permian rate 40m/My (Algeo *et al.*, 1992). The up-to-300m thick BSLM is testament to this. This puts the rate of lower rate of 80m/My suggested by forward modelling well within the range of possibility. Conversely, simulations of the SDP section show that similar successions can be created at low rates of subsidence when combined with specific other conditions. The rate of 10-45m/My is also supported by evidence from the Moscow-Mezen basin, which in the Moscovian was relatively quiescent.

It seems likely that this disparity in subsidence rates represents the major cause of divergence in style of stacking between the two sections. This echoes the findings of studies which similarly suggested that subsidence represented the major control on peritidal parasequence thickness (Burgess *et al.*, 2001). The accommodation difference effected by the subsidence rates is likely to represent the fundamental control. Although there must be a repetitive mechanism in place to generate the sedimentary cyclicity, the glacio-eustatic forcing does not serve to create different stacking patterns in geographically distant basins. Modelling therefore suggests that subsidence rate is the ultimate control on the thickness of HfSs. The studied section may therefore be best described as tectonically-modulated glacio-eustasy.

This is particularly important for the development of ice-house petroleum reservoirs: crucially, the salient forcing mechanism for stacking patterns is not the amplitude of glacio-eustasy but the subsidence regime of the basin. It seems likely that it is the subsidence regime which will dictate the thickness of sedimentary cycles and therefore the spacing of reservoir-prone facies within each HfS (discussed further in section 6.5.3).

6.5.2 Assessment of the presence of a sedimentary hierarchy

The quantitative definition of a hierarchy from section 4.1.3 states that: “a hierarchy is a series of sedimentary cycles, either parasequences or high-frequency sequences, each bounded by sub-aerial unconformities, in which there exist at least two discrete groups in terms of thicknesses... The opposite case would be a continuum of cycles, with no grouping apparent in the thicknesses.” The SDP section does not meet the criteria of this definition, and although in the FC section there are outliers in terms of cyclothem thickness (minimum thickness of 3.6m, maximum of 17.2m, average thickness of 9m) no discrete thickness groups indicative of a hierarchy are apparent. So, although a definitive judgement on this is perhaps not possible from the sedimentary sections, model simulations of the two sections can provide insight into the likelihood of a hierarchy.

Numerical forward modelling of both the FC and SDP sections suggests that high-frequency glacio-eustasy occurred during deposition, and moreover, is the only currently known way in which to generate the repeated sub-aerial exposure characteristic of the sections. However, modelling also indicates that if two eustatic oscillations were operating in conjunction, then HfS thicknesses and stacking patterns deviate significantly from the observed sections. It is only when one component dominates, and the remaining oscillations are of negligible amplitude that good-matches for HfS thickness are created (Figure 6.11). If two or more oscillations are of sufficient amplitude to affect deposition and non-deposition, then the modelled sections cease to bear resemblance to the studied sections. These however, are precisely the conditions that are a prerequisite for the generation of a sedimentary hierarchy. In this context the two things are mutually exclusive; a sedimentary hierarchy or a relatively realistic section can be generated, but not both. This outcome of the modelling is in line with conclusions drawn from Chapters 4 and 5, conclusions which also suggest that a sedimentary hierarchy is extremely unlikely and that sedimentary stacking in the Honaker Trail section, Utah, are likely to be the result of an interplay between one eustatic component of high-amplitude and tectonic subsidence.

Durbin-Watson analysis of the model simulation also highlights the fact that the majority of runs generate a sedimentary section in which the cycle thickness stacking pattern is indistinguishable from random (Figure 6.31). This statistical method specifically shows that each HfS thickness is independent in terms of thickness from the last. This does not satisfy the fuzzy definition of what constitutes a sedimentary hierarchy (e.g. Goldhammer *et al.*, 1991) and it certainly does not meet the more rigorous definition provided in section 4.1.3. Furthermore, it raises the question that if simulated successions generated by an entirely deterministic numerical model of simple glacio-eustatic periodic forcing are shown to be indistinguishable from random, how can the sedimentary record

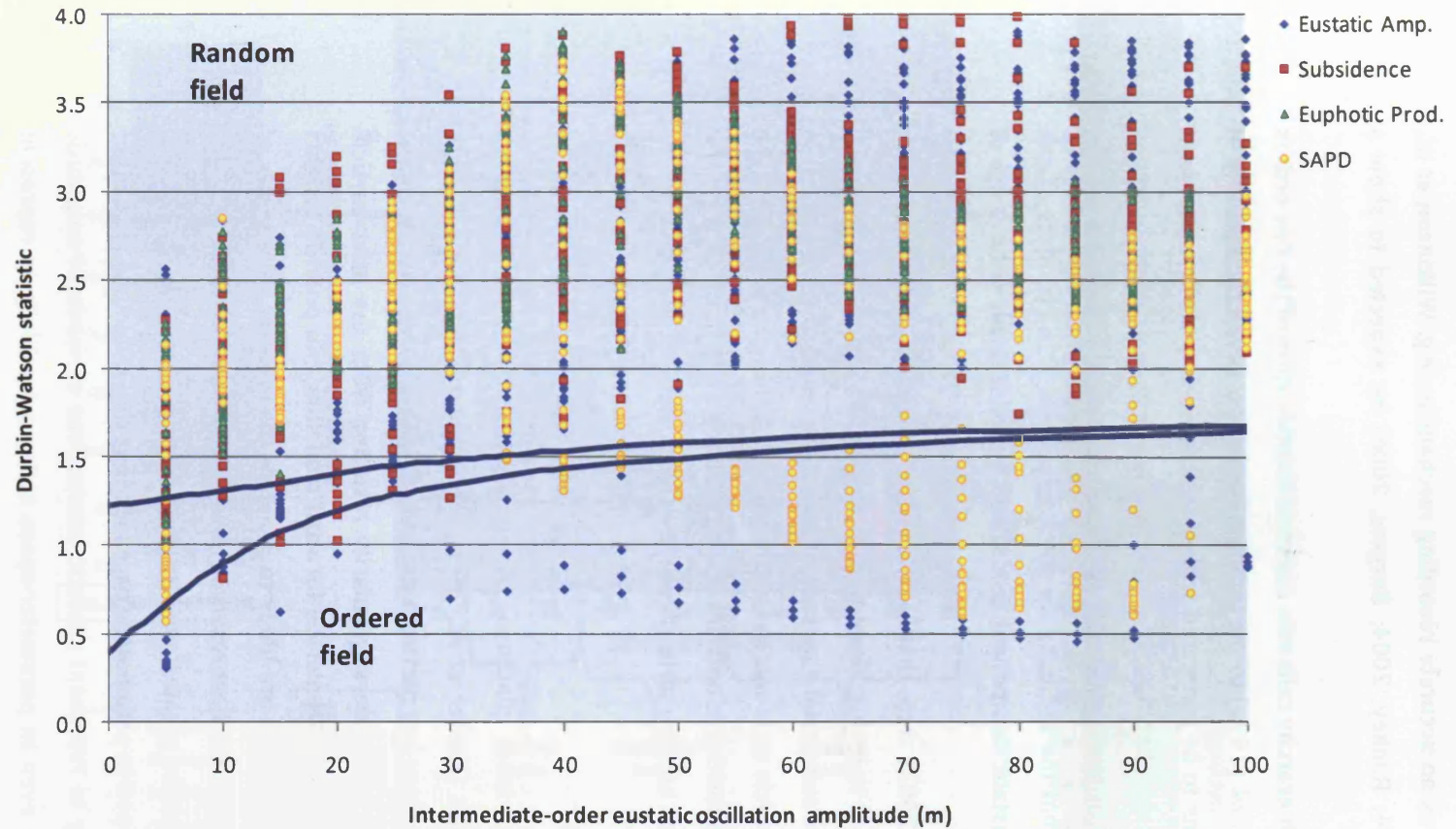


Figure 6.31: Plot of the Durbin-Watson statistic for all simulations outlined in Table 6.1. The plot shows that the overwhelming majority of runs generate a sedimentary section which is indistinguishable from random. This statistical method specifically shows that each HfS is independent in terms of thickness from the last. It is difficult to infer a hierarchy where each HfS has a thickness independent of the last, thus not forming trends. SAPD = Sub-aerial platform denudation. Runs addressing eustatic amplitude which plot in the ordered field represent interactions of very low amplitude sea-level oscillations (5-10m high- and intermediate-order) which generate similar-thickness cycles throughout a run. SAPD runs plotting in this field are the result of very high rates of sub-aerial denudation (<60m/My) which has the same effect.

(demonstrated to be dubious as an accurate recording mechanism; e.g. Wilkinson *et al.*, 2003; Burgess & Emery, 2004; Rankey, 2004; Burgess, 2006) be expected to show a greater degree of order?

The apparent lack of a hierarchy calls into question identification of the two orders of cyclicity invoked by Algeo *et al.* (1992) in the Gobbler Formation. Given the inability of appropriately-matching sections to be generated with more than one eustatic component of significant amplitude, it seems likely that the identification of two orders of cyclicity (inferring therefore the effect of two significant amplitude eustatic components) is not appropriate. It is more likely that the sedimentary stacking pattern is the product of one significant amplitude glacio-eustatic component modulated by the tectonic subsidence of the basin.

Similarly, Izart *et al.* (2003) state that “eustacy [sic] controlled sedimentation in the Moscow Basin.” Although it is highly likely that in most cases glacio-eustasy is the fundamental cause of repetitive sub-aerial exposure of carbonate, modelling suggests that the most important control on cycle style was in fact subsidence. Although eustasy dictates the presence or not of cycles, subsidence and the accommodation created as a result of it ultimately control sedimentation and the style of cyclicity produced.

6.5.3 Reservoir Implications

Stacked cyclothems of inner platform ice-house carbonates form important components of major reservoirs (Kenter *et al.*, 2006). The quantity and proportion of grainstone lithofacies in a cyclothem has particular importance, as it is the lithofacies with the best porosity-permeability parameters (primarily resulting from the inter-particle porosity in grain-supported textures). Numerical forward modelling can provide insights into the parameter-space locations that are likely to generate the greatest thicknesses of grainstone lithofacies and therefore the best reservoir properties.

Figure 6.32 suggests that the greatest average thickness of grainstone per HfS and averaged over a run are developed in parameter-space locations that modelling (and other studies) indicate are not likely to represent realistic interactions of sea-level amplitude and subsidence. Nevertheless, even in parameter-space zones more likely to represent realistic combinations of parameters, there are areas that show the potential to generate increased thicknesses of grainstones. This effect is most prominent at moderate rates of foreland basin subsidence (170-190m/My), where average grainstone thickness per HfS per run reaches 2.4m; a metre more than at subsidence rates of 140-160m/My. Although the grainstone thickness difference between simulations is relatively small, it is worth noting that these values are averaged over an entire section. The increase is simply the result of interactions between amplitude of sea-level oscillation and subsidence rate

combining to produce periods of sedimentation that predominantly occur in the euphotic zone, creating grainstones.

Increased grainstone thicknesses are also evident at lower subsidence rates of 110-140m/My, but to a lesser extent (2.1m average per HfS per run); the result of a less favourable interaction of eustatic amplitude and subsidence towards thicker grainstone production.

Sedimentary stacking patterns in these areas of increased subsidence are comparable with that seen in both outcrop and subsurface reservoirs. Grainstone lithofacies mainly occurs as one bed of significant thickness per HfS, and is located at the top of the HfS. Consequently, the greatest bed thickness developed per HfS also has important bearing on the potential reservoir quality of sequences in a given parameter-space zone.

Increased average grainstone thickness is supported by results of modelling of the greatest individual bed thickness per run (Figure 6.33). However, in contrast to the plot of average thickness per HfS per run, greatest individual bed thickness shows that the lower subsidence rate of 110-140m/My has a similar potential to create the greatest single grainstone beds, in comparison to the higher rate of 170-190m/My. So, although there is less grainstone generated in a sedimentary section created at a lower-rate of subsidence, there is still potential to develop significant individual grainstone beds.

Modelling of grainstone thicknesses therefore suggest subsidence rates comparable to moderately to rapidly subsiding extensional basins and moderately subsiding foreland basins will generate the greatest thicknesses of grainstone.

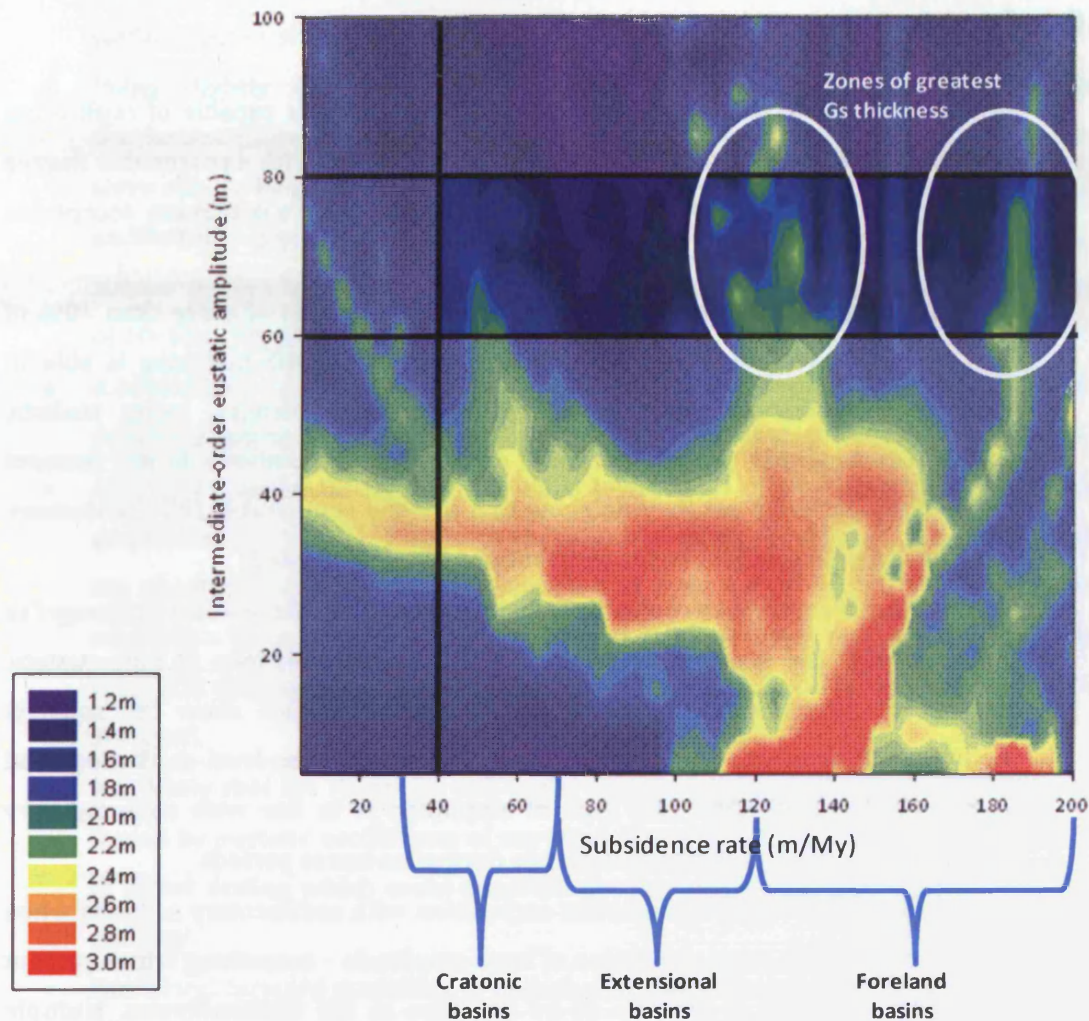


Figure 6.33: Parameter-space response surface plot of the greatest single bed thickness of grainstone lithofacies per run. Subsidence rate is the major variable. The shaded area represents zones of parameter-space which are not interpreted to represent realistic interactions of subsidence and intermediate-order amplitude based on numerical forward modelling. High-subsidence rates (above 150m/My) are included based on modelling results from Chapter 4. The results show that the greatest bed thicknesses of grainstone are developed in the same parameter-space locations as Figure 6.32. It is notable that in terms of greatest single bed thickness a subsidence rate of 100-140m/My shows a much more prominent response than it does in terms of average thickness per Hfs per run; suggesting that even though average thicknesses are not as significant as at higher rates, considerable individual thicknesses are still developed.

6.6 CONCLUSIONS

- A simple one-dimensional numerical forward modelling is capable of replicating observed sections comprising different stacking patterns with a reasonable degree of success (up to 87.5% of cycle thicknesses matched for a maximum acceptable 10% deviation from individual cycle thickness).
- Critically no simulation manages to replicate the thickness of more than 70% of HfSs in the FC section. It is encouraging however that HfS-matching is able to replicate a significant number of high-frequency sequences, using realistic parameters, to within a small margin of error. These simulations do not recreate the sections perfectly yet they do show that broadly comparable HfS thicknesses, stacking patterns and lithofacies distributions can be modelled.
- Simulations attempting to replicate cyclicity in both New Mexico and Arkhangel'sk Oblast display the greatest correlation with observed sections at high-eustatic amplitudes. Simulations addressing the FC section (which show the smallest model-matching errors) suggest it is likely that eustatic sea-level oscillations had an amplitude of 60-80m. This type of amplitude is in line with contemporary sedimentary evidence of sea-level change during ice-house periods.
- Simulations also display the greatest correlation with sedimentary sections when there is only one eustatic oscillation of large amplitude – something which current knowledge suggests is unlikely to be the case in the Carboniferous. Multiple eustatic components of similar amplitude but differing wavelength serve to increase the deviation from the observed section. This tends to agree with results from modelling of sea-level behaviour in Chapters 4 and 5.
- In the FC section, modelling suggests subsidence occurred at a rate of 80-130m/My. It is feasible that the FC section was developed at the lower limit of this range. This rate would be in line with sedimentary evidence and the intra-cratonic setting of the Orogrande Basin (given the elevated subsidence rates demonstrated from the Pennsylvanian).
- Modelling of euphotic production rates for both the FC and SDP sections show greatest correlation with the observed section at rates of 700-800m/My. These rates are lower than estimates of production for modern shallow-water frame-building organisms, but given the inner-platform setting, may not be unrealistic.
- Sub-aerial platform denudation is predicted to have negligible effect in the FC study area. Lowering of the platform surface is predicted by modelling to be of greater importance in the SDP section; a tentative estimate would predict slightly

elevated rates (from those quoted from comparable successions) of approximately 20m/My. This elevated rate is possible given the nature of the sub-aerial exposure surfaces in the study area.

- Using slightly elevated rates of sub-aerial erosion and euphotic carbonate production (20m/My and 800m/My respectively) good matches to the SDP section were able to be generated at low subsidence rates and high amplitudes of eustatic oscillation – parameters which are in line with other evidence. This suggests a similar section to the observed SDP succession could be create at subsidence rates of 10-45m/My and eustatic amplitudes of 45-60m.
- A subsidence rate of 10-45m/My is in-line with estimates for basin subsidence in a relatively quiescent intra-cratonic basin such as the Moscow-Mezen Syncline.
- Although 45-60m eustatic amplitude is lower than other estimates of oscillation amplitude, it is feasible that, with variations to other parameters, good matches to the observed section could be generated at even higher amplitudes of sea-level oscillation. Generation of SDP-style sections at moderately high amplitudes shows very thin sedimentary cycles can be created under relatively large oscillations of sea-level.
- It is likely that the repetitive sub-aerial exposure surface seen in both section are forced by eustatic oscillations of sea-level; there is no other mechanism operative in either setting which could generate the sub-aerial exposure which defines the cyclicity.
- Numerical forward modelling of both the FC and SDP sections indicates that a high amplitude of intermediate-order eustatic oscillation is the most likely candidate to generate a section of similar style to the observed successions.
- Through comparison of the simulations of the two studied sections it is apparent that whilst glacio-eustasy is fundamentally responsible for the creation of the sedimentary cyclicity it does not represent the fundamental control on cycle style. It seems likely that this disparity in subsidence rates represents the major cause of divergence in style of stacking between the two sections.
- This is particularly important for the development of ice-house petroleum reservoirs: crucially, the salient forcing mechanism for stacking patterns is not the amplitude of glacio-eustasy but the subsidence regime of the basin. It seems likely that it is the subsidence regime that will dictate the thickness of sedimentary cycles and therefore the spacing of reservoir-prone facies within each HfS.
- Modelling of grainstone thicknesses suggest moderately to rapidly subsiding extensional basins and moderately subsiding foreland basins will generate the greatest thicknesses of grainstone.

- The dominance of a single eustatic component combined with statistically disordered successions suggests that a sedimentary hierarchy is not present in either section.
- It seems likely that the identification of two orders of cyclicity in the Orogrande Basin by previous workers is not appropriate. It is more likely that the sedimentary stacking pattern is the product of significant amplitude glacio-eustatic oscillations subsequently modulated by the tectonic subsidence of the basin.

Chapter 7: PERITIDAL FACIES IN ICE-HOUSE SUCCESSIONS: RARITY RESULTING FROM LIMITED PRESERVATION POTENTIAL

7.1 INTRODUCTION

Metre-scale peritidal cyclothem, characterised by tidal flat laminites, are distinctive components of Lower Palaeozoic and many Mesozoic platform carbonates yet are not common in Upper Palaeozoic sequences (cf. Davies, 1984; Walkden, 1987; Koerschner & Read, 1989; Wright, 1992; Goldhammer *et al.*, 1994; Lehrmann & Goldhammer, 1999). The accepted interpretation is that during ice-house periods, large-amplitude high-frequency eustatic sea-level oscillations precluded extensive deposition of peritidal facies as a consequence of relatively rapid variations in base level (Walkden & Walkden, 1990; Wright, 1992). In contrast, small-amplitude low-frequency eustatic oscillations during greenhouse periods are considered to have allowed development of extensive, stacked cyclic sequences containing significant thickness of peritidal sediment (Wright, 1986; Tucker & Wright, 1990); although the degree to which both successions are truly cyclic has been called into question (Wilkinson *et al.*, 1996; Wilkinson *et al.*, 1997; Wilkinson *et al.*, 1998). Ice-house periods produced characteristically asymmetrical sub-tidal cycles which are truncated by abnormal sub-aerial exposure of sub-tidal facies (e.g. Hardie *et al.*, 1986; Goldhammer *et al.*, 1990; Saller *et al.*, 1994; Barnett *et al.*, 2002). Wright (1992) refers to the metre-scale, shoaling-upwards peritidal cycles as Type 1 platform cyclothem, and the irregular sub-tidal cycles with sub-aerial capping surfaces as Type 2 platform cyclothem. This nomenclature is maintained here.

There are notably few exceptions to the unwritten rule that ice-house periods cannot sustain peritidal conditions long enough to produce peritidal sedimentary facies. Wright (1986) documents extensive, well-developed peritidal cyclicity from South Wales (Chadian-Holkerian), although this was likely to be just prior to the onset of glacio-eustatic conditions. Similarly, Davies *et al.* (2004) noted well-developed peritidal capping units to cycles from the Holkerian-Asbian Leete Limestone of North Wales. Again, the temporal position of the unit is likely to be just before the onset of glacio-eustasy, and it is notable that the overlying Asbian ice-house unit, the Loggerheads Limestone, contains no peritidal facies. More convincing evidence is presented by Bridges (1982), in late Brigantian cyclothem from Derbyshire, England, who documents calcite pseudomorphs of gypsum preserved from what is interpreted as a sabkha setting. The caveat to this being that peritidal facies were seen capping only one of five cycles – a micritic laminated crust containing rhizocretions and pseudomorphs with a total thickness of 15mm. It is certainly

plausible that this extremely thin micritic crust had an alternate origin, and definitive evidence of peritidal facies existing within ice-house successions remains elusive.

The bipartite “greenhouse” versus “ice-house” model of cycle development is likely to be significantly complicated by the operation of autocyclic controls (e.g. Burgess & Wright, 2003). Given the uncertain ability of the sedimentary record to faithfully record the fundamental controls on sedimentation (e.g. Burgess & Wright, 2003), distinction between autocyclic and allocyclic controls cannot be reliably achieved. Moreover, it can be said that stratigraphic study of sedimentary sections does not allow detailed investigation of likely controlling parameters on the stacking patterns of these contrasting successions. Numerical forward modeling is a tool which does not have the same limitations as stratigraphy, and can therefore supplement our understanding on the controls of peritidal facies development derived from the study of the sedimentary record. This study aims, through one-dimensional forward modeling, to identify the major controls on peritidal facies development and preservation in the stratigraphic record.

7.1.1 Peritidal versus sub-tidal cyclicality

Under conditions of rapid base-level variation combined with amplitude changes of up to 100m or more (Heckel, 1986; Lehrmann & Goldhammer, 1999), the stable sea-level conditions which apparently favour peritidal carbonate deposition are rarely present. This has been cited as the major reason for the contrasting styles of sedimentary cyclicality between green-house and ice-house periods (Wright, 1992), possibly because the large-amplitude high-frequency oscillations overrode autocyclic controls on sedimentation which may promote tidal flat development. Autocyclicality may even represent the fundamental reason for the bipolar nature of shoaling-upwards cycles in inner-platform carbonates. It has been suggested that the lack of peritidal cyclothems in the Cenozoic may coincide with the spread of mangroves (Wright & Azerêdo, 2006). Furthermore, Wright & Azerêdo suggest that the rarity of tidal flat carbonates in the Cenozoic may, in part, reflect the spread of macrophytes (i.e. mangroves) in low energy tropical and subtropical settings. There is also evidence to suggest that disturbance by infaunal sediment burrowers and dwellers, and by marine grass and intertidal mangroves, would have been sufficient to rework the ‘original’ sediment completely (Beavington-Penney *et al.*, 2006). This would, in effect, result in the destruction of primary depositional surfaces and detailed lithological variations; the observed facies may therefore be better described as “taphofacies” rather than “depofacies.”

The sedimentary style of the Type 1 peritidal cyclothem reflects the ‘keep-up’ configuration of the carbonate factory in response to small-amplitude small-wavelength eustatic oscillations (Walkden, 1987; Wright, 1992). High production rates and

accommodation steadily created by subsidence meant these 'keep-up' platforms often experienced lateral basinward progradation and rapidly evolved into aggradational shelves (*sensu* Koerschner & Read, 1989). The relatively low accommodation created only by subsidence limits Type 1 cycles in thickness to approximately 1-5 metres. Type 1 cyclothems typically comprise thick sabkha cycles with extensive dolomitization, and commonly lack sub-aerial exposure features (although weakly-developed vadose caps may be present; Figure 7.1). This is interpreted as a result of subsidence out-pacing the sea-level falls combined with low-amplitude eustatic falls generating negligible relief on the exposed platform (Wright, 1992).

Type 2 cyclothems are much thicker as a result of the cumulative factors of subsidence and eustatic oscillations creating more accommodation, and range between approximately 5 and 15 metres thick (Figure 7.1). They exhibit extensive sub-aerial exposure features, including well-developed palaeokarstic surfaces and calcrete profiles. These cyclothems typically shallow-up from a wackestone-packstone base to a skeletal grainstone or oolitic grainstone unit displaying evidence of meteoric diagenesis. Peritidal carbonates are not a prominent component of Carboniferous platform systems, even within the upper part of the cycle which represents the eustatic fall. It may be expected that if peritidal facies were to be found anywhere in ice-house succession, it would be during a late high-stand of sea-level, as this represents the slowest rate of eustatic change. Most contemporary models of carbonate accumulation invoke a sea-level asymmetry of up to 95% on the falling limb (refer to Goldhammer *et al.*, 1991). This asymmetry is judged to reflect the relatively rapid sea-level rise from ice-melt, and the relatively slow fall as ice-caps and glaciers reform. Hays *et al.* (1976) documented an asymmetry of 85 % (i.e. 15% TST, 85% FSST) in Pleistocene data.

The differing styles of cyclicity are therefore considered to be affected not only by the amplitude and frequency of eustatic oscillations, but also by their degree of asymmetry. The relative sequence stratigraphic position of peritidal deposition may also play a critical factor; the taphonomy of the facies being a key element. To this end, the degree to which the platform undergoes sub-aerial exposure and meteoric diagenesis may play the most important role. In other words, are peritidal conditions not precluded by high rates of sea-level change, as currently thought? Rather, are they created in most situations, even at end-member extremes of subsidence and eustasy (and therefore accommodation), but have a low preservation potential, so as not to be recorded during ice-house periods? This study aims to address these questions.

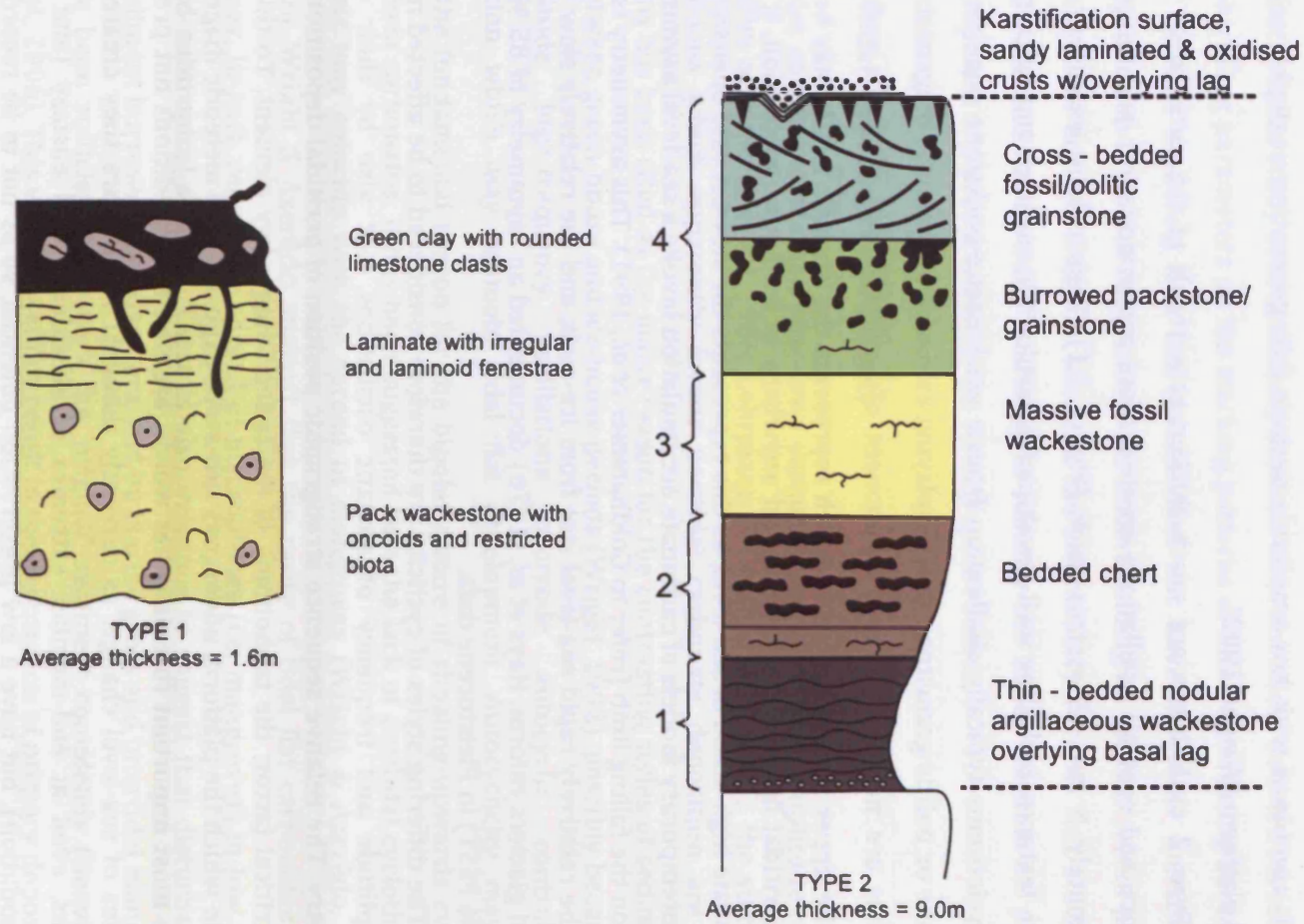


Figure 7.1: Schematic representation highlighting the thickness and facies differences of a typical Type 1 cycle from the Gobbler Formation (Pennsylvanian, New Mexico; modified from Algeo *et al.*, 1992) and a Type 2 cycle from the Rocha Forte Formation (Oxfordian, Portugal; redrawn from Wright & Azerêdo, 2006).

7.2 METHOD

TED models peritidal carbonate production in a simple way. In one-dimension peritidal carbonate production is a function only of depth. Other factors which may play a crucial role in the development of peritidal facies (such as a sheltered location or specific vegetation; refer to Beavington-Penney *et al.*, 2006) are not relevant in one-dimension. These factors essentially act as a modifier to either peritidal accumulation or dissipation and in one-dimension could only be modelled as a rate change in accumulation or removal of peritidal facies. Peritidal accumulation therefore only occurs in a specified depth range at a given rate. Modelling of large seas in the Upper Carboniferous (specifically the Northern European Seaway and the North American Midcontinent Seaway) suggests them to have a remarkably low tidal range (0.1m to 2m; Wells *et al.*, 2005; Wells *et al.*, 2007). A median value of 1m is adopted here, which serves as the boundary for peritidal carbonate accumulation. The thickness of sediment deposited in this depth range (<1m) is herein subsequently referred to as peritidal bed thickness.

Numerical forward modelling was employed in this study with two aims; firstly, to investigate and quantify the deposition of peritidal facies under ice-house conditions, and secondly to examine conditions which may lead to a depletion of peritidal facies in the ice-house portions of the sedimentary record. Simulations were conducted according to published parameters believed to be possible controls on peritidal sequence development during ice-house periods (Table 7.1; refer to section 3.3). Amplitude and asymmetry of eustatic oscillation were chosen as parameters as they represent the major discriminator in terms of sea-level change between ice-house and greenhouse periods. Sub-aerial platform denudation rate was chosen as it is the most likely cause of post-depositional modification of peritidal facies.

The results of simulations were compared in two terms: firstly by the average thickness of peritidal facies per high-frequency sequence (HfS) per run, and secondly by the single greatest bed thickness of peritidal facies per run. Average thickness (essentially cumulative peritidal bed thickness per HfS) allows a general appreciation of the thicknesses of peritidal sediment produced under certain parameters, while greatest bed thickness provides a better indication of the likelihood of such a bed being observed in a sedimentary succession.

Carbonate production rate was not included as a variable given that production rates for peritidal settings are relatively poorly constrained. A peritidal production rate of 500m/My represents an approximate mean between observed modern rates of peritidal accumulation and ancient rates of accumulation (Sadler, 1999). It should also be noted

Runs investigating:	Variables	Min. value	Max. value	Increment	Source
Eustatic amplitude	High-order amplitude	0m	50m	2.5m	Paterson <i>et al.</i> , 2006
	Intermediate-order amplitude	0m	90m	5m	Heckel, 1986; Wright & Vanstone, 2001
Intermediate-order asymmetry	Intermediate-order oscillation asymmetry	50%	95%	5%	Hays <i>et al.</i> , 1976; Goldhammer <i>et al.</i> , 1991
	Intermediate-order amplitude	10m	100m	5m	See above
High-order asymmetry	High-order oscillation asymmetry	50%	95%	5%	Hays <i>et al.</i> , 1976; Goldhammer <i>et al.</i> , 1991
	Intermediate-order amplitude	10m	100m	5m	See above
Sub-aerial exposure	Platform denudation rate	0m/My	100m/My	5m/My	Goldhammer <i>et al.</i> , 1991; Plan, 2005
	Intermediate-order amplitude	10m	100m	5m	See above

Table 7.1: List of the variables used in numerical simulations. Variables address a range of values according to an increment. For each run plan, the variables are modified one per run according to the increment, until each combination has been addressed. Duration was fixed at 3My.

that the rate of 500m/My is production, which is subsequent to modification by other parameters before accumulation occurs. Nevertheless, the rate employed here is likely to be somewhat higher than that of ancient successions (Sadler, 1994; Sadler, 1999). These simulations, which over-estimate peritidal carbonate production, can be considered to represent a best-case scenario for the accumulation and preservation of peritidal facies.

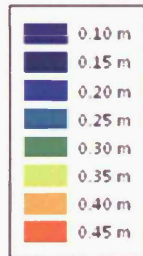
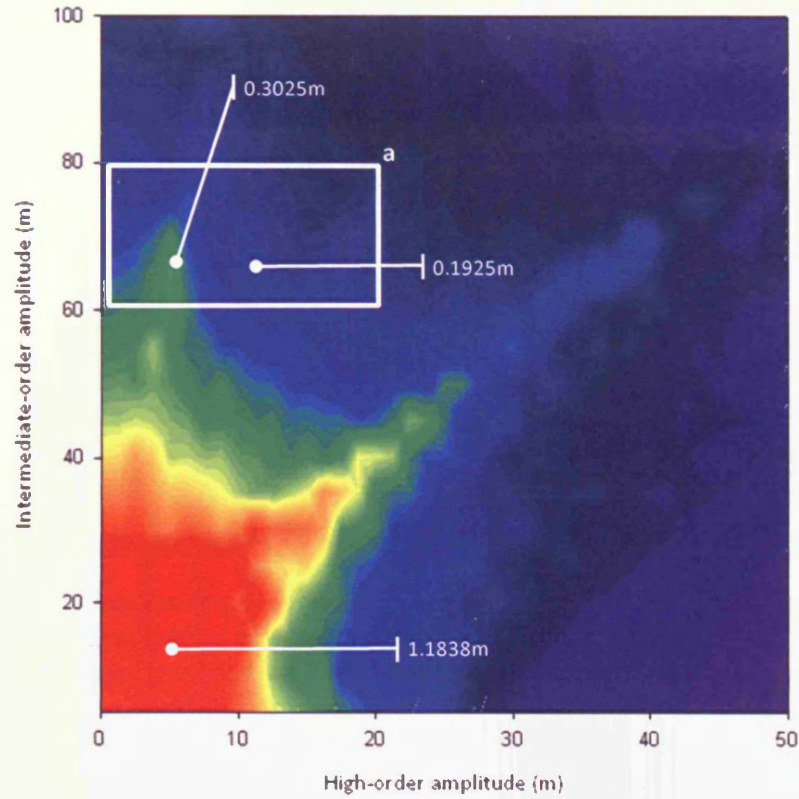
7.3 NUMERICAL MODELLING OF PERITIDAL CARBONATE ACCUMULATIONS

Modelling of the interaction between two eustatic sea-level oscillations; a high-order and intermediate-order component highlights parameter-space zones where significant thicknesses of peritidal facies accumulate. These zones can be sub-divided into two trends; significant thicknesses at low-amplitudes of sea level oscillation and within a parameter space zone where high-order amplitude is approximately 50-60% of intermediate-order amplitude (Figure 7.2).

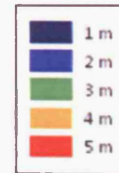
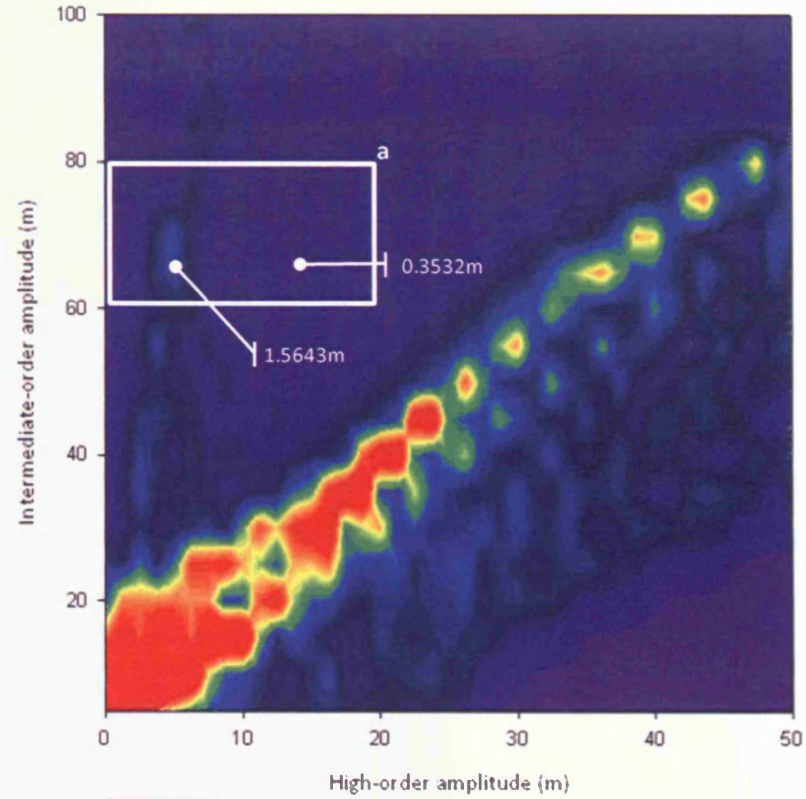
The latter trend is apparent only when observing the greatest bed thickness of peritidal facies developed per simulation, it is not immediately apparent in plots of average peritidal thickness per HfS. This suggests that the trend is caused by the relatively large-amplitude of the high-order component in comparison with the intermediate-order component. Under these conditions, there are a significantly fewer number of 'missed' high-order oscillations (i.e. those not recorded by a period of sedimentation on the platform top). The high-order oscillations which are recorded, due to their lesser amplitude than those of intermediate-order, are less likely to cause a significant relative sea-level rise; thus there is a greater chance of sedimentation taking place within the peritidal depth range. This is reinforced by observing that where high-order amplitude is greater than 50% of intermediate-order amplitude there is no increase in greatest bed thicknesses of peritidal facies; instead the thicknesses show a decrease. Increasingly similar amplitudes cause high-order oscillations to submerge the platform to a greater depth, making peritidal production less likely. This trend is maintained when the amplitude relationship becomes inverted. Although based on potentially unrealistic amplitude relationships (cf. Barnett *et al.*, 2002), it highlights that this trend is due to relatively large-amplitude high-order oscillations.

The large-amplitude high-order oscillations are, however, also likely to represent an unrealistic mode of sea-level behaviour. Although not prohibited by conventional estimates of amplitudes (e.g. Goldhammer *et al.*, 1991; Barnett *et al.*, 2002), they do conflict with numerical evidence presented in Chapter 4, Chapter 5 and Chapter 6. This evidence suggests that realistic matches with sedimentary sections are best achieved with low-amplitudes of high-order oscillation. It seems likely therefore, that this does not represent a realistic method of accumulating significant thicknesses of peritidal sediment.

In contrast to this, the tendency of pronounced sedimentation and accumulation of peritidal facies at very low interactions of eustatic sea-level oscillation does represent a realistic method of peritidal production – but crucially, only during greenhouse periods. Simulations conducted at less than 30m intermediate-order amplitude and 10m high-



Average peritidal facies thickness per HfS per run
(Note an upper cut-off of 0.5m is applied)



Greatest peritidal bed thickness per run
(Note an upper cut-off of 5m is applied)

Figure 7.2: Caption overleaf.

Figure 7.2: Parameter-space response surface plots for simulations investigating amplitude of sea-level change.

In both plots eustatic components are displayed on the axes, whilst the colour indicates average peritidal facies thickness per HfS per run (left) and greatest bed thickness of peritidal facies (right). Both variables measure thickness of peritidal facies, which is defined as the thickness of sediment deposited in a zone of peritidal water depth (<1m in TED). Blues colours indicate small thickness and red large thicknesses. Note the different scales. Subsequent parameter space plots conform to the same format.

Box (a) delineates a zone of parameters considered likely for ice-house periods (derived from other studies).

Large thicknesses of peritidal facies are primarily developed at small intermediate- and high-order amplitudes, which may be considered equivalent to greenhouse sea-level behaviour. Significant bed thickness values also tend to be developed where high-order amplitude is 50-60% of intermediate-order amplitude, however, this is not consistent with evidence of ice-house sea-level behaviour. Under ice-house conditions peritidal thicknesses are developed in all cases and can reach considerable individual bed thicknesses.

order amplitude display strong parallels with what may be expected in terms of peritidal facies from greenhouse period oscillations, despite a frequency difference (greenhouse oscillations are estimated to be small-amplitude, low-frequency; Lehrmann & Goldhammer, 1999). Figure 7.2, shows that simulations within this zone result in average peritidal thicknesses per HfS (approximately 1.2m) comparable to sedimentary cycles from peritidal greenhouse successions (compare with Figure 7.1).

The relatively thin cycle thickness and correspondingly large thickness of peritidal facies is entirely due to limited accommodation created by the low-amplitude oscillations. The increased frequency of oscillation in the simulations results in a thicker succession (because there are more cycles), but does not affect the cycle thickness or facies content. These simulated cycles may therefore be classed as Type 1 peritidal cyclothem. Their existence at low-amplitudes of sea-level oscillation not only confirms the veracity of the model in replicating peritidal successions, but also suggests the interactions of sea-level where peritidal facies are most likely to develop.

This trend rapidly diminishes as intermediate-order amplitude increases, to a point where, at probable amplitudes of intermediate-order oscillation during ice-house periods a maximum of 0.3m of peritidal facies can be produced per HfS (Figure 7.2; a). The greatest peritidal bed thickness under these conditions is still a sizeable 1.6m, however. Thus, based on modelling of sea-level oscillation amplitudes alone, it seems likely that observable thicknesses of peritidal facies are likely to be created, even with ice-house sea-level amplitudes.

Asymmetry of intermediate order oscillation was considered to be a probable control on peritidal facies development as it constitutes a significant difference between ice-house and greenhouse periods. Ice-house periods, characterised by the waxing and waning of continental glaciers, are thought to be best modelled using an asymmetry of 85-95% (Hays *et al.*, 1976; Goldhammer *et al.*, 1991); representative of the differential melting and growth of ice-sheets. Conversely, greenhouse sea-level oscillations are envisaged to be mainly symmetric in nature (Read *et al.*, 1995). This difference is borne out by simulations of peritidal facies accumulations under ice house conditions (Figure 7.3). Simulations which show both the greatest average peritidal thickness and the greatest individual peritidal bed thickness (approximately 0.5m and 5m respectively) exist in a parameter-space zone below 65% asymmetry. This corresponds with the symmetric eustatic sea-level oscillations invoked during greenhouse periods.

Low intermediate-order amplitudes and a high-degree of symmetry, do not lead, as may be expected to greater thickness of peritidal facies. Instead, modelling suggests that slightly higher oscillations are needed to generate the greatest average thicknesses of peritidal facies per run (40-70m). This is not entirely inconsistent with estimates of

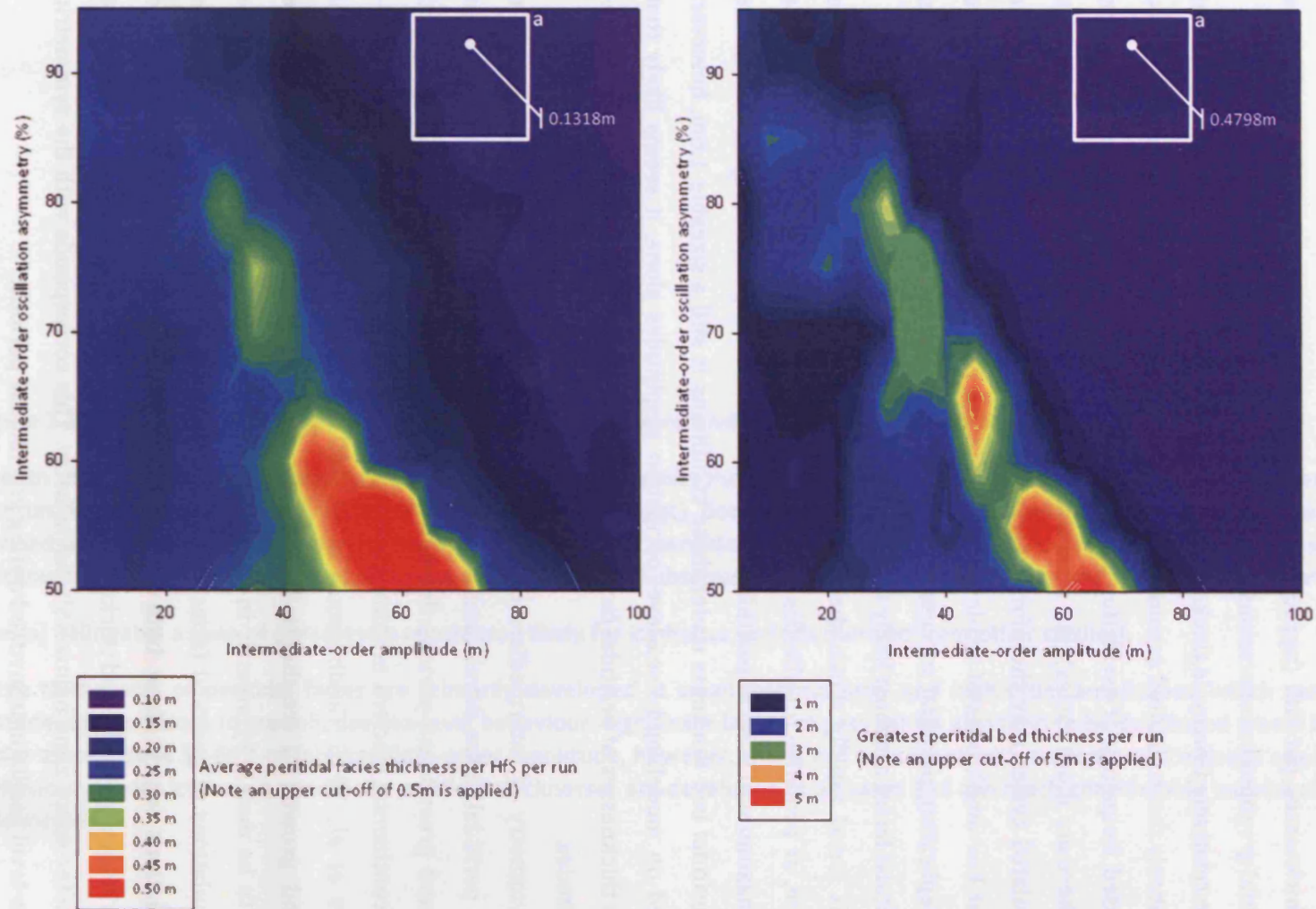


Figure 7.3: Parameter-space response surface plots for simulations investigating intermediate-order asymmetry, displaying average peritidal facies thickness per HfS per run (left) with the greatest bed thickness of peritidal facies (right). Box (a) denotes likely ice-house parameters (defined from other studies). Note the different scales. Simulations which show both the greatest average peritidal thickness, and the greatest individual peritidal bed thickness (approximately 0.5m and 5m respectively) exist in a parameter-space zone below 65% asymmetry; reminiscent of greenhouse conditions (50% asymmetry). At ice-house parameters, and above 70m amplitude, variation of asymmetry has little effect on peritidal facies development.

greenhouse sea-level oscillation (Immenhauser & Scott, 2002), but does not accurately match predicted amplitudes. A comparison of greatest bed thicknesses however, show that at 40-70m intermediate-order amplitude, cycles which are anomalously thick in comparison with Type 1 cyclothems are created. A better match is provided at 20-50m intermediate-order amplitude and below 60% asymmetry. In this parameter-space zone sub-2m beds of peritidal facies are created; a figure more in line with observed thicknesses from the sedimentary record. At oscillation asymmetries of greater than 85%, representative of ice-house configurations of sea-level change, varying asymmetry has no significant effect. Under these conditions, only very thin accumulations of peritidal sediment develop. Although these deposits are thin, peritidal facies do develop, and at thicknesses which may be expected to be observable in the sedimentary record (greatest bed thickness: 0.47m).

Given the demonstrable improbability of significant amplitude high-order eustatic oscillations, their asymmetry was not considered likely to be a major determining factor. Simulations were still conducted, however, in order to quantify the effect of high-order asymmetry and also to prevent unpredicted effects adversely affecting other parameters. A comparison of the parameter-space plots in Figure 7.4 shows that at ice-house high-order amplitudes asymmetry of high-order oscillation has a negligible effect; both in terms of average peritidal thickness per HfS and greatest bed thickness per run. This is a reflection of the high-order oscillations limited importance in dictating peritidal facies thickness, thus modifying its asymmetry has little effect. The only parameter-space zone where modification of asymmetry has significant effect is at large high-order amplitudes and with an asymmetry of above 70%. Under these conditions the FSST of a sea-level oscillation is sufficient to create thick (greater than 3m) beds of peritidal facies. However, these conditions are not likely to be realistic given previous modelling of sea-level behaviour, which as noted indicates that high-order amplitudes are likely to be negligible (<20m; refer to section 5.5.2).

Simulations addressing high-order asymmetry reiterate that greater-amplitude intermediate-order oscillations are a more important control on peritidal facies development. Despite this, even at ice-house amplitudes, between 0.17m and 0.26m are generated consistently in HfSs and greatest bed thickness is 0.29m. Asymmetry has little effect on either number, but again, significant thicknesses of peritidal facies are still being produced consistently under ice-house conditions. It may be expected that 0.3m of peritidal facies would be visible as such in an ice-house cycle; yet sedimentary evidence of peritidal facies is elusive.

Sub-aerial platform denudation rate has considerable effect on the thickness of peritidal facies observed in simulated successions. Greatest bed thickness is reduced from

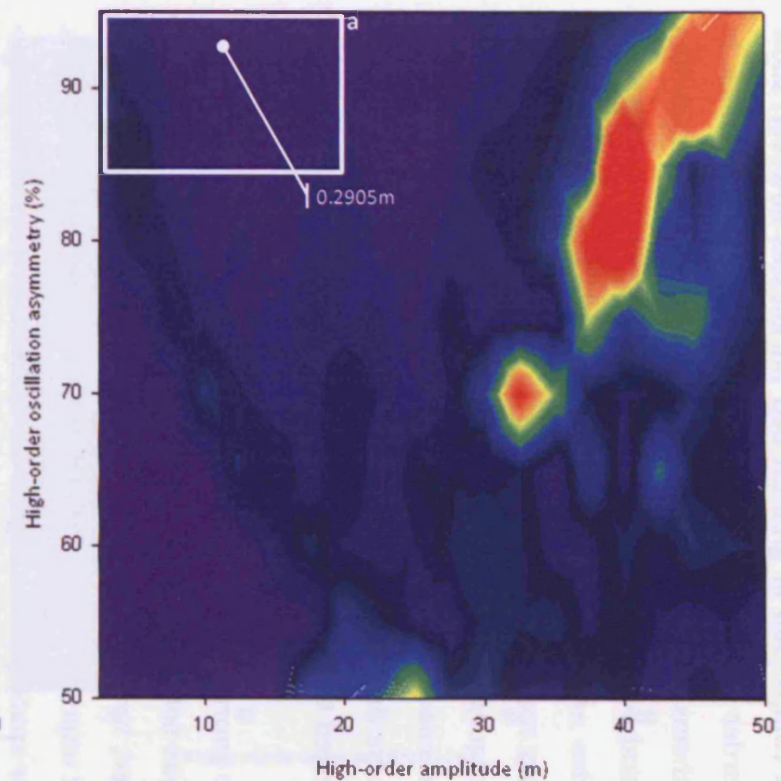
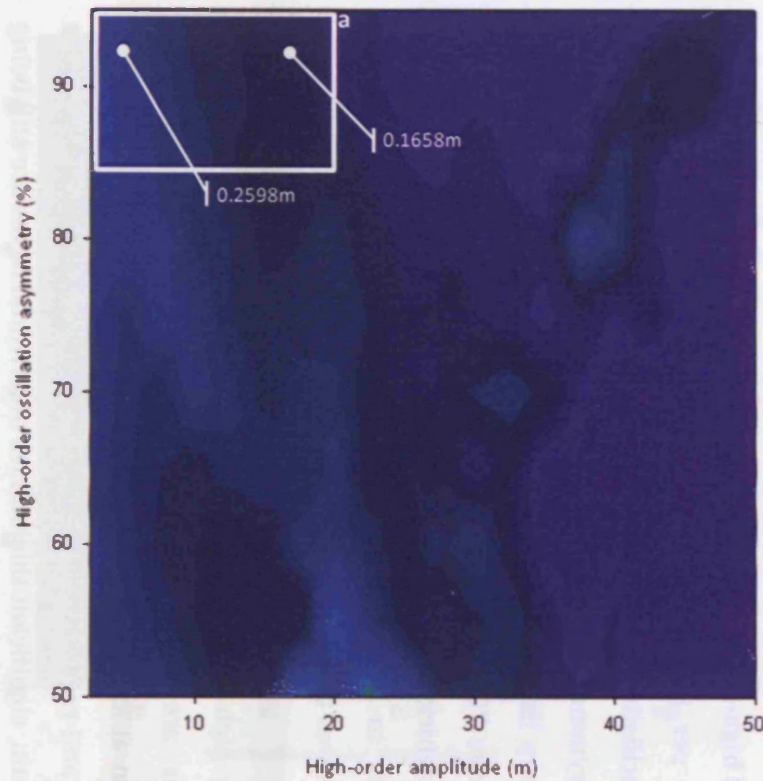


Figure 7.4: Parameter-space response surface plots for simulations investigating high-order asymmetry, displaying average peritidal facies thickness per HfS per run (left) with the greatest bed thickness of peritidal facies (right). Box (a) denotes likely ice-house parameters (defined from other studies). Note the different scales. At ice-house amplitudes, varying high-order asymmetry has negligible effect on peritidal thickness. The only parameter-space zone where modification of asymmetry has significant effect is at large high-order amplitudes and with an asymmetry of 70% and above. However, these conditions are not likely to be realistic given previous modelling of sea-level behaviour.

in excess of 5m at 0m/My sub-aerial platform denudation to approximately 3m at 100m/My (Figure 7.5). The latter rate may not be realistic (cf. Plan, 2005; modelling studies presented in Chapter 5 suggest a rate of 10m/My is appropriate for semi-humid climates) but emphasise the important role sub-aerial platform denudation plays. Simulations investigating sub-aerial platform denudation show an unusual relationship with intermediate-order amplitude, with the greatest average and bed thicknesses occurring at 35m amplitude. This can be explained by the interaction of intermediate- and high-order oscillations, which in these simulations are fixed at 20m. This amplitude is 57% of the intermediate-order amplitude, and therefore falls within the 50-60% range which display an anomalously high peritidal facies quotient. This is the same effect exhibited in Figure 7.2. The intermediate-order amplitude of 40m may be considered anomalously low for an ice-house interval.

At more realistic ice-house amplitudes of 60-80m sub-aerial erosion appears to have relatively little effect. However, if a run with no erosion is compared with a run incorporating a platform denudation rate of 5m/My, it is seen the thickness of peritidal facies per HfS is reduced by more than half (from 0.17m to 0.07m). There is less of a visible effect on greatest bed thickness; however there is still a reduction in bed thickness.

The implications of this are best seen by comparing simulations with no sub-aerial platform denudation with the same simulations but which incorporate a sub-aerial dissolution component of 10m (Figure 7.6). In terms of average peritidal facies thickness the difference is marked, with an overall reduction in significant thicknesses (Figure 7.6; a). An examination of peritidal thicknesses under ice-house amplitudes in particular reveals a reduction in average thickness per HfS per run by nearly an order of magnitude (0.19m to 0.04m). Bed thicknesses show a similar reduction from 1.56m to 0.19m. It is a matter of debate whether such thicknesses would be visible at outcrop (refer to section 7.4.2), but it seems likely that in a system with even a minor sub-aerial platform denudation component that there is a significantly reduced chance of preserving peritidal facies in the sedimentary record.

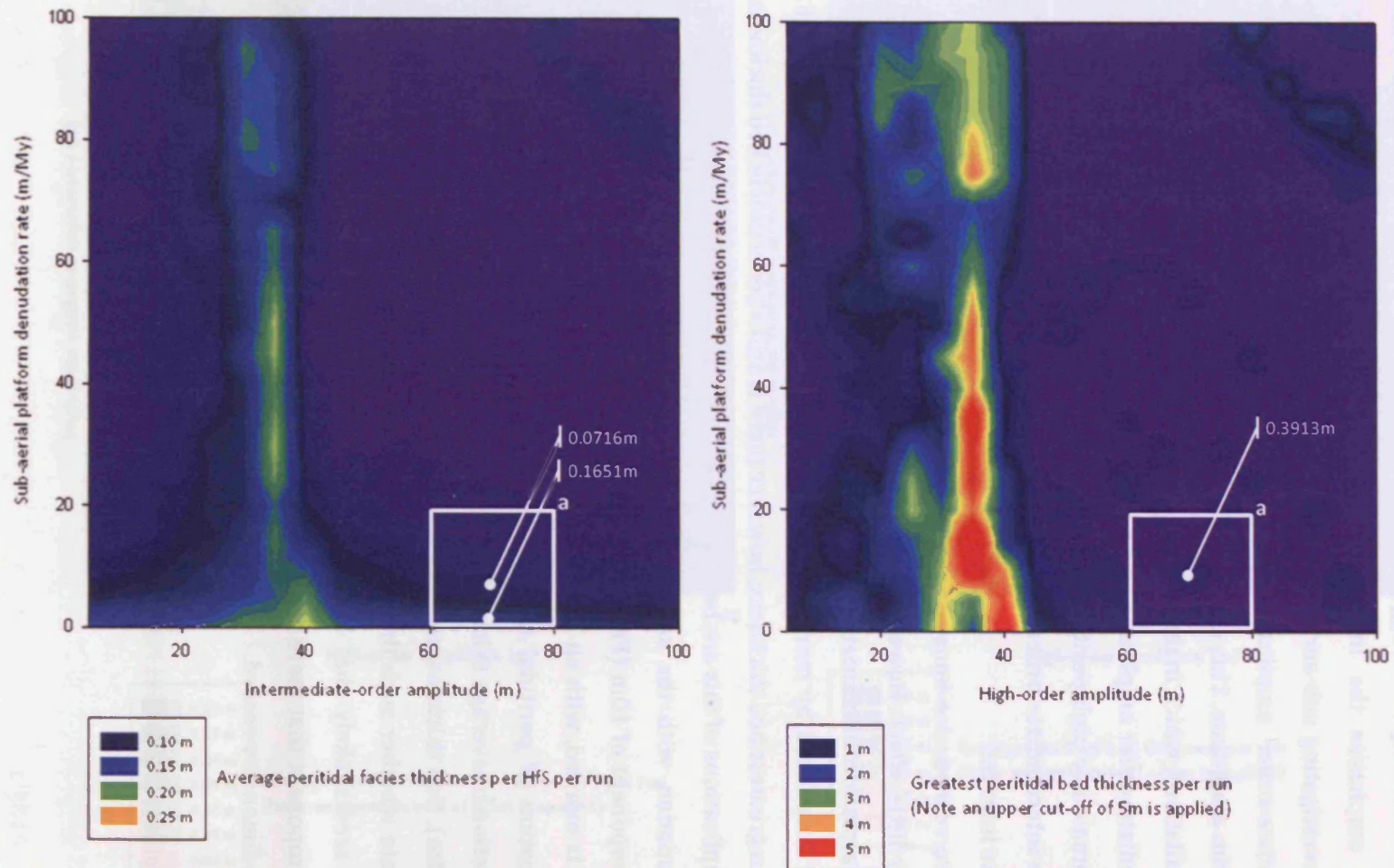
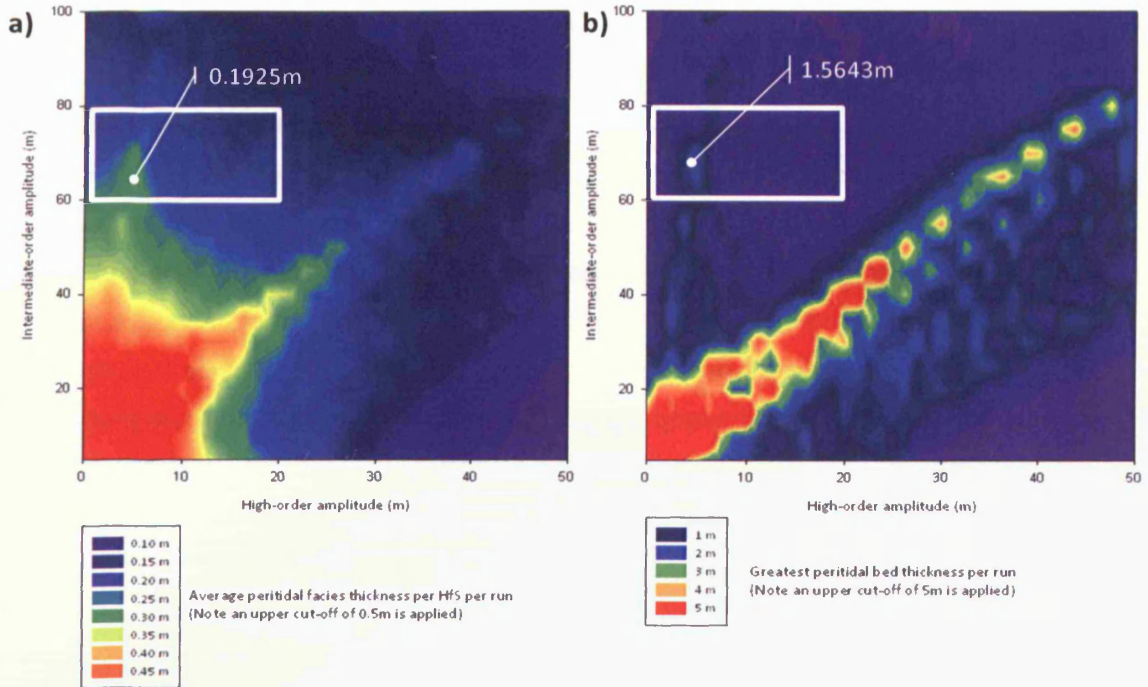


Figure 7.5: Parameter-space response surface plots displaying for simulations investigating sub-aerial platform denudation rate, average peritidal facies thickness per Hfs per run (left) with the greatest bed thickness of peritidal facies (right). Box (a) denotes likely ice-house parameters (defined from other studies). Note the different scales. Greatest average and bed thicknesses occurs at 35m amplitude. This is explained by the interaction of intermediate- and high-order oscillations, which in these simulations are fixed at 20m; representing 57% of the intermediate-order amplitude, and therefore falls within the 50-60% range which display an anomalously high peritidal facies quotient. This is the same effect exhibited in Figure 7.2. The intermediate-order amplitude of 40m may be considered anomalously low for an ice-house interval. At ice-house amplitudes, there is a rapid lowering of peritidal thickness values from 0m/My to 5m/My (from 0.1651m to 0.0716m).

Simulations with no sub-aerial platform denudation



Simulations with 10m/My sub-aerial platform denudation

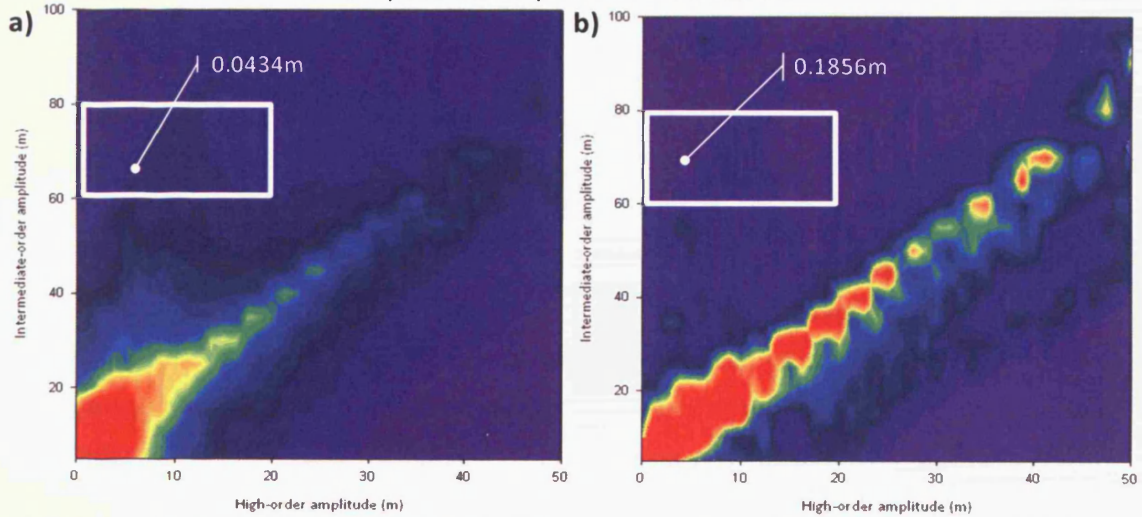


Figure 7.6: Parameter-space response surface plots comparing runs with no sub-aerial platform denudation component (top), and runs with 10m/My platform denudation (bottom). Results are shown in terms of average peritidal facies thickness per HfS per run (a) and greatest bed thickness of peritidal facies (b). White boxes denote likely ice-house parameters (defined from other studies). Note the different scales. Sub-aerial erosion reduces peritidal thicknesses in both cases to minimal amounts at ice-house parameters. With 10m/My sub-aerial platform denudation significant quantities of peritidal facies only develop at greenhouse amplitudes, and in the case of greatest bed thickness; where high-order amplitude is ~50-60% of intermediate-order amplitude.

7.4 INTERPRETATION

7.4.1 Accumulation of peritidal facies

Numerical simulations correspond well with what may be expected in terms of peritidal facies development within greenhouse sequences. Small-amplitudes of intermediate-order sea-level change show the greatest propensity for development of thick peritidal accumulations. When small intermediate-order amplitudes are coupled with small high-order amplitudes this effect is amplified. These are the precise conditions under which peritidal Type 1 sequences are envisaged to accumulate during greenhouse periods. This is despite the fact that both the frequency of high- and intermediate-order cyclicity in the modelled simulations is greater than that for predicted for oscillations during greenhouse periods. Greenhouse periods, with limited amounts of water locked as continental ice, are thought to oscillate on a longer-term frequency, possibly dictated by longer-term climate change or tectonic activity (Read *et al.*, 1995). This frequency discrepancy, however, in terms of simulations, only results in more cycles and thicker sequences, rather than a change in character of the facies proportions. As such the model is able to demonstrate an ability to reproduce the situations in which peritidal facies most prominently develop. This demonstrates a firm basis from which to test for the existence of peritidal facies in ice-house sequences.

Contemporary explanations for the absence of peritidal facies in ice-house sequences are not adequate. These are mostly based on the assumption that the large-amplitude eustatic oscillations characteristic of these periods prohibit extensive peritidal flat development due to associated rapid sea-level change (e.g. Wright, 1992). However, modelling reveals that even under ice-house sea-level amplitudes (i.e. large intermediate-order amplitude and small high-order amplitude) significant thicknesses of peritidal facies are still developed. Significance in this case is determined by the likelihood of detecting evidence of peritidal facies development in the sedimentary record. Whilst this is a difficult criterion to quantify, it seems probable that given the ubiquitous development of peritidal facies (both in terms of average thickness and greatest bed thickness) that peritidal facies may be recognised at single point in at least one ice-house succession globally. For instance, in runs examining amplitudes of eustatic change (Figure 7.2) the greatest bed thickness at likely ice-house amplitudes is 1.6m with average thicknesses ranging between 0.2m and 0.3m per simulation.

Other simulations display similar average thicknesses; runs modifying intermediate-order asymmetry generate an average of 0.13m, and high-order asymmetry

between 0.17m and 0.26m. Greatest bed thicknesses in these sections are never less than 0.29m. Based solely on the accumulation of peritidal facies it therefore seems likely that they would be able to be distinguished in a sedimentary section. Peritidal facies may not be visible in every parasequence given the low averages, but greatest bed thicknesses of between 0.29m and 1.6m would be highly likely to be visible at outcrop. The fact that no peritidal facies are recognised in ice-house sedimentary successions despite endemic presence in simulations suggests there is an alternate cause for their non-occurrence.

Analysis of oscillation asymmetry reiterates this point. The asymmetry of ice-house oscillations results in rapid sea-level rise, and a less rapid sea-level fall. Figure 7.7 displays the sequence stratigraphic position of periods of peritidal deposition. Despite the rapid sea-level rise, peritidal facies would still accumulate on the TST if a lag-depth were not incorporated into the model. The justification of utilising a lag-depth in a one-dimensional simulation is given in section 3.3.3.7, however it can also be considered to represent hydraulic action preventing deposition in the uppermost part of the water column. Transgressions of sea-level can be particularly destructive and are not likely to promote preservation of facies at the base of a HfS (e.g. cobble sized lithoclasts evidenced from northern Russia; section 6.3.2.2). Yet despite significant rates of sea-level fall peritidal accumulations still accumulate during the FSST. It would therefore seem that significant rates of sea-level fall do not preclude peritidal sequence development, which further suggests that there is another explanation for the non-occurrence of peritidal facies in ice-house sections.

One explanation may be that that these peritidal beds are not recognised by workers at outcrop. This is supported by statistical evidence, which suggests that studies of lithofacies distributions tend to group thin beds when compared against theoretical distributions (Burgess, 2007a; 2007b). This, however, does not seem likely given the scrutiny applied to exposure surfaces and the upper parts of HfSs (e.g. Vanstone, 1998; Budd *et al.*, 2002; Kabanov, 2003); precisely the stratigraphic position where peritidal facies are most likely to develop. If significant peritidal features developed here, they would most likely be identified. A further explanation is therefore necessary, and one is provided by the effect of sub-aerial exposure on peritidal facies.

7.4.2 Taphonomy of peritidal facies

Sub-aerial exposure has a significant detrimental effect on the probability of observing peritidal facies accumulations in the sedimentary record. Minor amounts of sub-aerial platform denudation have the effect of substantially reducing the thicknesses observed in comparison with diagenetically-unaltered simulated successions (Figure 7.6). Reduction in average peritidal thickness per HfS during ice-house periods (i.e. high-

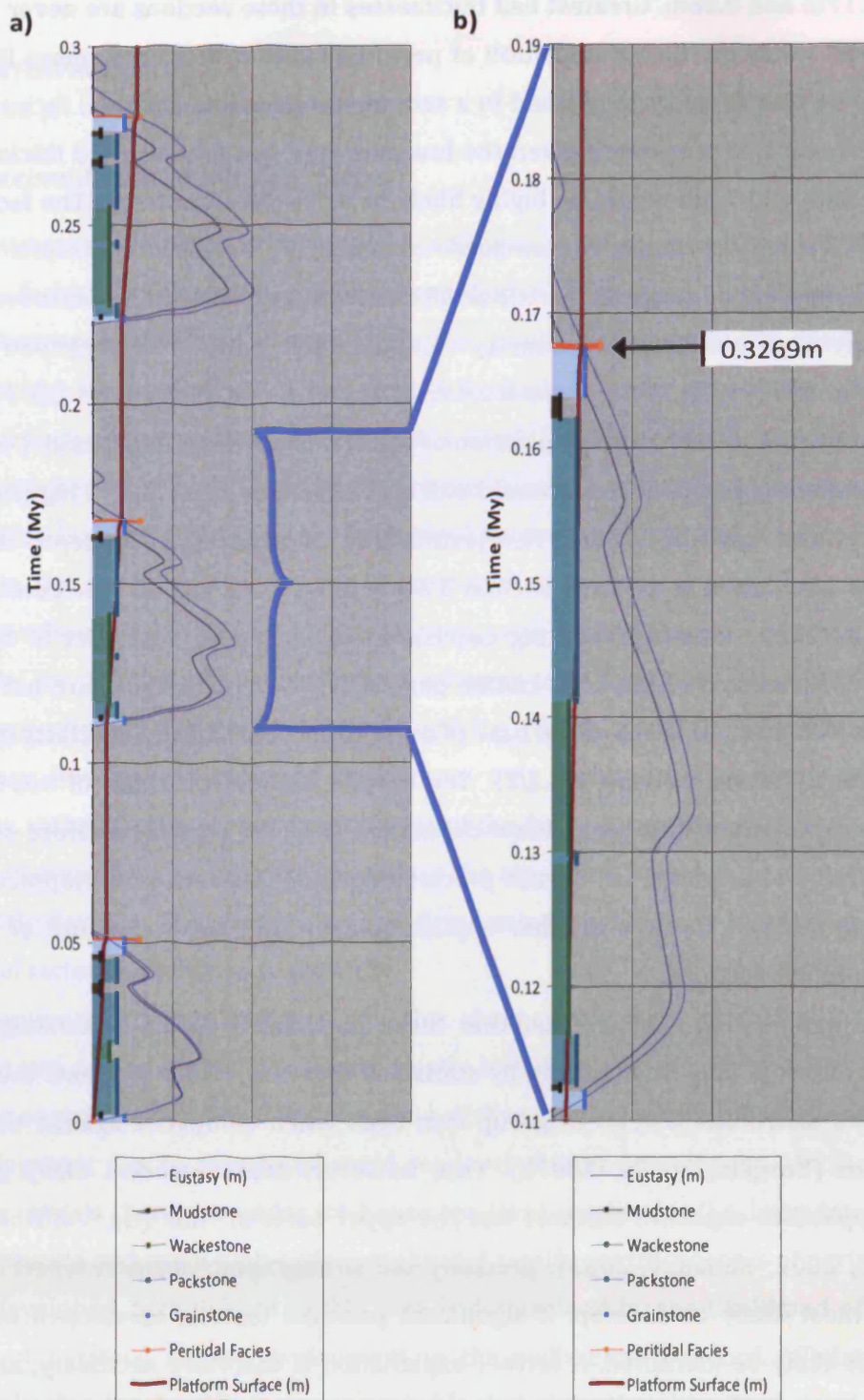


Figure 7.7: Chronostratigraphic plot of peritidal sequence development under ice-house conditions (70m intermediate-order amplitude, 20m high-order). Horizontal axis is metres (each vertical bar represents 20m), facies are assigned an arbitrary number to generate a synthetic section. Sedimentation occurs when relative sea-level (light blue line) passes to the right of the platform surface line. a) shows three HfSs, peritidal facies are developed at the top of each, despite rapid sea-level fall. Peritidal facies are not developed at the base of cycles due to sedimentation lag depth. b) zoom on one HfS showing peritidal thickness development at the top of the cycle.

frequency large-amplitude eustatic oscillations) amounts to an 80% reduction in thickness at 10m/My sub-aerial denudation rate. This rate is likely not to be excessive for climate in tropical latitudes in the Pennsylvanian, and has been employed by previous modelling studies to simulate sub-aerial diagenesis (Goldhammer *et al.*, 1991). This effect becomes even more pronounced when comparing greatest bed thickness which exhibit up to a 90% reduction in thickness. The reduction of greatest bed thickness from 1.6m to 0.19m significantly decreases the likelihood of recognising peritidal facies in the sedimentary record.

The reason relatively low rates of sub-aerial platform denudation have such a large effect is due to the stratigraphic position of peritidal facies occurrences. As previously mentioned (section 7.4.1) peritidal facies occur during TSTs of intermediate-order oscillations, which places them at the top of HfSs (Figure 7.7). During a lowstand, they therefore comprise the uppermost portions of the platform surface. If platform lowering by sub-aerial processes then occurs, these facies are the most likely to be removed. Figure 7.8 provides an illustration of this effect: peritidal thicknesses of up to 0.32m are completely removed during the subsequent period of exposure. These facies are the most vulnerable and are the first to be removed.

In reality, this is also likely to be compounded by the unlithified nature of peritidal deposits during exposure. Unlike the coarse-grained, and usually well-cemented, deposits characteristic of the upper units of ice-house cycles, peritidal facies are typically mud-dominated and fine grained. It is therefore likely that these facies have poorer preservation potential; not only because of carbonate dissolution but also through aeolian winnowing, particularly as increased erosion has been documented from sea-level lowstands (Schmitz & Pujalte, 2003).

Other factors, not able to be addressed by one-dimensional forward modelling may also have significant effect. Factors which may be detrimental to the presence of peritidal facies are likely to include the prominence of macrophytic vegetation (Wright & Azerêdo, 2006), the presence of infaunal burrowing organisms in the peritidal zone (Beavington-Penney *et al.*, 2006) and also climate, which in addition to determining the rate of platform denudation would also dictate pedogenesis. Furthermore, sub-marine sediment transport and wave action, with wave-base dictated by fetch, are also likely to be crucial (Burgess, 2006); peritidal facies are more likely to develop in sheltered areas.

It seems apparent that in ice-house periods peritidal facies have very limited preservation potential even before other modifiers to the existence of peritidal facies development are applied. Given the prevalence peritidal facies under ice-house conditions as seen in modelling, it seems likely that the limited preservation potential plays a

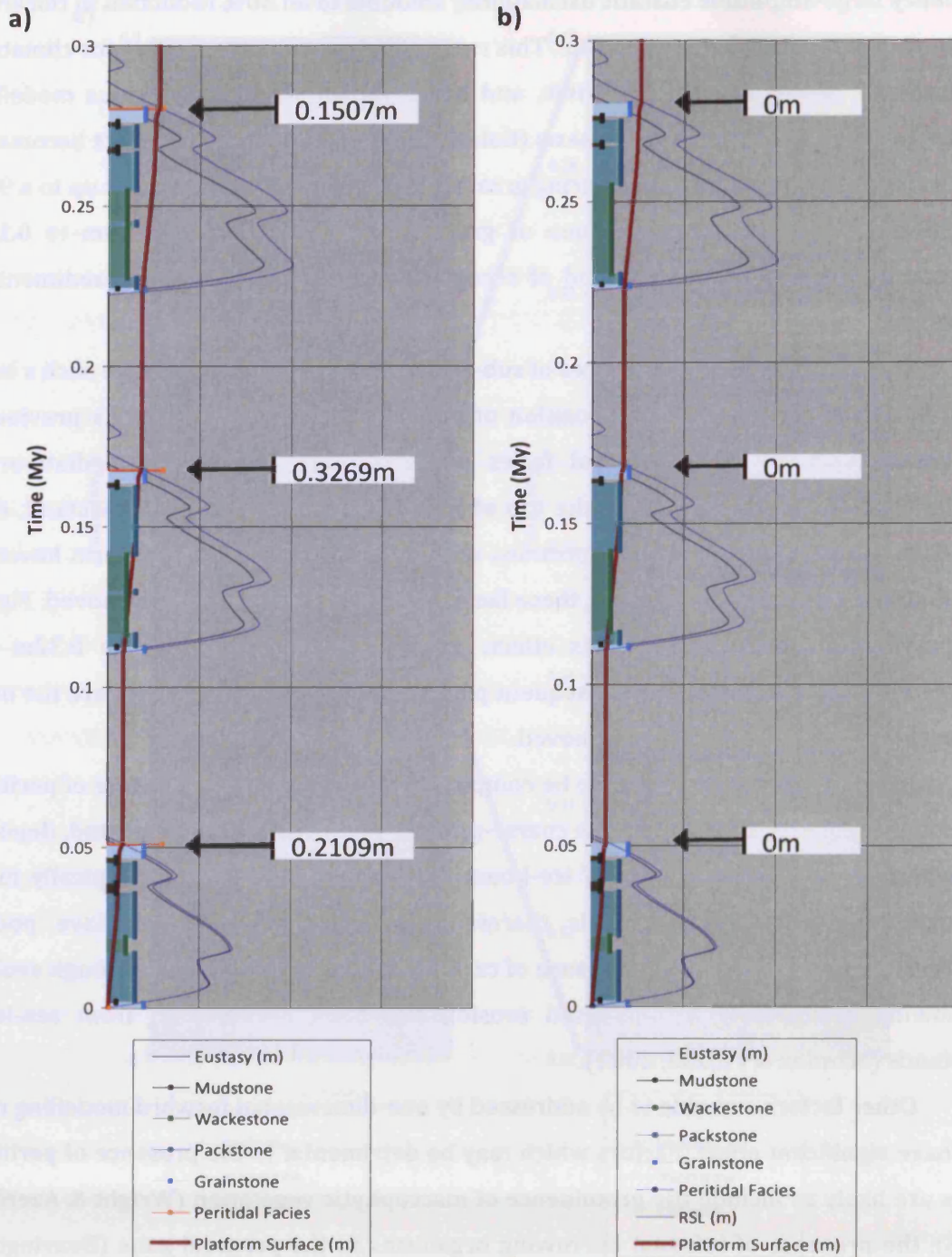


Figure 7.8: Chronostratigraphic diagrams comparing development of peritidal facies under ice-house sea-level amplitudes and conditions of a) no sub-aerial platform denudation and b) 10m/My platform denudation. This rate removes all peritidal facies in this run. a) is the same run as Figure 7.7; a.

significant role in ensuring peritidal facies are not recorded in ice-house portions of the stratigraphic record.

7.5 CONCLUSIONS

- Based upon a simple function for the generation of peritidal facies in one-dimension, numerical forward modelling of varying amplitudes of eustatic sea-level oscillation show a good ability to produce realistic quantities of peritidal facies under small-amplitude 'greenhouse' oscillations.
- All simulations conducted show at least some peritidal facies development. Under ice-house sea-level amplitudes and asymmetries this amounts to an average thickness per HfS per run of approximately 0.15-0.3m and greatest bed thicknesses per run of 0.3m-1.5m. While there may be some doubt surrounding the recognition of a 15cm-30cm in the sedimentary record, there can be less uncertainty in the ability to recognise a metre or more of peritidal facies. Based on sea-level alone, peritidal facies do not, therefore, have a particularly limited accumulation potential during ice-house periods.
- This finding casts doubt on the theory that the highly asymmetric, large-amplitude oscillations typical of ice-house periods prevented deposition of peritidal facies, and instead suggests there may be an alternate reason for their non-occurrence in ice-house portions of the stratigraphic record.
- The role of meteoric diagenesis is likely to be one of the greatest detrimental factors to the preservation of peritidal facies. Even very low amounts of sub-aerial platform diagenesis can remove all but the thickest occurrences of peritidal facies in a simulation, which are reduced by almost an order of magnitude.
- The sequence stratigraphic position of the greatest peritidal accumulations is likely to amplify this effect as peritidal facies are typically at the top of the stratigraphic column during exposure. The unlithified sediment is therefore likely to be more prone to weathering. The subsequent sea-level transgression is also not likely to aid preservation of these facies.
- There are also a number of other factors, unable to be addressed by one-dimensional forward modelling, but which are likely to be detrimental to accumulation (e.g. macrophytic vegetation, depositional setting) or preservation (infaunal burrowing, pedogenesis) of peritidal facies. It is suggested here that one or a combination of these factors serve to remove evidence of remaining peritidal facies subsequent to their sub-aerial erosion.

Chapter 8: CONCLUSIONS

8.1 MAJOR RESULTS

In attempting to address the objectives outlined in Chapter 1, several important observations can be made from results of these combined outcrop and modelling studies regarding the nature of ice-house carbonate successions. These findings are interdependent but can be broadly categorised into 4 major themes:

1. Carbonate thickness hierarchies; definition, controls and occurrence in the stratigraphic record;
2. Identification of possible best-fit parameter values for particular ancient successions;
3. Subsidence as the dominant control on ice-house stacking patterns.
4. Poor taphonomic potential of peritidal facies during ice-house periods.

8.1.1 The improbability of a sedimentary hierarchy

Given the emphasis placed on hierarchical stacking patterns in contemporary literature (e.g. Anderson, 2004), and their assumed predictive power, forward modelling indications that they are likely rare in the sedimentary record may be regarded as the most important outcome of this study. This finding derives from a quantitative definition of the term hierarchy hitherto only expressed in a qualitative and subjective way. The lack of a precise definition hampered previous efforts to conclusively test for the existence of a hierarchy because of confused assumptions of its properties. To determine when a hierarchy can objectively be said to exist, a robust set of simple criteria was created based on previous qualitative assumptions, and rigorously applied to sedimentary successions.

Furthermore, the reinterpretation of cycle boundaries made by previous workers calls into question the existence of a hierarchy in a section regarded as the best evidence of a sedimentary hierarchy: the Honaker Trail section (HTS), Utah. Vertical facies associations, shown by previous workers to be not fundamentally indicative of an excursion of relative sea-level, are not used to define cycle boundaries in this study. This eliminates another qualitative element of the definition of a sedimentary hierarchy, thereby eliminating significant uncertainty from the identification of a sedimentary hierarchy. A reinterpretation of the HTS and identification of cycle boundaries only where there is unambiguous evidence of direct sub-aerial exposure therefore represents a much more objective way of characterising HfSs. Importantly, a reinterpretation of cycle

boundaries based on objective identification of sub-aerial exposure surfaces results in the breakdown of the hierarchy identified by previous workers.

A more objective reinterpretation of cyclicity in the HTS also results in several refinements to the genetic stratigraphy of the succession as proposed by previous authors. "Double cycles" as proposed by Grammer *et al.* (2000) are found to be unsupported by sedimentary evidence. A more appropriate interpretation for HTS HfSs necessitates only one oscillation of relative sea-level to deposit both siliciclastic and carbonate sediment. Significantly, this finding is supported with evidence from numerical modelling which suggests that only one eustatic sea-level oscillation of significant amplitude is likely to be operative during ice-house periods.

In general, modelling indicates that a sedimentary hierarchy, while not impossible, is only likely to occur at very specific combinations of eustatic sea-level oscillation; that both modelling of sedimentary sections and previous knowledge of sea-level behaviour suggest are highly unlikely. Specifically, a thickness hierarchy will only be generated when there is an amplitude ratio of 3:4 between high-order and intermediate-order oscillations. This remains true within simple model scenarios where eustatic amplitude is the only variable. In more complex scenarios (with an additional variable) a sedimentary hierarchy is only created when unrealistic eustatic parameters are employed; suggesting that a sedimentary hierarchy is fundamentally unrealistic, as very high amplitudes of high-order oscillation are often needed to generate the differential thicknesses of sediment. This does not seem consistent with what we know about rates of sea-level change during ice-house conditions.

Modelling of HTS lithofacies supports this finding by suggesting that with two high-frequency (i.e. sub-My wavelength) glacio-eustatic components it is difficult to generate a simulated section comparable to the HTS. However, with one static eustatic component and a low-order oscillation, a HTS-equivalent section can be generated at a range of parameters. Hence, it seems improbable based on results of numerical forward modelling, that a single dominant large-amplitude high-frequency eustatic parameter can generate a good approximation of the HTS, with the same number of HfSs and similar thicknesses.

A similar interpretation to this is made from the results of modelling studies conducted on contemporaneous sections in New Mexico and northern Russia. In both of these cases numerical forward modelling indicates that a large amplitude of intermediate-order eustatic oscillation is the most likely method to generate a section of similar style to the observed successions. Given the dominance of a single eustatic component, combined with statistically disordered successions, it is maintained that a sedimentary hierarchy is also not present at either of these locations. The evidence provided by numerical

modelling of sections is also supported by statistical analysis of the outcrop stacking patterns, which suggests that runs of HfS thickness are not of sufficient length to disprove randomness.

These results strongly imply that a sedimentary hierarchy is not present in ice-house successions, even with the ordered, hierarchical forcing mechanism present in the numerical model. Furthermore the results are derived from processes taking place within a deterministic environment, the outcome of which is a perfect recording of these processes. It is highly doubtful that any portion sedimentary record would document the controls of its creation with such fidelity. The lack of a sedimentary hierarchy is further reinforced by modelling of the controlling parameters of geographically disparate sedimentary successions, which not only display remarkable correspondence in terms of parameter values, but universally suggest only one sea-level oscillation of significant amplitude is necessary to generate similar successions.

8.1.2 Identification of possible parameter values for ancient successions

The second point in the above list, the identification of likely controlling parameters of ice-house parameters, is also the result of numerical simulations of stacking patterns. These results, as mentioned, show remarkable parallels in producing different styles of sedimentary section using two similar components; notably, amplitude of eustatic oscillation, euphotic carbonate production rate, and a single significant major variable; subsidence rate. In addition to this, the fact that simulations of HTS HfSs did not create realistic representations of HTS lithofacies proportions reiterates that the knowledge of the fundamental controls on carbonate deposition and accumulation needs improvement. The deviation from observed lithofacies is likely to have a number of causes, not least of which is a significant complexity in the sedimentary environment which is not incorporated in the parameters, and represents an appraisal of the known limitations of the one-dimensional forward model implemented here.

Modelling of stacking patterns in cyclic successions also facilitates identification of parameters that show good correlation throughout the three sections, and the amplitude of eustatic oscillation can be placed in this category. Modelling studies of the HTS indicates an intermediate-order amplitude of 60-80m generates the most appropriate sections in comparison to stacking patterns observed in the HTS. Similarly, simulations attempting to replicate cyclicity in both New Mexico and Arkhangel'sk Oblast display the greatest correlation with observed sections at high-eustatic amplitudes (60-80m and 45-60m respectively). Furthermore, this type of amplitude is in line with contemporary sedimentary evidence of sea-level change during ice-house periods (yet this is only

meaningful if we assume that Carboniferous ice-houses were similar to those of the Pliocene-Holocene).

Euphotic production rates show a similar degree of correlation. Modelling of euphotic production rates for both all three studied successions show a best fit with the observed sections at rates of 700-800m/My. These rates are lower than estimates of production for modern shallow-water frame-building organisms, but given the inner-platform setting, may not be unrealistic.

In contrast to these parameters which show good correlation, one parameter likely to differ between sections is sub-aerial platform denudation, which although likely to be similar at the HTS and FC localities probably occurred at an elevated rate at the SDP section. Sub-aerial platform denudation is predicted to have negligible effect in the FC and HTS study areas. Lowering of the platform surface is predicted by modelling to be of greater importance in the SDP section; a tentative estimate would predict slightly elevated rates (from those quoted from comparable successions) of approximately 20m/My.

8.1.3 Subsidence as the primary control on ice-house stacking patterns

The primary divergence between the three sections, however, seems to be in terms of subsidence rate. For the SDP section modelling indicates that a subsidence rate of 10-45m/My produces good matches to the observed section; with such a rate being in-line with estimates for basin subsidence in a relatively quiescent intra-cratonic basin such as the Moscow-Mezen Syncline. In the FC section, modelling suggests subsidence occurred at a rate of 80-130m/My with it being likely that the FC section was developed at the lower limit of this range. This rate would be in line with sedimentary evidence and the intra-cratonic setting of the Orogrande Basin (given the elevated subsidence rates demonstrated from the Pennsylvanian).

Modelling of the HTS demonstrates that simulations which show that the most realistic stacking patterns, and the thicknesses which most resemble the HTS, are developed at relatively high rates of subsidence (greater than 150m/My). These subsidence rates are in line with rates cited for the Paradox Basin (Goldhammer *et al.*, 1991). Given that subsidence rate provides the basis for the best correlations, it is probable that the complex tectonic setting of the HTS and encompassing Paradox Basin plays a prominent role in dictating the nature of the sedimentary succession.

The different, but realistic, rates of subsidence for each tectonic setting illustrate the third major finding of this study; that whilst glacio-eustasy is primarily responsible for the creation of the sedimentary cyclicity it does not represent the fundamental control on cycle style. Furthermore, it seems likely that this disparity in subsidence rates represents the major cause of divergence in style of stacking between the two sections. In all cases, it

seems likely that the glacio-eustatic signal is significantly modulated by a combination of long- and short-term variations in subsidence, masking the glacio-eustatic signal and representing the greatest source of variation between the observed sections and numerical simulations.

8.1.4 Poor preservation potential of peritidal facies

It is less likely that the high-amplitude large-frequency glacio-eustatic oscillations explain the paucity of peritidal facies in ice-house periods. Modelling studies presented here cast doubt on the theory that highly asymmetric, large-amplitude oscillations thought to be typical of ice-house periods prevented deposition of peritidal facies, and instead demonstrates that peritidal facies have the capability of being created even under conditions of rapid base-level change. Instead, it is suggested here that the role of meteoric diagenesis of exposed peritidal facies is likely to be one of the greatest detrimental factors to their preservation. Even very low amounts of sub-aerial platform diagenesis have the potential to significantly reduce the thickness of peritidal facies, and therefore the probability of their preservation as recognisable units in the stratigraphic record.

8.2 WIDER IMPLICATIONS OF RESULTS

In Middle to Late Carboniferous carbonate platform sequences reservoir quality facies generally consist of grainstones (e.g. Saller *et al.*, 1999; Kenter *et al.*, 2006). Thickness of such facies is variable across a range of cyclothem types, but modelling studies (Chapter 6) suggest that subsidence rates comparable to moderately to rapidly subsiding extensional basins and moderately subsiding foreland basins will generate the greatest thicknesses of grainstone (110-140m/My and 170-190m/My respectively). This is a first-stage requirement to predict likely reservoir quality in a frontier basin where Carboniferous carbonates are a potential target.

Furthermore, the extreme improbability of a sedimentary hierarchy existing means 'bundled' stacking patterns should not be used as a predictive element to determine stacking patterns of inner-platform ice-house successions in the subsurface. This is particularly important for the development of ice-house petroleum reservoirs: crucially, the salient forcing mechanism for stacking patterns is not the amplitude of glacio-eustasy but the subsidence regime of the basin. It seems likely that it is the subsidence regime that will dictate the thickness of sedimentary cycles and therefore the spacing of reservoir-prone facies within each HfS.

8.3 FUTURE WORK

The primarily numerical approach used here represents a method to address problems which cannot be answered using conventional empirical techniques. A logical further step would be to conduct a larger-scale parameter-space study. Such a study would potentially incorporate variables which were not addressed here (such as non-linear subsidence). Potential, and indeed likely, outcomes of a study of this nature would be a better understanding of how parameters interact to control sedimentary stacking and lithofacies associations. One caveat is that any such study would have difficulties in visualisation of results. 3D plots are not ideal to convey complex relationships and it is suggested that response-surfaces are the most convenient way to convey relationships in parameter-space.

The quantitative definition presented here represents only one definition of a hierarchy – albeit one which is based on the objective application of sequence stratigraphy. It is proposed that this quantitative definition represents a significant improvement over previous qualitative models and definitions. It is suggested that future studies may benefit by rigorously applying and examining conceptual sequence-stratigraphic models within numerical models. Furthermore, it is possible that ongoing research can improve upon the definition of a sedimentary hierarchy and its application, and this represents an avenue for further research.

There also exists a need to further quantify the effect of interacting subsidence and eustatic oscillation in producing variable cycle and lithofacies thicknesses. A basis is presented here in the analysis of separate basins. It may be envisaged that analysis of a number of disparate basins, both geographically and in terms of tectonic regime, may populate a database that could provide a predictive tool for interpretation of stacking patterns in the subsurface. It is also suggested that further quantification is required of the interaction between eustasy and subsidence rates at an intra-basin scale. It is proposed that the Paradox Basin represents an ideal location for such a study. The complex tectonic regime in the basin is not uniform, and it is likely that stacking patterns differ among localities on the shelf. The superb exposure of this region, combined with the abundance of sub-surface data available for both basin and shelf locations would provide an excellent dataset. It is suggested that previous interpretations of cycle boundaries be re-evaluated at these localities and cycle boundaries inferred only where sub-aerial exposure is evident. This would facilitate objective analysis of stacking patterns with the aim of assessing the degree to which differential subsidence affects stacking.

The Orogrande Basin also represents an excellent location for an intra-basin subsidence-eustasy study. The opposing sides of the basin experienced different subsidence regimes, however it should be noted that the western margin is a ramp and not directly comparable with the eastern shelf.

REFERENCES

- Adams, A. E. & Cossey, P. J., 2004. Chapter 8: North Wales Shelf. In *British Lower Carboniferous Stratigraphy*, (ed. Cossey, P. J., Adams, A. E., Purnell, M. A., Whiteley, M. J., Whyte, M. A. & Wright, V. P.), Geological Conservation Review Series, **29**. Joint Nature Conservation Committee, Peterborough, p. 366-91.
- Adams, A. E., Horbury, A. D., Abdel & Aziz, A. A., 1990. Controls on Dinantian sedimentation in south Cumbria and surrounding areas of northwest England. *Proceedings of the Geologists' Association*, **101**, p. 19-30.
- Adams, J. M., Faue, H. & Petit-Maire, N., 1992. Methane and Milankovitch cycles. *Nature*, **355**, p. 214.
- Adhémar, J. A., 1842. *Révolutions de la Mer, Deluges Periodics*. Carilian-Goeury et V. Dalmont, Paris, 247 pp.
- Algeo, T. J., 1996. Meteoric water/rock ratios and the significance of sequence and parasequence boundaries in the Gobbler Formation (Middle Pennsylvanian) of south-central New Mexico. In *Paleozoic Sequence Stratigraphy: Views from the North American Craton*, (ed. Witzke, B. J., Ludvigson, G. A. & Day, J.), Geological Society of America Special Paper, **306**. Geological Society of America, Boulder, Colorado, p. 359-71.
- Algeo, T. J. & Hinnov, L. A., 2006. Milankovitch cyclicity in the Ohio and Sunbury shales: astronomical calibration of the Late Devonian-Early Carboniferous Timescale (Abstract). *Geological Society of America Abstracts with Programs*, **38**, p. 268.
- Algeo, T. J. & Wilkinson, B. H., 1988. Periodicity of mesoscale Phanerozoic sedimentary cycles and the role of Milankovitch orbital modulation. *Journal of Geology*, **96**, p. 313-22.
- Algeo, T. J., Wilkinson, B. H. & Lohmann, K. C., 1992. Meteoric-burial diagenesis of Middle Pennsylvanian limestones in the Orogrande Basin, New Mexico: water/rock interactions and basin geothermics. *Journal of Sedimentary Petrology*, **62**, p. 652-70.
- Algeo, T. J., Wilson, J. L. & Lohmann, K. C., 1991. Eustatic and tectonic controls on cyclic sediment accumulation patterns in Lower-Middle Pennsylvanian strata of the Orogrande Basin, New Mexico. In *Geology of the Sierra Blanca, Sacramento and Capitan Ranges, New Mexico: New Mexico Geological Society Guidebook. 42nd Field Conference*, (ed. Barker, J. M., Kues, B. S., Austin, G. S. & Lucas, S. G.), New Mexico Geological Society, 1991 Field Conference, p. 203-12.

- Allaby, A. & Allaby, M., 1999. *Oxford Dictionary of Earth Sciences*. Oxford University Press, Oxford, 649 pp.
- Allen, P. A. & Allen, J. R., 1990. *Basin Analysis*. Blackwell Scientific Publications, Oxford, 560 pp.
- Allen, P. A. & Allen, J. R., 2005. *Basin Analysis (Second Edition)*. Blackwell Scientific Publications, Oxford, 549 pp.
- Anderson, E. J., 2004. The cyclic hierarchy of the 'Purbeckian' Sierra del Pozo Section, Lower Cretaceous (Berriasian), southern Spain. *Sedimentology*, **51**, p. 455-77.
- Artyushkov, E. V., Chekhovich, P. A. & Tarling, D. H., 2003. The origin of water-depth changes in past epeiric seas. *Doklady Earth Sciences*, **388**, p. 515-20.
- Atchley, S. C. & Loope, D. B., 1993. Low-stand aeolian influence on stratigraphic completeness: upper member of the Hermosa Formation (latest Carboniferous), southeast Utah, USA. In *Aeolian Sediments: Ancient and Modern*, (ed. Pye, K. & Lancaster, N.), Spec. Publ. Int. Ass. Sediment., **16**. Blackwell, London, p. 127-49.
- Aurell, M., Bosence, D. W. J. & Waltham, D. A., 1995. Carbonate ramp depositional systems from a late Jurassic epeiric platform (Iberian Basin, Spain): a combined computer modelling and outcrop analysis. *Sedimentology*, **42**, p. 75-94.
- Aurell, M., Bosence, D. W. J. & Waltham, D. A., 1998. Carbonate production and offshore transport on a Late Jurassic carbonate ramp (Kimmeridgian, Iberian Basin, NE Spain): evidence from outcrops and computer modelling. In *Carbonate Ramps*, (ed. Wright, V. P. & Burchette, T. P.), Geological Society of London Special Publication, **149**. London.
- Baars, D. L., 1988. The Paradox Basin. In *Sedimentary Cover - North America Craton, US*, (ed. Sloss, L. L.), The Geology of North America, **D-2**. Geological Society of America, Boulder, Colorado.
- Baars, D. L. & Stevenson, G. M., 1981. Tectonic evolution of the Paradox basin, Utah and Colorado. *Geology of the Paradox Basin*, 1981 Field Conference. Rocky Mountain Association of Geologists. 23-31.
- Baars, D. L. & Stevenson, G. M., 1982. Subtle Stratigraphic Traps in Paleozoic Rocks of Paradox Basin. In *The Deliberate Search for the Subtle Trap*, (ed. Halbouty, M. T.), AAPG Memoir, **32**. AAPG, Tulsa, OK, p. 131-58.
- Balog, A., Haas, J., Read, J. F. & Coruh, C., 1997. Shallow marine record of orbitally forced cyclicity in a Late Triassic carbonate platform, Hungary. *Journal of Sedimentary Research*, **67**, p. 661-75.
- Barbeau, D. L., 2003. A flexural model for the Paradox Basin: implications for the tectonics of the Ancestral Rocky Mountains. *Basin Research*, **15**, p. 97-115.

- Barnett, A. J., 2002. *An investigation of the controls on stratigraphic cyclicity in late Mississippian-early Pennsylvanian (Carboniferous) platform carbonates*. Unpublished PhD thesis, Cardiff University, Cardiff.
- Barnett, A. J., Burgess, P. M. & Wright, V. P., 2002. Icehouse world sea-level behaviour and stratal patterns in late Visean (Mississippian) carbonate platforms; integration of numerical forward modelling and outcrop studies. *Basin Research*, **14**, p. 417-39.
- Barrick, J. E. & Heckel, P. H., 2000. A provisional conodont zonation for Late Pennsylvanian (late Late Carboniferous) strata in midcontinent region of North America. *Newsletter on Carboniferous Stratigraphy*, **18**, p. 15-22.
- Beavington-Penney, S. J., Wright, V. P. & Racey, A., 2006. The Middle Eocene Seeb Formation of Oman: An investigation of acyclicity, stratigraphic completeness, and accumulation rates in shallow marine carbonate settings. *Journal of Sedimentary Research*, **76**, p. 1137-61.
- Benne, R. E., 1975. *The stratigraphy of the lower Gobbler Formation, Sacramento Mountains, New Mexico*. M.S. Thesis, University of Oklahoma, Norman, OK.
- Berger, A. L., 1978a. Long-term variations of caloric insolation resulting from the Earth's orbital elements. *Quaternary Research*, **9**, p. 139-67.
- Berger, A. L., 1978b. Long-term variations of daily insolation and Quaternary climatic changes. *Journal of Atmospheric Science*, **35**, p. 2362-67.
- Berger, A. L. & Loutre, M. F., 1994. Astronomical forcing through geological time. In *Orbital forcing and cyclic sequences*, (ed. De Boer, P. L. & Smith, D. G.), **19**. Blackwell Scientific, London, p. 15-24.
- Berger, A. L., Loutre, M. F. & Dehant, V., 1989. Influences of the changing lunar orbit on the astronomical frequencies of pre-Quaternary insolation patterns. *Paleoceanography*, **4**, p. 555-64.
- Bice, D., 1988. Synthetic stratigraphy of carbonate platform and basin systems. *Geology*, **16**, p. 703-06.
- Borer, J. M. & Harris, P. M., 1989. Depositional facies and cycles in Yates Formation outcrops, Guadalupe Mountains, New Mexico. In *Subsurface and Outcrop Examination of the Capitan Shelf*, (ed. Harris, P. M. & Grover, G. A.), SEPM Core Workshop, **13**. p. 305-18.
- Bosence, D. W. J. & Waltham, D. A., 1990. Computer modeling the internal architecture of carbonate platforms. *Geology*, **18**, p. 26-30.
- Bosence, D. W. J., Wood, J. L., Rose, E. P. F. & Qing, H., 2000. Low- and high-frequency sea-level changes control peritidal carbonate cycles, facies and dolomitization in the Rock of

- Gibraltar (Early Jurassic, Iberian Peninsula). *Journal of the Geological Society*, **157**, p. 61-74.
- Boss, S. K. & Rasmussen, K. A., 1995. Misuse of Fischer plots as sea-level curves. *Geology*, **23**, p. 221-24.
- Bosscher, H. & Schlager, W., 1992. Computer simulation of reef growth. *Sedimentology*, **39**, p. 503-12.
- Bosscher, H. & Schlager, W., 1993. Accumulation rates of carbonate platforms. *Journal of Geology*, **101**, p. 345-55.
- Bowman, M. W. & Vail, P. R., 1999. Interpreting the stratigraphy of the Baltimore Canyon section, offshore New Jersey with PHIL, a stratigraphic simulator. In *Numerical Experiments in Stratigraphy: Recent Advances in Stratigraphic and Sedimentologic Computer Simulations*, (ed. Harbaugh, J. W., Watney, W. L., Rankey, E. C., Slingerland, R., Goldstein, R. H. & Franseen, E. K.), SEPM Special Publication, **62**. SEPM, Tulsa, OK, p. 117-38.
- Boylan, A. L., Waltham, D. A., Bosence, D. W. J., Badenas, B. & Aurell, M., 2002. Digital rocks: linking forward modelling to carbonate facies. *Basin Research*, **14**, p. 401-15.
- Bridges, P. H., 1982. The origin of cyclothems in the late Dinantian platform carbonates at Crich, Derbyshire. *Proceedings of the Yorkshire Geological Society*, **44**, p. 159-80.
- Budd, D. A., Gaswirth, S. B. & Oliver, W. L., 2002. Quantification of macroscopic subaerial exposure features in carbonate rocks. *Journal of Sedimentary Research*, **72**, p. 917-28.
- Burgess, P. M., 2001. Modelling carbonate sequence development without relative sea-level oscillations. *Geology*, **29**, p. 1127-30.
- Burgess, P. M., 2006. The signal and the noise: forward modeling of allocyclic and autocyclic processes influencing peritidal carbonate stacking patterns. *Journal of Sedimentary Research*, **76**, p. 962-77.
- Burgess, P. M., 2007a. Cyclicity in Carbonates: Simple Models Versus The World. In *2007 AAPG Annual Convention and Exhibition (April 1 - 4, 2007)*, AAPG, Long Beach, CA.
- Burgess, P. M., 2007b. The nature and meaning of shallow-water carbonate lithofacies thickness distributions. *In review*.
- Burgess, P. M. & Emery, D. J., 2004. Sensitive dependence, divergence and unpredictable behaviour in a stratigraphic forward model of a carbonate system. In *Geological Prior Information: Informing Science and Engineering*, (ed. Curtis, A. & Wood, R.), **239**. The Geological Society, London, p. 77-94.

- Burgess, P. M. & Wright, V. P., 2003. Numerical forward modelling of carbonate platform dynamics: an evaluation of complexity and completeness in carbonate strata. *Journal of Sedimentary Research*, **73**, p. 637-52.
- Burgess, P. M., Wright, V. P. & Emery, D. J., 2001. Numerical forward modelling of peritidal carbonate parasequence development: implications for outcrop interpretation. *Basin Research*, **13**, p. 1-16.
- Byers, C. W., 1977. Biofacies patterns in euxinic basins - a general model. In *Deep-Water Carbonate Environments*, (ed. Cook, H. E. & Enos, P.), SEPM Special Publication, **25**. SEPM, Tulsa, OK, p. 5-18.
- Carey, J. S., Swift, J. P. D., Steckler, M. S., Reed, C. W. & Niedoroda, A., 1999. High-resolution sequence stratigraphic modeling 2: effects of sedimentation processes. In *Numerical experiments in stratigraphy: recent advances in stratigraphic and sedimentologic computer simulations*, (ed. Harbaugh, J. W., Watney, W. L., Rankey, E. C., Slingerland, R., Goldstein, R. H. & Franseen, E. K.), SEPM Special Publication, **62**. SEPM, Tulsa, OK, p. 151-64.
- Cecil, C. B., 1990. Paleoclimate controls on stratigraphic repetition of chemical and siliciclastic rocks. *Geology*, **18**, p. 533-36.
- Cecil, C. B., 2004. *Eolian Dust and the Origin of Sedimentary Chert*. USGS Open-File Report 2004-1098 for U.S. Geological Survey, Reston, VA.
- Cherns, L. & Wright, V. P., 2000. Missing molluscs as evidence of large-scale, early skeletal aragonite dissolution in a Silurian sea. *Geology*, **28**, p. 791-94.
- Cisne, J. L., 1986. Earthquakes recorded stratigraphically on carbonate platforms. *Nature*, **323**, p. 320-22.
- Clark, P. U., Alley, R. B. & Pollard, D., 1999. Northern Hemisphere Ice-Sheet Influences on Global Climate Change. *Science*, **286**, p. 1104-18.
- Cloetingh, S., 1986. Intraplate stresses: a new tectonic mechanism for relative fluctuations of sea level. *Geology*, **14**, p. 617-20.
- Collier, R. E. L., Leeder, M. R. & Maynard, J. R., 1990. Transgressions and regressions: a model for the influence of tectonic subsidence, deposition and eustasy, with application to Quaternary and Carboniferous examples. *Geological Magazine*, **127**, p. 117-28.
- Cozzi, A., Hinnov, L. A. & Hardie, L. A., 2005. Orbitally forced Lofer cycles in the Dachstein Limestone of the Julian Alps (northeastern Italy). *Geology*, **33**, p. 789-92.
- Croll, J., 1875. *Climate and Time in Their Geological Relations. A theory of secular changes of the Earth's climate*. Appleton & Co., New York, 535 pp.

- Cross, T. A. & Lessenger, M. A., 1999. Construction and application of a stratigraphic inverse model. In *Numerical experiments in stratigraphy: recent advances in stratigraphic and sedimentologic computer simulations*, (ed. Harbaugh, J. W., Watney, W. L., Rankey, E. C., Slingerland, R., Goldstein, R. H. & Franseen, E. K.), SEPM Special Publication, **62**. SEPM, Tulsa, OK, p. 69-83.
- Crowley, T. J. & Baum, S. K., 1991. Estimating Carboniferous sea-level fluctuations from Gondwanan ice-extent. *Geology*, **19**, p. 975-77.
- D'Argenio, B., Ferreri, V., Raspini, A., Amodio, S. & Buonocunto, F. P., 1999. Cyclostratigraphy of a carbonate platform as a tool for high-precision correlation. *Tectonophysics*, **315**, p. 357-84.
- Davies, J. R., 1984. Sedimentary cyclicity in the late Asbian and early Brigantian (Dinantian) limestones of the Anglesey and Llandudno districts, North Wales. *Proceedings of the Geologists' Association*, **95**, p. 392-93.
- Davies, J. R., 1991. Karstification and pedogenesis on a late Dinantian carbonate platform, Anglesey, North Wales. *Proceedings of the Yorkshire Geological Society*, **48**, p. 297-321.
- Davies, J. R., Wilson, D. & Williamson, I. T., 2004. *Geology of the country around Flint. British Geological Survey Memoir for 1:50000 Geological Sheet 108 (England and Wales)*. British Geological Survey, Keyworth, Nottingham, 196 pp.
- Davis, J. C., 2002. *Statistics and Data Analysis in Geology*. John Wiley & Sons, New York, 638 pp.
- Davis, J. C. & Herzfeld, U. C., 1993. *Computers in Geology: 25 Years of Progress*. Oxford University Press, New York, 316 pp.
- de Benedictis, D., Bosence, D. W. J. & Waltham, D. A., 2007. Tectonic control on peritidal carbonate parasequence formation: an investigation using forward tectono-stratigraphic modelling. *Sedimentology*, **54**, p. 587-605.
- de Boer, P. L. & Smith, D. G., 1994. Orbital forcing and cyclic sequences. In *Orbital Forcing and Cyclic Sequences*, (ed. de Boer, P. L. & Smith, D. G.), IAS Special Publication, **19**. IAS, Oxford, p. 1-14.
- de Gibert, J. M., Netto, R. G., Tognoli, F. M. W. & Grangeiro, M. E., 2006. Commensal worm traces and possible juvenile thalassinidean burrows associated with *Ophiomorpha nodosa*, Pleistocene, southern Brazil. *Palaeogeography, Palaeoclimatology, Palaeoecology*, **230**, p. 70-84.
- Della Porta, G., Kenter, J. A. M. & Bahamonde, J. R., 2004. Depositional facies and stratal geometry of an Upper Carboniferous prograding and aggrading high-relief carbonate platform (Cantabrian Mountains, N Spain). *Sedimentology*, **51**, p. 267-95.

- Della Porta, G., Kenter, J. A. M., Immenhauser, A. & Bahamonde, J. R., 2002. Lithofacies character and architecture across a Pennsylvanian inner-platform transect (Sierra de Cuera, Asturias, Spain). *Journal of Sedimentary Research*, **72**, p. 898-916.
- Demicco, R. V. & Hardie, L. A., 2002. The "carbonate factory" revisited: a re-examination of sediment production functions used to model deposition on carbonate platforms. *Journal of Sedimentary Research*, **72**, p. 849-57.
- Dickinson, W. R. & Lawton, T. F., 2003. Sequential intercontinental suturing as the ultimate control for Pennsylvanian Ancestral Rocky Mountains deformation. *Geology*, **31**, p. 609-12.
- Driese, S. G. & Dott, R. H., 1984. Model for sandstone-carbonate "cyclothems" based on upper member of Morgan Formation (Middle Pennsylvanian) of northern Utah and Colorado. *American Association of Petroleum Geologists Bulletin*, **68**, p. 574-97.
- Drummond, C. N. & Wilkinson, B. H., 1993a. Carbonate cycle stacking patterns and hierarchies of orbitally forced eustatic sea-level change. *Journal of Sedimentary Petrology*, **63**, p. 369-77.
- Drummond, C. N. & Wilkinson, B. H., 1993b. On the Use of Cycle Thickness Diagrams as Records of Long-Term Sealevel Change during Accumulation of Carbonate Sequences. *The Journal of Geology*, **101**, p. 687-702.
- Drummond, C. N. & Wilkinson, B. H., 1996. Stratal thickness frequencies of orderedness in stratigraphic sequences. *Journal of Geology*, **104**, p. 1-18.
- Dunn, P. A., 1991. *Diagenesis and cyclostratigraphy: an example from the Middle Triassic Latemar platform, Dolomites Mountains, northern Italy*. Unpublished PhD Thesis, The John Hopkins University, Baltimore.
- Dunn, P. A., Goldhammer, R. K. & Hardie, L. A., 1986. Mr. Sediment - A computer model for carbonate cyclicity (Abstract). *Geol. Soc. Am. Abstracts with Programs*, **18**, p. 590.
- Dunn, P. A., Goldhammer, R. K., Hardie, L. A. & Nguyen, C. T., 1991. Two-dimensional forward modelling of Lower Ordovician platform carbonate sequences (Beekmantown Gp, central Appalachians): the search for high-frequency autocycles (Abstract). *American Association of Petroleum Geologists Bulletin*, **75**, p. 565.
- Durbin, J. & Watson, G. S., 1950. Testing for Serial Correlation in Least Squares Regression, I. *Biometrika*, **37**, p. 409-28.
- Durbin, J. & Watson, G. S., 1951. Testing for Serial Correlation in Least Squares Regression, II. *Biometrika*, **38**, p. 159-79.

- Eberli, G. P., Schwab, A. M. & Grammer, G. M., 2000. Anatomy of Ismay algal fields - a comparison of outcrop and 3-D seismic data. In *Genetic Stratigraphy on the Exploration and Production Scales*, (ed. Homewood, P. W. & Eberli, G. P.), ELF EP, Pau, France, p. 93-107.
- Elias, G. K., 1963. Habitat of Pennsylvanian algal bioherms, Four Corners area. In *Shelf Carbonates of the Paradox Basin*, (Ed, Bass, R. O.) Four Corners Geological Society, 4th Field Conference Guidebook, p. 185-203.
- Elrick, M. & Read, J. F., 1991. Cyclic ramp-to-basin carbonate deposits, Lower Mississippian, Wyoming and Montana: a combined field and computer modeling study. *Journal of Sedimentary Petrology*, **61**, p. 1194-224.
- Enos, P., 1991. Sedimentary Parameters for Computer Modelling. In *Sedimentary Modeling: Computer Simulations and Methods for Improved Parameter Definition*, (ed. Franseen, E. K., Watney, W. L., Kendall, C. G. S. C. & Ross, W.), **233**. Kansas Geological Survey Bulletin, Lawrence, KS, p. 63-99.
- Evans, J. E. & Reed, J. M., 2007. Integrated loessite-paleokarst depositional system, early Pennsylvanian Molas Formation, Paradox Basin, southwestern Colorado, U.S.A. *Sedimentary Geology*, **195**, p. 161-81.
- Fisher, R. A., 1922. On the interpretation of χ^2 from contingency tables, and the calculation of P. *Journal of the Royal Statistical Society*, **85**, p. 87-94.
- Foos, A., 1996. Comparison of subaerial exposure surfaces at major unconformities and capping shallowing-upward carbonate cycles. In *Paleozoic Sequence Stratigraphy: Views from the North American Craton*, (ed. Witzke, B. J., Ludvigson, G. A. & Day, J.), Geological Society of America Special Paper, **306**. Geological Society of America, Boulder, Colorado, p. 419-24.
- Foos, A., 1991. Aluminous lateritic soils, Eleuthera, Bahamas: a modern analog to carbonate paleosols. *Journal of Sedimentary Petrology*, **61**, p. 340-48.
- Gawthorpe, R. L., 1986. Sedimentation during carbonate ramp-to-slope evolution in a tectonically active area: Bowland Basin (Dinantian), northern England. *Sedimentology*, **33**, p. 185-206.
- Ginsburg, R. N., 1971. Landward movement of carbonate mud: New model for regressive cycles in carbonates [abstract]. *American Association of Petroleum Geologists, Annual Meeting, Abstract with Programs*, **55**, p. 340.
- Gischler, E., 2002. Subsurface Geology of a Prograding Carbonate Platform Margin, Great Bahama Bank. *Palaios*, **17**, p. 526-27.

- Goldhammer, R. K., Dunn, P. A. & Hardie, L. A., 1987. High frequency glacio-eustatic sealevel oscillations with Milankovitch characteristics recorded in Middle Triassic platform carbonates in northern Italy. *American Journal of Science*, **287**, p. 853-92.
- Goldhammer, R. K., Dunn, P. A. & Hardie, L. A., 1990. Depositional cycles, composite sea level changes, cycle stacking patterns, and the hierarchy of stratigraphic forcing: example from platform carbonates of the Alpine Triassic. *Geological Society of America Bulletin*, **102**, p. 535-62.
- Goldhammer, R. K., Oswald, E. J. & Dunn, P. A., 1991. Hierarchy of stratigraphic forcing: example from Middle Pennsylvanian shelf carbonates of the Paradox Basin. In *Sedimentary Modeling: Computer Simulations and Methods for Improved Parameter Definition*, (ed. Franseen, E. K., Watney, W. L., Kendall, C. G. S. C. & Ross, W.), Kansas Geological Survey Bulletin, **233**. Kansas Geological Survey, Lawrence, KS, p. 361-414.
- Goldhammer, R. K., Oswald, E. J. & Dunn, P. A., 1994. High-frequency, glacio-eustatic cyclicity in the Middle Pennsylvanian of the Paradox Basin: an evaluation of Milankovitch forcing. In *Orbital Forcing and Cyclic Sequences*, (ed. de Boer, P. L. & Smith, D. G.), **19**. IAS Special Publication, Oxford, p. 243-83.
- Gradstein, F. M., Ogg, J. G. & Smith, A. G., 2004. *A Geologic Time Scale 2004*. Cambridge University Press, Cambridge, 610 pp.
- Grammer, G. M., Eberli, G. P., Van Buchem, F. S. P., Stevenson, G. M. & Homewood, P. W., 2000. Application of high resolution sequence stratigraphy in developing an exploration and production strategy for a mixed carbonate/siliciclastic system (Carboniferous) Paradox Basin, Utah, USA. In *Genetic Stratigraphy on the Exploration and Production Scales*, (ed. Homewood, P. W. & Eberli, G. P.), ELF EP, Pau, France, p. 29-69.
- Greenwood, E., Kottowski, F. E. & Thomson, S. I., 1977. Petroleum potential and stratigraphy of Pedregosa basin: comparison with Permian and Orogrande basins. *American Association of Petroleum Geologists Bulletin*, **61**, p. 1448-69.
- Grinstead, C. M. & Snell, J. L., 1997. *Introduction to Probability*. American Mathematical Society, Providence, RI, USA, 510 pp.
- Grotzinger, J. P., 1986. Cyclicity and paleoenvironmental dynamics, Rocknest platform, northwest Canada. *Geological Society of America Bulletin*, **97**, p. 1208-31.
- Guidish, T. M., Lerche, I., Kendall, C. G. S. C. & O'Brien, J. J., 1984. Relationship between eustatic sea-level changes and basin subsidence. *American Association of Petroleum Geologists Bulletin*, **68**, p. 164-77.

- Haas, J., 2004. Characteristics of peritidal facies and evidences for subaerial exposures in Dachstein-type cyclic platform carbonates in the Transdanubian Range, Hungary. *Facies*, **50**, p. 263-86.
- Hallock, P. & Schlager, W., 1986. Nutrient excess and the demise of coral reefs and carbonate platforms. *Palaios*, **1**, p. 389-98.
- Hardie, L. A., Bosellini, A. & Goldhammer, R. K., 1986. Repeated subaerial exposure of subtidal carbonate platforms, Triassic, northern Italy: Evidence for high frequency sea level oscillations on a 10^4 year scale. *Paleoceanography*, **1**, p. 447-57.
- Hardie, L. A., Dunn, P. A. & Goldhammer, R. K., 1991. Field and modelling studies of Cambrian carbonate cycles, Virginia Appalachians - discussion. *Journal of Sedimentary Petrology*, **61**, p. 636-46.
- Hardie, L. A. & Shinn, E. A., 1986. Carbonate depositional environments, modern and ancient: part 3: tidal flats. *Colorado School of Mines Quarterly*, **81**, p. 1-74.
- Hattori, I., 1976. Entropy in Markov Chains and Discrimination of Cyclic Patterns in Lithologic Successions. *Mathematical Geology*, **8**, p. 477-97.
- Hays, J. D., Imbrie, J. & Shackleton, J. J., 1976. Variations in the Earth's orbit - pacemaker of the ice ages. *Science*, **194**, p. 1121-31.
- Heckel, P. H., 1986. Sea-level curve for Pennsylvanian eustatic marine transgressive-regressive depositional cycles along midcontinent outcrop belt, North America. *Geology*, **14**, p. 330-34.
- Hilgen, F. J., 1991. Extension of the astronomically calibrated (polarity) time scale to the Miocene/Pliocene boundary. *Earth and Planetary Science Letters*, **107**, p. 349-68.
- Hite, R. J. & Buckner, D. H., 1981. Stratigraphic correlations, facies concepts, and cyclicity in Pennsylvanian rocks of the Paradox Basin. In *Geology of the Paradox Basin*, (ed. Wiegand, D. L.), Rocky Mountain Association of Geologists, 1981 Field Conference, p. 147-59.
- Horbury, A. D., 1989. The relative roles of tectonism and eustasy in the deposition of the Urswick Limestone in south Cumbria and north Lancashire. In *The role of tectonics in Devonian and Carboniferous sedimentation in the British Isles*, (ed. Arthurton, R. S., Gutteridge, P. & Nolan, S. C.), **6**, Yorkshire Geological Society Occasional Publication, p. 153-69.
- Horbury, A. D. & Adams, A. E., 1996. Microfacies associations in Asbian carbonates: an example from the Urswick Limestone Formation of the southern Lake District, northern England. In *Recent Advances in Lower Carboniferous Geology*, (ed. Strogon, P.,

- Somerville, I. D. & Jones, G. L.), Geological Society Special Publication, **107**. The Geological Society, London, p. 221-38.
- Imbrie, J. & Imbrie, J. Z., 1980. Modeling the climatic response to orbital variations. *Science*, **207**, p. 943-53.
- Immenhauser, A. & Scott, R. W., 2002. An estimate of Albian sea-level amplitudes and its implication for the duration of stratigraphic hiatuses. *Sedimentary Geology*, **152**, p. 19-28.
- Izart, A., Le Nindre, Y., Stephenson, R., Vaslet, D. & Stovba, S., 2003. Quantification of the control of sequences by tectonics and eustasy in the Dniepr-Donets Basin and on the Russian Platform during Carboniferous and Permian. *Bulletin de la Société Géologique de France*, **174**, p. 93-100.
- James, N. P. & Choquette, P. W., 1988. *Paleokarst*. Springer-Verlag, New York, 416 pp.
- Jurdy, D. M., Stefanick, M. & Scotese, C. R., 1995. Paleozoic plate dynamics. *Journal of Geophysical Research*, **100**, p. 17965-75.
- Kabanov, P. B., 2003a. The Upper Moscovian and Basal Kasimovian (Pennsylvanian) of Central European Russia: Facies, Subaerial Exposures and Depositional Model. *Facies*, **49**, p. 243-70.
- Kabanov, P. B., 2003b. The Upper Moscovian and basal Kasimovian (Upper Carboniferous) of central European Russia: facies, subaerial exposures, and depositional model. *Facies*, **49**, p. 243-70.
- Kabanov, P. B., 2005. Traces of terrestrial biota in the upper Moscovian paleosols of central and northern European Russia. *Paleontological Journal*, **39**, p. 372-85.
- Kabanov, P. B. & Baranova, D. V., 2007. Cyclothems and stratigraphy of the Upper Moscovian - basal Kasimovian succession of central and northern European Russia. In *Proceedings of the 15th International Congress on the Carboniferous and Permian*, Royal Netherlands Academy of Arts and Sciences, Amsterdam, p. 147-60.
- Kamola, D. L. & Huntoon, J. E., 1995. Repetitive stratal patterns in a foreland basin sandstone and their possible tectonic significance. *Geology*, **23**, p. 177-80.
- Kendall, C. G. S. C. & Lerche, I., 1988. The rise and fall of eustasy. In *Sea-Level Changes - An Integrated Approach*, (ed. Wilgus, C. K., Posamentier, H., Ross, C. A. & Kendall, C. G. S. C.), Society of Economic Paleontologists and Mineralogists, Special Publication **42**. p. 3-17.
- Kenter, J. A. M., Harris, P. M., Collins, J. F., Weber, L. J., Kuanysheva, G. & Fischer, D. J., 2006. Late Visean to Bashkirian platform cyclicity in the central Tengiz buildup, Precaspian

- Basin, Kazakhstan: Depositional evolution and reservoir development. In *Giant hydrocarbon reservoirs of the world: From rocks to reservoir characterization and modeling*, (ed. Harris, P. M. & Weber, L. J.), AAPG Memoir, **88**. SEPM Special Publication, SEPM, Tulsa, OK, p. 7-54.
- Kenter, J. A. M., Vizika, O., Rosenberg, E., Skalinski, M., Harris, P. M. & Buoniconti, M., 2007. Assessment of Permeability and Porosity Using High Resolution CT and NMR: An Example From The Central Tengiz Platform Reservoir, Pricaspian Basin, Kazakhstan (abstract). *American Association of Petroleum Geologists AGM*, Long Beach, California.
- Kindler, P., 1992. Coastal response to the Holocene transgression in the Bahamas: episodic sedimentation versus continuous sea-level rise. *Sedimentary Geology*, **80**, p. 319-29.
- Klein, G. d. V., 1994. Depth determination and quantitative distinction of influence of tectonic subsidence and climate on changing sea level during deposition of midcontinent Pennsylvanian cyclothems. In *Tectonic and Eustatic Controls on Sedimentary Cycles*, (ed. Dennison, J. M. & Ettensohn, F. R.), Concepts in Sedimentology and Palaeontology, **4**. SEPM, p. 35-50.
- Kluth, C. F. & Coney, P. J., 1981. Plate tectonics of the ancestral Rocky Mountains. *Geology*, **9**, p. 10-15.
- Koerschner, W. F. & Read, J. F., 1989. Field and modelling studies of Cambrian carbonate cycles, Virginia Appalachians. *Journal of Sedimentary Petrology*, **59**, p. 654-87.
- Košir, A., 2004. Microcodium Revisited: Root Calcification Products of Terrestrial Plants on Carbonate-Rich Substrates. *Journal of Sedimentary Research*, **74**, p. 845-57.
- Kottlowski, F. E., 1963. *Paleozoic and Mesozoic strata of south-western and south-central New Mexico*. New Mexico Bureau of Mines & Mineral Resources, Bulletin 79, Socorro, NM, 100 pp.
- Kottlowski, F. E., 1965. Sedimentary basins of south central New Mexico. *American Association of Petroleum Geologists Bulletin*, **49**, p. 2120-39.
- Kottlowski, F. E., Flower, R. H., Thompson, M. L. & Foster, R. W., 1956. *Stratigraphic studies of the San Andres Mountains, New Mexico*. New Mexico Bureau of Mines & Mineral Resources Bulletin, Memoir 1, Socorro, NM, 132 pp.
- Kutzback, J. E. & Otto-Bliesner, B. L., 1982. The sensitivity of the African - Asian monsoonal climate to orbital parameter changes for 9000 years BP in a low-resolution general circulation model. *Journal of Atmospheric Science*, **39**, p. 1177-88.
- Lapeter, D. & Holterhoff, P., 2007. Evolving Middle Pennsylvanian Inner Platform Carbonate Stacking Architectures, Bug Scuffle Member, Gobbler Formation, New Mexico. 2007

- GSA Denver Annual Meeting (28–31 October 2007)*, Denver, CO. Geological Society of America Abstracts with Programs. **39**, p. 338.
- Laskar, J., 1989. A numerical experiment on the chaotic behaviour of the solar system. *Nature*, **338**, p. 237-38.
- Laskar, J., 1999. The limits of Earth orbital calculations for geological time-scale use. *Philosophical Transactions of the Royal Society of London*, **357**, p. 1735-59.
- Laskar, J., Robutel, P., Joutel, F., Gastineau, M., Correia, A. C. M. & Levrard, B., 2004. A long-term numerical solution for the insolation quantities of the Earth. *Astronomy & Astrophysics*, **428**, p. 261-85.
- Lehrmann, D. J. & Goldhammer, R. K., 1999. Secular variation in parasequence and facies stacking patterns of platform carbonates: a guide to application of stacking patterns analysis in strata of diverse ages and settings. In *Advances in Carbonate Sequence Stratigraphy: Applications to Reservoirs, Outcrops and Models*, (ed. Saller, A. H., Harris, P. M. & Simo, J. A.), SEPM Special Publication, **63**. SEPM, Tulsa, Oklahoma, p. 187-225.
- Lerat, O., Van Buchem, F. S. P., Eschard, R., Grammer, G. M. & Homewood, P. W., 2000. Facies distribution and control by accommodation within high-frequency cycles of the Upper Ismay interval (Pennsylvanian, Paradox Basin, Utah). In *Genetic Stratigraphy at the Exploration and Production Scales*, (ed. Homewood, P. W. & Eberli, G. P.), Elf EP, Pau, France, p. 71-91.
- Lerche, I., Dromzook, E., Kendall, C. G. S. C., Walter, C. M. & Seaturro, D., 1987. Geometry of carbonate bodies; a quantitative investigation of the factors influencing their evaluation. *Carbonates & Evaporites*, **2**, p. 15-42.
- Loope, D. B. & Haverland, Z. E., 1988. Giant desiccation fissures filled with calcareous eolian sand, Hermosa Formation (Pennsylvanian), southeastern Utah. *Sedimentary Geology*, **56**, p. 403-13.
- MacArthur, R. H. & Wilson, E. O., 1967. *The theory of island biogeography*. Princeton University Press, Princeton, 203 pp.
- Matthews, R. K., Frohlich, C. & Duffy, A., 1997. Orbital forcing of global change throughout the Phanerozoic: A possible stratigraphic solution to the eccentricity phase problem. *Geology*, **25**, p. 807-10.
- Maynard, J. R. & Leeder, M. R., 1992. On the periodicity and magnitude of Late Carboniferous glacioeustatic sea-level changes. *Journal of the Geological Society*, **149**, p. 303-11.
- Mazzullo, S. J., 1999. Eustatic and tectonic controls on cyclic deposition in Lower Permian ramp facies (Chase Group and Basal Wellington Formation) in the US midcontinent. In

- Advances in Carbonate Sequence Stratigraphy: Applications to Reservoirs, Outcrops and Models*, (ed. Saller, A. H., Harris, P. M. & Simo, J. A.), SEPM Special Publication, **63**. SEPM, Tulsa, Oklahoma, p. 151-68.
- McKerrow, W. S. & Scotese, C. R., 1990. Revised world maps and introduction. In *Paleozoic paleogeography and biogeography*, (ed. McKerrow, W. S. & Scotese, C. R.), Memoir of the Geological Society, London, **12**. Geological Society of London, London, p. 1-24.
- Melnyk, D. H. & Smith, D. G., 1989. Outcrop to sub-surface cycle correlation in the Milankovitch frequency band: Middle Cretaceous, central Italy. *Terra Nova*, **1**, p. 432-36.
- Miall, A. D., 1997. *The Geology of Stratigraphic Sequences*. Springer-Verlag, Berlin, pp.
- Milankovitch, M., 1941. *Kanon der Erdbestrahlung und seine Anwendung auf das Eiszeitenproblem*. Royal Serbian Academy, Belgrade, 633 pp.
- Milliman, J. D., 1974. *Marine Carbonates. Part 1, Recent Sedimentary Carbonates*. Springer-Verlag, New York, 375 pp.
- Montañez, I. P. & Read, J. F., 1992. Eustatic control on early dolomitization of cyclic peritidal carbonates: Evidence from the Early Ordovician Upper Knox Group, Appalachians. *Geological Society of America Bulletin*, **104**, p. 872-86.
- Nagy, Z. R., Somerville, I. D., Gregg, J. M., Becker, S. P., Shelton, K. L. & Sleeman, A. G., 2005. Sedimentation in an actively tilting half-graben: sedimentology and stratigraphy of Late Tournaisian-Viséan (Mississippian, Lower Carboniferous) carbonate rocks in south County Wexford, Ireland. *Sedimentology*, **52**, p. 489-512.
- Nikishin, A. M., Ziegler, P. A., Stephenson, R. A., Cloetingh, S. A. P. L., Furne, A. V., Fokin, P. A., Ershov, A. V., Bolotov, S. N., Korotaev, M. V., Alekseev, A. S., Gorbachev, V. I., Shipilov, E. V., Lankreijer, A., Bembinova, E. Y. & Shalimov, I. V., 1996. Late Precambrian to Triassic history of the East European Craton: dynamics of sedimentary basin evolution. *Tectonophysics*, **268**, p. 23-63.
- Norris, J. R., 1997. *Markov Chains*. Cambridge University Press, New York, 253 pp.
- Ohlen, H. R. & McIntyre, L. B., 1965. Stratigraphy and tectonic features of Paradox Basin, Four Corners Area. *American Association of Petroleum Geologists Bulletin*, **49**, p. 2020-40.
- Osleger, D. A., 1991. Subtidal carbonate cycles: Implications for allocyclic vs. autocyclic controls. *Geology*, **19**, p. 917-20.
- Osleger, D. A. & Read, J. F., 1991. Relation of eustasy to stacking patterns of meter-scale carbonate cycles, Late Cambrian, U.S.A. *Journal of Sedimentary Petrology*, **61**, p. 1225-52.

- Paterson, R. J., Whitaker, F. F., Jones, G. D., Smart, P. L., Waltham, D. A. & Felce, G., 2006. Accommodation and sedimentary architecture of isolated icehouse carbonate platforms: insights from forward modeling with CARB3D+. *Journal of Sedimentary Research*, **76**, p. 1162-82.
- Patterson, W. P. & Walter, L. M., 1994. Syndepositional diagenesis of modern platform carbonates; evidence from isotopic and minor element data. *Geology*, **22**, p. 127-30.
- Paulay, G. & McEdward, L. R., 1990. A simulation model of island reef morphology: the effects of sea-level fluctuations, growth, subsidence and erosion. *Coral Reefs*, **9**, p. 51-62.
- Perlmutter, M. A., De Boer, P. L. & Syvitski, J. R. L., 1999. Geological observations and parameterizations. In *Numerical experiments in stratigraphy: recent advances in stratigraphic and sedimentologic computer simulations*, (ed. Harbaugh, J. W., Watney, W. L., Rankey, E. C., Slingerland, R., Goldstein, R. H. & Franseen, E. K.), SEPM Special Publication, **62**. SEPM, Tulsa, OK, p. 25-31.
- Peterson, J. A. & Hite, R. J., 1969. Pennsylvanian evaporite-carbonate cycles and their relation to petroleum occurrence, southern Rocky Mountains. *American Association of Petroleum Geologists Bulletin*, **53**, p. 884-908.
- Pindell, J. L. & Dewey, J. F., 1982. Permo-Triassic reconstruction of western Pangea and the evolution of the Gulf of Mexico/Caribbean region. *Tectonics*, **1**, p. 179-211.
- Plan, L., 2005. Factors controlling carbonate dissolution rates quantified in a field test in the Austrian alps. *Geomorphology*, **68**, p. 201-12.
- Pomar, L., 2001a. Ecological control of sedimentary accommodation: evolution from a carbonate ramp to rimmed shelf, Upper Miocene, Balearic Islands. *Palaeogeography, Palaeoclimatology, Palaeoecology*, **175**, p. 249-72.
- Pomar, L., 2001b. Types of carbonate platforms: a genetic approach. *Basin Research*, **13**, p. 313-34.
- Pomar, L., Brandano, M. & Westphal, H., 2004. Environmental factors influencing skeletal grain sediment associations: a critical review of Miocene examples from the western Mediterranean. *Sedimentology*, **51**, p. 627-51.
- Pray, L. C., 1961. *Geology of the Sacramento Mountains Escarpment, Otero County, New Mexico*. New Mexico Bureau of Mines & Mineral Resources, Bulletin 35, Socorro, NM, 144 pp.
- Pray, L. C. & Wray, J. L., 1963. Porous algal facies (Pennsylvanian) Honaker Trail, San Juan Canyon, Utah. In *Shelf Carbonates of the Paradox Basin*, (ed. Bass, R. O.), Four Corners Geological Society, 4th Field Conference Guidebook, p. 204-34.

- Quinn, T. M. & Matthews, R. K., 1990. Post-Miocene diagenetic and eustatic history of Enewetak atoll: model and data comparison. *Geology*, **18**, p. 942-45.
- Quiquerez, A., Allemand, P., Dromart, G. & Garcia, J.-P., 2004. Impact of storms on mixed carbonate and siliciclastic shelves: insights from combined diffusive and fluid-flow transport stratigraphic forward model. *Basin Research*, **16**, p. 431-49.
- Ramsay, A. T. S., 1989. Tectonics and sedimentation of late Dinantian limestones in South Wales. In *The Role of Tectonics in Devonian and Carboniferous Sedimentation in the British Isles*, (ed. Arthurton, R. S., Gutteridge, P. & Nolan, S. C.), **6**. Yorkshire Geological Society Occasional Publication, p. 225-41.
- Rankey, E. C., 2004. On the Interpretation of Shallow Shelf Carbonate Facies and Habitats: How Much Does Water Depth Matter? *Journal of Sedimentary Research*, **74**, p. 2-6.
- Read, J. F. & Goldhammer, R. K., 1988. Use of Fischer diagrams to define third-order sea-level curves in Ordovician peritidal cyclic carbonates, Appalachians. *Geology*, **16**, p. 895-99.
- Read, J. F., Grotzinger, J. P., Bova, J. A. & Koerschner, W. F., 1986. Models for generation of carbonate cycles. *Geology*, **14**, p. 107-10.
- Read, J. F., Kerans, C., Weber, J. J., Sarg, J. F. & Wright, F. M., 1995. *Milankovitch Sea-level Changes, Cycles and Reservoirs on Carbonate Platforms in Greenhouse and Ice-house Worlds*. SEPM Short Course Notes Series 35, Tulsa, OK, 102 pp.
- Riebeek, H., 2006. *Paleoclimatology: Explaining the Evidence*. NASA Earth Observatory. Available: http://earthobservatory.nasa.gov/Study/Paleoclimatology_Evidence/. Last accessed: 20 May 2006.
- Riley, N. J., 1993. Dinantian (Lower Carboniferous) biostratigraphy and chronostratigraphy in the British Isles. *Journal of the Geological Society*, **150**, p. 427-46.
- Ritter, S. M., Barrick, J. E. & Skinner, M. R., 2002. Conodont sequence biostratigraphy of the Hermosa Group (Pennsylvanian) at Honaker Trail, Paradox Basin, Utah. *Journal of Paleontology*, **76**, p. 495-517.
- Ross, C. A., 1979. Late Paleozoic collision of North and South America. *Geology*, **7**, p. 41-44.
- Ross, C. A., 1986. Paleozoic evolution of southern margin of Permian Basin. *Geological Society of America Bulletin*, **97**, p. 536-54.
- Ross, C. A. & Ross, J. P., 1987. Late Paleozoic sea levels and depositional sequences. In *Timing and Depositional History of Eustatic Sequences: Constraints on Seismic Stratigraphy*, (ed. Ross, C. A. & Haman, D.), Cushman Foundation for Foraminiferal Research Special Publication, **24**. Cushman Foundation, Washington, D.C., p. 137-49.

- Roylance, M. H., 1990. Depositional and diagenetic history of a Pennsylvanian algal-mound complex; Bug and Papoose Canyon fields, Paradox Basin, Utah and Colorado. *American Association of Petroleum Geologists Bulletin*, **74**, p. 1087-99.
- Sadler, P. M., 1994. The expected duration of upward-shallowing peritidal carbonate cycles and their terminal hiatuses. *Geological Society of America Bulletin*, **106**, p. 791-802.
- Sadler, P. M., 1999. The influence of hiatuses on sediment accumulation rates. In *On the Determination of Sediment Accumulation Rates*, (ed. Bruns, P. & Hass, H. C.), GeoResearch Forum, **5**. Trans Tech Publications, Switzerland, p. 15-40.
- Sadler, P. M., Osleger, D. A. & Montanez, I. P., 1993. On the labelling, length and objective basis of Fischer plots. *Journal of Sedimentary Petrology*, **63**, p. 360-68.
- Saller, A. H., Dickson, J. A. D. & Boyd, S. A., 1994. Cycle stratigraphy and porosity in Pennsylvanian and Lower Permian shelf limestone, Eastern Central Basin Platform, Texas. *American Association of Petroleum Geologists Bulletin*, **83**, p. 1835-54.
- Saller, A. H., Dickson, J. A. D. & Matsuda, F., 1999a. Evolution and distribution of porosity associated with subaerial exposure in Upper Paleozoic platform limestones, West Texas. *American Association of Petroleum Geologists Bulletin*, **83**, p. 1835-54.
- Saller, A. H., Dickson, J. A. D., Rasbury, E. T. & Ebato, T., 1999b. Effects of long-term accommodation change on short-term cycles, Upper Palaeozoic platform limestones, West Texas. In *Advances in Carbonate Sequence Stratigraphy: Applications to Reservoirs, Outcrops and Models*, (ed. Saller, A. H., Harris, P. M. & Simo, J. A.), SEPM Special Publication, **63**. SEPM, Tulsa, p. 227-46.
- Sander, B., 1951. *Contributions to the study of depositional fabrics (rhythmically deposited Triassic limestones and dolomites)*. American Association of Petroleum Geologists, Tulsa, Oklahoma, 207 p. pp.
- Sattler, U., Immenhauser, A., Hillgärtner, H. & Esteban, M., 2005. Characterization, lateral variability and lateral extent of discontinuity surfaces on a Carbonate Platform (Barremian to Lower Aptian, Oman). *Sedimentology*, **52**, p. 339-61.
- Schlager, W., 2003. Benthic carbonate factories of the Phanerozoic. *International Journal of Earth Sciences*, **92**, p. 445-64.
- Schmitz, B. & Pujalte, V., 2003. Sea-level, humidity, and land-erosion records across the initial Eocene thermal maximum from a continental-marine transect in northern Spain. *Geology*, **31**, p. 689-92.

- Scholle, P. A. & Goldstein, R. H., 1991. *Classic Upper Paleozoic reefs and bioherms of west Texas and New Mexico (A field guide to the Guadalupe and Sacramento Mountains)*. AAPG Classic Carbonate Course, Tulsa, OK, 246 pp.
- Scholle, P. A. & Spearing, D., 1982. *Sandstone depositional environments*. AAPG Memoir 31. AAPG, Tulsa, OK, 410 pp.
- Schwarzacher, W., 1975. *Sedimentation models and quantitative stratigraphy*. Elsevier, New York, 382 p. pp.
- Schwarzacher, W., 2005. The stratification and cyclicity of the Dachstein Limestone in Lofer, Leogang and Steinernes Meer (Northern Calcareous Alps, Austria). *Sedimentary Geology*, **181**, p. 93-106.
- Sinclair, H. D., 1997. Tectonostratigraphic model for underfilled peripheral foreland basins: An Alpine perspective. *Geological Society of America Bulletin*, **109**, p. 324-246.
- Smith, L. B. & Read, J. F., 2000. Rapid onset of late Paleozoic glaciation on Gondwana: Evidence from Upper Mississippian strata of the Midcontinent, United States. *Geology*, **28**, p. 279-82.
- Smith, S. V. & Kinsey, D. W., 1976. Calcium carbonate budget production, coral reef growth and sea-level changes. *Science*, **194**, p. 937-39.
- Somerville, I. D., 1979. A sedimentary cyclicity in early Asbian (lower D1) limestones in the Llangollen district of North Wales. *Proceedings of the Yorkshire Geological Society*, **42**, p. 397-404.
- Soreghan, G. S., 1992. Preservation and paleoclimate significance of eolian dust in the Ancestral Rocky Mountains province. *Geology*, **20**.
- Soreghan, G. S., 2002. How high were the Ancestral Rocky Mountains? *Geological Society of America AGM; Abstracts Volume, 2002 Denver Annual Meeting*. Geological Society of America. **22**. p. 13.
- Soreghan, G. S., Elmore, R. D. & Lewchuk, M. T., 2002. Sedimentologic-magnetic record of western Pangean climate in upper Paleozoic loessite (lower Cutler beds, Utah). *Geological Society of America Bulletin*, **114**, p. 1019-35.
- Soreghan, G. S., Moses, A. M., Soreghan, M. J., Hamilton, M. A., Mark Fanning, C. & Link, P. K., 2007a. Palaeoclimatic inferences from upper Palaeozoic siltstone of the Earp Formation and equivalents, Arizona-New Mexico (USA). *Sedimentology*, **54**, p. 701-19.
- Soreghan, G. S., Soreghan, M. J. & Hamilton, M. A., 2007b. Reconciling indicators of cold and warmth in Late Paleozoic tropical Pangaea: high-magnitude glacial-interglacial climate change? *Geological Society of America AGM*.

- Spence, G. H. & Tucker, M. E., 1999. Modeling carbonate microfacies in the context of high-frequency dynamic relative sea-level and environmental changes. *Journal of Sedimentary Research*, **69**, p. 947-61.
- Spence, G. H. & Tucker, M. E., 2007. A Proposed Integrated Multi-Signature Model for Peritidal Cycles in Carbonates. *Journal of Sedimentary Research*, **77**, p. 797-808.
- Steckler, M. S., 1999. High-resolution sequence stratigraphic modeling 1: the interplay of sedimentation, erosion and subsidence. In *Numerical experiments in stratigraphy: recent advances in stratigraphic and sedimentologic computer simulations*, (ed. Harbaugh, J. W., Watney, W. L., Rankey, E. C., Slingerland, R., Goldstein, R. H. & Franseen, E. K.), SEPM Special Publication, **62**. SEPM, Tulsa, OK, p. 139-49.
- Stemmerik, L., 1996. High frequency sequence stratigraphy of a siliciclastic influenced carbonate platform, lower Moscovian, Amdrup Land, North Greenland. In *High Resolution Sequence Stratigraphy: Innovations and Applications*, (ed. Howell, J. A. & Aitken, J. F.), Geological Society Special Publication, **104**. The Geological Society, London, p. 347-65.
- Stevenson, G. M. & Baars, D. L., 1986. The Paradox: A Pull-Apart Basin of Pennsylvanian Age. In *Paleotectonics and sedimentation in the Rocky Mountain region, United States*, (ed. Peterson, J. A.), American Association of Petroleum Geologists Memoir, **41**. AAPG, Tulsa, OK, p. 513-39.
- Stevenson, G. M. & Baars, D. L., 1988. Overview - carbonate reservoirs of the Paradox basin. *1988 Carbonate Symposium*, Rocky Mountain Association of Geologists. 149-62.
- Strasser, A. & Samankassou, E., 2003. Carbonate Sedimentation Rates Today and in the Past: Holocene of Florida Bay, Bahamas, and Bermuda vs. Upper Jurassic and Lower Cretaceous of the Jura Mountains (Switzerland and France). *Geologia Croatica*, **56**, p. 1-18.
- Tedesco, L. P. & Wanless, H. R., 1991. Generation of sedimentary fabrics and facies by repetitive excavation and storm filling of burrow networks, Holocene of South Florida and Caicos Platform, B.W.I. *Palaios*, **6**, p. 326-43.
- Tinker, S. W., 1998. Shelf-to-basin facies distributions and sequence stratigraphy of a steep-rimmed carbonate margin; Capitan depositional system, McKittrick Canyon, New Mexico and Texas. *Journal of Sedimentary Research*, **68**, p. 1146-74.
- Tipper, J. C., 1997. Modeling carbonate platform sedimentation - Lag comes naturally. *Geology*, **25**, p. 495-98.

- Tipper, J. C., 2000. Patterns of stratigraphic cyclicity. *Journal of Sedimentary Research*, **70**, p. 1262-79.
- Titus, A. & Riley, N. J., 1997. Recognition and correlation of eustatic flooding events in the late Visean of Utah (southwest USA) and Britain (northwest Europe). *Newsletter on Carboniferous Stratigraphy*, **15**, p. 19-22.
- Trudgill, S., 1985. *Limestone geomorphology*. Longman, London, 196 pp.
- Tucker, M. E. & Wright, V. P., 1990. *Carbonate Sedimentology*. Blackwell Scientific, Oxford, 482 pp.
- Vail, P. R., Mitchum, R. M. J., Todd, R. G., Widmier, J. M., Thompson, S. I., Sangree, J. B., Bubb, J. N. & Hatlelid, W. G., 1977. Seismic stratigraphy and global changes of sea level. In *Seismic Stratigraphy: Applications to Hydrocarbon Exploration*, (ed. Payton, C. E.), AAPG Memoir, **26**. AAPG, Houston, p. 49-212.
- Van Buchem, F. S. P., Doligez, B., Eschard, R., Lerat, O., Grammer, G. M. & Ravenne, C., 2000. Stratigraphic architecture and stochastic reservoir simulation of a mixed carbonate/siliciclastic platform (Upper Carboniferous, Paradox Basin, USA). In *Genetic Stratigraphy at the Exploration and Production Scales*, (ed. Homewood, P. W. & Eberli, G. P.), Elf EP, Pau, France, p. 109-29.
- Van Wagoner, J. C., Posamentier, H. W., Mitchum, R. M. J., Vail, P. R., Sarg, J. F., Loutit, T. S. & Hardenbol, J., 1988. An overview of the fundamentals of sequence stratigraphy and key definitions. In *Sea-Level Changes: an Integrated Approach*, (ed. Wilgus, C. K., Hastings, B. S., Kendall, C. G. S. C., Posamentier, H., Ross, C. A. & Van Wagoner, J. C.), SEPM Special Publication, **42**. SEPM, Tulsa, OK, p. 38-45.
- Vanstone, S. D., 1993. *Soil development and the use of palaeosols in the assessment of palaeoclimate: a case study from the late Dinantian of Britain and Newfoundland*. Unpublished PhD thesis, University of Reading, Reading.
- Vanstone, S. D., 1996. The influence of climatic change on exposure surface developments: a case study from the Late Dinantian of England and Wales. In *Recent Advances in Lower Carboniferous Geology*, (ed. Strogon, P., Somerville, I. D. & Jones, G. L.), Geological Society Special Publication, **107**. The Geological Society, London, p. 281-301.
- Vanstone, S. D., 1998. Late Dinantian palaeokarst of England and Wales: implications for exposure surface development. *Sedimentology*, **45**, p. 19-37.
- Veevers, J. J. & Powell, C. M., 1987. Late Palaeozoic glacial episodes in Gondwanaland reflected in transgressive-regressive depositional sequences in Euramerica. *Geological Society of America Bulletin*, **98**, p. 475-87.

- Vollbrecht, R. & Kudrass, H. R., 1990. Geological results of a pre-site survey for ODP drill sites in the SE Sulu Basin. In *Proceedings of the Ocean Drilling Program, Initial Reports*, (ed. Rangin, C., Silver, E. & von Breyman, M. T.), **124**, p. 105-11.
- Walkden, G. D., 1974. Paleokarstic surface in Upper Viséan (Carboniferous) limestone of the Derbyshire Block, England. *Journal of Sedimentary Petrology*, **44**, p. 1232-47.
- Walkden, G. M., 1987. Sedimentary and diagenetic styles in Late Dinantian Carbonates of Britain. In *European Dinantian Environments*, (ed. Miller, J., Adams, A. E. & Wright, V. P.), J Wiley & Sons Ltd., Chichester, p. 131-55.
- Walkden, G. M. & Davies, J. R., 1983. Polyphase erosion of subaerial omission surfaces in the Late Dinantian of Anglesey, North Wales. *Sedimentology*, **30**, p. 861-78.
- Walkden, G. M. & Walkden, G. D., 1990. Cyclic sedimentation in carbonate and mixed carbonate clastic environments: four simulation programs for a desktop computer. In *Carbonate Platforms (Facies, Sequences and Evolution)*, (ed. Tucker, M. E., Wilson, J. L., Crevello, P. D., Sarg, J. F. & Read, J. F.), IAS Special Publication, **9**, p. 55-78.
- Walker, R. G. & James, N. P., 1992. *Facies models : response to sea level change*. Geological Association of Canada. St. John's, Newfoundland, Canada, 409 pp.
- Warburton, J., 1990. An Alpine Proglacial Fluvial Sediment Budget. *Geografiska Annaler. Series A, Physical Geography*, **72**, p. 261-72.
- Warrlich, G. M. D., Waltham, D. A. & Bosence, D. W. J., 2002. Quantifying the sequence stratigraphy and drowning mechanisms of atolls using a new 3-D forward stratigraphic modelling program (CARBONATE 3D). *Basin Research*, **14**, p. 379-400.
- Watney, W. L., Wong, J.-C. & French, J. A. J., 1991. Computer simulation of Upper Pennsylvanian (Missourian) carbonate-dominated cycles in western Kansas. In *Sedimentary Modeling: Computer Simulations and Methods for Improved Parameter Definition*, (ed. Franseen, E. K., Watney, W. L., Kendall, C. G. S. C. & Ross, W.), **233**. Kansas Geological Survey Bulletin, Lawrence, KS, p. 415-30.
- Weedon, G., 2003. *Time-Series Analysis and Cyclostratigraphy: Examining Stratigraphic Records of Environmental Cycles*. Cambridge University Press, Cambridge UK, 259 pp.
- Wells, M. R., Allison, P. A., Piggott, M. D., Gorman, G. J., Hampson, G. J., Pain, C. C. & Fang, F., 2007. Numerical Modeling of Tides in the Late Pennsylvanian Midcontinent Seaway of North America with Implications for Hydrography and Sedimentation. *Journal of Sedimentary Research*, **77**, p. 843-65.

- Wells, M. R., Allison, P. A., Piggott, M. D., Pain, C. C., Hampson, G. J. & De Oliveira, C. R. E., 2005. Large sea, small tides: the Late Carboniferous seaway of NW Europe. *Journal of the Geological Society*, **162**, p. 417-20.
- Wengard, S. A., 1962. Pennsylvanian sedimentation in Paradox Basin, Four Corners region. In *Pennsylvanian system in the United States, a symposium.*, (ed. Branson, C. C.), AAPG, Tulsa, OK, p. 264-330.
- Wengard, S. A., 1963. Stratigraphic section at Honaker Trail, San Juan Canyon, San Juan County, Utah. In *Shelf Carbonates of the Paradox Basin*, (Ed, Bass, R. O.) Four Corners Geological Society, 4th Field Conference Guidebook, p. 235-43.
- Wengard, S. A. & Matheny, M. L., 1958. Pennsylvanian system of Four Corners Region. *American Association of Petroleum Geologists Bulletin*, **42**, p. 2048-106.
- Wengerd, S. A., 1959. Pennsylvanian oil possibilities of San Juan Basin, Four Corners region; Colorado-New Mexico. *American Association of Petroleum Geologists Bulletin*, **43**, p. 2214-27.
- Wilkinson, B. H., Diedrich, N. W. & Drummond, C. N., 1996. Facies successions in peritidal carbonate sequences. *Journal of Sedimentary Research*, **66**, p. 1065-78.
- Wilkinson, B. H., Diedrich, N. W., Drummond, C. N. & Rothman, E. D., 1998. Michigan hockey, meteoric precipitation, and rhythmicity of accumulation on peritidal carbonate platforms. *Geological Society of America Bulletin*, **110**, p. 1075-93.
- Wilkinson, B. H., Drummond, C. N., Diedrich, N. W. & Rothman, E. D., 1997a. Biological mediation of stochastic peritidal carbonate accumulation. *Geology*, **25**, p. 847-50.
- Wilkinson, B. H., Drummond, C. N., Diedrich, N. W. & Rothman, E. D., 1999. Poisson processes of carbonate accumulation on Paleozoic and Holocene platforms. *Journal of Sedimentary Research*, **69**, p. 338-50.
- Wilkinson, B. H., Drummond, C. N., Rothman, E. D. & Diedrich, N. W., 1997b. Stratal order in peritidal carbonate sequences. *Journal of Sedimentary Research*, **67**, p. 1068-82.
- Wilkinson, B. H., Merrill, G. K. & Kivett, S. J., 2003. Stratal order in Pennsylvanian cyclothems. *Geological Society of America Bulletin*, **115**, p. 1068-87.
- Wilson, J. L., 1972. Influence of local structure in sedimentary cycles of Beeman and Holder Formations, Sacramento Mountains, Otero County, New Mexico. In *Cyclic Sedimentation in the Permian Basin, A Symposium*, (ed. Elam, J. C. & Chuber, S.), West Texas Geological Society, Midland, TX, p. 100-14.
- Wright, V. P., 1982a. Calcrete paleosols from the Lower Carboniferous Llanelly Formation, South Wales. *Sedimentary Geology*, **33**, p. 1-33.

- Wright, V. P., 1982b. The recognition and interpretation of paleokarsts: two examples from the Lower Carboniferous of South Wales. *Journal of Sedimentary Petrology*, **52**, p. 83-94.
- Wright, V. P., 1986. Facies sequences on a carbonate ramp: the Carboniferous Limestone of South Wales. *Sedimentology*, **33**, p. 221-41.
- Wright, V. P., 1992. Speculations on the controls on cyclic peritidal carbonates: ice-house versus greenhouse eustatic controls. *Sedimentary Geology*, **76**, p. 1-5.
- Wright, V. P., 1994. Paleosols in shallow marine carbonate sequences. *Earth-Science Reviews*, **35**, p. 367-95.
- Wright, V. P., 1996. Use of palaeosols in sequence stratigraphy of peritidal carbonates. In *Sequence Stratigraphy in British Geology*, (ed. Hesselbo, S. P. & Parkinson, D. N.), Geological Society Special Publication, **103**. The Geological Society, London, p. 63-74.
- Wright, V. P., 2005. *Carbonate Depositional Systems, Reservoir Sedimentology and Diagenesis*. Unpublished Report for Nautilus Geoscience Training Alliance, Houston.
- Wright, V. P. & Azerêdo, A. C., 2006. How relevant is the role of macrophytic vegetation in controlling peritidal carbonate facies?: Clues from the Upper Jurassic of Portugal. *Sedimentary Geology*, **186**, p. 147-56.
- Wright, V. P. & Chernes, L., 2004. Are there "black holes" in carbonate deposystems? *Geologica Acta*, **2**, p. 285-90.
- Wright, V. P. & Vanstone, S. D., 2001. Onset of Late Palaeozoic glacio-eustasy and the evolving climates of low latitude areas: a synthesis of current understanding. *Journal of the Geological Society*, **158**, p. 579-82.

Appendices

**Appendix 1:
Pilot lateral variability study of Dinantian platform
carbonates, Anglesey, UK**

A1.1	Aims	2
A1.2	Introduction	2
A1.3	Executive Summary	3
	A1.3.1 Recommendations	6
A1.4	Sampling & methods.....	7
	A1.4.1 Logs	8
A1.5	Facies	9
	A1.5.1 Facies F1	13
	A1.5.1.1 F1 Environmental Interpretation	16
	A1.5.2 Facies F2	17
	A1.5.2.1 F2 Environmental Interpretation	17
	A1.5.3 Facies F1(ES)	18
	A1.5.4 Facies F2(ES)	19
	A1.5.4.1 F1(ES) & F2(ES) Environmental Interpretation	19
	A1.5.5 Summary	20
A1.6	Lateral Variability.....	20
	A1.6.1 Unit 1 (Representative sample: C8.)	20
	A1.6.2 Unit 2 (Representative sample: C5, C6.)	22
	A1.6.3 Unit 3 (Representative sample: C16.)	22
	A1.6.4 Unit 4 (Representative sample: C13.)	26
	A1.6.5 Unit 5 (Representative sample: C10.)	26
	A1.6.6 Unit 6, 7, 8	26
	A1.6.7 Summary	29
A1.7	Cyclicity	29
	A1.7.1 Cycle 1	29
	A1.7.2 Cycle 2	31
	A1.7.3 Cycle 3	31
	A1.7.4 Cycles 4 & 5	32
	A1.7.5 Cycle 6	32
	A1.7.6 Summary	33
A1.8	Analogue Studies.....	34
	A1.8.1 Facies	34
A1.9	Cyclicity	36
	A1.9.1 Comparison with the Sierra de Cuera Platform, Spain	38
A1.10	Conclusions	40
A1.11	References.....	42

APPENDIX 1: PILOT STUDY OF LATERAL MICROFACIES VARIABILITY AND SEDIMENTARY CYCLICITY OF THE DINANTIAN OF ANGLESEY, UK

A1.1 AIMS

The general aim of this study is to provide information on the architecture of ice-house cyclothem-bearing reservoirs of the Pricaspian Basin, and globally, through the interpretation of a reservoir analogue cropping out in Anglesey; specifically addressing the inherent cyclicity and lateral variability of microfacies. In particular the following contributions are provided in the present report:

- A modern facies framework for the late Viséan of Anglesey; incorporating a facies characterisation, an assessment of the ability to correlate these facies laterally and a study of any observed lateral variability in these facies.
- An assessment of the sedimentary cyclicity of the analogue and its relation to reservoirs of the Pricaspian Basin.
- Comparison of the facies and cyclicity of the analogue with those observed in reservoirs of the Pricaspian Basin.

A1.2 INTRODUCTION

Anglesey, by the late Viséan (Asbian-Brigantian) had evolved from a land attached ramp to a reef-rimmed carbonate shelf (Adams & Cossey, 2004). Part of the inner-platform facies of this shelf are represented at outcrop near the village of Moelfre, on the North coast of the island (Figure 1). Viséan strata crop out as shallow-dipping (approximately 7° south-east) beds with a clear sedimentary cyclicity (Figure 2). The inherent cycles are clearly defined at frequent intervals (one to ten metres) by cycle-capping palaeokarstic surfaces representing sub-aerial exposure. Anglesey presents an ideal opportunity to study strata analogous to Viséan reservoirs in the Pricaspian Basin of Kazakhstan.

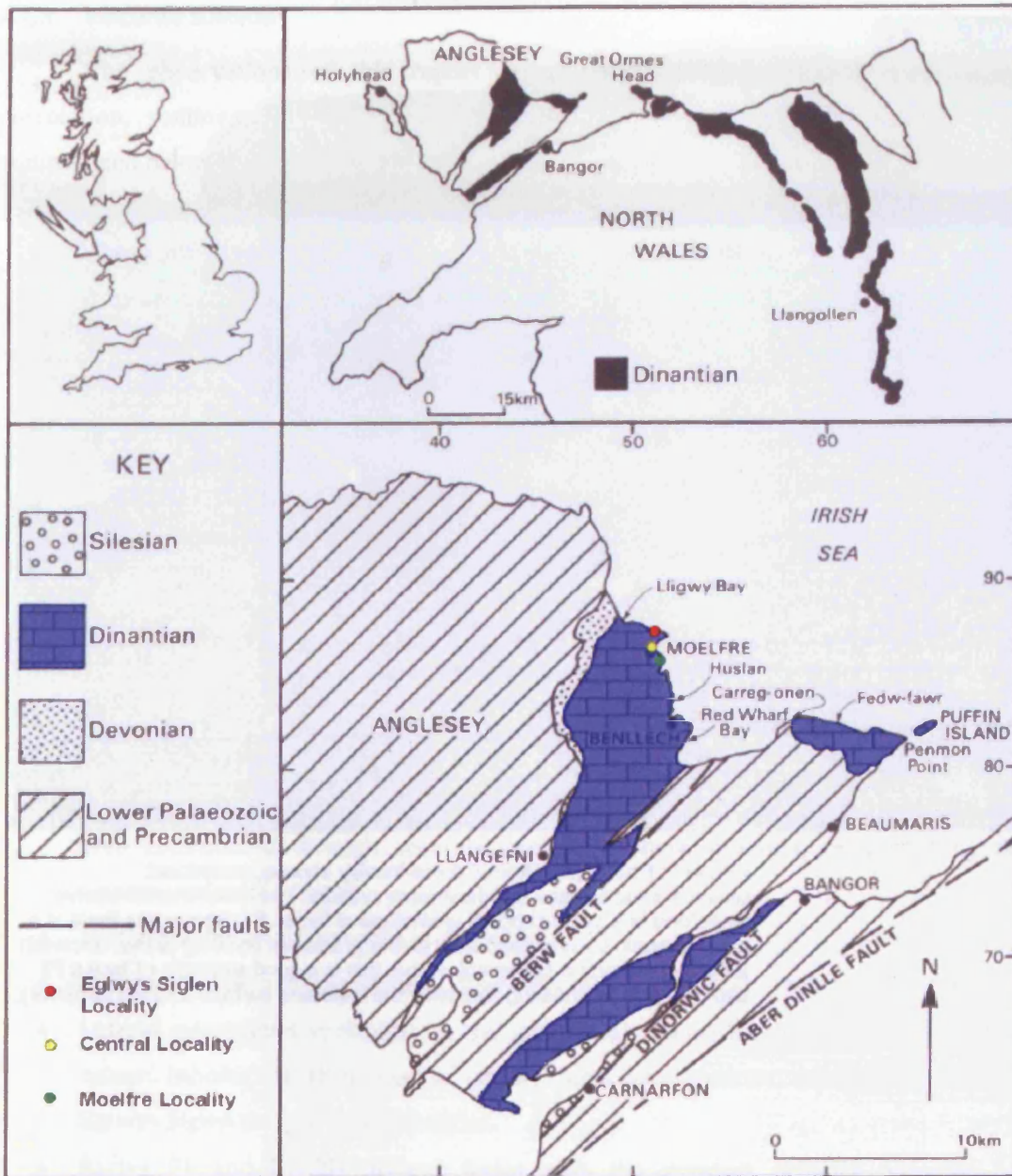


Figure 1: Geological map showing the distribution of Dinantian carbonates in Anglesey and North Wales, as well as localities sampled in the November survey (modified from Davies, 1991).

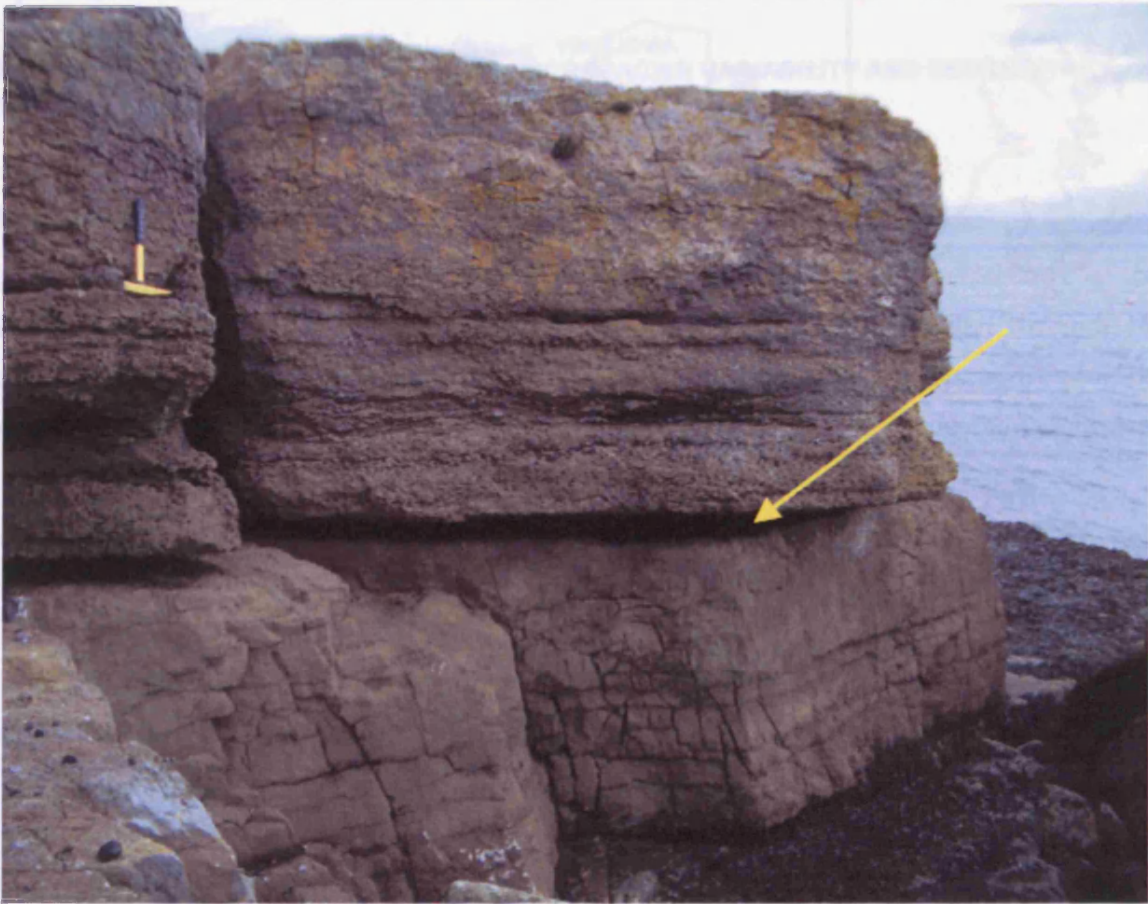


Figure 2: Photograph from Central locality showing prominent palaeokarstic surface and illustrating cyclicality. The lower more massive limestone is a cycle-capping grainstone of facies F1. Above this there is a palaeokarstic surface (apparent as the prominent bedding plane, arrowed) although missing a palaeosol. Above this is a good example of facies F2 showing burrow mottling (between the exposure surface and the hammer).

A1.3 EXECUTIVE SUMMARY

The observations of this report regarding the facies, microfacies, lithological correlation, sedimentary cyclicity and application as an outcrop analogue are briefly summarised below:

- There are two major facies types which occur in the Asbian and Brigantian of Anglesey: F1, a bioclastic grainstone and F2, a peloidal packstone. There are also two minor facies characterised; these are associated with facies seen exclusively at the Eglwys Siglen locality: these are observed to be of the same genetic facies as F1 and F2, but display proportionally more micritic material.
- Facies F1 is interpreted as a cycle-top grainstone unit, displaying shallow-water (less than ten metres) biota, and deposited in a high energy environment, consistent with classic cycle top packages. It displays a palaeokarstic top with evidence of pedogenesis.
- Facies F2 is regarded as a basal transgressive unit, comprising biota preferring slightly deeper conditions and displaying evidence of deposition in a deeper environment, including burrowing and bioturbation.
- Correlation of these facies as units across the three localities is generally good and well constrained through accurate sampling where possible, reinforced by field interpretation of outcrop.
- Biohermal facies are not seen in Anglesey.
- Stratal architecture is essentially layer-cake in Anglesey.
- Lateral microfacies variability in the late Viséan seems limited. Although there are minor lithological thickness variations between localities, particularly between Eglwys Siglen and the other localities.
- Facies F1 and F1(ES) present facies with the greatest primary porosity, now represented by calcite spar. These would make the best reservoirs facies.
- A significant lateral change is notable in the prominence of the 'muddier' facies F1(ES) and F2(ES) at Eglwys Siglen, as opposed to facies F1 and F2 which are observed to be laterally adjacent at the other localities (refer to Chapter 7). The reasons for this change are unknown at this time. In terms of reservoir properties any increase in the micrite content of the sediment is likely to have a detrimental affect on porosity and permeability.

- Cyclicity in the study interval at Anglesey is characterised by two well defined classical ice-house cycles, three indeterminate cycles which are poorly constrained, and a cycle demonstrating a significant deepening event combined with a change in the nature of cyclicity in the Brigantian.
- The Asbian-early Brigantian cycles display classic ice-house, shallow-water shoaling-up cycles. They consist of a basal transgressive unit containing packstone (F2) facies which grade upwards into shallower grainstone (F1) units capped by a palaeokarst displaying pedogenic features.
- Later Brigantian cycles exhibit a style consistent with deposition at a greater depth, with considerably deeper water facies being deposited, possibly preserving minor cyclicity. The causes and precise effects of this deepening event are not understood at this time.
- Facies F1 is considered to be an analogue of Karachaganak facies C2.3C.
- Facies F2 is considered to be an analogue of Karachaganak facies C3.1C.
- There is a deepening event described as being 'late Viséan-early Serpukhovian' in Karachaganak which is likely to be the equivalent of the event seen in the Brigantian of Anglesey.
- The Anglesey platform presents significant dissimilarities in its architecture compared to the Sierra de Cuera platform. It is likely to represent a shallow end-member of an evolution of the Sierra de Cuera platform.

A1.3.1 Recommendations

One of the main issues not directly addressed in this study was dolomitisation and diagenetic history of the facies. A study of mineralogy of analogous facies in Karachaganak using x-ray diffraction analysis (Di Giovanni et al, 2001a) showed that pure limestone was the dominant lithology, while dolomite accounted for only 2-7% of the lithology in less than one third of samples. On this basis, dolomitisation alone may not warrant further investigation. A study of the origin of calcite cements however, could provide useful insights into the diagenetic history and reservoir potential of the analogous reservoir facies comparable to Karachaganak. This work could be completed from the existing data set.

The changing nature of the lithology and the apparent deepening event in the Brigantian could potentially provide information regarding changing eustatic sea-level patterns in the Lower Carboniferous. The fact that this deepening is observed in both Kazakhstan and Anglesey suggests that this is a major event of some importance. A more

detailed study of the Brigantian and Serpukhovian strata would be needed, probably using a different analogue to Anglesey.

The presence of slightly muddier lithologies at the Eglwys Siglen locality may not necessarily warrant further investigation. If the lithology is not significantly varied so as to affect reservoir properties then further study would be wasted, particularly as this would require a new data set on an anomaly which may not yield predictive results.

This study does not incorporate one-dimensional forward modelling. This work is planned and can be accomplished using the existing data set and information contained in this report.

Finally, in order to accurately assess any implications for reservoir development that the distinction between the lensoid bioherms described by Della Porta et al (2004) and Anglesey may have, a study accurately quantifying the distinctions between the two architectural styles, if any, must be undertaken.

A1.4 SAMPLING & METHODS

The boundaries of the study area fall around the village of Moelfre (SH 512864; Figure 1). The regional strike is approximately north-east to south-west, meaning that beds crop out as cliff exposures along the headlands around Moelfre. These cliff exposures present ideal opportunity for study due to ease of access and their stratigraphic location. Specifically, three localities were chosen for logging and sampling, all selected as they repeated the same strata either side of the Asbian-Brigantian boundary over a lateral distance of approximately 1.2km. A natural limit was imposed upon the scale of the lateral variability study by the geology. The shallow-dipping Asbian beds are truncated by a fault at SH 515868, limiting lateral tracing beyond this major fault. To the south the Brigantian strata are overlain by siliclastic Namurian sediments, defining the southern lateral extent at SH 515857. Between these two boundaries, however, outcrop was relatively continuous.

The first locality (refer to Figure 1) was south of the town of Moelfre (SH 513858; sample prefix 'M'). Sampling was conducted over approximately 200 metres laterally and 11 metres stratigraphically. Effort was made to conduct sampling of the stratigraphic column over as small an area as possible to preserve the maximum achievable distance between each locality. The major limitation on sampling was the limited vertical extent of the cliff faces.

Eglwys Siglen (SH 516869; sample prefix 'ES') is the second locality, located on the headland north of Moelfre. Lateral sampling here could be accomplished using a compact section due to high cliffs and relatively safe access, and was therefore completed over a

distance of approximately 100m. The high cliffs also afforded vertical sampling equal to that achieved at Moelfre: 11 metres.

The third locality is sited 600 metres north of Moelfre locality, and 600 metres south of Eglwys Siglen (SH 515864). It is located as close as possible to the mid-point between the first two localities to act as a control point, and is known as Central (sample prefix 'C'). Due to the small cliffs at this locality, only 5 metres vertically could be sampled. This meant lateral sampling was completed over a distance of no more than twenty metres.

The sampling plan called for samples every half metre or at every major (visible) lithological change. This was adhered to as closely as possible, however there were points where this plan could not be followed. The base of the Brigantian at Moelfre and Eglwys Siglen were the primary examples of this problem, where the beds appeared too cyclic, or thin vertically, to sample each 'cycle'. For occasions like these, sampling every 30cm was undertaken where possible.

71 samples were taken (Figure 3), from which, over 50 acetate peels were made. From these peels the facies characterisation was developed. A representative selection of 15 thin sections is also in production at the Open University, which will be used to refine the characterisation at a later date.

A1.4.1 Logs

Figure 4 shows the sedimentary logs produced primarily as a result of the analysis of acetate peels. The logs also incorporate data from the author's field notebooks, including rock type classifications made in the field, and stratigraphic information, such as the location of palaeokarstic horizons and macro-scale petrographic features.

Figure 5 is the key to the logs, which was adapted from (Davies,1991). The key divides principle grain types and macrofauna; grain types are shown in the schematic diagram of the lithological column, whereas macrofauna (taken to be accessories to the principle facies components) are shown alongside the horizon from which the sample came. Sedimentary structures are also shown within the column. Numbers between the scale bar and lithological column are sample points, shown at the correct stratigraphic horizon.

Comparison of these logs to those of Davies (1981; Figure 6) shows an excellent correlation between the two studies. The use of Davies' logs, produced before sequence stratigraphy was widely accepted, and cyclostratigraphy thought of, introduces a measure of control to this research. In that light, comparison between the two sets of logs shows that this study located every major lithological change and hiatus.

Samples Record: Moelfre, Nov 2004

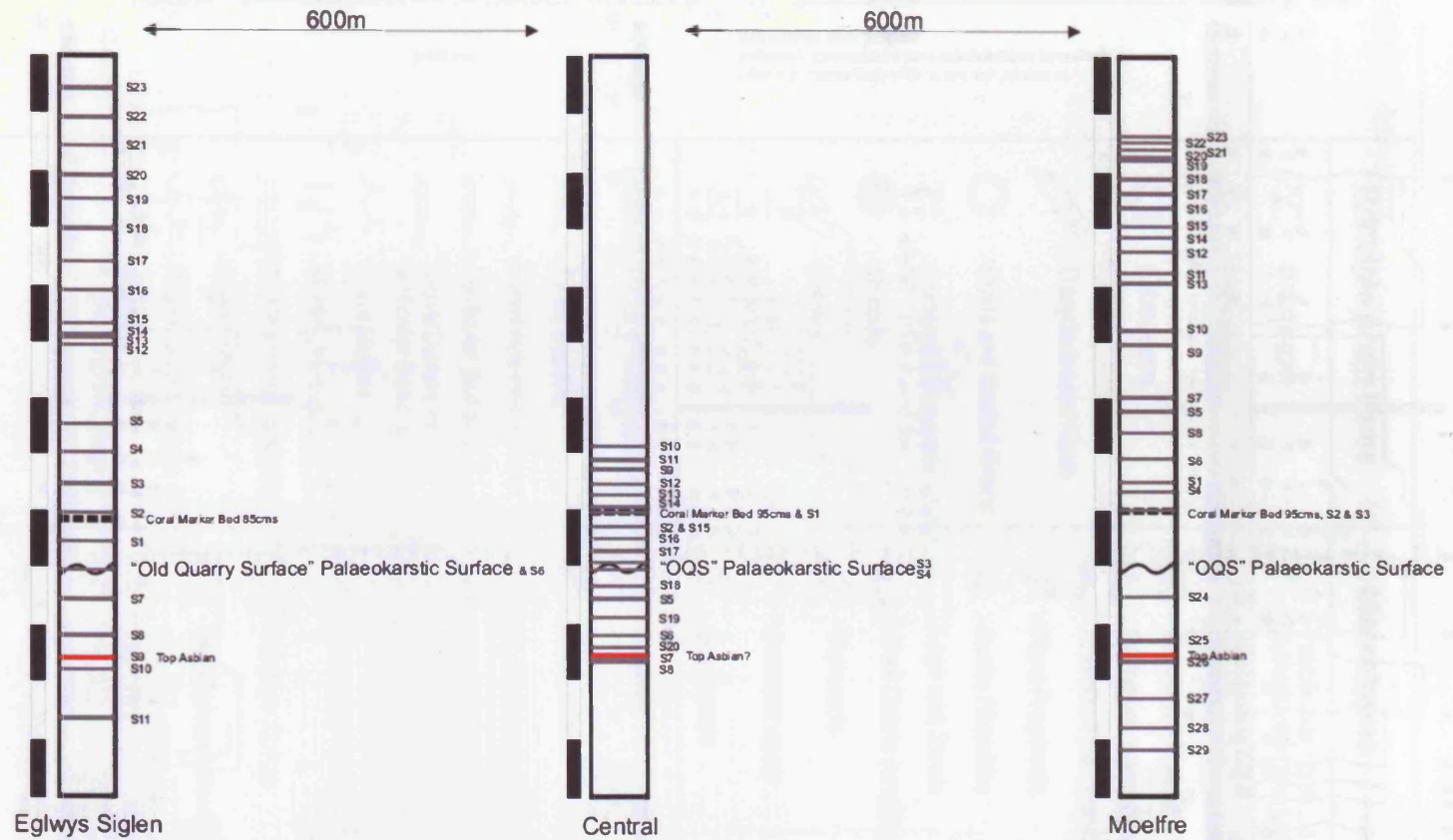


Figure 3: Diagram showing positions of samples taken from the Asbian/Brigantian of Anglesey relative to the *Lithostrotion* marker bed.

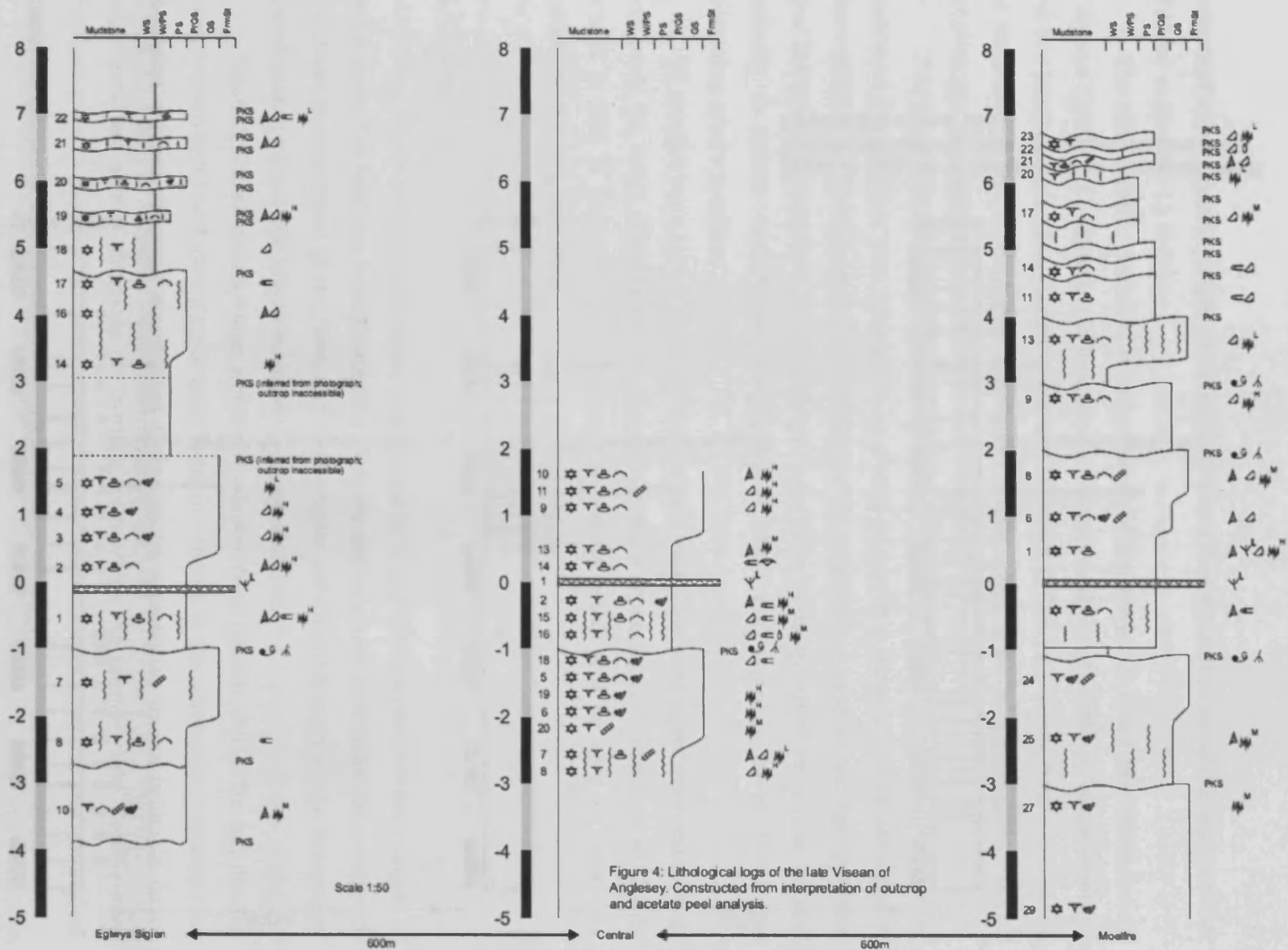


Figure 4: Lithological logs of the late Viséan of Anglesey. Constructed from interpretation of outcrop and acetate peel analysis.

Principle grain types	Macrofauna
 Brachiopod	 Fasciculate coral (Lithostrotion and Lonsdalia)
 Foraminifera	 Fasciculate coral (Syringopora)
 Echinoderm	 Carbonate Nodule
 Dasycladacean Algae	 Pedogenic calcrete nodule
 Ooids and Coated Grains	 Reworked pedogenic nodule
 Carbonate Intraclasts	 Plant Fragments
 Oncoids	 In situ Rhizoliths
 Peloids	 Logs and Stems
 Quartz Sand	 Shell Debris (undifferentiated)
 Molluscs	 Ostracods
	 Saccaminopsis
	 Gastropods
Sedimentary structures	 Bivalves
 Cross Bedding	 Bryozoans
 Current ripple cross lamination	 Palaeoberesellids
 Lenticular Bedding	 Sponges
 Wave/Current formed lenticular Bedding	 Solitary Rugose Coral
 Wave Ripples	 Colonial Rugose Coral
 Mottling/bioturbation	 Tabulate Corals
 Cryptmicrobial lamination	 Stromatoporoids - lamellar
 Chert nodule	 Stromatoporoids - hemispherical/bulbous
 Palaeokarstic surface	 Stromatoporoids branching
 Stylolites (Light, Medium, Heavy)	 Gigantoproductid
	 Daviesiella
	 Triobite Remains

Figure 5: Key of structures used in sedimentary logs (adapted from Davies, 1991)

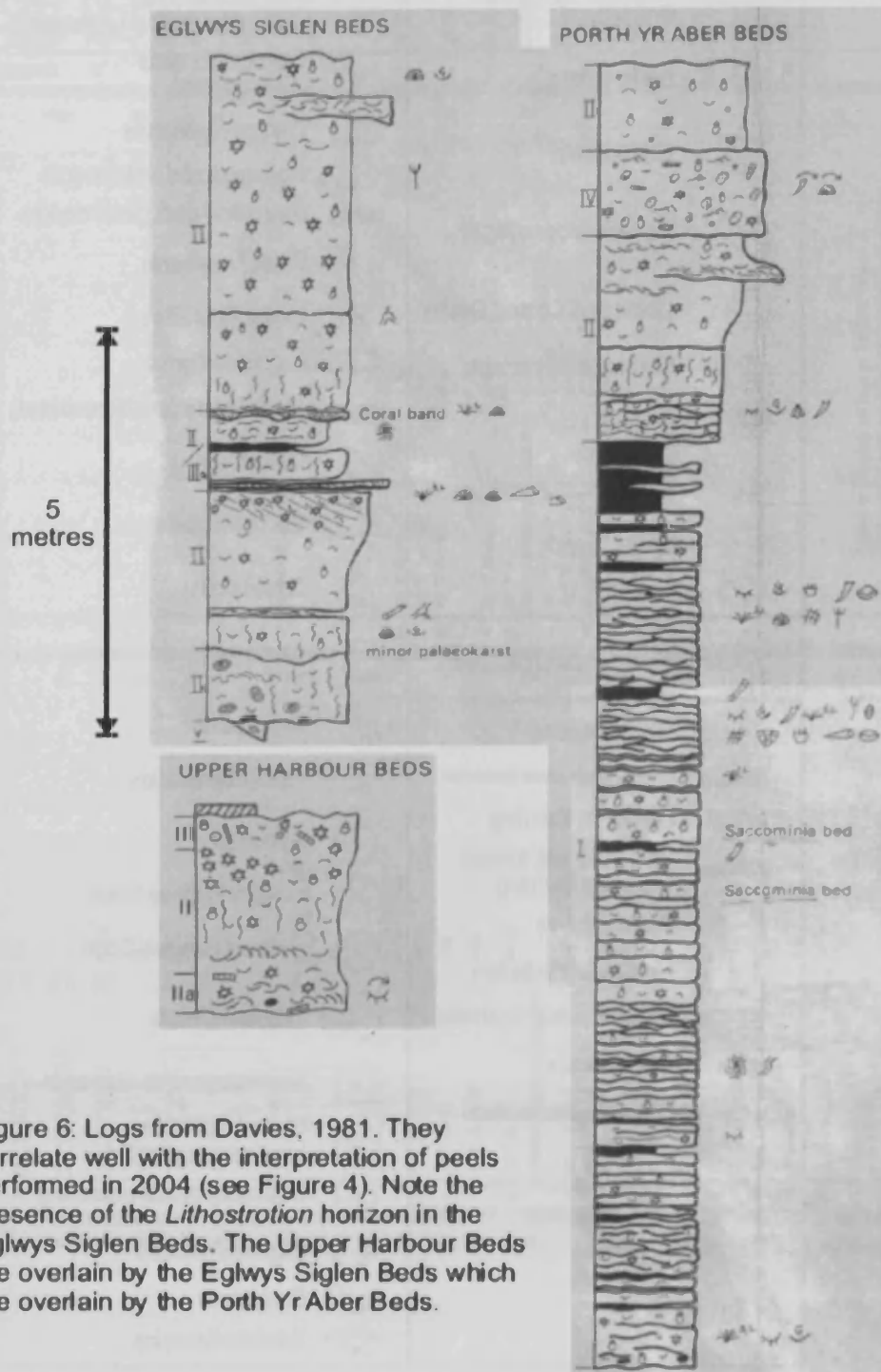


Figure 6: Logs from Davies, 1981. They correlate well with the interpretation of peels performed in 2004 (see Figure 4). Note the presence of the *Lithostrotion* horizon in the Eglwys Siglen Beds. The Upper Harbour Beds are overlain by the Eglwys Siglen Beds which are overlain by the Porth Yr Aber Beds.

A1.5 FACIES

There are two major and two minor facies that this study recognises. The reason for the limited number of facies is three-fold. Fundamentally, the cycles are usually seen to be less than 3 metres in thickness, from cycle-bottom to cycle-top, which is the average top Asbian cycle thickness in Anglesey (Davies, 1984). In a typical cycle there may be only 4 samples, and of these samples there was not seen to be a sufficient difference to warrant the inclusion of multiple facies types. Secondly the endemic burrowing of sediment noted in each facies caused severe mixing, which, after subsequent compaction and diagenesis, produced local areas of different composition. Consequently it was felt that the addition of wackestone/packstone qualifiers would only serve to cloud the issue. Finally, the limited number of facies types is beneficial for numerical forward modelling. The fundamental distinction between a 'muddier' deep-water facies and a 'cleaner' shallow-water facies makes it much easier to replicate the cyclicity seen at Anglesey using computer models.

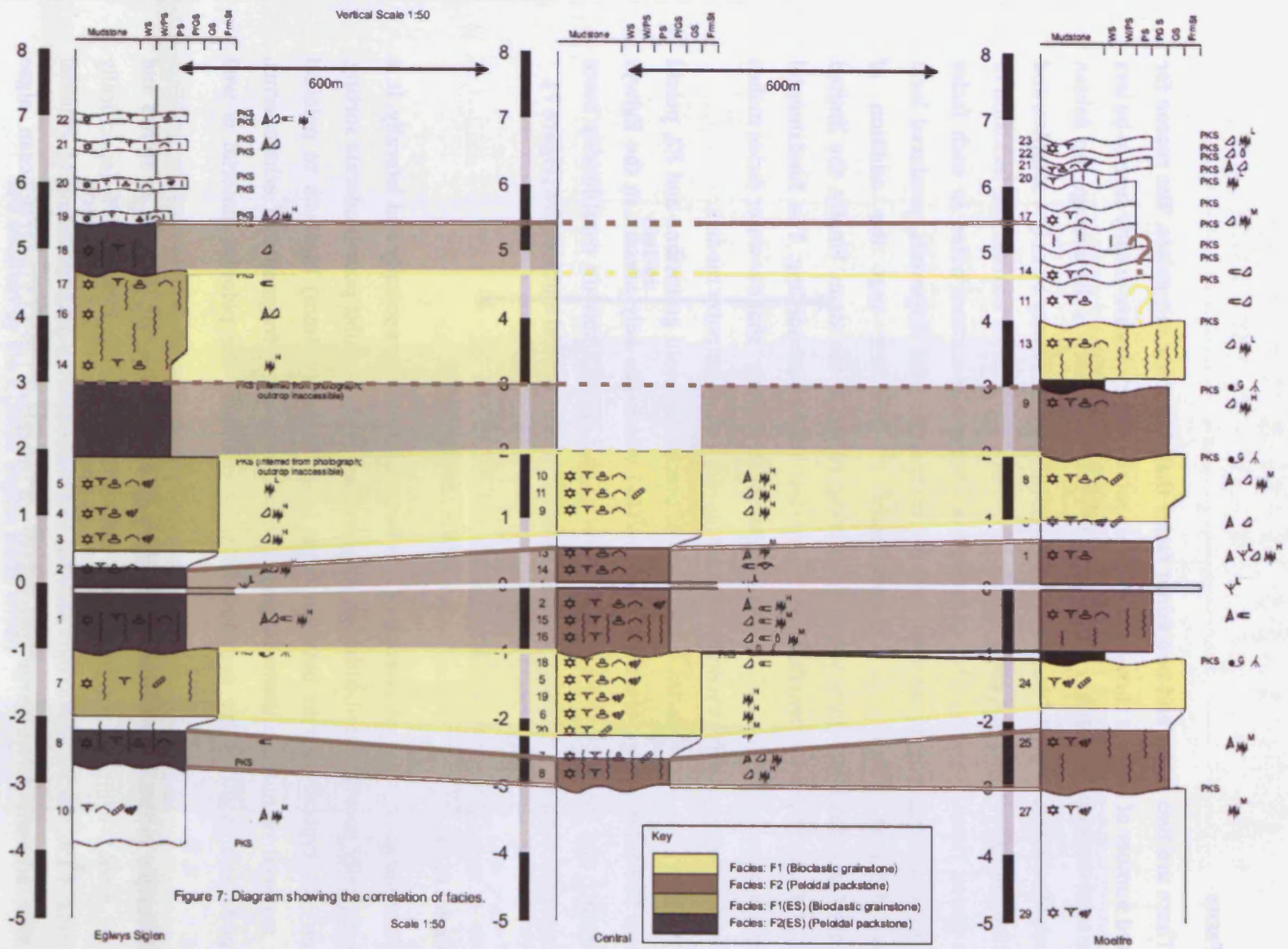
Therefore the major facies types are: F1, bioclastic peloid grainstone and F2, peloid packstone. The minor types are F1(ES) and F2(ES) which are only present in the Eglwys Siglen locality and highlight the fact that facies at this locality contain considerably more micritic material than their laterally adjacent counterparts at Central and Moelfre (Figure 7).

A1.5.1 Facies F1

There is good, clear correlation of this facies both stratigraphically and laterally. It is characteristically poorly sorted, although some examples may exhibit poor-moderate sorting. The grain size typically varies between large (approximately 4mm) bioclasts to peloidal micritic material of indeterminate original composition. Large fragments of echinoderms, brachiopods and molluscs are common. In some examples the peloidal material is well rounded.

Principle grains in this facies (see Figure 8) are brachiopods (present as spines and fragments; 6.6%), echinoderms (fragments and ossicles; 7.1%), foraminifera (specifically endothyrids; 4.1%, see Photomicrograph M8b) and miscellaneous fragments (5.9%). Peloidal grains also account for a large percentage of material (29%). Dasycladacean algae (palaeoberesellids), gastropods and ostracods are present as rare fragments but are not principle grains. Cement is predominantly calcite spar (34%).

This facies commonly displays burrowing and reworking as a result of bioturbation. As a result portions of a sample can appear to have a packstone fabric, when in reality they



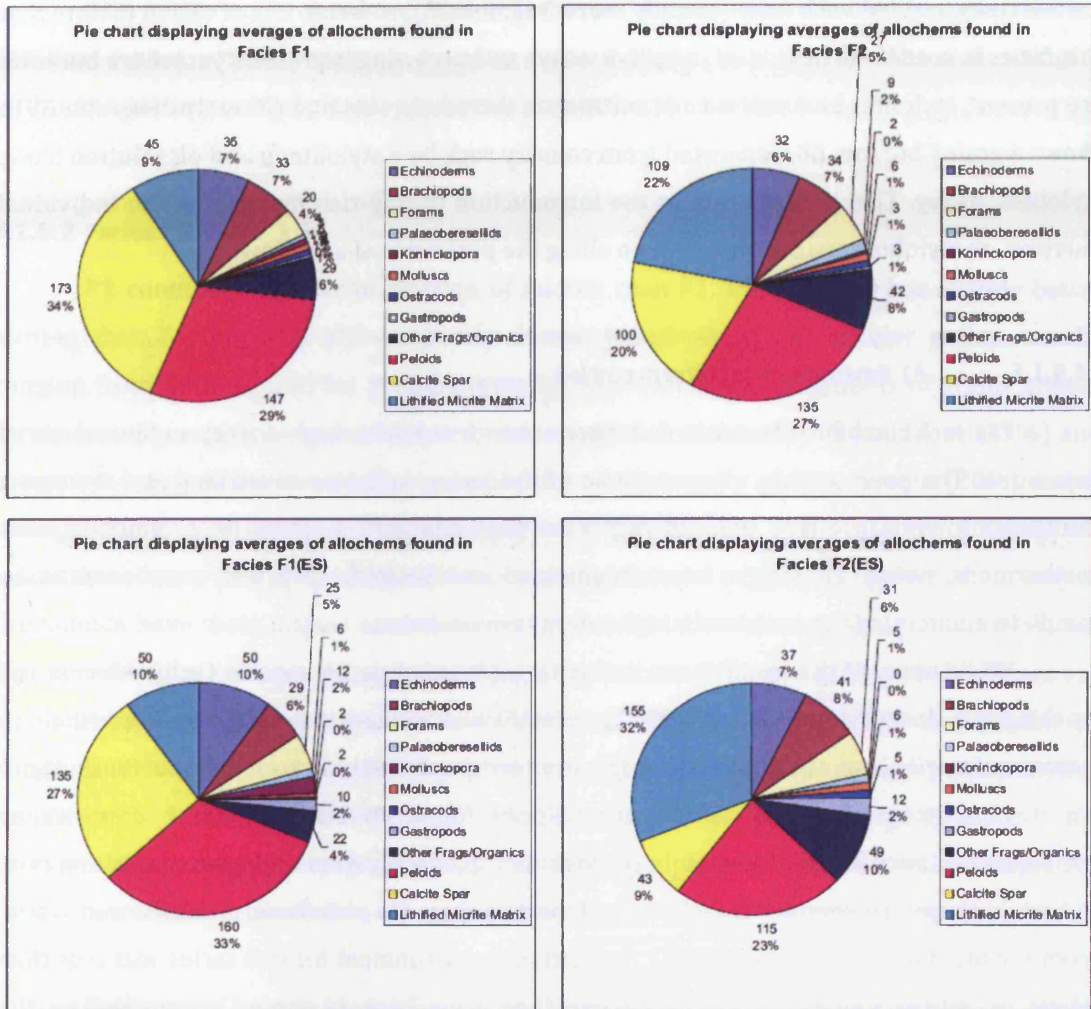


Figure 8: Diagram showing allochem and cement proportions in facies types.

are burrows in-filled with finer (usually more fragmented) material. It is of worth to note that this facies is seen to be devoid of stylolites where no burrowing is present, yet where burrows are present, stylolites and evidence of solution is extremely common (Photomicrograph ES1a shows a grainy burrow fill, separated from country rock by a stylolites); and dissolution along stylolites, heavy. This is likely due to the introduction of clay-rich material in the individual burrows, as stylolites are commonly seen along the perimeter of a burrow.

A1.5.1.1 F1 Environmental Interpretation

Facies F1 exhibits features consistent with a subtidal, high-energy environment of deposition. The poor sorting, characteristic of the facies, indicates reworking and transport mechanisms were in effect, but did not move the sediment far from its production area. Furthermore, nearly all fossils were fragmented and broken; very few were seen to be complete, reinforcing the notion of a high-energy environment.

While many of the fossils seen in this facies are non-depth specific (echinoderms and brachiopods; Horbury and Adams, 1996), several favour shallow water depths of less than 10 metres; primarily dasycladacean algae (Photomicrograph ES1b; bottom). Importantly there are no instances of grains which are seldom found in shallow water depositional environments, such as trilobites or bryozoans. Ostracods, bivalves and gastropods are rare, and while these are commonly cycle base bioclasts they are also found in shallower water. From the biota it is fair to say that the depositional environment for this facies was less than 10 metres water depth and above fair-weather wave base (a theory supported by the reworking and poor sorting of grains).

There are several examples within this facies of brittle deformation of grains; concordant with the interpretation of this facies as being deficient in carbonate mud – as would be expected in a shallow environment.

Burrowing is evident (Photomicrograph ES8b) in this facies in the muddier cycles closer to the fine packstones and wackestones of the Brigantian. One way of interpreting this (if 5th order, or minor, cyclicity is accepted) is that as the 5th order rhythms become more prominent in the Brigantian, the amplitude of wave base fluctuation on a rising limb becomes greater, submerging the grainstones deeper and thus allowing bioturbation and burrowing to take place, introducing the finer packstone material into the host rock. This would explain the source of finer, more micritic material within the grainstones higher in the stratigraphic column, which is not seen in the Asbian.

At a macro-scale, at outcrop, this facies forms the palaeokarstic caps to cycles. During the next transgression pedogenic features were stripped leaving rhizoliths and stringers within the grainstone and gigantoproductids encrusting the hardground.

A1.5.2 Facies F2

F2 contains a greater proportion of micrite than F1. It commonly has slightly better sorting than F1, but may still be poorly sorted. Relatively, it has smaller grains, usually ranging from 2mm to micritic peloidal material, however larger fragments of grains appear rarely (usually echinoderm, mollusc or brachiopod). Peloidal matter is abundant (27%) and comprises much of the material in a sample, the relative rarity of spar cement (20%) makes distinguishing such material from the matrix (22%) difficult. The presence of significant quantities of very-fine grained miscellaneous shelly material suggests, however, that many of the peloids have their origins as skeletal grains. Yet the abundance of shelly material shows this facies is grain-supported and therefore a packstone. Principle grains in this facies are similar to F1: echnioderms (6.5%), brachiopods (6.7%), molluscs (1.1%) and peloids all dominate. Foraminifera (endothyrids; 5.3%) are rarer. Principle grains are predominantly fragmented. Good 'depth-indicating' bioclasts such as bryozoans, trilobites and Saccamminopsis are extremely rare, with only one example of each in the entire sample set. Other macrofauna is limited in F2 with ostracods (0.7%) and gastropods appearing rarely (0.5%).

Evidence of burrowing is inherent to this facies and is present in nearly all examples (Photomicrograph ES3a shows how varied the microfacies on a millimetre scale). Burrow mottling presents an often confusing texture in peels and locally some samples can be interpreted as wackestones due to infilling of burrows with finer material (Photomicrograph ES8b shows a burrow infilled with grainier material, including Koninckopora). Heavy stylolitisation and evidence of pressure solution is also common, along with associated localised clay enrichment. Lithified micrite matrix is abundant in this facies, although some blocky spar cement is common in bioturbated samples.

A1.5.2.1 F2 Environmental Interpretation

The composition of facies F2 suggests it was deposited in a lower energy environment than that of F1. The absence of binding organisms as principle grains does not suggest that this facies was bound by the biota. It contains significantly more lithified micrite denoting a

relatively distal position from the loci of shallow-water carbonate production. Proportionally, micritic cement has a much greater presence (49% including peloids and micrite matrix) in this facies than spar cement (20%), in contrast to F1 (34% spar) and is supportive of a deeper environmental setting. The moderate degree of sorting coupled with a smaller grain-size relative to F1 reinforces this statement.

In terms of biota there is not a significant difference between this facies and that of F1. Echinoderm, brachiopod and foram debris all dominate, but do not give any clear indication of depth. The large amount of peloidal grains and indistinct peloidal material also reflects the deeper water depth and lower-energy setting. Foraminifera, gastropods and ostracods are more common in these facies and comprise a greater total percentage of the rock than in facies F1. While these accessory grains are also found in shallow water their abundance in this facies, combined with other indicators, suggest a relatively deep depositional environment. Rarely, this facies contains bioclasts which are found exclusively in deeper water (10-20m) including trilobites, *Saccamminopsis* and bryozoans, although these cannot be regarded as definitive due to their rarity.

Burrowing is common in almost all instances of this facies. This facies is likely to have been deposited below fair-weather wave base and therefore prone to benthic organisms bioturbating the otherwise undisturbed sediment.

A1.5.3 Facies F1(ES)

Facies F1(ES) has the same characteristics as F1 for the most part. Sorting remains poor (although one case has moderate sorting), there is a large range of grain size, and an abundance of the bioclasts common in F1 (echinoderms; 10%, brachiopods; 5.8%, foraminifera; 5%, and molluscs; 1.1% – usually displayed as fragments). *Palaeoberesellids* (1.1%) and *Koninckopora* (2.3%) are also rarely present, but *Koninckopora* in particular is relatively abundant in one sample, ES7 (Photomicrograph ES7b), forcing the average up.

The only fundamental difference between facies F1 and F1(ES) is that F1(ES) contains a considerably greater proportion of micrite. An additional minor difference is that individual grains can often be seen to be smaller and exhibit a greater degree of fragmentation. Crucially, while there is an increased micrite content in F1(ES), it is not of the quantities seen in a true packstone of F2 and it would therefore be appropriate to label F1(ES) a bioclastic pack-grainstone.

A1.5.4 Facies F2(ES)

As in facies F1(ES) the only major difference between F2(ES) and F2 is the increase in micrite content (54%) and fragmentation, and a relative overall decrease in grain size. F2 has been labelled a fine-grained peloidal packstone due to the overall similarities between this facies and F2.

A1.5.4.1 F1(ES) & F2(ES) Environmental Interpretation

Significantly both F1(ES) and F2(ES) seem to be genetically related to their corresponding facies at Moelfre and Central localities. Characteristics of the fabric in general (including biota, grain types, grain size and sorting) are correlative with the other localities. The major difference, as noted, is the greater amount of micritic material in these facies.

A simple interpretation would place Eglwys Siglen in a distal position relative to the source of carbonate production, explaining the abundance of mud. This would not, however, allow for the increase in the micrite content of both F1 grainstone and F2 packstone units.

There is little evidence that the thickness variations are as a result of biohermal mounding causing pre-existing palaeobathymetric relief. Bioherm producing biota are largely absent.

An alternative explanation is that the palaeobathymetry of the area was such that a shallow bathymetric low existed. This would adequately accommodate the increase in detrital material and sorting, and decrease in grain size; as broken shelly material would accumulate in a low, while carbonate mud was swept from the surrounding highs. This would make little difference in terms of facies variability when considering relative sea-level rises and falls, as the depression would likely be on the order of several metres. It would, however, significantly affect deposition as sea-level transgressed: packstones (F2) would be deposited on the high-ground, but in the low area accumulation rates would be slightly lower, allowing for a build-up of mud. This would also be true for F1 facies later in the cycle. The problem with this explanation is that once the hollow was filled facies F1(ES) and F2(ES) would no longer be produced. Therefore long-term, slow subsidence is required. A source of this may be the fault that truncates Asbian strata less than twenty metres to the north of where the majority of Eglwys Siglen samples were taken. If this were an extension of a major fault in the basement then the subsidence could be accommodated. However, at this time the origin of the relatively micrite-rich facies at Eglwys Siglen is unknown.

A1.5.5 Summary

By comparing the results from point counting, visually represented in Figure 8, several trends are apparent, which, as they are based on quantitative data, are useful to note.

Most importantly there are clear trends in the quantities of calcite spar cement found in each individual facies. Facies F1 and F1(ES), as expected, show the most extensively developed calcite cement. Facies F2 and F2(ES) have correspondingly lower cement values. Importantly facies F2 is less cement rich (20%) than F1 (34%), while F2(ES) is less cement rich (9%) than F1(ES) (27%). The inverse is true of micrite content (Figure 8). This is important to note when considering Anglesey as a reservoir analogue to the Pricaspian Basin. The best potential reservoirs are facies F1 and F1(ES), whose original primary porosity is now represented by spar cement.

Several factors are apparent which support the theory that facies F1(ES) and F2(ES) were deposited in depression, or at least, an area distal from the loci of production. Echinoderm fragments, in many cases having undergone significant dissolution, are most common in these facies, suggesting that they were transported away from the meadows in which they grew. Swept from the higher energy shoreward facies, they settled in low-energy areas. This is echoed by the increased quantities of miscellaneous detrital shelly material and forams, which are also most abundant in F1(ES) and F2(ES). Furthermore, minor allochems, including ostracods and gastropods (indicative of a deeper environment) are also most abundant in these facies.

Two critical caveats to the results of point counting must be noted. Firstly, most of the samples had undergone severe bioturbation. This has the potential to confuse any findings, although there appears to be no major anomalous results in the dataset. Secondly, significant difficulty was encountered defining peloids as distinct from micritic matrix in facies F2 and F2(ES). When interpreting point counting from these facies, it may be useful to combine the totals for peloids and matrix.

A1.6 LATERAL VARIABILITY

For accurate assessment of lateral variation, each major lithological change was classified as a unit (Figure 9). The lateral variability of each of these units is described below.

A1.6.1 Unit 1 (Representative sample: C8.)

Good correlation exists in Unit 1 between all three cycles, albeit from only 4 samples over the three localities. Central and Moelfre display samples presenting the same facies, F2.

Eglwys Siglen characteristically shows a facies with a much lower sparry cement content (5.8% in Eglwys Siglen, compared with 13% and 26% at Central and Moelfre, respectively), and more prominent detrital shelly material (bioclasts comprise 41% of facies F2(ES) and an average of 30% in F2 samples from this unit). This is consistent with the variation between Eglwys Siglen and the other two localities. Beyond this, lateral variation in this facies is negligible.

A1.6.2 Unit 2 (Representative sample: C5, C6.)

Excellent constraint on this unit is afforded by 5 samples from Central locality. It should be noted that while Figure 9 shows a pronounced thickening of Unit 2 at Central, which is misleading as the actual thickening is less than thirty centimetres (compare with Figure 10). This apparent thickening may itself only be due to poor lithostratigraphic constraint because of limited availability of samples in Moelfre and Eglwys Siglen.

Samples from Central display F1 facies (with no burrowing) which is also replicated in the samples from Moelfre. Eglwys Siglen displays facies F1(ES) with burrowing in this unit (from acetate peel analysis), point counting reveals no significant variations in proportions of cement or allochems (Figure 11). This was probably caused as the thin section cut a burrow, infilled with grainier material thus giving an anomalous count. An example of this grainy burrow fill is shown in Photomicrograph ES8b, from the extensively burrowed Lithological Unit 1.

A1.6.3 Unit 3 (Representative sample: C16.)

Unit 3 is correlative over all three localities, although no sample was taken at Moelfre, notes taken at outcrop were used. Burrowing is pervasive in this unit. At Central, textures range from peloidal wackestone to packstone depending on whether or not the sample was taken from within a burrow. Observations at outcrop, logs from Davies (pers. comm., 2004) and peel analysis were used to constrain that this was the same facies over all three localities.

The facies at Eglwys Siglen is richer in bioclasts (37% compared to 31% at Central) and is determined to be of facies F2(ES), whereas those at Moelfre and Central are heavily bioturbated examples of F2. Point counting data supports this; Figure 12 showing the increased micrite content at the expense of calcite spar, characteristic of Facies F2(ES). This unit therefore shows the same lateral variability as Units 1 and 2.

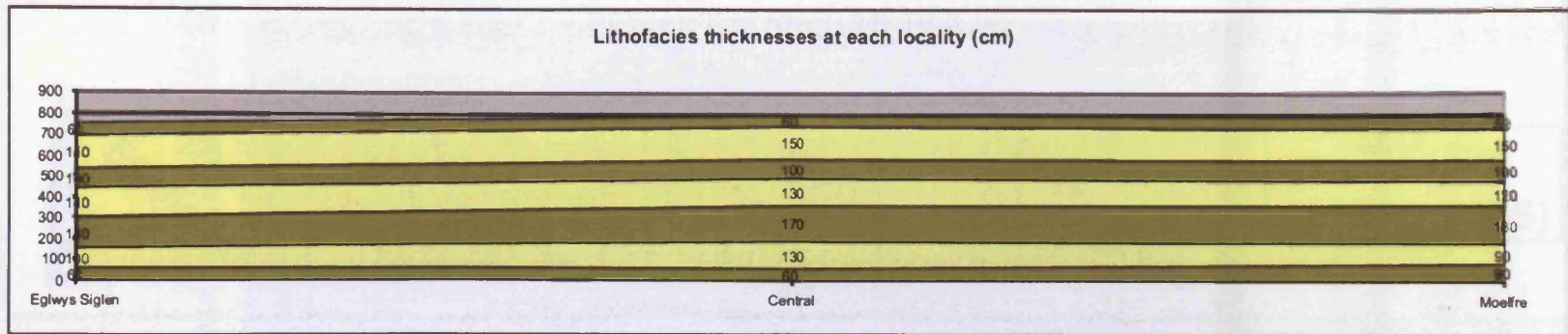


Figure 10: Schematic showing representative cross section based on stratal thickness measurements at each locality. Not to scale.

Comparison of facies and allochems in Lithological Unit 2

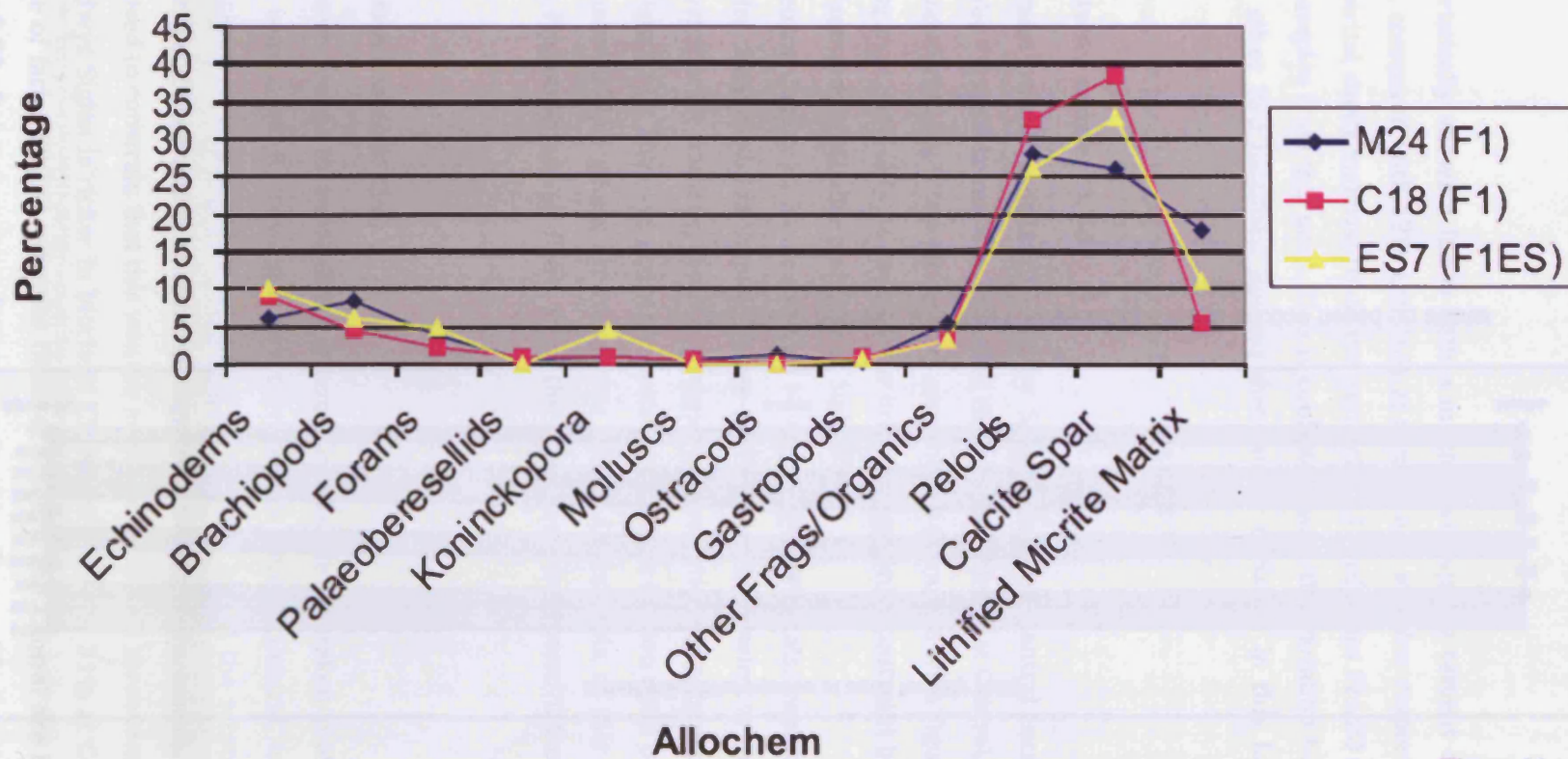


Figure 11

Comparison of facies and allochems in Lithological Unit 3

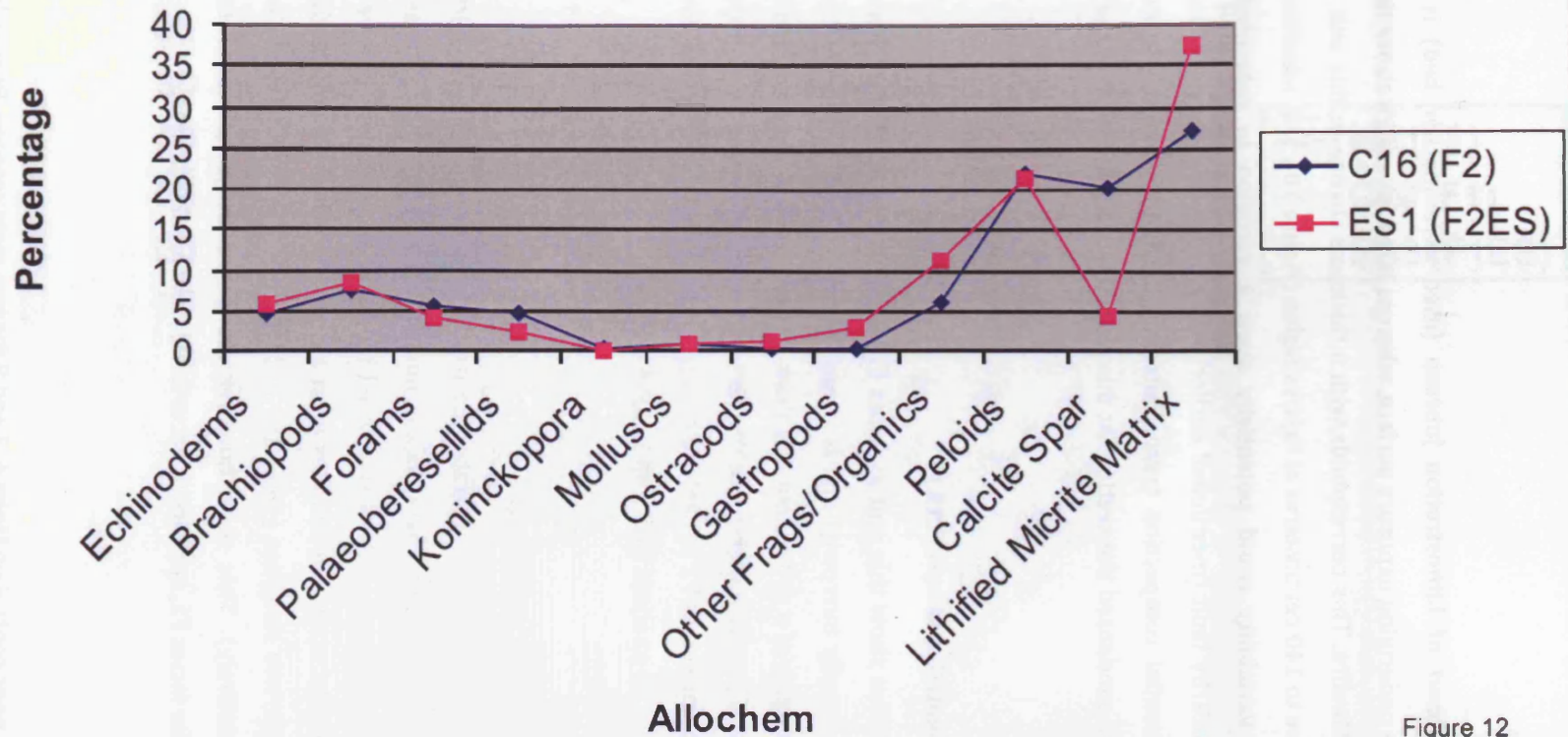


Figure 12

Notably the band of Lithostrotion juncean (used as a marker bed) is only 80 centimetres from the underlying exposure surface, whereas it is a full metre above the surface at both Central and Moelfre. This corresponds with a thickness change in this unit from 180 centimetres at Moelfre to 140 centimetres at Eglwys Siglen (Figure 10). This admittedly minor indicator of lateral variability could potentially show a variation in palaeobathymetry. Alternatively, if the nearby fault (mentioned earlier) was causing preferential subsidence of this area, then differential compaction (exacerbated by the large amounts of mud in the depression) may have condensed the section. At this time however, the cause of the variation is unclear.

A1.6.4 Unit 4 (Representative sample: C13.)

All three localities show this unit as facies F2, although characterised from only four samples. The unit is heavily burrowed and is almost certainly the same unit as Unit 3. The reasons for the occurrence of a prominent and thick Lithostrotion juncean horizon in a cycle base packstone unit are poorly understood. The fact that one sample was taken from Eglwys Siglen, and was characterised as F2 is likely to be largely due to burrow mottling. From study at outcrop and microfacies analysis Unit 3 and Unit 4 are seen to be the same unit.

A1.6.5 Unit 5 (Representative sample: C10.)

Good control of Unit 5 is demonstrated across all three localities. There is little lateral variability over this unit, which, petrographically, does not display the normal transition into muddier facies at Eglwys Siglen. This is supported by point counting data (Figure 13). The only change in variability occurs in samples from Moelfre, which are significantly grainier than those of the other two localities (48% spar at Moelfre to 25% and 21% at Central and Eglwys Siglen, respectively). This may, however, be a product of bioturbation, which, uncharacteristically for facies F1, appears to occur in this unit at all localities.

A1.6.6 Unit 6, 7, 8

There is very poor control on Units 6, 7 and 8 for two main reasons. Primarily, none of these units are present at Central. Secondly, the apparent minor cyclicity which comes into affect in the Brigantian (and in any case, the more confusing nature of the cycles in this part of the column) makes tracing any units laterally very difficult (Figure 14). It would therefore be

Comparison of facies and allochems in Lithological Unit 5

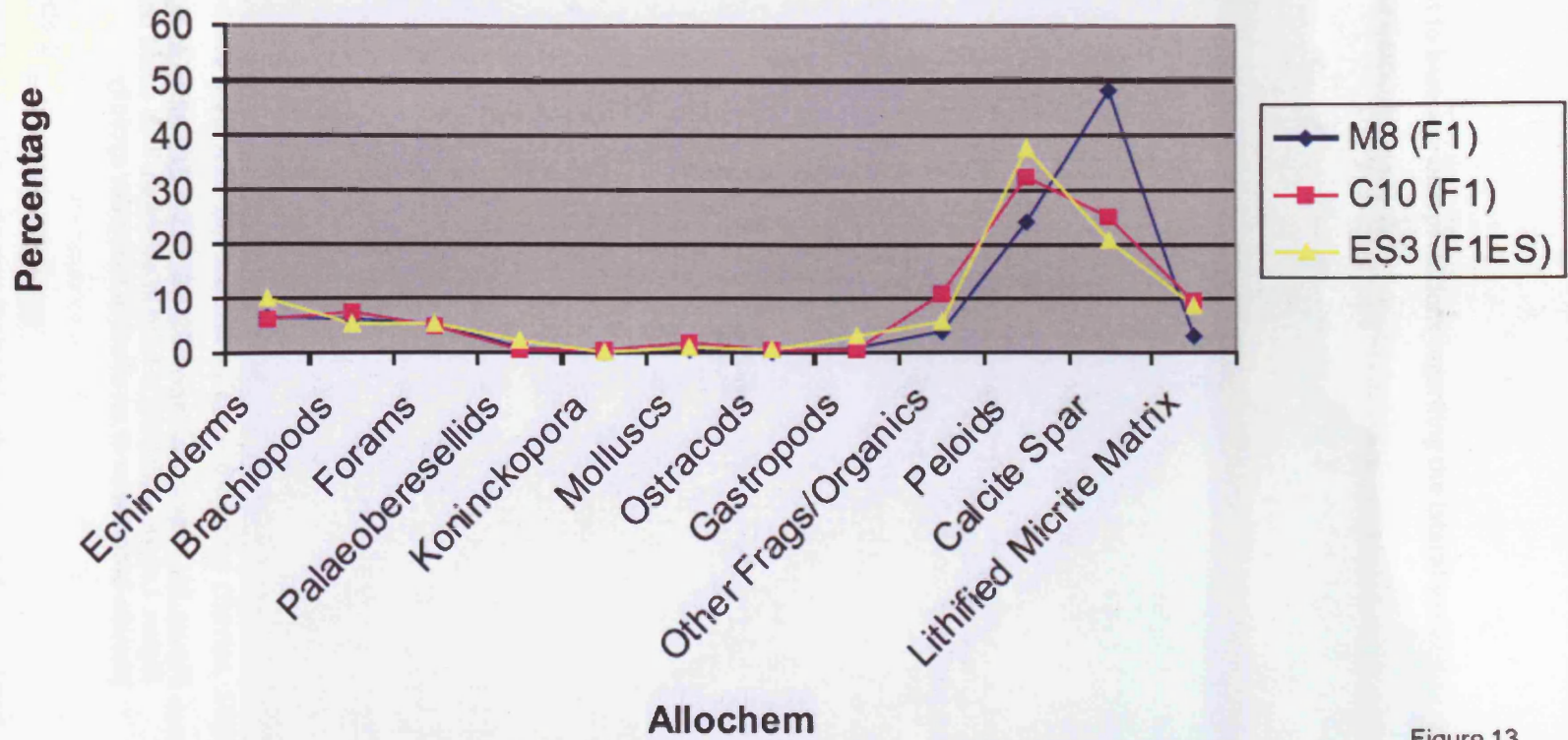


Figure 13



Figure 14: example of facies F2(ES) of the Brigantian at Eglwys Siglen. Lateral variability is hard to establish. This could be pseudo-brecciation or an effect of fifth order cyclicity.

imprudent to base any interpretations regarding the lateral variability of facies or microfacies upon these units.

A1.6.7 Summary

Lateral microfacies variability in the late Viséan appears to be limited. There are, however, notable lithological thickness variations between localities, particularly between Eglwys Siglen and the other two localities, which show good correlation of thicknesses (Figure 10). One interpretation of the cause of this could be differential compaction, either related to the nearby fault, palaeobathymetry or compaction due to the greater amounts of mud. Having said this, there is the potential for human error due to the limited outcrop at Central and the pervasive bioturbation in many of the lithologies.

There is little evidence that the thickness variations are as a result of biohermal mounding causing pre-existing palaeobathymetric relief. Bioherm producing biota are largely absent.

The prominence of F1(ES) and F2(ES) seen at Eglwys Siglen as opposed to F1 and F2 seen laterally at the other localities is the only major change seen laterally. As mentioned, the reasons for this change are unknown at this time. In terms of reservoir properties any increase in the micrite content of the sediment is likely to have a detrimental affect on porosity and permeability. If, however, this facies change is fault controlled, it will not present a predictive tool for understanding the lateral distribution of reservoir properties on a platform.

A1.7 CYCLICITY

Cyclicality in the studied sections is limited to six (possibly only five) cycles (Figure 15). This correlates well with the traditional cycle thickness (Davies, 1984) for the Viséan of Anglesey. Each cycle and its accompanying palaeokarstic features are described below.

A1.7.1 Cycle 1

Sampling of this cycle was limited by the present day sea-level, and meant only two samples from Moelfre and one from Eglwys Siglen could be acquired. At outcrop there is distinct cyclicality traceable at both localities, capped by a prominent palaeokarst with a weathered-back (inaccessible) palaeosol. The facies comprising the cycle at Moelfre is a

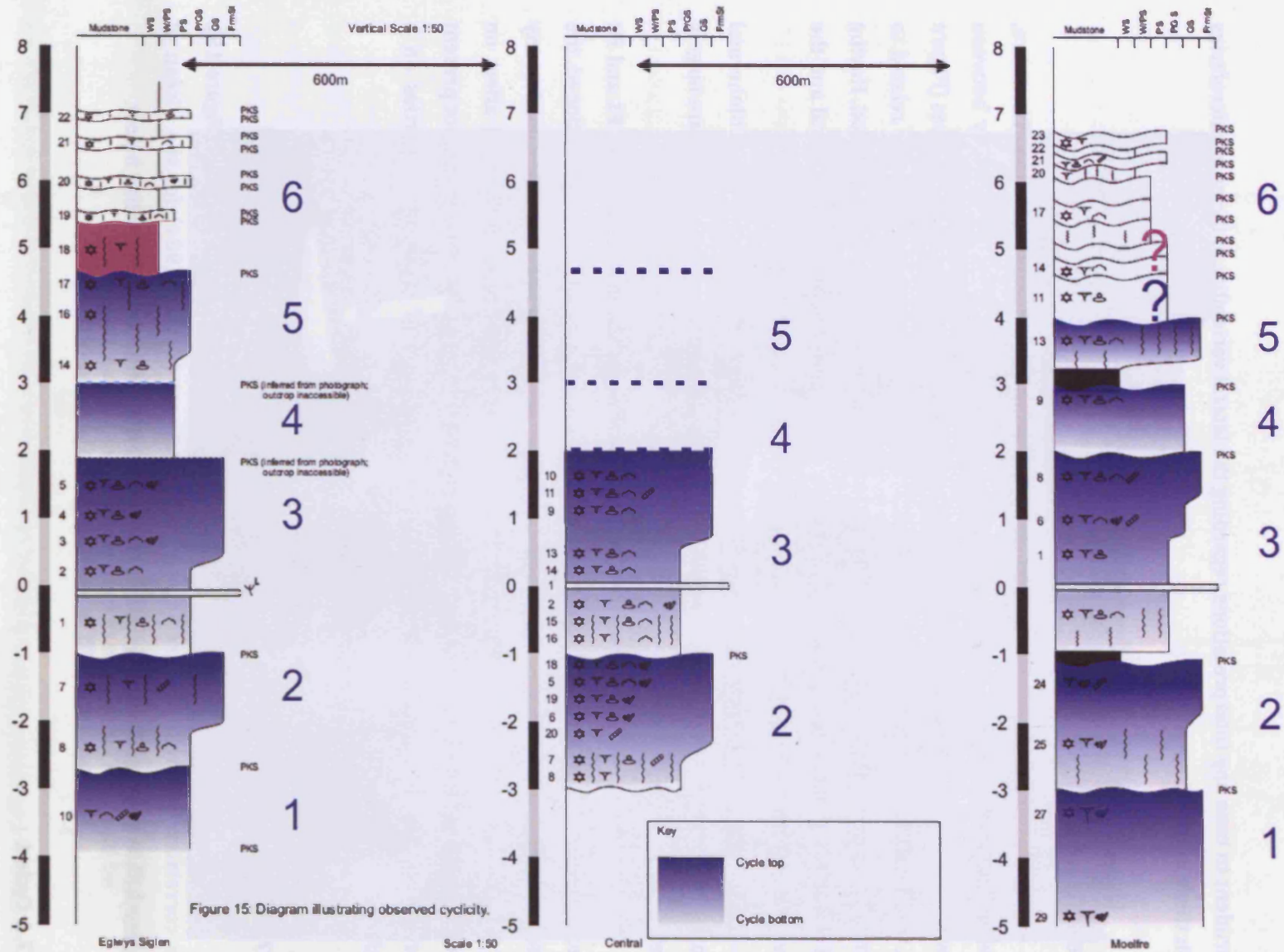


Figure 15: Diagram illustrating observed cyclicty.

standard cycle top grainstone (F1) with rhizocretions and encrusting biota. At Eglwys Siglen no facies characterisation was completed as the single sample could not be said to be representative, although it is likely to be a packstone – concordant with the muddier facies seen at Eglwys Siglen. Although interpretation of this cycle is poor, the important thing to note is that there is definitely a correlative palaeokarstic surface between Cycles 1 and 2, and it is likely to be capping a fourth order cycle.

A1.7.2 Cycle 2

There is excellent constraint upon both the boundaries and facies of Cycle 2. It is seen at all three localities, bounded at its top by a major palaeokarstic surface and is covered by 11 samples, 7 of which are in the central locality. Cycle 2 displays a classic shallowing-up lithology composed of burrowed F2 facies at the base and grading into cycle-top F1 facies. The palaeokarstic surface at the top of this cycle is very well developed with a prominent thick (approximately ten centimetres) palaeosol. Below the palaeokarstic horizon, pedogenic features can be seen for approximately twenty centimetres, the most abundant of which are rhizocretions. Gigantoproductids and solitary corals are seen encrusting the hardground on the palaeokarstic surface. This prominent cycle cap is a very well developed 4th order boundary.

A1.7.3 Cycle 3

Almost identical in nature to Cycle 2, Cycle 3 again records a classical shallowing-upwards cycle. The basal facies is F2 and heavily burrowed across all three localities. Interestingly, this cycle contains the ten centimetre thick Lithostrotion juncean marker horizon, although its origin and implications are unclear. Above the Lithostrotion band burrows are not seen and the facies grades up to F1. There is a prominent palaeokarstic surface developed at Moelfre, however this surface is covered by vegetation at Central (although the topography indicates it is present) and the cliff face at Eglwys Siglen does not permit close inspection, although there is a laterally extensive break in the limestone at the corresponding height. This, along with data from Davies (2004, pers. comm.), allows a certain level of confidence in saying that that the palaeokarstic surface is laterally extensive.

A1.7.4 Cycles 4 & 5

The nature of the cyclicity becomes more confusing higher in the Brigantian. Whereas cycles 2 and 3 display distinct cyclicity packaged between prominent well-developed exposure surfaces, Brigantian cycles display more variation. The basal boundary of Cycle 4, complete with well-developed palaeokarstic features as mentioned above, cannot be traced laterally but is taken to be present with a high degree of confidence. Cycle 4 is only displayed and accessible at Moelfre, and it may only be the bottom package of Cycle 5. The major problem with this is that there is a distinct palaeokarstic at the top of Cycle 4, complete with pedogenic features, a palaeosol and evidence of a hardground. This however is not traceable at Central due to the absence of outcrop, and at Eglwys Siglen due to the sheer cliff. If this is accepted as a small 4th order cycle then it would fit the classic interpretation that cycles thin upwards as they approach a major lowstand boundary. The capping exposure surface seems to fit this interpretation as, save for the massive grainstone unit directly above it, it marks the transition into less distinct Brigantian cyclicity.

A1.7.5 Cycle 6

This is difficult to interpret as one cycle alone (Figure 16). The facies here are noticeably muddier here from visual inspection of the outcrop. They are less massive and almost form nodular bedding in places. It is clear that there is a lithological change, with the beds incorporating more micrite than those lower in the stratigraphic column. The lithological aspects of this change have been well documented by Somerville (1979a, 1979b) and Davies (1984). However, the cause of this change is uncertain and would necessitate further study. This change in facies could be indicative of a 5th order oscillation being recorded in the rock record, piggybacking on a 4th order sea-level change. In this scenario, subsequent to the major lowstand exposure of Cycle 4/5, sea level may have rapidly risen beyond the rate of carbonate production, backstepping the production areas and depositing wackestones at Eglwys Siglen and Moelfre. A 5th order lowstand may have allowed carbonate production to prograde producing grainier lithologies, while catch-up was slowly occurring to the overriding 4th order curve. Fundamentally, it can be demonstrated from the logs in this study that there was a significant overall deepening at the top of cycle 4/5.



Figure 16: The Brigantian facies F2 at Moelfre. These are laterally adjacent to those shown in Figure 14. They are more massive but still difficult to trace laterally.

A1.7.6 Summary

Cyclicality in the study interval at Anglesey is characterised by the two well defined cycles (2 and 3), the three that are poorly constrained (1, 4 and 5), and the changing nature of cyclicality into the Brigantian (6).

Cycles 2 and 3 display classic ice-house, shallow-water shoaling-up cycles. They consist of a basal transgressive unit consisting of packstone (F2) facies which grades upwards into a shallower grainstone (F1) unit capped by a palaeokarst displaying pedogenic features. From the samples taken from Cycle 1, and notes taken at outcrop, it is reasonable to predict that Cycle 1, although poorly sampled, displays a similar, classical style of cycle architecture as 2 and 3.

Cycles 4 and 5 do not display ice-house style architecture, and any stacking patterns at all are hard to define. It is likely that transition into the Brigantian, deeper cycles are affecting these units. Cycle 6 represents this Brigantian style, with deeper water facies being deposited. Although the causes and precise effects of this deepening affect are not understood at this time.

A1.8 ANALOGUE STUDIES

The study of lateral variability and assessment of cyclicality in Anglesey was always intended as an analogue study for reservoirs of the Pricaspian Basin. The results of this study are compared here to the geological reports of three wells from Karachaganak; K152 (Di Giovanni et al, 2001b), K200 (Gorla et al, 2002) and K700 (Di Giovanni et al, 2001a).

A1.8.1 Facies

While the reports focus on the Serpukhovian of Karachaganak and the study in Anglesey was of the Viséan, the facies of the platform are likely to be similar and comparable. Indeed, the two facies described in this study correspond well, in terms of microfacies and wider geological setting, to those seen at Karachaganak.

Facies F1 in Anglesey is considered to be an analogue of facies C2.3C (a foram-rich skeletal packstone-grainstone) in Karachaganak. C2.3C is envisaged to have been deposited in a shallow-depth platform interior setting, possibly a skeletal shoal (Figure 17). Algal components (specifically Palaeoberesellidae, Koninckopora and Calcifolium) are very rare, whereas benthic foraminifera are abundant (Endothyriidae), and are considered to be

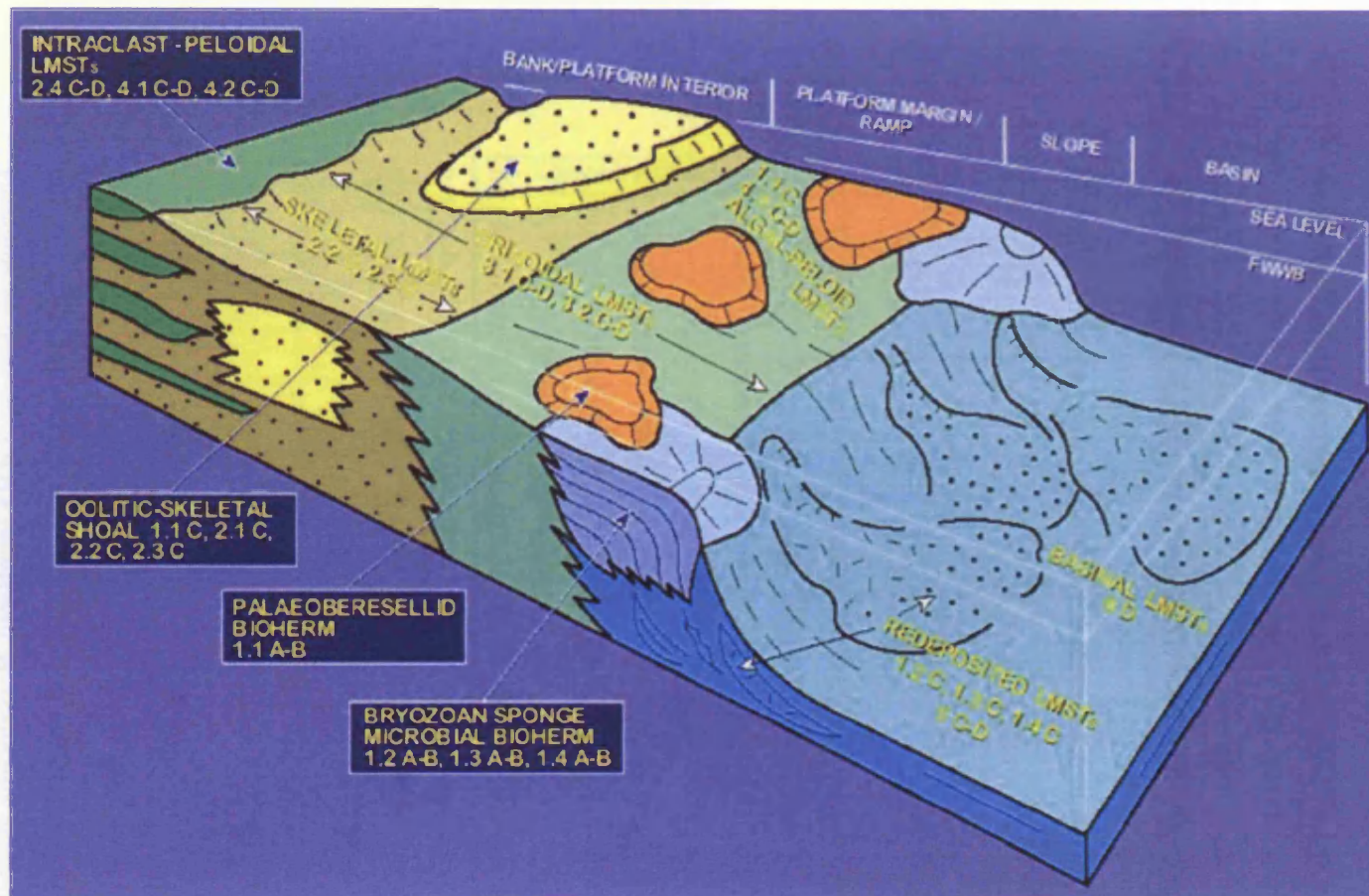


Figure 17: Lower Carboniferous biofacies of the Karachaganak platform: of which Anglesey is an analogue. Facies F1 and F2 are envisaged to be analogous to C2.3C and C3.1C respectively (from Di Giovanni *et al*, 2001a).

relatively shallow-water taxa. This biotic assemblage is concordant with that of facies F1 in Anglesey. The envisaged depth of deposition was between five and ten metres, which also corresponds well with the environmental interpretation of facies F1.

There is also a fitting analogue for facies F2 in Karachaganak. Facies C3.1C is mainly composed of crinoids and brachiopoda fragments. Algae are very rare or absent and the benthic fraction is generally poor. These sediments are considered transgressive and deposited in a relatively deep environment, consistent with the stratigraphic location and environmental interpretation of facies F2.

A1.9 CYCLICITY

The cyclicity evident in Anglesey is largely congruent with that recorded in the Karachaganak geological reports. However, although the style of the cyclicity fits well, it should be noted that Viséan cyclicity is likely to exhibit significant differences to that of the Serpukhovian due to variations in the global ice-house environment.

A theoretical individual shallowing-upward cycle from the Serpukhovian of Karachaganak is shown in Figure 18. It grades up from transgressive bioclastic crinoidal packstone-grainstones (C3.1C/F2) to foram-rich skeletal packstone-grainstones (C2.3C/F1). Capping cycles in Karachaganak are green-algal, foram skeletal packstone-grainstones, which are not seen at Anglesey. This discrepancy may be accommodated by considering the different age of the analogue to Karachaganak and the abundance of green algae in many of its facies.

The cycles both in Anglesey and Karachaganak are considered to have been deposited on a shallow bank interior setting, where sea level variations were a major control on sedimentation. This finding is in agreement with the global architecture of the Late Viséan-Serpukhovian shallow water sediments, which is characterised globally by a small-scale cyclicity related to glacio-eustatic sea level oscillations. Facies parasequences in older wells are not always easily detectable from core sampling as the spacing of approximately ten metres can be lower than the average thickness of individual cycles, as seen at Anglesey (where cycle thickness does not exceed four metres).

As in Anglesey, with the appearance of apparently deeper-water cycles and facies in the Brigantian, the late Viséan-early Serpukhovian section in Karachaganak seems to represent a period of relative drowning of the platform. Di Giovanni et al (2001a) recognises this as a period "in which 'rather deep' microbial bioherms were able to colonise the inner platform location'; a transgression in other words. Like the origin of the Anglesey deepening-

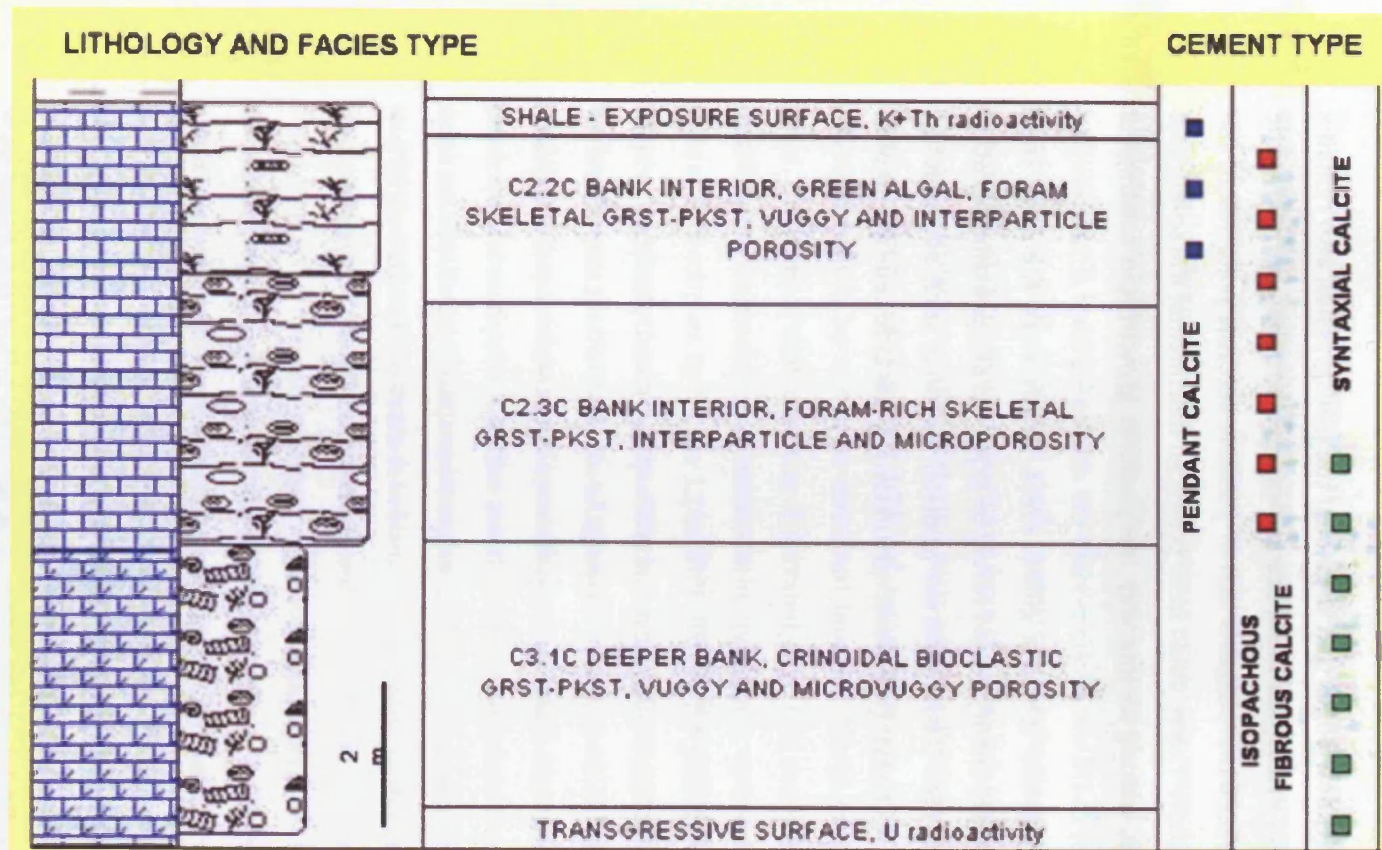


Figure 18: Ideal early Serpukhovian shallowing-upward cycle as seen in Karachaganak. Facies C3.1C and C2.3C have analogous facies in Anglesey (from Di Giovanni *et al*, 2001a).

event, Di Giovanni et al (2001a) acknowledges that at present the transgression also remains an enigma at Karachaganak. In the Pricaspian Basin the drowning event is placed above the Tula volcanics. Di Giovanni et al, (2001a) suggests that a “possible volcanic pollution of the Pre-Caspian waters during the middle Viséan could have produced detrimental life conditions for the carbonate producer biota, halting in this way the platform growth and causing its relative drowning”. This, however, could not accommodate the deepening seen at Anglesey (if there is truly a marked change) unless it was a global event. If this were the case, then complete destruction of the carbonate factory would surely be expected at a proximal location to the eruption such as the Pricaspian Basin, whereas at distal locations such as Anglesey, production may only be slowed. A change (for whatever reason) in eustatic sea-level would explain this deepening better.

A1.9.1 Comparison with the Sierra de Cuera Platform, Spain

Della Porta et al (2002; 2004) describe a steep-margined platform, which, although younger (lower Pennsylvanian) than Anglesey, is useful for a comparison of architectural styles and facies patterns. A fundamental difference in the style of sedimentation is apparent at Sierra de Cuera. Unlike Anglesey, there is no evidence of subaerial exposure developed on subtidal lithofacies, although the cycles do shallow-upwards. Della Porta et al explained this increased accommodation space using subsidence rates of 70-140 metres per million years. Regardless of the cause, the cycles deposited consist of packstone-grainstone shoals interlaced with algal (*Donezella*) bioherms.

The algal bioherms dictate the depositional style of the area, generating a palaeobathymetric relief of up to ten metres. These wackestone-packestone bioherms build-ups (Della Porta et al's Lithofacies B) can be laterally extensive for tens of kilometres and which developed in the oligophotic zone between 20-30m and 70-90m. Consequently this facies inter-fingers with Lithofacies Association D, a crinoidal-rich bioclastic packestone-grainstone which forms lenses 5m thick and 200-500 metres in width. Lithofacies Association D is interpreted to represent a subtidal shoal or bioclastic bar reflecting the reworking of crinoid meadows. Overall, due to both the mounded bioherms and grainstone shoaling more margin-ward, a complex mosaic of facies types is present in Sierra de Cuera, causing significant lateral variation between units of good and bad reservoir properties.

In contrast to the Sierra de Cuera platform, the facies in Anglesey are demonstrated to be relatively layer cake (Figure 10). The maximum lithofacies thickness deviation over the one kilometre study area was by forty centimetres, and interpretation of the logs along with

Figure 10, does not suggest that the platform at Anglesey was overly influenced by bioherms or a mounded palaeobathymetry. This concurs with the results of the point counting carried out as part of this study. Organisms which construct the bioherms units in Sierra de Cuera, principally *Donezella* and dasycladacean algae are rare in Anglesey. Palaeoberesellids in Anglesey compose less than 3% in most samples, and the highest percentage is 4.6%. *Koninckopora* is equally rare, usually occurring as less than 2% of total grains, also with a maximum of 4.6%. This is in stark contrast to the findings of Horbury & Adams (1996), who noted that of cycle-middle allochems from the Urswick Limestone Cumbria, palaeoberesellids may constitute up to 95% of the bioclasts present. Prior to this study, Adams (1992) recorded similar results stating that 67% of samples taken from Ilston, South Wales contained palaeoberesellids as the most abundant bioclast. These studies are not mirrored by results from Anglesey. Point counting illustrated that the most abundant bioclasts were forams, brachiopod fragments and echinoderm fragments, averaging 5.1%, 6.8% and 7.7% in all facies. This eclipses by far the 1.2% total average for palaeoberesellids.

One hypothesis for the differing styles of sedimentation between Anglesey and other Carboniferous platforms is that Anglesey represents an end-member of an evolution from the architecture presented at Sierra de Cuera. While the mechanism causing deposition to produce cycles deeper than the norm in an icehouse environment may be debatable, the fact remains that rates of accumulation were still significant at depths up to 90m; (Della Porta et al, 2004). At Sierra de Cuera it is feasible that the oligophotic carbonate-producing organisms formed delicate bioherms, which due to their fragile nature of their colonial communities could only exist sub-fair-weather wave-base (Figure 19). Bioherm growth logically gives rise to the inner-platform lensoid stratal geometries seen at Sierra de Cuera. Anglesey, however, may reflect the same segment (inner-platform) of a shelf without a mechanism for developing a large water column above the sea-bed. Under these conditions sedimentation may have been regulated by fair-weather wave-base, forcing uniform sedimentation and redistribution of sediment; preventing any algal build-ups. Storm conditions would occasionally damage the oligophotic algal factory further towards the margin, distributing minor amounts of algal fragments into the shallower landward parts of the shelf (and causing the minor algal fragment quantities seen during point counting). Simplified, this theory accepts there are two loci of carbonate accumulation; a deeper-water margin-ward oligophotic factory producing strata with a lensoid geometry, and one more shoreward, lacking bioherms builders and depositing layer-cake strata. To accurately assess any implications for reservoir development this may have, a study accurately quantifying the distinctions between the two factories, if any, must be undertaken.

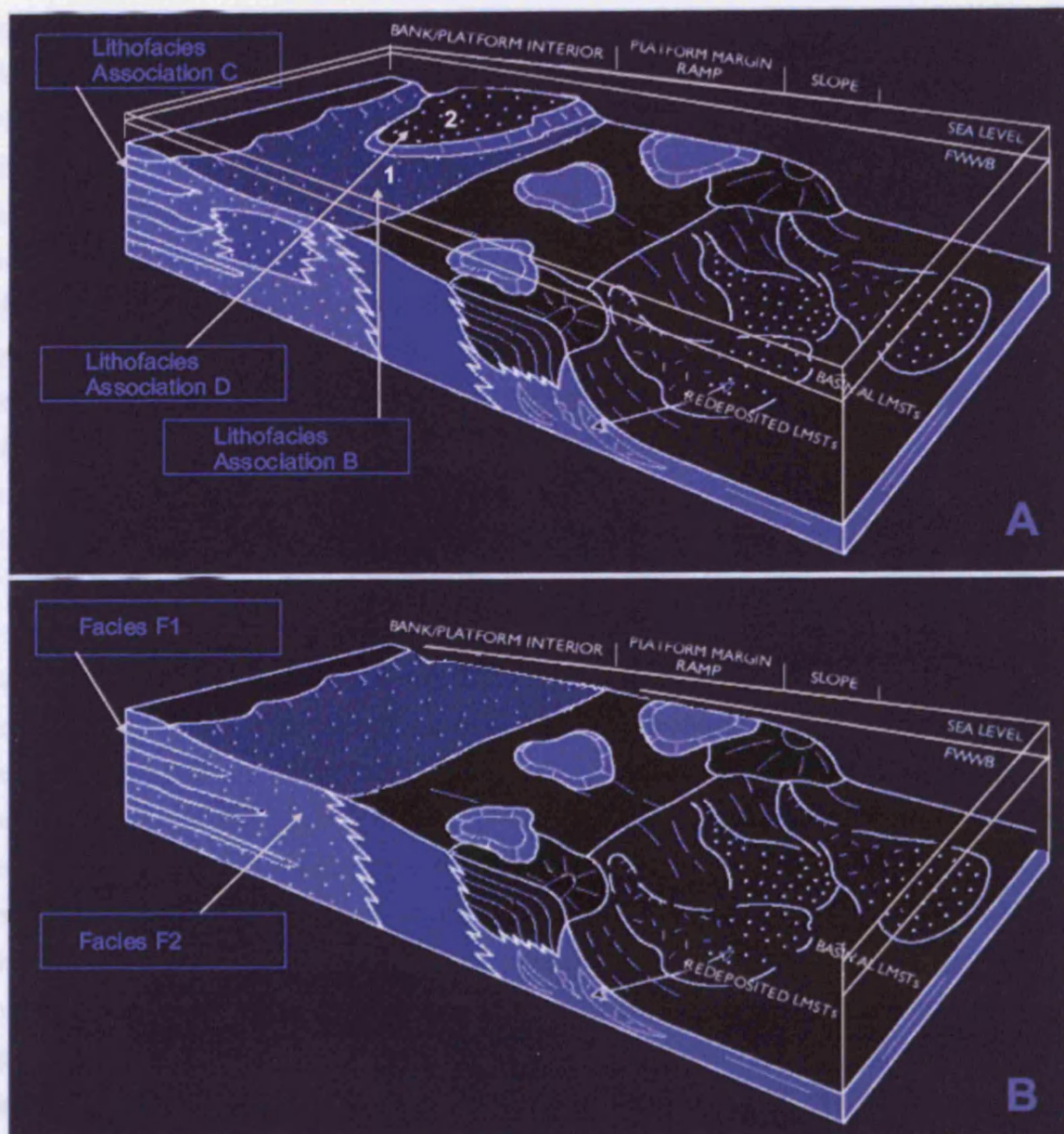


Figure 19: A) Block diagram of facies relationships of the Sierra de Cuera Platform (from Della Porta *et al.*, 2002) during a transgressive systems tract. Lithofacies Association B occurs as thin, sheet-like wackestone to packstone *Donezella* buildups, which developed in the oligophotic zone, 3-10m thick and laterally extensive for tens of kilometers. Laterally adjacent to this facies is Lithofacies Association D, a crinoid-rich bioclastic pack-grainstone which forms lenses 5m thick and 200-500m in width. This facies group is interpreted to represent a subtidal shoal or bioclastic bar formed from reworking of crinoid meadows. Note the overall greater water depth in comparison to Anglesey.

B) Block diagram of interpreted facies relationships in Anglesey during a transgressive systems tract. Compared to Sierra de Cuera the inner-platform facies are layer-cake and show no marked lateral thickness variation over the 1km study area. Both facies F1 and F2 occur as tabular beds between 1.5m and 2m thick. Diagram modified from Di Giovanni *et al.*, 2001a).

A1.10 CONCLUSIONS

The facies recognised at Anglesey by this study correspond well with what would be expected on a typical Lower Carboniferous carbonate platform. Additionally they conform to previous interpretations of the lithofacies of the area (Davies, 1984; 1991).

The theorised geological setting is also concordant with the lithofacies seen at outcrop and on a microfacies scale. On the whole, correlation between facies is good to excellent, and the only lateral variability seen occurs between Central and Eglwys Siglen locality, where the facies have relatively high micrite content.

Cyclicity too is conformable with what is expected from late Viséan inner platform cycles. Cycles are less than 4 metres in thickness, which in turn corresponds well with what is seen at Karachaganak, as do the facies.

It is not possible at this time to delineate a single petrographic characteristic that can distinguish Sierra de Cuera facies from those of Anglesey. It is likely that the presence of *Donezella* is one such characteristic. Further study is needed to quantify this.

A1.11 REFERENCES

- Adams, A. E. & Cossey, P. J., 2004. Chapter 8: North Wales Shelf. In *British Lower Carboniferous Stratigraphy*, (ed. by Cossey, P. J., et al), Geological Conservation Review Series, 29. Joint Nature Conservation Committee, Peterborough, pp. 366-91.
- Adams, A. E., Horbury, A. D. & Ramsay, A. T., 1992. Significance of palaeoberesellids (Chlorophyta) in Dinantian sedimentation, UK. *Lethaia*, 25, 375-382.
- Davies, J. R., 1981. Unpublished PhD Thesis, University of Wales, Aberystwyth.
- Davies, J. R., 1984. Sedimentary cyclicity in the late Asbian and early Brigantian (Dinantian) limestones of the Anglesey and Llandudno districts, North Wales. *Proceedings of the Geologists' Association*, 95, pp. 392-3.
- Davies, J. R., 1991. Karstification and pedogenesis on a late Dinantian carbonate platform, Anglesey, North Wales. *Proceedings of the Yorkshire Geological Society*, 48, pp. 297-321.
- Davies, J.R., 2004, Personal Communication via e-mail.
- Della Porta, G., Kenter, J.A.M., Immenhauser, A. & Bahamonde, J. R., 2002. Lithofacies character and architecture across a Pennsylvanian inner-platform transect (Sierra de Cuera, Asturias, Spain). *Journal of Sedimentary Research*, 72, pp. 898-916.
- Della Porta, G., Kenter, J.A.M. & Bahamonde, J. R., 2004. Depositional facies and stratal geometry of an Upper Carboniferous prograding and aggrading high-relief carbonate platform (Cantabrian Mountains, N. Spain). *Sedimentology*, 51, pp. 267-295.
- Di Giovanni, R., Balossino, P., Bigoni, F., Giovannelli, A., Caccialanza, P. G., Ferrini, C., Gorza, M., Meazza, O., Pampuri, F. & Venturini C., 2001a. Karachaganak Well 700: Geology, Petrophysics and Log Interpretation Report. Unpublished internal report for Karachaganak Integrated Organisation, Milan.

Di Giovanni, R., Balossino, P., Bigoni, F., Borromeo, O., Caccialanza, P. G., Ferrini, C., Gorza, M., Meazza, O., Pampuri, F. & Venturini C., 2001b. Karachaganak Well 152: Geology, Petrophysics and Log Interpretation Report. Unpublished internal report for Karachaganak Integrated Organisation, Milan.

Gorla, L., Miraglia, S., Nardon, S. & Zacchetti, O., 2002. Karachaganak Well 200: Geological Report. Unpublished internal report for Karachaganak Integrated Organisation, Milan.

Horbury, A. D. & Adams, A. E., 1996. Microfacies associations in Asbian carbonates: an example from the Urswick Limestone Formation of the southern Lake District, northern England. In *Recent Advances in Lower Carboniferous Geology*, (ed. by Strogon, P., et al), Geological Society Special Publication, 107. The Geological Society, London, pp. 221-38.

Somerville, I. D., 1979a. A sedimentary cyclicity in early Asbian (lower D1) limestones in the Llangollen district of North Wales. *Proceedings of the Yorkshire Geological Society*, 42, pp. 397-404.

Somerville, I. D., 1979b. A cyclicity in the early Brigantian (D2) limestones east of the Clwydian Range, North Wales and its use in correlation. *Geological Journal*, 14, pp. 69-86.

Appendix 2:
1:100 stratigraphic log of the Honaker Trail Section,
Utah, USA

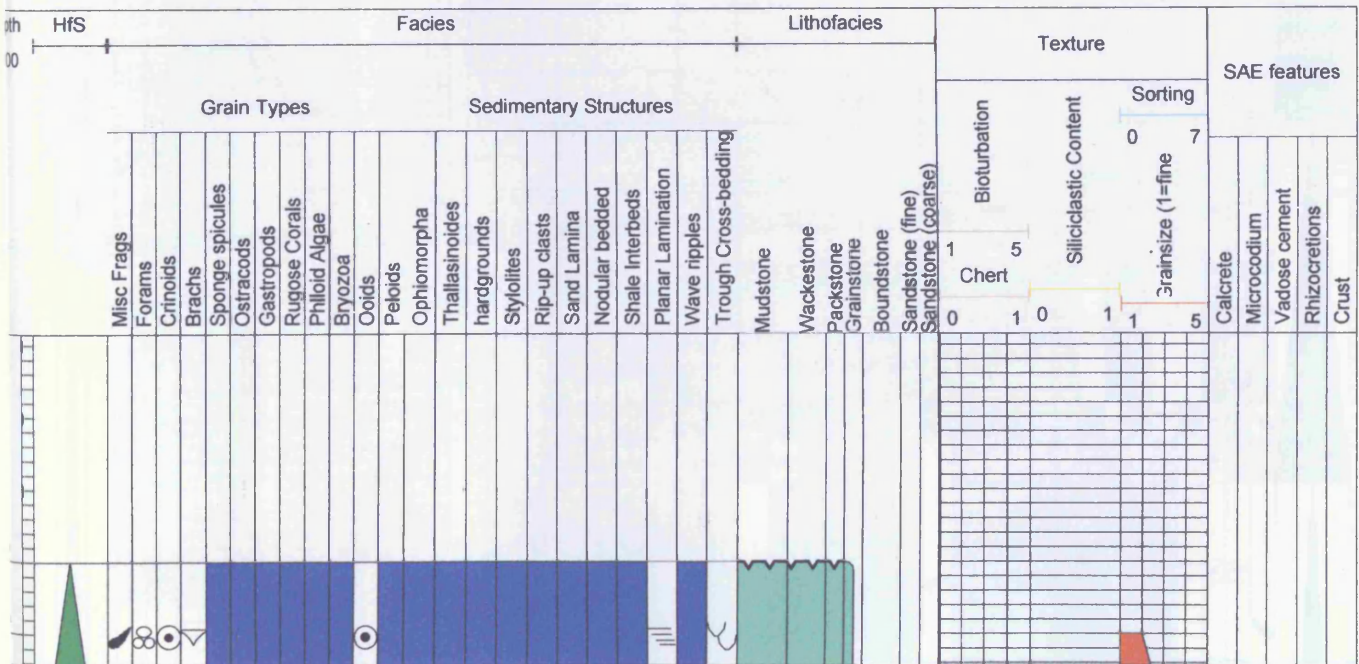
SECTION: Honaker Trail
LOCATION: Utah, USA
DATA TYPE: Stratigraphic log
DATA DEPTHS: 0-154.11m
LOGGED BY: David Pollitt
DATE: December, 2006

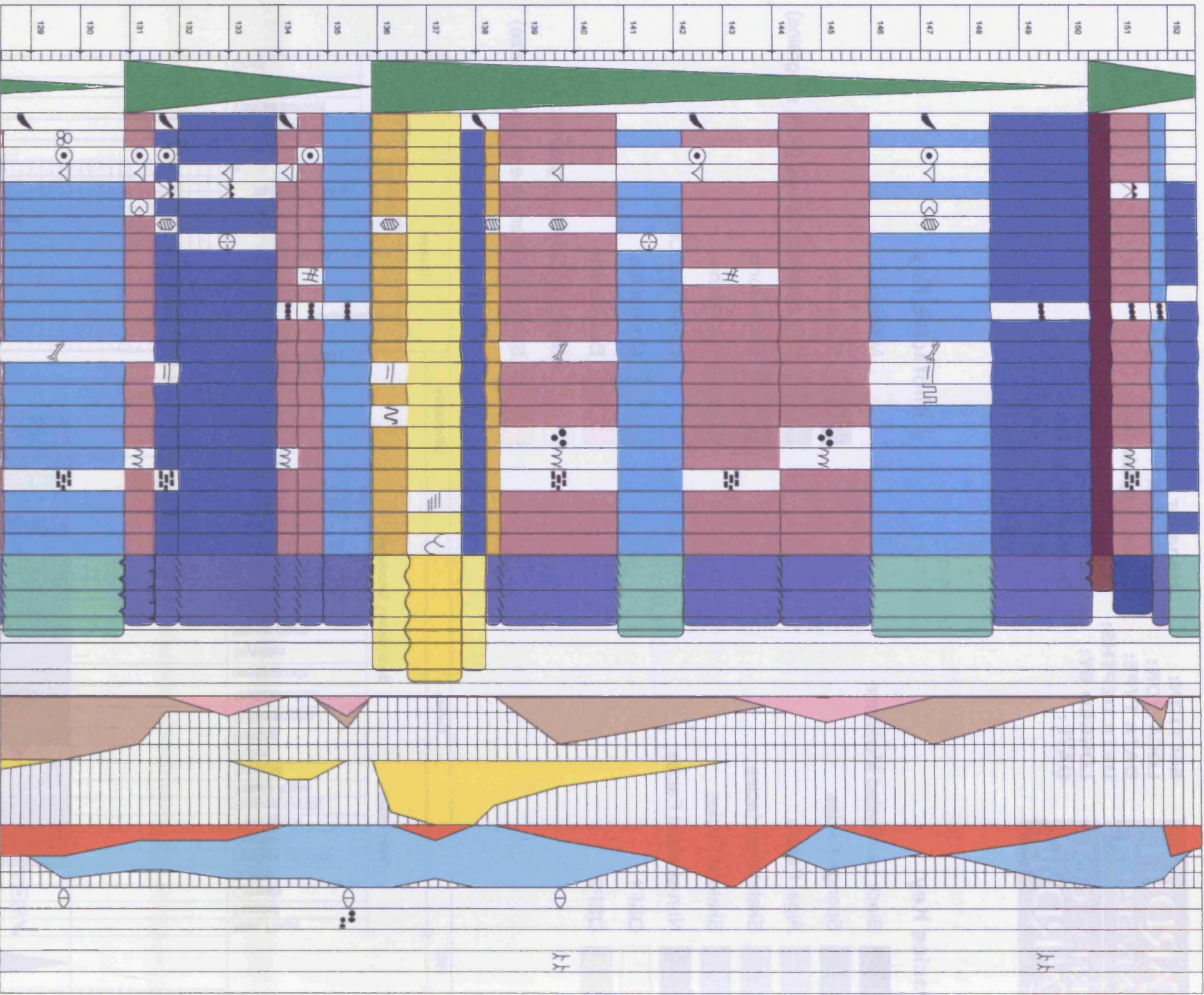
Facies Key

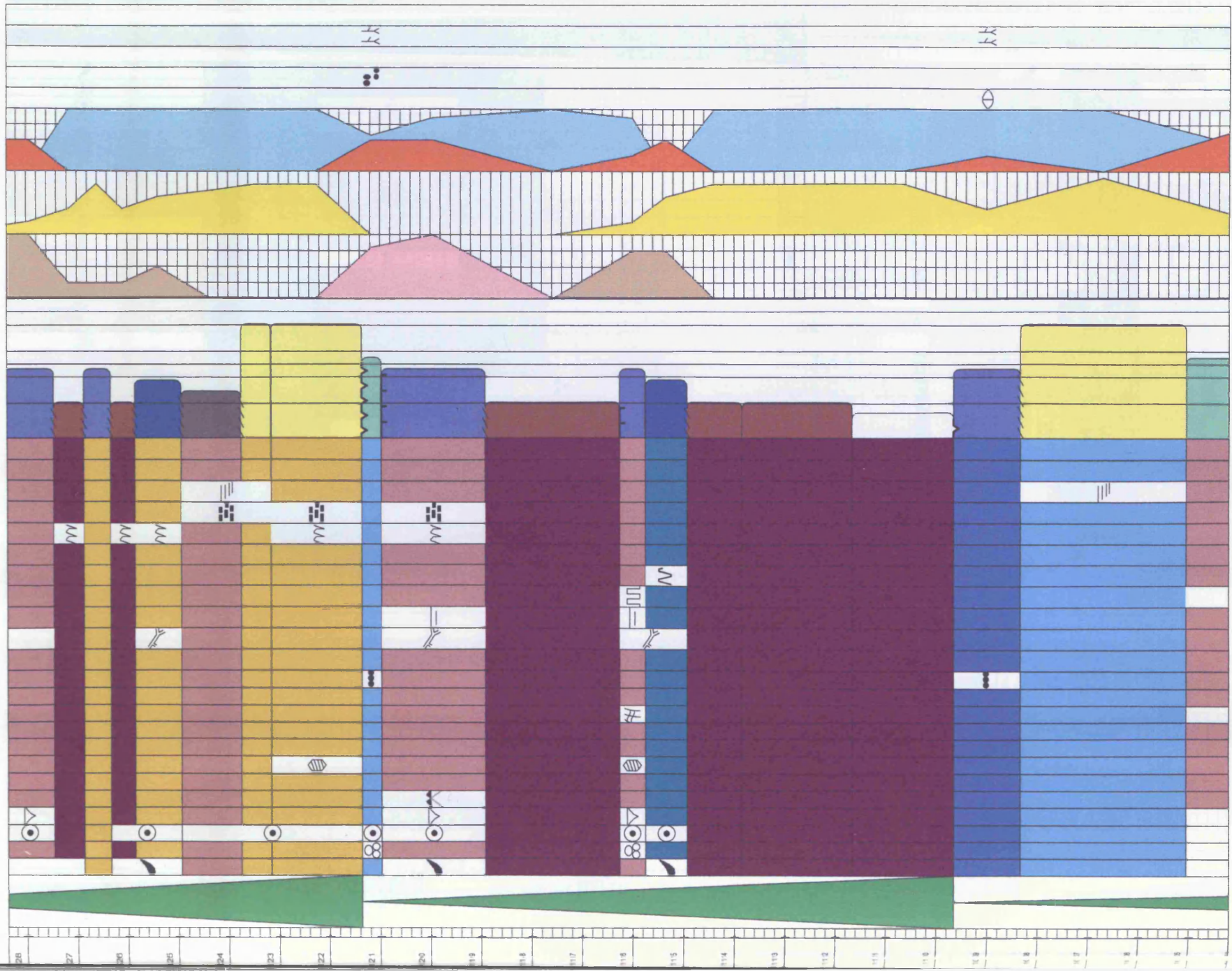
-  Black Laminated Mudstone
-  Sponge Facies
-  Algal Facies
-  Skeletal-silt facies
-  Skeletal Facies
-  Non-skeletal Facies
-  QSF1
-  QSF2

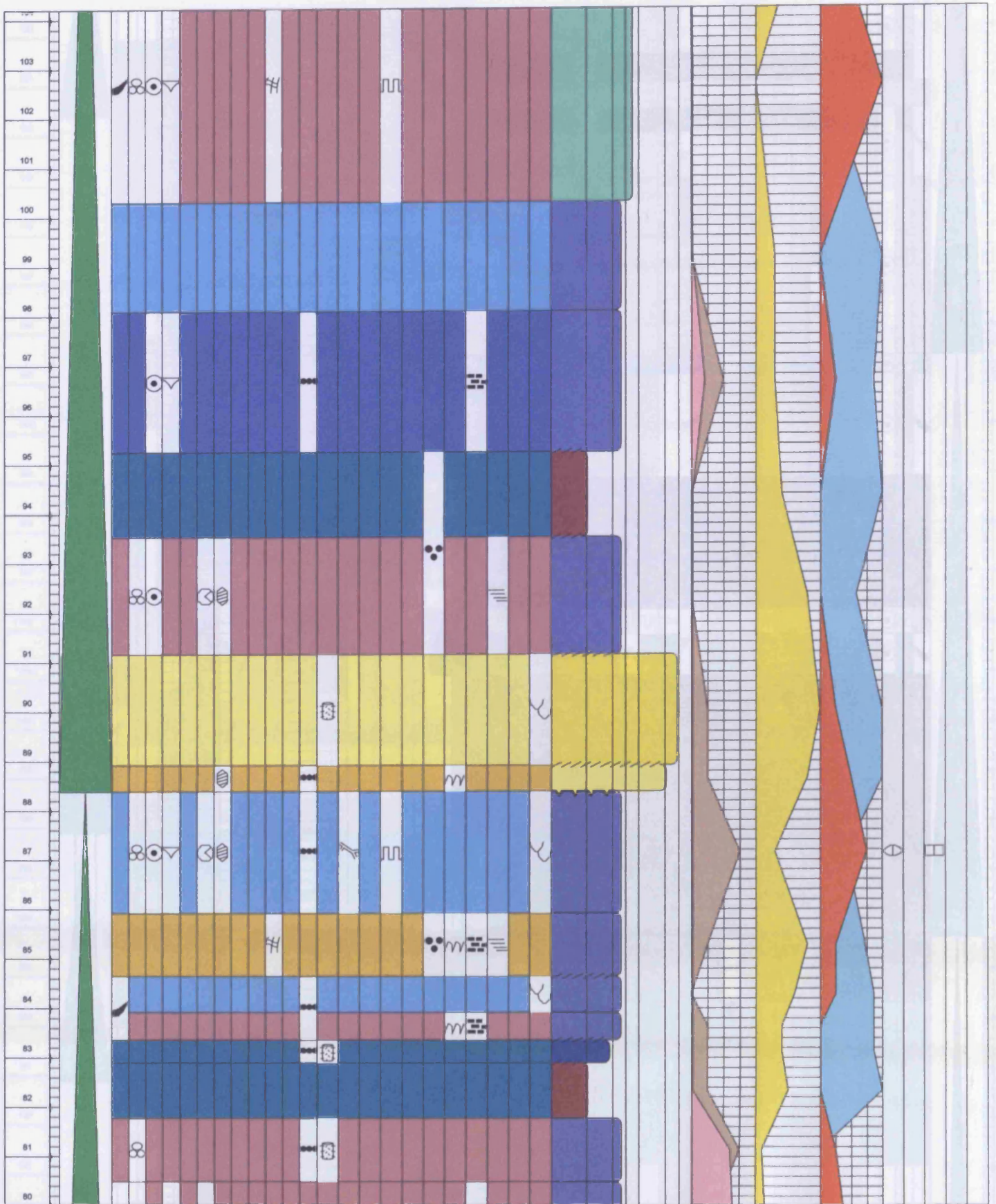
Lithofacies Key

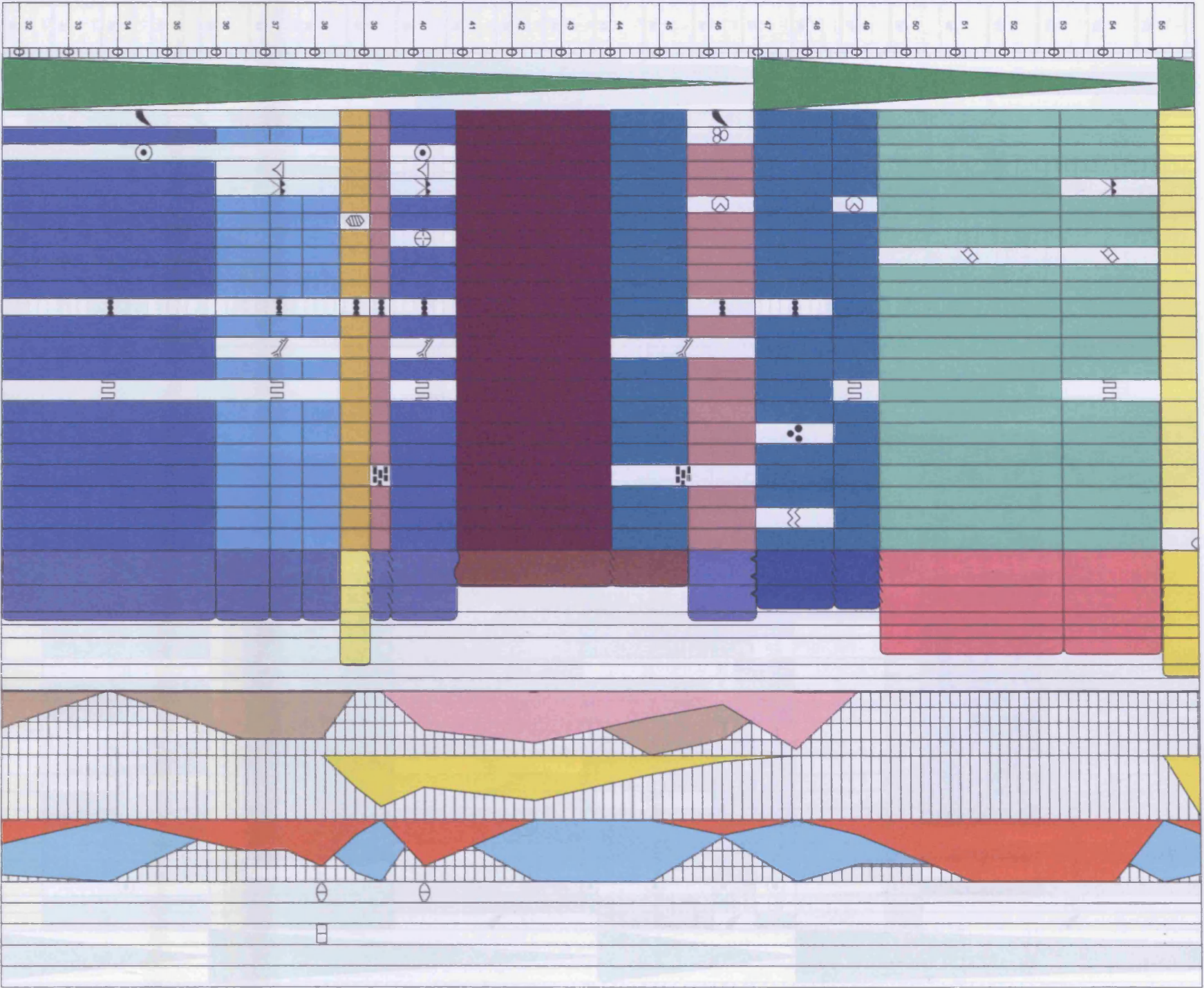
-  Missing
-  Mudstone
-  Silty carbonate shale (50% silt grains)
-  Wackstone
-  Packstone
-  Diagenetic Crust
-  Grainstone
-  Boundstone
-  Siltstone (20-63um grain size)
-  Sandstone (very fine to granule size)

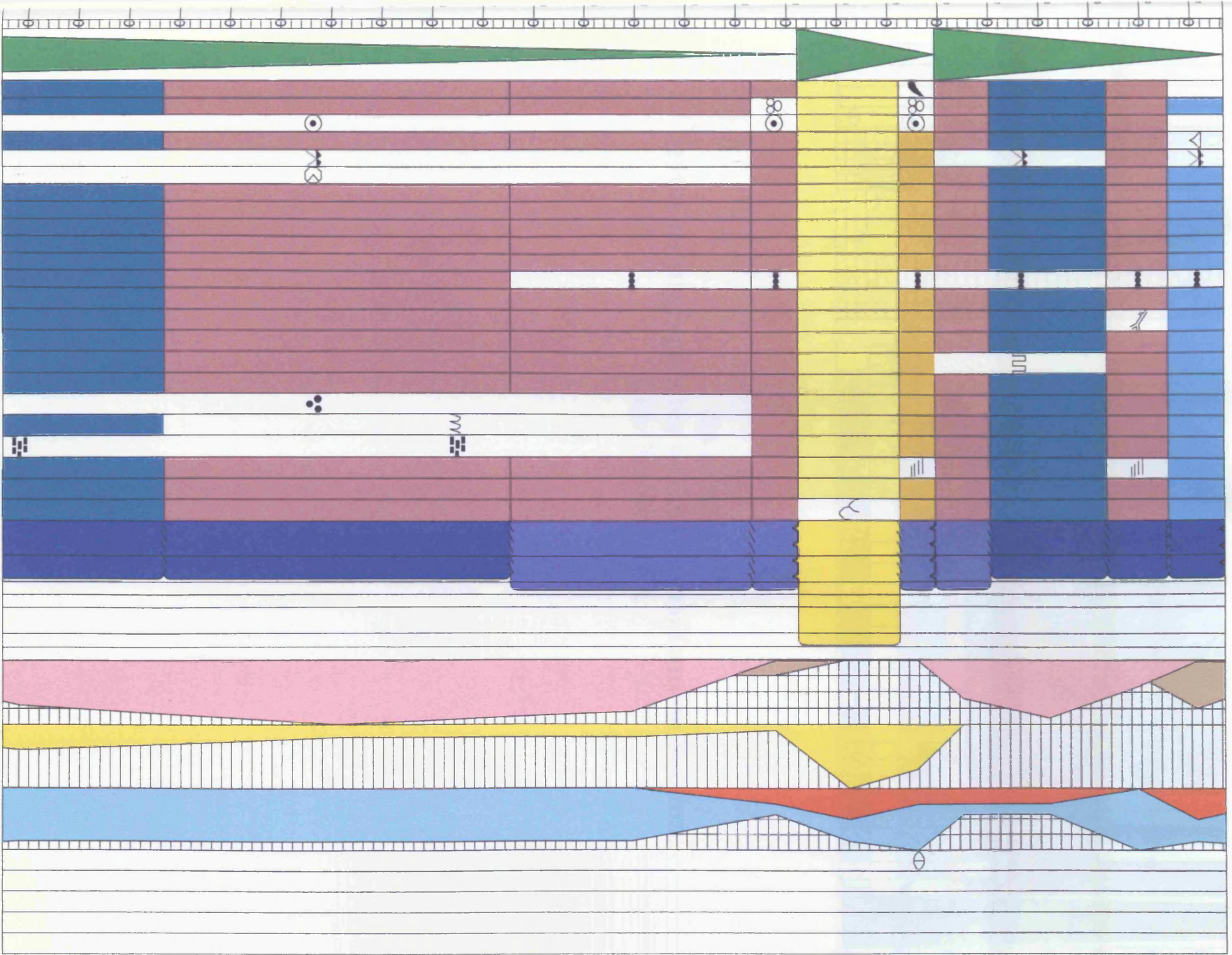












Appendix 3:
1:100 stratigraphic log of the Fresnal Canyon Section,
New Mexico, USA

SECTION: Fresno Canyon
LOCATION: New Mexico, USA
DATA TYPE: Stratigraphic log
DATA DEPTHS: 0-124m
LOGGED BY: David Pollitt
DATE: November, 2005

Lithofacies Key

-  Missing
-  Mudstone
-  Silty carbonate shale (50% silt grains)
-  Wackstone
-  Packstone
-  Grainstone
-  Sandstone (very fine to granule size)

